ENRICHMENT OF DENITRIFYING ANAEROBIC METHANE OXIDATION (DAMO) AND ANAEROBIC AMMONIUM OXIDATION (ANAMMOX) CO-CULTURE FOR THE TREATMENT OF ANAEROBIC DIGESTER EFFLUENT

A THESIS SUBMITTED TO
THE GRADUATE SCHOOL OF NATURAL AND APPLIED SCIENCES
OF
MIDDLE EAST TECHNICAL UNIVERSITY

BY

RAYAAN HARB

IN PARTIAL FULFILLMENT OF THE REQUIREMENTS
FOR
THE DEGREE OF DOCTOR OF PHILOSOPHY
IN
ENVIRONMENTAL ENGINEERING

JANUARY 2023

Approval of the thesis:

ENRICHMENT OF DENITRIFYING ANAEROBIC METHANE OXIDATION (DAMO) AND ANAEROBIC AMMONIUM OXIDATION (ANAMMOX) CO-CULTURE FOR THE TREATMENT OF ANAEROBIC DIGESTER EFFLUENT

submitted by **RAYAAN HARB** in partial fulfillment of the requirements for the degree of Doctor of Philosophy i**n** Environmental Engineering**, Middle East Technical University** by,

Prof. Dr. Halil Kalıpçılar
Dean, Graduate School of **Natural and Applied Sciences** _____

Prof. Dr. Bülent İçgen
Head of the Department, **Environmental Engineering** _____

Prof. Dr. Tuba Hande Bayramoğlu
Supervisor, **Environmental Engineering, METU** _____

Examining Committee Members:

Prof. Dr. Filiz B. Dilek
Environmental Engineering, METU _____

Prof. Dr. Tuba Hande Bayramoğlu
Environmental Engineering, METU _____

Prof. Dr. Bilge Kocamemi
Environmental Engineering, Marmara University _____

Prof. Dr. F. Dilek Sanin
Environmental Engineering, METU _____

Prof. Dr. Ayşenur Uğurlu
Environmental Engineering, Hacettepe University _____

Date: 20.01.2023

I hereby declare that all information in this document has been obtained and presented in accordance with academic rules and ethical conduct. I also declare that, as required by these rules and conduct, I have fully cited and referenced all material and results that are not original to this work.

Name Last name : Rayaan Harb
Signature :

ABSTRACT

ENRICHMENT OF DENITRIFYING ANAEROBIC METHANE OXIDATION (DAMO) AND ANAEROBIC AMMONIUM OXIDATION (ANAMMOX) CO-CULTURE FOR THE TREATMENT OF ANAEROBIC DIGESTER EFFLUENT

Harb, Rayaan
Doctor of Philosophy, Environmental Engineering
Supervisor: Prof. Dr. Tuba Hande Bayramoğlu

January 2023, 421 pages

Recently, the implementation of next-generation biological nutrient removal techniques aimed at recycling nutrients such as nitrogen and phosphorus while generating energy, producing value-added products and mitigating greenhouse gas emissions, in wastewater treatment plants is being emphasized. In this regard, investigating the development and applicability of a DAMO-Anammox co-culture and a novel DAMO-Anammox-Microalgae sequential treatment unit in the treatment of anaerobic digester (AD) effluent was the main goal of this PhD research. A DAMO-Anammox co-culture is capable of oxidizing methane into carbon dioxide, oxidizing ammonium and reducing nitrite and nitrate into nitrogen gas. A DAMO-Anammox co-culture was enriched in an SBR and the effect of hydraulic retention time (HRT), thus nitrogen loading rate was assessed on the co-culture performance. The relative abundance in the microbial consortium of the target phyla were 8% *Planctomycetota*, 0.5% NC10, and 0.16% *Euryarchaeota*. Since the co-culture was Anammox dominated, the reduction in HRT from 6 to 4 days did not allow the DAMO microorganisms, especially DAMO bacteria any chance of competition with the Anammox bacteria. The short-term effect of ammonium to dissolved methane ratios (0, ¼, 1), which has not been investigated in the current literature, was assessed in batch reactors. The results illustrated DAMO bacteria dominance at ratios less

than 1, and Anammox dominance at ratio of 1 constraining the DAMO bacteria activity in turn facilitating the increase in DAMO archaea activity. The effect of various combinations of nitrogen sources on the enrichment of the DAMO microorganisms and the DAMO-Anammox co-culture were researched. The results revealed that in the absence of a dominant Anammox culture, the DAMO (DAMO bacteria and DAMO archaea) activity was prominent which may allow a shorter enrichment period of a DAMO culture. A DAMO-Anammox co-culture consisting of 7% *Planctomycetota*, 0.2% NC10 and 0.3% *Euryarchaeota* was employed to treat an AD effluent with concentrations of about 222±8 mg TN/L (166±15 mg TAN/L and 56±6 mg NO_2^--N/L), achieving a TN removal rate of 12.1±2.6 mg N/L·day. The DAMO-Anammox-Microalgae system was successful in completely removing nitrogen and phosphorus from an AD effluent. Regarding the promising nature of this integrated system, an innovative wastewater treatment system was further proposed.

Keywords: DAMO, Anammox, microalgae, anaerobic, denitrification

ÖZ

ANAEROBİK ÇÜRÜTÜCÜ ÇIKIŞ SUYUNUN ARITIMI İÇİN DENİTRİFİYE ANAEROBİK METAN OKSİDASYONU (DAMO) VE ANAEROBİK AMONYUM OKSİDASYONU (ANAMMOX) BİRLEŞİK KÜLTÜRÜNÜN ZENGİNLEŞTİRİLMESİ

Harb, Rayaan
Doktora, Çevre Mühendisliği
Tez Yöneticisi: Prof. Dr. Tuba Hande Bayramoğlu

Ocak 2023, 421 sayfa

Son zamanlarda, atıksu arıtma tesislerinde enerji ve katma değerli ürünlerin üretiminin yanında sera gazı emisyonlarının azaltımı, azot ve fosfor gibi besin maddelerinin geri dönüştürülmesini amaçlayan yeni nesil biyolojik besin giderim tekniklerinin üzerinde durulmaktadır. Bu bağlamda, bu doktora tezinin temel amacı, bir DAMO-Anammox birleşik kültürünün ve yeni bir DAMO-Anammox-Mikroalg ardışık arıtma ünitesinin anaerobik çürütücü (AÇ) çıkış sularının arıtımı için geliştirilmesini ve uygulanabilirliğini araştırmaktır. DAMO-Anammox birleşik kültürü metanı oksitleyerek karbon dioksite dönüştürebilir, amonyumu oksitleyebilir, ve nitrit ve nitratı azot gazına indirgeyebilir. DAMO-Anammox birleşik kültürü, bir AKR'de (Ardışık kesikli reaktör) zenginleştirilmiş ve hidrolik bekletme süresinin (HBS), dolayısıyla azot yükleme hızının birleşik kültür performansına etkisi araştırılmıştır. Hedef filumun mikrobiyal konsorsiyumundaki göreceli bolluğu %8 *Planctomycetota*, %0,5 NC10 ve %0,16 *Euryarchaeota* olarak gözlemlenmiştir. Birleşik kültür Anammox ağırlıklı olduğundan, HBS'nin 6 günden 4 güne düşürülmesi, DAMO mikroorganizmalarının, özellikle DAMO bakterilerinin Anammox bakterileriyle rekabet etmesine izin vermemiştir. Amonyum-çözünmüş metan oranının (0, ¼, 1) kısa vadeli etkisi, mevcut literatürde araştırılmamış olup, bu çalışma kapsamında kesikli reaktörlerde araştırılmıştır. Sonuçlar, 1'den küçük

oranlarda DAMO bakteri baskınlığını, 1 oranında ise Anammox baskınlığını ve bu koşulda DAMO bakteri aktivitesinin kısıtlanırken DAMO arke aktivitesindeki artışın kolaylaştığını göstermiştir. Azot türlerinin çeşitli kombinasyonlarının DAMO mikroorganizmaların ve DAMO-Anammox birleşik kültürünün zenginleştirilmesine etkisi araştırılmıştır. Sonuçlar, baskın bir Anammox kültürü olmadığında, DAMO (DAMO bakteri ve DAMO arke) aktivitesinin belirgin olduğunu ve bunun da DAMO kültürü için daha kısa bir zenginleştirme süresine yol açabileceğini göstermiştir. %7 *Planctomycetota*, %0,2 NC10 ve %0,3 *Euryarchaeota*'dan oluşan bir DAMO-Anammox birleşik kültürü, yaklaşık 222±8 mg TN/L (166±15 mg TAN/L ve 56±6 mg NO_2^--N/L) derişime sahip bir AÇ çıkış suyunu arıtmak için kullanılmış ve 12,1±2,6 mg N/L·gün'lük bir TN giderim hızı elde edilmiştir. DAMO-Anammox-Mikroalg sistemi, AÇ çıkış suyundan azot ve fosforu tamamen gidermede başarılı olmuştur. Bu entegre sistemin gelecek vadeden özellikleri doğrultusunda yenilikçi bir atıksu arıtma sistemi de önerilmiştir.

Anahtar Kelimeler: DAMO, Anammox, mikroalg, anaerobik, denitrifikasyon

Dedicated To

My Beloved Parents

Abu Rayaan and Um Rayaan

ACKNOWLEDGMENTS

This thesis saw the light with the kind support and help of many individuals. I would like to extend my sincere thanks to all of them. Foremost, I would like to express my sincere gratitude to my advisor Prof. Dr. Tuba H. Ergüder Bayramoğlu for her guidance, support, and encouragement in my PhD study and research. I would also like to thank the members of the examining committee, especially the members of the Thesis Monitoring Committee, Prof. Dr. Filiz B. Dilek, Prof. Dr. Bilge Kocamemi, Prof. Dr. F. Dilek Sanin and Prof. Dr. Ayşenur Uğurlu for their significant contributions, insightful comments and remarks. I would like to thank Prof. Dr. Bilge Kocamemi for her support during the research.

I gratefully acknowledge the financial support provided by the Scientific and Technological Research Council of Turkey (TÜBİTAK) for the project (Project No. 118Y195) from which this thesis has emerged

I would like to express my gratitude towards my family, Douraid, Iman, Lama and Yazan Harb for their unconditional encouragement, patience, motivation and support throughout my life.

In addition, I would like to thank all my colleagues and friends for their support especially Irmak Subaşı, Tercan Çataklı, Nihan Kalaycıoğlu, Tuğba Çelik Çağlar, Ertan Hoşafcı, Dilan Laçin, Simgenur Sağdiç, Feride Ece Kutlar, Mohsin Ali, Mert Şanlı, Amin Ghaderi Kia, Riyadh El Alami, Elif Sena Uzunpınar, Engin Koç, Bora Kiraz, Mert Erkanlı, Yunus Emre Beyribey and Emre Yıldırım, for the stimulating discussions, chess nights at the bar, and for all the fun we had in the past five years. Finally, I would like to thank Hüseyin Çalışkan and Alper Çalışkan for their technical support and advice.

TABLE OF CONTENTS

LIST OF TABLES

TABLES

LIST OF FIGURES

FIGURES

LIST OF ABBREVIATIONS

ABBREVIATIONS

AD	Anaerobic digester
AFBR	Anaerobic fixed bed reactor
AH	Anaerobic hybrid
Al	Aluminium
AMO-D	Anaerobic methane oxidation coupled to denitrification
AMX	Anaerobic ammonium oxidation
ANME-d	Anaerobic methane oxidation coupled to denitrification
AOB	Ammonia-oxidizing bacteria
AOM	Anaerobic oxidation of methane
Ar	Argon
ATP	Adenosine triphosphate
Ba	Barium
BBM	Bold's basal medium
BNR	Biological nutrient removal
BOD	Biochemical oxygen demand
C/N	Carbon to Nitrogen
$CaCO_3$	Calcium carbonate
C_{final}	Final concentration
CH_4	Methane

$C_{initial}$	Initial concentration
Co	Cobalt
CO_2	Carbon dioxide
CO_3^{2-}	Carbonate
COD	Chemical oxygen demand
CSTR	Completely stirred-tank reactor
Cu^{2+}	Copper (II)
Cy5	Red fluorophore Cyanine 5
DAMO	Denitrifying anaerobic methane oxidation
DAMOa	Denitrifying anaerobic methane oxidizing archaea
DAMOb	Denitrifying anaerobic methane oxidizing bacteria
DAMX	DAMO-Anammox
DAPI	4′,6-diamidino-2-phenylindole
DCW	Dry cell weight
DEN	Denitrifiers
DHS	Down-flow hanging sponge reactor
dNTP	Deoxyribonucleotide triphosphate
DO	Dissolved oxygen
EPS	Extracellular Polymeric Substances
Fe^{2+}	Iron (II)
Fe^{3+}	Iron (III)
FISH	Fluorescent In-Situ Hybridization

FNA	Free nitrous acid
GC	Gas chromatograph
GFP	Green fluorescent protein
GHG	Greenhouse gas
GWP	Global warming potential
H.D.	Heterotrophic Denitrification
$H_2PO_4^-$	Dihydrogen phosphate
H_2S	Hydrogen sulfide
HCO_3^-	Bicarbonate
He	Helium
HfMBR	Hollow-fiber membrane bioreactor
HPO_4^{2-}	Hydrogen phosphate
HRT	Hydraulic retention time
IC	Ion chromatograph
ICM	Intracytoplasmic membrane
$K_{CH_4}^{D_a}$	Methane saturation constant for DAMOa
$K_{CH_4}^{D_b}$	Methane saturation constant for DAMOb
$K_{NO_2^-}^{D_b}$	Nitrite saturation constant for DAMOb
$K_{NO_2^-}^{An}$	Nitrite saturation constant for Anammox
KNO_3	Potassium nitrate
LEL	Low explosion limit

LOD	Limit of detection
LOQ	Limit of quantification
MAMBR	Membrane aerated membrane bioreactor
MBfBR	Membrane Biofilm Bioreactor
MBR	Membrane Bioreactor
Mn	Manganese
Mo^{2+}	Molybdenum (II)
MOB	Aerobic methane oxidizing bacteria
MSGLR	Magnetically stirred gas lift reactor
N	Nitrogen
N_2	Nitrogen gas
N_2O	Nitrous oxide
NaCl	Sodium chloride
$NaHCO_3$	Sodium bicarbonate
$NaNO_2$	Sodium nitrite
NGS	Next-Generation Sequencing
NH_3-N	Ammonia-nitrogen
NH_4^+	Ammonium
NH_4^+-N	Ammonium-nitrogen
$[NH_4^+\text{-}N]_f$	Final Ammonium-nitrogen concentration
$[NH_4^+\text{-}N]_i$	Initial Ammonium-nitrogen concentration
NH_4Cl	Ammonium chloride

Ni	Nickel
NiR	Nitrate reductase
NLR	Nitrogen Loading Rate
NO	Nitric oxide
NO_2^-	Nitrite
NO_2^--N	Nitrite-nitrogen
$[NO_2^-\text{-}N]_f$	Final Nitrite-nitrogen concentration
$[NO_2^-\text{-}N]_i$	Initial Nitrite-nitrogen concentration
NO_3^-	Nitrate
NO_3^--N	Nitrate-nitrogen
$[NO_3^-\text{-}N]_f$	Final Nitrate-nitrogen concentration
$[NO_3^-\text{-}N]_i$	Initial Nitrate-nitrogen concentration
O_2	Oxygen
O2DN	Oxygenic denitrification
OD	Optical density
OH^-	Hydroxide
OLR	Organic loading rate
P	Phosphorus
PAR	Photosynthetically active radiation
PBR	Photobioreactor
PBS	Phosphate Buffer Saline
PCR	Polymerase Chain Reaction

PFA	Paraformaldehyde
PLR	Phosphate loading rate
pMMO	Particulate methane mono-oxygenase
PO_4^{3-}	Orthophosphate
PO_4^{3-}-P	Orthophosphate-phosphorus
PQQ	Pyrroloquinoline quinone
RAS	Recycle activated sludge
$r_{NH_4^+}$	Ammonium removal rate
$r_{NO_2^-}$	Nitrite removal rate
$r_{NO_3^-}$	Nitrate removal rate
$r_{Anammox\ NO_2^-}$	Nitrite-based Anammox reaction rate
$r_{DAMOa\ NO_3^-}$	Nitrate-based DAMOa reaction rate
$r_{DAMOb\ NO_2^-}$	Nitrite-based DAMOb reaction rate
rpm	Rounds per minute
rRNA	Ribosomal ribonucleic acid
SBR	Sequencing Batch Reactor
SCADA	Supervisory control and data acquisition
sCOD	Soluble Chemical Oxygen Demand
S-DAMO	Sulfate-dependent anaerobic methane oxidation
SFBR	Semi-fed batch reactor
Si	Silicon

SND	Simultaneous Nitrification and Denitrification
SO_4^{2-}	Sulfate
SOB	Sulfur-Oxidizing Bacteria
SOP	Soluble Ortho-Phosphate
SRB	Sulfate-Reducing Bacteria
SRT	Solid Retention Time
SRT_{min}	Minimum solid retention time
SWW	Synthetic wastewater
TAN	Total Ammonium Nitrogen
TCD	Thermal Conductivity Detector
tCOD	Total chemical oxygen demand
TN	Total Nitrogen
$TN_{available}$	Available Total Nitrogen concentration
TN_f	Final Total Nitrogen concentration
TN_i	Initial Total Nitrogen concentration
$TN_{removed}^{AMX}$	Total Nitrogen removed by Anammox
$TN_{removed}^{DAMOa}$	Total Nitrogen removed by DAMOa
$TN_{removed}^{DAMOb}$	Total Nitrogen removed by DAMOb
$TN_{removed}^{microorganism}$	Total Nitrogen removed by each target microorganism
TOC	Total Organic Carbon
TP	Total phosphorus
TSS	Total suspended solids

UASB	Up-flow anaerobic sludge blanket
UASBR	Up-flow Anaerobic Sludge Blanket Reactor
UEL	Upper explosion limit
UV	Ultraviolet
v/v	Volume to volume
VAP	Value-added product
VFA	Volatile fatty acid
VSS	Volatile suspended solids
vvm	Volume of gas per unit volume of growth medium per minute
WAS	Waste activated sludge
WWTP	Wastewater treatment plant
Zn	Zinc
$\%CATN_{removed}$	Percentage contribution to the available TN removal
ΔG^0	Gibbs free energy
Δ C	Change in concentration
$\Delta[NH_4^+\text{-}N]$	Change in ammonium-nitrogen concentration
$\Delta[NO_2^-\text{-}N]_{AMX}$	Nitrite-nitrogen concentration consumed by Anammox
$\Delta[NO_2^-\text{-}N]_{DAMOa}$	Nitrite-nitrogen concentration produced by DAMOa
$\Delta[NO_2^-\text{-}N]_{DAMOb}$	Nitrite-nitrogen concentration consumed by DAMOb
$\Delta[NO_3^-\text{-}N]_{AMX}$	Nitrate-nitrogen concentration produced by Anammox
$\Delta[NO_3^-\text{-}N]_{DAMOa}$	Nitrate-nitrogen concentration consumed by DAMOa

CHAPTER 1

INTRODUCTION

1.1 Statement of the Problem

Biological nutrient removal (BNR) techniques in wastewater treatment plants (WWTPs) began with the purpose of removing nutrients such as nitrogen and phosphorus. Nowadays, we are searching for alternatives and modifications that can generate energy, produce value-added products and mitigate the greenhouse gas (GHG) emissions while treating the wastewater. This is achieved with the understanding that wastewater is a valuable resource that can be utilized to recycle nutrients back to the environment and to harvest energy whilst reducing the carbon footprint of WWTPs.

Conventional BNR processes have a high energy demand that results in little or no recovery of resources and energy. These processes often require external chemical inputs (Ahn, 2006; Modin et al., 2007). However, wastewater containing both organic carbon and nutrients such as nitrogen and phosphorus has the potential for resource and energy recovery if the appropriate processes were implemented. This has led to a transformation in wastewater treatment practices that focus on energy and resource recovery whilst increasing treatment efficiency. In that scope, anaerobic processes are emphasized for energy recovery since they require a very low energy input compared to aerobic processes.

Despite the controllable production and collection of methane in WWTPs in the form of biogas, as a sustainable and renewable form of energy, a portion of the methane is also uncontrollably emitted to the environment. This occurs at various steps of the units and processes in operation at WWTPs. The methane emissions from WWTPs account for approximately 7% of the global emission (U.S. EPA, 2012) and contribute to 20% of global warming.

Therefore, a compact system aimed at biological nutrient removal in its various forms along with GHG emissions mitigation, at a low operation cost whilst having the potential of producing numerous value added products is crucial at this critical period. Hence nitrogen driven methane oxidation appears to provide prospect in wastewater treatment systems (Wang et al., 2017a). The Denitrifying Anaerobic Methane Oxidizing (DAMO) microorganisms are responsible of undertaking such a process by linking the carbon and nitrogen cycles (Shen et al., 2012). The DAMO microorganisms target NO_2^-, NO_3^- and CH_4 and convert them to N_2 and CO_2. Additionally, it has been found that DAMO microorganisms can function very well in a co-culture with Anaerobic Ammonium Oxidizing (Anammox) bacteria providing an extra dimension in nutrient removal by targeting NH_4^+ as well (Zhu et al., 2011). Therefore, implementing a DAMO-Anammox co-culture for wastewater treatment seems to be promising, especially that an external carbon source or energy input is not required when compared to conventional nitrogen removal techniques.

Research focusing on the cultivation and enrichment of the DAMO microorganisms and the DAMO-Anammox co-culture has been conducted. These studies determined the critical factors and their ranges such as temperature, pH, nitrogen source provided and their ratios, trace metals, DO concentration, reactor configuration and inoculum source. Nevertheless, studies aim at evaluating the effects of factors such as CO_2 and H_2S (Wang et al., 2017a), biodegradable organic matter, heavy metals, salinity, suspended solids, hydraulic shock loadings, NH_4^+:CH_4 molar ratios should be conducted (Harb et al., 2021). Since such parameters might be present in potential wastewater to be treated by DAMO processes, such as AD liquor and/or landfill leachate.

The DAMO-Anammox co-culture has been only tested on lab-scale (Wang et al., 2017a). In order to implement full-scale DAMO-based technologies for wastewater treatment, scaling up is required. In this scope, challenges that need to be addressed will emerge. For instance, the long startup time for a DAMO-Anammox co-culture, dissolved methane concentration and its bioavailability and biomass retention are

some of the major concerns. The choice of appropriate inoculum and reactor configuration may resolve some of these challenges.

The DAMO process has been integrated with Anammox so far but not combined with any sequential system. DAMO-Anammox systems are capable of removing nitrogen species and CH_4, yet phosphorus remains unremoved, therefore, further treatment would be required. Employing microalgae for the treatment of phosphorus may be useful. An integrated DAMO-Anammox-Microalgae proposed in this thesis has the potential to remove dissolved methane, ammonium, nitrite, and nitrate, phosphate, and even carbon dioxide. The microalgae can be further recycled to an AD for energy extraction or can be the source of value-added products. This will also help mitigate GHG emissions and decrease the carbon and energy footprint of WWTPs.

1.2 Scopes and Objectives

The scope of this PhD research is to investigate the development of a DAMO-Anammox co-culture in sequencing batch reactors (SBRs) and its use in treatment of nutrients from synthetic and original wastewaters. A schematic flowchart of the scope of the thesis is illustrated in Figure 1.1 and the objectives to be researched are detailed as follows:

- Enrichment of DAMO-Anammox co-culture in SBRs.
    - Investigation of the effect of the hydraulic retention time (HRT) and in turn the nitrogen loading rate (NLR) in SBR on the co-culture activity, removal efficiency and population dynamics, which have not been investigated in the current literature.
    - Investigation of the effect of Fe^{2+} and Cu^{2+} concentrations on the DAMO-Anammox co-culture activity, performance, and removal efficiency.
    - Investigation of the effects of specific parameters, namely, NH_4^+/CH_4 ratio on the DAMO-Anammox co-culture in batch reactors.

NH_4^+/CH_4 ratio is of concern because it indicates the balance between DAMO and Anammox microorganisms in terms of their relative activity in the system, since CH_4 can be removed by DAMO microorganisms while NH_4^+ is only removed by Anammox. The optimum ratio leading to the highest efficiency of the DAMO-Anammox activity will be determined.

- Assessment of the effect of different nitrogen sources in the enrichment of DAMO microorganisms was performed.
- Investigation of the DAMO-Anammox co-culture performance in SBR by treating an original wastewater, namely, Anaerobic Digester (AD) effluent, which was not investigated in the literature until recently, in 2021, a study was published. Lim et al. (2021) investigated the applicability of a DAMO-Anammox membrane biofilm reactor in treating mainstream (domestic wastewater) and side-stream wastewater (AD effluent).
    - Determining the optimum dilution ratio for AD effluent in batch reactors by comparing their performance with batch reactors provided with equivalent concentrations of synthetic wastewater.
- Investigation of the integration of the DAMO-Anammox co-culture with a sequential microalga culture with an attempt to completely remove nutrients (both nitrogen and phosphorus) and CH_4 to produce a carbon source, i.e., microalgae, of both value-added products and also energy. A schematic diagram of the integrated sequential DAMO-Anammox-Microalgae system is shown in Figure 1.2.
    - Investigation of the treatment of AD effluent using this novel DAMO-Anammox-Microalgae sequential treatment unit.

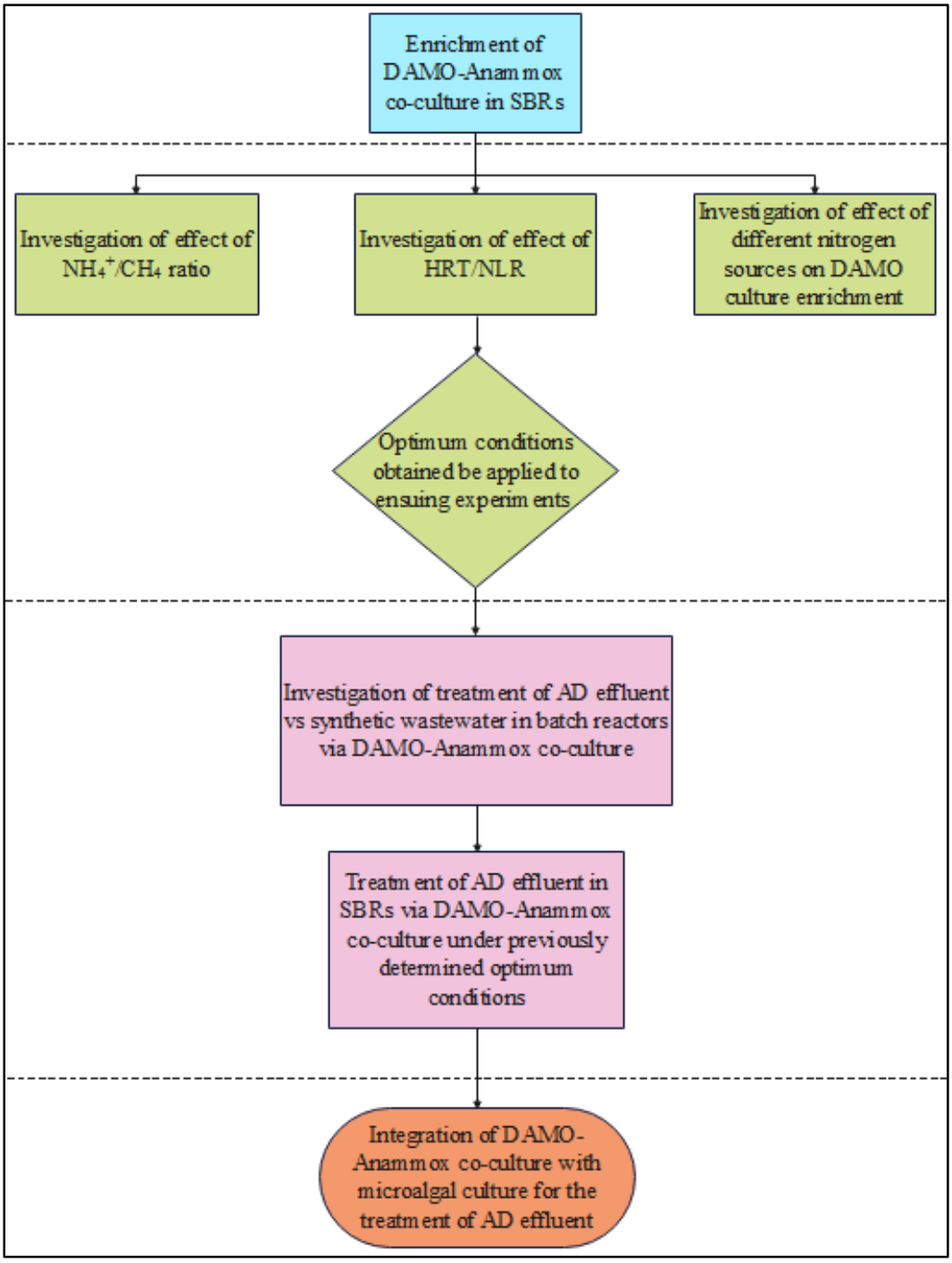

Figure 1.1 Schematic representation of the scope of the thesis

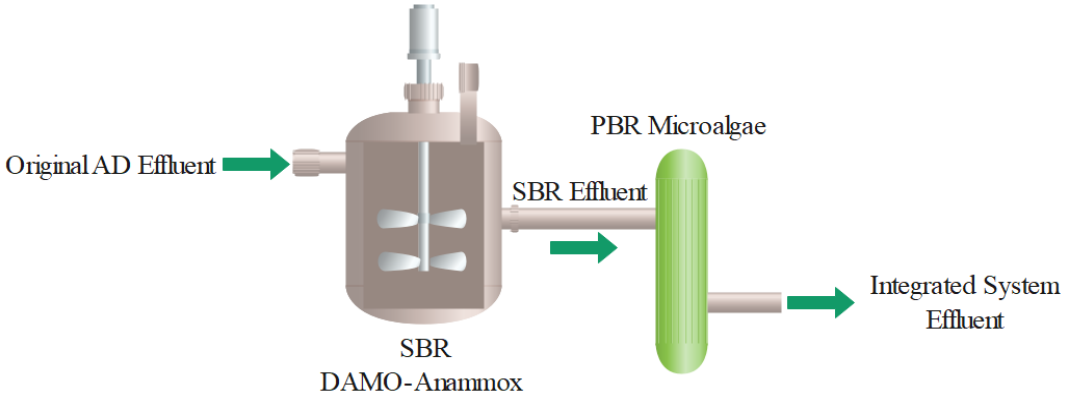

Figure 1.2 Proposed Integrated DAMO-Anammox-Microalgae System for AD effluent treatment

1.3 Organization of the Dissertation

The PhD dissertation is composed of six chapters, where it commences with an introduction including a statement of the problem, a summary of the objectives and motivations that helped shape this research and an insight into the organization of this thesis. The second chapter comprises of a review of the literature and research, highlighting the gaps in the literature.

Chapters 3, 4 and 5 discuss the experimental studies performed for this PhD thesis. It should be noted that these chapters were written as separate chapters each including its specific introduction, materials and methods, results and discussion and conclusion. In this respect, the third chapter discusses the enrichment of the DAMO-Anammox co-culture in SBRs including the specific activity batch tests conducted and the parameters assessed, such as HRT, NLR, Fe^{2+} and Cu^{2+} concentrations and the NH_4^+/CH_4 ratio and their effects on the co-culture. The fourth chapter includes the investigation of the effects of various combinations of nitrogen sources on the enrichment of DAMO microorganisms. To this purpose, two reactors were established, each provided with different nitrogen sources and comparing the performance of these reactors with the DAMO-Anammox co-culture discussed in the third chapter. Furthermore, the fifth chapter includes the application of the

original AD effluent on the DAMO-Anammox co-culture and the integration of the DAMO-Anammox co-culture with a sequential microalga PBR. The possible application of such a system, namely, the integrated sequential DAMO-Anammox-Microalgae system for the treatment of original AD effluent, is discussed.

The sixth chapter comprises of a final conclusion to the research performed through the whole thesis study. It also involves recommendations that might aid future research conducted in this field.

CHAPTER 2

LITERATURE REVIEW

2.1 Methane Removal

Methane (CH_4), another GHG mainly produced in the anaerobic digestion process, is reported to be emitted from conventional WWTPs. About 1% of the amount of COD entering the facility is released in the form of CH_4 (Campos et al., 2016). CH_4 emission from anaerobic digestion of primary and secondary sludge is stated to represent 75% of the overall methane emissions produced from WWTPs (Daelman et al., 2012). According to Crone et al. (2016), estimates of methane losses from anaerobic effluents treating domestic wastewater range between 11-100%. Considering that the GWP of CH_4 is 28 times more than that of CO_2 (Stocker et al., 2013), mitigating the release of methane from WWTPs is of crucial importance. According to Noyola et al. (2006) more than 60% of the total methane gas produced in anaerobic digesters (ADs) is dissolved in the effluent at low temperatures. The dissolved CH_4 must be removed from AD effluents to avoid generating potentially explosive atmospheres. Usually the AD effluent is recycled back to the WWTP, in this case the CH_4 changes phase and is emitted into the atmosphere.

CH_4 recovery techniques used to mitigate the concentrations of dissolved methane in wastewater treatment effluents have been tested. Membranes employed to remove the dissolved gas have shown removal efficiencies for methane of about 86% (Luo, 2014), while, stripping of the gas via aeration of the effluent can lead to a removal efficiency of around 86% (Khan et al., 2011). Electrochemical method has lower removal efficiency, 82%, than the latter two (Dutta et al., 2010), moreover, other techniques include micro-aeration along with stripping and dissipation methods. Stripping and dissipation provide a removal efficiency of 73% for methane (Glória et al., 2016). The main drawbacks of stripping include low efficiency in cold

weather, scaling due to the addition of lime during pH adjustment and the need for pre and post treatment to remove suspended solids before stripping and reduce the dissolved oxygen concentration after stripping. Another method used is flaring or incineration, but the gases should be concentrated usually by membrane separation (Glória et al., 2016). Conditioning steps are required before flaring which includes de-foaming, water and H_2S removal and compression of the biogas (Noyola et al., 2006), this increases the cost of operation of this method.

On the other hand, a recent approach is the biological CH_4 consumption via DAMO and similar methanotrophs represents an important global CH_4 sink. DAMO microorganisms are capable of removing nitrite and nitrate using dissolved CH_4 as the electron donor. This presents a promising opportunity in replacing conventional CH_4 and nitrogen removal techniques in WWTPs. Nevertheless, the applicability and full-scale installation are some of the main challenges especially that these microorganisms are slow-growing. The detailed information on the DAMO process and the microorganisms involved are provided in Section 2.4.

2.2 Biological Nutrient Removal

In water and wastewater treatment the target nutrients to be removed are nitrogen and phosphorus. Three main mechanisms utilized for nutrient removal are biological, physical and chemical (W.E.F., 2011). Different processes to remove nitrogen exist that include the conversion of nitrogen to the gaseous form N_2, this is done by biological treatment systems that mainly employ nitrification and denitrification (W.E.F., 2011). Nevertheless, the denitrification process will lead to by-products such as nitrous oxide and nitric oxide that have negative effects on the atmosphere. Another process employs the biological uptake of nitrogenous compounds utilized for biomass growth. On the other hand, physical processes involve membrane separation processes such as reverse-osmosis and nano-filtration to remove the dissolved nitrogen species. Alternatively, ammonia stripping at high pH and selective ion exchange are physico-chemical processes that can be utilized to remove

ammonium and nitrate ions (Eliassen and Tchobanoglous, 1968). However, biological nitrogen removal is the most prominent process since it is the process most widely employed.

Different reactor configurations and processes were developed to utilize the different aspects of the biological removal processes. Some are separate processes where specific nitrogen or phosphorus species are intended to be removed. Whereas staged processes or sequential processes are utilized to create alternating aerobic and anaerobic environments that provide suitable conditions for processes such as nitrification, denitrification, polyphosphate accumulation and release. Such configurations include Bardenpho, modified Lutzack-Ettinger and A2O processes. On the other hand, integrated nitrification and denitrification processes are conducted by having the two processes occurring in the same reactor, namely, simultaneous nitrification and denitrification (SND) by providing suitable reactor conditions, especially with respect to dissolved oxygen (DO) concentration.

The sequential configurations that employ nitrification and denitrification are space, cost and energy intensive. About 55.6% of the total energy consumption of WWTP is allocated to aeration in conventional nitrification and for advanced treatment with nitrification 40% more energy is required compared to the conventional process (Morgenroth et al., 2004; Halim, 2012). In addition, conventional nitrification and denitrification processes lead to the formation and release of nitrous oxide (N_2O), which has a global warming potential (GWP) of about 265 times that of CO_2 (Stocker et al., 2013). Estimates show that the N_2O produced from WWTP represents about 3% of all U.S. national sources and is listed as the sixth highest contributor to GHG emissions in the U.S. (Ahn et al., 2010). The nitrogenous compounds released into the environment can cause a cascade of environmental issues, particularly an escalation in freshwater nitrate levels and a rise in nitrous oxide production that may heighten global climate change (Duce et al., 2008).

Next generation nitrogen removal technologies are promising for decreased energy and chemical demand for the processes, such as, partial nitritation/Anammox,

completely autotrophic nitrogen-removal over nitrite (CANON) and microbial electrochemical cells. The latter process is energy efficient at recovering nitrogen from side-streams, yet low effluent levels are not achieved in comparison to other processes (Winkler and Straka, 2019). Since it is one of the nitrogen removal mechanisms studied in this PhD thesis, the details of the Anammox process are discussed in the following section, Section 2.3.

2.3 Anaerobic Ammonium Oxidation

2.3.1 Historical Background

One of the significant processes in the biogeochemical nitrogen cycle also presumed to be one of the major sources of nitric and nitrous oxide emission is denitrification. A broad range of microorganisms can perform heterotrophic denitrification through the reduction of nitrate via nitrite into nitric oxide and nitrous oxide and finally dinitrogen gas. In anoxic conditions, denitrification was thought to be the main nitrate removal pathway (Jetten, 2008).

Figure 2.1 shows the nitrogen cycle and the processes involved. Nitrification is a two-step aerobic oxidation process where microorganisms such as *Nitrosomonas* spp. are responsible for the first step shown in Equation 2.1 while microorganisms such as *Nitrobacter* spp. are responsible for the second step shown in Equation 2.2 (Koch et al., 2019). Furthermore, heterotrophic denitrification occurs in oxygen-limited conditions where NO_3^- acts as the final electron acceptor instead of O_2, in the presence of a source organic carbon such as COD (chemical oxygen demand), shown in Equation 2.3 (Latham et al., 2016).

$2\ NH_4^+ + 3\ O_2 \rightarrow 2\ NO_2^- + 2\ H_2O + 4\ H^+$ ($\Delta G^0 = -275$ kJ/mol NH_4^+) .Equation 2.1

$2\ NO_2^- + O_2 \rightarrow 2\ NO_3^-$ ($\Delta G^0 = -74$ kJ/mol NO_2^-) ..... Equation 2.2

$2\ NO_3^- + 10\ e^- + 12\ H^+ \rightarrow N_2 + 6\ H_2O$ ($\Delta G^0 = -1120$ kJ/mol NO_3^-) ... Equation 2.3

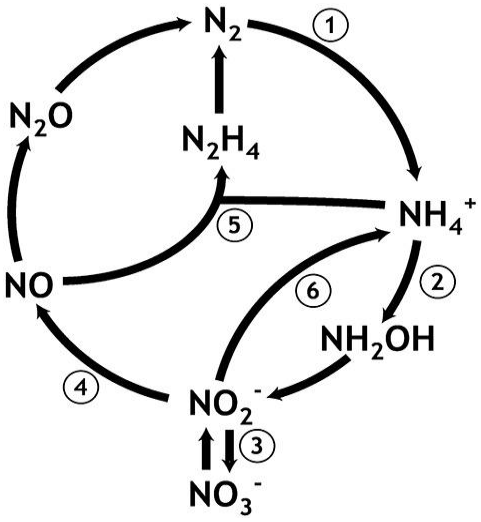

Figure 2.1. The nitrogen cycle. 1. Dinitrogen gas fixation. 2. Aerobic ammonium oxidation by bacteria and archaea. 3. Aerobic nitrite oxidation. 4. Denitrification. 5. Anaerobic ammonium oxidation. 6. Dissimilatory nitrate and nitrite reduction to ammonium (Jetten, 2008).

Ammonium is biochemically difficult to activate and the enrichment and detection of anaerobic microorganisms utilizing ammonium as a food source was unsuccessful, it was believed that ammonium was inert under anoxic conditions. However, this claim gradually changed after observations made from a denitrifying pilot plant belonging to Gist Brocades Fermentation Company. A decrease in NH_4^+ concentration at the cost of NO_3^- and an apparent N_2 gas production was observed. These observations paved the path to the discovery of the Anammox process and bacteria (Kuenen, 2008). The anaerobic ammonium oxidation (Anammox) a chemolithoautotrophic process may be one of the main sinks of inorganic nitrogen (Burgin and Hamilton, 2007). Furthermore, a medium supporting autotropic growth using carbon dioxide, ammonium and nitrite along with biomass retention was developed and that was the base for enrichment of Anammox bacteria (Kuenen, 2008). Although various strains of Anammox bacteria have been enriched and detected, the diversity of these bacteria is relatively unknown.

2.3.2 Phylogeny, Biochemical Reaction and Pathway

The Anammox bacteria belong to the order *Planctomycetales* (van Niftrik and Jetten, 2012). *Brocadia*, *Kuenenia*, *Jettenia*, *Scalindua*, *Anammoxoglobus*, and *Anammoximicrobium* are the six Anammox genera that have been described (Li et al., 2018b). Most of the anammox bacteria were identified from WWTPs or lab-scale reactors, for the exception of the genus *Scalindua*, which was identified in marine sediments. Identification methods include fluorescence in situ hybridization (FISH) and phylogenetic analysis of partial 16S rRNA genes (Schmid et al., 2007). A phylogenetic analysis was conducted by isolating the RNA of Anammox cells and amplifying the targeted sequences through PCR. The level of relation between different Anammox species was found by comparing the 16S rRNA gene sequences (Schmid et al., 2007). The phylogenetic tree of the Anammox bacteria is illustrated in Figure 2.2.

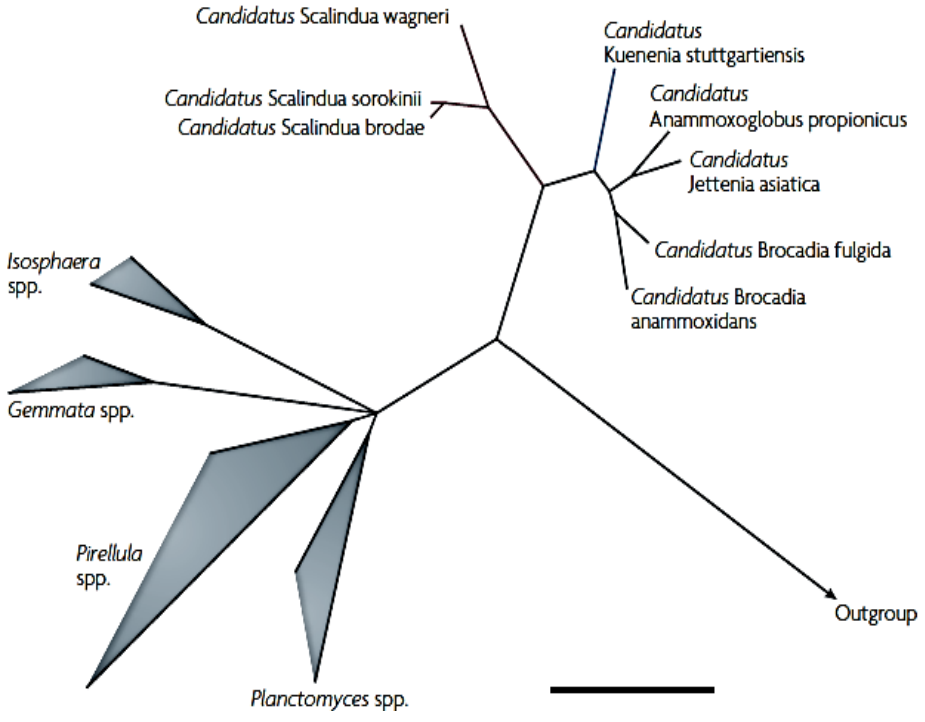

Figure 2.2 16S rRNA-based Anammox bacteria phylogenetic tree. The scale bar represents 10% sequence divergence (Kuenen, 2008).

It was thought that Anammox bacteria are strictly chemolithoautotrophs, but recent research shows that their metabolic pathway may be more flexible. Some Anammox species, for instance '*Candidatus* Anammoxglobus propionicus' and '*Candidatus* Brocadia fulgida', are capable of utilizing organic carboxylic acids, such as propionate and acetate, as electron donors. Moreover, Fe^{2+} can be utilized along with NH_4^+ as an electron donor (Strous et al., 2006; Kartal et al., 2007b; Kartal et al., 2008; van Niftrik and Jetten, 2012). In addition, Anammox bacteria can also utilize Fe^{3+}, manganese oxides and nitrate as electron acceptors (Strous et al., 2006). Yet, the general chemolithoautotrophic Anammox process converts NH_4^+ using NO_2^- as the electron acceptor to N_2 and NO_3^-, as illustrated in Equation 2.4 (Dapena-Mora et al., 2007). Utilizing stable nitrogen isotopes as tracers was utilized to differentiate denitrification and the Anammox processes, since isolating Anammox bacteria and obtaining pure cultures was found to be difficult, since they were found in nature along with other bacterial species that helped provide suitable conditions for the survival of the Anammox bacteria (Dalsgaard et al., 2003; 2005). Figure 2.3 shows the general Anammox process in comparison to the nitrification and denitrification processes.

$$NH_4^+ + 1.32\ NO_2^- + 0.066\ HCO_3^- + 0.13\ H^+ \rightarrow 1.02\ N_2 + 0.26\ NO_3^- + 0.066\ CH_2O_{0.5}N_{0.15} + 2.03\ H_2O\ (\Delta G^0 = -357\ \text{kJ/mol}\ NH_4^+)$$ ……..…... Equation 2.4

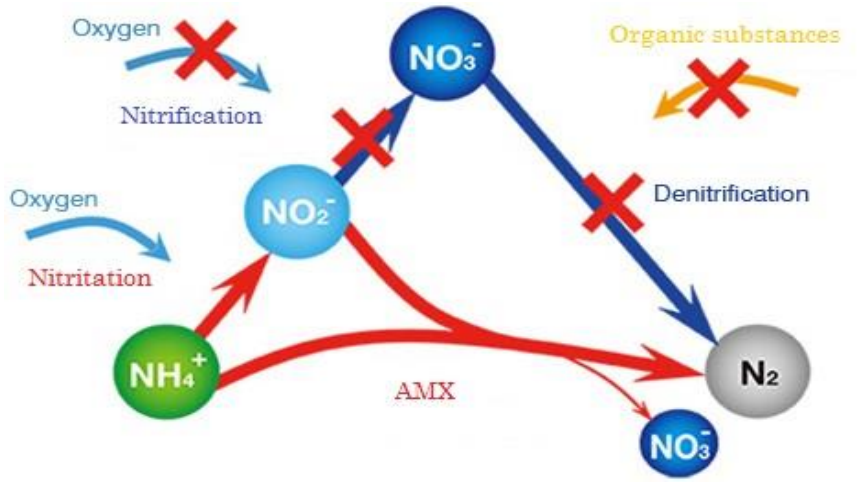

Figure 2.3 The Anammox process (Meidensha, 2015).

2.3.3 Ultrastructure of Anammox bacteria

The isolation of Anammox cultures aided in the molecular identification of the Anammox bacteria which provided an understanding of their physiology that includes a unique prokaryotic organelle (van Niftrik et al., 2008), as well as the identification of the unique ladderane lipids (Rattray et al., 2008). This knowledge provided an important base to understand the role of Anammox in the global nitrogen cycle of marine and terrestrial environments. The Anammox bacteria are generally round in shape or coccoid having a diameter that ranges from 800 to 1,100 nm (van Niftrik and Jetten, 2012). The cellular structure of the Anammox bacteria is different in various ways to other known strains of bacteria. The main difference is the presence of single bilayer membrane-bound organelle containing ladderane lipids, where all the catabolic reactions occur called the anammoxosome (van Niftrik et al., 2004). Those lipids are specific to the Anammox bacteria. The lipids that are contained in the anammoxosome membrane suggest that these bacteria have evolved and diverged early in the bacterial lineage (Jetten et al., 2005). Furthermore, Anammox bacteria differ from other bacterial cells by having a proteinaceous cell wall lacking the cell wall polymer peptidoglycan, and instead of the cell wall being bound by an outer cell membrane, there are two cell membranes on the inner side of the cell wall. Moreover, since ladderane lipids are unique to Anammox bacteria then lipid analysis can help identify the bacteria. The fatty acid sample collected from the bacteria was analyzed through gas chromatography to identify the ladderane lipids (Brandes et al., 2007). Figure 2.4 shows the cellular structure of the Anammox bacteria. The cytoplasm of Anammox bacteria is divided into three sections (van Niftrik et al., 2004):

1. Paraphyoplasm, bounded by the cytoplasmic membrane and intracytoplasmic membrane.
2. Riboplasm, containing the nucleoid.
3. Anammoxosome, where the Anammox process occurs.

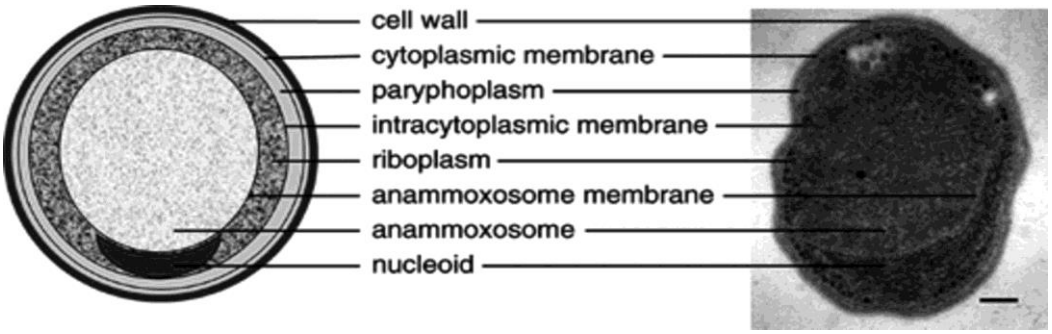

Figure 2.4 Cellular structure of the Anammox bacteria (van Niftrik et al., 2004).

Anammox bacteria divide through the mechanism of constrictive binary fission, versus the other Planctomycetes, which divide through budding. The Anammox bacteria have a slow growth time ranging from 10-30 days. Doubling time measured in the laboratory under optimal conditions was found to be 11 days. The reason behind slow growth rate is thought to be low substrate conversion rate (Strous et al., 2002).

2.3.4 Potential Niches in Natural and Engineered Systems

Various sources of seed sludge from natural and engineered systems have been used to enrich Anammox bacteria. Some studies have enriched Anammox bacteria from inocula taken from marine sediments (van de Vossenberg et al., 2008; Kindaichi et al., 2011; Nozhevnikova et al., 2012). On the other hand, most of enrichment studies have obtained inocula from sludge of different processes in wastewater treatment facilities. This led to an increase in the studies conducted to test for the presence of Anammox in WWTPs of various wastewater types in order to evaluate the potential of the sludge to be utilized as Anammox seed sludge (Kocamemi et al., 2018). Inocula from activated sludge (Chamchoi and Nitisoravut, 2007; Kartal et al., 2008; Lopez et al., 2008; Noophan et al., 2009; Bae et al., 2010; Sun et al., 2011; Saricheewin et al., 2010; Kocamemi et al., 2018), anaerobic digester sludge (Chamchoi and Nitisoravut, 2007; Sun et al., 2011) methanogenic granular sludge (Sun et al., 2011) were utilized in various studies. Therefore, additional research

studies should be conducted to assess the viability of utilizing mixed local sludge in contrast to using imported Anammox seed sludge as an enrichment inoculum (Kocamemi et al., 2018).

2.4 Denitrifying Anaerobic Methane Oxidation

2.4.1 Historical Background

The biological conversion of methane was believed to occur only under oxic conditions and enrichment cultures capable of utilizing methane with nitrate or nitrite were not discovered until recently. This claim changed when oxidation of methane was discovered in anoxic marine sediments in 1976 (Figure 2.5), it was later referred to as the anaerobic oxidation of methane (AOM) and was found to be coupled with sulfate reduction (Reeburgh, 1976). The species responsible for this process were identified as methanotrophs that are within a sub-group of the methylotrophic bacteria, utilizing one-carbon compounds as a source of carbon and energy while assimilating formaldehyde (Hanson and Hanson, 1996; Chistoserdova et al., 2005). However, the microorganisms responsible for this process were identified about 20 years later (Hinrichs et al., 1999; Boetius et al., 2000; Bian et al., 2001). In 2006, an enrichment medium capable of sustaining DAMO microorganisms, also known as nitrate/nitrite dependent anaerobic methane oxidation (N-DAMO) microorganisms, was described (Raghoebarsing et al., 2006). Ettwig et al. (2008) indicated that the bacteria related to the NC10 phylum are responsible of converting methane and nitrite under anoxic conditions into carbon dioxide and nitrogen gas, respectively. The methanotrophic archaea, *Methanoperedens nitroreducens* were classified under the anaerobic methanotrophic archaea group 2 (ANME-2d) by Haroon et al. in 2013 (Figure 2.5). Co-existence of DAMO and Anammox microorganisms revealed in the last decade (Luesken et al., 2011b) was of significance for DAMO enrichment studies.

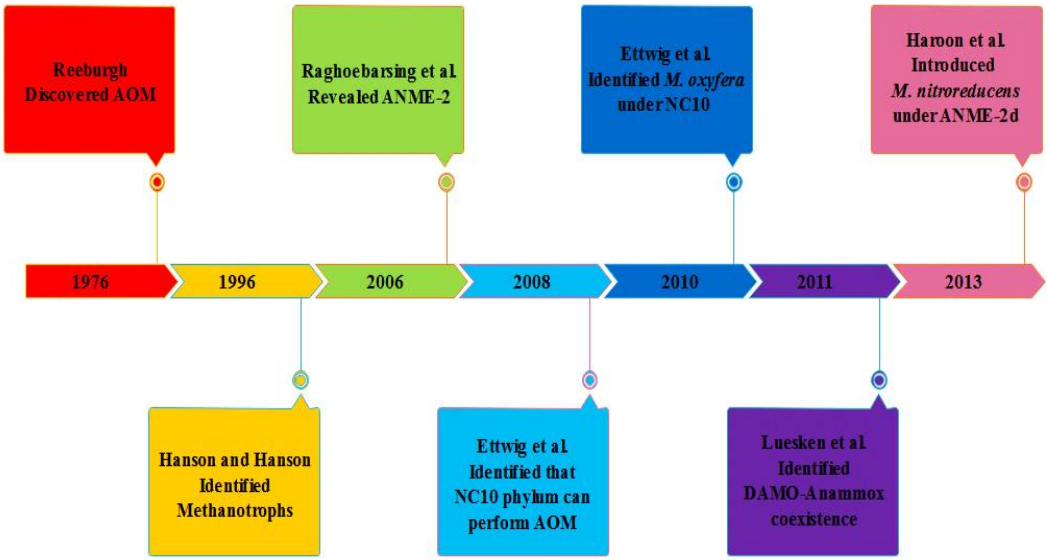

Figure 2.5 Timeline showing the important events since the discovery of anaerobic oxidation of methane (AOM) (Harb et al., 2021)

2.4.2 Phylogeny, Biochemical Reactions and Pathways

Phylogenetically different microorganisms are responsible for the DAMO process. DAMO bacteria, namely, '*Candidatus* Methylomirabilis oxyfera' (*M. oxyfera*), belonging to the NC10 phylum (Ettwig et al., 2010) and DAMO archaea, namely, '*Candidatus* Methanoperedens nitroreducens' (*M. nitroreducens*), belonging to ANME-2d (Raghoebarsing et al., 2006; Haroon et al., 2013; Cui et al., 2015), are the two main microorganisms responsible for the process. While *Gammaproteobacteria* strain HdN1 (Zedelius et al., 2011) and *Dechloromonas* aromatica strain RCB (*D. aromatica* RCB) in *Betaproteobacterium* (Chakraborty et al., 2005) are two microorganisms that partner with *M. nitroreducens*. Figure 2.6 and Figure 2.7 illustrate the 16S rRNA phylogenetic trees of *M. oxyfera* and *M. nitroreducens*, respectively.

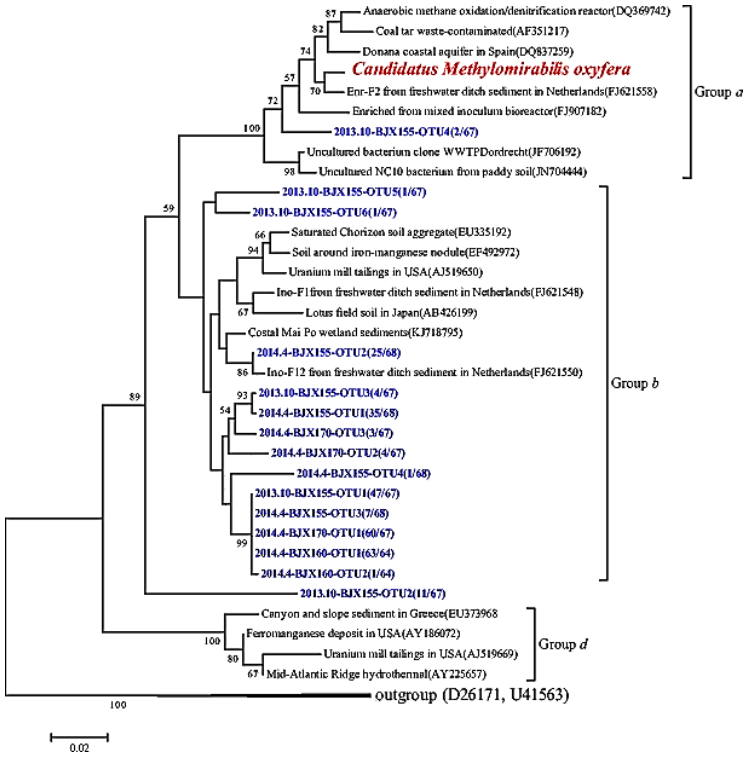

Figure 2.6 The 16S rRNA phylogenetic tree of *M. oxyfera* (Wang et al., 2016)

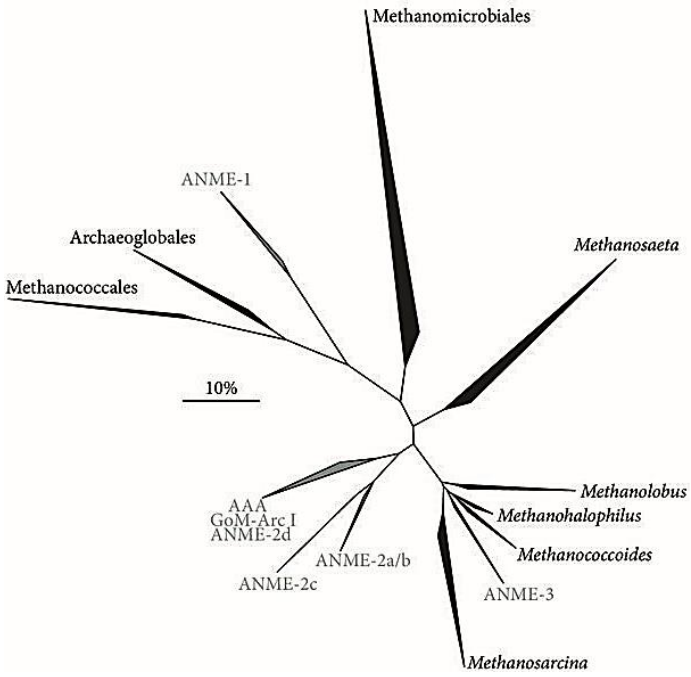

Figure 2.7 The 16S rRNA phylogenetic tree showing methanotrophic archaea (grey) and other archaeal clades (black) (Timmers et al., 2017)

M. nitroreducens convert nitrate to nitrite using methane as an electron donor, while the *M. oxyfera* reduce nitrite to nitrogen gas using methane as an electron donor as well. In both reactions, the methane is converted to carbon dioxide. Equation 2.5 and Equation 2.6 refer to the reactions conducted by *M. nitroreducens* and *M. oxyfera*, respectively (Winkler et al., 2015; Wang et al., 2017a).

$CH_4 + 4\ NO_3^- \rightarrow 4\ NO_2^- + 2\ H_2O + CO_2$ (ΔG^0= -503 kJ/mol CH_4) ….. Equation 2.5

$3\ CH_4 + 8\ NO_2^- + 8\ H^+ \rightarrow 3\ CO_2 + 4\ N_2 + 10\ H_2O$ (ΔG^0= -928 kJ/mol CH_4) ..Equation 2.6

Anaerobic methane oxidation was thought to be heavily based on reverse methanogenesis, given that methane is chemically unreactive (Chistoserdova et al., 2005). This has been clarified with data showing that methanotrophic archaea have homologs of the genes for all three subunits of the methyl-coenzyme M reductase-like (MCR) enzyme, enabling the oxidation of methane anaerobically (Hallam et al., 2003). In addition, acetate is produced by '*M. nitroreducens*' through the complete reductive acetyl-CoA (carbon fixation) pathway and acetyl-CoA synthetase (Hallam et al., 2003). In addition, electrons produced in reverse methanogenesis may be used by other denitrifying partners or by '*M. nitroreducens*' itself for further denitrification (Wang et al., 2017a). The reactions and pathways of the denitrifying partners should be further investigated. Metagenomic, transcriptomic and genomic assays showed that reverse methanogenesis is realized with a terminal electron acceptor of nitrate (Hallam et al., 2003; Heller et al., 2008; Meyerdierks et al., 2010; Scheller et al., 2010; Stokke et al., 2012).

In *M. oxyfera*, the enzyme responsible for the AOM, i.e., pMMO (particulate methane monooxygenase), was found in the cytoplasmic membrane (Wu et al., 2012a) instead of in the envelope called intracytoplasmic membrane (ICM) as in the other proteobacterial methanotrophs (Hanson and Hanson, 1996; Wu et al., 2012a). It was found that the metabolic pathway taking place in *M. oxyfera* was an intra-aerobic pathway, in other words, *M. oxyfera* produces its own oxygen rather than obtaining it from the environment. This is done by metabolizing nitrite via nitric oxide (NO) into oxygen and nitrogen gas (Figure 2.8). The intracellular oxygen

produced can be used for methane oxidation via the classical aerobic methane oxidation pathway involving pMMO (Wu et al., 2011). This pathway was later referred to as oxygenic denitrification (O2DN), where methane or other alkanes are utilized as electron donors to reduce NO_3^- or NO_2^- into N_2 (He et al., 2018b). *M. oxyfera* expresses enzymes for the reduction of NO_2^- to NO (cytochrome cd1-type nitrite reductase; NirS) located in periplasm of *M. oxyfera* (Wu et al., 2012a).

Various ionic compounds could be utilized as electron acceptors for AOM, like nitrite and nitrate (Bussmann, 2005; Lopes et al., 2011). However, Hu et al. (2009) indicates that the DAMO archaea prefer NO_3^- reduction to NO_2^- reduction. Therefore, DAMO bacteria are required to remove NO_2^-, which might have inhibitory effects on *M. oxyfera* and Anammox (Hu et al., 2011). This effect needs to be further investigated. *M. nitroreducens* is capable of reducing nitrate to nitrite, as shown in Equation 2.5; further reduction of NO_2^- to N_2 can only be achieved through other microorganisms such as *M. oxyfera*, Anammox, *Gammaproteobacteria* or *Betaproteobacteria* (Wang et al., 2017a). Consequently, DAMO archaea tend to form syntrophic partnerships with the previously stated microorganisms.

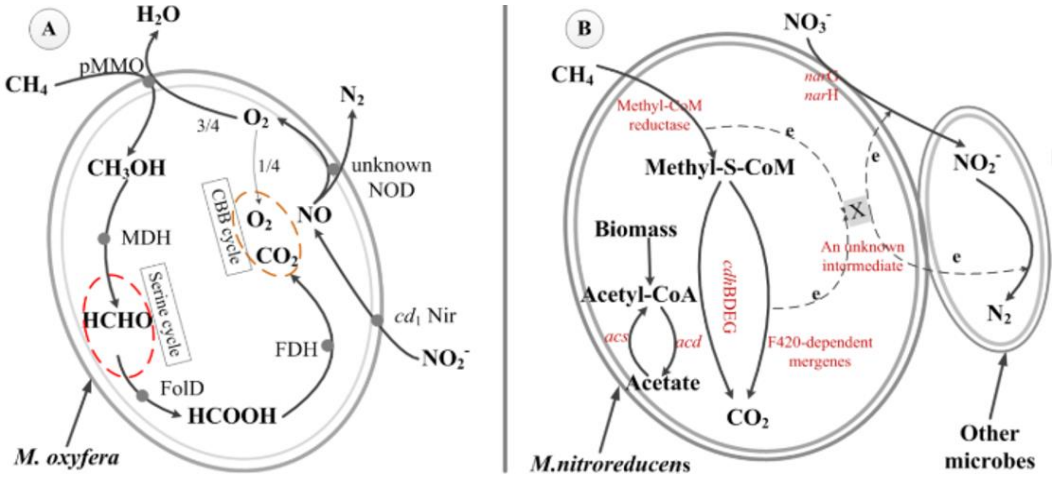

Figure 2.8 Two different pathways of *M. oxyfera* and *M. nitroreducens* (Wang et al., 2017a). (A) 'Inter-aerobic denitrification' dominated by *M. oxyfera*, and (B) 'Reverse methanogenesis' dominated by *M. nitroreducens* with a syntrophic relationship.

2.4.3 Ultrastructure of DAMO Microorganisms

M. nitroreducens has an irregular cocci shape with a diameter of 1–3 mm and typically found as sarcina-like clusters in mesophilic conditions (Haroon et al., 2013). As Ettwig et al. (2010) revealed, *M. oxyfera* is a Gram-negative rod bacterium with a diameter of 0.25–0.50 mm and a length of 0.8–1.1 mm and prefers mesophilic conditions and has a slow growth metabolism. The *M. oxyfera* cellular ultrastructure is an unusual polygon cell shape with an additional layer as the outermost sheath (Wu et al., 2012b), which is thought to be the exoskeleton-like (glycoprotein) surface layer (S-layer) that plays a role in osmotic and mechanical cell stabilization with peptidoglycan components (Engelhardt, 2007; Cabeen and Jacobs-Wagner, 2005; Sleytr and Beveridge, 1999).

The specific maximum growth rate (μmax) reported for DAMO bacteria ranges from 0.043-0.121 d^{-1} with a biomass yield of 0.055-0.094 g COD/g COD, corresponding to a doubling time of 5.7-16 days. While the reported μmax for DAMO archaea, which was not found experimentally rather in a modelling study, was 0.036 d^{-1} with

a biomass yield of 0.071 g COD/g COD corresponding to a doubling time of 19 days (Chen et al., 2014; Yu et al., 2017).

2.4.4 Potential Niches in Natural and Engineered Systems

Molecular studies conducted on freshwater samples from river and lake sediments as well as oligotrophic freshwater lakes, proved the presence of active *M. oxyfera*-like bacteria in those niches (Raghoebarsing et al., 2006; Smemo and Yavitt, 2008; Ettwig et al., 2008; Ettwig et al., 2009; Hu et al., 2009; Deutzmann and Schink, 2011; Luesken et al., 2011a; Kojima et al., 2012; Kampman et al., 2012; Yang et al., 2012; Wang et al., 2012; Shen et al., 2012; Zhu et al., 2012; Shen et al., 2013; Zhu et al., 2013). Moreover, the DAMO activity was predicted to be seen in anoxic-oxic interphase in freshwaters (Thauer and Shima, 2006; Oremland, 2010).

DAMO species have highly variable diversity among various niches (Han and Gu, 2013). Zhang et al. (2018) stated that high diversity has been observed in marine and ocean ecosystems. Active DAMO archaea and DAMO bacteria were identified in estuarine intertidal sediment with a higher diversity of DAMO archaea than DAMO bacteria (Chen et al., 2020). As it was already revealed by others (Raghoebarsing et al., 2006; Ettwig et al., 2009; Deutzmann and Schink, 2011; Kojima et al., 2012), freshwater habitats and wastewater have high abundance of the aforementioned species rather than rice paddy bed and reed beds. *M. oxyfera*-like bacteria were detected in paddy field soil registering the highest abundance of *M. oxyfera*-like bacteria in the nature (Hatamoto et al., 2014; Zhou et al., 2014; Xu et al., 2017). Inoculum from the paddy field soils was utilized to enrich the DAMO microorganisms using continuous-flow and batch cultures fed with either nitrate or nitrite as a sole electron acceptor (Hatamoto et al., 2014; Xu et al., 2017). Recently, Graf et al. (2018) reported a new species belonging to NC10, '*Ca*. Methylomirabilis limnetica', which dominates the planktonic microbial community in anoxic zones of the deep stratified Lake Zug, Switzerland.

Apart from the natural environments, DAMO activities were also observed in both municipal and industrial WWTPs sludge samples (Luesken et al., 2011a; Xu et al., 2017). Moreover, denitrifying methanotrophic bacteria, i.e., *M. oxyfera*-like bacteria were enriched from municipal WWTP sludge samples (Kampman et al., 2014; Hu et al., 2009). Similarly, DAMO culture was enriched from methanogenic granular sludge samples (He et al., 2014). Another possible niche for NC10 bacteria was found to be food waste digestate collected from an anaerobic digestion facility (Xu et al., 2017).

2.5 Integrated DAMO-Anammox System

The DAMO process is an energy-efficient alternative of conventional nitrogen and methane removal processes from wastewaters. Its application has the potential to provide the existing technologies with solutions to problems they are currently facing. The two key issues confronted in WWTPs are the lack of carbon sources for nitrogen removal and the substantial emission of greenhouse gases (GHG) (Wang et al., 2017a). In this scope, DAMO integration with other processes was studied, in particular with Anammox as a co-culture. The environmental conditions leading to the enrichment of DAMO-Anammox co-culture were investigated (Luesken et al., 2011b; Zhu et al., 2011; Haroon et al., 2013; Ding et al., 2014; Ding et al., 2017; Fu et al., 2017a; Silva et al., 2017; Lu et al., 2018). A different DAMO integrated system with aerobic methane oxidation coupled to denitrification (AMO-D) was achieved by Silva-Teira et al. (2017) and Sánchez et al. (2016).

The Anammox process is considered as an innovative alternative for conventional nitrification-denitrification processes (Strous et al., 1999). In comparison to DAMO, enrichment, cultivation, and applicability of the Anammox process in wastewater treatment and nitrogen removal is much more established. There are even various established full-scale applications in the Netherlands, USA, Spain, South Korea and Turkey (Kocamemi et al., 2018). However, nitrate is a by-product of the Anammox process which leads to incomplete nitrogen removal (Luesken et al., 2011b) and

requires a fixed NO_2^-/NH_4^+ molar ratio of 1.32 (Gao and Tao, 2011), as shown in Equation 2.4. According to the stoichiometry of Anammox reaction, the NO_3^- produced corresponds to 11% of the influent total N (NH_4^+ and NO_2^-) (Du et al., 2019). Therefore, with the establishment of an integrated DAMO-Anammox system, the DAMO archaea would complement the Anammox by reducing the $NO_3^-$to NO_2^- (Equation 2.5) and preventing the accumulation of NO_3^-, hence achieving complete nitrogen removal while oxidizing methane into carbon dioxide (Lu et al., 2018), as shown in Figure 2.9. Therefore, combining the DAMO and Anammox processes has a high potential of removing NH_4^+, NO_2^-, NO_3^-, and dissolved CH_4 from wastewaters (Luesken et al., 2011b) such as the anaerobic digester (AD) liquor and landfill leachate. The supply of CH_4 enables the complete nitrogen removal containing varying NH_4^+, NO_2^-, and NO_3^- ratios (Shi et al., 2013).

Employing a nitritation reactor and a DAMO fed batch reactor to treat the effluent of an upflow anaerobic sludge blanket (UASB) was performed (Kampman et al., 2012). One reactor, referred to as SFBR−, was fed with this synthetic medium. The other reactor, referred to as SFBR+, was fed with medium containing 10% (v/v) filtered effluent from the aerobic sewage treatment Bennekom. However, pilot-scale and full-scale applications are yet to be applied. In order to incorporate the DAMO process or a DAMO-Anammox process in full-scale WWTP, nitritation and organic matter degradation are required to be performed prior to the DAMO or DAMO-Anammox processes in order to convert the NH_4^+ to NO_2^- and the organic matter into CH_4 (Wang et al., 2017b; Van Kessel et al., 2018). Wang et al. (2017b) conceptually proposes two possibilities of full-scale applications. The first is the incorporation of a nitritation-DAMO-Anammox process to the side-stream of a WWTP treating the AD liquor before it is recirculated into the main wastewater line. The second is the integration of a nitritation-DAMO-Anammox process to the main-stream preceded by an activated sludge process or similar advanced treatment processes that degrade organic matter. Furthermore, a DAMO-Anammox membrane biofilm reactor preceded by nitritation may be applied to treat landfill leachate to achieve high-rate nitrogen removal (Nie et al., 2020). Lim et al. (2021) demonstrated the first and only

real wastewater application on a lab-scale DAMO-Anammox co-culture. A DAMO-Anammox membrane biofilm reactor (MBfR) was employed to treat mainstream and sidestream wastewater. The effluent of a high-rate activated sludge (HRAS) system was the source of the mainstream wastewater, where three different scenarios were studied. On the other hand, AD liquor was used a sidestream wastewater and studied under one scenario. This study demonstrated the applicability of using a DAMO-Anammox co-culture to remove nitrogen from both mainstream and sidestream wastewater.

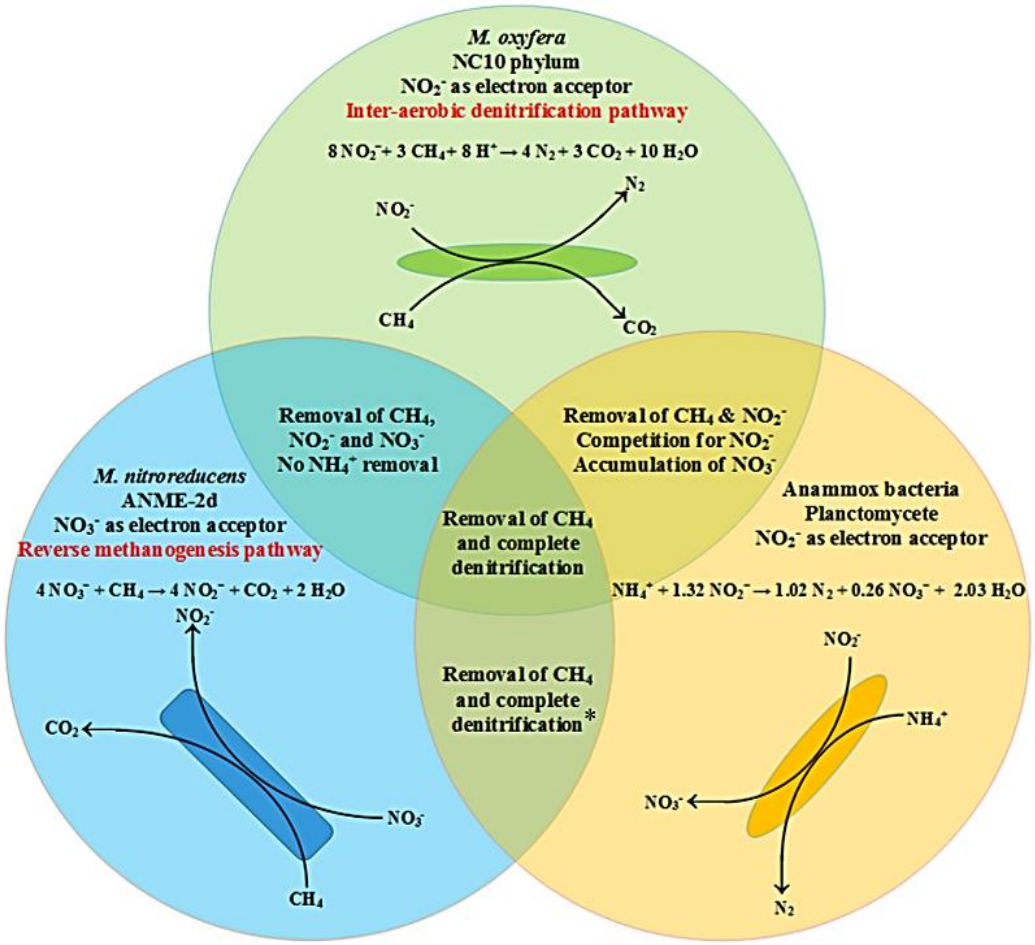

Figure 2.9 The reactions of DAMO microorganisms (*M. oxyfera* and *M. nitroreducens*) and Anammox cultures and the possible outcomes of treatment with different combinations. * Complete denitrification is dependent on the N molar and CH_4: N ratios (Harb et al., 2021)

2.6 Factors Affecting the Enrichment of DAMO-Anammox Co-culture

The earliest successful enrichment of DAMO microorganisms (Raghoebarsing et al., 2006) marked the starting point of studies aimed at enrichment and cultivation of DAMO microorganisms and their co-cultures. Few studies tested the effect of some factors on the activity of DAMO microorganisms, while others applied the operational conditions and tested the performance of the enriched DAMO microorganisms. Reducing the enrichment period, improving biomass retention, and increasing the nitrogen consumption rates were the focus of many enrichment studies (Kampman et al., 2014). In order to minimize the drawbacks of DAMO cultures, the operational conditions applied for their enrichment and operation should be well known. Consequently, the factors including, temperature (Hu et al., 2009; Kampman et al., 2014; He et al., 2015b), pH (He et al., 2015b; Zhu et al., 2012), inoculum type (He et al., 2014), feed type in terms of the nitrogen sources and their concentrations, (Raghoebarsing et al., 2006; Ettwig et al., 2008; Ettwig et al., 2009; Hu et al., 2009; Luesken et al., 2011a; He et al., 2014; Kampman et al., 2012; Hu et al., 2014; Kampman et al., 2014; Wang et al., 2015; He et al., 2015b; Bhattacharjee et al., 2016; Hatamoto et al., 2017), trace metal concentrations (He et al., 2015a; Kampman et al., 2014), chemical oxygen demand (COD) (Silva-Teira et al., 2017; He et al., 2018a), sulfate (Li et al., 2020a), salinity (He et al., 2015b), methane content (Fu et al., 2015), dissolved oxygen (DO) (Luesken et al., 2012) reactor configuration (Ettwig et al., 2009; Hu et al., 2009; Luesken et al., 2011a; Kampman et al., 2012; Hatamoto et al., 2014; He et al., 2014; Hu et al., 2014; Kampman et al., 2014; Wang et al., 2015; Hatamoto et al., 2017; Li et al., 2018a; Fu et al., 2019) and hydraulic retention time (HRT) (Kampman et al., 2014; Hatamoto et al., 2014) were revealed in line with the observed effects on the growth and activity of DAMO microbial consortia. This section clearly defines the abovementioned factors that were either investigated or applied in the studies for the enrichment of DAMO cultures. The operational ranges studied leading to the highest conversion rates are also summarized for the related factors. Table 2.1 is a summary of some of the conditions applied in cultivation of DAMO cultures and obtained activity rates.

The introduction of an Anammox culture might reduce the enrichment time of DAMO microorganisms and promote the activity of DAMO archaea (Ding et al., 2014). In this respect, the DAMO-Anammox co-culture enrichment and operation studies were also reviewed in this section for factors having the potential to affect the establishment of a co-culture, its enrichment and activity. Table 2.2 summarizes the DAMO-Anammox co-culture studies with respect to the inocula used, reactor types operated and the operational conditions such as HRT, temperature, and pH. The composition of the DAMO microorganisms enriched is also shown in Table 2.2 and Table 2.3, on the other hand, summarizes other DAMO-Anammox co-cultures studies with emphasis on conversion (activity) rates and composition of both Anammox and DAMO cultures, together with influent N concentrations, pH, temperature, and reactor type information.

2.6.1 Temperature

Experiments showed that temperature has a significant effect on the growth and activity of DAMO microorganisms. The temperatures studied range from 10 to 45°C (Wang et al., 2015; Luesken et al., 2011a; He et al., 2014; Hu et al., 2009; Hatamoto et al., 2017). The optimal temperature for DAMO growth regarding both short-term and long-term effects was found to be about 35°C (He et al., 2015b). These studies are summarized in Table 2.1, some of which have important details that are worth mentioning. Hu et al. (2009) compared the enrichment of the DAMO microorganisms at two different temperatures, 35°C and 22°C. The results showed that both bacteria and archaea were found in the reactor operated at 35°C while only bacteria were enriched in the second reactor. Li et al. (2018a) observed DAMO activity after 75 days in the reactor operated at 30°C, while the DAMO activity started after 100 days in the reactor operated at 20°C.

Li et al. (2020b) assessed the long-term (>350 days) DAMO performance under stepwise cooling conditions (from 30 to 20°C in 120 days) and at ambient temperatures fluctuating from 13 to 38°C through April to November (230 days). Stepwise cooling conditions led to a hindrance of DAMO activity at first, yet DAMO

cultures then adapted and had similar activities both at 20°C and 30°C (nitrate removal rate (NRR) of 7.61 mg NO_3^--N/L·day). Thus, despite a delay in the activity at low temperatures such as 20°C (Li et al, 2018a), DAMO activity was likely to recover in time. On the other hand, at ambient temperatures that fluctuate through the year and during the day, the highest NRR (7.14 mg N/L·day) obtained at the beginning decreased about 5 times after 230 days. This suggests that long-term temperature fluctuation (as experienced at ambient conditions) irreversibly inhibited DAMO activity (Li et al., 2020b).

Similar to DAMO, DAMO-Anammox co-cultures were operated at temperatures ranging from 22 to 35°C (Luesken et al., 2011b; Zhu et al., 2011; Ding et al. 2014; He et al. 2015; Hu et al. 2009) (Table 2.2). The best co-culture activity was found at 35°C (Ding et al., 2017). Temperatures of 15, 25, 35°C were tested and the results showed that a decrease in temperature causes a reduction in the consumption rate of nitrate from about 55 to 30 mg N/L·day while the ammonium consumption rate decreased from 15 to 8 mg N/L·day (Ding et al., 2017).

Table 2.1 Operational conditions and reactor types used in cultivation of DAMO cultures and obtained activity rates (Harb et al., 2021)

[a] N-feed	Influent Concentration	[d] Reactor Type	Specific Activity/Conversion rate		
			NO_2^-	NO_3^-	CH_4
[1] NO_2^-, NO_3^-	Up to 84 mg NO_2^--N/L Up to 84 mg NO_3^--N/L	SBR	11.76 mg N/day	10.89 mg N/day	528 µmol C/day
[2] NO_2^-, NO_3^-	42-210 mg NO_2^--N/L 42-140 mg NO_3^--N/L	CSTR with external settler	74.59 µg N/day (mg protein)	1.12 mg N/day	2.45 µmol C/day (mg protein)
[3] NO_2^-, NO_3^-	7-280 mg NO_2^--N/L 70 mg NO_3^--N/L	SBR	0.07-0.11 mg N/day (mg protein)	NG	2.3-3.17 µmol C/day (mg protein)
[4] NO_3^- (35 °C)	NG	SBR	24.2 mg N/L·day	28 mg N/L·day	2.4 mmol C/day
[4] NO_3^- (22 °C)	NG	SBR	NG	0.91 mg N/L·day	0.038 mmol C/day
[5] NO_2^-	1.4-84 mg NO_2^--N/L 7-42 mg NO_3^--N/L	SBR	18.14 µg N/day (mg protein)	NG	0.43 µmol C/day (mg protein)
[6] NO_2^-	7-21 mg NO_2^--N/L	SBR	2.38-4.76 mg N/L·day	NG	19.2-33.6 µmol C/day (mg protein)
[7] NO_2^-	0.91-9.13 mg NO_2^--N/L	SFBR with gas recirculation	0.46-10.96 mg N/L·day	NG	NG
[8] NO_2^-	40-140 mg NO_2^--N/L 30-70 mg N/L·day ([b] NLR)	SBR CSTR MSGLR	11.4 mg N/L·day ([c] NRR) 26.4 mg N/L·day ([c] NRR) 76.9 mg N/L·day ([c] NRR)	NG	NG
[9] NO_2^-, NO_3^-	14-980 mg NO_2^--N/L 56-120 mg NO_3^--N/L	MBR	8-36 mg N/L·day	NG	NG
[10] NO_3^- or NO_2^-	0.15 g NO_2^--N/L 0.1 g NO_3^--N/L	MBfBR	14.84 mg N/L·day	7.56 mg N/L·day	NG
[11] NO_2^-, NO_3^-	16 mg NO_2^--N/L 7 mg NO_3^--N/L	SBR	40.32 mg N/L·day	NG	21-190 µM C/day
[12] NO_2^-, NO_3^-	7-9.8 mg NO_2^--N/L 7-14 mg NO_3^--N/L	DHS	70.4 mg N/L·day	39 mg N/L·day 22.4 mg N/L·day	2.7 mM C/day
[12] Only NO_3^-	9.8-14 mg NO_3^--N/L	DHS	60.2 mg N/L·day	84.4 mg N/L·day 70 mg N/L·day	3.3 mM C/day

[a] References: [1] Raghoebarsing et al., 2006; [2] Ettwig et al., 2008; [3] Ettwig et al., 2009; [4] Hu et al., 2009; [5] Luesken et al., 2011a; [6] He et al., 2014; [7] Kampman et al., 2012; [8] Hu et al., 2014; [9] Kampman et al., 2014; [10] Wang et al., 2015; [11] Bhattacharjee et al., 2016; [12] Hatamoto et al., 2017.
[b] Nitrogen Loading Rate [c] Nitrogen Removal Rate NG: Not Given
[d] Reactor type: SBR: Sequencing batch reactor, CSTR: Continuously Stirred Tank Reactor, MBR: Membrane Bioreactor, MBfBR: Membrane Biofilm Bioreactor, DHS: Down-flow hanging sponge reactor, MSGLR: Magnetically stirred gas lift reactor.

Table 2.2 Environmental and operational conditions of DAMO-Anammox co-culture systems with the obtained DAMO culture compositions (Harb et al., 2021)

[a] Inocula	[b] Reactor Type	HRT(day)	Temperature (°C)	pH	Composition (%) DAMO archaea	Composition (%) DAMO bacteria
[1] Anoxic freshwater sediment	SBR	NG	25	7	10	80
[2] Anoxic freshwater sediment (ditch sediment)	CSTR	NG	30	7.3–7.6	0	70
[3] Sediment from a eutrophic ditch	SBR	2.2-15	30	6.9-7.5	0	70
[4] Mixture of sediments from freshwater lake, anaerobic digester sludge and return sludge	SBR	NG	35	NG	40	30
[4] Mixture of sediments from freshwater lake, anaerobic digester sludge and return sludge	SBR	NG	22	NG	0	15
[5] Industrial wastewater treatment plant	SBR	NG	20-23	6.8-7.3	NG	60-70
[6] Methanogenic sludge, paddy soil, freshwater sediment	SBR	6	30	7.0-7.2	NG	50
[7] Freshwater sediment	SBR with gas recirculation	4.8-55	30	7.0-8.0	NG	70-80
[8] A previous SBR enrichment culture	SBR, CSTR, MSGLR	2	30	7.0-7.2	NG	NG
[9] Mixture of digested primary sludge, secondary sludge and digested secondary sludge	Submerged MBR	1.4–67	20	6.5–8	NG	60-70
[10] Freshwater sediment	MBfBR	NG	10-25	7	NG	73
[11] River sediment	Intermittently fed SBR	29	35	7.5	0	73
[12] Enriched culture sludge from a laboratory-scale continuous-flow	Closed-type DHS Reactor	0.08-0.17	30	NG	5	50-70

[a] References: [1] Raghoebarsing et al., 2006; [2] Ettwig et al., 2008; [3] Ettwig et al., 2009; [4] Hu et al., 2009; [5] Luesken et al., 2011a; [6] He et al., 2014; [7] Kampman et al., 2012; [8] Hu et al., 2014; [9] Kampman et al., 2014; [10] Wang et al., 2015; [11] Bhattacharjee et al., 2016; [12] Hatamoto et al., 2017.
[b] Reactor type: SBR: Sequencing batch reactor, CSTR: Continuously Stirred Tank Reactor, MBR: Membrane Bioreactor, MBfBR: Membrane Biofilm Bioreactor, DHS: Down-flow hanging sponge reactor, MSGLR: Magnetically stirred gas lift reactor.
NG: Not Given

Table 2.3 Operational conditions, obtained consortium compositions, and nitrogen and methane conversion rates in DAMO-Anammox reactors (Harb et al., 2021)

[a] Reactor Type	Temperature (°C)	pH	N-feed	Influent Concentration	Composition (%)			Activity Rate
					DAMO bacteria	DAMO archaea	Anammox	
[1] SBR	30	7.3-7.6	NH_4^+, NO_2^-	14-280 mg NH_4^+-N/L 525 mg NO_2^--N/L	50	NG	50	100 mg NO_2^--N/L·day 81.6 mg NH_4^+-N/L·day
[2] SBR	25	7.2	NH_4^+, NO_2^-	4:3 (NO_2^-: NH_4^+) (0-60 day) Excess NO_2^- and limited NH_4^+ (after 60 days)	NG	NG	NG	0.7 mmol CH_4-C/L·day 117.6 mg NH_3-N/L·day 175 mg NO_2^--N/L·day
[3] CSTR	22	7.0-7.5	NH_4^+, NO_3^-	80 g NO_3^--N/L 48 g NH_4^+-N/L	-	78	3	1.06 mmol CH_4-C/day 6.68 mmol N_2-N/day 46.62 mg NH_4^+-N/day 49.56 mg NO_3^--N/day
[4] CSTR	35	7-8.5	NH_4^+, NO_3^-	9.8-196 mg NH_4^+-N/L 9.8-196 mg NO_3^--N/L	12	29	21	67.76 mg NO_3^--N/L·day 56.98 mg NH_4^+-N/L·day
[5] HfMBR	35	7.0-8.1	NO_3^-, NO_2^-, NH_4^+	10 mg NO_2^--N/L 40 mg NH_4^+-N/L 60 mg NO_3^--N/L	38.8	26.2	6.2	78 mg NO_3^--N/L·day 26 mg NH_4^+-N/L·day
[6] CSTR	NG	NG	NO_3^-, NO_2^-, NH_4^+	50 mg NO_3^--N/L 10 mg NO_2^--N/L 50 mg NH_4^+-N/L	51.3	NG	6.77	0.24 mg NO_3^--N/day 2.24 mg NO_2^--N/day 1.16 mg NH_4^+-N/day 63.44 µmol CH_4-C/day
			NO_3^-, NH_4^+		40.2		NG	144.62 µg NO_3^--N/day 11.34 µg NH_4^+-N/day 52.00 µmol CH_4-C/day
			NO_3^-		38.9		NG	51.24 µg NO_3^--N/day 47.42 µmol CH_4-C/day
			NO_2^-, NH_4^+		46.6		11.68	1.99 mg NO_2^--N/day 1.11 mg NH_4^+-N/day 97.27 µmol CH_4-C/day
			NO_2^-		64.7		NG	3.63 mg NO_2^--N/day 128.33 µmol CH_4-C/day
[7] MBR	22	NG	NH_4^+, NO_3^-	NG	20-30	20-30	20-30	190 mg NO_3^--N/L·day 60 mg NH_3-N/L·day

Table 2.3 Operational conditions, obtained consortium compositions, and nitrogen and methane conversion rates in DAMO-Anammox reactors (Harb et al., 2021) (Continued)

[8] MBR	22	7-8	NH_4^+, NO_3^-	NG	20	50	20	684 mg NO_3^--N/L·day 684 mg NO_2^--N/L·day
[9] MBR	35	7-8	NH_3, NO_2^-	-	-	-	-	560 mg NO_2^--N/L·day 470 mg NH_4^+-N/L·day
[10] HfMBR	35	7.3-7.8	NH_4^+, NO_3^-	-	14	79	7	16.13 mg NO_3^--N/L·day 75.70 mg NO_2^--N/L·day 47.26 mg NH_4^+-N/L·day
[11] Semi continuous CSTR	35	7-7.5	NO_2^-, NH_4^+	-	-	-	-	-

[a] References: [1] Luesken et al., 2011b; [2] Zhu et al., 2011; [3] Haroon et al., 2013; [4] Ding et al., 2014; [5] Ding et al., 2017; [6] Fu et al., 2017a; [7] Shi et al., 2013; [8] Cai et al., 2015; [9] Xie et al., 2016; [10] Fu et al., 2017b; [11] Hu et al., 2015

SBR: Sequencing batch reactor, CSTR: Continuously Stirred-Tank Reactor, MBR: Membrane Bioreactor, DHS: Down-flow hanging sponge reactor, MSGLR: Magnetically stirred gas lift reactor.

NG: Not Given

2.6.2 pH

Weakly alkaline conditions in the range of 7.0-9.0 are favored by most heterotrophic denitrifying microorganisms (Tang et al., 2011). The studies using DAMO cultures used previously described optimal pH ranges of 6.5-8.0 for their growth (Ettwig et al., 2009; Luesken et al., 2011a; He et al., 2014; Kampman et al., 2014), while others worked to find the optimal pH with the range of 5.9-9.0 (Zhu et al., 2012; He et al., 2015b). Results showed that the activity (1.2-1.6 nmol CH_4 /min·(mg protein)) was higher in the range of 6.75-7.4 compared to the range of 5.9-6.7 (0.4-1.0 nmol CH_4 /min·(mg protein)) (Zhu et al., 2012). An optimum pH range was found between 7.0-8.0 and within this range the optimum pH was recorded as 7.6 (He et al., 2015b). Although He et al. (2015b) found that the DAMO activity decreases by 50% at pH 9.0, NC10 bacteria were detected in food waste digestate at pH 9.24 (Xu et al., 2018) (Table 2.1).

Considering the DAMO-Anammox co-culture studies, Table 2.3 shows the operation pH of these studies to be in the range of 7.0-8.5 (Luesken et al., 2011b; Zhu et al., 2011; Haroon et al., 2013; Ding et al., 2014; Ding et al., 2017; Fu et al., 2017a; Shi et al., 2013; Cai et al., 2015; Xie et al., 2016; Fu et al., 2017b; Hu et al., 2015). The most commonly applied pH range throughout the aforementioned studies was 7.3-7.5, which is likely to support both DAMO and Anammox cultures (Luesken et al., 2011b; Haroon et al., 2013; Ding et al., 2014; Ding et al., 2017; Cai et al., 2015; Xie et al., 2016; Fu et al., 2017b; Hu et al., 2015).

2.6.3 Inoculum type

Enrichment studies mainly focused on the detection of NC10 bacteria and the inoculum type for the cultivation. Different types of inocula sources and enrichment strategies for the DAMO bacteria were tested over time. It is understood that the enrichment period ranges from as low as 75 days (Hu et al., 2014) to about a year (Luesken et al., 2011a; Zhu et al., 2011; Raghoebarsing et al., 2006), which is affected by the inocula type.

Natural ecosystems contaminated with nitrogen, such as peatlands, are potential sources for the enrichment of DAMO organisms (Raghoebarsing et al., 2006; Ettwig et al., 2008; Ettwig et al., 2009; Luesken et al., 2011a; Zhu et al., 2011; Kampman et al., 2012; Wang et al., 2012; Zhu et al., 2012; Hatamoto et al., 2014; He et al., 2014; Hu et al., 2014; Shen et al., 2014; Shen et al., 2015; Bhattacharjee et al., 2016; Wang et al., 2015). The target gene (*pmoA*) was detected in three paddy soil samples inferring the existence of *M. oxyfera* (Hatamoto et al., 2014).

Other inocula sources include municipal and industrial WWTP sludge especially methanogenic sludge due to the presence of significant amounts of methane and nitrite (Luesken et al., 2011a; He et al., 2014). A mixture of municipal wastewater sludge containing primary sludge, secondary sludge and digested secondary sludge was used to inoculate membrane bioreactors (MBRs) and after 12 months of operation, the culture was dominated by *M. oxyfera* (Kampman et al., 2014). Luesken et al. (2011a) screened ten WWTPs for *M. oxyfera* via 16S rRNA screening and identified NC10 bacteria in nine of the selected WWTPs. *M. oxyfera*-type bacteria have been successfully enriched from a mixture of sludge composed of the AD sludge and return sludge from municipal WWTP and freshwater sediment (Hu et al., 2009).

Paddy soil, freshwater sediment and methanogenic sludge were compared as inocula in three sequencing batch reactors (SBRs). The highest NO_2^- consumption with respect to methane was observed in the reactor inoculated with the methanogenic sludge (He et al., 2014). Moreover, the ratios of the consumption rates of CH_4 to nitrite were 3:8.9, 3:8.6 and 3:7.6 for methanogenic sludge, paddy soil and freshwater sediment, respectively. Furthermore, a mixture of the three previous inocula was successfully used in the enrichment of a DAMO consortia with an Archaea to Bacteria ratio of 1.77 suggesting that a mixed inoculum may have an advantage over a sole inoculum source (Li et al., 2018a).

Various approaches were employed to enrich a DAMO-Anammox co-culture. One approach to successfully establish a co-culture was to use an already established

DAMO culture; thus, in turn decrease the enrichment period from 75 to 30 days (Luesken et al., 2011b; Fu et al., 2017a). Luesken et al. (2011b) successfully established the co-culture by enriching the Anammox bacteria using an inoculum of a pre-established stable DAMO culture containing 70 to 80% DAMO bacteria and achieved a co-culture of equal microbial composition of DAMO and Anammox after 161 days (Table 2.2). A second approach was to use a stable Anammox culture as the inoculum source (Zhu et al., 2011). After inoculation with Anammox granules and stabilization of the culture, CH_4 and NO_2^- were supplied to the culture in excess under NH_4^+ limited conditions to enrich the DAMO bacteria. The co-culture enrichment from Anammox granules took one year of enrichment period (Zhu et al., 2011). A third approach was to use of sludge mixtures from different sources for the co-culture enrichment such as a mixture of methanogenic sludge and activated sludge from a WWTP, successful enrichment was achieved in 4.5 months (Ding et al., 2014). It was observed that Anammox and DAMO bacteria were present in the outer layer of the microbial clusters, surrounding DAMO archaea aggregates (Ding et al., 2014). Finally, the fourth approach was to enrich the DAMO and Anammox microorganisms in separate reactors and then combine them in one reactor to establish the co-culture.

In conclusion, freshwater sediments are significant inoculum sources for successful enrichment of co-cultures of DAMO microorganisms and Anammox bacteria (Fu et al., 2017a; Ding et al., 2017) as well as paddy soils (Laçin, 2021). However, due to the physical characteristics such as high mineral content like silicon and high viscosity as observed in paddy field soils, direct usage of these inocula may not be practival (Laçin, 2021). Nevertheless, a mixed inoculum may have an advantage over using a sole inocula source (Li et al., 2018a). On a different note, granule size of the biomass is an important factor that affects removal efficiencies and might have an effect on enrichment; therefore, requires a further investigation. Simulation results reveal that smaller granules enabled higher simultaneous ammonium and methane removal efficiencies (Winkler et al., 2015).

2.6.4 Feed

Feed Type

In the enrichment studies carried out, mostly synthetic wastewater with nitrite or nitrate, or nitrite and nitrate along at different concentrations (Table 2.2) with trace elements was used as the feed and methane was supplied as the carbon source (Raghoebarsing et al., 2006; Ettwig et al., 2008; Ettwig et al., 2009; Hu et al., 2009; He et al., 2014; Wang et al., 2015; Bhattacharjee et al., 2016; Hatamoto et al., 2014; Hatamoto et al., 2017). To our knowledge, there is limited number of enrichment studies using an original wastewater as the feed such as filtered effluent of an activated sludge process (Kampman et al., 2012).

Recently, Lim et al. (2021) published a study that is the first and only real wastewater application on a lab-scale DAMO-Anammox co-culture, up to this date. A DAMO-Anammox MBfR was established to treat main-stream and side-stream wastewater under four different scenarios. Three main-stream scenarios operated at a temperature of 22°C were studied where the source of was the effluent of a HRAS system. In the first scenario, nitritation was applied to the HRAS effluent prior to the DAMO-Anammox MBfR and was operated at an HRT of 1 day. In the second scenario partial nitritation was applied prior to the DAMO-Anammox MBfR and was also operated at an HRT of 1 day, while in the third scenario, partial nitritation and Anammox was performed prior to the DAMO-Anammox MBfR, which was operated at an HRT of 0.5 days. On the other hand, AD liquor was used the side-stream wastewater and studied under one scenario. In this scenario the AD effluent was partially nitrified prior to the DAMO-Anammox MBfR, which was operated at a temperature of 35°C and HRT of 2 days.

In order to investigate the effects of synthetic wastewater and original wastewater on enrichment of DAMO microorganisms, Kampman et al. (2012) operated two sequencing fed-batch reactors (SFBRs). The first was fed with a medium made of 10% (v/v) filtered activated sludge process effluent containing 1.3 mg biochemical

oxygen demand (BOD)/L, 2.1 mg Kjeldahl-N/L and 3.8 mg (NO_2^- + NO_3^-)-N/L. On the other hand, the second was fed with synthetic wastewater containing a source of alkalinity, calcium (Ca), magnesium (Mg), the necessary trace elements, 14–980 mg NO_2^--N/L and 14–126 mg NO_3^--N/L and no source of BOD. The maximum nitrite consumption rate in the first reactor was 11% higher (Kampman et al., 2012). The activated sludge effluent provided potential growth factors that may be absent in the reactor fed with synthetic wastewater (Kampman et al., 2012).

In Lim et al. (2021) the influent concentrations in the mainstream scenarios applied to the DAMO-Anammox MBfR were 12 mg NH_4^+-N/L, 62 mg NO_2^--N/L and 1-22 mg NO_3^--N/L (Scenario I), 20 mg NH_4^+-N/L, 31 mg NO_2^--N/L and 0-14 mg NO_3^--N/L, (Scenario II) and 5 mg NH_4^+-N/L, 0.5 mg NO_2^--N/L and 10 mg NO_3^--N/L, (Scenario III). While the influent NH_4^+, NO_2^- and NO_3^- concentrations in the side-stream scenario were 455, 590 and 0 mg N/L, respectively. The removal rates achieved were 12 mg NH_4^+-N/L·day, 62 mg NO_2^--N/L·day and 1-22 mg NO_3^--N/L·day (Scenario I), 16 mg NH_4^+-N/L·day, 31 mg NO_2^--N/L·day and 0-14 mg NO_3^--N/L·day, (Scenario II) and 4 mg NH_4^+-N/L·day, 1 mg NO_2^--N/L·day and 14 mg NO_3^--N/L·day, (Scenario III) and 225 mg NH_4^+-N/L·day and 290 mg NO_2^--N/L·day in the side-stream scenario. Moreover, in the main-stream scenarios DAMOa had the highest abundance and DAMOb was the second while Anammox had the least abundance within the DAMO-Anammox co-culture. On the other hand, in the side-stream scenario DAMOa had the highest abundance, while Anammox was the second highest and the lowest abundance was found to be DAMOb.

Nitrogen

The effect of different nitrogen feeds on DAMO microorganisms and their microbial composition was assessed in enrichment studies (Hu et al., 2011; Hatamoto et al., 2014; Fu et al., 2017a). The nitrogen supplied in DAMO enrichment studies involve nitrite in the range of 3-15 mM (Ettwig et al., 2008; Raghoebarsing et al., 2006; Luesken et al., 2011a) and nitrate in the range of 0.5-8.6 mM (Hatamoto et al., 2017; Kampman et al., 2014; Bhattacharjee et al., 2016) (Table 2.2). A study using two

separate cultures fed separately with NO_3^- and NO_2^- revealed that when supplied with NO_2^-, DAMO bacteria dominated over DAMO archaea (Hu et al., 2011). Another study using batch and continuous flow cultures provided with only NO_2^- and only NO_3^-, reported that the enriched NC10 bacterial communities were different (Hatamoto et al., 2014). The nitrite-fed continuous flow reactor exhibited a shorter lag period and a higher maximum NO_2^- consumption rate compared to the nitrate-fed continuous flow reactor (Hatamoto et al., 2014). In addition, DAMO archaea were not detected in the nitrite-fed reactor while they had a composition of around 7% in the nitrate-fed reactor (Hatamoto et al., 2014). The DAMO bacteria constituted about 68% in the nitrite-fed reactor and 58% in the nitrate-fed reactor (Hatamoto et al., 2014). It was also reported that both DAMO archaea and DAMO bacteria can survive in NO_3^- and CH_4 conditions, since nitrite accumulation was not observed (Li et al., 2018a).

The effect of nitrite on a DAMO co-system (DAMO bacteria and DAMO archaea) was investigated in terms of nitrogen removal and microbial community. The short-term studies showed that nitrite concentrations below 100 mg N/L did not inhibit the co-system (Lou et al., 2019). As the nitrite concentration was increased to 950 mg N/L, nitrogen removal efficiency was completely inhibited. On the other hand, the long-term studies illustrated that nitrogen removal performance was completely inhibited at 650 mg N/L. This led to a decrease in the DAMO co-system species abundance and diversity, changing the microbial community structure. NO_2^- consumption is inhibited by the formation of free nitrous acid (FNA) under acidic conditions and the ionized form of NO_2^- under alkaline conditions (Lou et al., 2019).

Regarding the DAMO-Anammox co-culture, different combinations and concentrations of NO_3^-, NO_2^- and NH_4^+ feed affect the microbial composition of the co-culture (Table 2.2 and Table 2.3). Low concentration of NO_2^- was identified as an important factor in maintaining a high activity of *M. nitroreducens* (Luesken et al., 2011b; Zhu et al., 2011; Ding et al., 2014; Fu et al., 2017a). In addition, Anammox can outcompete *M. oxyfera* over NO_2^- since they have a higher NO_2^-

affinity ($K_{NO_2^-}^{An}$ of 0.1 mg N/L and $K_{NO_2^-}^{D_b}$ of 0.6 mg N/L, respectively) (Winkler et al., 2015; Zhu et al., 2011), while the NO_3^- affinity of *M. nitroreducens* $K_{NO_3^-}^{D_a}$ is 2.1 mg N/L (Lu et al., 2019). Therefore, for a successful enrichment of the co-culture, CH_4 and NO_2^- should be supplied in excess while keeping the NH_4^+ concentration limited (Luesken et al., 2011b). In most of the co-culture studies, Anammox was reported to be responsible of the majority of the total NO_2^- removal. Moreover, theoretically NO_3^- produced by the Anammox bacteria (Equation 2.4) can be completely removed by *M. nitroreducens* (Equation 2.5) and the NO_2^- is converted to N_2 gas by *M. oxyfera* (Equation 2.6) and Anammox bacteria (Equation 2.4) (Xie et al., 2016).

Hu et al. (2015) investigated the effect of nitrogen source on the removal of nitrogen and methane by using two separate anoxic reactors, one fed with NO_3^- while the other fed with NO_2^- at a loading rate between 10.5-38.4 mg N/day along with NH_4^+ and CH_4 supply to both reactors. The NO_3^--fed and NO_2^--fed reactors showed the presence of DAMO archaea composition of 70% and 26%, respectively (Table 2.3). The study claims that the disappearance of DAMO bacteria in both reactors was due to the competition with Anammox bacteria. Fu et al. (2017a), on the other hand, observed the domination of DAMO bacteria in their study conducted in six reactors with different combinations of NO_2^-, NO_3^- and NH_4^+ (Table 2.3). The study claims that DAMO archaea were not found in the co-culture under NO_3^--fed conditions, possibly due to the absence of the microorganisms in the inocula. It was also reported in another study that the NH_4^+ feed leads to an increase in the percentage of Anammox bacteria in the consortium and improves the nitrogen removal rate, while no archaea thrived in the NO_3^--fed reactor in contrast to previous studies (Hu et al., 2009; Hu et al., 2010).

In a co-culture study, the NH_4^+ concentration was gradually increased to 280 mg N/L·day while the nitrite concentration was increased to 525 mg N/L·day (Luesken et al., 2011b) (Table 2.3). The developed co-culture was composed of equal percentage of DAMO bacteria and Anammox bacteria, achieving a NO_2^- removal rate of 100 mg N/L·day (Luesken et al., 2011b). Haroon et al. (2013) supplied NH_4^+

and NO_3^- in the feed and enriched a co-culture of DAMO archaea and Anammox bacteria where CH_4 was intermittently flushed into the headspace. The NO_3^- and NH_4^+ removal rates were both about 15 mg N/L·day.

Since DAMO bacteria and Anammox bacteria compete for NO_2^-, the NO_2^- to NH_4^+ ratio is an important parameter. Xie et al. (2016) used a NO_2^- to NH_4^+ molar ratio of 1.19 and achieved a NO_2^- and NH_4^+ removal rate of 560 mg N/L·day and 470 mg N/L·day, respectively. Furthermore, a synthetic wastewater mimicking the effluent of a mainstream partial nitritation process was used as feed to investigate the applicability of the co-culture in the treatment of domestic mainstream wastewater, since this wastewater has lower total nitrogen compared to that of anaerobic digestion (Xie et al., 2018). Setting the NO_2^-:NH_4^+ molar ratio in the synthetic feed within the range of 1.17-1.55 resulted in a high TN removal range of 91.7–94.7% (Xie et al., 2018). On the other hand, modelling a NO_2^-:NH_4^+ molar ratio of 1 showed the highest TN removal with microbial composition of 65% Anammox, 23% DAMO archaea and 12% DAMO bacteria (Chen et al., 2014). However, further rise in the molar ratio would eliminate DAMO archaea due to the methane competition with DAMO bacteria, consequently, causing a decline in TN removal (Chen et al., 2014). Similarly, DAMO and Anammox co-existence in a single granule was evaluated and it was found that the NO_2^- : NH_4^+ influent molar ratio is critical for the survival of DAMO microorganisms (Winkler et al., 2015).

It can be inferred that the influent N concentration, N source type and NO_2^- : NH_4^+ molar ratio as well as other potential N source molar ratios (NO_3^- : NO_2^- and NO_3^- : NH_4^+) are decisive parameters in the composition of the DAMO co-system and the DAMO-Anammox co-culture, their activities and TN removal. It should be noted that DAMO archaea and Anammox co-culture may be a self-sustaining system since each of the microorganisms is producing the electron acceptor of the other (Equation 2.4 and Equation 2.5). At balanced molar ratios, high N removal efficiencies might be achieved. On the other hand, obtaining a balanced ratio, may require the involvement of pretreatment units such as partial nitritation in Anammox systems.

Yet, the arrangement of the consortium and its activity might be only possible if the inoculum contains the microorganisms of concern (Fu et al., 2017a).

Trace Metals

It was revealed that *M. oxyfera* does not have genes for pyrroloquinoline quinone (PQQ) biosynthesis (Wu et al., 2011) that would be necessary for better DAMO activity. Moreover, Cu^{2+} (Copper) is a key element for pMMO enzyme activity (Glass and Orphan, 2012; Wu et al., 2011; Hatamoto et al., 2018); therefore, Hatamoto et al. (2018) tested the addition of Cu^{2+} and PQQ to the medium of DAMO culture and results showed that when Cu^{2+} and PQQ concentrations were increased from 0.19 to 0.38 mg/L and 0 to 2 nM, respectively, the nitrite consumption rate doubled. Furthermore, the results of the studies conducted by He et al. (2015a) investigating the effect of iron (Fe^{2+}) and Cu^{2+} showed that an Fe^{2+} and Cu^{2+} concentrations of 1.12 mg/L and 0.63 mg/L, respectively, stimulated the activity and the growth of DAMO bacteria in an SBR. Cu^{2+} concentrations exceeding 1.57 mg/L may inhibit the DAMO process (He et al., 2015a). Enzymes responsible for CH_4 oxidation are activated by Cu^{2+}, while enzymes responsible for NO_2^- reduction are activated by Fe^{2+} (He et al., 2015a). Jiang et al. (2018) investigated the effects of Fe^{3+} (0, 10, 50 mg/L), Cu^{2+} (0, 1, 5 mg/L) and molybdenum (Mo^{2+}) (0, 1, 5 mg/L) on the activity of a DAMO and methanogenic bacteria co-culture. The results showed that Fe^{3+}, Cu^{2+} and Mo^{2+} concentrations of 50 mg/L, 1 mg/L and 5 mg/L, respectively, enabled NO_2^- removal, while Cu^{2+} and Mo^{2+} concentrations of 5 mg/L and 1 mg/L, respectively, inhibited microbial activity. Conversely, trace metal elements such as Mo, zinc (Zn), cobalt (Co), manganese (Mn), and nickel (Ni) had no significant effect on DAMO specific activity (He et al., 2015a).

Regarding DAMO-Anammox co-culture, the effect of Fe^{2+} concentration was investigated (Lu et al., 2018). Fe^{2+} was found to have an important role in the competition among DAMO bacteria, DAMO archaea and Anammox bacteria. Anammox activity significantly increased with increasing Fe^{2+} concentrations in turn out-competing the DAMO bacteria, since Anammox bacteria require Fe^{2+} to

function. This is evident since they possess an anammoxosome compartment, that stores iron particles (van Niftrik et al., 2008). NO_3^- production via the Anammox reaction will improve the growth of the DAMO archaea (Lu et al., 2018).

Chemical Oxygen Demand

Except the one experimental research (Silva-Teira et al., 2017), the majority of the studies investigating the effect of COD on DAMO activity are mainly modelling studies. Silva-Teira et al. (2017) supplied an integrated DAMO and AMO-D pre-anoxic MBR with a synthetic effluent of an up-flow anaerobic sludge blanket reactor (UASBR) containing 35 mg soluble COD/L, 36 mg TN/L of which 34 mg N/L was ammonia. The results suggest that the COD functioned as an electron donor for Anammox that were behind a relatively small fraction of nitrogen removal in the pre-anoxic MBR. The achieved CH_4 and N-removal rates were 180 mg/L·day and 150 mg/L·day, respectively (Silva-Teira et al., 2017). In another study, He et al. (2018a) established a mathematical model to explain the microbial processes and interactions between DAMO bacteria and associated heterotrophic bacteria in an SBR. The results showed that adding small amounts of organic matter in the influent promoted the growth of DAMO bacteria, which was highest at 0.34 mg COD/mg N and 24 mg/L COD conditions. This was attributed to the increased excretion of growth factors by the heterotrophic bacteria, which unexpectedly decreased at those COD conditions, and to the indirect positive effect of these growth factors on DAMO bacteria. Yet, over-supply of COD decreased the DAMO biomass while improving the heterotrophic biomass. The stimulation of DAMO bacteria growth compared to heterotrophic bacteria at low substrate concentrations was also linked to the low nitrite concentration due to higher affinity of the former for nitrite. Higher nitrite concentrations (21 mg/L N) further weakened the nitrite competition and led to increased heterotrophic biomass. Apparently, nitrogen source, its concentration and nitrogen affinity constants should be considered to comment about the COD effect on a consortium where COD-degraders and DAMO cultures potentially co-exist.

Sulfate

Li et al. (2020a) studied the effect of sulfate on NO_2^--DAMO process, by testing the performance and microbial structure of the DAMO bacteria at a sulfate concentration ranging between 0-200 mg SO_4^{2-}/L. The activity of the microorganisms initially increased and reached a maximum denitrification rate of 1.26 mg N/L·day at 80 mg SO_4^{2-}/L and was inhibited above that concentration. The SO_4^{2-} was proposed to affect the mass transfer rate of methane and in turn the methane oxidation of nitrite-DAMO process. While in a study performed by Lou et al. (2022) to investigate the effect of SO_4^{2-} on the DAMO process. The results illustrated that the activity of the DAMO system was slightly enhanced with the addition of SO_4^{2-} up to a concentration of 40 mg SO_4^{2-}/L but then decreased by 50% up to concentrations of 80 mg SO_4^{2-}/L. Inhibition of the DAMO process was observed at concentrations above 80 mg SO_4^{2-}/L. These two studies are the only studies conducted on the effect of sulfate on DAMO microorganisms.

In the presence of sulfate, DAMO archaea may couple with sulfate reducing bacteria (SRB), a process called S-DAMO (sulfate-dependent anaerobic methane oxidation). The product of methane oxidation, hydrogen, will be utilized to reduce sulfate to sulfide by the SRB (Knittel and Boetius, 2009; Cui et al., 2015). On the other hand, sulfate-dependent anaerobic ammonium oxidation is a reaction that may occur since it has a low ΔG^0 value (-16.6 kJ/mol) but it is not likely to prevail (Zhang et al., 2009) since the Anammox and DAMO processes have lower ΔG^0 values. The inhibitory effect of sulfide on Anammox was found to be dictated by substrate and sulfide levels, as well as exposure time. Anammox activity diminished by 50% at a sulfide concentration of 32 mg S/L, while at 160 mg S/L the Anammox was completely inhibited. On the other hand, acclimation of the Anammox was achieved at a concentration of 8 mg S/L (Jin et al., 2013). In contrast, the effects of sulfide on the DAMO co-system are yet to be investigated.

Salinity

The activity of DAMO microorganisms from freshwater sediments was assessed under increasing salt concentrations (He et al., 2015b). It was observed that, in an inoculum dominant with 60% *M. oxyfera*, the highest specific activity was obtained at 0 g NaCl/L, while increasing the salt concentration up to 15 g NaCl/L decreased the specific activity. The increase in cell osmotic pressure led to the inhibition of the microorganisms (He et al., 2015b). Nevertheless, *M. oxyfera* can adapt to high salt concentrations of 20 g NaCl/L recovering its activity after 90 days of incubation, which reveals that DAMO process can possibly occur in saline ecosystems (He et al., 2015b).

Regarding the use of DAMO-Anammox co-cultures, one should consider the salinity effect on Anammox bacteria. According to various studies conducted to evaluate the effect of salinity on Anammox activity indicated that Anammox can tolerate concentrations in the range of 4-30 g NaCl/L (Yi et al., 2011; Jin et al., 2011; Wang et al., 2019). At low temperatures of 15 °C, efficient Anammox activity was detected below 4 g NaCl/L (Wang et al., 2019). Freshwater Anammox bacteria were found to be able to adapt to 7g NaCl/L concentrations (Yi et al., 2011), while the IC50 (50% inhibition concentration) of freshwater Anammox bacteria was found to be 9.1 g NaCl/L (Lin et al., 2020). The Anammox activity of adapted and non-adapted cultures to salt concentrations was compared. The results showed that the Anammox activity of the adapted and non-adapted cultures was similar at about 20 g NaCl/L (Engelbrecht et al., 2019) and 30 g NaCl/L (Jin et al., 2011). Apparently, DAMO bacteria and Anammox co-cultures can adapt to wastewaters with high salinity. The existence of the DAMO archaea in this consortium depends on the salinity effect on DAMO archaea which remains to be investigated.

2.6.5 Methane Content

The solubility of CH_4 is low, so DAMO processes may be at a disadvantage (Islas-Lima et al., 2004; He et al., 2013). Hence, one way to overcome this issue, presented in nearly all enrichment studies is to supply excess CH_4 (Raghoebarsing et al., 2006; Kampman et al., 2014; Luesken et al., 2011b; Chen et al., 2016a). Another approach is to improve the CH_4 solubility, through the addition of paraffin oil, where paraffin oil acts as a second liquid phase increasing CH_4 solubility by 25% significantly aided DAMO activity (Fu et al., 2015). According to Fu et al. (2015), CH_4 solubility at 35 °C was 2.93% (v/v CH_4/liquid) (1.2 mmol/L). Increasing the CH_4 solubility to 3.96% (v/v) (1.62 mmol/L) led to an increase in DAMO activity from 0.298 to 0.585 mg NO_3^--N/day, which was caused by the addition of 5% paraffin oil (v/v paraffin/liquid) (Fu et al., 2015). The consumption rates of a DAMO-Anammox co-culture with 5% paraffin oil (3.18 mg NO_3^--N/day and 5.14 mg NH_4^+-N/day) were twice as much as the consumption rates with 0% paraffin oil (Fu et al., 2015).

In the research studies, applied methane flow rate was usually in the range of 2-10 mL/min (Hu et al. 2014; Hatamoto et al., 2017; Kampman et al., 2012) at 95%:5% (CH_4: CO_2) (Raghoebarsing et al., 2006; Ettwig et al., 2008; Ettwig et al., 2009; Luesken et al., 2011a; Bhattacharjee et al., 2016). Increased CH_4 partial pressure was found to improve the AOM activity (Nauhaus et al., 2002; Cai et al., 2018; He et al., 2013). Similarly, a decline in nitrite and nitrate consumption rates was caused by a decrease in CH_4 partial pressure (Ding et al., 2017). In a DAMO co-system, the decline in CH_4 partial pressure will first affect DAMO archaea due to the lower CH_4 affinity compared to DAMO bacteria ($K_{CH_4}^{D_a}$ of 8 mg CH_4/L and $K_{CH_4}^{D_b}$ of 0.042 mg CH_4/L, respectively) (Guerrero-Cruz et al., 2019; Lu et al., 2019).

Chen et al. (2014), in their modeling study with a membrane biofilm bioreactor (MBfBR), showed that the Anammox bacteria mainly located on the outer layer of the biofilm while that of DAMO organisms were close to the membrane surface. In this respect, low surface methane loading (<0.0001 g/m^2·hr) was found to result in a low fraction of DAMO microorganisms while Anammox being dominant, whereas

high surface methane loadings (>0.0001 $g/m^2 \cdot hr$) caused a DAMO bacteria prosperity (Chen et al., 2014). Fu et al. (2019) pointed out the similar significant effect of the gas-phase transfer of CH_4 on the activity of the granular DAMO-Anammox co-culture compared to nitrogen compounds' transfer. They explained that CH_4 could not be transferred to the interior of the granules and caused the granules to be disrupted into flocs.

It is claimed that the DAMO cultures and the DAMO-Anammox co-culture are suitable for processes for the treatment of wastewaters with low C/N ratio, such as anaerobic digester supernatants (Islas-Lima et al., 2004). DAMO enrichment studies reported CH_4:NO_2^- molar consumption ratio as 0.38 (Kampman et al., 2012), 0.34, 0.35 and 0.39 (He et al., 2014), while the CH_4:NO_3^- molar consumption ratio as 0.58 (Hatamoto et al., 2014) and 0.54 (Islas-Lima et al., 2004). These findings are close to the theoretical stoichiometry ratios of the DAMO reactions (Equation 2.5 and Equation 2.6), CH_4:NO_2^- and CH_4:NO_3^- molar ratios of 0.38 and 0.63, respectively (Islas-Lima et al., 2004; Raghoebarsing et al., 2006).

To our knowledge, there has been no study so far aimed at testing the effect of CH_4:NH_4^+ ratio. This ratio might be of significance for the arrangement of the consortia in DAMO-Anammox co-cultures and in turn the treatment of wastewaters such as anaerobic digester effluent or landfill leachate. Theoretically, the CH_4:NH_4^+ molar consumption ratio should indicate the dominant species in the co-culture since Anammox culture consume NH_4^+ and DAMO cultures consume CH_4. Therefore, finding the optimal ratio is vital for the target removal efficiency.

Landfill leachate composition depends on different factors some of which are the type of waste disposed and the age of the landfill. It has been found that leachate consists of a COD ranging from 100-70,900 mg/L, BOD in the range of 3-26,800 mg/L, NH_3-N ranging from 0.2-13,000 mg N/L, salinity ranging from 4,000-15,100 mg NaCl/L and pH between 5.8-8.5, with old landfills containing low COD and BOD content (Chu et al., 1994; Renou et al., 2008). Moreover, the heavy metal content of leachate included Fe ranging from 2.7-76 mg/L, Mn in the range of 0.028-16.4 mg/L,

barium (Ba) between 0.006-0.164 mg/L, Cu between 0.005-0.78 mg/L, aluminum (Al) less than 2 mg/L and silicon (Si) in the range of 3.72-10.48 mg/L (Renou et al., 2008). The heavy metal content in leachate is low but the effect of some of the metals such as Ba, Al, and Si on a DAMO-Anammox co-culture needs to be further investigated. However, high salinity of leachate (Diamantis et al., 2013) may cause a challenge for its application to a DAMO-Anammox system. On the other hand, the anaerobic digester effluent composition is NH_4^+ 800-1000 mg N/L, NO_2^- 30-70 mg N/L, CH_4 10-25 mg/L, PO_4^{3-} 20-87 mg P/L and COD of 180-280 mg/L (Zhang et al., 2011; Cookney et al., 2016; Liu et al., 2016b). Provided that nitritation, anaerobic digestion of organic matter (in the case of young age landfill leachate) and salinity regulation (in the case of leachate) are performed, the composition and concentrations of the constituents of leachate, especially old age, and anaerobic digester liquor seem suitable for treatment by a DAMO-Anammox co-culture.

2.6.6 Dissolved Oxygen (DO)

Luesken et al. (2012) and Kampman et al. (2018) tested the effect of DO concentration on the activity of *M. oxyfera*. Chen et al. (2014) and Castro-Barros et al. (2017) modelled the effects of DO concentration on DAMO activity in different DAMO-based integrated systems. It was found that DO concentrations of 0.35 mg O_2/L slightly increased the denitrifying methanotrophic activity which returned to its original level after oxygen had been removed, while exposure to a concentration of 1.0 mg O_2/L inhibited anaerobic methanotrophs, even after the removal of O_2 (Luesken et al., 2012; Kampman et al., 2018). This occurred due to downregulation of the biosynthesis of nucleic acids and proteins, consequently, decreasing cell division processes in *M. oxyfera* (Luesken et al., 2012).

Chen et al. (2014) modelled a single-stage MBfBR coupling nitritation-Anammox-DAMO for complete nitrogen removal to investigate the effects of DO concentration (Chen et al., 2014) and to construct a relation between the oxygen surface loading rate and the system performance (Chen et al., 2015). The best TN removal of a DAMO, AOB and Anammox biofilm co-culture was achieved at a DO concentration

of 0.17 mg/L (Chen et al., 2014). On the other hand, an aerobic granular sludge reactor with AOB, Anammox, DAMO and aerobic methane oxidizing bacteria (MOB) was modelled to investigate the effect of DO concentration on the nitrogen and methane removal (Castro-Barros et al., 2017). The results indicated that the effective nitrogen and methane removal can be reached at DO concentrations less than 0.5 mg/L. Therefore, balance of the microbial consortium and system performance can be maintained through the operational control of the oxygen supply (Chen et al., 2015).

2.6.7 Reactor Configuration

DAMO enrichment was performed in various reactor types (Table 2.2), such as SBRs (Ettwig et al., 2009; Hu et al., 2009; Luesken et al., 2011a; Kampman et al., 2012; He et al., 2014; Hu et al., 2014; Li et al., 2018a), up-flow continuous reactors and batch reactors (Hatamoto et al., 2014), continuous stirred tank reactors (CSTRs) (Ettwig et al., 2008; Hu et al., 2014), MBRs (Wang et al., 2015; Kampman et al., 2014), continuous down-flow sponge bioreactor (Hatamoto et al., 2017) and a magnetically stirred gas lift reactor (MSGLR) (Hu et al., 2014). Moreover, the effect of different reactor configuration on the specific activities of DAMO microorganisms was investigated (Hatamoto et al., 2014; Hu et al., 2014; Fu et al., 2019).

In enrichment studies, DAMO microorganisms were reported as having a slow growth rate with a doubling time of 1-2 weeks for *M. oxyfera* and several weeks for *M. nitroreducens* (Raghoebarsing et al., 2006; Hu et al., 2009; Ettwig et al., 2010; Luesken et al., 2012; Hatamoto et al., 2014; Kampman et al., 2012; He et al., 2014; He et al., 2015a; Wang et al., 2015; Bhattacharjee et al., 2016). As a result of homogeneous distribution of substrate and biomass, long-term reliable operation, and stability under limiting conditions, SBRs proved to be suitable for the enrichment of slowly growing microorganisms, such as Anammox (Strous et al., 1999). Thus, in the earlier enrichment studies, SBRs were the common choice of enrichment reactors (Raghoebarsing et al., 2006; Ettwig et al., 2009; Hu et al., 2009;

Luesken et al., 2011a). Although SBRs are chosen for their potential biomass retention in comparison to CSTRs, however in comparison to MBRs, enrichment in SBRs takes longer periods due to eventual biomass washout. This is evident since the minimum solid retention time (SRT_{min}) of the DAMO and Anammox microorganisms calculated from μ_{max} is in the order of a few days to a few weeks. The SRT_{min} of DAMO bacteria was found to be 8.3-23.3 days, while that of DAMO archaea was found to be 29.3 days (Chen et al., 2014; Yu et al., 2017). On the other hand, the SRT_{min} of Anammox, was calculated to be 4.8-13.9 days (Chen et al., 2014; Lotti et al., 2014). Therefore, converting the SBR into an MBR by adding a membrane to increase the biomass retention was tested and resulted in an increase in the nitrite consumption rate (Kampman et al., 2012). Nevertheless, an enrichment study carried out with MBRs indicated that limited biomass retention is not the main reason for the decrease in the nitrite consumption rates (Kampman et al., 2014). The long-term results showed that the growth was unstable, and that the activity decreased after a couple of years of operation (Kampman et al., 2014). Internal recirculation in an MBR is an important parameter that governs methane removal (Sánchez et al., 2016; Silva-Teira et al., 2017).

In order to understand the reason behind the SBR limitation in DAMO enrichment, comparison studies on the effect of different reactor types should be analyzed. Hu et al. (2014) investigated the effect of three different reactor types (MSGLR, SBR and CSTR) on the performance of a DAMO culture. The MSGLR showed the best performance with the highest total and specific DAMO activities with a nitrogen removal rate of 76.9 mg N/L·day compared to removal rates of 26.4 mg N/L·day and 11.4 mg N/L·day in the CSTR and SBR, respectively. This was due to the improvement in the mass transfer of gas-liquid phases and the mixing of liquid-solid phases (Hu et al., 2014).

The system configuration employed is important in the successful application of DAMO-Anammox co-culture. Since both microorganisms are slow-growers, biomass retention, which is dependent on the reactor configuration, is one of the factors to be considered. Enrichment of the DAMO and Anammox co-culture was

first achieved using an SBR (Luesken et al., 2011b; Zhu et al., 2011; Langone et al., 2014). Luesken et al. (2011b) established a co-culture containing equal amounts of DAMO and Anammox in one year, which can remove NH_4^+ and NO_2^- at a rate of 81.6 mg NH_4^+-N/L·day and 100 mg NO_2^--N/L·day, respectively (Table 2.3). The membrane biofilm bioreactor (MBfBR) was also employed to establish the co-culture and investigate the specific activity (Shi et al., 2013; Cai et al., 2015; Hu et al., 2015; Xie et al., 2016; Sánchez et al., 2016; Silva-Teira et al., 2017; Xie et al., 2018). This configuration eliminates potential methane supply problems with respect to flammability, low solubility, and high energy demand when sparging, meanwhile enhancing biomass retention and gas transfer (Shi et al., 2013). MBfBR configuration is also reported to be able to withstand NO_2^-: NH_4^+ ratio changes in the influent (Xie et al., 2018). Species distribution of DAMO bacteria, DAMO archaea and Anammox bacteria in the MBfBR was of equal percentages in the microbial consortia (Shi et al., 2013; Xie et al., 2016). Different microbial composition of 50% DAMO archaea, 20% DAMO bacteria and 20% Anammox bacteria was developed also using an MBfBR (Cai et al., 2015), where 3.6 times more nitrate removal rate was obtained compared to the previous composition enriched by Shi et al. (2013). Indeed, one of the highest recorded removal rates for DAMO reactors, namely, 684 mg NO_2^--N/L·day, 684 mg NO_3^--N/L·day and 268 mg NH_4^+-N/L·day, were achieved with this microbial composition in an MBfBR (Cai et al., 2015) (Table 2.3).

Hollow-fiber membrane bioreactor (HfMBR) was also employed to establish DAMO and Anammox co-culture (Ding et al., 2017; Fu et al., 2017b; Lu et al., 2018). Ding et al. (2017) achieved a co-culture dominated by DAMO microorganisms by 65% (38.8% DAMO bacteria and 26.2% DAMO archaea), 13.8% *Proteobacteria* and 6.2% Anammox. While Fu et al. (2017b) also obtained a co-culture in an HfMBR consisting of 86% of DAMO microorganisms (74.3% DAMO archaea and 11.8 DAMO bacteria) and 5.6% Anammox bacteria. In a recent study aimed to enrich a DAMO-Anammox co-culture, a novel reactor configuration namely, the membrane aerated membrane bioreactor (MAMBR) was employed (Nie et al., 2019). The MAMBR provides efficient CH_4 distribution via a permeable

membrane and ultrafiltration membrane that completely retains the biomass. The NRR of the previously enriched microorganisms increased after inoculating the MAMBR, from 76.7 mg NH_4^+-N/L·day and 87.9 mg NO_3^--N/L·day to 126.9 mg NH_4^+-N/L·day and 158.8 mg NO_3^--N/L·day. The total nitrogen removal rate reached a maximum of 2.5 g N/L·day in 200 days of operation.

In a comparative study using SBR and HfMBR, the importance of liquid-phase mass transfer and gas-phase mass transfer on the co-culture system was investigated (Fu et al., 2019). The SBR was inoculated with granules from an HfMBR system, yet lower nitrogen removal was observed compared to the HfMBR. The nitrate removal rate decreased, but then recovered. The methane gas-phase transfer was claimed to be the cause of the reduced nitrogen removal of the system. Moreover, the microbial morphology was affected through the unbalance of nutrient requirement, which caused the granules to disrupt into flocs and the microbial interactions were affected where the DAMO archaea population decreased (Fu et al., 2019).

In summary, biomass retention and methane transfer are the two main factors dictated by reactor configuration that affect the enrichment of DAMO microorganisms. Although SBRs support biomass retention, the SBR configuration does not facilitate methane gas transfer. On the other hand, CSTR configuration does not facilitate biomass retention. Therefore, modifications that improve biomass retention and gas transfer can be applied to the SBR and CSTR configurations. Reactor configurations such as MBRs and HfMBRs are superior to other configurations with regard to supporting biomass retention and facilitating gas transfer.

2.6.8 Hydraulic Retention Time

Since biomass retention is an important concern regarding the DAMO microorganisms, HRT is expected to have a significant effect on the enrichment and specific activity of those microorganisms. However, purposely the HRT effect on the nitrogen and CH_4 removal via a DAMO-Anammox co-culture was not examined. Studies conducted on nitrogen and dissolved methane removal using co-cultures in

various reactor configurations applied different HRTs in the range of 1-8 days (Shi et al., 2013; He et al., 2014; Cai et al., 2015; Xie et al., 2016; Ding et al., 2017; Fu et al., 2017b). The studies performed using SBRs applied higher HRTs than those employing biofilm reactors in all their forms. The effect of a gradual decrease in HRT from 8 days to 1 day on the complete nitrogen removal of a DAMO-Anammox MBR was assessed (Xie et al., 2016). A complete nitrogen removal rate of 1300 mg N/L·day was achieved without nitrate buildup, which is comparable to the practical rates reported for side-stream nitrogen removal processes (Xie et al., 2016).

Kampman et al. (2014) claimed that lowering the HRT of a DAMO culture from 61 to 1.4 days while maintaining the nitrite loading rate, which was done by decreasing the influent nitrite concentration, increased the nitrite consumption rate from 8 to 31 mg N/L. Kampman et al. (2014) claims that lower HRT helps wash out inhibitory by-products. Moreover, results show increased nitrite consumption rates at HRTs of 1.3 days (Kampman et al., 2014). The highest nitrite removal rate of 985.6 mg N/L·day was achieved by reducing HRT from 4.2 to 2.1 hours (Hatamoto et al., 2014). On the other hand, a modelling study illustrated that, in an MBfBR operated at an HRT less than 5.25 days no major removal of dissolved CH_4 occurred, while at HRT of 5.75-8 days dissolved CH_4 removal efficiency reached more than 90% (Chen et al., 2015). This may be due to the washout of the DAMO microorganisms from the biofilm at lower HRTs (Chen et al., 2015). Moreover, it is found that the optimum HRT is inversely proportional to the oxygen surface loading rate (Chen et al., 2016b).

Since the DAMO and Anammox are slow-growing microorganisms, the starting HRT of enrichment should be long enough in order to accommodate the growth period of those microorganisms and prevent biomass washout. Once enrichment is achieved, HRT may be reduced depending on the reactor configuration. Since MBRs have a higher capacity of biomass retention than SBRs, HRT reduction will be better administered in MBR configuration.

2.6.9 Conclusion

In order to address the current issues regarding GHG emissions and release of pollutants into the environment, in a biological treatment perspective, focus should shift towards anaerobic processes (Harb et al., 2021). Therefore, applying the DAMO process for wastewater treatment seems to be promising, especially when combining it with the Anammox process (Wang et al., 2017a; Wang et al., 2017b; van Kessel et al., 2018). Considering the information conveyed herein about the parameters or factors affecting the DAMO co-system and DAMO-Anammox co-culture, nitrogen driven methane oxidation appears to have an auspicious prospect in wastewater treatment systems (Wang et al., 2017a). This can be achieved via the mitigation of nitrate and methane discharged from WWTPs into the environment and atmosphere. Nitrate is the final main form of nitrogen oxides and more abundant than nitrite in wastewater and in the natural environment due to WWTP effluents or agricultural runoff. Thus, DAMO archaea's environmental role in the global carbon and nitrogen cycles should be better defined and investigated. Therefore, a DAMO archaeon–Anammox co-culture is likely to be more significant than a DAMO bacterium–Anammox co-culture. Nevertheless, a DAMO-Anammox containing DAMO bacteria provides an additional degree of freedom making the process more flexible in terms of the NO_2^- : NH_4^+ molar ratio required (Harb et al., 2021).

Consequently, a temperature between 30-35 °C and a pH between 7.0-7.6 are required for the enrichment of DAMO microorganisms (Harb et al., 2021). The nitrogen source provided, and their ratios play an important role in changing the microbial composition of the DAMO co-system and DAMO-Anammox co-culture. Adjusting the nitrogen molar ratios may help to provide a stable and balanced DAMO-Anammox co-culture that can target all the nitrogen species. In addition, the presence of trace metals such as iron and copper are vital for their enrichment. Mixed inocula from natural sources and WWTPs are convenient for the enrichment of the microorganisms. Methane solubility is an important factor in the enrichment of DAMO microorganisms, therefore increasing the solubility from 1.2 mmol/L to 1.62

mmol/L may lead to doubling the DAMO-Anammox activity. In contrast, DO concentration should remain below the inhibitory concentration of 1.0 mg O_2/L, preferably at around 0.35 mg O_2/L. Moreover, reactor configurations of MBR, HfMBR or MAMBR provide the highest activity due to their biomass retention and gas (methane) transfer characteristics, the two main factors of reactor configuration regarding the DAMO enrichment. Furthermore, controlling HRT is critical for preventing washout and allowing enough time for the DAMO enrichment and activity.

However, the DAMO-Anammox system has been only tested on lab-scale (Wang et al., 2017a). Therefore, further studies aimed at assessing the effects of factors such as CO_2 and H_2S (Wang et al., 2017a), biodegradable organic matter, heavy metals, salinity, hydraulic shock loadings, NO_2^-:NO_3^- and CH_4:NH_4^+ molar ratios should be conducted since such compounds might be available in potential influent of DAMO processes such as anaerobic digester liquor or landfill leachate. DAMO-Anammox co-culture has been applied with an original partially nitrified anaerobic digester effluent in one study up to this date (Lim et al., 2021). Therefore, investigating the application of a DAMO-Anammox system seems critical for understanding the potentials of this co-culture system. Moreover, the DO effect on the growth and activity of the DAMO microorganisms through the competition with the ammonia oxidizers has not been studied (van Kessel et al., 2018).

In order to implement full-scale DAMO-based technologies for wastewater treatment, scaling up is required (Harb et al., 2021). This will give rise to challenges that need to be addressed. Independent of the wastewater type, dissolved methane concentration and its bioavailability and biomass retention are some of the major concerns of DAMO and DAMO-Anammox systems. These issues may be solved through the proper reactor selection such HfMBR or MAMBR (Harb et al., 2021). Yet, SBRs are advantageous with respect to cycle time, operational simplicitiy and low cost in comparison membrane reactors (Kitanou et al., 2021). Although the DAMO-Anammox co-culture exhibits a potential in treating side-stream wastewater such as anaerobic digestor liquor and also landfill leachate, pretreatment will be

required to remove potential inhibitory compounds such as heavy metals (Zn, Al), salinity, COD, sulfide, suspended solids, and provide the necessary nitrite, nitrate, and methane (Harb et al., 2021). Another challenge for full-scale implementation is the long start-up time for a DAMO-Anammox co-culture. In addition, modelling, monitoring, and optimization are required in order to integrate the DAMO process into the current WWTPs (Wang et al., 2017a) and utilize the benefits this process presents in terms of GHG mitigation, energy conservation and sustainability.

Further modifications of the DAMO-Anammox system might be explored such as integrating this co-culture with microalgae (Harb et al., 2021). This integration can target a wider range of pollutants including phosphorus, increase the removal efficiency of residual ammonium and recover energy from the consumed methane. Lab-scale integration of Anammox and microalgae has been performed by Gutwinski and Cema (2016) and Manser et al. (2016). The CO_2 produced from the oxidation of CH_4 in a DAMO-Anammox system can be further used by microalgae through photosynthesis, and the microalgae can then be processed and digested in the anaerobic digester. Such a novel configuration might close the energy cycle making it self-sustainable and energy efficient (Harb et al., 2021).

2.7 Microalgae and *Chlorella vulgaris*

Incrementing trends of global warming caused by GHG production and accumulation in the atmosphere, due to the dependence of the world economies on conventional energy production through fossil fuels, has sparked the research in the field of carbon sequestration. The major greenhouse gases responsible for the phenomenon of global warming are CO_2 and CH_4 (Singh and Ahluwalia, 2012). Research on the capture and storage of those gases is becoming a prominent tool to reduce the power plant gas emissions. The basis of most research if not all is the surrounding natural environment. Since photosynthetic organisms are natural carbon sequesters or fixers, the promising solution could be using microalgae since they exhibit superior advantages over higher plants through their fast growth rate (Khan

et al., 2009). Microalgae have a relatively high yield with a minimal land use (Collet et al., 2010). They can be easily cultivated and encompass the main primary producers on the planet. In addition, microalgae have a short doubling time and have a much higher photosynthetic efficiency than terrestrial plants. Furthermore, microalgae are considered to be a carbon neutral biofuel since they capture and store the atmospheric carbon dioxide (Chisti, 2007). Figure 2.10 shows the relation between CO_2 reduction and other climate changing gases.

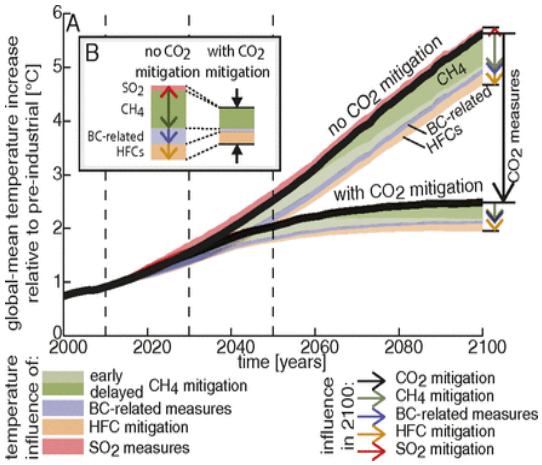

Figure 2.10 Influence of short-lived climate forcers (SLCF) and CO_2 linkage with varying CO_2 mitigation (BC: black carbon; HFC: hydrofluorocarbons) (Rogelj et al., 2014).

There are ample advantages to the microalgae utilization which include their tolerance to high CO_2 concentration, low light intensity conditions, and being industrially attractive for investment through the co-products such food supplements, animal feed, oil extraction, its trans-esterification into biodiesel, electricity production by converting the algae to methane anaerobically. Furthermore, it is possible to produce algal biodiesel at low cost with a significant greenhouse gas and energy balance benefit over fossil diesel. However, when scaled up to commercial production levels, the costs may surpass those for fossil diesel (Kadam, 2001). Biodiesel from microalgae seems to be the main renewable biofuel that has the potential to displace conventional transport fuels without negatively affecting the

food supply. Moreover, oil crops such as oil palm and bioethanol from sugarcane cannot match the sustainability of biodiesel from microalgae (Chisti, 2008).

All microalgae species tested have similar amino acid content, and are rich in the essential amino acids, while the polysaccharides are variable in sugar composition, but most of the species had high proportions of glucose (21-87%) (Richmond, 2004). This provides support that the anaerobic digestion of microalgae is preferable option since the microalgae contain the basic nutritional content needed for the different processes of anaerobic digestion. It is expected that the combination of microalgae in AD biogas production and processing methods will enhance the cost efficiency of the process, facilitating it to develop economically viable and environmentally sustainable energy (Richmond, 2004).

2.7.1 Phylogeny

Microalgae are a biodiverse group that includes about 40,000 described and analyzed species (Hu et al., 2008). One of the most studied specie is *Chlorella vulgaris*, which belongs to the following classification: Domain: *Eukaryota*, Kingdom: *Viridiplantae*, Phylum: *Chlorophyta*, Class: *Trebouxiophyceae*, Order: *Chlorellales*, Family: *Chlorellaceae*, Genus: *Chlorella*, Specie: *Vulgaris*. In 1890, Martinus Willem Beijerinck first discovered it as the first microalga with a defined nucleus. *C. vulgaris*, a unicellular microalga that flourishes in freshwater, is thought to be present on earth since the pre-Cambrian period, 2.5 billion years ago (Safi et al., 2014).

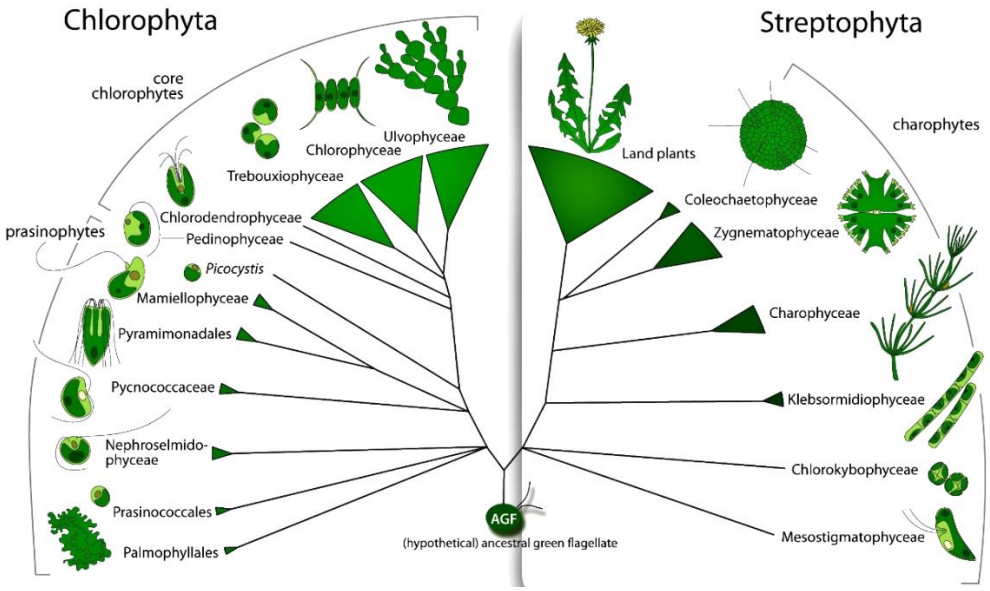

Figure 2.11 Schematic illustrating the phylogeny of green algae (Leliaert et al., 2012)

2.7.2 Biochemical Reactions and Pathways

C. vulgaris like all green algae undergo oxygenic photosynthesis, where light is utilized to convert CO_2 into carbohydrates, hence, such organisms are known as photoautotrophs. On the other hand, in the absence of light, respiration takes place, where the stored carbohydrates are broken down into CO_2 using O_2 as the electron acceptor. According to the presence of light and availability of organic and inorganic, green algae can undergo different growth modes that utilize different carbon sources (Hammed et al., 2016).

The three metabolism modes are autotrophic, heterotrophic and mixotrophic, displayed in Table 2.4. Autotrophic metabolism also referred to photosynthesis utilizes light and inorganic carbon mainly in the form of CO_2 or HCO_3^-. The captured CO_2 is fixed via the Calvin-Benson cycle to produce carbohydrates necessary for the growth of the cell (Hildebrand et al., 2013). Equation 2.7 illustrates the autotrophic metabolism (Park et al., 2021). On the other hand, heterotrophic metabolism is a non-photosynthetic, also referred to as dark metabolism. This mode of metabolism

utilizes organic carbon for energy production (Morales-Sánchez et al., 2015). Three major steps take place in heterotrophic metabolism; the first is the uptake of the organic carbon source, then this carbon source is processed via glycolysis, tricarboxylic acid cycle and the glyoxylate cycle pathways. The last step is the storage or utilization of the metabolites created through these pathways (Morales-Sánchez et al., 2015). Equation 2.8 illustrates the heterotrophic metabolism (Park et al., 2021). Simultaneous autotrophic and heterotrophic metabolism is called mixotrophic metabolism (Wang et al., 2014). Both inorganic and organic carbon sources are utilized (Kang et al., 2004). This allows for the adaptability of the *C. vulgaris* to conditions and to the availability of different carbon sources and light (Liang et al., 2009; Min et al., 2011). Equation 2.9 displays the mixotrophic metabolism.

Table 2.4 Modes of microalgae metabolism (Perez-Garcia et al., 2011)

Metabolism Mode	Energy Source	Carbon Source	Light Presence
Autotrophic	Light	Inorganic	Compulsory
Heterotrophic	Organic carbon	Organic	Not required
Mixotrophic	Light and Organic carbon	Both	Not compulsory

$HCO_3^- + H_2O \rightarrow C\ (Biomass) + 1/2\ O_2 + 3\ OH^-$ ……..……. Equation 2.7

$(1+a)\ CH_2O + O_2 \rightarrow C\ (Biomass) + a\ CO_2 + (1+a)\ H_2O$ ……..…… Equation 2.8

$b\ HCO_3^- + c\ CH_2O \rightarrow (b+(c-a))\ C\ (Biomass) + 3\ OH^- + a\ CO_2$ ……... Equation 2.9

2.7.3 Ultrastructure of *C. vulgaris*

C. vulgaris is a spherical microscopic cell containing many structural characteristics similar to plant cells. It has a diameter of 2–10 μm (Yamamoto et al., 2004; Yamamoto et al., 2005). Like plant cells, *C. vulgaris* contains a cell wall that preserves the cell's integrity and protects it against invaders and harsh conditions.

The thickness of this cell wall is related to the growth phase of the cell and the environment conditions. At early stages of development, the cell wall is relatively thin but at maturation reaches 17-21 nm in thickness (Yamamoto et al., 2004; Yamamoto et al., 2005). The cytoplasm contains the internal organelles such as the nucleus, the mitochondria, vacuoles, a single chloroplast, and the Golgi body. The mitochondrion is responsible of the respiratory activity of the cell by converting carbohydrates into energy in the form adenosine triphosphate (ATP). While the chloroplast is where the process of photosynthesis takes place by fixing CO_2 into carbohydrates. In addition, during nitrogen stress conditions the cytoplasm and chloroplast accumulate lipid globules that will be utilized by the cell as a source of energy. Figure 2.12 shows a schematic of the *C. vulgaris* cell.

C. vulgaris is a non-motile cell that reproduces asexually. It reproduces rapidly; one cell in optimal conditions multiplies by autosporulation into four daughter cells within 24 hours. The daughter cells will form their cell walls inside the mother cell and after maturation; the mother cell wall will rupture releasing the daughter cells that will feed on the remnants of the mother cell (Yamamoto et al., 2004; 2005).

Chlorophyll located in the thylakoids is the most abundant pigment in *C. vulgaris*. Moreover, *C. vulgaris* also contains accessory pigments such as carotenoids to increase the amount of light utilized by the cell. In addition, β-carotene is associated with the lipid droplets in the chloroplast, and primary carotenoids are associated with chlorophyll in thylakoids where they trap light energy and transfer it into the photosystem (Safi et al., 2014).

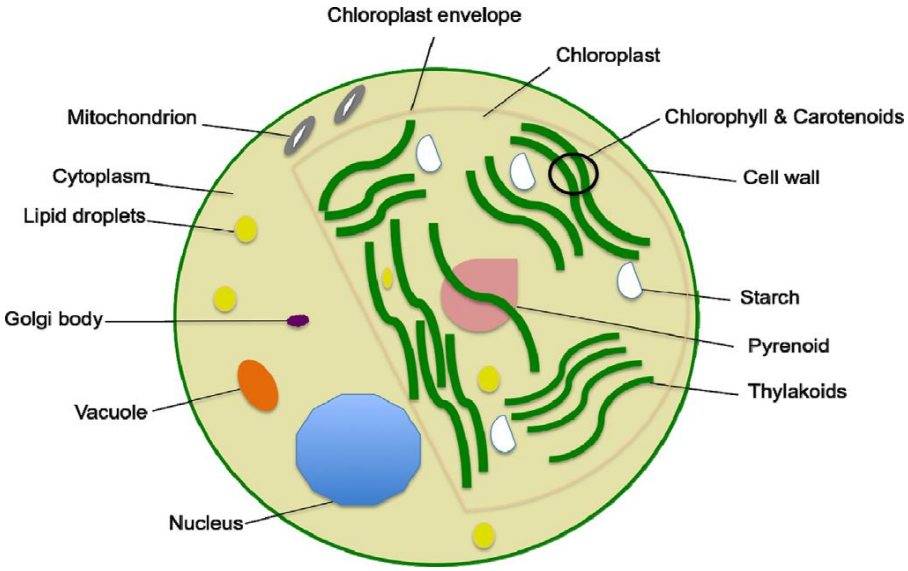

Figure 2.12 Schematic of *C. vulgaris* showing the different organelles present (Safi et al., 2014).

2.7.4 Factors Affecting the Enrichment of *C. vulgaris*

There are two categories of factors that affect microalgal growth; environmental factors (physical) and nutritional factors (chemical). Physical factors include pH, temperature, light intensity, illumination period, and aeration. On the other hand, carbon, nitrogen, phosphorus, silicon, metals such as iron, copper, zinc, and vitamins are some of the main nutritional factors vital for microalgal growth (Daliry et al., 2017). The optimum conditions for the enrichment of *C. Vulgaris* are summarized in Table 2.5 (Subaşı, 2022). The conditions to be employed dictate the metabolism modes of the cultured microalgae and vary depending on the intended application of the microalgae. The various applications of microalgae are displayed in Section 2.7.5.

Table 2.5 Optimum conditions for *C. vulgaris* enrichment. Modified from (Subaşı, 2022)

Parameter	Optimum Condition	Reference
pH	6.5-10.0	Deniz (2020)
Temperature	15-25°C	Falkowski & Owens (1980); Deniz (2020)
Growth Metabolism	Mixotrophic	Daliry et al. (2017)
Nitrogen Source	NH_4^+	Liu et al. (2016a)
Phosphorus Source	$H_2PO_4^-$	Larsdotter (2006)
N:P Ratio	5-15 g/g 8 g/g	Aslan and Kapdan (2006) Subaşı (2022)
Inorganic Carbon Source	HCO_3^- and CO_3^{2-}	Carvalho et al. (2006)
Organic Carbon Source	Glucose	Daliry et al. (2017)
Aeration	0.4 vvm	Anjos et al. (2013)
Light Intensity	50-220 µmol/m^2·s	Khalili et al. (2015); Daliry et al. (2017)
Illumination Period (light: dark) (hours)	24:0 (autotrophic) 16:8 (heterotrophic)	Deniz (2020); Subaşı (2022) Daliry et al. (2017)
HRT	2-8 days 4 days	Larsdotter (2006) Subaşı (2022)
NLR	8-42 mg/L·day	Subaşı (2022); Danesh et al. (2020)
PLR	1-5 mg/L·day	Şentürk and Yıldız (2020)
OLR	36-100 g/L·day	Kamyab et al. (2014); Subaşı (2022)

Temperature

Microalgae generally operate at temperatures between 15-30˚C. This is due to the fact that enzyme activity to perform photosynthesis and cell division is best within this range (Falkowski and Owens, 1980). In addition, some studies claim that temperatures above 25˚C reduce protein synthesis by the cell (Konopka and Brock, 1978). With respect to *C. vulgaris*, Deniz (2020) states that the optimum temperature is 25˚C.

pH

pH is very vital in dictating the mode of metabolism and the biosynthesis of secondary metabolites, since the pH level determines the proton concentration in the water (Khalil et al., 2010). There are ample studies involving the enrichment of microalgae at pH ranging between 2.5-11.5 (Sakarika and Kornaros, 2016). Moreover, depending on the intended application of the microalgae, different pH ranges are employed. For instance, biomass productivity was the highest at a pH range of 9.0-10.0 (Daliry et al., 2017). On the other hand, Wang et al. (2010) found that the optimum growth of *C. vulgaris* occurred at a pH ranging between 6.5-7.0.

Light Intensity and Illumination Period

Light is a vital parameter since it is the source of photons that initiate photosynthesis. Light intensity dictates the cellular activity performed by the microalgae (Daliry et al., 2017). For instance, microalgae enriched under limited light intensity tend to convert carbon into amino acids, while cultures enriched with saturated light intensities tend to utilize the carbon to produce sugars, such as starch (Daliry et al., 2017). Moreover, the optimum light intensity varies with different strains of microalgae and depends on the culture age (Khalili et al., 2015). The optimum light intensity for *C. vulgaris* was found to be 50-200 μmol/m^2·s (Daliry et al., 2017). Since different reactions and metabolism modes occur in the presence and absence of light, the period of illumination is an important factor to consider while operating a microalgae culture. Cell growth is the highest during light periods, while cell division occurs during the dark period. Therefore, cell division, cell growth, chlorophyll production, and lipid and carbohydrate contents as well as nutrient removal are affected by illumination periods (Daliry et al., 2017). The optimum growth rate of *C. vulgaris* was found at an illumination period of 24:0 hr (light: dark) (Deniz, 2020). Nevertheless, some studies were performed at an illumination period of 16:8 hr and 12:12 hr (light: dark) to increase the lipid content (Daliry et al., 2017).

Cultivation Systems

Different methods of cultivating the microalgae have been utilized such as open pond or closed photobioreactor (PBR) systems (Singh and Ahluwalia, 2012). Open ponds come in various shapes and are usually concrete or compacted soil systems. Open pond systems are ideal for large-scale biomass production since they are cheap to construct (Safi et al., 2014). Open ponds include natural water bodies, such as lakes, lagoons, and ponds, as well as wastewater or artificial ponds. To increase the sunlight exposure, the optimal depth of such ponds is usually 15-50 cm and medium stirring is required (Brennan and Owende, 2010). These ponds have some disadvantages that include environmental control to prevent contamination, water loss by evaporation and growth of undesired bacterial strains (Safi et al., 2014; Zuccaro et al., 2019). Temperature changes caused by seasonal change as well as changes in CO_2 concentration pose challenges to manage those ponds. However, mutual beneficial interactions between the microbial communities and the microalgae culture may arise. These symbiotic relations may improve the nutrient removal efficiencies and microalgal growth (Kumar et al., 2015; Ryu et al., 2014).

Closed PBRs were developed to provide a controlled environment where parameters that were difficult to control in open ponds, especially temperature, CO_2 concentration and light exposure are managed. This technique is more suitable for the growth of sensitive strains that are not able to compete and flourish in harsh conditions (Safi et al., 2014). The microalgae are fed with CO_2 through tubes, and fluorescent lights are used in case there is insufficient sunlight exposure. There are different configurations of PBRs that include flat-plate, tubular, and column PBRs (Qiang and Richmond, 1996; Zhang et al., 2001; Molina Grima et al., 2003; Kojima and Zhang, 1999). The typical diameter of these reactors is usually 20 cm or less, while the thickness is a few millimeters to allow enough light absorption (Chisti, 2007). On the other hand, such systems are costly to construct, possess limited illumination area and have sterilizing costs (Lee, 2001). In addition, biofilm formation, a disadvantage for such systems, causes a decrease in the photosynthetic

ability of the microalgae culture by preventing light penetration (Zuccaro et al., 2019).

Aeration

Aeration is another physical parameter that provides the microalgae with the required CO_2 for photosynthesis. However, aeration also helps with mixing, hence preventing precipitation of the microalgae in some microalgal systems. This allows for a homogeneous culture which in turn improves light penetration (Daliry et al., 2017). Thus, the type of microalgal system affects the optimum aeration rate to be provided (Daliry et al., 2017). In bubble column PBRs, Anjos et al. (2013) found that the optimum CO_2 concentration and flowrate for CO_2 biofixation of *C. vulgaris* were 6.5% and 0.4 vvm (0.044 L/L·min), respectively.

Nutrient Source

NH_4^+ and NO_3^- are both used as inorganic sources of nitrogen by the microalgae. But NH_4^+ is the preferred source of nitrogen since its uptake requires less energy compared to NO_3^- (Liu et al., 2016a). Moreover, the assimilated NO_3^- is later converted to NH_4^+ via nitrate reductase (NiR) (Fernandez and Galvan, 2008; Guerrero et al., 1981).

Regarding phosphorus, its assimilation takes place simultaneously along with the uptake of nitrogen via photosynthesis and respiration (Molinuevo-salces et al., 2019). The preferred phosphorus species are $H_2PO_4^-$, HPO_4^{2-}, and PO_4^{3-} (Solovchenko et al., 2020). Moreover, organic phosphorus species are assimilated (Singh et al., 2018). The charge and pH of the cell membrane determine the affinity for different inorganic phosphate species (Singh et al., 2018).

Since nitrogen and phosphorus are simultaneously assimilated, the nitrogen to phosphorus (N:P) ratio is an important parameter to be assessed. The optimum range of the N:P ratio for *C. Vulgaris* was found to be between 5-15 (g N: g P). Nevertheless, the optimum ratio may vary depending on the intended application of

the microalgae culture in terms of biomass productivity, lipid and protein content (Aslan and Kapdan, 2006; Choi and Lee, 2015; Anbalagan et al., 2016).

The nitrogen loading rate (NLR) is an essential parameter since they affect the quality of the microalgae culture in terms of the nutrient and organic removal efficiencies. Danesh et al. (2020) applied NLRs of 10, 20, 32.5, 42 and 63 mg N/L·day to mixed microalgae culture. The nitrogen was fully removed at all loading rates except 63 mg N/L·day, where the removal efficiency reached only 68%. Moreover, it was found that the *C. sorokiniana* and *C. vulgaris* were the dominant species at NLRs of 32.5 and 42 mg N/L·day, and the highest lipid and starch content was observed at 42 mg N/L·day.

The phosphorus loading rate (PLR) is another essential parameter that affects chlorophyll, carotenoid, and lipid content (Şentürk and Yıldız, 2020). According to Şentürk and Yıldız (2020), increasing the PLR from 5 to 20 mg/L·day of *C. vulgaris* culture, improved chlorophyll, carotenoid, and lipid content, yet the phosphorus removal efficiency decreased gradually. Whereas Lovio-Fragoso et al. (2019) found that for a culture of *C. muelleri* a PLR of 4.5 mg/L·day led to a higher cell number, while a PLR of 2.25 mg/L·day led to a higher dry cell weight concentration and chlorophyll-a content.

Carbon Source

During autotrophic metabolism, *C. vulgaris* utilize gaseous CO_2 but prefers its soluble forms HCO_3^- and CO_3^{2-} as sources of inorganic carbon (Carvalho et al., 2006; Znad et al., 2012;). Since the atmospheric CO_2 concentration of about 0.04% may not be sufficient for optimum microalgal growth, increased CO_2 concentration can be supplied, such as flue gas (Larsdotter, 2006; Singh and Singh, 2014). However, high CO_2 concentrations lead to a decrease in pH levels causing chemical precipitation of CO_3^{2-}, OH^-, and PO_4^{3-}, which in turn may cause cell damage (Carvalho et al., 2006). Therefore, pH regulation is required.

During heterotrophic and mixotrophic metabolism, organic carbon sources are

utilized such as glucose, starch, sucrose, acetate, and glycerol. Glucose provides the maximum specific growth rate since it is readily utilized by *C. vulgaris* (Liang et al., 2009). Moreover, supplementing the microalgae with organic carbon may increase the biosynthesis of lipids and carbohydrates but at the same time decrease the biosynthesis of photosynthetic proteins and pigments (Kong et al., 2011). However, increased cell growth and cell density can also be observed in mixotrophic and heterotrophic cultures (Chinnasamy et al., 2009; Bashir et al., 2019).

Organic loading rate (OLR) is also an important parameter that affects the enrichment and growth of microalgae. Kamyab et al. (2014) applied different OLRs of 36, 48, 72 and 96 g COD/L·day to a culture of *C. pyrenoidosa*. The results showed an increase in biomass productivity and specific growth rate meanwhile a decrease in lipid productivity was also observed.

Solid Retention Time and Hydraulic Retention Time

The SRT directly affects the light penetration which in turn influences the nutrient removal efficiencies. Longer SRT will increase the chance of biofilm formation and hence decrease the light penetration, especially in PBR systems (Xu et al., 2014).

On the other hand, HRT affects the nutrient loading rate and hence affects the biomass activity. This is because of the HRT effect on the microalgae biomass concentration, in turn affecting the light penetration (Cromar and Fallowfield, 1997; Garcia et al., 2000). In addition, the HRT should not exceed the time necessary to sustain the microalgae growth rate (Molina Grima et al., 1996; Larsdotter, 2006). According to ample studies conducted, it can be concluded that the optimum HRT ranges between 2-8 days (Larsdotter, 2006; Muñoz and Guieysse, 2006; Posadas et al., 2014). Hence controlling SRT, HRT and SRT/HRT ratio is critical in boosting microalgal productivity as well as nutrient removal (Xu et al., 2014).

2.7.5 Applications of Microalgae

Wastewater Treatment Applications

Since microalgal systems have low operational cost, less sludge formation, low energy requirements, mitigate GHG emissions and can be harvested for value-added products, they are considered as advantageous over some conventional wastewater treatment systems (Cai et al., 2013). Moreover, microalgae can remove carbon, nitrogen, and phosphorus and accumulating heavy metals simultaneously (Rawat et al., 2011; Abdel-Raouf et al., 2012; Cai et al., 2013). Therefore, integration of microalgal systems as a tertiary or quaternary treatment have been employed (Abdel-Raouf et al., 2012). Microalgae systems have been employed in the treatment of different wastewater types, such as domestic, slaughterhouse, swine manure, chicken manure, pharmaceutical, landfill leachate, olive mill, agro-industry and wastewater from mines (González et al., 1997; De Godos et al., 2009; Molinuevo-salces et al., 2010; Riaño et al., 2011; Abdel-Raouf et al., 2012; Cai et al., 2013; Escapa et al., 2015; Hernañdez et al., 2016; Di Caprio et al., 2018; Ülgüdür et al., 2019; Khanzada, 2020; Al-Jabri et al., 2021; Han et al., 2021).

Commercial Applications

Due to its protein content, which is about 55% of its dry weight, *C. vulgaris* is studied for the possibility of its utilization as an unconventional food source (Safi et al., 2014). Japan became the world leader in utilizing *C. vulgaris* for medical treatment since it was found to contain immune-modulating and anti-cancer characteristics. In addition, consuming it can stimulate collagen synthesis for skin rejuvenation (Safi et al., 2014). Pigments such as phycobiliproteins, carotenoids and chlorophylls found in microalgae have ample health benefits and can be utilized as a substitute for commercial colorants (Rodrigues et al., 2015).

In recent years due to the climate change issue, research has been focused on CO_2 mitigation. *C. vulgaris* provides a sustainable option to reduce atmospheric CO_2

concentrations since it is easily cultured. Furthermore, since it is capable of accumulating lipids, *C. vulgaris* is appropriate for biodiesel production. Many studies have targeted to assess the potential of *C. vulgaris* growth and harvesting for biofuel purposes. The extracted oil from microalgae can be a source of different nutrient supplements, emulsifiers, and biofuels (Sharma et al., 2018). Different processes are performed to attain biodiesel, bioethanol, and biogas. Transesterification of lipids is performed to synthesize biodiesel, while fermentation of the microalgae produces bioethanol. On the other hand, anaerobic digestion is conducted to obtain biogas from microalgae (Molina Grima et al., 2003; Pragya et al., 2013). In addition, the fact that microalgae can grow using low quality water, removing the pollutants and sequestering CO_2 provided a cost and energy efficient alternative for the conventional methods previously employed (Chisti, 2007; Frank et al., 2013; Barreiro et al., 2013; Bennion et al., 2015).

2.7.6 Conclusion

Microalgae are fast-growing microorganisms capable of achieving nutrient and carbon removal, concurrently mitigating GHG emissions. Moreover, microalgae systems have relatively low operation and maintenance costs and short start-up time compared to conventional wastewater treatment processes. Microalgal systems can be utilized in the treatment of various wastewater types. Depending on the type of wastewater, intended treatment and application objective, different metabolism modes can be employed in the growth of microalgae. Parameters such as temperature, pH, light intensity, illumination period, HRT, NLR, PLR and OLR may affect the enrichment and growth of microalgae. *C. Vulgaris*, compared to other microalgae species, are more robust and resistant to varying environmental factors, able to accumulate high lipid content. In addition, microalgae harvesting can yield various value-added products in many different forms, such as, biofuel, vitamins, proteins, and drugs, which provide a positive economic perspective to the utilization of microalgae.

CHAPTER 3

ENRICHMENT OF THE DAMO-ANAMMOX CO-CULTURE AND ASSESSING THE EFFECT OF VARIOUS PARAMETERS ON THE CO-CULTURE

3.1 Introduction

The application of the DAMO process for wastewater treatment seems to be auspicious, particularly when integrating it with the Anammox process (Wang et al., 2017a; Wang et al., 2017b; van Kessel et al., 2018). Important parameters that should be taken into consideration for the enrichment of a DAMO-Anammox co-culture include temperature (30-35 °C), pH (7.0-7.6), DO concentration, source of inocula, reactor configuration, nitrogen source and their corresponding molar ratios, trace metals concentration, HRT and NLR, and NH_4^+:CH_4 molar ratio (Harb et al., 2021).

Due to the slow growth of DAMO and Anammox microorganisms, the HRT applied during the enrichment should be enough to allow the activity of those microorganisms and prevent biomass washout. Depending on the reactor configuration the HRT may be reduced, but this in turn would increase the NLR, which can play a role in changing the population dynamics of the reactor. Studies performed on nitrogen and methane removal employing DAMO-Anammox co-cultures applied various HRTs ranging from 1-8 days depending on the reactor configuration used (Shi et al., 2013; Hu et al., 2014; Cai et al., 2015; Xie et al., 2016; Ding et al., 2017; Fu et al., 2017b;). For instance, Hu et al. (2014) employed a SBR and applied an HRT of 6 days. While Xie et al. (2016) demonstrated the effect of a gradual decrease in HRT from 8 days to 1 day on a previously enriched DAMO-Anammox MBR and the results suggest that a complete nitrogen removal rate of 1300 mg N/L·day was achieved without NO_3^- accumulation, which was comparable to practical rates reported for side-stream nitrogen removal processes. Moreover,

Kampman et al. (2014) claimed that lowering the HRT from 61 to 1.4 days while maintaining the NO_2^- loading rate, increased the NO_2^-consumption rate from 8 to 31 mg N/L in an MBR. Moreover, it is claimed that lower HRT aids in the wash out of inhibitory by-products that might have accumulated in longer HRT conditions. Meanwhile, the highest NO_2^- removal rate of 985.6 mg N/L·day was observed by reducing HRT from 4.2 to 2.1 hours in continuous biofilm reactors (Hatamoto et al., 2014). As seen in these studies, a wide range of HRTs applied in various reactor configurations may have different effects, which remains to be researched for removal efficiencies.

As well as HRT and, in turn, the NLR parameters, molar ratios of nitrogen species have a vital effect on the microbial population dynamics and, thus, nitrogen removal efficiencies. The molar ratio of NO_2^- : NH_4^+ ranging between 1.17-1.55 was tested by Xie et al. (2018) and a high TN removal range of 91.7–94.7% was achieved. While Chen et al. (2014) modelled a microbial composition of Anammox, DAMOa and DAMOb of 65%, 23% and 12%, respectively, and obtained the highest TN removal at a NO_2^-: NH_4^+ ratio of 1. Nevertheless, further increase in the molar ratio suggested the elimination of DAMOa due to the CH_4 competition with DAMOb, consequently, causing a decline in TN removal.

Ample DAMO enrichment studies reported various CH_4:NO_2^- molar consumption ratio. For instance, Kampman et al. (2012) reported a CH_4:NO_2^- ratio of 0.38, while He et al. (2014) reported a CH_4:NO_2^- ratio of 0.34, 0.35 and 0.39. These ratios are attributed to DAMOb since the theoretical CH_4:NO_2^- molar ratio is 0.38 (Equation 2.5 in Section 2.4.2). However, the effect of the NH_4^+:CH_4 ratio was not tested so far on a DAMO-Anammox co-culture. In a DAMO-Anammox co-culture, NH_4^+ and CH4 are the electron donors supporting the Anammox and DAMO activities, respectively. In addition, dissolved CH_4 and its bioavailability is critical for the enrichment and growth of DAMO microorganisms. Therefore, the solubility of CH_4 is the limiting factor that determines the NH_4^+:CH_4 ratios to be applied, due to its maximum saturation and dissolution constants. Theoretically, the NH_4^+:CH_4 molar

consumption ratio would indicate the dominant species in the co-culture since. Therefore, finding the optimal ratio in terms of removal efficiency is vital.

In this chapter, a DAMO-Anammox co-culture was aimed to be enriched in an SBR and the effect of HRT and NLR changes were to be evaluated, meanwhile the effect of Fe^{2+} and Cu^{2+} concentrations was also investigated. In addition, the effect of various NH_4^+:CH_4 ratios on the enriched co-culture was assessed in order to determine the shift in dynamics in terms of which of the target microorganisms would dominate the co-culture.

3.2 Materials and Methods

The first step of enriching the DAMO-Anammox co-culture was the enrichment of the Anammox bacteria. The co-culture was planned to be enriched using Anammox bacteria as the seed along with other inocula that may have the potential to contain DAMO microorganisms. Using Anammox as the base of co-culture enrichment reduces the enrichment period since the Anammox provides nitrate for the DAMO archaea (shown in Equation 2.4 and 2.5, in Section 2.3.2 and Section 2.4.2, respectively) (Zhu et al., 2012). Therefore, an Anammox SBR was established to enrich the Anammox bacteria, and it was operated throughout the duration of the research, this ensured the availability of Anammox seed at any point for seeding. After operating the Anammox SBR for about a year, the DAMO-Anammox SBR was established to enrich the co-culture and operated for 202 cycles (780 days). Section 3.3.2 discusses the results of the DAMO-Anammox enrichment.

The effect of Fe^{2+} and Cu^{2+} concentrations and HRT and NLR were examined through the operation of the DAMO-Anammox SBR by monitoring the reactor performance using the various analytical and molecular methods specifically during the phases that involve the changes applied. On the other hand, the experiments evaluating the effect of the NH_4^+/CH_4 ratio were performed in batch reactors operated for 6 days, hence, the short-term effect of the NH_4^+/CH_4 ratio are covered in this chapter.

3.2.1 Reactor Setup and Operational Conditions

3.2.1.1 Anammox SBR

An air-tight stainless-steel SBR was used to enrich the Anammox bacteria. The total reactor volume was 2.4 L while the effective volume was 2.1 L, leaving a headspace of 0.3 L, shown in Figure 3.1. The reactor was operated in a 24-hour cycle as follows, reaction period of 22.5 hours and settling of 1.5 hours, while feeding and decanting were performed manually and lasted for few minutes each. The exchange volume was 1 L making an HRT of 2.1 days (Zekker et al. 2019; 2021).

Figure 3.1 Anammox SBR

The inoculum used was a mixture of Anammox granular seed (1 L) obtained from Marmara University Environmental Engineering Department (Figure 3.2) and BNR recycling activated sludge (RAS) from Istanbul Paşaköy Advanced Biological WWTP (0.6 L). The Anammox granular seed sludge used had been enriched within the scope of TÜBİTAK 108Y120 project (Kocamemi et al., 2018). The enrichment of this culture started in 2008 using activated sludge obtained from Istanbul Paşaköy Advanced Biological WWTP; meanwhile the Anammox bacteria were kept active through regular feeding.

The Anammox granular seed contained a total suspended solids (TSS) of 1.4 g/L and volatile suspended solids (VSS) of 1.3 g/L making a 91% of VSS/TSS percentage, while the RAS contained a TSS and VSS of 25.5 g/L and 19.3 g/L, respectively, yielding a VSS/TSS percentage of 76%. Before the startup of the reactor, the mixed seed sludge contained a TSS and VSS of 9.7 g/L and 7.3 g/L, respectively, leading to a VSS/TSS percentage of 76%.

Figure 3.2 Anammox granular sludge in the Anammox SBR

The reactor was operated under the following conditions, pH in the range of 7-7.5, temperature of 35°C, DO was kept close to 0 mg/L by purging the reactor with an Ar/CO_2 mixture (95%:5%) for about 10-15 min every cycle (Chamchoi and Nitisoravut, 2007). While the mixing was performed using an orbital shaker at 120 rpm.

The feed consists of the constituents and related concentrations according to Dapena-Mora et al. (2007) and Guerrero et al. (2013), as shown in Table 3.1. During the startup period of the Anammox reactor, NH_4^+, NO_2^- and NO_3^- were added to the medium to reach concentrations of 15, 22.5, 20 mg N/L, respectively, in the reactor at the beginning of each cycle's reaction period (t=0). These concentrations were chosen since the Anammox seed used had been previously acclimated at those concentrations and the ratio of NH_4^+: NO_2^- should be 1:1.5 (Chamchoi and Nitisoravut, 2007). NO_3^- was added at the beginning of the enrichment period (first 77 days) in order to provide the denitrifiers that may be present in the sludge with a

nitrogen source other than NO_2^- that should be consumed by the Anammox. Samples were taken and analyzed, accordingly the removal efficiencies, removal rates and consumption ratios were calculated, to assess the performance of the system in comparison to the expected theoretical ratios of Anammox. Furthermore, any biomass removed from the reactor after decanting or during sampling was placed back into the reactor manually, reducing any sludge loss and maximizing the solid retention time (SRT).

The enrichment process proceeded until steady-state conditions were reached. In order to maintain steady-state conditions, NH_4^+ and NO_2^- analyses were performed at the end of each cycle and according to their consumption, the required amount was added to the feed to maintain the target initial concentrations of 15 mg N/L of NH_4^+ and 22.5 mg N/L of NO_2^-. Nitrate was not added in the feed after the first 77 days of operation, but it was monitored to check the ratio of the ions to track the Anammox activity. Maintaining an Anammox SBR for seeding would be helpful for the enrichment of the DAMO-Anammox co-culture activity. Thus, Anammox SBR was operated for about 200 days. Because the main focus of this thesis study is to enrich a DAMO-Anammox co-culture, the results of the Anammox SBR was summarized the Results and Discussion Section (Section 3.3.1) Yet the detailed results of the Anammox SBR are shown in APPENDIX A.

Table 3.1 Anammox feed constituents and concentrations (Dapena-Mora et al., 2007; Guerrero et al., 2013)

Compound	Concentration (g/L)
NH_4Cl	0.1314
$NaNO_2$	0.2543
KNO_3	0.1444
KH_2PO_4	0.0272
$MgSO_4.7H_2O$	0.3
$CaCl_2.2H_2O$	0.18
$KHCO_3$	0.75
Mineral Solution 1 (1 mL/L)	
$C_{10}H_{14}N_2Na_2O_8 \cdot 2H_2O$	15
$ZnSO_4.7H_2O$	0.43
$CoCl_2$	0.12
$MnCl_2 \cdot 4H_2O$	0.99
$CuSO_4.5H_2O$	0.25
$NaMoO_4.2H_2O$	0.22
$NiCl_2.6H_2O$	0.19
Na_2SeO_3	0.1
H_3BO_3	0.011
Mineral Solution 2 (1 mL/L)	
$C_{10}H_{14}N_2Na_2O_8 \cdot 2H_2O$	5
$FeSO_4.7H_2O$	5

3.2.1.2 DAMO-Anammox SBR

The enrichment of the DAMO-Anammox co-culture was conducted in an air-tight stainless-steel SBR (Figure 3.3). The SBR has a total volume of 3.3 L, effective volume of 2.6 L making a headspace of 0.7 L. The exchange volume ratio is 0.5 corresponding to an exchange volume of 1.3 L.

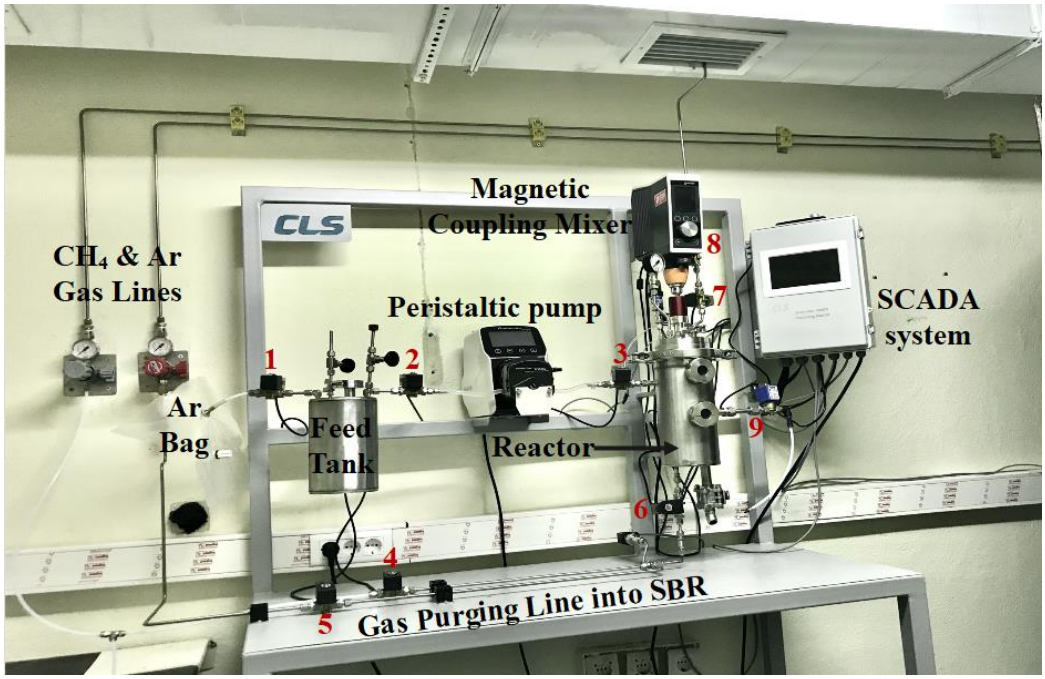

Figure 3.3 DAMO-Anammox SBR

The DAMO-Anammox SBR was controlled using an automated SCADA system, to ensure full control and safe operation of the system. The screen is shown in Figure 3.4. The electrical solenoid gas and liquid valves can be seen numbered in Figure 3.3 and their corresponding locations in Figure 3.4 were controlled by the pre-programmed SCADA system according to the cycle period and the safety features designed to prevent any leakage of CH_4 out of the reactor and any entry of air into the reactor. Ar and CH_4 were purged from the bottom of the reactor using a digital pressure gauge, electric solenoid gas valves and a check valve (non-return valve) to

ensure the pressure in the gas line was higher than in the reactor at the time of purging and to prevent any liquid from flowing into the gas lines.

The CH_4 tank was located outside the hot room in a cabinet equipped with a CH_4 sensor and a suction ventilation system. Moreover, a methane sensor was also installed in the hot room next to the reactor. These sensors were setup according to the low explosion limit (LEL) and upper explosion limit (UEL) for methane which are 5% and 15%, respectively, with respect to air. The safety limit for methane set in the SCADA system was 0.2%. Above 0.2%, the system including all electric solenoid valves would stop and a warning SMS would be sent to all the laboratory staff. If a methane percentage of 0.8% was to be detected, the electricity in the hot room would be shut down, keeping only the ventilation systems working to aerate the room.

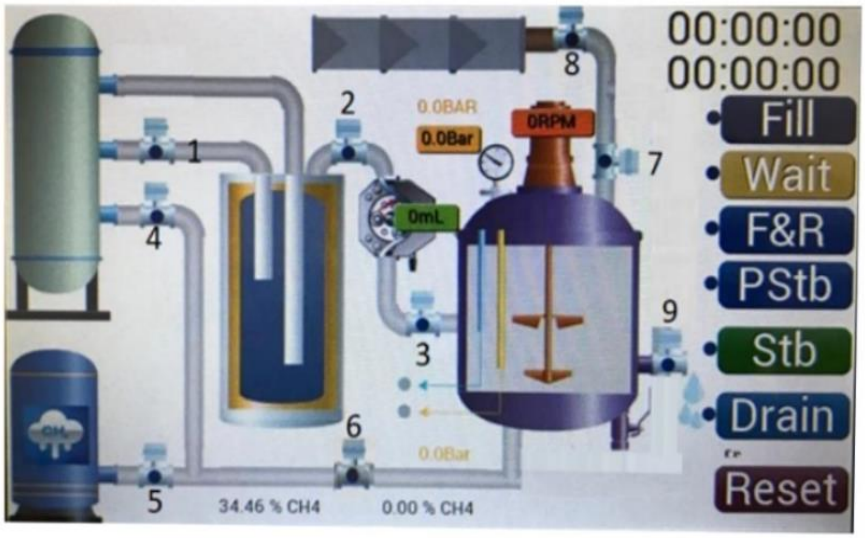

Figure 3.4 The initial screen of the SCADA system

The reactor was operated initially in a 72 hr cycle, in the following order feeding and reaction, settling and decanting periods of 70.5 hr, 1 hr, and 0.5 hr, respectively. This ensures an HRT of 6 days (Luesken et al., 2011b; He et al., 2014; He et al., 2015). In order to prevent any biomass loss due to washout, any sludge removed after decanting or sampling was placed back into the reactor manually, in turn maximizing

the SRT. The operation temperature and pH were 35°C and 7-7.5, respectively; mixing was applied at 150 rpm. DO was maintained close to 0 mg/L by purging the reactor with an Ar/CO_2 mixture (95%:5%) for about 3-5 min every cycle. The synthetic wastewater was purged with the Ar/CO_2 mixture for 10-15 min and its pH was adjusted to about 7.5, before being fed into the reactor. Then the reactor was purged a few times with a mixture of CH_4: CO_2 at 95%:5% to flush the Ar out and the pressure of the headspace was stabilized at 1.5 atm (absolute pressure) at the beginning of each cycle (Ettwig et al., 2009; Zhu et al., 2012; He et al., 2014, He et al., 2015a; Zhao et al., 2017). The methane was kept in excess compared to the NO_2^- and NO_3^- provided.

The DAMO-Anammox SBR was seeded with the previously enriched Anammox (0.6 L), Anaerobic Digester (AD) sludge from the return line from ASKI Ankara Central WWTP in Tatlar village, Sincan, Ankara (1 L) and freshwater sediment from Eymir Lake, Ankara (1 L). The pH of the AD sludge was recorded as 7.44. Eymir Lake is a very eutrophic lake close to the center of Ankara. The sediment samples of Eymir Lake were collected from three different locations of the lake, as shown in Figure 3.5, at a depth of 30 cm at shallow and still regions (Laçin, 2021). The corresponding coordinates of Location 1, Location 2 and Location 3 were 39°48'51.16" N 32°49'14.76" E; 39°49'4.53" N 32°49'13.88" E; and 39°49'19.70" N 32°49'46.90" E, respectively. The pH of each location was recorded as 7.33, 7.36 and 7.95, respectively, in addition, the sediment samples were passed through a 1 mm sieve to obtain a homogeneous mixture. In order to prevent contact with air during sampling and transportation, the sludge and sediment samples were packed in sealed bottles without headspace gas. The samples were stored at 4°C in anaerobic conditions. Some of the samples were stored at -20°C for use in molecular analysis.

Figure 3.5 Eymir Lake freshwater sediment sampling locations (Laçin, 2021)

The seed sludge mixture was thoroughly washed with a feed solution lacking any nitrogen source in order to remove or decrease the concentration of any existing nitrogen source and COD present in the sludge. This was done to reduce the activity of denitrifiers that require COD and nitrite or nitrate. Among the three sludges, the lake sediment contained the highest TSS with 248±8 g/L and a VSS of 18.2±2.4 g/L leading to the lowest VSS/TSS percentage of 7%. The AD sludge comprised of 20.3±0.2 g/L TSS and 9.6±0.2 g/L VSS making a VSS/TSS percentage of 47%, while the Anammox sludge contained a TSS and VSS of 2.9±0.3 g/L and 2.3±0.3 g/L, respectively, leading to the highest VSS/TSS percentage of 80%. Moreover, the mixed initial seed sludge contained a TSS and VSS of 271±10 g/L and 11.2±0.8 g/L making a VSS/TSS percentage of 4%. The seed sludges are shown in Figure 3.6.

Figure 3.6 Different sludge used to inoculate the reactor. (a) Anammox sludge from the Anammox reactor (b) AD sludge (c) Sediment from Eymir Lake

The DAMO-Anammox SBR was operated in five main phases as described in Table 3.2 where the change in the operational conditions performed in each phase is shown. Initially heterotrophic denitrification was expected to be the dominant reaction taking place in the reactor due to the potential sCOD content, thus, the NO_3^- consumption in the initial 25 cycles can be attributed to heterotrophic denitrification. This period was not considered as a phase of operation of the DAMO-Anammox SBR, rather defined as heterotrophic denitrification period. The initial concentrations of NO_2^-, NO_3^- and NH_4^+ during this period were 15 mg N/L, 15 mg N/L and 7 mg N/L, respectively (influent NH_4^+: NO_2^- molar ratio of 0.47) (Ettwig et al., 2009; Luesken et al., 2011; Cai et al., 2015). The end of this period marks the beginning of Phase I (Cycle 26-78) where the same initial concentrations as the heterotrophic denitrification period were applied. Limited NH_4^+ was supplied to limit the Anammox activity in order to support the enrichment of the DAMO microorganisms. The initial concentrations of NO_2^-, NO_3^- and NH_4^+ were chosen to be 15 mg N/L, 15 mg N/L and 7 mg N/L since theoretically Anammox will consume NO_2^- at about 1.5 times the concentration of NH_4^+ (shown in Equation 2.4, in Section 2.3.2), that is 10.5 mg N/L, so the remaining NO_2^- (4.5 mg N/L) will be available for DAMOb, as shown in Equation 2.6 in Section 2.4.2. Moreover, the DAMOa will consume NO_3^-

to produce NO_2^-, as illustrated in Equation 2.5 in Section 2.4.2, and that will also be available for the DAMOb.

In Phase II, the concentration of NO_2^- was increased to 25 mg N/L at Cycle 79, achieving an influent NH_4^+: NO_2^- molar ratio of 0.28, while the concentration of NO_3^- was increased to 25 mg N/L at Cycle 85. In Phase III, the NH_4^+ concentration was increased to 12 mg N/L at Cycle 115, achieving an influent NH_4^+: NO_2^- molar ratio similar to the startup of the reactor of 0.48. The increments in the concentration were conducted after analyzing the results of the specific activity tests. After observing a decrease in DAMO microorganisms' activity from Cycle 115 to 120, an increase in the concentrations of Fe^{2+} and Cu^{2+} was decided during Phase III. This was due to the fact that at Fe^{2+} concentrations more than that of the unmodified feed used by Ettwig et al. (2009), microbial activity was found to be higher (Lu et al., 2018). Therefore, at Cycle 120, the initial Fe^{2+} and Cu^{2+} concentrations were increased from 3.75 to 50 μM and 0.5 to 10 μM, respectively. The required amount of NH_4^+ (as NH_4Cl), NO_2^- (as $NaNO_2$) and NO_3^- (as KNO_3) to be added in the feed was calculated according to the analyses performed at the end of each cycle to maintain the target initial concentrations of each of the nitrogen species. The synthetic feed's micro and macro nutrient content required for the DAMO-Anammox co-culture enrichment are presented in Table 3.3.

As seen in Table 3.2, after Cycle 160 of Phase III, all influent concentrations and nitrogen molar ratios were kept the same, except the HRT. In order to investigate the effect of HRT on the DAMO-Anammox co-culture, the HRT of 6 days applied at the beginning of the study, was decreased to 4 days in Phase IV (Cycle 161-188). Due to the performances that are discussed in the Results and Discussion section (Section 3.3.2), the HRT was increased back to 6 days by Cycle 189 in Phase V.

Table 3.2 Phase changes of the DAMO-Anammox SBR with respect to the operational conditions

Phase	Cycle No.	NH_4^+ (mg N/L)	NO_2^- (mg N/L)	NO_3^- (mg N/L)	Fe^{2+} (μM)	Cu^{2+} (μM)	HRT (days)	Influent Molar Ratio		
								NH_4^+/ NO_2^-	NH_4^+/NO_3^-	NO_2^-/ NO_3^-
Heterotrophic Denitrification	1-25	7	15	15	3.75	0.5	6	0.47	0.47	1
I	26-78	7	15	15	3.75	0.5	6	0.47	0.47	1
II	79-114	7	25	25*	3.75	0.5	6	0.28	0.28	1
III	115-160	12	25	25	50	10	6	0.48	0.48	1
IV	161-188	12	25	25	50	10	4	0.48	0.48	1
V	189-205	12	25	25	50	10	6	0.48	0.48	1

* The increase in NO3- concentration from 15 to 25 mg N/L occurred at Cycle 85

Table 3.3 DAMO-Anammox feed (Ettwig et al., 2009; Luesken et al., 2011b)

Compound	Concentration (g/L)[a]
NH_4Cl	0.0535/0.0917[b]
$NaNO_2$	0.1479/0.2464[b]
KNO_3	0.2167/0.3611[b]
$KHCO_3$	0.5
KH_2PO_4	0.05
$CaCl_2 \cdot 2H_2O$	0.3
$MgSO_4 \cdot 7H_2O$	0.2
Acidic Trace Elements 0.5 mL/L (100 mM HCl)	
$FeSO_4 \cdot 7H_2O$	2.085/55.602[c]
$ZnSO_4 \cdot 7H_2O$	0.068
$CoCl_2 \cdot 6H_2O$	0.12
$MnCl_2 \cdot 4H_2O$	0.5
$CuSO_4$	0.32/6.384[c]
$NiCl_2 \cdot 6H_2O$	0.095
H_3BO_3	0.014
Alkali Trace Elements 0.2 mL/L (10 mM NaOH)	
SeO_2	0.067
$Na_2WO_4 \cdot 2H_2O$	0.05
Na_2MoO_4	0.242

[a] The dilution factor of the feed to the initial reactor concentrations is 2

[b] The incremental increases in N species with respect to the Phases

[c] Modified DAMO-Anammox feed according to Lu et al. (2018)

Specific Activity Tests

The batch specific activity tests were conducted to assess the activity of each of the microorganism groups that were targeted to be enriched (Anammox, DAMOa and DAMOb). Batch reactors containing sludge from the DAMO-Anammox SBR withdrawn at Cycle 75 for Phase I, at Cycle 105 for Phase II and at Cycle 145 for

Phase III were provided with synthetic feed specific for each microorganism group. Five test reactor types and two control reactor types were set up. The test reactors were operated in triplicates, divided into the following categories: DAMOb, DAMOa, Anammox (AMX), DAMO-Anammox (DAMX) and denitrifiers (DEN) (Table 3.4). Each reactor type contained specific synthetic feed that supports the target microorganism category. The control reactors contained sludge and nitrogen-free synthetic feed, one of the controls was provided with methane while the other was not.

Table 3.4 Different reactor types operated for the specific activity test

Reactor type	Synthetic Feed	Intended Activity
DAMX	NH_4^+, NO_2^-, NO_3^-, CH_4	DAMO-Anammox co-culture Mimicking main reactor
AMX	NH_4^+, NO_2^-, NO_3^-	Anammox bacteria
DAMOb	NO_2^-, CH_4	DAMO bacteria
DAMOa	NO_3^-, CH_4	DAMO archaea
DEN	NO_2^-, NO_3^-	Denitrifiers
Control 1	Nitrogen-free, purged with Ar	Negative control
Control 2	Nitrogen-free, purged with CH_4	Negative methane control

Each reactor has a total volume of 56 mL, and the operated effective volume was 35 mL, making a headspace volume of 21 mL (Figure 3.7). Each reactor contained 15 mL of DAMO-Anammox SBR sludge that was previously washed multiple times with nitrogen-free synthetic feed, to ensure that the concentrations of the nitrogen species in the sludge were approximately 0 mg N/L. According to the categories shown in Table 3.4, 20 mL of different synthetic feed, corresponding to the nitrogen species provided in Table 3.4 and the nutrient solution in Table 3.3 were added to each reactor. The initial nitrogen species concentrations reflected the values applied in the DAMO-Anammox SBR for the specific phase in which the activity tests were prepared (Table 3.5). The pH values of the sludge and feed were adjusted separately to 7.5 by purging with Ar and CO_2 before seeding the reactors.

Figure 3.7 The specific activity batch test setup

After seeding the reactors, the AMX, DEN and Control 1 reactor types were purged with 4 L/min of Ar and 0.05 L/min of CO_2 for 1 min. The reactors were tightly closed, and the headspace was purged for 1 min with Ar and pressurized. The DAMX, DAMOb, DAMOa and Control 2 reactor types were purged with 4 L/min of Ar for 4 min and then purged with 0.2 L/min of CH_4/CO_2 gas mixture for 1 min. The reactors were tightly closed, and the headspace was purged for 1 min with CH_4/CO_2 gas mixture and pressurized to achieve about 1.2 atm CH_4 partial pressure. By performing this procedure, DO was maintained as low as possible, pH was adjusted to around 7.5 and the headspace was pressurized with CH_4, the latter only for the related test and control reactors receiving CH_4, as shown in Table 3.4.

The reactors were operated for the duration of a cycle corresponding to 72 hours (3 days) under the operational conditions shown in Table 3.5. Liquid samples were taken at the start of the experiment and every 12 hours for 72 hours. They were filtered and analyzed for the different nitrogen species and TOC. Similarly, gas samples were taken at the same time intervals, but after each GC analysis, the headspace of the reactors was purged again for 1 min with the CH_4/CO_2 gas mixture to obtain a CH_4 partial pressure of about 1.14 atm.

Table 3.5 The conditions for the specific activity batch tests

Parameter	Condition
Incubation period (day)	3
Total Volume (mL)	56
Headspace (mL)	21
Effective Volume (mL)	35
Inoculum (mL)	15
Medium (mL)	20
Initial NH_4^+ (mg N/L)	7^{I} / 7^{II} / 12^{III}
Initial NO_2^- (mg N/L)	15^{I} / 25^{II} / 25^{III}
Initial NO_3^- (mg N/L)	15^{I} / 25^{II} / 25^{III}
Total pressure in the headspace (atm)	1.20
Methane partial pressure (atm)	1.14
pH	7.50
rpm	127

I: Phase I specific activity

II: Phase II specific activity

III: Phase III specific activity

Assessing of the Effect of Fe^{2+} and Cu^{2+} on the DAMO-Anammox Co-culture

As aforementioned, the Fe^{2+} and Cu^{2+} concentrations were increased at Cycle 120, the activity of the three target microorganisms in terms of the removal rates, removal efficiencies and population dynamics of Phase II (Cycles 79-114) and Phase III (Cycles 115-160) were compared to assess the effect of the increase in Fe^{2+} and Cu^{2+} concentrations. The initial Fe^{2+} and Cu^{2+} concentrations were increased from 3.75 to 50 μM and 0.5 to 10 μM, respectively. According to Lu et al. (2018), the optimum Fe^{2+} concentration for Anammox, DAMO archaea (DAMOa) and DAMO bacteria (DAMOb) was found to be 80 μM, 80 μM and 20 μM, respectively. Lu et al. (2018) also noted that increasing Fe^{2+} concentration over the optimum concentrations does

not negatively affect the DAMO-Anammox co-culture activity. On other hand, the optimum Cu^{2+} concentration for a DAMO bacteria culture was found to be 10μM (He et al., 2015a).

The only other parameter to change from Phase II to Phase III was the NH_4^+ concentration, which was increased from 7 to 12 mg N/L, at Cycle 115. Furthermore, the results of the batch specific activity tests performed in Phase II and Phase III were compared in terms of the activity of each of the target microorganisms to evaluate the effect of the Fe^{2+} and Cu^{2+} concentrations.

Assessing of the Effect of HRT and NLR on the DAMO-Anammox Co-culture

As mentioned previously, the effect of HRT and NLR was investigated by comparing Phase III, Phase IV, and Phase V. The HRT was 6 days in Phase III and decreased to 4 days at Phase IV, and then increased back to 6 days at Phase V. Changing the HRT in turn changed the NLR. The theoretical NLR was 20.7 mg N/L·day in Phase III, and it was increased to 30 mg N/L·day in Phase IV and then decreased back to 20.7 mg N/L·day in Phase V. The removal rates, removal efficiencies and population dynamics of the co-culture were assessed during this period to examine the effect of the HRT and NLR.

3.2.1.3 BATCH SET: Short-term Effect of NH_4^+/CH_4 Ratio on DAMO-Anammox Activity

The aim of this batch study was to investigate the effect of the NH_4^+/CH_4 ratio on the DAMO-Anammox co-culture. NH_4^+ and CH_4 are the two electron donors in a DAMO-Anammox co-culture activity. Therefore, the following ratios were chosen since they represent different activity states of the co-culture. The NH_4^+/CH_4 of 0 only favors the DAMO activity, while the NH_4^+/CH_4 of ¼ provides 4 times more CH_4 than NH_4^+, and the NH_4^+/CH_4 of 1 provides equal concentrations of CH_4 and NH_4^+.

10 batch reactors were set up, each with a total volume of 24 mL inoculated with 10 mL of sludge from the DAMO-Anammox SBR and 10 mL of feed, making a headspace volume of 4 mL. The sludge was withdrawn at Cycle 194 (Phase V) and was washed with nitrogen-free synthetic feed to ensure that the concentrations of the nitrogen species were zero prior to the start of the experiment. The reactors to be purged with CH_4 were purged for 5 mins taking into consideration the pH reduction of the sludge that might be caused by CH_4/CO_2 gas mixture. The nitrogen species, dissolved CH_4 and gaseous CH_4 concentrations were measured periodically. Each time the dissolved CH_4 was measured using the salting-out method (Daelman et al., 2012), the sludge was discarded since the procedure requires mixing the sludge with a salt solution to strip out the CH_4. Therefore, the test reactors decreased in number throughout the 6-day experiment.

The reactor types are shown in Table 3.6. Moreover, Table 3.7 represents the conditions applied during this experiment. All the reactors were supplied with NO_2^- and NO_3^- each at an initial concentration of 25 mg N/L. The control reactor was not supplied with CH_4, to assess the non-methanotrophic denitrification activity. Two test reactors, named N0, were not supplied with NH_4^+, forming an NH_4^+/CH_4 of 0. Three test reactors, labelled N2 supplied with an initial NH_4^+ concentration of about 2 mg N/L, creating an NH_4^+/CH_4 of ¼. While four other test reactors, labelled N8 were supplied with initial NH_4^+ concentration of about 8 mg N/L, forming an NH_4^+/CH_4 of 1. One of the reactors labelled N8 was used at the start to measure the initial dissolved CH_4 concentration and then discarded. Since only the NH_4^+ concentrations were changed in the test reactors to obtain different NH_4^+/CH_4 ratios, the T0 reactor (Table 3.6) reflected the initial CH_4 concentration in all the test reactors.

Table 3.6 Different reactor types operated for the NH_4^+/CH_4 ratio batch test

Reactor type	Number of Reactors	Synthetic Feed	Intended Activity
Control	1	NO_2^-, NO_3^-	Heterotrophic denitrification
N0	2	NO_2^-, NO_3^-, CH_4	DAMOb & DAMOa
N2	3	NH_4^+, NO_2^-, NO_3^-, CH_4	Anammox, DAMOb & DAMOa
N8	3	NH_4^+, NO_2^-, NO_3^-, CH_4	Anammox, DAMOb & DAMOa
T0	1	NH_4^+, NO_2^-, NO_3^-, CH_4	Intended to measure the initial dissolved CH_4 supplied in the test reactors

Table 3.7 The conditions for the NH_4^+/CH_4 ratio batch test

Parameter	Condition
Incubation period (day)	6
Total Volume (mL)	24
Headspace (mL)	4
Effective Volume (mL)	20
Inoculum (mL)	10
Medium (mL)	10
Initial NH_4^+ (mg N/L)	0^1 / 1.93^2 / 7.7^3
Initial NO_2^- (mg N/L)	25
Initial NO_3^- (mg N/L)	25
Initial Dissolved CH_4 (mmol/L)	0.55
pH	7.50
rpm	127

1: N0 reactors

2: N2 reactors

3: N8 reactors

3.2.2 Analytical Methods

The activity of the DAMO-Anammox SBR was assessed to evaluate the enrichment of the co-culture and the composition of the biomass in terms of the target species. This was performed through the assessment of the removal rates, removal efficiencies, removal molar ratios of the nitrogen species and total nitrogen removal in comparison to the theoretical values present in the literature. Furthermore, molecular analysis through Fluorescent In-situ Hybridization (FISH) and Next-Generation Sequencing (NGS) 16S Metagenome Analysis were performed to assess the change in the microbial consortium focusing on the DAMO and Anammox microorganisms.

3.2.2.1 Volumetric and Chromatographic Analyses

Anions such as NO_2^-, NO_3^- and SO_4^{2-} were analyzed using Ion Chromatography (IC) (IC -Shimadzu Prominence HIC-SP). The IC was operated under the following conditions, highest pressure limit of 150 bar, oven temperature of 45°C, and a flow rate of 0.8 mL/min. The analyses were performed in duplicates or triplicates, depending on the presence of enough sample volume. The calibration curves, the limit of detection (LOD) and the limit of quantification (LOQ) are shown in APPENDIX C.

Total Ammonium Nitrogen (TAN as NH_4^+-N + NH_3-N) was analyzed using the Hach Nessler Method (Hach, 2012). The analyses were performed in triplicates. The calibration curves, LOD and LOQ are illustrated in APPENDIX D.

Soluble chemical oxygen demand (sCOD) was evaluated using medium range kits and low range kits (Hach, 2012). The analyses were performed in duplicates or triplicates, depending on the presence of enough sample volume. The Total Organic Carbon (TOC) was analyzed using the TOC analyzer. The analyses were performed in triplicates. The calibration, LOD and LOQ of the sCOD and TOC tests are shown in APPENDIX E.

Total Solids (TS), Volatile Solids (VS), Total Suspended Solids (TSS) and Volatile Suspended Solids (VSS) were analyzed using Standard Method (APHA, AWWA, WEF, 2005). The analyses were performed in triplicates. On the other hand, the pH and DO of the feed and the effluent of each reactor was measured using a pH-meter and DO-meter, as well as the temperature of the room was recorded.

CO_2, CH_4 and N_2 gases were analyzed using the Thermal Conductivity Detector (TCD) equipped in the Gas Chromatograph (GC) (Trace GC Ultra: Thermo Electron Corporation). The following settings were applied in the GC, injector temperature 80°C, oven temperature 40°C, detector temperature 80°C, while the carrier gas used was Helium (He) maintained at a pressure of 100 kPa. The analyses were performed in triplicates. The calibration and the LOD and LOQ of the GC analyses were performed and shown in APPENDIX F.

Dissolved methane was analyzed by performing the salting-out method adopted from Daelman et al. (2012) with some alterations. These alterations were performed after several trials to optimize the method. Although Daelman et al. (2012) used 20 g of NaCl for a 60 mL sample, a comparison between 10 g of NaCl and 100 g NaCl/L solution was performed using 10 mL of AD sludge previously sparged with CH_4/CO_2 gas mixture for different periods (1 min, 5 mins, 10 mins and 15 mins). It was found that 100 g NaCl/L solution resulted in higher CH_4 in the headspace while the 10 g of NaCl resulted in higher CO_2 in the headspace. Therefore, 100 g NaCl/L solution was adopted for the salting-out of CH_4. The modified salting-out method used in the experiments is as follows:

A solution of 100 g NaCl/L was placed in a 25 mL serum bottle, then a sludge sample was placed carefully into the salt solution. The bottom of the cap and the top of the liquid phase was marked on the bottle. The cap of the bottle was tightly closed and shook vigorously for 2 minutes. The bottle was left for 1 minute and then the gas expansion volume was measured using a water displacement device. The headspace gas composition was analyzed using the GC as described above. The last step was measuring the headspace of the bottle by filling the marked empty bottle with ultrapure water to the liquid phase mark first and measuring the mass of the bottle and then to the bottom of the cap and measuring the mass of the bottle. The difference between the two would signify the headspace volume. The headspace volume was added to the expansion volume and that volume was used along with the GC molar fraction to find the moles of CH_4 in the headspace by employing the ideal gas law at 35°C. The salting-out analyses were performed in duplicates.

3.2.2.2 Determination of the Reaction Rate of Each Target Microorganism

The NO_2^- and NO_3^--based reaction rates of the target microorganisms, namely Anammox, DAMOa and DAMOb were calculated throughout the operation of the SBR and the batch test. These reaction rates were computed according to the stoichiometric Equations 2.4, 2.5 and 2.6 in Section 2.3.2 and Section 2.4.2 (Hu et al., 2015). Equations 3.1, 3.2 and 3.3 were used to compute the reaction rates of each microorganism.

- $r_{Anammox\ NO_2^-} = -1.32 * r_{NH_4^+}$ ..... Equation 3.1
- $r_{DAMOa\ NO_3^-} = -r_{NO_3^-} + (0.26/1.32) * r_{Anammox\ NO_2^-}$ ..... Equation 3.2
- $r_{DAMOb\ NO_2^-} = -r_{NO_2^-} - r_{Anammox\ NO_2^-} + r_{DAMOa\ NO_2^-}$ ..... Equation 3.3

The Anammox and DAMOb reaction rates were calculated based on the NO_2^- consumption. Since Anammox is the only species among the three target microorganisms that oxidizes NH_4^+, the consumed NO_2^- by Anammox was computed using the measured NH_4^+ consumption rate ($r_{NH_4^+}$), and the NO_2^- removal reaction rate of Anammox ($r_{Anammox\ NO_2^-}$) was computed accordingly, as shown in Equation 3.1. The reaction rate of DAMOa ($r_{DAMOa\ NO_3^-}$) was calculated using the measured NO_3^- ($r_{NO_3^-}$) consumption rate, that includes the produced NO_3^- ($(0.26/1.32) * r_{Anammox\ NO_2^-}$) from the Anammox reaction, illustrated in Equation 3.2. The DAMOb reaction rate ($r_{DAMOb\ NO_2^-}$) was calculated using the measured NO_2^- consumption rate ($r_{NO_2^-}$) by considering the Anammox NO_2^- consumption rate ($r_{Anammox\ NO_2^-}$) and the DAMOa production rate of NO_2^- which is equal to ($r_{DAMOa\ NO_3^-}$) (Hu et al., 2015), as shown in Equation 3.3.

3.2.2.3 Determination of the Contribution of Each Target Microorganism to the Available Total Nitrogen Removed

The contribution of each of the target microorganisms to the Total Nitrogen (TN) removal was assessed to examine their activity and to further understand the composition of the consortium in correlation with the molar ratio calculations and the molecular analysis. A sample calculation is displayed in APPENDIX H. The TN removed by each target microorganism, namely Anammox, DAMOb and DAMOa was calculated by considering the consumed and produced nitrogen with respect to each reaction (Equations 2.4, 2.5 and 2.6 in Section 2.3.2 and Section 2.4.2). Equations 3.4-3.14 were used in the calculations of the percent contribution of each microorganism to the TN removed. This was calculated as a percentage from the available TN that takes into consideration the produced nitrogen in the intermediate reactions, which cannot be observed by only considering the initial and final nitrogen

concentrations. The initial TN was calculated by the summation of the initial concentrations of the nitrogen species analyzed experimentally (Equation 3.4). The final TN was calculated by the summation of the final concentrations of the nitrogen species (Equation 3.5).

The available TN is a term used via this thesis study for the first time. $TN_{available}$ is the summation of the initial nitrogen species and the produced nitrogen species via the reactions taking place, such as NO_3^- from Anammox and NO_2^- from DAMOa (Equation 3.6). Utilizing the available TN is critical since it allows the calculation of the actual consumption of each of the target species, otherwise, the real activity of DAMOa and DAMOb would not be recognized by just monitoring the initial and final concentrations of the nitrogen species. While the percentage contribution to the available TN removed ($\%CATN_{removed}$) was computed according to Equation 3.7.

$$TN_i=[NH_4^+\text{-}N]_i+[NO_2^-\text{-}N]_i+[NO_3^-\text{-}N]_i \quad \text{Equation 3.4}$$

$$TN_f=[NH_4^+\text{-}N]_f+[NO_2^-\text{-}N]_f+[NO_3^-\text{-}N]_f \quad \text{Equation 3.5}$$

$$TN_{available}=[NH_4^+\text{-}N]_i+[NO_2^-\text{-}N]_i+[NO_3^-\text{-}N]_i+\Delta[NO_3^-\text{-}N]_{AMX}+\Delta[NO_2^-\text{-}N]_{DAMOa} \quad \text{Equation 3.6}$$

$$\%CATN_{removed}^{microorganism}=(TN_{removed}^{microorganism}/TN_{available})*100 \quad \text{Equation 3.7}$$

where,

TN_i: initial TN concentration at each cycle, the sum of the initial concentrations of all the nitrogen species, (mg N/L)

$[NH_4^+\text{-}N]_i$: initial NH_4^+ concentration at each cycle, (mg N/L)

$[NO_2^-\text{-}N]_i$: initial NO_2^- concentration at each cycle, (mg N/L)

$[NO_3^-\text{-}N]_i$: initial NO_3^- concentration at each cycle, (mg N/L)

TN_f: final TN concentration at each cycle, the sum of the final concentrations of all the nitrogen species, (mg N/L)

$[NH_4^+\text{-}N]_f$: final NH_4^+ concentration at each cycle, (mg N/L)

$[NO_2^-\text{-}N]_f$: final NO_2^- concentration at each cycle, (mg N/L)

$[NO_3^-\text{-}N]_f$: final NO_3^- concentration at each cycle, (mg N/L)

$TN_{available}$: available TN concentration that is available for consumption by the target microorganisms which includes the summation of any nitrogen species to be produced via the target microorganisms, (mg N/L)

$\Delta[NO_3^-\text{-}N]_{AMX}$: NO_3^- concentration to be produced stoichiometrically by Anammox in each cycle computed regarding the consumed NH_4^+-N, (mg N/L)

$\Delta[NO_2^-\text{-}N]_{DAMOa}$: NO_2^- concentration to be produced stoichiometrically by DAMOa in each cycle, (mg N/L)

$TN_{removed}^{microorganism}$: TN removed by each microorganism calculated in Equations 3.11, 3.12 and 3.14, (mg N/L)

$\%CATN_{removed}^{microorganism}$: Percentage contribution of each microorganism to the available TN removal (%)

Since NH_4^+ is only consumed by Anammox and the Anammox bacteria were observed to be the most active of the three microorganisms, NH_4^+ was chosen to be the starting point of this calculation. The consumed NH_4^+ by Anammox was computed (Equation 3.8). While the corresponding consumed NO_2^- and produced NO_3^- by Anammox was then computed, according to Equations 3.9 and 3.10, respectively. Hence the summation of the consumed nitrogen species while deducting the produced nitrogen yields the TN removed by Anammox (Equation 3.11).

AMX:

$\Delta[NH_4^+\text{-}N]=[NH_4^+\text{-}N]_i-[NH_4^+\text{-}N]_f$……..……..... Equation 3.8

$\Delta[NO_2^-\text{-}N]_{AMX}= 1.32*\Delta[NH_4^+\text{-}N]$….....……..…...…….... Equation 3.9

$\Delta[NO_3^-\text{-}N]_{AMX}= 0.11*(\Delta[NH_4^+\text{-}N]+\Delta[NO_2^-\text{-}N]_{AMX})$……..…..... Equation 3.10

$TN_{removed}^{AMX}=\Delta[NH_4^+\text{-}N]+\Delta[NO_2^-\text{-}N]_{AMX}-\Delta[NO_3^-\text{-}N]_{AMX}$……..…..... Equation 3.11

where,

$\Delta[NH_4^+\text{-}N]$: NH_4^+ concentration consumed by Anammox in each cycle, (mg N/L)

$\Delta[NO_2^-\text{-}N]_{AMX}$: NO_2^- concentration consumed by Anammox in each cycle, (mg N/L)

$TN_{removed}^{AMX}$: TN concentration consumed by Anammox in each cycle, (mg N/L)

The available NO_3^- for DAMOa consumption includes the initial NO_3^- concentration and the produced NO_3^- by Anammox. Accordingly, the consumed NO_3^- by DAMOa can be computed, and subsequently the TN removed by DAMOa can be computed as well (Equation 3.12).

DAMOa:

$TN_{removed}^{DAMOa}=\Delta[NO_3^-\text{-}N]_{DAMOa}=[NO_3^-\text{-}N]_i-[NO_3^-\text{-}N]_f+\Delta[NO_3^-\text{-}N]_{AMX}$.. Equation 3.12

$\Delta[NO_2^-\text{-}N]_{DAMOa}=\Delta[NO_3^-\text{-}N]_{DAMOa}$……..…... Equation 3.13

where,

$\Delta[NO_3^-\text{-}N]_{DAMOa}$: NO_3^- concentration consumed by DAMOa in each cycle, (mg N/L)

$TN_{removed}^{DAMOa}$: TN concentration consumed by DAMOa in each cycle, (mg N/L)

On the other hand, the available NO_2^- for DAMOb consumption is the remaining NO_2^- after the Anammox reaction, since Anammox has a higher affinity to NO_2^- in comparison to DAMOb, and the produced NO_2^- by DAMOa. Hence, the consumed NO_2^- by DAMOb can be computed, hence, the TN removed by DAMOb can be deduced (Equation 3.14).

DAMOb:

$TN_{removed}^{DAMOb}=\Delta[NO_2^-\text{-}N]_{DAMOb}=[NO_2^-\text{-}N]_i-\Delta[NO_2^-\text{-}N]_{AMX}+\Delta[NO_2^-\text{-}N]_{DAMOa}-[NO_2^-\text{-}N]_f$ ……...…….. Equation 3.14

where,

$\Delta[NO_2^-\text{-}N]_{DAMOb}$: NO_2^- concentration consumed by DAMOb in each cycle, (mg N/L)

$TN_{removed}^{DAMOb}$: TN concentration consumed by DAMOb in each cycle, (mg N/L)

3.2.2.4 Determination of the Stoichiometric Ratio of the Consortium

The different combinations of nitrogen ratios were examined to further assess the performance and status of the reactor in terms of the co-culture present. In other words, it was aimed to reveal the potential culture combinations and dominance by following the theoretical stoichiometric ratios of the nitrogen species, which might be the indicator of the reactions of the target microorganisms. Four different ratios were calculated and compared to the stoichiometric molar ratios, $\Delta NO_2^-/\Delta NH_4^+$; $\Delta NO_3^-/\Delta NH_4^+$; $\Delta NO_3^-/\Delta NO_2^-$ and $\Delta NO_3^-/ (\Delta NO_2^- + \Delta NH_4^+)$. These ratios were examined under six different cases of the co-cultures that might be occurring in the reactor. The assumptions followed in these cases are given below:

- The main four cases are as follows: AMX, AMX & DAMOa, AMX & DAMOb and DAMX, (Equations 3.15, 3.16, 3.18 and 3.19);
    i. AMX: The SBR only contains Anammox culture.
    ii. AMX & DAMOa: The SBR contains both Anammox and DAMOa.
    iii. AMX & DAMOb: The SBR contains both Anammox and DAMOb.
    iv. DAMX: The SBR contains Anammox, DAMOa and DAMOb.
- For all cases (i.e., for all the potential combinations of cultures)
    i. Each culture is 100% active.
    ii. Anammox is present since they have been enriched and provided with the necessary conditions to thrive.
- The change of concentration in each cycle was calculated as follows $\Delta C = C_{initial} - C_{final}$. Therefore, consumption of the nitrogen species is positive, while production is negative.

The theoretical stoichiometric ratios were calculated according to the stoichiometry present in the reaction equations (Equations 2.4, 2.5 and 2.6 in Section 2.3.2 and Section 2.4.2). For Equations 2.4, 2.5 and 2.6, the limiting reagent in each reaction was considered. The limiting reagent in each reaction is NH_4^+, NO_3^- and NO_2^- for Anammox, DAMOa and DAMOb reactions, respectively. Accordingly, the equations were adjusted for 1 mole of the specified limiting reagent.

In addition to the four main cases mentioned above, a special incident, where DAMOa is able to consume only the NO_3^- produced by the Anammox, was constructed by equating the moles of NO_3^- consumed to the moles of NO_3^- produced in the two cases, namely, *AMX & DAMOa and *DAMX, as displayed in Equations 3.17 and 3.20, respectively. In these two cases, the activity of DAMOa was not assumed to be 100%. Incorporating this special case may improve the characterization of the co-culture composition via the molar ratio calculation.

All calculations of each culture combination (six cases) are given in Equations 3.15-3.20 and accordingly, the theoretical stoichiometric molar values were obtained in Table 3.8.

AMX: $NH_4^+ + 1.32\ NO_2^- \rightarrow 0.26\ NO_3^- + 1.02\ N_2$……... Equation 3.15

AMX & DAMOa: $NH_4^+ + 0.32\ NO_2^- + 0.74\ NO_3^- \rightarrow 1.02\ N_2$…..... Equation 3.16

*AMX & DAMOa: $NH_4^+ + 1.06\ NO_2^- \rightarrow 1.02\ N_2$……...…….. Equation 3.17

AMX & DAMOb: $NH_4^+ + 2.32\ NO_2^- \rightarrow 0.26\ NO_3^- + 1.52\ N_2$…….... Equation 3.18

DAMX: $NH_4^+ + 1.32\ NO_2^- + 0.74\ NO_3^- \rightarrow 1.52\ N_2$……...…… Equation 3.19

*DAMX: $NH_4^+ + 2.06\ NO_2^- \rightarrow 1.52\ N_2$……....…. Equation 3.20

Table 3.8 Theoretical stoichiometric molar ratio values of nitrogen species for the different consortium cases

Microbial consortium cases	ΔNH_4^+	ΔNO_2^-	ΔNO_3^-	$\Delta NO_2^-/\Delta NH_4^+$	$\Delta NO_3^-/(\Delta NO_2^-+\Delta NH_4^+)$	$\Delta NO_3^-/\Delta NO_2^-$	$\Delta NO_3^-/\Delta NH_4^+$
AMX	1.00	1.32	-0.26	1.32	-0.11	-0.2	-0.26
AMX & DAMOa	1.00	0.32	0.74	0.32	0.56	2.31	0.74
*AMX & DAMOa	1.00	1.06	0	1.06	0	0	0
AMX & DAMOb	1.00	2.32	-0.26	2.32	-0.08	-0.11	-0.26
DAMX	1.00	1.32	0.74	1.32	0.32	0.56	0.74
*DAMX	1.00	2.06	0	2.06	0	0	0

3.2.3 Molecular Analysis Methods

Two molecular analyses methods were employed in this study, the Fluorescent In-Situ Hybridization (FISH) and the Next-Generation Sequencing (NGS) 16S Metagenome. The FISH method was performed periodically to detect, identify, and determine the relative abundance of the target species among the whole archaeal and bacterial consortium. On the other hand, the NGS 16S Metagenome method was performed to determine all the microorganisms present in the consortium and their relative abundance.

3.2.3.1 Fluorescent In-Situ Hybridization Analysis

The FISH analyses were performed during the different phases of operation of the DAMO-Anammox SBR for morphological detection and determination of the relative abundance of the target species (Nielsen et al., 2009).

About 5 ml of sample was used, where the supernatant was separated by centrifugation at 10,000 g for 5 min and then it was discarded. The remaining sludge was fixed with an equal volume of 4% paraformaldehyde (PFA) in phosphate buffered saline (PBS), which was then stored overnight at 4°C. The next day the sample was centrifuged at 10,000 g for 5 min to separate the PFA, which was then discarded. The remaining fixed biomass was then dissolved in 5 mL of 1:1 PBS/Ethanol (Daims et al., 2009). The samples were then stored overnight at -20°C. The following day the samples were carefully placed on slides and dehydration of the samples on the slides was conducted. This was carried out with sequential washing with 50%, 80%, and 99% ethanol (Daims et al., 2009). The next step was permeabilization of the microbial cells which was performed by incubating the slides for 1 hr at 37°C after the addition of lysozyme (Daims et al., 2009).

Hybridization solutions of different probes targeting *M. nitroreducens*, *M. oxyfera*, General Bacteria, General Archaea and Anammox were prepared considering their relative formamide and NaCl concentrations. The stringency conditions (formamide and NaCl concentrations) were optimized prior to the FISH analyses to ensure better results of probe hybridization. The probes used in the scope of these experiments are

summarized in Table 3.9. Five hybridization mixtures were prepared using different combinations of the previously described solutions (Table 3.10). The mixtures containing only General Archaea and General Bacteria were counterstained with DAPI to determine the content of bacteria and archaea in the microbial consortium. Five slides were prepared for each biomass sample analyzed. The hybridization mixtures were added carefully on the slides and the slides were incubated at 46°C for about 5 hr (Daims et al., 2009). After hybridization, the slides were washed at 48°C for 15 min with a washing buffer containing the same formamide concentration as the hybridization buffer (Daims et al., 2009).

After washing and drying the slides, imaging can commence. FISH imaging was performed using Carl Zeiss Axio Vision A1 UV microscope under suitable filters of the chosen probes. At least 3 representative microscopy images were chosen for each slide. The images were analyzed via the ImageJ software. The obtained images from the microscope were then processed using ImageJ, where the colored areas were converted to pixels. The pixel areas represent the presence of the probe and hence the target cell. The average area occupied by the pixels in the three chosen images and the relative abundance of each slide was computed. These computations were conducted in relativeness to the area occupied by the General Bacteria and General Archaea which were performed in relativeness to DAPI counterstaining. A summary of the steps performed using ImageJ, the resulting images and the obtained relative abundance in each slide are illustrated in APPENDIX I.

Table 3.9 Sequences, labels and formamide concentrations of chosen FISH probes

Target Species	Probe	Label	Formamide Concentration (%)	Reference
M. nitroreducens	S-*-Darc-872-a-A-18-GGC TCC ACC CGT TGT AGT	GFP and Cy5	40	Hu et al. (2015)
M. oxyfera	S-*-DBACT-0193-a-A-18-CGC TCG CCC CCT TTG GTC	Alexa Fluor 350	40	Ettwig et al. (2009)
General Anammox	S-*-Amx-0368-a-A-18-CCT TTC GGG CAT TGC GAA	Cy5	20	Schmid et al. (2005)
General Bacteria	EUB1 -GCT GCC TCC CGT AGG AGT	GFP	40	Daims et al. (2009)
	EUB2 -GCA GCC ACC CGT AGG TGT			
	EUB3-GCT GCC ACC CGT AGG TGT			
General Archaea	S-Darc-0915-a-A-20-GTG CTC CCC CGC CAA TTC CT	GFP	40	Knittel et al. (2005)

Table 3.10 The hybridization mixture and aim of each slide

Slide	Hybridization mixture content	Aim
1	General Bacteria and DAPI counterstaining	Determine the content of bacteria in the microbial consortium
2	General Archaea and DAPI counterstaining	Determine the content of archaea in the microbial consortium
3	*M. oxyfera*, Anammox and General Bacteria	Determine the abundance of *M. oxyfera* and Anammox relative to General Bacteria
4	*M. nitroreducens* and General Archaea	Determine the abundance of *M. nitroreducens* relative to General Archaea
5	*M. oxyfera*, *M. nitroreducens* and Anammox	Determine the relative abundance of the target species among each other

3.2.3.2 Next-Generation Sequencing (NGS) 16S Metagenome Analysis

The introduction of NGS or high-throughput sequencing has transformed the area of microbial ecology and allowed major advances in environmental studies (Oulas et al., 2015). Moreover, this founded the field of "metagenomics", which refers to the direct genetic analysis of genomes within an environmental sample without prior cultivation of clonal cultures (Oulas et al., 2015).

Primarily, functional and sequence-based analysis of collective microbial genomes in an environmental sample, referred to as "full shotgun metagenomics" was applied. This technique allows for full sequencing of the available genomes within a sample, creating a biodiversity profile that can be linked with functional composition analysis of known and unknown organism lineages (Oulas et al., 2015). Furthermore, the issues of what microorganisms are present in a consortium, their function, and their interactions with one another can be addressed. Later, polymerase chain reaction (PCR) amplification of specific genes of interest, referred to as "marker gene

amplification metagenomics" or "16S ribosomal RNA gene", started to be applied (Oulas et al., 2015). This technique allows achieving a taxonomic distribution profile using PCR amplification and sequencing of the 16S rRNA gene where the taxonomic distribution can be linked with environmental data obtained from the sample under study (Oulas et al., 2015). Subsequently, various metagenomics statistical and computational tools as well as databases were developed to cope with the vast influx of data collected. Hence, allowing the quick and detailed generation of a genomic profile of an environmental sample (Oulas et al., 2015).

Four sludge samples were withdrawn from the DAMO-Anammox SBR at different cycles, stored at -20°C and then sent for Next-Generation Sequencing (NGS) analysis to be performed by BM LABOSIS. The sampling cycles were the first cycle (the beginning of the SBR operation), Cycle 55, Cycle 130 and Cycle 202, each representing a different phase of the reactor operation. The change in the population dynamics was examined at the cycles stated above. The NGS 16S Metagenome Analysis procedure followed by BM LABOSIS is the procedure described by Boylen et al. (2019), the summary of which is given in Figure 3.8. The procedure is also summarized in the following text.

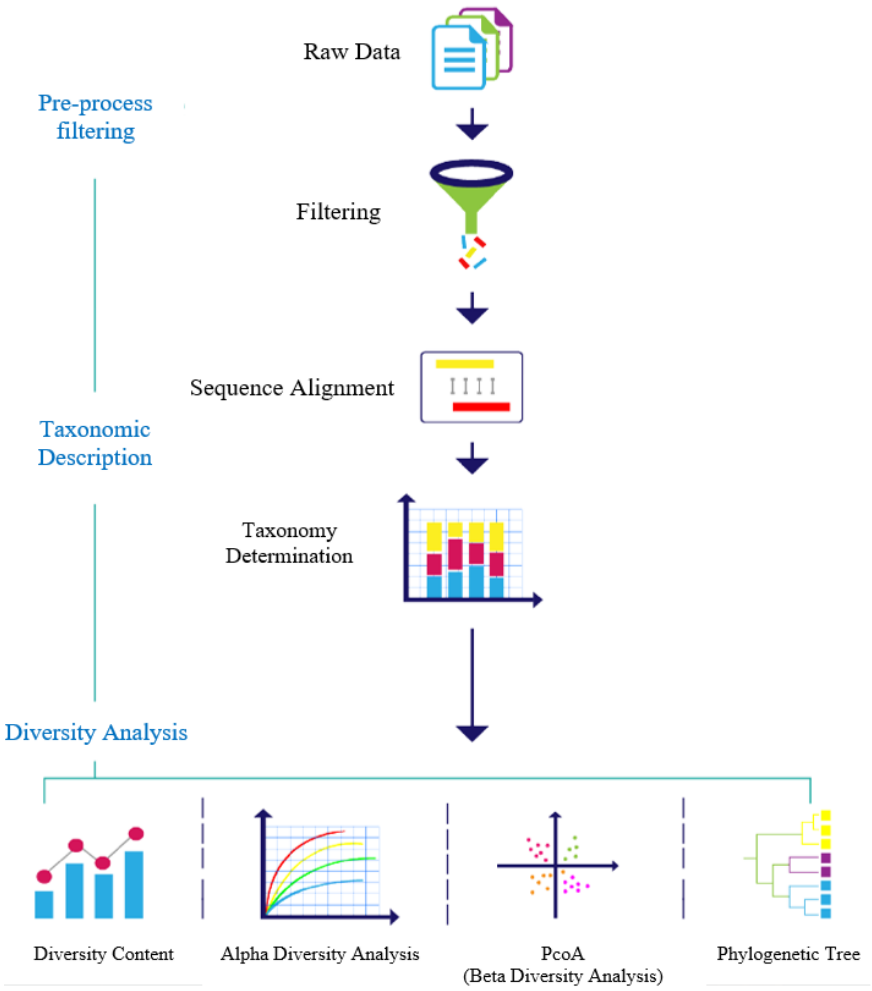

Figure 3.8 NGS 16S Metagenome Analysis procedure (Boylen et al., 2019)

1. Sample preparation: DNA isolation and quality control are performed to create libraries.
2. Creating a library: The 16S rRNA gene is used with specific primers, which were then replicated and purified. The concentration of libraries generated by real time PCR is diluted to 4 nM and normalization is done.
3. Sequencing: After the library is prepared sequencing using the synthesis method is done with each new dNTP added. The added base fluoresces are optically observed and recorded.
4. Raw Data Processing: The data generated after sequencing is analyzed in FASTA format.
5. Raw Data Quality Control: The quality of the fastqc files (FASTQC) are examined using QIIME2.

6. Determination of Chimeric Readings using DADA2
7. Filtering: Reads, primers and barcodes with Phred quality scores less than 20 are filtered out using DADA2.
8. Determination of Taxonomy: Determination of taxonomic species for each sample using QIIME2.
9. Diversity Analysis: Alpha and Beta Rarefaction Analysis using QIIME2 is performed.

3.3 Results and Discussion

3.3.1 The Results of Anammox SBR Operation

The Anammox SBR was operated throughout the research period of about 1 year. In this thesis study, only the first 200 cycles are presented covering the cycles at which the seed Anammox sludge was withdrawn for the DAMO-Anammox SBR. Moreover, the Anammox activity during this period was used for comparison with the Anammox activity in the co-culture in the various reactors that were established in this study. The operational results are briefly summarized in this section to reveal the state and activity of the Anammox seed (Figure 3.9, Figure 3.10 and Figure 3.11). The detailed results are presented in Appendix A.

The Anammox SBR was operated at 35°C, the pH of the influent at the beginning of each cycle was maintained between 7.0-7.3 and the HRT of the reactor was set as 2 days. The pH of the effluent ranged from 6.9-8.3 throughout the 200 cycles, as shown in Figure A-1. Although the pH was set between 7.0-7.5 before the start of every cycle using Ar/CO_2 mixture, the average pH of the effluent during the first 7 cycles was 7.73, which can be attributed to the activity of heterotrophic denitrification (H.D.) in the presence of sCOD (Figure A-2). On the other hand, the average pH from Cycle 7-200 was 7.28. The activity of H.D. can be observed till Cycle 32, where complete removal of NO_3^- can be seen in Figure 3.9c and Figure A-3c.

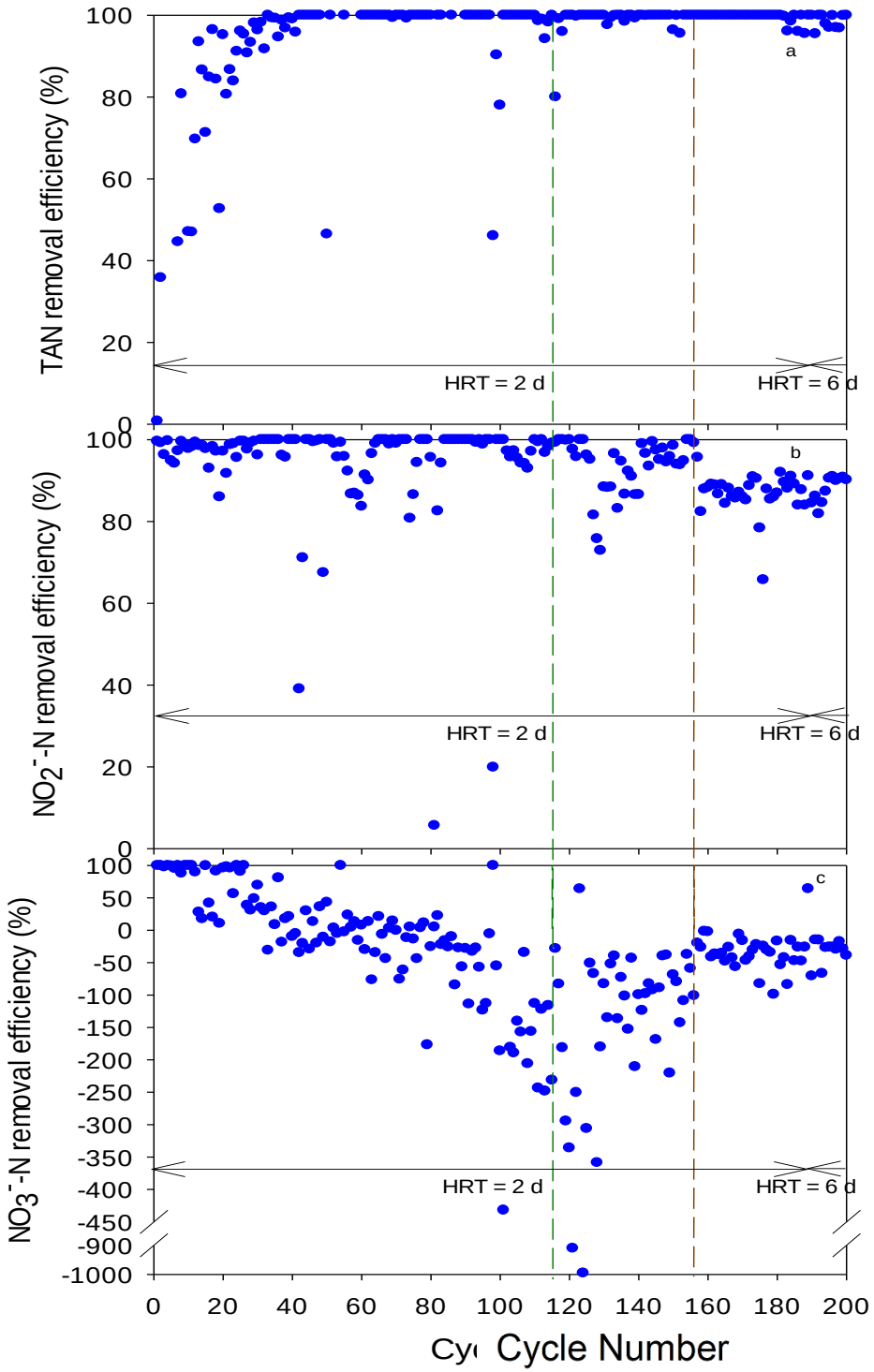

Figure 3.9 Removal efficiencies of (a) TAN, (b) NO_2^- and (c) NO_3^- in each cycle of the Anammox SBR (the negative values of removal emphasize production or accumulation; green dashed line at Cycle 115 refers to removal of 0.25 L of sludge from the reactor; brown dashed line at Cycle 156 refers to removal of 0.6 L of sludge for DAMO-Anammox SBR seeding)

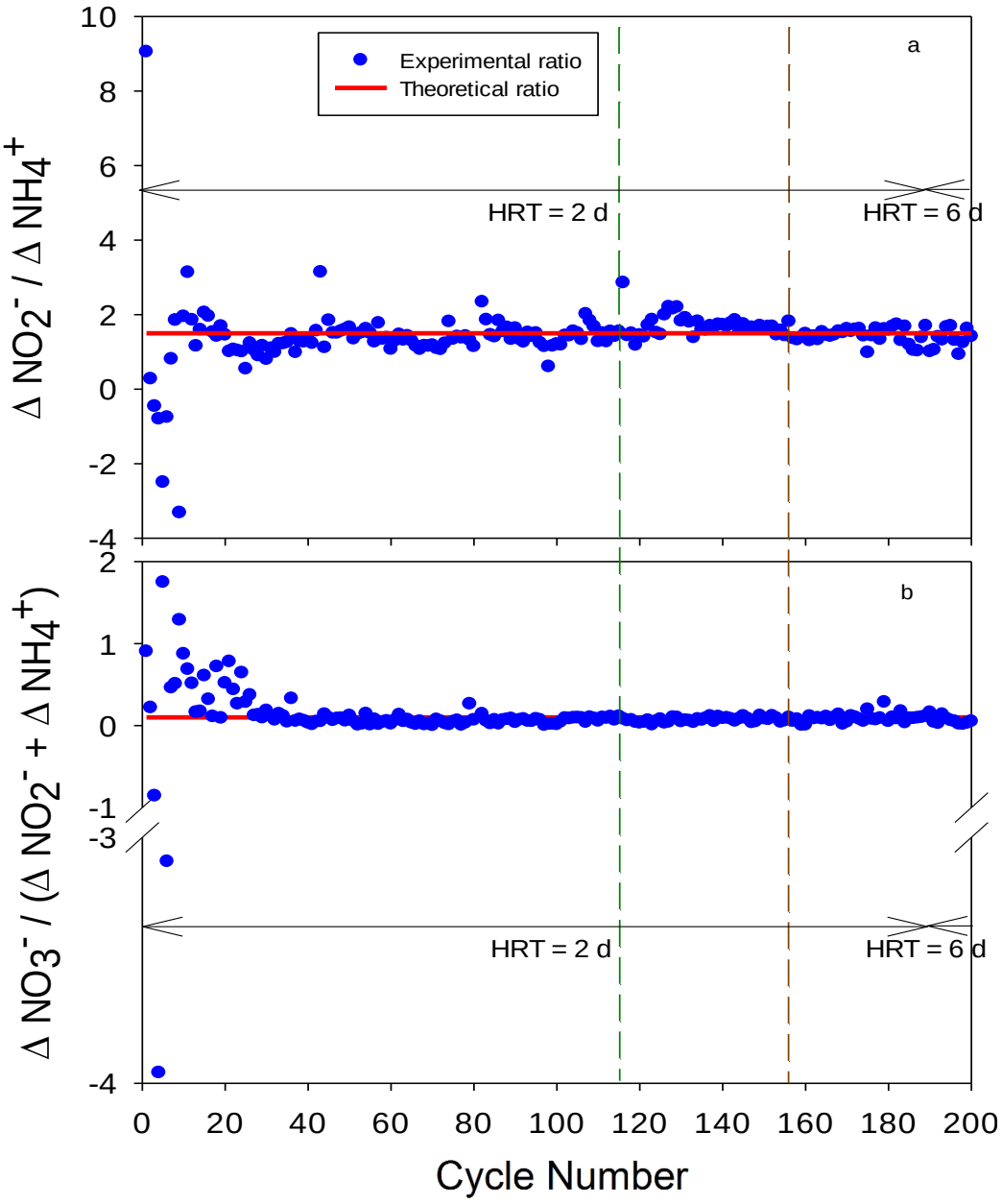

Figure 3.10 The comparison of the experimental and theoretical ratios of (a) ΔNO_2^- /ΔNH_4^+ and (b) ΔNO_3^-/ (ΔNO_2^- + ΔNH_4^+) in the Anammox SBR (green dashed line at Cycle 115 refers to removal of 0.25 L of sludge from the reactor; brown dashed line at Cycle 156 refers to removal of 0.6 L of sludge for DAMO-Anammox SBR seeding)

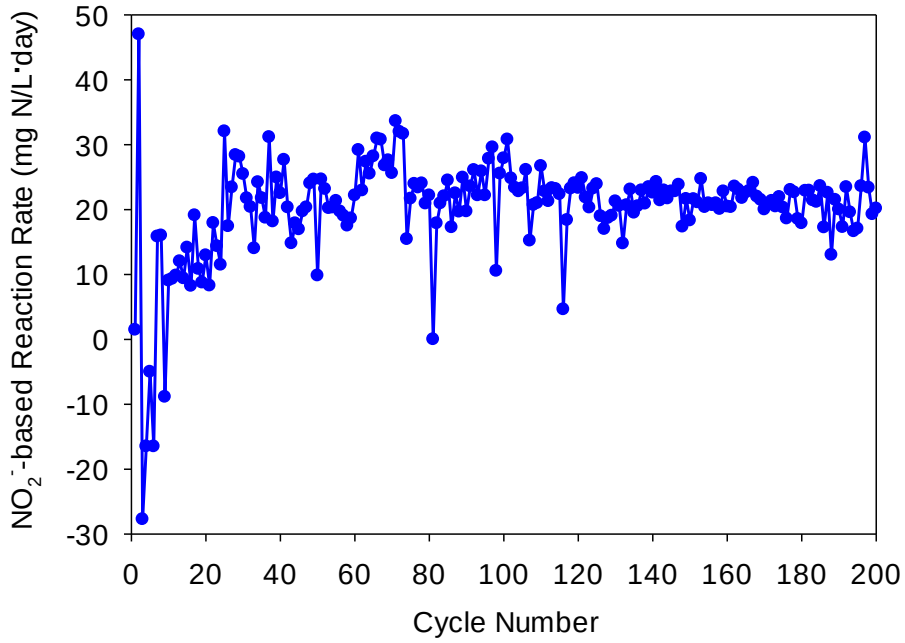

Figure 3.11 The calculated NO_2^--based reaction rate of the Anammox SBR in each cycle

The initial TAN concentration at Cycle 1 was found to be 139 mg N/L, therefore NH_4^+ was not added to the feed (Figure A-3a). On the other hand, NO_2^- and NO_3^- were each added to establish an initial theoretical concentration of 10 mg N/L (Figure A-3b and Figure A-3c). After the 10th cycle, the initial TAN concentration reached levels lower than 15 mg N/L in the reactor, so NH_4^+, NO_2^- and NO_3^- were added in the feed creating initial theoretical concentrations of NH_4^+, NO_2^- and NO_3^- of 15, 22.5 and 20 mg N/L, respectively, up till Cycle 77. After Cycle 77, NO_3^- was not added in the feed since it became unnecessary due to the extremely low H.D. activity. Hence, the consequent theoretical NLR was 57.5 mg N/L·day up to Cycle 77 and reduced to 37.5 mg N/L·day after Cycle 77. The feed was prepared according to the consumption of TAN and NO_2^-, to maintain the initial theoretical concentrations in the reactor. These concentrations were chosen since the Anammox seed used was acclimated at those concentrations and the ratio of NH_4^+: NO_2^- was 1:1.5 (Chamchoi and Nitisoravut, 2007).

The removal efficiencies, removal rates and consumption ratios were calculated to assess the performance of the system in comparison to the expected stoichiometric ratios of Anammox. TAN removal efficiency increased gradually from 35 to 85% in

the first 16 cycles and reached 95-100% by Cycle 32, indicating the enrichment of the Anammox culture. After Cycle 32 the average TAN removal efficiency was about 98±8 %, (Figure 3.9a), while the average removal rate of TAN was 16.4±3.3 mg N/L·day (Figure A-4a). The average removal efficiency of NO_2^- was 93±12 % (Figure 3.9b), while the NO_2^- average removal rate was 23.6±4.8 mg N/L·day (Figure A-4b). On the other hand, NO_3^- was expected to be produced as a by-product of the Anammox process, as shown in Equation 2.4 in Section 2.3.2. This is observed in Figure A-3c, where the concentration of NO_3^- increased in each cycle. The positive removal efficiency signifying the consumption of NO_3^-, mainly due to H.D., occurred from Cycle 1-32 at an average of 74±14 % (Figure 3.9c). Meanwhile the negative removal efficiency of NO_3^-, signifying the production became the general trend after Cycle 32 due to the dominant activity of Anammox, averaging a production rate of 2.8±1.8 mg N/L·day as shown in Figure A-4c.

At Cycle 98 due to the low pH of 6.36, the TAN removal ability of the Anammox was affected greatly, the removal efficiency and removal rate of TAN was 46% and 8mg N/L·day, respectively. After the pH was regulated within the desired range, the Anammox activity increased back to its regular state of above 90% of TAN removal efficiency.

Samples were taken at various cycles for TSS and VSS analysis and reported in Table A-1. The TSS and VSS analyses were not performed frequently in order not to lose any biomass since this reactor was planned to be used as a stock reactor to seed the DAMO-Anammox SBR. In addition, since the Anammox sludge was mainly in granular form, the TSS and VSS analyses conducted on the suspended (non-granular) biomass would not have correctly represented the actual biomass present in the reactor.

At Cycle 115, 250 mL of Anammox sludge was removed from the reactor for seeding purposes, which reduced the NO_2^- removal efficiency to about 70%. The removal efficiency recovered back to above 90% at Cycle 141. Furthermore, at Cycle 156, 600 mL of Anammox sludge was removed to seed the DAMO-Anammox SBR. The removal efficiency of TAN was not affected much by the removal of biomass. The

removal efficiency of NO_2^- decreased to around 85%. This was expected since the removed biomass volume was 60% of the total sludge volume.

The NO_2^--based reaction rate of Anammox was calculated as described in Section 3.2.2.4. Figure 3.11 shows the calculated reaction rate of each cycle. The average NO_2^--based reaction rate after Cycle 32 (the end of H.D.) of the Anammox bacteria was found to be 21.8±4.4 mg N/L·day, reaching a maximum of 33.6 mg N/L·day at cycle 71.

Regarding the ratio of $\Delta NO_2^-/\Delta NH_4^+$ consumption, it was found to be on average 1.49±0.31 which is close to the theoretical consumption ratio of 1.32. The results showed that the reactor activity was constant at this ratio, as seen from Figure 3.10a. On the other hand, the ratio of $\Delta NO_3^-/ (\Delta NO_2^- + \Delta NH_4^+)$ was found to be on average 0.07±0.05 which is close to the theoretical ratio of 0.11, as shown in Figure 3.10b. The overall performance of the Anammox can be considered as stable and reached steady state with constant removal efficiencies and removal rates and with ratios similar to the theoretical stoichiometric ratios (Equation 2.4, Section 2.3.2).

3.3.2 The Results of DAMO-Anammox SBR Operation

The DAMO-Anammox SBR was established aiming to enrich the DAMO-Anammox co-culture. Moreover, the effect of HRT and, in turn, NLR and meanwhile the effect of Fe^{2+} and Cu^{2+} concentrations were to be investigated. The effect of these parameters was tested on the reactor performance and the population dynamics of the microbial consortium enriched in the DAMO-Anammox SBR. The DAMO-Anammox SBR was operated for about 780 days (202 cycles) and the results are presented in two main sections, namely, the results of reactor performance and the results of molecular analyses.

3.3.2.1 Results of Reactor Performance

The results of the reactor performance were divided into two sections, a section discussing the pH, TOC and TSS and VSS analyses conducted (Section 3.3.2.1.1)

and a section discussing the results of the nitrogen species analyses (3.3.2.1.2), including the removal efficiencies, removal rates, TN removal and the contribution of each of the target species and reaction rates of each of the target species.

3.3.2.1.1 pH, TOC and TSS and VSS

The DAMO-Anammox SBR was operated at a temperature of 35°C, while the pH of the influent was maintained at a pH of 7.2-7.6. The effluent pH ranged from 7.0-7.6, throughout 202 cycles, as shown in Figure 3.12. The average pH in the different phases of operation was 7.33, 7.34, 7.26, 7.28 and 7.31, in Phases I, II, III, IV and V, respectively. These pH values were in the range of the most commonly applied pH throughout DAMO-Anammox enrichment studies (7.3-7.5) (Luesken et al., 2011; Haroon et al., 2013; Ding et al., 2014; Hu et al., 2015; Cai et al., 2015; Xie et al., 2016; Fu et al., 2017; Ding et al., 2017). This pH range was defined as the optimal pH range for the enrichment of the DAMO-Anammox co-culture.

The TOC of Cycle 0 was found to be 24.6 mg/L and by Cycle 11, the TOC was measured to be about 12 mg/L. If this TOC source would have been methanol (whichwas not aimed and thus was not analyzed), 8-14% of the initial NO_2^- and NO_3^- concentration would be consumed via heterotrophic denitrification (H.D.). This reveals that the NO_2^- and NO_3^- consumed via H.D. only lasted till Cycle 25 and after that the H.D. activity was minimal. The H.D. refers to denitrification that utilizes organic carbon excluding the supplied CH_4. This was further supported by the results of the specific activity tests performed in Phases I, II and III. This was mainly due to the fact that the mixed sludge was washed multiple times with feed solutions in the absence of any nitrogen source to diminish the sCOD and initial NH_4^+ concentrations. However, the TOC concentration reached about 5.5 mg/L by Cycle 120. At Cycle 192, the measured TOC was found to be about 14.4 mg/L as shown in Figure 3.13. This reveals that despite no addition of organics in the feed, there was production of organics. This might be due to the release of extracellular polymeric substances (EPS) as well as degradation of microorganisms which were not supported by the operational conditions. Nevertheless, very low TOC degradation measured in Cycle 120 indicates that, even if there is H.D., it is not the main NO_2^-

and NO_3^- removal mechanism. Since organic carbon was not added in the feed, the effluent concentration would decrease following the trend shown by the theoretical effluent concentration line shown in Figure 3.13.

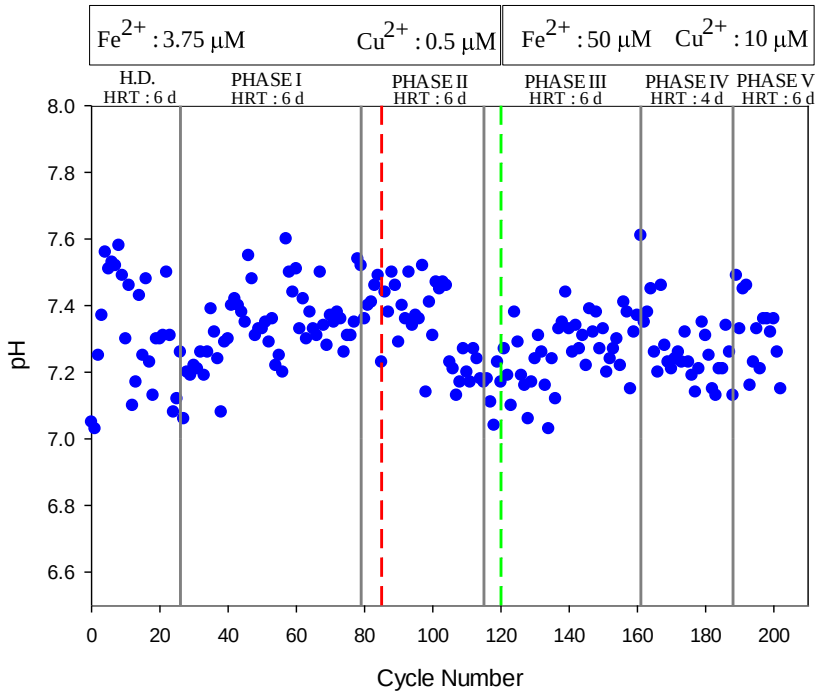

Figure 3.12 pH values of the effluent samples of the DAMO-Anammox SBR (red dashed line: increase in NO_3^- concentration at Cycle 85; green dashed line: increase in Fe^{2+} and Cu^{2+} concentrations at Cycle 120)

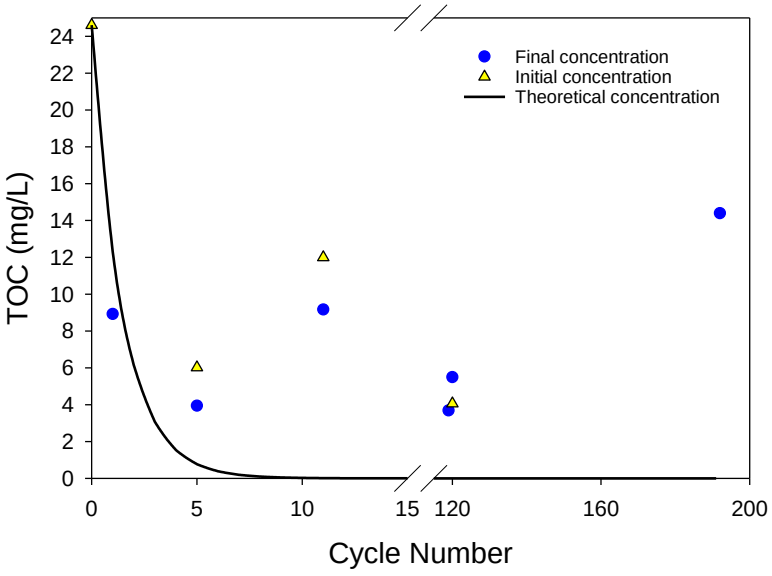

Figure 3.13 The results of TOC analyses of the DAMO-Anammox SBR

The initial TSS and VSS were 271.2±9.6 and 11.2±0.8 g/L, by Cycle 72 the TSS and VSS decreased to 12.6±1.3 and 5.9±0.1 g/L, respectively (Table 3.11 and Figure 3.14). Moreover, by Cycle 105 the TSS and VSS decreased slightly to reach levels of 12.2±0.6 and 5.7±0.3 g/L, respectively. Although the initial concentration of VSS decreased by Cycle 105, the VSS/TSS percentage increased from 4% to 47%. This was due to the washout of decayed microorganisms and suspended particles mainly found in the lake sediment. At Cycle 129, a decrease in the VSS concentration (3.2±0.2 g/L) was observed along with a decrease in VSS/TSS percentage (24%). While at Cycle 160 the VSS was 1.0±0.02 g/L, and the TSS was 5.1±0.2 g/L making a VSS/TSS percentage of 19%. An increase in TSS and VSS, 9.3±0.3g/L and 2.4±0.1 g/L, respectively, was then observed at Cycle 181, making a VSS/TSS percentage of 26%. This might be due to the growth of Anammox bacteria during Phase IV. At Cycle 192 a slight decrease in TSS (7.9±0.6 g/L) and VSS (1.9±0.2 g/L) was noticed which corresponds to a VSS/TSS percentage of 24%.

Table 3.11 TSS and VSS results of the sludge in the DAMO-Anammox SBR

Sludge	Phase	TSS (g/L)	VSS (g/L)	VSS/TSS (%)
Mixed initial seed	-	271.2±9.6	11.2±0.8	4
Cycle 2	H.D.	78.4±1.9	12.2±0.3	16
Cycle 72	I	12.6±1.3	5.9±0.1	47
Cycle 105	II	12.2±0.6	5.7±0.3	47
Cycle 129	III	13.1±0.4	3.2±0.2	24
Cycle 160	III	5.1±0.2	1.0±0.02	19
Cycle 181	IV	9.3±0.3	2.4±0.1	26
Cycle 192	V	7.9±0.6	1.9±0.2	24

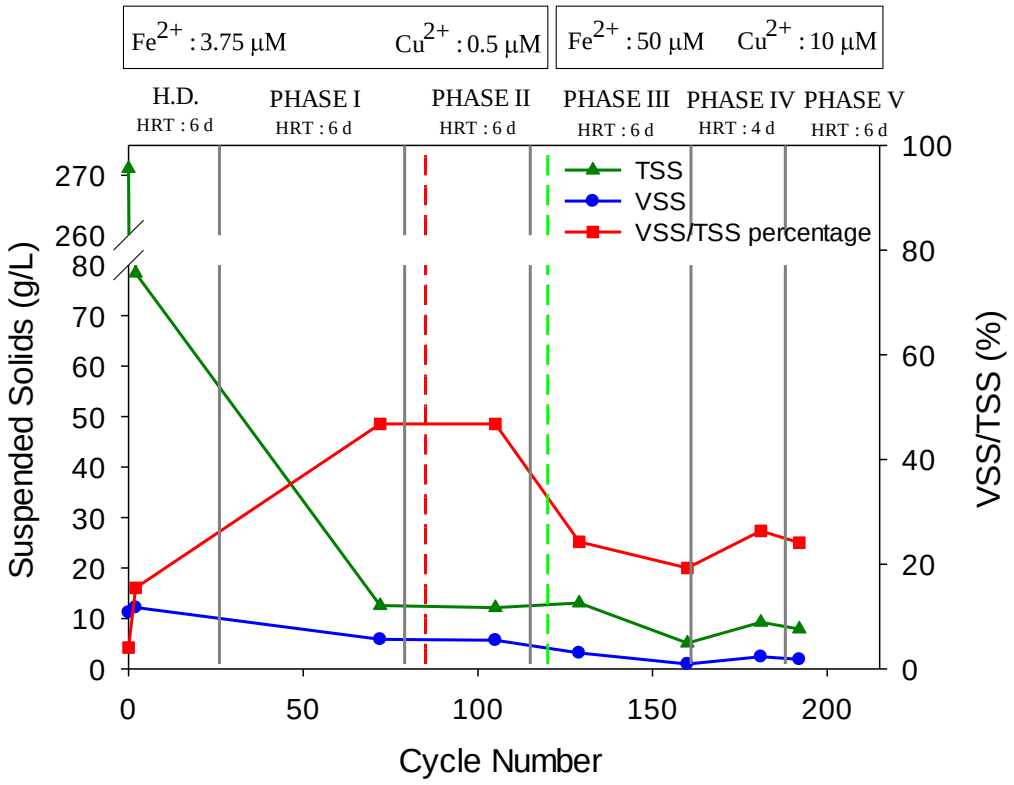

Figure 3.14 TSS, VSS and VSS/TSS percentage of the biomass in the DAMO-Anammox SBR (red dashed line: increase in NO_3^- concentration at Cycle 85; green dashed line: increase in Fe^{2+} and Cu^{2+} concentrations at Cycle 120)

3.3.2.1.2 Results of Nitrogen Species Analyses

The results of the analyses conducted show that a DAMO-Anammox co-culture was enriched. The contribution of each of the target microorganisms to the TN removal, stoichiometric molar ratios of the nitrogen species and the reaction rates of the target microorganisms were computed. The results illustrated Anammox dominance throughout the operation of the DAMO-Anammox SBR, while DAMOb and DAMOa activities fluctuated throughout the different operational phases of the DAMO-Anammox SBR. This is also observed in the specific activity tests that were performed for Phases I, II and III. The specific activity tests were conducted to assess the activity of each of the target microorganisms, namely, Anammox, DAMOa and DAMOb, via separate batch reactors. Some differences in the results of the specific activity tests and the DAMO-Anammox SBR were observed. This was attributed to

the difference in reactor volume, where the batch tests had a much smaller reactor volume. This allowed for higher contact between the microorganisms and the medium and dissolved CH_4 may be more available for the utilization of the microorganisms.

According to the TOC of the first 25 cycles, H.D (i.e., non-methanotrophic denitrification) was the dominant reaction taking place in the reactor. Therefore, the period of the first 25 cycles was referred to as the heterotrophic denitrification (H.D.) phase. During the H.D. phase of the DAMO-Anammox SBR, NH_4^+ was not added in the feed since the NH_4^+ concentration existing in the mixed sludge was found to be 80 mg N/L, higher than the desired initial concentration (7 mg N/L) (Figure 3.15). Only NO_2^- and NO_3^- were added creating a theoretical initial concentration of 15 mg N/L of each. Once NH_4^+ concentration reached to levels lower than 7 mg N/L in the reactor, it was then added to the feed. It took three cycles for the NH_4^+ concentration to decrease to the desired initial concentration. NH_4^+, NO_2^- and NO_3^- were added to the feed at the beginning of each cycle according to their consumption to fulfill the theoretical initial targeted concentrations.

Phase I

After observing a halt in the consumption of NO_3^-, H.D. dominance in the DAMO-Anammox SBR was considered to have ended and this marked the beginning of Phase I (Cycle 26-78). In Phase I, the theoretical initial concentrations of NH_4^+, NO_2^- and NO_3^- remained 7, 15 and 15 mg N/L, respectively (Figure 3.15). The applied HRT was 6 days establishing a theoretical NLR of 12.3 mg N/L·day, while the average experimental NLR was 11.5±1.8 mg N/L·day (Figure 3.16a). The average removal efficiencies of TAN NO_2^- and NO_3^- were 94±8 % (Figure 3.16b), 74±10 % (Figure 3.16c) and 26±19 % (Figure 3.16d), respectively. In addition, the average removal rates of TAN NO_2^- and NO_3^- were 2.2±0.4 (**Hata! Başvuru kaynağı b ulunamadı.**b), 3.4±0.9 (**Hata! Başvuru kaynağı bulunamadı.**c) and 3.4±2.7 mg N/L·day (Figure 3.17d) respectively.

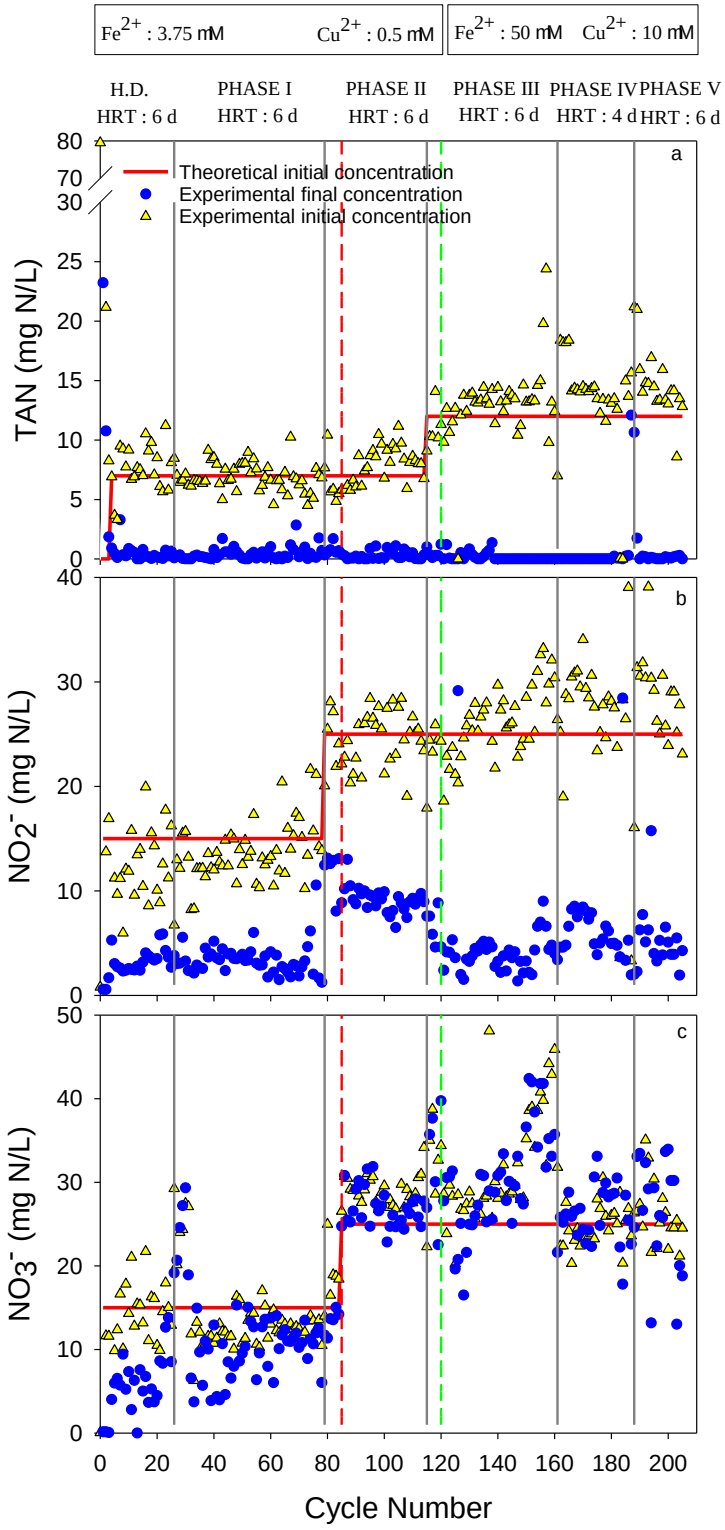

Figure 3.15 Initial and final concentrations of (a) TAN, (b) NO_2^--N and (c) NO_3^--N during each cycle of the DAMO-Anammox SBR (red dashed line: increase in NO_3^- concentration at Cycle 85; green dashed line: increase in Fe^{2+} and Cu^{2+} concentrations at Cycle 120; the S.D of each measurement was <5%)

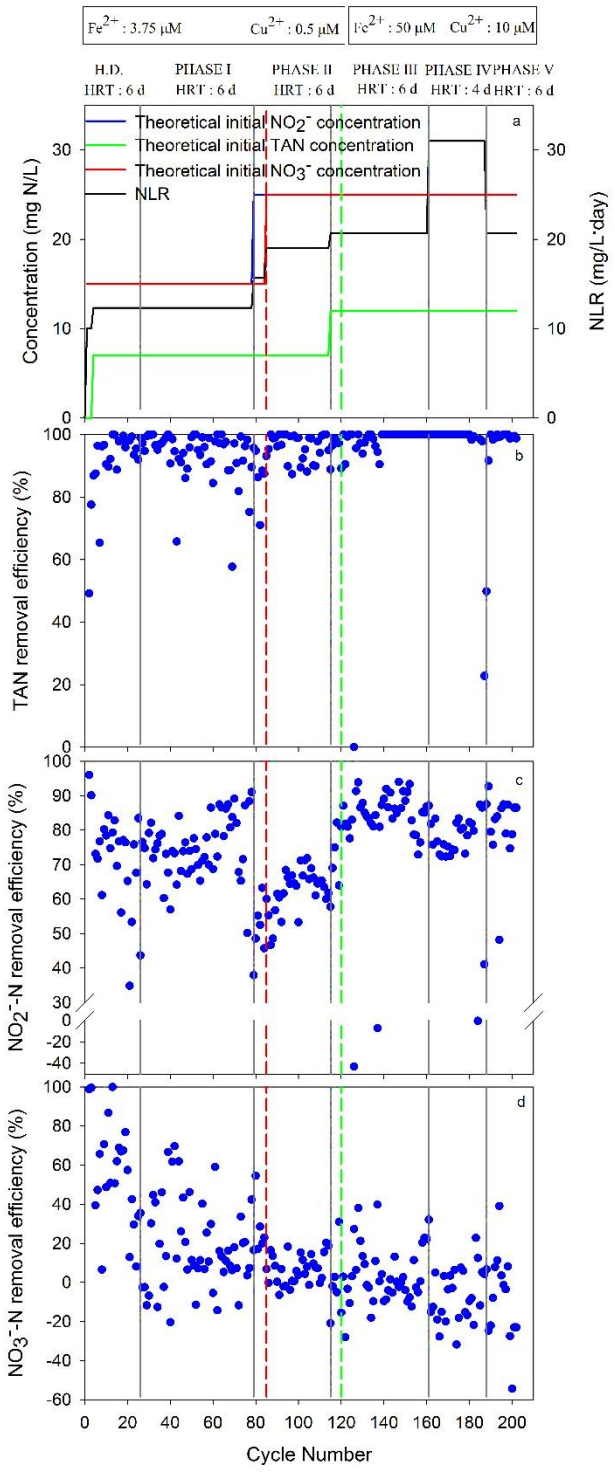

Figure 3.16 (a) Theoretical nitrogen influent concentrations and NLR. The removal efficiencies of (b) TAN, (c) NO_2^- and (d) NO_3^- in each cycle of the DAMO-Anammox SBR (The negative values emphasize production; red dashed line: increase in NO_3^- concentration at Cycle 85; green dashed line: increase in Fe^{2+} and Cu^{2+} concentrations at Cycle 120)

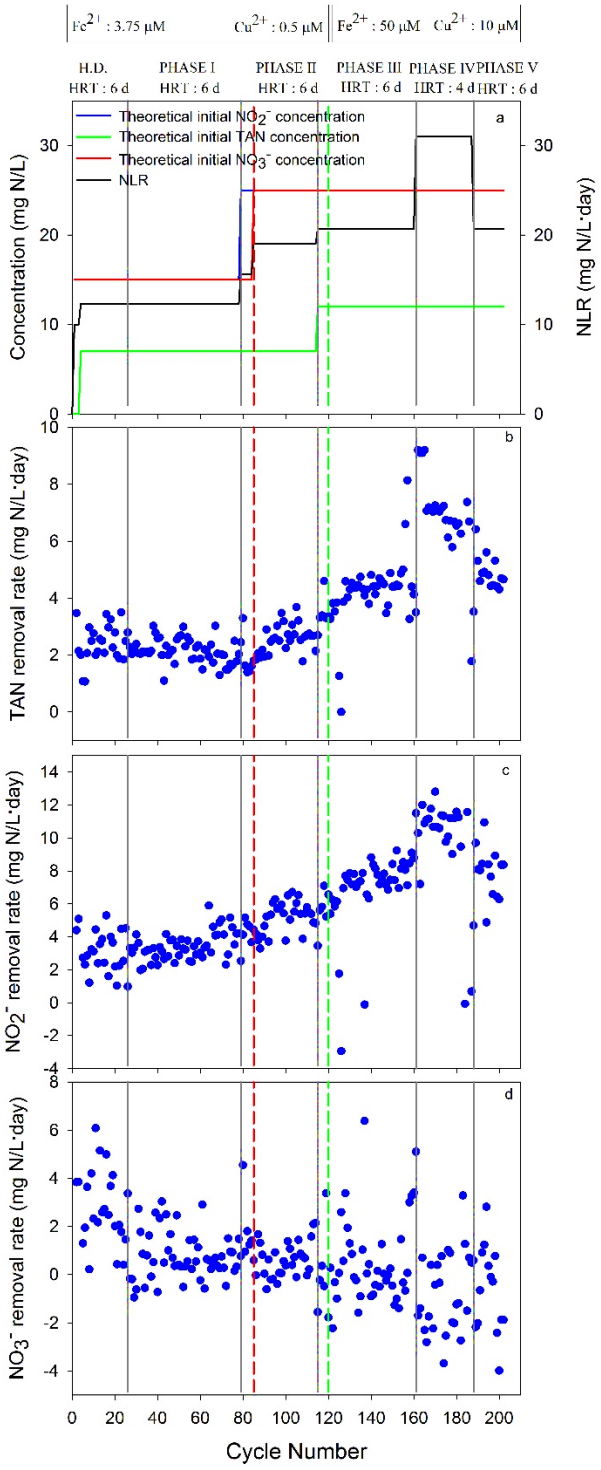

Figure 3.17 (a) Theoretical nitrogen influent concentrations and NLR. Removal rates of (b) TAN, (c) NO_2^- and (d) NO_3^- in the DAMO-Anammox SBR (The negative values imply production; red dashed line: increase in NO_3^- concentration at Cycle 85; green dashed line: increase in Fe^{2+} and Cu^{2+} concentrations at Cycle 120)

The removal efficiencies and removal rates of the nitrogen species illustrate that the Anammox microorganisms were fully functional and active in the reactor, while a fluctuation in the DAMOa and DAMOb activity was observed. The reason of low NO_3^- removal rate and efficiency were due to masking of the DAMOa activity by the Anammox activity where the NO_3^- production via Anammox masks the consumption of NO_3^-.

Nitrate removal was fluctuating, in some of the cycles a net production of NO_3^-, while in other cycles a net consumption was observed. This was due to the ability of DAMOa to consume the produced NO_3^- by the Anammox microorganisms. Although net production was visible in these cycles, the net increase in NO_3^- concentration was less than the theoretically produced NO_3^- amount due to Anammox. Therefore, DAMOa activity was present but not high enough to counteract the production of NO_3^- via the Anammox process. The results of the specific activity batch tests display the activity of each of the target microorganisms excluding the effects of the other competitive species. Therefore, the net change in all the nitrogen species, especially NO_3^-, was computed as the final concentration minus the initial concentration. Accordingly, average consumption and production rates and efficiencies were calculated as shown in Table 3.12 and Table 3.13.

Considering the influent and effluent concentration differences it can be revealed that NH_4^+ production was not observed throughout the operation of the DAMO-Anammox SBR (Table 3.12 and Table 3.13). This suggests that DNRA activity, which is the reduction of NO_3^- to NH_4^+, was not observable in the reactor. The frequency of occurrence of net NO_3^- consumption was about four-fold the occurrence of net NO_3^- production as shown in Figure 3.18. Furthermore, the average of the net NO_3^- production rate during Phase I was 1.4±0.8 mg N/L·day (Figure 3.19). Nevertheless, during Phase I, the average net consumption rate of NO_3^- was 3.4±2.7 mg N/L·day (Figure 3.19).

Table 3.12 Consumption and production rates of nitrogen species in each phase

Phase	Consumption Rate (mg N/L·day)				Production Rate (mg N/L·day)			
	TAN	NO_2^-	NO_3^-	TN[a]	TAN	NO_2^-	NO_3^-	TN[a]
I	2.2±0.4	3.4±0.9	3.4±2.7	9.0	-	-	1.4±0.8	1.4
II	2.5±0.6	5.0±0.9	3.3±2.7	10.8	-	-	1.2±1.5	1.2
III	4.3±1.0	7.2±1.3	4.6±4.9	16.1	-	1.5[b]	2.3±1.8	3.8
IV	6.9±1.6	10.6±2.6	2.7±2.8	20.2	-	0.1[b]	3.7±1.7	3.8
V	4.8±0.7	7.7±1.7	3.3±2.8	15.8	-	-	5.1±3.6	5.1

[a]Calculated as the sum of the rates of all the nitrogen species

[b]Occurred in 2 cycles in each phase due to the absence of NH_4^+ in the feed

Table 3.13 Consumption and production efficiencies of nitrogen species in each phase

Phase	Consumption Efficiency (%)				Production Efficiency (%)			
	TAN	NO_2^-	NO_3^-	TN[a]	TAN	NO_2^-	NO_3^-	TN[a]
I	94±8	74±10	26±19	65	-	-	9±6	3
II	94±6	61±7	13±11	56	-	-	5±7	2
III	96±3	84±6	13±12	64	-	25[b]	8±7	11
IV	97±15	77±9	10±9	61	-	1[b]	16±8	6
V	96±13	81±10	14±14	64	-	-	21±16	7

[a]Calculated as the average of the efficiencies of all the nitrogen species

[b]Occurred in 2 cycles in each phase due to the absence of NH_4^+ in the feed

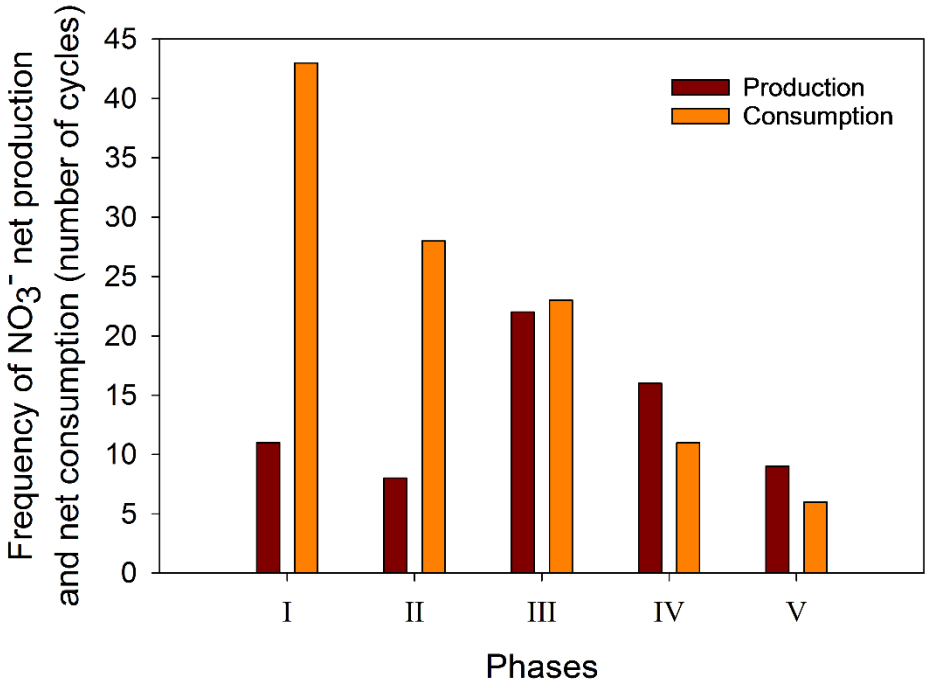

Figure 3.18 The frequency of net production and net consumption of NO_3^- in each phase of the DAMO-Anammox SBR operation

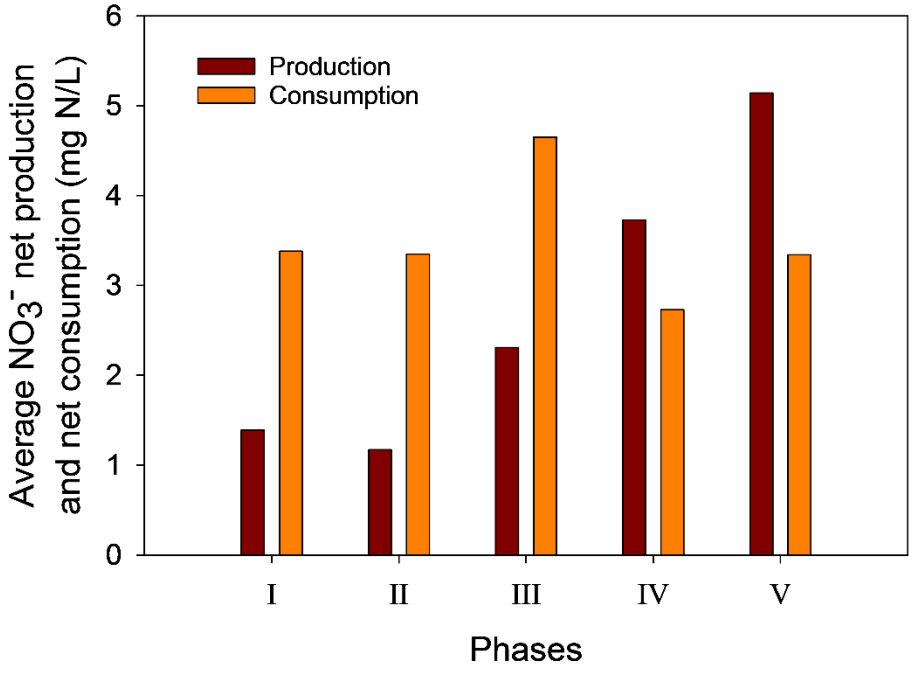

Figure 3.19 The average net production and net consumption of NO_3^- in each phase of the DAMO-Anammox SBR operation

The contribution to TN removal and the NO_2^- and NO_3^--based reaction rates calculations illustrated the dominance of Anammox, while DAMOb and DAMOa were second and third in activity, respectively. In Phase I, the TN average removal efficiency was calculated as 56±12 % while the average TN removed was calculated to be 6.3±1.3 mg N/L·day (Figure 3.20). The average $\%CATN_{removed}$ of Anammox, DAMOa and DAMOb were found to be 34±7 %, 10±7 % and 14±9 %, respectively. While the average $r_{Anammox\ NO_2^-}$, $r_{DAMOb\ NO_2^-}$ and $r_{DAMOa\ NO_3^-}$ were found to be 2.9±0.6 mg N/L·day, 1.9±1.4 mg N/L·day, and 1.4±1.0 mg N/L·day, respectively (Figure 3.22).

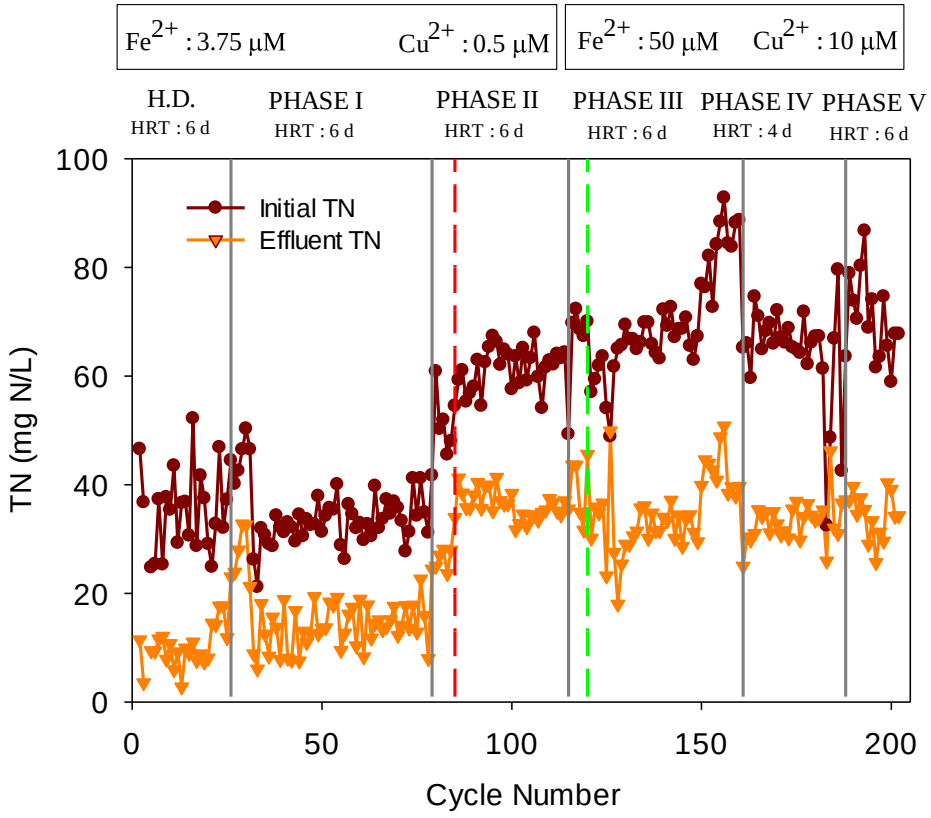

Figure 3.20 The initial and final TN concentrations in the DAMO-Anammox SBR (red dashed line: increase in NO_3^- concentration at Cycle 85; green dashed line: increase in Fe^{2+} and Cu^{2+} concentrations at Cycle 120)

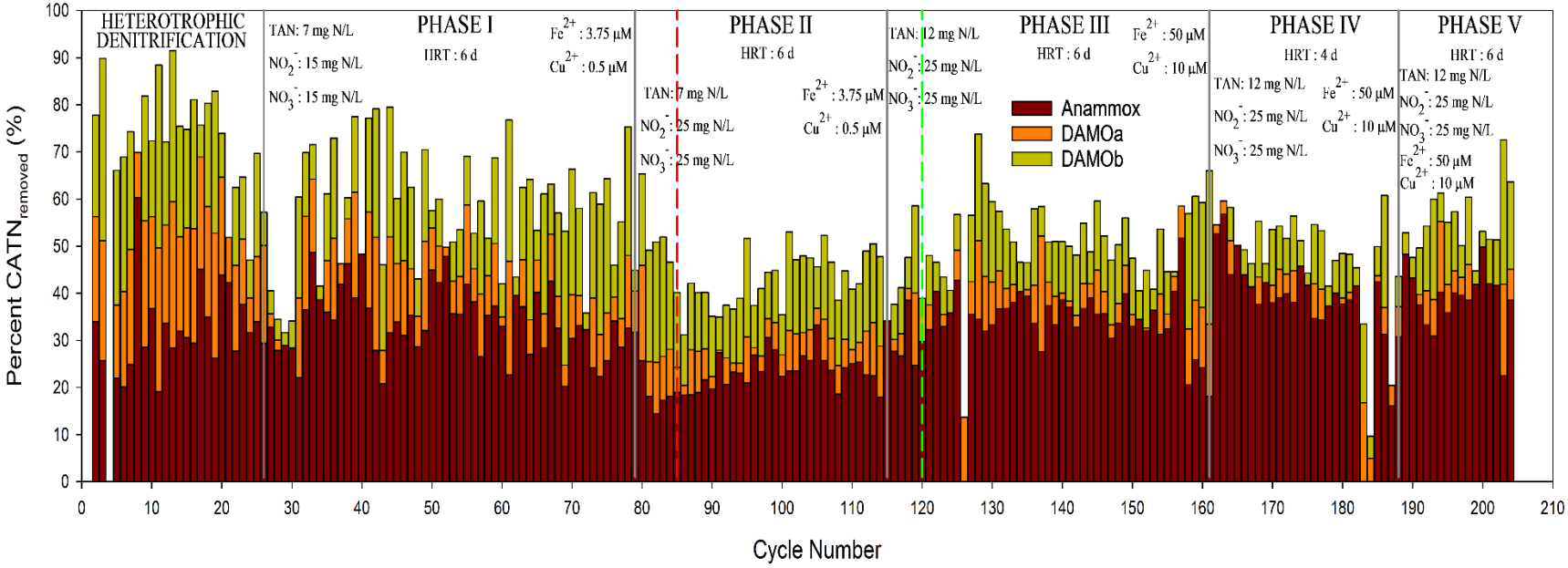

Figure 3.21 The %CATN$_{removed}$ of each microorganism (red dashed line: increase in NO_3^- concentration at Cycle 85; green dashed line: increase in Fe^{2+} and Cu^{2+} concentrations at Cycle 120)

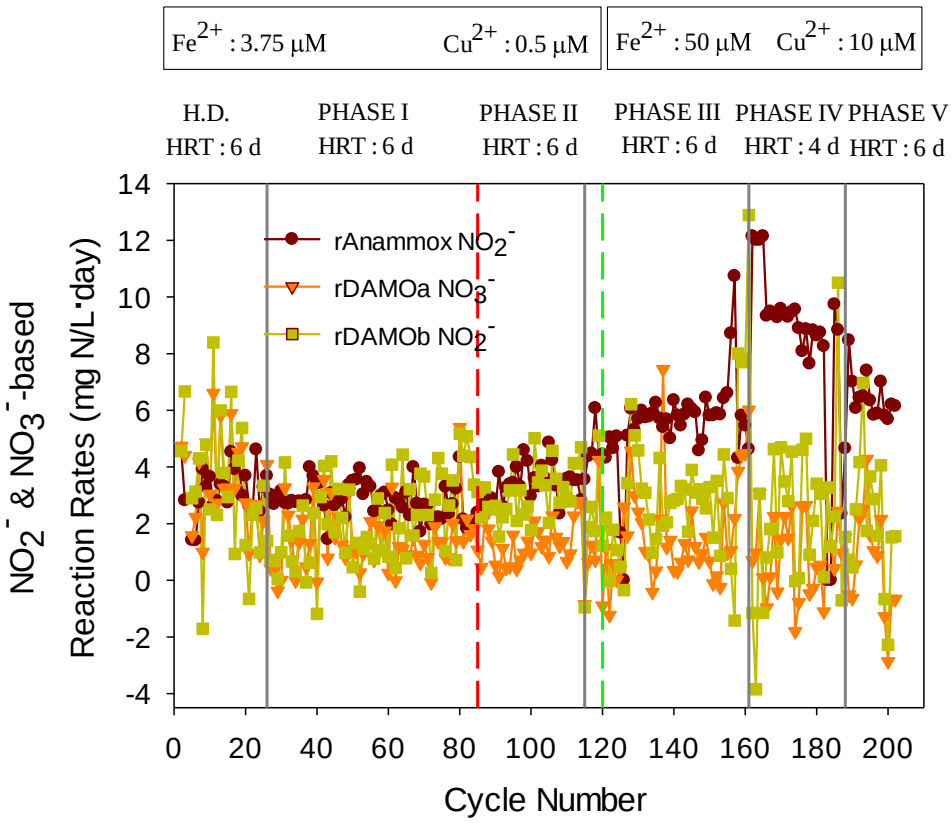

Figure 3.22 The calculated NO_2^- and NO_3^--based reaction rates of each target microorganism throughout the operation of the DAMO-Anammox SBR (red dashed line: increase in NO_3^- concentration at Cycle 85; green dashed line: increase in Fe^{2+} and Cu^{2+} concentrations at Cycle 120)

Phase I Specific Activity Test

The Phase I specific activity test was conducted using sludge extracted from the DAMO-Anammox SBR at Cycle 75. The related figures detailing the change in all nitrogen species in all the reactors with respect to the incubation period of 72 hrs are given in APPENDIX B (Figures B-1, B-2, B-3 and B-4). The summary of the results is shown in Table 3.14. The results showed that among the three target microorganisms, Anammox was the most active, while DAMOa was more active than DAMOb. The control reactor types did not show any changes with respect to liquid and gas analysis. The Denitrifiers (DEN) reactors, set up to assess the H.D.

activity, thus was not fed with CH_4, displayed negligible activity since NO_2^- concentration did not change and NO_3^- concentration decreased by about 2 mg N/L, in comparison to the other reactor types (Figure B-1a).

The nitrogen removal in the DAMX reactors, resembling the DAMO-Anammox SBR (Figure B-1c), was similar to the Anammox (AMX) reactors (Figure B-1e). As seen in Figure B-1c, the Anammox reaction was occurring dominantly before the DAMO reactions. Once the NH_4^+ is depleted, the DAMO reactions become evident. Nevertheless, an increase in the NO_2^- concentration was observed in the last 24 hr, which is speculated to be due to the DAMOa activity. Moreover, the NO_2^- concentration further decreased after the consumption of NH_4^+, this was due to the DAMOb activity. In the DAMOb reactors (Figure B-1b), the NO_2^- concentration decreased while there was a negligible change in the NO_3^- concentration. On the other hand, the results of the DAMOa reactors (Figure B-1d) illustrated a decrease in the NO_3^- concentration and an increase in NO_2^- concentration. In all the previously mentioned reactors except the DAMOb reactor, the concentration of the targeted ions reached a plateau zone.

The activities of DAMOb and DAMOa in their corresponding specific reactors was more evident than in the DAMX reactors. This is due to the presence of a dominant Anammox culture that outcompetes the DAMOb for NO_2^- and its production of NO_3^- masks the activity of DAMOa, therefore Anammox bacteria impose their activity in the reactor during Phase I.

The removal efficiencies and removal rates observed in the specific activity of Phase I resembled the ones found in the DAMO-Anammox SBR. The removal efficiencies of TAN, NO_2^- and NO_3^- in the DAMX reactors from the Phase I specific activity were 100%, 63% and 22%, respectively. In comparison the average removal efficiencies of TAN, NO_2^- and NO_3^- of the DAMO-Anammox SBR operation were 94±8 %, 74±10 % and 26±19 %, respectively. The average removal rates of TAN, NO_2^- and NO_3^- in the DAMX reactors in comparison to the DAMO-Anammox SBR were very similar. The average removal rates of TAN, NO_2^- and NO_3^- in the DAMX

reactors were 2.9, 3.7 and 0.5 mg N/L·day, respectively, while those of the DAMO-Anammox SBR were 2.2±0.4, 3.4±0.9 and 3.4±2.7 mg N/L·day, respectively.

The NO_2^- and NO_3^--based reaction rates of Anammox, DAMOb and DAMOa obtained from the DAMX reactors of the Phase I specific activity tests (Figure 3.23a) were 3.9, 1.0 and 1.2 mg N/L·day, respectively, while the average $r_{\text{Anammox } NO_2^-}$, $r_{\text{DAMOb } NO_2^-}$ and $r_{\text{DAMOa } NO_3^-}$ calculated from Phase I operation of the DAMO-Anammox SBR were 2.9±0.6, 1.9±1.4, and 1.4±1.0 mg N/L·day, respectively.

Table 3.14 Average removal rates and specific removal rates obtained via the specific activity tests performed for Phases I, II and III (negative values represent production)

Reactor	Average Removal Rates (mg N/L·day)									[a]Specific Removal Rates (mg N/g VSS·day)									Specific Removal Rates from the Literature (mg N/ g VSS·day)		
	TAN			NO_2^-			NO_3^-			TAN			NO_2^-			NO_3^-			NH_4^+	NO_2^-	NO_3^-
	I	II	III	I	II	III	I	II	III	I	II	III	I	II	III	I	II	III			
AMX	2.5	1.9	1.8	4.0	4.0	5.1	-0.5	-0.7	-1.3	1.3	0.5	1.5	2.1	1.0	4.3	-0.2	-0.2	-1.1			
DAMX	2.9	3.8	2.7	3.7	7.3	7.8	0.5	-0.9	4.1	1.5	0.9	2.2	1.9	1.8	6.5	0.2	-0.2	3.4	[5]11 & 12	[5]12	[5]12
DAMOb	-			1.9	2.2	2.6	-			-			1.0	0.5	2.2	-			-	[1]23 [2]29 [3]15-102 [4]0.7-[b]4.8	-
DAMOa	-			-1.5	-0.2	-0.1	2.1	0.7	2.6	-			-0.8	-0.04	-0.04	1.1	0.2	2.1	-	-	[1]136 [2]33 [3]7.8
DEN	-			0.0	0.9		0.7	-0.7	-1.0	-			0.0	0.2	0.6	0.4	-0.2	-0.8	-	-	-

[a]Phase I VSS = 1.93 g VSS/L Phase II VSS = 4.11 g VSS/L Phase III VSS = 1.21 g VSS/L

[b]The values were removal rates and not specific removal rates (mg N/L·day)

[1]Raghoebarsing et al. (2006); [2]Hu et al. (2009); [3]Hu et al. (2011); [4]He et al. (2014); [5]Hu et al. (2015)

- No change in concentration was observed

Table 3.15 Summary of the average NO_2^- and NO_3^--based reaction rates of the specific activity tests in Phases I, II and III

	Phase I			Phase II			Phase III		
	AMX NO_2^-	DAMOb NO_2^-	DAMOa NO_3^-	AMX NO_2^-	DAMOb NO_2^-	DAMOa NO_3^-	AMX NO_2^-	DAMOb NO_2^-	DAMOa NO_3^-
Respective reactors from Specific Activity (mg N/L·day)[a]	3.3	1.9	2.1	2.5	2.2	0.7	2.4	2.6	2.6
DAMX reactors from Specific Activity (mg N/L·day)[b]	3.9	1.0	1.2	5.0	2.4	0.1	3.5	9.0	4.8

[a] Respective reactors refers to AMX, DAMOa and DAMOb reactors

[b] DAMX reactors were fed with all the nitrogen sources and CH_4

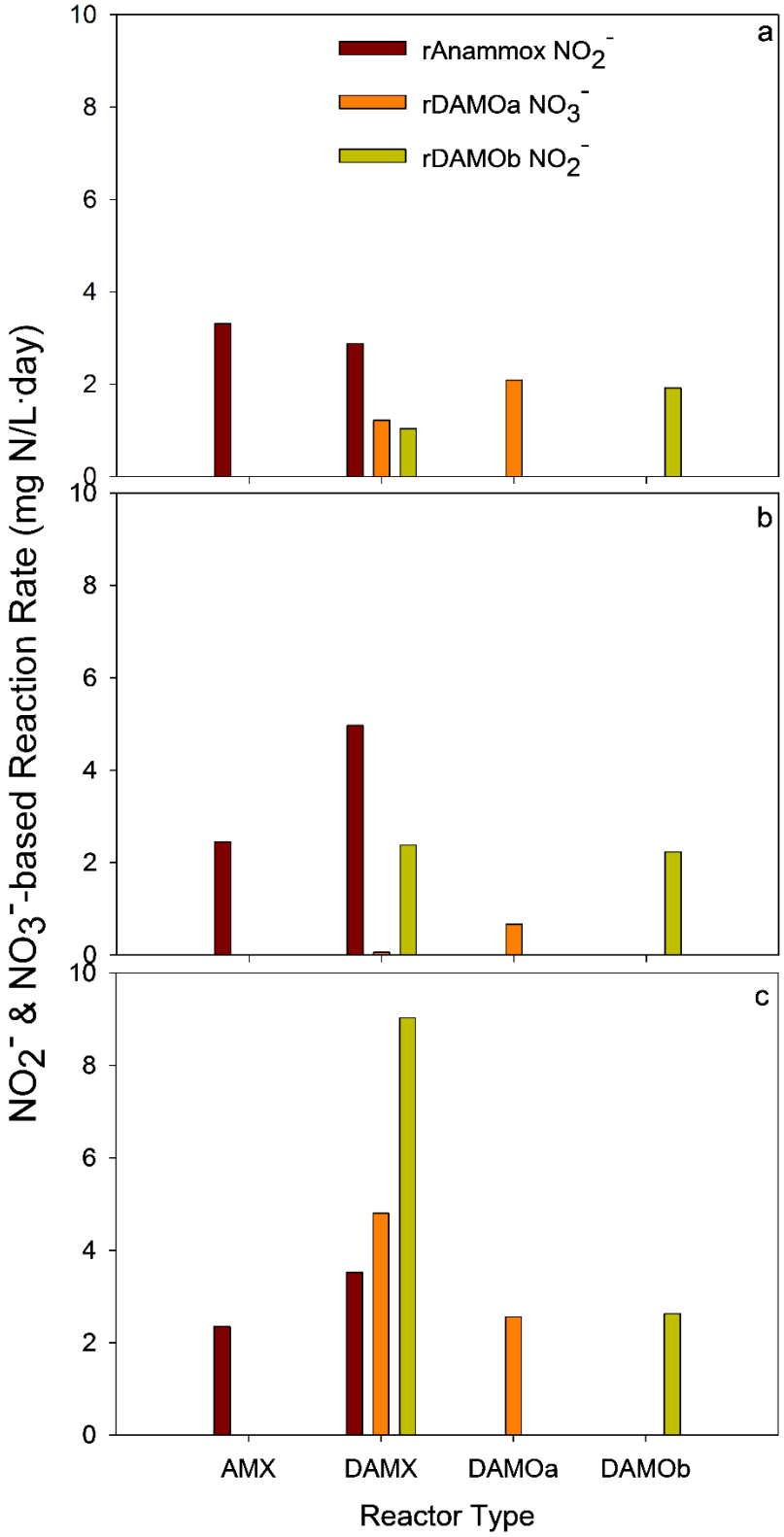

Figure 3.23 Calculated NO_2^- and NO_3^--based reaction rates from the specific activity batch tests (a) Phase I (b) Phase II (c) Phase III; AMX (Anammox), DAMX (DAMO-Anammox co-culture)

Phase II

In Phase II (Cycle 79-115), the theoretical initial concentrations of NO_2^- and NO_3^- were increased to 25 mg N/L each, while that of NH_4^+ remained at 7 mg N/L (Figure 3.15). It was aimed to support the enrichment of DAMO microorganisms over Anammox bacteria. The HRT was kept at 6 days, increasing the theoretical NLR to 19 mg N/L·day, while the average experimental NLR was 19.9±1.9 mg N/L·day (Figure 3.16a). Under these conditions, the average removal efficiencies of TAN, NO_2^- and NO_3^- were 94±6 % (Figure 3.16b), 61±7 % (Figure 3.16c) and 13±11 % (Figure 3.16d), respectively. In addition, the average removal rates of TAN, NO_2^- and NO_3^- were 2.5±0.6 (**Hata! Başvuru kaynağı bulunamadı.**b), 5.0±0.9 (**Hata! Başvuru kaynağı bulunamadı.**c) and 3.3±2.7 mg N/L·day (**Hata! Başvuru kaynağı bulunamadı.**d), respectively.

Despite the decrease in the NO_2^- average removal efficiency in Phase II compared to Phase I, Anammox was still fully functional and active in the reactor since the NH_4^+ did not decrease. Moreover, since the influent NH_4^+: NO_2^- ratio decreased from 0.47 to 0.28, limited NH_4^+ dictates the Anammox activity. Therefore, NO_2^- removal efficiency would decrease if DAMOb cannot sustain the same removal as Anammox. Furthermore, if the DAMOa activity has increased, the concentration of NO_2^- would be increasing. Similar to Phase I, the frequency of occurrence of net NO_3^- consumption was about four-fold the occurrence of net NO_3^- production (Figure 3.18). While the average of the net NO_3^- production rate slightly decreased from 1.4±0.8 to 1.2±1.5 mg N/L·day (Table 3.12). Nevertheless, during Phase II, the average net consumption rate of NO_3^- remained relatively the same as in Phase I at 3.3±2.7 mg N/L·day.

These results illustrate that although Anammox removal of NO_2^- decreased, its activity was still dominant in the reactor. This was due to the limited NH_4^+ provided. On the other hand, the activity of DAMOa slightly decreased, as observed with the decrease in the NO_3^- removal efficiency. This can be attributed to the increase in NO_2^- and NO_3^- concentrations which allowed the DAMOb a competitive advantage over Anammox and DAMOa. Since the limited NH_4^+ concentration prevented

Anammox from removing the same amount of NO_2^- as in Phase I, and DAMOb has a higher affinity to CH_4 in comparison to DAMOa.

In Phase II, the contribution of Anammox to TN removal slightly decreased in comparison to Phase I, while that of DAMOb TN removal remained higher than that of DAMOa. The contribution to TN removal and the reaction rates calculations still illustrated the dominance of Anammox, while the activity DAMOb was still higher than that of DAMOa. The total percentage of TN removed declined mainly due to the decline in Anammox contribution to the TN removal. The TN average removal efficiency was calculated as 41±6 % while the average TN removed was calculated to be 8.3±1.6 mg N/L·day (Figure 3.20). The average $\%CATN_{removed}$ of Anammox, DAMOa and DAMOb were found to be 23±4 %, 6±4 % and 15±5 %, respectively. While the average $r_{Anammox\,NO_2^-}$, $r_{DAMOb\,NO_2^-}$ and $r_{DAMOa\,NO_3^-}$ were found to be 3.3±0.8 mg N/L·day, 3.2±1.2 mg N/L·day, and 1.4±1.0 mg N/L·day, respectively (Figure 3.22).

Phase II Specific Activity Test

The Phase II specific activity test was conducted using sludge extracted from Cycle 105. The results showed that among the three target microorganisms, Anammox was the most active, while DAMOb was more active than DAMOa. The detailed results of the nitrogen species analyses are shown in Figure B-5. The control reactor types did not show any changes with respect to liquid and gas analysis. The DEN reactors, (Figure B-5a) show negligible activity due to heterotrophic compared to the other test reactors.

The AMX reactors (Figure B-5e), did not show similar activity to the Anammox activity in the DAMX reactors due to being operated at a low pH of 6.94. The low pH in these reactors occurred due to a slight increase in purging time using CO_2. The highest nitrogen removal was observed in the DAMX reactors (Figure B-5c), where initially the NO_2^- concentration decreased and the NO_3^- concentration increased, due to the Anammox reaction. Then the NO_3^- concentration slightly decreased and the NO_2^- concentration slightly increased, which is speculated to be due to the DAMOa activity. In the DAMOb reactors (Figure B-5b), the NO_2^- decreased with a negligible

change in the NO_3^- concentration. On the other hand, the results of the DAMOa reactors (Figure B-5d) exhibited a decrease in NO_3^- concentration and a slight increase in NO_2^- concentration.

The DAMOa activity was less than that in the Phase I specific activity, while that of DAMOb was higher in the Phase II specific activity tests. This signifies a shift in dominance between Phase I and Phase II due to the increase in NO_2^- and NO_3^-, while applying the same NH_4^+ concentration.

The gas analysis of the DAMX, DAMOb and DAMOa reactors of the Phase I specific activity showed CH_4 consumption of about 317, 319 and 323 μmol, respectively (Figure B-6 and Figure B-7). The CH_4 consumption in the Phase II specific activity was 2 to 10-fold the CH_4 consumption exhibited in the Phase I specific activity. This suggests that the activity of the methanotrophic microorganisms increased immensely from Phase I to Phase II. On the other hand, the DAMX and DAMOa reactors illustrated total N_2 production of about 31 and 8 μmol, respectively (Figure B-6 and Figure B-7). In the DAMOb, inexplicably, showed N_2 consumption of about 8 μmol. CH_4 production was still observed in Phase II, suggesting the existence of methanogenic microorganisms in the consortium.

The removal efficiencies and removal rates observed in the specific activity of Phase II resembled the ones found in the DAMO-Anammox SBR except for NO_3^-. The removal efficiencies of TAN, NO_2^- and NO_3^- in the DAMX reactors from the Phase II specific activity were 89%, 72% and -12%, respectively. In comparison the average removal efficiencies of TAN, NO_2^- and NO_3^- of the DAMO-Anammox SBR operation were 94±6 %, 61±7 % and 13±11 %, respectively. Nevertheless, the average removal efficiency of NO_3^- from the DAMOa reactors in the Phase II specific activity (9%) resembled that of the DAMO-Anammox SBR. The average removal rates of TAN, NO_2^- and NO_3^- in the DAMX reactors in comparison to the DAMO-Anammox SBR were very similar. The average removal rates of TAN, NO_2^- and NO_3^- in the DAMX reactors were 3.8, 7.3 and -0.9 mg N/L·day, respectively, while those of the DAMO-Anammox SBR were 2.5±0.6, 5.0±0.9 and 3.3±2.7 mg N/L·day, respectively. While the average removal rate of NO_3^- in the DAMOa reactors was 0.7 mg N/L·day. This suggests that the activity of DAMOa diminished

in the co-culture, but when provided the opportunity in less competitive and more favorable conditions, by only providing NO_3^- as the nitrogen source, DAMOa becomes prevalent.

The average $r_{Anammox\ NO_2^-}$, $r_{DAMOb\ NO_2^-}$ and $r_{DAMOa\ NO_3^-}$ computed from DAMX reactors in Phase II specific activity test were 5.0, 2.4 and 0.1 mg N/L·day, respectively (Figure 3.23b). In comparison the average $r_{Anammox\ NO_2^-}$, $r_{DAMOb\ NO_2^-}$ and $r_{DAMOa\ NO_3^-}$ from Phase II operation of the DAMO-Anammox SBR were 3.3±0.8, 3.2±1.2, and 1.4±1.0 mg N/L·day, respectively.

Phase III

In Phase III (Cycle 116-160), an increase in the theoretical initial concentrations of NH_4^+ from 7 to 12 mg N/L was planned. Yet, keeping the concentrations of NO_2^- and NO_3^- at 25 mg N/L each (Figure 3.15). The HRT was kept at 6 days, subsequentially increasing the NLR to 20.7 mg N/L·day while the average experimental NLR was 23.4±3.1 mg N/L·day (Figure 3.16a). Nevertheless, after observing a reduction in activity of the target microorganisms, especially DAMOa, an increase in the concentrations of Fe^{2+} and Cu^{2+} was opted for. The initial concentrations of Fe^{2+} and Cu^{2+} were increased from 3.75 to 50 µM and 0.5 to 10 µM, respectively. The average removal efficiencies of TAN, NO_2^- and NO_3^- were 96±3 % (Figure 3.16b), 84±6 % (Figure 3.16c) and 13±12 % (Figure 3.16d), respectively. In addition, the average removal rates of TAN, NO_2^- and NO_3^- were 4.3±1.0 (**Hata! Başvuru kaynağı bulunamadı.**b), 7.2±1.3 (**Hata! Başvuru ka ynağı bulunamadı.**c) and 4.6±4.9 mg N/L·day (**Hata! Başvuru kaynağı bulunamadı.**d), respectively.

The Effect of Fe^{2+} and Cu^{2+} on the DAMO-Anammox Co-culture

The increased initial Fe^{2+} and Cu^{2+} concentrations should improve the activity of the three target microorganisms. Since the optimum Fe^{2+} concentration for Anammox, DAMO archaea (DAMOa) and DAMO bacteria (DAMOb) was found to be 80 µM, 80 µM and 20 µM, respectively (Lu et al., 2018). After the increase in Fe^{2+} and Cu^{2+} concentrations, the NO_3^- removal efficiency increased due to favorable conditions for DAMOa. Nevertheless, these conditions were also favorable for Anammox and

once again Anammox production of NO_3^- dominated over its removal. Improved activity of the three target microorganisms was observed after the increase in Fe^{2+} and Cu^{2+} concentrations, however, due to the Anammox dominance the increase in activity was not observable in DAMO-Anammox SBR as in the specific activity tests. The specific activity tests evidently displayed the increase in DAMOb and DAMOa activity. These results comply with the results shown in the work of Lu et al. (2018) and Luesken et al. (2011), where higher Fe^{2+} and Cu^{2+} concentrations were employed than in Ettwig et al. (2009) and that improved the activity of the DAMO and Anammox microorganism.

To better differentiate the effect of Fe on Anammox activity, that is if it was due to an additional Feammox activity or enzyme-related increase in Anammox bacteria, specific activity tests can be performed with Fe control reactors, which remains to be investigated.

The average removal efficiencies of TAN and NO_2^- increased from 94±6 % to 96±3 % and from 61±7 % to 84±6 %, respectively, from Phase II to Phase III (Table 3.13). Meanwhile, the average removal rates of TAN and NO_2^- increased from 2.5±0.6 to 4.3±1.0 mg N/L·day and 5.0±0.9 to 7.2±1.3 mg N/L·day, respectively, from Phase II to Phase III (Table 3.12). This may be caused by the increase in theoretical initial NH_4^+ concentration from 7 to 12 mg N/L, which improved the NO_2^- removal by the Anammox bacteria. Nevertheless, the increase in Fe^{2+} and Cu^{2+} concentrations may have also aided the activity of DAMOb.

The frequency of occurrence of NO_3^- net production increased from 22% to 49% of the cycles in Phase III, while NO_3^- net consumption reached 51%, as shown in Figure 3.18. However, the average NO_3^- consumption rate increased from 3.3±2.7 mg N/L in Phase II to 4.6±4.9 mg N/L in Phase III, which was about double the average net production rate (2.3±1.8 mg N/L), as shown in Table 3.12. This signifies that the ability of NO_3^- removal improved due to the increase in Fe^{2+} and Cu^{2+} concentrations. The average removal efficiency of NO_3^- remained the same from Phase II to Phase III at 13±11 % (Table 3.13). This was due to the increased Anammox activity which increased the NO_3^- production. This can be seen in the average production efficiency of NO_3^- which increased from 5±7 % in Phase II to

8±7 % in Phase III. On the other hand, despite the increased in the average NO_3^- removal rate from 3.3±2.7 mg N/L·day in Phase II to 4.6±4.9 mg N/L·day in Phase III (Figure 3.16). When considering only the cycles in which net NO_3^- removal had occurred, the average consumption rate of NO_3^- increased from 3.3±2.7 mg N/L·day in Phase II to 4.6±4.9 mg N/L·day. Meanwhile considering only the cycles where net NO_3^- production had occurred, the average production rate increased as well from 1.2±1.5 mg N/L·day in Phase II to 2.3±1.8 mg N/L·day in Phase III (Table 3.12).

In Cycle 126, with the absence of NH_4^+ in the feed, the DAMOa removal of NO_3^- was evident reaching a removal efficiency of 27%. The absence of Anammox activity during this cycle cleared the masking effect caused on the DAMOa removal of NO_3^-. Although both NO_2^- and NO_3^- were present in the feed in the same cycle, DAMOa activity was prevalent over DAMOb activity since an increase in NO_2^- concentration was observed.

The average TN removed in Phase III was calculated to be 11.6±2.8 mg N/L□day (Figure 3.20). The total percentage of TN removed increased from Phase II back to the levels observed in Phase I, after the increase in NH_4^+ concentration, which allowed more nitrogen removal via Anammox. Moreover, the increase in Fe^{2+} and Cu^{2+} concentrations to levels favorable for Anammox and DAMOa might have increased their contribution to TN removal. The average $\%CATN_{removed}$ of Anammox increased to 34±8 % (Figure 3.21). However, the average $\%CATN_{removed}$ of DAMOb decreased to 11±5 % (Figure 3.21). On the other hand, the average $\%CATN_{removed}$ of DAMOa was relatively the same as in Phase II at 6±5 % (Figure 3.21).

The average $r_{\text{Anammox } NO_2^-}$ increased from 3.3±0.8 mg N/L·day in Phase II to 5.5±1.5 mg N/L·day in Phase III. Meanwhile the average $r_{\text{DAMOb } NO_2^-}$ slightly decreased from 3.2±1.2 mg N/L·day in Phase II to 2.8±2.0 mg N/L·day in Phase III, due to the increased Anammox activity. On the other hand, the average $r_{\text{DAMOa } NO_3^-}$ increased from 1.4±1.0 mg N/L·day in Phase II to 1.5±1.7 mg N/L·day in Phase III, as shown in Figure 3.22.

Phase III Specific Activity Test

The Phase III specific activity test was conducted using sludge extracted from Cycle 145. Amongst the three target microorganisms, Anammox was the most active, while DAMOa and DAMOb were relatively similar in activity. The detailed results of the nitrogen species analyses are shown in Figure B-8. The control reactor types did not show any changes with respect to liquid and gas analysis. The DEN reactors, (Figure B-8a) show negligible activity due to heterotrophic compared to the other test reactors.

In the AMX reactors (Figure B-8e), the NH_4^+ and NO_2^- concentrations decreased throughout the experiment. The increase in NO_3^- concentration which is a by-product of the Anammox process was also visible. The nitrogen removal in the DAMX reactors (Figure B-8c) was slightly higher than the AMX reactors. The concentration of NO_2^- in the DAMX reactors decreased to levels lower than in the AMX reactors which suggests that DAMOb was responsible for this difference between DAMX and AMX reactors. The NO_3^- concentration increased due to the Anammox process by the 36th hour but then decreased due to the DAMOa activity (Figure B-8c). In the DAMOb reactors (Figure B-8b), the NO_2^- decreased, while a negligible change was observed in the NO_3^- concentration. On the other hand, the results of the DAMOa reactors (Figure B-8d) illustrated a decrease in NO_3^- concentration. The gas analysis for the Phase III specific activity test was not conducted due to the malfunction of the GC machine during the run of the experiment.

The removal efficiencies and removal rates of TAN observed in the specific activity of Phase III were lower than those found in the DAMO-Anammox SBR. While the removal efficiencies and removal rates of NO_2^- and NO_3^- from the specific activity were higher than those observed from the DAMO-Anammox SBR operation. The removal efficiencies of TAN, NO_2^- and NO_3^- in the DAMX reactors from the Phase III specific activity were 71%, 79% and 45%, respectively. In comparison the average removal efficiencies of TAN, NO_2^- and NO_3^- of the DAMO-Anammox SBR operation were 96±3 %, 84±6 % and 13±12 %, respectively. The average removal

rates of TAN, NO_2^- and NO_3^- in the DAMX reactors in comparison to the DAMO-Anammox SBR were very similar. The average removal rates of TAN, NO_2^- and NO_3^- in the DAMX reactors were 2.7, 7.8 and 4.1 mg N/L·day, respectively, while those of the DAMO-Anammox SBR were 4.3±1.0, 7.2±1.3 and 4.6±4.9 mg N/L·day, respectively. This shows that the activity of Anammox was lower in the DAMX reactors in comparison to the DAMO-Anammox SBR, while the activity of DAMOa was very similar in both the DAMX reactors from the specific activity test and the DAMO-Anammox SBR.

The Phase III specific activity average $r_{Anammox\ NO_2^-}$, $r_{DAMOb\ NO_2^-}$ and $r_{DAMOa\ NO_3^-}$ from the DAMX reactors were 3.5, 9.0 and 4.8 mg N/L·day, respectively, as seen from Figure 3.23c. In contrast, the average $r_{Anammox\ NO_2^-}$, $r_{DAMOb\ NO_2^-}$ and $r_{DAMOa\ NO_3^-}$ in Phase III operation of the DAMO-Anammox SBR were 5.5±1.5, 2.8±2.0 and 1.5±1.7 mg N/L·day, respectively.

The results attained from the NO_2^- and NO_3^--based reaction rate calculations from the specific activity batch tests performed in Phase II and Phase III clearly illustrated an increase in the $r_{DAMOa\ NO_3^-}$ in the DAMOa batch reactors from 0.7 mg N/L·day in Phase II to 2.6 mg N/L·day in Phase III (Figure 3.23). Moreover, the $r_{DAMOa\ NO_3^-}$ in the DAMX batch reactors increased from 0.1 mg N/L·day in Phase II to 4.8 mg N/L·day in Phase III, as shown in Figure 3.23. On the other hand, the $r_{Anammox\ NO_2^-}$ in the AMX batch reactors slightly decreased from 2.5 mg N/L·day in Phase II to 2.4 mg N/L·day in Phase III, due to the low pH applied in Phase II specific activity, as shown in Figure 3.23. In addition, the $r_{Anammox\ NO_2^-}$decreased in the DAMX batch reactors from 5.0 mg N/L·day in Phase II to 3.5 mg N/L·day in Phase III. Meanwhile, in the DAMX batch reactors the $r_{DAMOb\ NO_2^-}$ reaction rate increased about four-fold from 2.4 mg N/L·day in Phase II to 9.0 mg N/L·day in Phase III. However, the calculated $r_{DAMOb\ NO_2^-}$ in the DAMOb batch reactors showed comparatively a smaller increase from 2.2 mg N/L·day in Phase II to 2.6 mg N/L·day in Phase III (Figure 3.23).

The maximum specific removal rates of NH_4^+, NO_2^- and NO_3^- achieved by Hu et al. (2015) were 12, 12 and 12 mg N/ g VSS·day, respectively. The specific average

removal rates calculated from the specific activity batch tests in this study were lower than the values found in the literature. The removal rates found in the literature were of reactors inoculated with pre-enriched sludge that contained much higher DAMOb and DAMOa content compared to the sludge used in this study. Nevertheless, the reaction rates from Hu et al. (2015) were comparable with the reaction rates calculated in this study.

Phase IV

In Phase IV (Cycle 161-188), the initial theoretical NH_4^+, NO_2^- and NO_3^- concentrations were kept at 12, 25 and 25 mg N/L. Yet the HRT was decreased from 6 to 4 days, subsequentially increasing the NLR to 31 mg N/L·day while the average experimental NLR increased to 32.2±4.8 mg N/L·day (Figure 3.16a). The average removal efficiency of TAN slightly increased to 97±15 % (Figure 3.16b). Despite the slight increase in the average TAN removal efficiency, the NO_2^- average removal efficiency decreased to 77±9 % (Figure 3.16c). This decrease in NO_2^- average removal efficiency may be associated with a decrease in DAMOb activity. In addition, the average NO_3^- removal efficiency decreased to 10±9 % (Figure 3.16d). Likewise, the average TAN removal rate increased to 6.9±1.6 mg N/L·day (**Hata! B aşvuru kaynağı bulunamadı.**b), after the increase in the NLR. Despite the decrease in the average NO_2^- removal efficiency in Phase IV, the average NO_2^- removal rate increased to 9.9±2.6 mg N/L·day (**Hata! Başvuru kaynağı bulunamadı.**c). In addition, the average removal rate of NO_3^- decreased to 2.7±2.8 mg N/L·day (**Hata! Başvuru kaynağı bulunamadı.**d).

In Phase IV, the frequency of net production of NO_3^- became more prominent than the frequency of net consumption of NO_3^- as shown in Figure 3.18. The consumption efficiency and consumption rate of NO_3^- decreased to 10±9 % (Table 3.13) and 2.7±2.8 mg N/L·day (Table 3.12), respectively, after the reduction in HRT. On the other hand, the production efficiency and production rate of NO_3^- increased to 16±8 % (Table 3.13) and 3.7±1.7 mg N/L·day (Table 3.12), respectively. This signifies that the production of NO_3^- by Anammox bacteria were able to cope with the increase in NLR, which caused a decrease in DAMOb activity due to the competition.

Meanwhile DAMOa was not able to cope with the increased NO_3^- production by Anammox under an HRT of 4 days.

In order to clearly observe the DAMOa activity, in Cycle 183, NH_4^+ and NO_2^- were not added in the feed, while in Cycle 184 only NH_4^+ was not added in the feed. In both Cycle 183 and Cycle 184 the NO_3^- concentration decreased while that of NO_2^- remained relatively the same. About 7 mg N/L of NO_3^- was consumed in Cycle 183 and about 3 mg N/L was consumed in Cycle 184.

The average TN removed calculated in Phase IV was 15.7±5.4 mg N/L·day (Figure 3.20). Moreover, the average TN removal percentage decreased from 49±10 % in Phase III to 47±13% in Phase IV after the decrease in HRT to 4 days. The average $\%CATN_{removed}$ of Anammox increased from 34±8 % to 37±13 %. While the average $\%CATN_{removed}$ of DAMOb and DAMOa diminished to 8±7 % and 4±4 %, respectively, due to the reduced HRT of 4 days. This outcome indicates that the cycle period of 2 days was not adequate for the DAMO activity, in comparison to the Anammox activity. Meanwhile, the average $r_{Anammox\,NO_2^-}$ reached 9.1±2.2 mg N/L·day, while the average $r_{DAMOb\,NO_2^-}$ and $r_{DAMOa\,NO_3^-}$ decreased to 2.6±3.4 mg N/L·day and 1.1±1.7 mg N/L·day, respectively, after the decrease in HRT from 6 days to 4 days.

After observing a clear increase in Anammox activity on behalf of the DAMO microorganisms, an increase of HRT back to 6 days was opted for, which might aid the activity of the DAMO microorganisms and increase their contribution to the TN removal.

Phase V

In Phase V (Cycle 189-202), the initial theoretical NH_4^+, NO_2^- and NO_3^- concentrations were kept at 12, 25 and 25 mg N/L. Yet the HRT was increased back to 6 days from 4 days in Phase IV, subsequentially decreasing the theoretical NLR and the average experimental NLR back to 20.7 mg N/L·day and 23.5±2.6 mg N/L·day, respectively (Figure 3.16a). The average removal efficiency of TAN slightly decreased back to the same level as Phase III at 96±13 % (Figure 3.16b). The NO_2^- average removal efficiency increased to 81±10 % in Phase V after the

increase in HRT back to 6 days (Figure 3.16c). While the average NO_3^- removal efficiency further decreased to 14±14 % (Figure 3.16d). Likewise, the average TAN removal rate decreased to 4.8±0.7 mg N/L·day, back to Phase III levels, as displayed in (**Hata! Başvuru kaynağı bulunamadı.**b). On the other hand, the average NO_2^- r emoval rate increased to 7.7±1.7 mg N/L·day in Phase V (**Hata! Başvuru kaynağı bulunamadı.**c). Meanwhile, the average NO_3^- removal rate remained at 3.3±2.8 mg N/L·day (**Hata! Başvuru kaynağı bulunamadı.**d).

Although the NO_3^- average removal efficiency and average removal rate was 14±14% and 3.3±28 mg N/L·day, respectively, in Phase V, which indicates an average net production of NO_3^-. The consumption efficiency of NO_3^- increased from 10±9 % in Phase IV to 14±14 % in Phase V (Table 3.13). While the consumption rate of NO_3^- increased from 2.7±2.8 mg N/L·day in Phase IV to 3.3±2.8 mg N/L·day in Phase V (Table 3.12)

In Phase V, the frequency of net production of NO_3^- remained more prominent than the frequency of net consumption of NO_3^- as in Phase IV (Figure 3.18). However, both the consumption efficiency and production efficiency of NO_3^- increased to 14±14 % and 21±16 %, respectively (Table 3.13). Likewise, the consumption rate and production rate of NO_3^- increased to 3.3±2.8 and 5.1±3.6 mg N/L·day, respectively (Table 3.12).

The average TN removal rate was calculated in Phase V was 12.0±2.7 mg N/L□day. The average percentage TN removed increased to 51±8 % in Phase V. A slight increase was observed in DAMOa and DAMOb contribution to the TN removal shown in Figure 3.21. The average $\%CATN_{removed}$ of Anammox, DAMOa and DAMOb, in Phase V, were 40±5 %, 4±4 % and 9±5 %, respectively. Meanwhile, in Phase V, the average $r_{Anammox\,NO_2^-}$ witnessed a decrease to reach 6.1±1.0 mg N/L·day, while the average $r_{DAMOb\,NO_2^-}$ and $r_{DAMOa\,NO_3^-}$ decreased slightly to 2.6±2.5 mg N/L·day and 1.0±2.0 mg N/L·day, respectively.

The Effects of HRT and NLR on the DAMO-Anammox Co-culture

The Anammox activity increased with the increase in NLR (decrease in HRT). The DAMOb activity, on the other hand, decreased due to the competition by Anammox

over NO_2^-. Furthermore, the increased Anammox activity caused an increase in NO_3^- production that DAMOa could not cope with in the shorter cycle period, hence, a decrease in DAMOa activity was observed.

The average TN percentage removed displayed a decline from 49% in Phase III to 47% in Phase IV. Nevertheless, the average $\%CATN_{removed}$ of Anammox to the TN removal, it increased from 34% in Phase III to 37% in Phase IV. On the other hand, the average $\%CATN_{removed}$ of DAMOb and DAMOa decreased from 11 % in Phase III to 8% in Phase IV and from 6% in Phase III to 4 % in Phase IV, respectively.

With the decrease in HRT, the dominance of Anammox was also evident through the average NO_2^- and NO_3^--based reaction rate calculations. The average $r_{Anammox\ NO_2^-}$ increased from 5.5 mg N/L·day in Phase III to 9.1 mg N/L·day in Phase IV. While the average $r_{DAMOb\ NO_2^-}$ and $r_{DAMOa\ NO_3^-}$ decreased from 2.8 mg N/L·day in Phase III to 2.6 mg N/L·day in Phase IV and 1.5 mg N/L·day in Phase III to 1.1 mg N/L·day in Phase IV, respectively. The main reason behind the decrease in the average $r_{DAMOb\ NO_2^-}$ and $r_{DAMOa\ NO_3^-}$ compared to the average $r_{Anammox\ NO_2^-}$ was that they did not have enough reaction time during the 2-day cycle period.

After the increase in HRT back to 6 days in Phase V, the average TN removed rose to 51 %. The average % $CATN_{removed}$ of Anammox increased to 40 % while that of DAMOb and DAMOa were 9 % and 4 %, respectively. The average $r_{Anammox\ NO_2^-}$ experienced a decrease to 6.1 mg N/L·day, while the average $r_{DAMOb\ NO_2^-}$ and $r_{DAMOa\ NO_3^-}$ remained relatively the same at 2.6 mg N/L·day and 1.0 mg N/L·day, respectively. In Phase V, the contribution to the TN removal and the NO_2^- and NO_3^--based reaction rates seemed to revert gradually to levels achieved in Phase III.

In comparison to the Anammox SBR, the TAN average removal efficiency in the DAMO-Anammox SBR was similar, nevertheless, the average NO_2^- removal efficiency in the Anammox SBR (93 %) was higher than that of the DAMO-Anammox SBR (81 %). Moreover, the TAN and NO_2^- average removal rates in the Anammox SBR, 15.3 and 22.7 mg N/L·day respectively, were higher than the that of the DAMO-Anammox SBR (6.9 and 9.9 mg N/L·day, respectively). This indicates that the Anammox bacteria were more active in the Anammox SBR. This was due

to the fact that the Anammox SBR was supplied with adequate NH_4^+ for the Anammox consumption of NO_2^-, while in the DAMO-Anammox limited NH_4^+ was supplied and the NO_2^- removal was shared by Anammox and DAMOb. Moreover, the highest $r_{Anammox\ NO_2^-}$ in the DAMO-Anammox SBR was found to be 12.1 mg N/L·day in Phase IV. This was less than the average $r_{Anammox\ NO_2^-}$ in the Anammox SBR, which was 21.7 mg N/L·day.

In comparison to similar studies performed in the literature, the removal rates achieved in this study were lower than those found in He et al. (2014), Hu et al. (2015) and Fu et al. (2017a), nevertheless, they were relatively comparable despite the microbial consortium of the previously mentioned contained higher content of *M. nitroreducens* and *M. oxyfera* than in this thesis.

He et al. (2014), setup three SBRs inoculated with different seed source each containing *M. oxyfera*. Methanogenic sludge, paddy soil and freshwater sediment were used. The reactors were provided with NO_2^- (7-21 mg N/L) and operated at an HRT of 6 days. The NO_2^- removal rate achieved was between 0.7-4.8 mg N/L·day which is comparable to the DAMOb average removal rates achieved in this study.

Two SBRs were established by Hu et al. (2015), one fed with NH_4^+ (0.21 g N/L), NO_2^- (6.6-20 mg N/L) and CH_4 while the second was fed with NH_4^+ (0.21 g N/L), NO_3^-(0.21 g N/L) and CH_4. The reactors were operated at an HRT of 112 days. The removal rates of NH_4^+ and NO_2^- achieved in the first reactor were 13.3 and 13.1 mg N/L□day, respectively. On the other hand, the removal rates of NH_4^+ and NO_3^- attained in the second reactor were 11.7 and 13.0 mg N/L·day, respectively. Furthermore, the calculated average $r_{Anammox\ NO_2^-}$ and $r_{DAMOa\ NO_3^-}$ from the first reactor were found to be 15.4 mg N/L·day and 9.9 mg N/L·day, respectively, while negligible activity was observed for DAMOb after 80 days of operation. On the other hand, the calculated average$r_{Anammox\ NO_2^-}$ and $r_{DAMOa\ NO_3^-}$ from the second reactor were found to be about 24 mg N/L·day and 4.4 mg N/L·day, respectively, while that of DAMOb was about 8.75 mg N/L·day up to Day 75 of operation and then gradually decreased to become negligible by Day 125.

In addition, Fu et al. (2017a) set a batch reactor fed with NH_4^+ (50 mg N/L), NO_2^- (10 mg N/L) and NO_3^- (50 mg N/L), operated at an HRT of 90 days. The achieved NH_4^+, NO_2^- and NO_3^- removal rates were 28, 37 and 41 mg N/L·day, respectively.

Furthermore, the denitrification rate was calculated using the VSS was found to be 6.3 mg N/g VSS·day. These denitrification rates computed were about 3-fold less than the denitrification rate found in Hu et al. (2015) and two orders of magnitude lower than the denitrification rates attainable using methanol (Nyberg et al., 1996).

The main reasons behind lower removal rates attained in this study compared to the literature were the content of the DAMO microorganisms in the inoculum to begin with and the reactor configuration which plays an important role in the CH_4 availability to the DAMO microorganisms. In addition, the applied HRT in the mentioned studies above was much higher than that applied in this study. This permitted more time for the DAMO activity. It should be also noted that the microorganisms, in particular, the DAMO cultures' abundance, may differ in the studies, which requires to reveal the specific rates. However, because the content of the DAMO in the population is not known, one should be careful while comparing the data because the VSS concentration would not totally reveal the DAMO abundance.

3.3.2.1.3 Determination of the Stoichiometric Ratio of the Microbial Consortium

The theoretical and experimental molar ratios were calculated according to Section 3.2.2.4 and the results are shown in Figure 3.24. The reactor status in terms of the composition of the co-culture was assessed by comparing the experimental stoichiometric ratio obtained in the reactor to the theoretical ratios of the different consortium cases. In each ratio graph, there are three general zones, one dominated by AMX or AMX & DAMOb, another dominated by AMX & DAMOa and a third zone lying in between the DAMX and *DAMX ratios representing the co-culture with various combinations of microbial composition.

$\Delta NO_2^-/\Delta NH_4^+$ molar ratio

According to the $\Delta NO_2^-/\Delta NH_4^+$ molar ratio (Figure 3.24a), the reactor had less fluctuation in Phases II, III, IV and V compared to Phase I. The average $\Delta NO_2^-/\Delta NH_4^+$ experimental ratio in Phase I was 1.64, which indicates that the co-culture was in the region AMX or DAMX, and *DAMX. This illustrates that Anammox activity was higher than the activity of the DAMO microorganisms and that DAMOa and DAMOb activity were relatively similar, as the results of the removal efficiencies and removal rates of Section 3.3.2.1.2 verified. This is also observed in the results of the TN removal contribution in Section 3.3.2.1.2. During Phase II, the average $\Delta NO_2^-/\Delta NH_4^+$ molar ratio was 2.11. This ratio signifies that the microbial consortium was between AMX & DAMOb and *DAMX, which means a decreasing DAMOa dominance in comparison with DAMOb. Although both NO_2^- and NO_3^- concentrations were both increased in Phase II, DAMOb proliferation was more prominent than DAMOa. Furthermore, in Phase III, the average $\Delta NO_2^-/\Delta NH_4^+$ molar ratio decreased to 1.68 going back to the same region of Phase I. In Phase IV, the average $\Delta NO_2^-/\Delta NH_4^+$ ratio decreased to 1.58 and then increased slightly to 1.60 in Phase V. The microbial consortium stayed in the same region as in Phase III and Phase I.

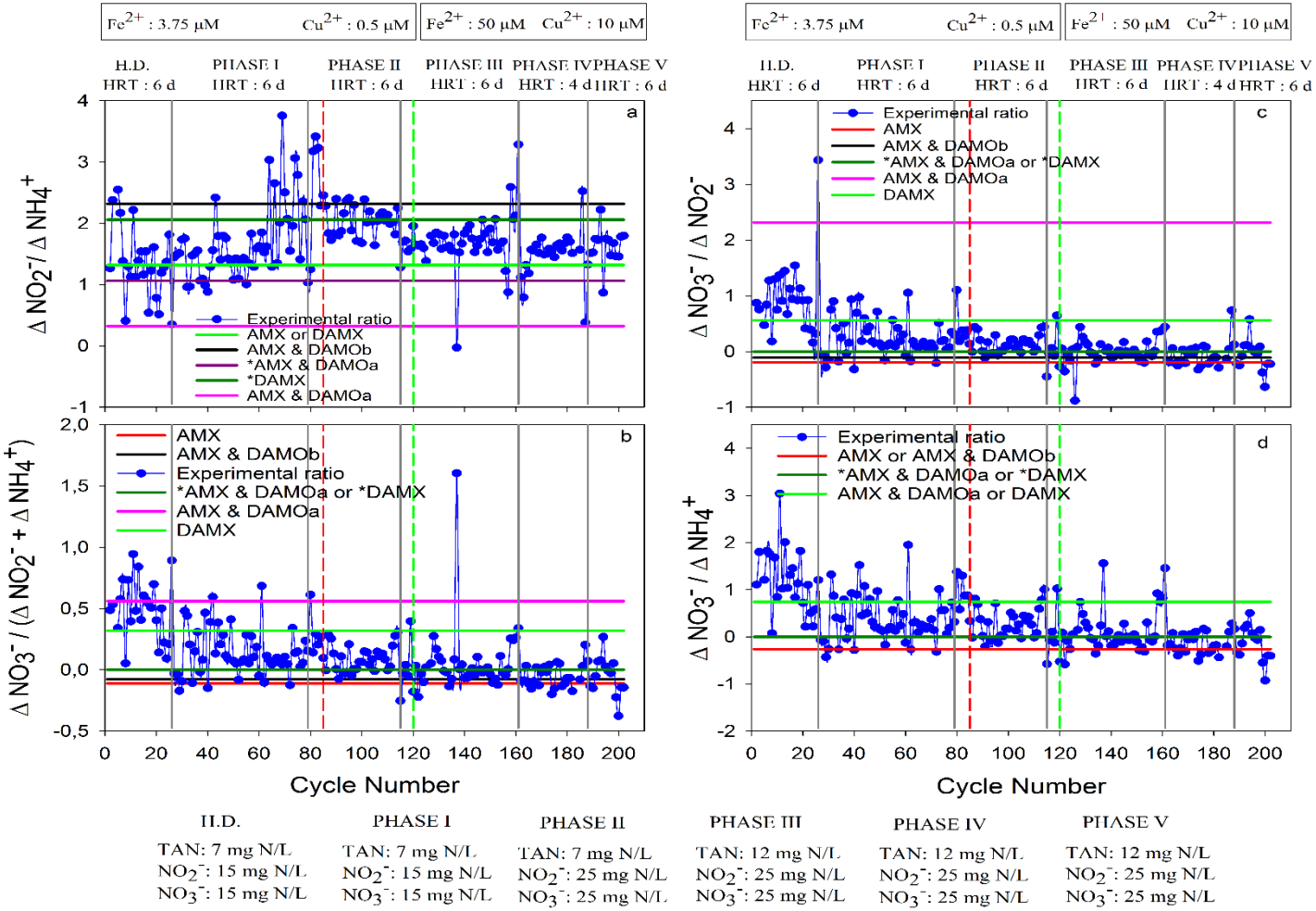

Figure 3.24 The cyclic molar ratios of (a) $\Delta NO_2^-/\Delta NH_4^+$, (b) $\Delta NO_3^-/(\Delta NO_2^- + \Delta NH_4^+)$, (c) $\Delta NO_3^-/\Delta NO_2^-$ and (d) $\Delta NO_3^-/\Delta NH_4^+$ in the DAMO-Anammox SBR compared to the theoretical ratio of each case (red dashed line: increase in NO_3^- concentration at Cycle 85; green dashed line: increase in Fe^{2+} and Cu^{2+} concentrations at Cycle 120)

$\Delta NO_3^-/(\Delta NO_2^- + \Delta NH_4^+)$ molar ratio

Regarding the $\Delta NO_3^-/(\Delta NO_2^- + \Delta NH_4^+)$ molar ratio, shown in Figure 3.24b, the reactor also appeared to experience less fluctuation in Phases II, III, IV and V compared to Phase I. Through Phase I, the average $\Delta NO_3^-/(\Delta NO_2^- + \Delta NH_4^+)$ molar ratio was 0.15. This indicates that the microbial consortium exhibited a $\Delta NO_3^-/(\Delta NO_2^- + \Delta NH_4^+)$ molar ratio in the region of *DAMX or *AMX & DAMOa, and DAMX, suggesting a consortium containing all three microorganisms where the activity of DAMOa and DAMOb were relatively similar without the absolute dominance of one over the other. In Phase II, the average $\Delta NO_3^-/(\Delta NO_2^- + \Delta NH_4^+)$ molar ratio trend was found to be 0.11, which illustrated the consortium remained in the same region as in Phase I. On the other hand, in Phase III, the average $\Delta NO_3^-/(\Delta NO_2^- + \Delta NH_4^+)$ molar ratio decreased to 0.06, signifying that the conosortium remained in the same region as Phases I and II, yet NO_3^- production by Anammox is becoming more prominent that its consumption by DAMOa. In Phase IV, the $\Delta NO_3^-/(\Delta NO_2^- + \Delta NH_4^+)$ molar ratio further decreased to -0.04 and later decreased slightly to -0.05 by Phase V. In Phase IV and Phase V, the microbial consortium in terms of the $\Delta NO_3^-/(\Delta NO_2^- + \Delta NH_4^+)$ molar ratio, was in the region between *DAMX or *AMX & DAMOa, and AMX & DAMOb which shows a further decrease in DAMOa activity since the production of NO_3^- by Anammox seems to be more prominent than its consumption.

$\Delta NO_3^-/\Delta NO_2^-$ molar ratio

As for the $\Delta NO_3^-/\Delta NO_2^-$ molar ratio, illustrated in Figure 3.24c, less fluctuation can be observed compared to the other ratios. The average $\Delta NO_3^-/\Delta NO_2^-$ molar ratio in Phase I was found to be 0.29, corresponding to the region between *DAMX or *AMX & DAMOa, and DAMX, signifying a co-culture containing the three microorganisms. In Phase II, the average $\Delta NO_3^-/\Delta NO_2^-$ molar ratio decreased to 0.17, remaining in the same region as Phase I. On the other hand, in Phase III, the average $\Delta NO_3^-/\Delta NO_2^-$ ratio decreased to -1.21, corresponding to a microbial consortium where production of NO_3^- by Anammox and its accumulation is much more prominent that its consumption, hence a reduction in DAMOa activity. The

average $\Delta NO_3^-/\Delta NO_2^-$ molar ratio later increased to -0.05 in Phase IV but slightly decreased to -0.07 in Phase V. In Phase IV and Phase V, the microbial consortium was in the region AMX & DAMOb and *DAMX or *AMX & DAMOa. This signifies an improvement in NO_3^- consumption by DAMOa in comparison to Phase III, yet DAMOb activity seems to be higher than that of DAMOa, which is also verified in the results of the $\%CATN_{removed}$ of Section 3.3.2.1.2.

$\Delta NO_3^-/\Delta NH_4^+$ molar ratio

The $\Delta NO_3^-/\Delta NH_4^+$ molar ratio, shown in Figure 3.24d, exhibited a microbial consortium in the region *DAMX or *AMX & DAMOa and DAMX or AMX & DAMOa in Phase I and Phase II. The average $\Delta NO_3^-/\Delta NH_4^+$ ratio in Phase I and Phase II was 0.38 and 0.35, respectively. In Phase III, the average $\Delta NO_3^-/\Delta NH_4^+$ molar ratio decreased to 0.09, corresponding to a microbial consortium close to the *DAMX and *AMX & DAMOa cases. But in Phase IV and Phase V, the average $\Delta NO_3^-/\Delta NH_4^+$ molar ratio decreased to -0.07 and -0.13, respectively. Corresponding to the region between *DAMX or *AMX & DAMOa and AMX or AMX & DAMOb, which signifies that DAMOa activity decreased since the production of NO_3^- by Anammox became more prominent than NO_3^- consumption by DAMOa. This may have been caused by the decrease in the HRT applied in Phase IV.

These results show that the co-culture enriched was fluctuating between composition percentages of the target species, showing in the majority of the phases the presence of the three target species. This was also verified via the molecular analyses (Section 3.3.2.2). The results of the $\%CATN_{removed}$ by each species can be correlated to the results presented by the stoichiometric molar ratio calculations. The high fluctuations observed in almost all stoichiometric ratios illustrated in Figure 3.24 decreased towards the end of Phase II and became smooth by Phase III, which remained similar in Phase IV and Phase V. This reveals that the microbial consortium became more stable in terms of percentages. This was also revealed by the TN removal contribution percentages of each target microorganism.

Observing the DAMO-Anammox co-culture transition under all the stoichiometric molar ratios described above, one can notice that the co-culture was closer to the

theoretical ratios of *DAMX and *AMX & DAMOa. This signifies that the DAMOa activity was not high enough to remove the provided NO_3^- and rather capable of removing the portion produced by the Anammox reaction. This might be due to the location of the DAMOa cells in the co-culture, suggesting that they were in close proximity to Anammox and probably within a granule, presenting a difficulty for the access to the provided NO_3^- in the feed.

The results of the stoichiometric molar ratios $\Delta NO_3^-/ (\Delta NO_2^- + \Delta NH_4^+)$ and $\Delta NO_3^- /\Delta NH_4^+$ were similar in terms of the change in the target microorganisms' population dynamics. Yet, since the theoretical stoichiometric molar ratios of $\Delta NO_3^-/\Delta NH_4^+$ of the different cases were overlapping with one another, it is difficult to attribute the change in the experimental molar ratios to one case or the other. In addition, the theoretical stoichiometric molar ratio $\Delta NO_3^-/\Delta NO_2^-$ of the cases AMX, AMX & DAMOb, *DAMX and *AMX & DAMOa were very close to one another, assessing the change in the target microorganisms' population dynamics was difficult. One can use the molar ratios of $\Delta NO_2^-/\Delta NH_4^+$ and $\Delta NO_3^-/ (\Delta NO_2^- + \Delta NH_4^+)$ to describe the presence of the DAMO-Anammox co-culture and the potential combinations of the target species.

3.3.2.2 Molecular Analyses Results

3.3.2.2.1 FISH Analyses Results of DAMO-Anammox SBR

Sludge samples from the DAMO-Anammox SBR were taken periodically to perform the FISH analysis, to observe the changes in the microbial composition existing in the reactor with respect to time. The target cells were identified with the corresponding probes given in Table 3.9 that can visually distinguish *M. oxyfera*, *M. nitroreducens* and Anammox. General bacteria, general archaea and DAPI probes were used to quantify the relative abundance of the target species in the reactor. Hence, the enrichment progress was tracked by assessing the composition change of the consortium. Samples from Cycles 2, 16, 34, 55, 75, 100, 130, 150, 175, 190 and 202 were analyzed and the microscope images are shown in Figure . These images

were analyzed using ImageJ to evaluate the relative abundance of the target microorganisms in each phase and the results are reported in Figure 3.26. It is noticeable from Figure that after Cycle 130 the proximity of Anammox and DAMOa was relatively closer to one another compared to DAMOb probably since DAMOa consumes the NO_3^- produced by the Anammox.

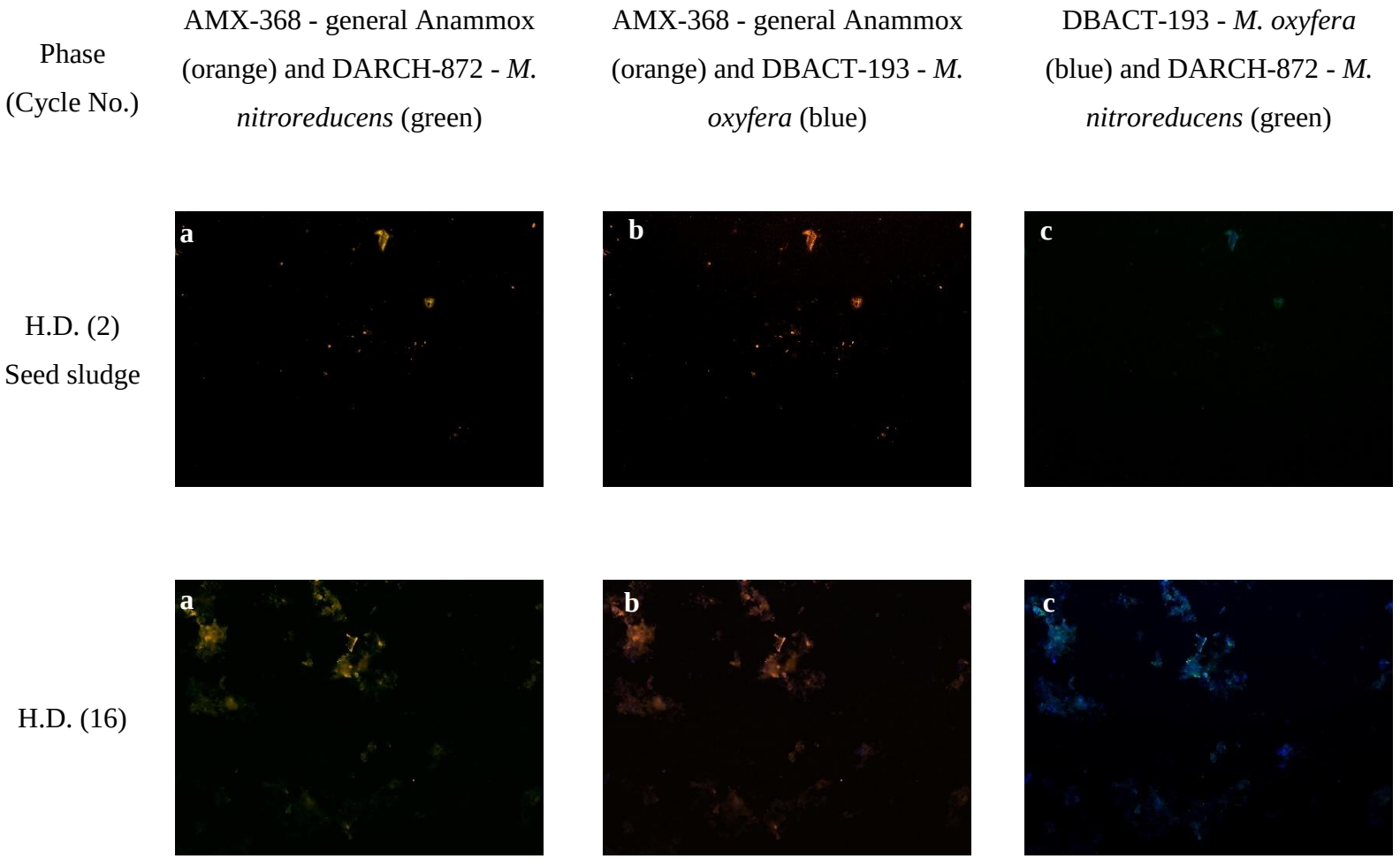

Figure 3.25 FISH images of DAMO-Anammox SBR sludge samples withdrawn at Cycle 2 to 202

Phase (Cycle No.)	AMX-368 - general Anammox (orange) and DARCH-872 - *M. nitroreducens* (green)	AMX-368 - general Anammox (orange) and DBACT-193 - *M. oxyfera* (blue)	DBACT-193 - *M. oxyfera* (blue) and DARCH-872 - *M. nitroreducens* (green)
I (34)	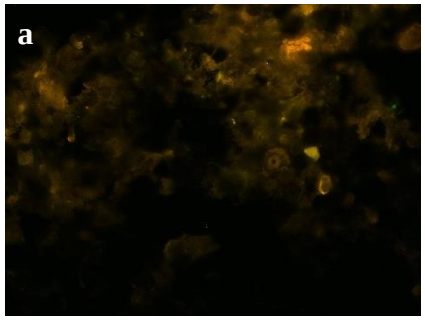	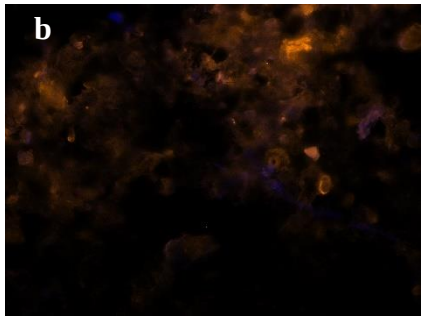	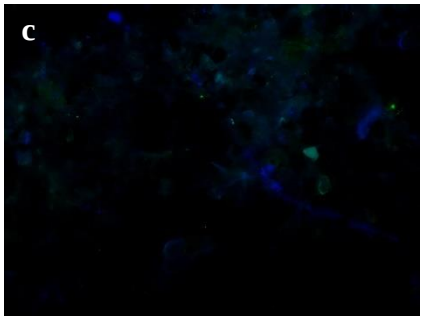
I (55)	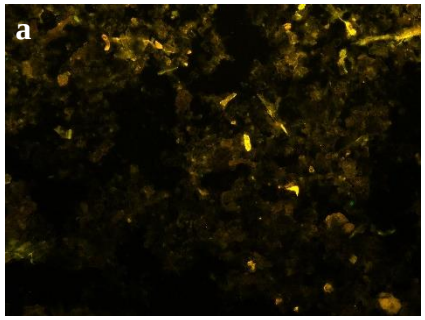	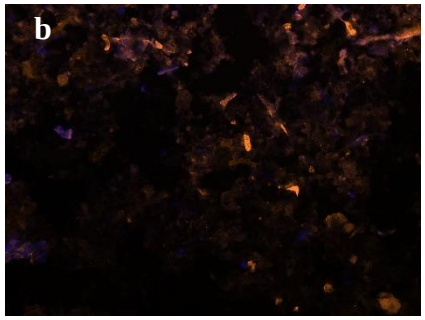	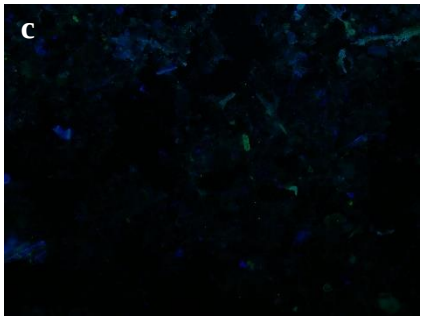

Figure 3.25 FISH images of DAMO-Anammox SBR sludge samples withdrawn at Cycle 2 to 202 (Continued)

Phase (Cycle No.)	AMX-368 - general Anammox (orange) and DARCH-872 - *M. nitroreducens* (green)	AMX-368 - general Anammox (orange) and DBACT-193 - *M. oxyfera* (blue)	DBACT-193 - *M. oxyfera* (blue) and DARCH-872 - *M. nitroreducens* (green)
I (75)	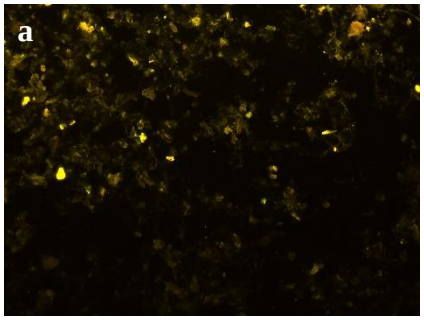	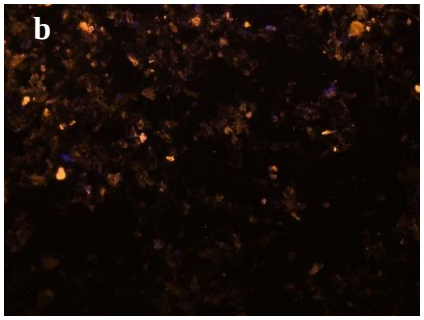	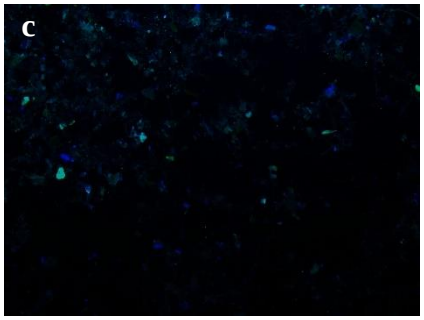
II (100)	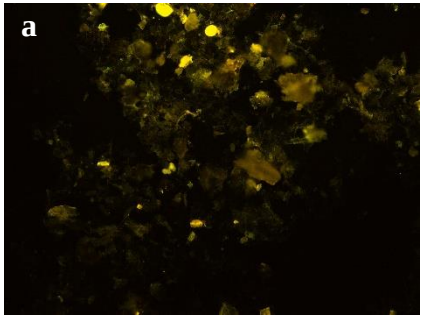	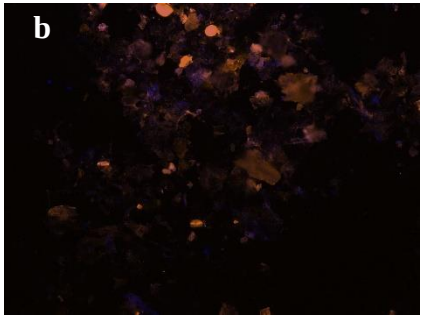	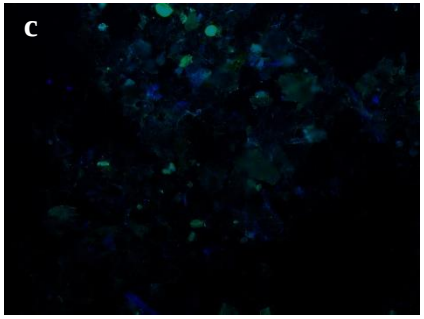

Figure 3.25 FISH images of DAMO-Anammox SBR sludge samples withdrawn at Cycle 2 to 202 (Continued)

Phase (Cycle No.)	AMX-368 - general Anammox (orange) and DARCH-872 - *M. nitroreducens* (green)	AMX-368 - general Anammox (orange) and DBACT-193 - *M. oxyfera* (blue)	DBACT-193 - *M. oxyfera* (blue) and DARCH-872 - *M. nitroreducens* (green)
III (130)	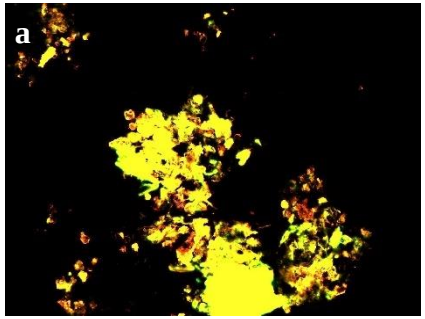	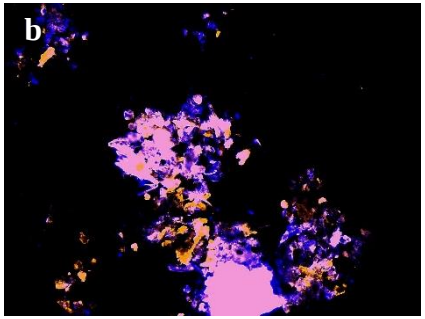	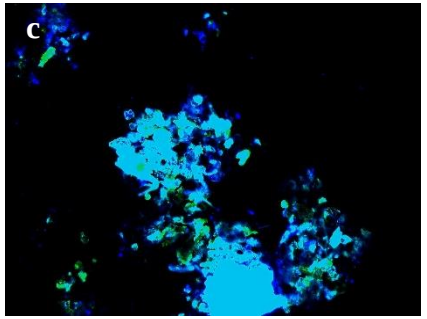
IV (175)	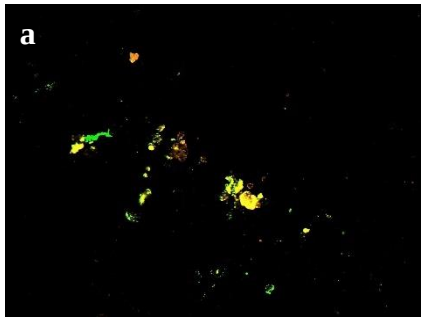	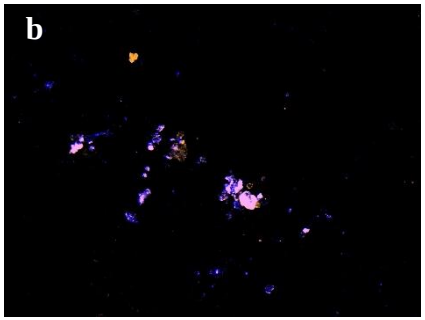	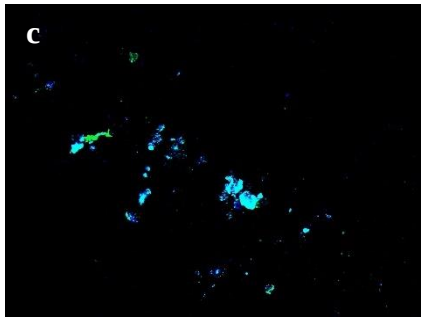

Figure 3.25 FISH images of DAMO-Anammox SBR sludge samples withdrawn at Cycle 2 to 202 (Continued)

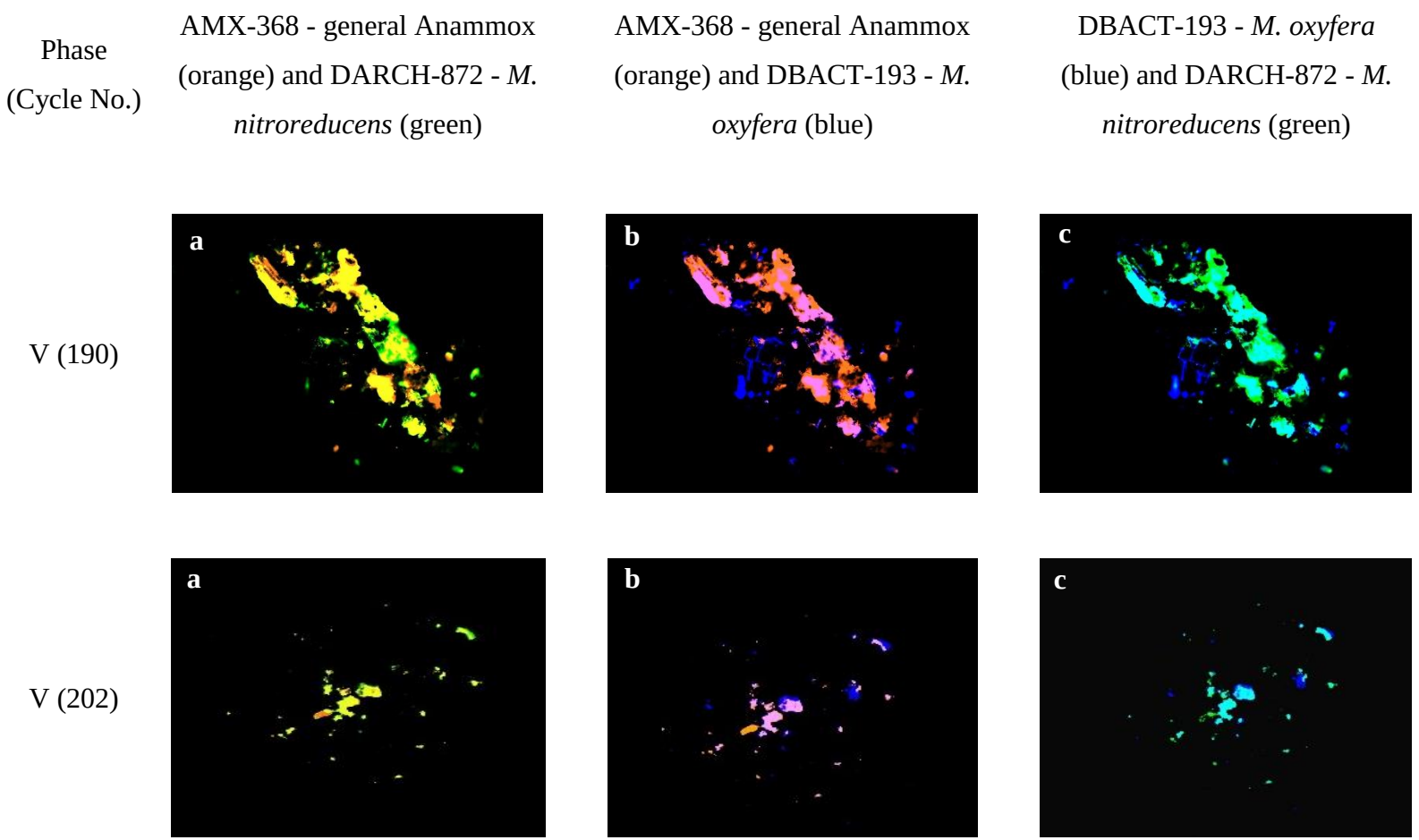

Figure 3.25 FISH images of DAMO-Anammox SBR sludge samples withdrawn at Cycle 2 to 202 (Continued)

The abundance of the three target species increased significantly from Cycle 2-202. The images and Figure 3.26 show Anammox dominance in the co-culture throughout the operation of the SBR. Nevertheless, the images also illustrate that the relative abundance of the DAMO microorganisms increased throughout the operation of the DAMO-Anammox SBR. This outcome was also verified by the nitrogen mass balance and the stoichiometric molar ratios calculations.

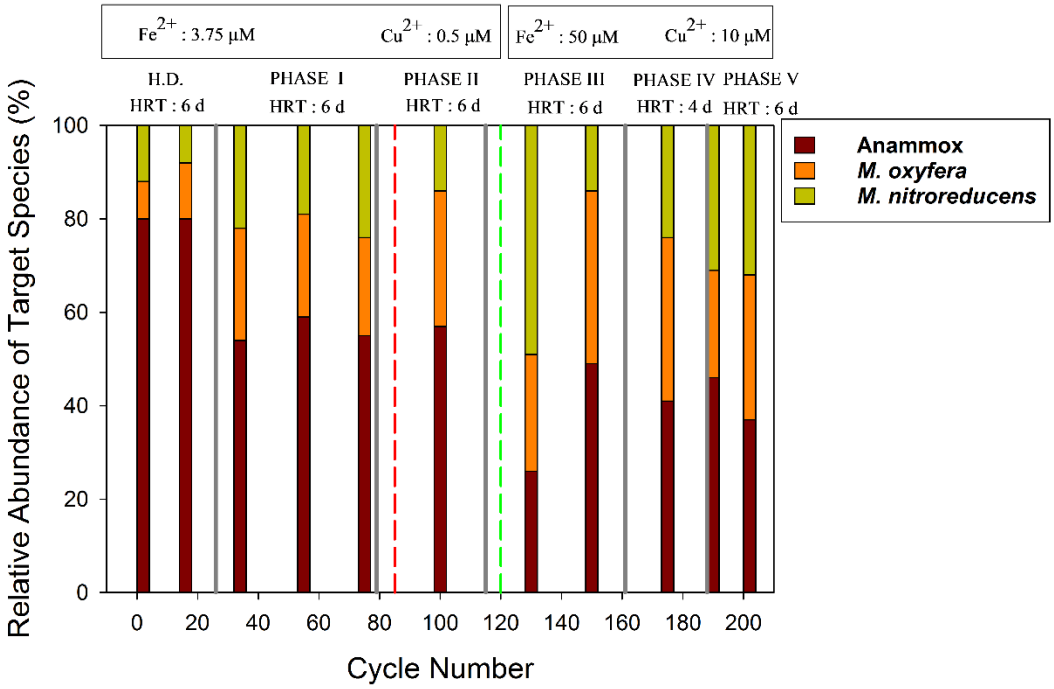

Figure 3.26 The relative abundance of target species with respect to each other in the DAMO-Anammox SBR. Increase in NO_3^- concentration at Cycle 85 (red dashed line); increase in Fe^{2+} and Cu^{2+} concentrations at Cycle 120 (green dashed line)

The initial sludge constituted of AD sludge, lake sediment and granular Anammox sludge. For that reason, the average relative abundance of Anammox to the target microorganisms was high (80±3 %) in the H.D. phase (Cycle 2 and 16) (Figure 3.26). On the other hand, the average relative abundance of *M. oxyfera* and *M. nitroreducens* was found to be 10±3 % each.

In Phase I (Cycles 34, 55 and 75), the average relative abundance of Anammox had decreased to 56±5 % but remained higher than that of *M. oxyfera* and *M. nitroreducens*. Yet, the average relative abundance of *M. oxyfera* and *M. nitroreducens* increased and was similar at 22±5 % (Figure 3.26).

In Phase II (Cycle 100), with the increase in NO_2^- and NO_3^- concentrations, the relative abundance of Anammox remained relatively the same at 57±8 %, while the relative abundance of *M. oxyfera* increased to about 29±7 % and that of *M. nitroreducens* decreased to about 14±1 % (Figure 3.26). The increase in NO_2^- and NO_3^- initial concentrations, while maintaining the initial NH_4^+ concentrations, allowed *M. oxyfera* an advantage over *M. nitroreducens*. The changes in the relative abundance of *M. oxyfera* and *M. nitroreducens* comply with the results of the nitrogen species analyses discussed in Section 3.3.2.1.2.

At the start of Phase III (Cycle 130), the relative abundance of Anammox, *M. oxyfera* and *M. nitroreducens* was 35±2 %, 34±2 % and 31±3 %, respectively (Figure 3.26). Yet, towards the end of Phase III (Cycle 150), the relative abundance of Anammox, *M. oxyfera* and *M. nitroreducens* changed to 42±6 %, 31±3 % and 27±7 %, respectively (Figure 3.26). The average relative abundance of Anammox, *M. oxyfera* and *M. nitroreducens* were calculated as 38±5 %, 32±3 % and 29±6 %, respectively, in Phase III. This illustrated that the increase in Fe^{2+} and Cu^{2+} concentrations gave *M. nitroreducens* an advantage at the beginning. Despite, the improvement in the relative abundance of *M. nitroreducens* at the start of Phase III, it could not compete and stay in a dominant state in the co-culture. These results also comply with the results of Section 3.3.2.1.2.

Although a slight increase in the average relative abundance of Anammox to 40±3 % was observed in Phase IV (Cycle 175), the relative abundance of *M. oxyfera* witnessed a slight increase to 35±5 %, while that of *M. nitroreducens* slightly decreased to 24±8 % (Figure 3.26). It should be noted that, the results of the nitrogen species analysis discussed in Section 3.3.2.1.2 illustrate an increase in Anammox activity, meanwhile a decline in DAMOb and DAMOa activity. It was expected to

see an increase in Anammox composition, and a decrease in *M. oxyfera* composition in Phase IV at an HRT of 4 days. The composition obtained at Cycle 175 might be the resultant of a delayed effect of the 6-day HRT of Phase III. Therefore, the composition obtained in Phase V, Cycle 190, might better reveal the effect of the 4-day HRT because the sampling was done just at the very beginning of Phase V. Thus, Cycle 190 samples are much better indicators of Phase IV, i.e, 4-day HRT effect. Indeed, it is seen in Figure 3.26 at Cycle 190 that Anammox composition in the sludge increased to 46±5% while *M. oxyfera* decreased to 23±2 %. *M. nitroreducens* composition, on the other hand, slightly increased to 31±5%. Also considering the removal efficiency results indicating the negative effect of lowering HRT on DAMO microorganisms, it can be concluded that HRT of 4 days might have a lower negative effect on DAMOa microorganisms compared to DAMOb. This might be due to close proximity of DAMOa cells to Anammox cells and thus the NO_3^- source. On the other hand, DAMOb is already in competition for NO_2^- with Anammox bacteria. Thus, at HRT of 4 days where mainly Anammox bacteria was supported, the negative effect on the DAMOb was more evident.

In Phase V (Cycle 202), the relative abundance of Anammox was 37%, while the relative abundance of *M. oxyfera* decreased to about 31% and that of *M. nitroreducens* increased to about 31% (Figure 3.26). This suggests that shifting the HRT back to 6 days provided an advantage for the *M. oxyfera* again, while the Anammox bacteria decreased slightly compared to Cycle 190, yet still close to 32%. Therefore, it can be said that the change in HRT from 6 to 4 days did not affect the Anammox negatively as much it did the DAMO microorganisms. HRT of 4 days even improved the Anammox activity, yet DAMO microorganisms were favored at the 6-day HRT. 4-day HRT negatively affected the DAMO microorganisms, especially the DAMOb.

3.3.2.2.2 NGS 16S Metagenome Analyses Results of DAMO-Anammox SBR

The results involving the target microorganisms and their relative target phyla were analyzed at the genus level, while the general results of the samples analyzed were discussed at the order level with respect to the main metabolic activities detected in the DAMO-Anammox SBR. These activities include methanotrophic, methylotrophic, denitrification, and non-methanotrophic anaerobic chemoorganotrophic reactions.

The results of the NGS analysis illustrated that the target phyla, namely, *Planctomycetota*, NC10 and *Euryarchaeota*, were present in the microbial consortium. Anammox belong to the phylum *Planctomycetota*, while *M. oxyfera* (DAMOb) belong to phylum NC10 and *M. nitroreducens* belong to the phylum *Euryarchaeota*. Figure 3.27 illustrates the actual percentages of the target phyla at different cycles of the DAMO-Anammox SBR. The initial cycle, that is the microbial consortium in the seed sludge, contained 0.6% *Planctomycetota*, 2% *Euryarchaeota*, while NC10 was not detected. At Cycle 55 (Phase I), *Planctomycetota*, NC10 and *Euryarchaeota* composed of 5%, 0.02% and 0.03%, respectively. In Phase III (Cycle 130), NC10 was not detected, on the other hand, the microbial composition consisted of 3% *Planctomycetota* and 0.3% *Euryarchaeota*. Furthermore, at Cycle 202 (Phase V), *Planctomycetota*, NC10, and *Euryarchaeota* were found to be 8%, 0.5%, and 0.16%, respectively, of the microbial consortium. This illustrates that the percentage abundance of the target phyla changed and usually displayed an increasing trend throughout the operation of the DAMO-Anammox SBR. The changes in their abundance with respect to the changes implemented at each phase concurs with the removal efficiency and removal rate results exhibited in Section 3.3.2.1.2.

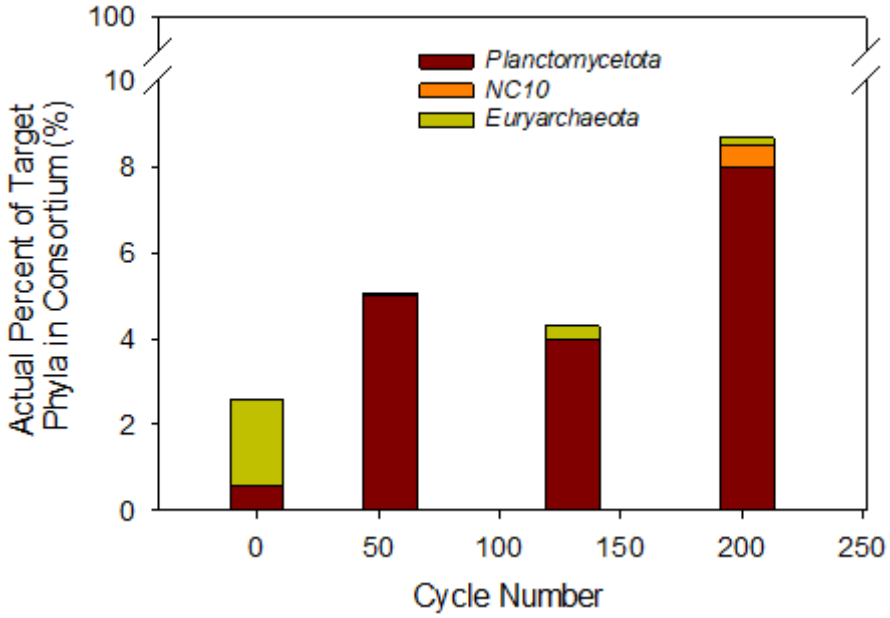

Figure 3.27 The actual percentage of the target phyla in the DAMO-Anammox SBR

The results of the NGS analysis illustrated the existence of species from the classes *Candidatus Brocadiae*, *Phycisphaerae* and *Planctomycetia*, in the *Planctomycetota* phylum (Figure 3.28). These classes were represented at different percentages in each cycle. The Anammox SBR was the source of the *Candidatus Brocadiae anammoxidans* belonging to the class *Candidatus Brocadiae* (Kocamemi et al., 2018). Since the initial seed sludge of the DAMO-Anammox SBR composed of AD sludge (38% by volume), freshwater sediment (38% by volume) and granular Anammox sludge (24% by volume) and the initial sample taken was mainly suspended sludge, the abundance of species belonging to the class *Candidatus Brocadiae* was found to be as low as 3% from the phylum *Planctomycetota*. The percentage of *Candidatus Brocadiae* increased from 3% at the initial cycle to 33% at Cycle 55, 58% at Cycle 130 and reached 60% at Cycle 202. This shows that, within the phylum *Planctomycetota*, *Candidatus Brocadiae* became the most dominant class throughout the operation of the DAMO-Anammox SBR (Figure 3.28).

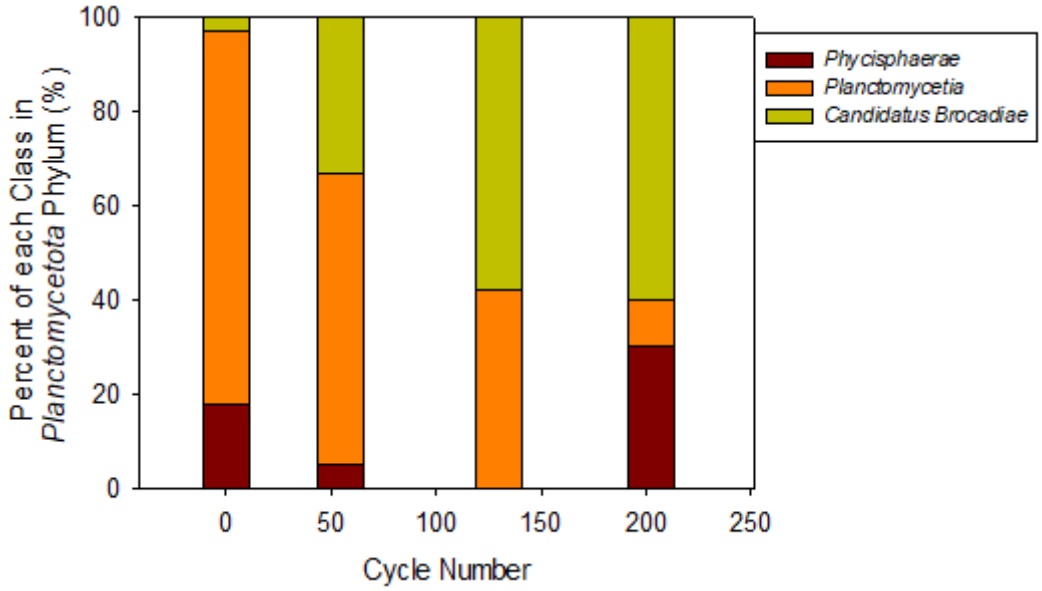

Figure 3.28 The percentage of each class in the phylum *Planctomycetota* from the DAMO-Anammox SBR

Within the *Euryarchaeota* phylum, there are various classes that consist of methanotrophic, methylotrophic, hydrogen-dependent methylotrophic, hydrogenotrophic, aceticlastic, alkanotrophic and methanogenic archaea. *Methanomicrobia*, *Methanobacteria*, *Candidatus Methanofastidiosia* and *Thermoplasmata* are classes within the phylum *Euryarchaeota* that were detected in the DAMO-Anammox SBR (Figure 3.29). The class *Methanomicrobia* includes the genera *Candidatus Methanophagales* and *Candidatus Methanoperedens*, which includes the species *Methanoperedens nitroreducens* (Evans et al., 2019). Nevertheless, the many methanogenic species belong to the class *Methanomicrobia*.

At the initial cycle, *Euryarchaeota* was distributed as 93% *Methanomicrobia*, 3% *Methanobacteria*, 1% *Candidatus Methanofastidiosia*, and 2% *Thermoplasmata*, as shown in Figure 3.29. The majority of the species detected in the initial cycle were methanogenic, especially that the seed inoculum was from AD sludge. Yet, in the Phase I sample (Cycle 55), all the *Euryarchaeota* detected was found to be composed of *Methanobacteria*. *Methanobacteria* mainly contain hydrogenotrophic, aceticlastic and methylotrophic microorganisms (Evans et al., 2019). The presence of organic

carbon (excluding CH_4) in Phase I (Figure 3.13) and the production of hydrogen through methane oxidation allowed the prosperity of this group of microorganisms. Yet, with the decrease in organic carbon (excluding CH_4) by Phase III (Cycle 130), the abundance of *Methanobacteria* within the phylum *Euryarchaeota* decreased to 27%. The composition of *Euryarchaeota* in Phase III was distributed as 51% *Methanomicrobia*, 27% *Methanobacteria* and 22% *Thermoplasmata*. Finally, by Phase V (Cycle 202), the composition of *Euryarchaeota* became 73% *Methanomicrobia* and 27% *Methanobacteria* (Figure 3.29).

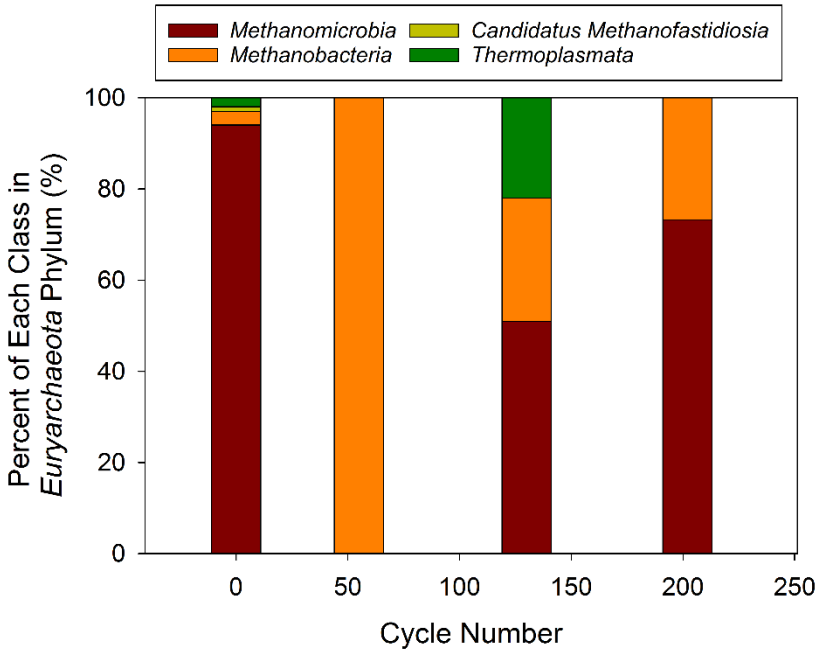

Figure 3.29 The percentage of each class in the phylum *Euryarchaeota* from the DAMO-Anammox SBR

The general NGS analyses results of the consortium is presented at the phylum level in Figure 3.30, Figure 3.31, Figure 3.32 and Figure 3.33. *Proteobacteria* was the dominant phylum in the initial mixed sludge, followed by *Chloroflexota* and *Bacteroidota* (Figure 3.30). At Cycle 55 representing Phase I, *Firmicutes* was the dominant phylum followed by *Proteobacteria* and *Bacteroidota* (Figure 3.31), while *Planctomycetota* was the fifth most abundant phylum reaching 5% of the microbial consortium. Furthermore, in Phase III (Cycle 130), *Firmicutes* remained the

dominant phylum, followed by *Proteobacteria*, while *Planctomycetota* remained the fifth most abundant phylum found in the microbial consortium at 4%, as seen in Figure 3.32. On the other hand, the sample from Phase V (Cycle 202) *Chloroflexota* was the most dominant phylum followed by *Proteobacteria* and *Acidobacteriota*. *Planctomycetota* was the fourth dominant phylum reaching 8% of the microbial consortium, as illustrated in Figure 3.33. A clear increase in *Planctomycetota* content of the microbial consortium is visible from the NGS results.

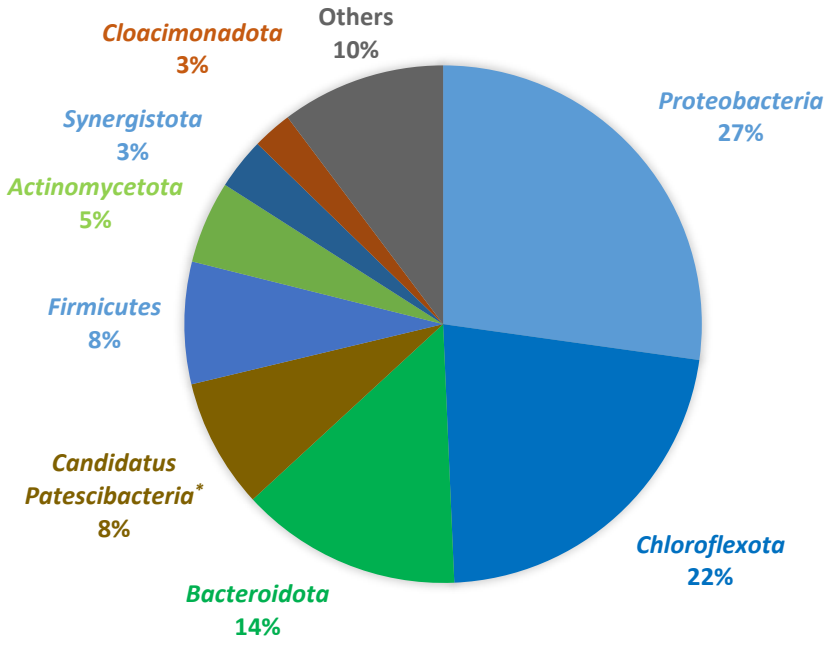

Figure 3.30 Phylum level composition of the DAMO-Anammox SBR sludge at Cycle 0 (seed sludge) **Candidatus Patescibacteria* is a superphylum

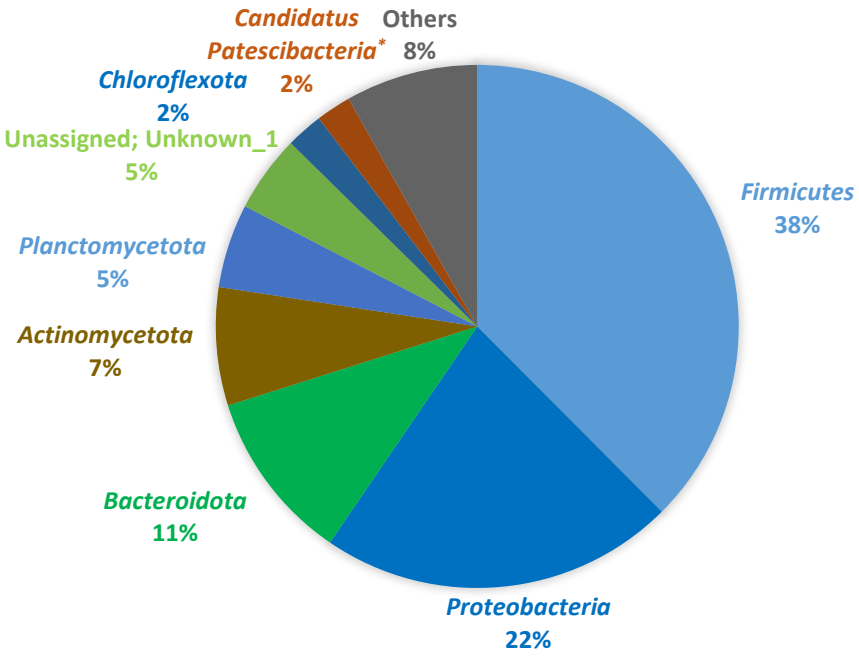

Figure 3.31 Phylum level composition of the DAMO-Anammox SBR sludge at Cycle 55 (Phase I) **Candidatus Patescibacteria* is a superphylum

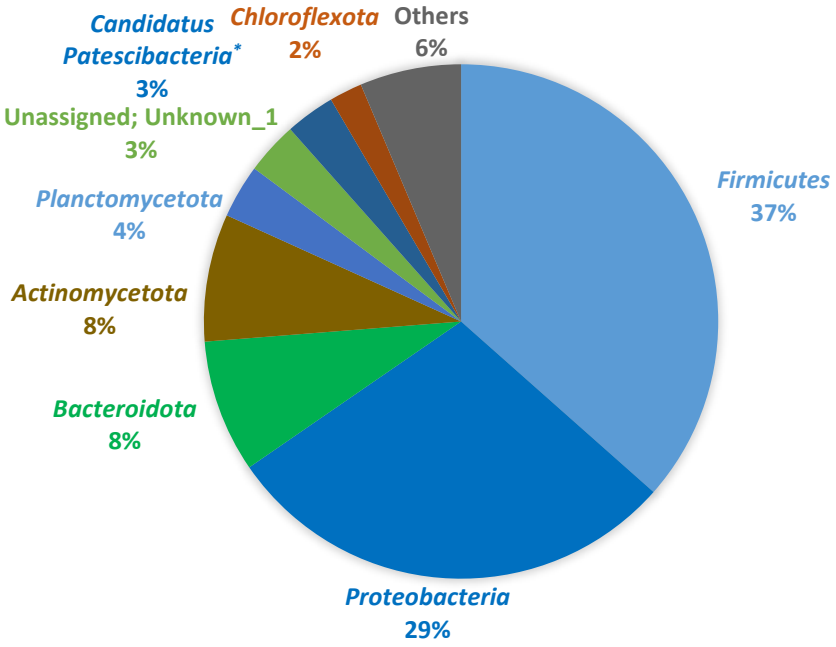

Figure 3.32 Phylum level composition of the DAMO-Anammox SBR sludge at Cycle 130 (Phase III) **Candidatus Patescibacteria* is a superphylum

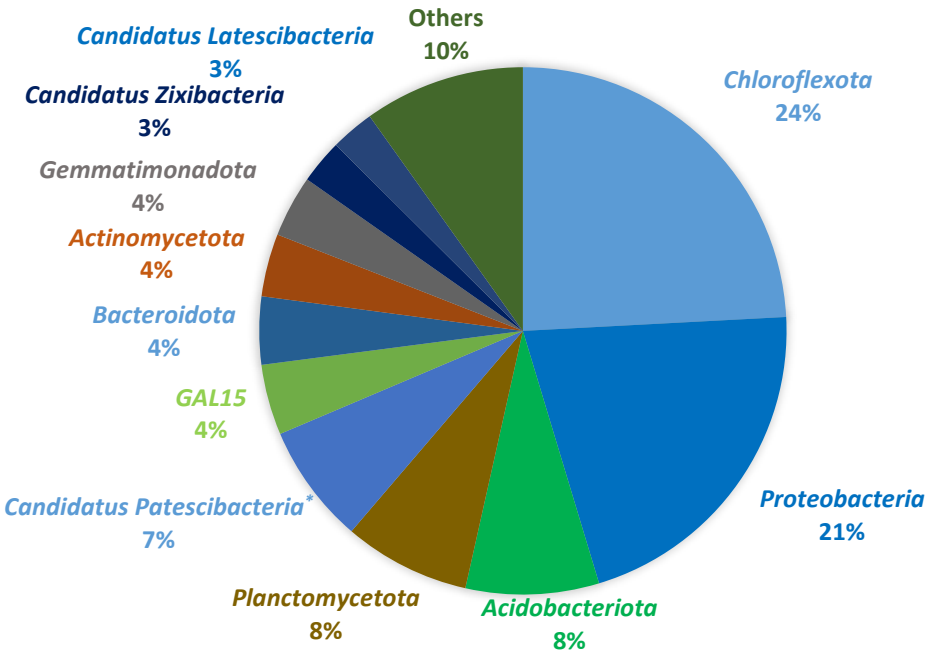

Figure 3.33 Phylum level composition of the DAMO-Anammox SBR sludge at Cycle 202 (Phase V) **Candidatus Patescibacteria* is a superphylum

In the context of the study, the general results of the NGS analysis were interpreted and described within two main metabolic groups that were the highest in abundance. The two main metabolic groups are methanotrophic and methylotrophic and non-methanotrophic anaerobic chemoorganotrophic.

Apart from the methanotrophic and methylotrophic species belonging to the phyla NC10 and *Euryarchaeota*, species belonging to the phyla *Proteobacteria* and *Verrucomicrobiota* were also detected in the DAMO-Anammox SBR. *Verrucomicrobiota* are considered as thermoacidophilic methanotrophs (Op den Camp et al., 2009), while *Proteobacteria* or now known as *Pseudomonadota* was one of the most dominant phyla detected in the DAMO-Anammox SBR. This phylum is one of the largest phyla and is a diverse phylogenetic division that constitutes of Gram-negative bacteria. Some of the numerous methanotrophic and methylotrophic species in the phylum *Proteobacteria* belong to the orders *Hyphomicrobiales*, *Rhodobacterales*, *Nitrosomonadales*, *Burkholderiales* and

Methylococcales. These species act as denitrifying methylotrophs in the absence of oxygen (Chistoserdova et al., 2010). *Hyphomicrobiales* and *Rhodobacterales* belong to the class *Alphaproteobacteria,* while *Burkholderiales* and *Nitrosomonadales* belong to the class *Betaproteobacteria,* and *Methylococcales* belongs to the class *Gammaproteobacteria*.

Despite the absence of any COD in the feed, non-methanotrophic anaerobic chemoorganotrophs were detected in the DAMO-Anammox SBR. This group includes species from the phyla *Proteobacteria*, *Firmicutes*, *Bacteroidota*, *Chloroflexota*, *Actinomycetota*, and *Acidobacteriota*. The reason behind the proliferation of this group of microorganisms is the possibility that COD is released by either dying biomass or in the form of acetate and succinate by some of the microorganisms.

The anaerobic chemoorganotrophic species in the phylum *Proteobacteria* belong to the orders *Burkholderiales*, *Nitrosomonadales*, *Rhodocyclales*, *Pseudomonadales*, *Enterobacterales*, *Myxococcales* and *Syntrophobacterales*. *Burkholderiales*, *Nitrosomonadales* and *Rhodocyclales* belong to the class *Betaproteobacteria*, while *Pseudomonadales* and *Enterobacterales* belong to the class *Gammaproteobacteria*. On the other hand, *Myxococcales* and *Syntrophobacterales* belong to the class *Deltaproteobacteria*.

Firmicutes now known as *Bacillota,* are mainly anaerobic chemoorganotrophic heterotrophs and can perform dissimilatory sulfate or sulfite reduction (Boone et al., 2005). The classes detected were *Clostridia*, *Bacilli*, and *Negativicutes*. Meanwhile, the *Bacteroidota* detected in the DAMO-Anammox SBR were anaerobic or facultatively anaerobic, saccharolytic microorganisms that are known to perform fermentation producing mainly succinate and acetate (Boone et al., 2005).

In addition, *Anaerolineae, Chloroflexia,* and *Dehalococcoidia* are the main classes detected from the *Chloroflexota* phylum. Microorganisms from the class *Anaerolineae* are anaerobic chemoorganotrophs but *Chloroflexia* can perform nitrite oxidation. Microorganisms from the classes *Actinomycetes* and *Acidimicrobiia*

belonging to the phylum *Actinomycetota* were detected in the DAMO-Anammox SBR. These microorganisms are either strictly or facultatively anaerobic and are mainly chemoorganotrophs (Boone et al., 2005). Species from the classes *Acidobacteriia*, *Holophagae*, and *Thermoanaerobaculia* from the *Acidobacteriota* phylum were found in the DAMO-Anammox SBR. Such microorganisms are mainly anaerobic chemoorganotrophic heterotrophs (Boone et al., 2005).

A small portion of heterotrophic denitrifiers was detected, which include species from the phylum *Proteobacteria*. Such species belong to the orders *Rhizobiales*, *Burkholderiales*, *Nitrosomonadales*, *Rhodocyclales* and *Pseudomonadales*. The order *Rhizobiales* belongs to the class *Alphaproteobacteria*, and *Burkholderiales*, *Nitrosomonadales* and *Rhodocyclales* belong to the class *Betaproteobacteria*. While the order *Pseudomonadales* belongs to the class *Gammaproteobacteria*. Their activity as discussed in Section 3.3.2.1.2 was low in comparison to the activities of the target microorganisms.

Microorganisms from the superphylum *Candidatus Patescibacteria*, also known as candidate phyla radiation (CPR) were detected in the DAMO-Anammox SBR. These microorganisms belong to various phyla such as *Candidatus Microgenomates*, *Candidatus Gracilibacteria*, *Candidatus Parcubacteria*, *Candidatus Pacebacteria*, ABY1, *Candidatus Komeilibacteria* and *Candidatus Saccharibacteria*. The species from the phylum *Candidatus Parcubacteria* are capable of producing H_2, SO_4^{2-} reduction and NO_2^- reduction; however, the majority of the microorganisms belonging to the other phyla are obligate fermenters that use heterolactic fermentation pathways, such as glycolysis and the pentose phosphate pathway but lack the tricarboxylic acid cycle and release fermentation by-products such as acetate, lactate, and formate (Danczak et al., 2017; Chaudhari et al., 2021; Hosokawa et al., 2021; Fujii et al., 2022).

AS mentioned above, the results obtained from the NGS analysis show an Anammox dominance over the DAMOa and DAMOb during the operation of the DAMO-Anammox SBR. Moreover, the NGS Metagenome analysis illustrates that DAMO

along with other denitrifying methanotrophs and methylotrophs belonging to the phyla *Proteobacteria*, *Verrucomicrobiota* and archaeal classes *Methanobacteria*, *Candidatus Methanofastidiosia* and *Thermoplasmata* were responsible for methane removal in the DAMO-Anammox SBR. In addition, the nitrogen removal was performed mainly by Anammox, DAMO and species from the *Proteobacteria* phylum.

Ding et al. (2017) achieved a microbial consortium of 39% NC10, 26% *Euryarchaeota*, 14% *Proteobacteria*, 6% *Planctomycetota* and 4% *Chlorobi* after 420 days of enrichment. An HfMBR inoculated with surface sediment of a freshwater river located in Suzhou, China, was operated at NH_4^+, NO_2^- and NO_3^- initial concentrations of 20-100, 10, and 20-200 mg N/L, respectively, at an HRT of 4-12 days. Moreover, the microbial consortium of the inoculum had relative abundances of about 0.6%, 3.5%, 20%, 1.8%, and 4% of NC10, *Euryarchaeota*, *Proteobacteria*, *Planctomycetota*, and *Chlorobi*, respectively. The percentage of NC10 and *Euryarchaeota* were much higher than in Ding et al. (2017), mainly due to the higher abundance of these microorganisms in the initial inoculum compared to this thesis. Yet, the percentage of *Planctomycetota* and *Proteobacteria* are relatively similar to the percentages found in Cycle 202.

Fu et al. (2017a) set a batch reactor supplied with NH_4^+ (50 mg N/L), NO_2^- (10 mg N/L) and NO_3^- (50 mg N/L) and operated at an HRT of 90 days. The inoculum used was sediment from a freshwater lake in Suzhou, China. The microbial consortium of the reactor fed with NH_4^+, NO_2^- and NO_3^- contained 51% NC10, 7% *Candidatus Brocadiae* and 3% *Proteobacteria*, while DAMOa were unexpectedly not enriched. A small proportion of archaea (0-5%) was detected in the inoculum and DAMOa were not detected in the enriched cultures. This signifies that DAMOa were not present in the inoculum, rather than the enrichment period or operational conditions were not sufficient. Fu et al. (2017a) claims that DAMOa are more difficult to enrich than DAMOb and the studies that claim enriching the DAMOa may be unusual since similarly they have used original mixed inocula, that include freshwater sediments, anaerobic digester sludge, methanogenic sludge, and activated sludge. Wang et al.

(2016) could not enrich DAMOa from an inoculum of freshwater sediment under nitrate and methane, after 13 months of operation. These results suggest that the choice of inoculum is critical to successfully enrich DAMOa.

3.3.3 Results of BATCH SET: Short-term Effect of NH_4^+:CH_4 Ratio on DAMO-Anammox Activity

The experiment was aimed at assessing the ratio of NH_4^+ to dissolved CH_4, since both are the electron donors dictating the activity of the three target microorganisms in a DAMO-Anammox co-culture. NH_4^+ is only consumed by Anammox and CH_4 is consumed by the DAMO microorganisms, the NH_4^+ to dissolved CH_4 ratio illustrates the balance between the Anammox and DAMO microorganisms. Moreover, due to the limitation of CH_4 dissolution, this ratio plays a key role in determining which of the microorganisms will display dominance.

Sludge was extracted from the DAMO-Anammox SBR at Cycle 194 (Phase V). N0, N2 and N8 represent the different test reactors with different NH_4^+:CH_4 ratios. The initial CH_4 content, in both the gas and liquid phase, was kept the same in all the reactor types. Moreover, the dissolved CH_4 was used in the calculation of the NH_4^+:CH_4 ratio since it is considered as the available CH_4 concentration. N0 reactors contained no NH_4^+ forming a NH_4^+:CH_4 ratio of 0, N2 reactors contained about 2 mg N/L of NH_4^+ forming a NH_4^+:CH_4 ratio of ¼ and N8 reactors contained about 8 mg N/L of NH_4^+ forming a NH_4^+:CH_4 ratio of 1. All reactors contained 25 mg N/L of NO_2^- and NO_3^- each. The Control reactor was only provided with 25 mg N/L of NO_2^- and NO_3^- each as the nitrogen source and was not supplied with any CH_4.

The results of the salting-out method show that there is decrease in the dissolved CH_4 content in the test reactors (Figure 3.34). At the same time, the headspace gas analysis of the test reactors displayed a decrease in the amount of CH_4 in the headspace (Figure 3.35). It can be inferred that CH_4 consumption occurred, since less gaseous CH_4 was available in the headspace and the soluble concentration

diminished. The initial dissolved CH_4 concentration was 0.56 mmol/L and reached a concentration of 0.32, 0.24 and 0.29 mmol/L in the N0, N2 and N8 reactors, respectively. The consumption of the dissolved CH_4 in all the reactor types followed a zero-order reaction. The consumption rate constants in N0, N2 and N8 reactor types were found as 1.6, 2.1 and 1.9 µM/hr, respectively. Although NH_4^+ was added to the N2 and N8 reactor types, which stimulated Anammox activity and by that allowing for competition over NO_2^- with DAMOb, dissolved CH_4 was consumed the fastest in N2 reactor types, while N8 and N0 reactor types were the second and third, respectively.

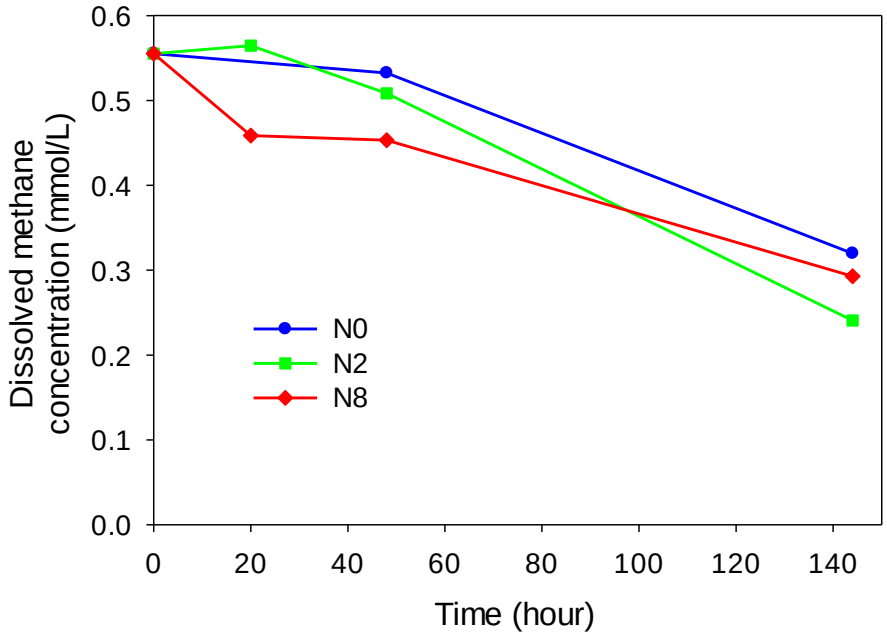

Figure 3.34 The dissolved methane concentration in each of the test reactor types

Since there was a limited amount of CH_4 in the headspace, the amount of dissolved CH_4 would decrease as it is consumed by the microorganisms. The concentration of gaseous CH_4 in the test reactors decreased while the concentration of N_2 increased in the headspace of the test reactors. The N2 reactors consumed the highest amount of CH_4 compared to the other reactor types and hence had the lowest dissolved CH_4 by the end of the experiment. After 6 days the reactors with N0, N2, and N8 consumed 460.7 µmol, 504.9 µmol and 407.6 µmol, respectively, as shown in Figure

3.35. N_2 production occurred in the test reactors but not in the control reactor (Figure 3.35a), revealing that there is no heterotrophic denitrification. The N2 reactors produced the highest amount of N_2 as 72.7 μmol, while the N0 and N8 reactors produced 61.2 μmol and 63.6 μmol of N_2, respectively. The CO_2 in the headspace decreased in the test reactors during the first 20 hours and then remained rather constant throughout the remaining duration of the experiment. The short-term effect of the NH_4^+:CH_4 showed that the N2 reactors with an NH_4^+:CH_4 ratio of 1/4 was slightly better than N0 and N8 reactors with the ratios of 0 and 1, respectively, in terms of N_2 production rate and CH_4 consumption rate.

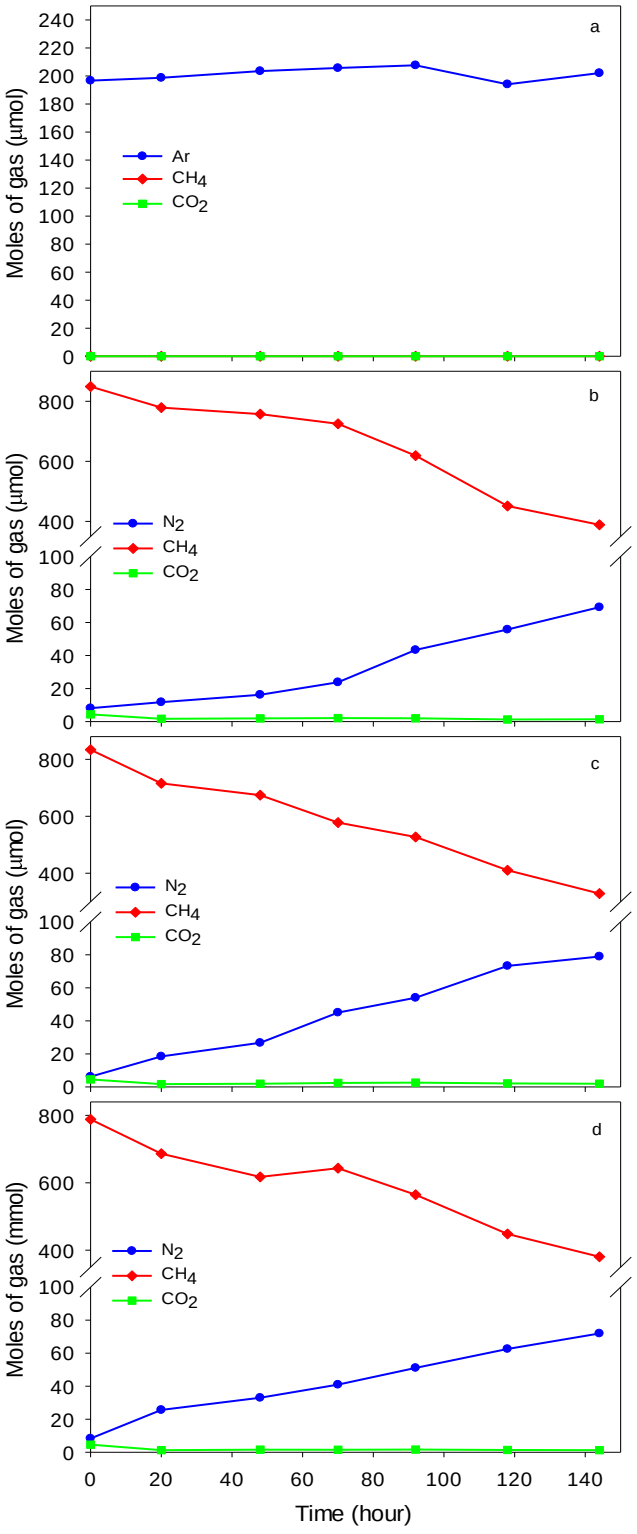

Figure 3.35 The gas composition in the headspace of each reactor type (a) control (b) N0 (c) N2 (d) N8

The initial TN concentrations in the Control, N0, N2 and N8 reactors were 53, 53, 57 and 64 mg N/L, respectively. The TN concentration in the Control reactor relatively did not change throughout the duration of the experiment which signifies that no heterotrophic denitrification activity was detected. On the other hand, among the test reactors, the lowest TN removal (17.8 mg N/L) was observed in the N0 reactor types, while the N2 and N8 reactor types showed 20.5 and 20.4 mg N/L, respectively (Figure 3.36). These correspond to a TN removal percentage of 34%, 36% and 32% in the N0, N2 and N8 reactors, respectively. Despite the relatively higher NH_4^+ concentration in the N8 in comparison to the N2 reactors, therefore supporting the Anammox activity, the highest amount of TN removal and highest TN removal percentage were achieved in the N2 reactors. This might be due to the limited production of NO_3^- by the Anammox bacteria since their activity was limited in the N2 reactors.

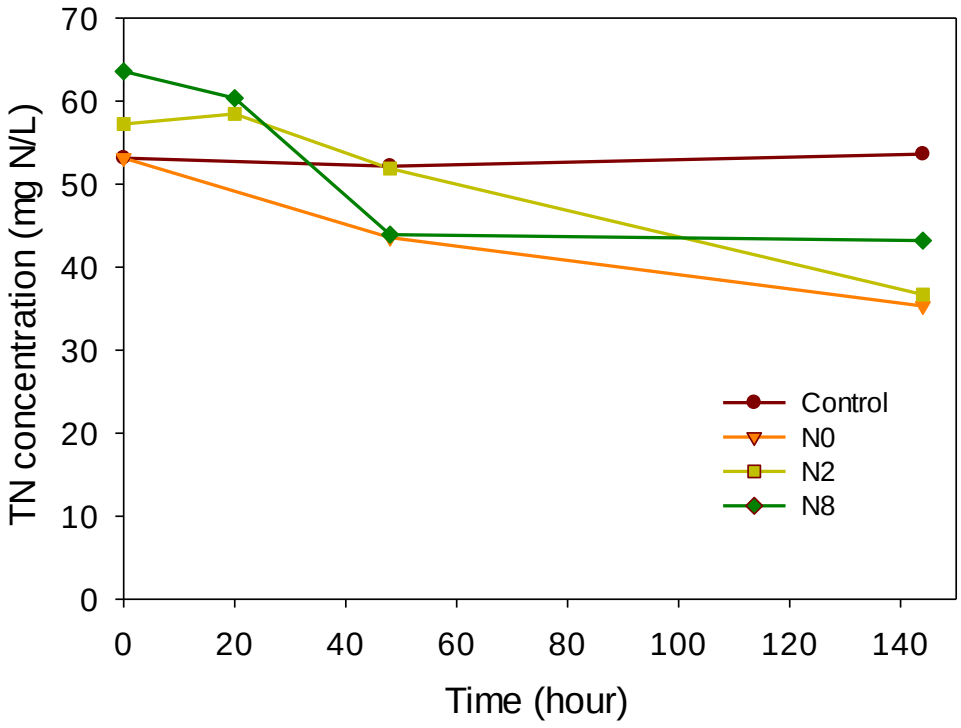

Figure 3.36 TN concentration in each reactor type

The reactors with NH_4^+ showed Anammox activity through NO_3^- production that was observed in the first 20 hours (Figure 3.37b), which was not the case in the N0 reactors as expected due to the absence of NH_4^+. After the consumption of most of the NH_4^+ (Figure 3.37c), DAMO activity was observed by the decrease in concentration of NO_3^- and NO_2^-. In the N8 reactors, DAMOa activity was more visible since the concentration of NO_2^- increased from the 48th hour till the end of the experiment (Figure 3.37a). The lowest final NO_3^- and NO_2^- concentrations were observed in the N0 and N2 reactors. In N8 reactor types, the highest consumption of NO_2^- can be observed. While the second highest NO_2^- consumption was observed in the N0 reactor types, which can be attributed to the DAMOb. On the other hand, NH_4^+ was consumed according to first-order reaction in N2 and N8 reactor types with rate constants 0.019 and 0.021 hr^{-1}, respectively. As expected higher NH_4^+ resulted in slightly higher rate. The NO_3^- consumption rates were similar in the N2 and N8 reactors, despite the Anammox activity in the N8 reactors. The NO_3^- consumption followed a zero-order reaction (Figure 3.37b), thus independent of the initial NO_3^- concentration. The rate constants of NO_3^- consumption in N0, N2 and N8 reactors were 0.028, 0.055 and 0.055 hr^{-1}, respectively. Moreover, the NO_2^- consumption in the three test reactor types followed a zero-order reaction. The rate constants of NO_2^- consumption in N0, N2 and N8 were 0.098, 0.089 and 0.35 hr^{-1}, respectively. However, the NO_2^- production observed in N8 reactors from Hour 48 to Hour 144 followed a zero-order reaction with a rate constant of 0.068 hr^{-1}. This was relatively similar to the rate constant of NO_3^- consumption in the N8 reactors (0.055 hr^{-1}), therefore, we can attribute the production of NO_2^- to the DAMOa activity.

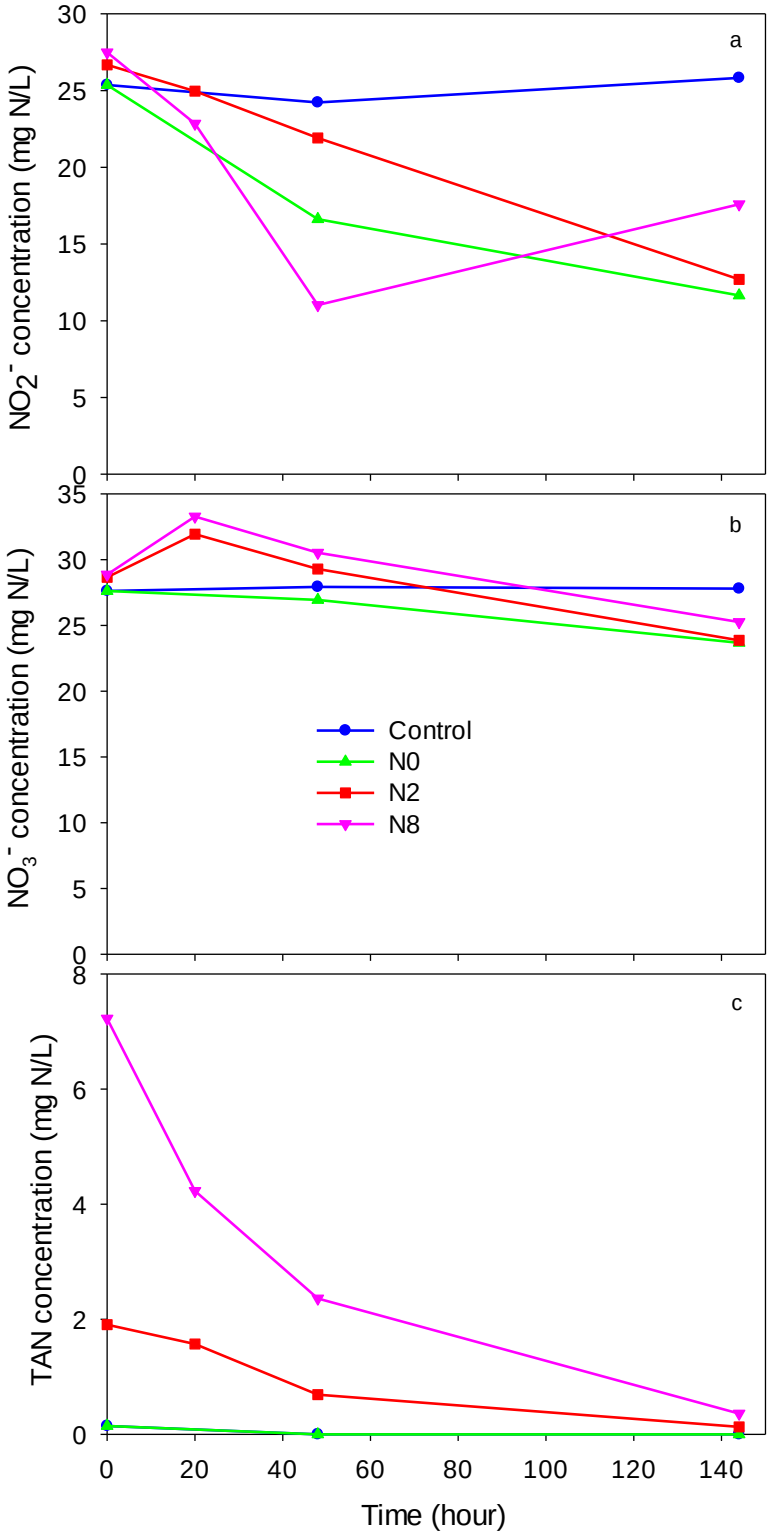

Figure 3.37 The concentrations of (a) NO_2^- (b) NO_3^- and (c) TAN in the batch reactors

The NO_2^- and NO_3^--based reaction rates of each target microorganism were calculated for the different reactor types, as shown in Figure 3.38. At higher NH_4^+ concentration the $r_{Anammox\ NO_2^-}$ increased, as also stated above. In N8 reactor type, the highest $r_{Anammox\ NO_2^-}$ of 1.6 mg N/L□day was observed, while $r_{Anammox\ NO_2^-}$ was 0.4 and 0 mg N/L·day in N2 and N0 reactor types, respectively. Moreover, in N2 and N0 reactor types, $r_{DAMOb\ NO_2^-}$ was the highest at 2.8 and 2.9 mg N/L·day, respectively, while in N8 reactor types, the $r_{DAMOb\ NO_2^-}$ was found to be 1.3 mg N/L·day. $r_{DAMOa\ NO_3^-}$ was the lowest at 1.2 mg N/L·day in the N8 reactors, while in the N2 and N0 reactor types, the $r_{DAMOa\ NO_3^-}$ was 0.9 and 0.7 mg N/L□day, respectively. Due to the higher CH_4 affinity of DAMOb compared to DAMOa and the limited available dissolved CH_4, DAMOb outcompeted DAMOa in all reactor types. On the other hand, due to the higher NO_2^- affinity of Anammox compared to DAMOb, once enough NH_4^+ was available for the Anammox stoichiometry, Anammox bacteria outcompeted DAMOb in N8 reactor types. Between the three NH_4^+:CH_4 ratios, the NH_4^+:CH_4 ratio of 1 displayed a more balanced activity of the three target microorganisms compared to the NH_4^+:CH_4 ratios of ¼ and 0. It should be noted that this parameter also needs to be tested to assess its long-term effect on the culture and nitrogen removal.

The addition of NH_4^+ supported the activity of Anammox bacteria, which in turn, triggered or improved the DAMOa activity. Yet, a dominant Anammox activity, may end up with NO_2^- buildup if limited NH_4^+ is present as observed in the N8 reactors.

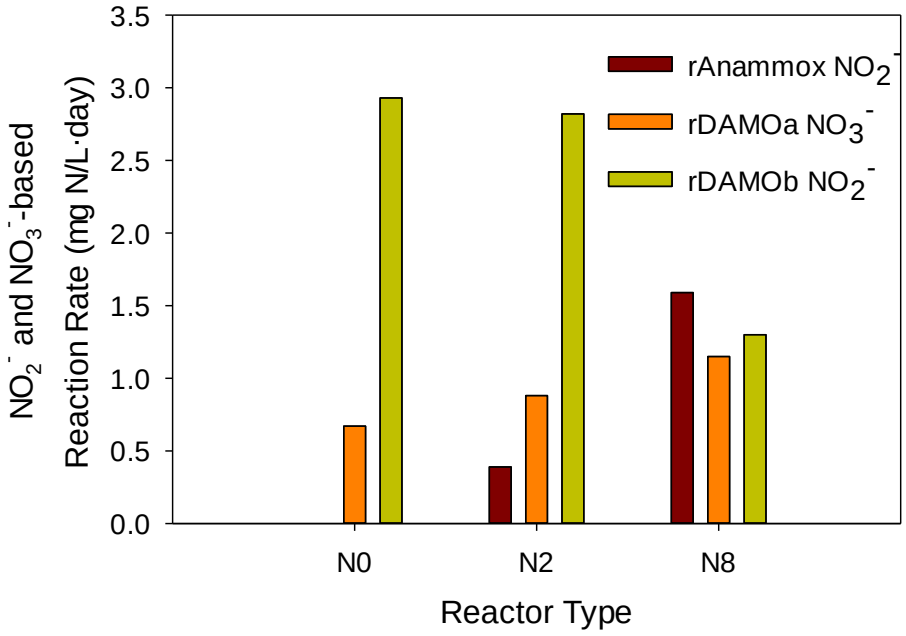

Figure 3.38 The calculated reaction rates of each of the target microorganisms in each reactor type

3.3.4 Conclusion

Two different reactors were operated to enrich a DAMO-Anammox co-culture. The first reactor was the Anammox SBR which was established to enrich an Anammox culture that would be used as a seed sludge to inoculate the later established DAMO-Anammox SBR. The DAMO-Anammox SBR was the main reactor to enrich the co-culture. This reactor was subject to five phases where various parameters such as influent nitrogen concentrations, HRT and NLR and influent Fe^{2+} and Cu^{2+} concentrations were changed in each phase during the operation of this reactor.

DAMO-Anammox co-culture was enriched in the DAMO-Anammox SBR where Anammox was the most dominant of the three target microorganisms. According to the NGS analysis *Planctomycetota*, NC10, and *Euryarchaeota* were found to be 8%, 0.5%, and 0.16%, respectively, of the microbial consortium. The enrichment of the DAMO-Anammox co-culture was verified via the results of the specific activity tests, $\%CATN_{removed}$ calculations, stoichiometric molar ratios calculations, NO_2^- and

NO_3^--based reaction rates calculations, FISH analysis and NGS Metagenome analysis performed at different periods of the DAMO-Anammox SBR operation. In order to understand the true yields of the target species, the concept of $\%CATN_{removed}$ by each target microorganism was developed. Moreover, the best indicatory stoichiometric molar ratios for a DAMO-Anammox co-culture are $\Delta NO_2^-/\Delta NH_4^+$ and $\Delta NO_3^-/ (\Delta NO_2^- + \Delta NH_4^+)$ to describe the presence of the DAMO-Anammox co-culture and the potential combinations of the target species.

The highest TN removal rate of the enriched DAMO-Anammox co-culture was achieved under the operational conditions of HRT 6 days and NLR of 21 mg N/L·day, in Phase V. The initial concentrations of TAN, NO_2^- and NO_3^- were 12, 25 and 25 mg N/L, respectively, while the initial Fe^{2+} and Cu^{2+} concentrations were 50 and 10 μM, respectively. The average TAN, NO_2^--N and NO_3^--N removal efficiencies were 96±13 %, 81±10 % and 14±14 %, respectively, while the TN removal was calculated as 51±8 %. The NO_3^- removal efficiency was low since in some of the cycles net production was observed, thus its removal efficiency was calculated excluding the cycles where net production had occurred. Nevertheless, NO_3^- production and consumption may be occurring simultaneously.

The average TAN, NO_2^- and NO_3^- removal rates under these operational conditions were 4.8±0.7, 7.7±1.7 and 3.3±2.8 mg N/L·day. The influent TN concentration of the DAMO-Anammox SBR, operated at 50% volume exchange rate was 141±15 mg N/L and this TN concentration was removed with an efficiency of 75±4 %. According to the influent concentration, the calculated TN removal rate was 35.4±5.1 mg N/L·day.

Reduction in the influent NH_4^+/NO_2^- or NH_4^+/NO_3^- molar ratios from 0.47 to 0.28 reduced the $\%CATN_{removed}$ of Anammox to an average of 23±4 %. This change in the influent molar ratios reduced the $\%CATN_{removed}$ of DAMOa by about 4% but did not cause any change in the $\%CATN_{removed}$ of DAMOb. Although due to the reduced Anammox activity and hence in TN removal, DAMO microorganisms were more stable and active.

Since Anammox was dominant over the DAMO microorganisms, the decrease in HRT from 6 to 4 days and simultaneously the increase in NLR, negatively affected the activity of the DAMO microorganisms while the Anammox activity increased. With the increase in HRT back to 6 days, the activities of the three target microorganisms reverted to levels relatively similar prior to the decrease in HRT. An HRT of 6 days was better than 4 days for the enriched co-culture in terms of performance of the three target microorganisms.

The increase in the Fe^{2+} and Cu^{2+} initial concentrations from 3.75 to 50 μM and 0.5 to 10 μM, respectively, improved the activity of the three target microorganisms. Nevertheless, due to the dominance of the Anammox bacteria this improvement was not observable as in the specific activity tests. The specific activity tests clearly illustrated the increase in the DAMOb and DAMOa activity.

From this enrichment study it can be deduced that the main reasons behind lower removal rates attained in this study in comparison to the literature were the content of the DAMO microorganisms in the inoculum and the reactor configuration, which plays a critical role in the CH_4 availability to the DAMO microorganisms.

Since NH_4^+ and CH_4 are the electron donors of the Anammox and DAMO reactions, respectively, the NH_4^+ to dissolved CH_4 ratio would illustrate the balance between the Anammox and DAMO microorganisms. This ratio would determine which of the microorganisms will display dominance in the co-culture. The ratios evaluated in batch reactors were 0, ¼, and 1 for a period of 3 days. At ratios of 0 and ¼, DAMOb was the dominant microorganism of the three since it has higher affinity to CH_4 compared to DAMOa. At the ratio of 1, balanced activity of the DAMO-Anammox co-culture was observed. The Anammox activity increased due to the increased presence of NH_4^+, this limited the activity of DAMOb since Anammox has higher affinity to NO_2^-. Furthermore, this allowed the increase in DAMOa activity. A longer period should also be assessed to observe the effect of this parameter on the performance of the co-culture.

CHAPTER 4

ASSESSING THE EFFECT OF DIFFERENT NITROGEN SOURCES ON THE ENRICHMENT OF DAMO CULTURES AND DAMO-ANAMMOX CO-CULTURES

4.1 Introduction

The nitrogen source provided, and their corresponding ratios play a significant role in changing the microbial composition of the DAMO co-system and DAMO-Anammox co-culture. Achieving a stable and balanced DAMO-Anammox co-culture that can target all the nitrogen species might be done by adjusting the nitrogen molar ratios.

Some enrichment studies assessed the effect of suppling various nitrogen feeds on the resulting microbial composition of DAMO microorganisms and DAMO-Anammox co-culture (Hu et al., 2011; Hu et al., 2015; Fu et al., 2017a). Maintaining a high activity of *M. nitroreducens* required a low concentration of NO_2^- in comparison to NO_3^- (Luesken et al., 2011b; Zhu et al., 2011; Ding et al., 2014; Fu et al., 2017a). Hu et al. (2011) demonstrated that a culture provided with NO_2^- showed DAMOb domination over DAMOa. On the other hand, Hu et al. (2015) claimed that in the presence of Anammox bacteria, DAMOb disappeared due to the competition over NO_2^-, while DAMOa proliferated. Hu et al. (2015) studied the effect of nitrogen source on the removal of nitrogen and methane, by setting two reactors. Both reactors were supplied with NH_4^+ and CH_4, one was fed with NO_3^- while the second was fed with NO_2^- at a loading rate between 10.5-38.4 mg N/day. DAMOa was present in both reactors at percentages of 70% and 26% in the NO_3^--fed and NO_2^--fed reactors, respectively.

Fu et al. (2017a) researched the effect of different nitrogen source combinations on DAMO microorganisms and Anammox bacteria. Six reactors seeded with freshwater lake sediment were setup as follows: N1 (NH_4^+, NO_2^-, NO_3^- and CH_4), N2 (NH_4^+, NO_3^- and CH_4), N3 (NO_3^- and CH_4), N4 (NH_4^+, NO_2^- and CH_4), N5 (NO_2^- and CH_4) and a control reactor. The initial concentrations of NH_4^+, NO_2^- and NO_3^- were 50, 10 and 50 mg N/L, respectively, and the reactors were operated at an HRT of 90 days. On the contrary to the previous studies mentioned, Fu et al. (2017a) observed the dominance of DAMOb in their study, while DAMOa were not found in the co-cultures, probably due to their absence in the inocula.

The results exhibited the highest and second highest TN removal rate were achieved by N1 and N4 reactors, respectively. In addition, N5 achieved the third highest TN removal rate, while the TN removal rate in N2 and N3 was lower than 2 mg N/L·day. This signifies that providing NO_2^-, NO_3^- and NH_4^+ as the nitrogen sources diminished the enrichment time from 75 to 30 days and enhanced the total nitrogen removal (Fu et al., 2017a). Indeed, it took Raghoebarsing et al. (2006) 480 days to enrich a DAMO culture when providing NO_2^- and NO_3^-, while He et al. (2015b) managed to enrich DAMO bacteria in 600 days by only providing NO_2^-. Whereas Haroon et al. (2013) enriched DAMO archaea in 350 days supplying NO_3^- and NH_4^+, instead of the nitrogen sources.

Therefore, the nitrogen source type, as well as influent nitrogen concentrations and the corresponding molar ratios are important factors in determining the composition of a DAMO co-system and a DAMO-Anammox co-culture, by dictating the activities of the three target microorganisms.

The aim in this part of the thesis is to investigate the effect of providing different nitrogen sources on the enrichment of DAMO cultures and DAMO-Anammox co-culture. This was performed by establishing two new reactors aimed at enriching the DAMO microorganisms, which were provided with different nitrogen sources. The first reactor was aimed at enriching a DAMO co-system (DAMO bacteria and DAMO archaea) called DAMO SBR. This reactor was provided with NO_2^-, NO_3^-

and CH_4 as the feed source. The second reactor aimed at enriching DAMO archaea and Anammox and possibly DAMOb, called DAA SBR, was provided with NH_4^+, NO_3^- and CH_4. Due to the potential DAMOa activity, it might be still possible to observe DAMOb in this DAA SBR, despite of the Anammox activity consuming NO_2^- like DAMOb.

It should be noted that this study was performed towards the end of the studies revealed in Chapter 3 of this PhD thesis, where the DAMO-Anammox SBR sludge was decreasing. Since the biomass concentration in the DAMO-Anammox SBR was gradually decreasing and the concern of not having enough sludge to perform the following experiments of this research was arising, the DAMO microorganism to be enriched in the DAMO SBR and DAA SBR along with the sludge from the DAMO-Anammox SBR would also serve as a seed sludge source for the reactor to be established in Chapter 5.

4.2 Material and Methods

Two reactors were established and operated under similar conditions with a variation in the nitrogen source. DAMO SBR was supplied with NO_2^- and NO_3^-, while DAA SBR was supplied with NH_4^+ and NO_3^-. The performances and microbial of the two reactors were compared with one another as well as with the DAMO-Anammox SBR to assess the effect of supplying different nitrogen sources on the subsequent enriched culture.

In both the DAMO SBR and DAA SBR, excess NO_3^- was provided in comparison to NH_4^+ and NO_2^-, in order to facilitate a competitive advantage for DAMOa. Since DAMOa converts NO_3^- into NO_2^- (Equation 2.5, Section 2.4.2), its activity was considered to set the rate of reaction in both reactors. The reactors' performances were monitored using the various analytical and molecular methods to evaluate the resulting enriched culture with respect to the different nitrogen sources provided. Section 4.3 discusses the results of both the DAMO SBR and DAA SBR.

4.2.1 Reactor Setup and Operational Conditions

4.2.1.1 DAMO and DAA SBRs

DAMO SBR was an air-tight stainless-steel SBR with total volume of 3.0 L (Figure 4.1a) used to enrich DAMOb and DAMOa. An effective volume of 2.5 L was established creating a headspace volume of 0.5 L. DAA SBR was also an air-tight stainless-steel SBR with total volume of 0.4 L (Figure 4.1b) used to enrich **D**AMO**a** and **A**nammox and possibly DAMOb as well. An effective volume of 0.3 L was established creating a headspace volume of 0.1 L. The exchange volume ratio for both reactors was set at 0.5 corresponding to an exchange volume of 1.25 L for the DAMO SBR and 0.15L for the DAA SBR. The cycle period for both reactors was 48 hr, making an HRT of 4 days. This was decided since these SBRs were run in parallel to the DAMO-Anammox SBR study.

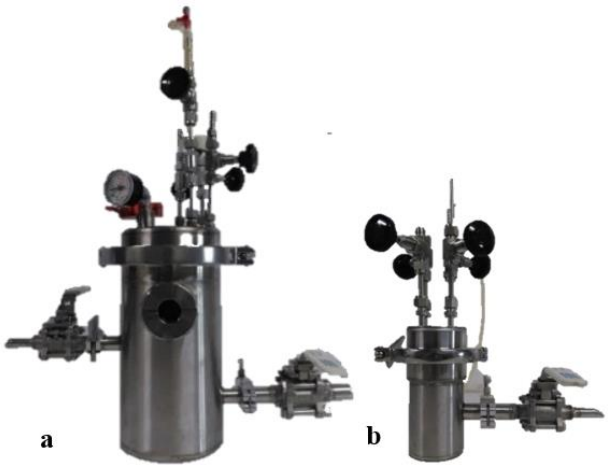

Figure 4.1 (a) DAMO SBR; (b) DAA SBR

The DAMO SBR was inoculated with AD sludge from ASKI Ankara Central WWTP in Tatlar village, Sincan, Ankara (2 L), shown in Figure 4.2. The pH of the AD sludge was recorded as 7.56, while the DAA SBR was inoculated with 0.2 L of the same AD sludge used for the DAMO SBR. Before inoculation, the AD sludge was thoroughly washed with a feed solution lacking any nitrogen source in order to

remove or decrease the concentration of any existing nitrogen source and COD present in the sludge. This was performed to reduce the activity of denitrifiers that require COD and nitrite or nitrate. The TSS and VSS of the initial sludge was 36.1 g/L and 15.1 g/L, respectively, yielding a VSS/TSS percentage of 42%.

Unlike the DAMO-Anammox SBR, the DAMO SBR and DAA SBR were inoculated only with AD sludge and not with freshwater lake sediment. The TSS concentration found in the freshwater lake sediment was very high (248±8 g/L) in comparison to the AD sludge (20.3±0.2 g/L) and this would increase the acclimation period of the reactors to washout the unwanted suspended solids.

Figure 4.2 AD sludge used to inoculate the DAMO SBR and DAA SBR

The operation temperature and pH values were 35°C and 7-7.5, respectively. Mixing was done using an orbital shaker at 120 rpm. DO was maintained close to 0 mg/L by purging the reactor with an Ar/CO_2 mixture (95%:5%) for about 3-5 min at the beginning of every cycle.

The feed solution was purged with the Ar/CO_2 mixture for 10-15 min and its pH was adjusted, before being fed into the reactor. Then the reactor was purged with a mixture of CH_4: CO_2 at 95%:5% to flush the Ar out and the pressure of the headspace was stabilized at 1.5 atm (absolute pressure) at the beginning of each cycle (Ettwig et al., 2009; Zhu et al., 2012; He et al., 2014, He et al., 2015a; Zhao et al., 2017). The

methane was kept in excess compared to the NO_2^- and NO_3^- provided in the DAMO SBR as well as in excess compared to the NO_3^- and NH_4^+ provided in the DAA SBR.

The feed solution supplied to the co-culture is as shown in Table 4.1 with the addition of NO_2^- and NO_3^- initial concentrations of 10 mg N/L and 25 mg N/L, respectively, in the DAMO SBR (Ettwig et al., 2009; Luesken et al., 2011; Cai et al., 2015). The same feed solution was supplied to the DAA SBR but with the addition of NO_3^- and NH_4^+ at initial concentrations of 25 mg N/L and 12 mg N/L, respectively. As seen in Table 4.1, this feed solution was modified from the solution shown in Table 3.3 and would provide the reactor with initial concentrations of Fe^{2+} and Cu^{2+} of 20 μM and 2.5 μM, respectively. These values are lower than that applied in the DAMO-Anammox SBR. Since the optimum Fe^{2+} DAMO bacteria (DAMOb) was found to be 20 μM, above this concentration the activity of DAMOb decreased without any obvious inhibitory effect (Lu et al., 2018). In the DAMO SBR, it was intended to supply NO_3^- at a higher concentration than NO_2^- in order to provide DAMOa an edge over DAMOb, since DAMOb has a higher affinity to CH_4 ($K_{CH_4}^{D_b}$ = 0.042 mg CH_4/L) than DAMOa ($K_{CH_4}^{D_a}$ = 8 mg CH_4/L) (Guerrero-Cruz et al., 2019; Lu et al., 2019). Moreover, NO_2^- is the outcome of the DAMOa reaction and so the DAMOa activity will be the rate-determining for nitrogen removal in this reactor. Nevertheless, in the DAA SBR, NO_2^- was not supplied and was expected to be provided by the DAMOa reaction. This in turn would initiate the Anammox reaction since NH_4^+ is supplied in the feed. In addition, the DAMOa activity will be the rate-determining for nitrogen removal in this reactor as well.

Table 4.1 Modified feed solution of DAMO and DAA SBRs (Ettwig et al., 2009; Luesken et al., 2011)

Compound	Concentration (g/L)
$KHCO_3$	0.5
KH_2PO_4	0.05
$CaCl_2 \cdot 2H_2O$	0.3
$MgSO_4 \cdot 7H_2O$	0.2
Acidic Trace Elements 0.5 mL/L (100 mM HCl)	
$FeSO_4 \cdot 7H_2O$	22.24
$ZnSO_4 \cdot 7H_2O$	0.068
$CoCl_2 \cdot 6H_2O$	0.12
$MnCl_2 \cdot 4H_2O$	0.5
$CuSO_4$	1.596
$NiCl_2 \cdot 6H_2O$	0.095
H_3BO_3	0.014
Alkali Trace Elements 0.2 mL/L (10 mM NaOH)	
SeO_2	0.067
$Na_2WO_4 \cdot 2H_2O$	0.05
Na_2MoO_4	0.242

4.2.2 Analytical Methods

The activities of the DAMO SBR and the DAA SBR were assessed to evaluate the composition of the biomass in terms of the microorganisms. This was performed through the assessment of the removal rates, removal efficiencies, removal molar ratios of the nitrogen species and total nitrogen removal in comparison to the theoretical values present in the literature. Furthermore, molecular analysis through FISH analysis was performed to assess the change in the microbial consortium focusing on the DAMO and Anammox microorganisms.

4.2.2.1 Volumetric and Chromatographic Analyses

Anions such as NO_2^-, NO_3^- and SO_4^{2-} were analyzed using IC (IC -Shimadzu Prominence HIC-SP). The IC was operated under the following conditions, highest pressure limit of 150 bar, oven temperature of 45°C, and a flow rate of 0.8 mL/min. The analyses were performed in duplicates or triplicates, depending on the presence of enough sample volume. The calibration curves, the limit of detection LOD and LOQ are shown in APPENDIX C.

TAN (NH_4^+-N + NH_3-N) was analyzed using the Hach Nessler Method (Hach, 2012). The analyses were performed in triplicates. The calibration curves, LOD and LOQ are illustrated in APPENDIX D.

sCOD was evaluated using medium range kits and low range kits (Hach, 2012). The analyses were performed in duplicates or triplicates, depending on the presence of enough sample volume. TOC was analyzed using the TOC analyzer. The analyses were performed in triplicates. The calibration, LOD and LOQ of the sCOD and TOC tests are shown in APPENDIX E.

TS, VS, TSS and VSS were analyzed using Standard Method (APHA, AWWA, WEF, 2005). The analyses were performed in triplicates. On the other hand, the pH and DO of the feed and the effluent of each reactor was measured using a pH-meter and DO-meter, as well as the temperature of the room was recorded.

CO_2, CH_4 and N_2 gases were analyzed using the TCD equipped in the GC (Trace GC Ultra: Thermo Electron Corporation). The following settings were applied in the GC, injector temperature 80°C, oven temperature 40°C, detector temperature 80°C, while the carrier gas used was He maintained at a pressure of 100 kPa. The analyses were performed in triplicates. The calibration and the LOD and LOQ of the GC analyses were performed and shown in APPENDIX F.

4.2.2.2 Determination of the Reaction Rate of Each Target Microorganism

The NO_2^- and NO_3^--based reaction rates of the target microorganisms, namely Anammox, DAMOa and DAMOb were calculated throughout the operation of the SBR and the batch test. These reaction rates were computed according to the stoichiometric Equations 2.4, 2.5 and 2.6 in Section 2.3.2 and Section 2.4.2 (Hu et al., 2015). Equations 4.1, 4.2 and 4.3 were used to compute the reaction rates of each microorganism.

- $r_{\text{Anammox } NO_2^-} = -1.32 * r_{NH_4^+}$ ..... Equation 4.1
- $r_{\text{DAMOa } NO_3^-} = -r_{NO_3^-} + (0.26/1.32) * r_{\text{Anammox } NO_2^-}$ ..... Equation 4.2
- $r_{\text{DAMOb } NO_2^-} = -r_{NO_2^-} - r_{\text{Anammox } NO_2^-} + r_{\text{DAMOa } NO_2^-}$ ..... Equation 4.3

The Anammox and DAMOb reaction rates were calculated based on the NO_2^- consumption. Since Anammox is the only species among the three target microorganisms that oxidizes NH_4^+, the consumed NO_2^- by Anammox was computed using the measured NH_4^+ consumption rate ($r_{NH_4^+}$), and the NO_2^- removal reaction rate of Anammox ($r_{\text{Anammox } NO_2^-}$) was computed accordingly, as shown in Equation 4.1. The reaction rate of DAMOa ($r_{\text{DAMOa } NO_3^-}$) was calculated using the measured NO_3^- ($r_{NO_3^-}$) consumption rate, that includes the produced NO_3^- ($(0.26/1.32) * r_{\text{Anammox } NO_2^-}$) from the Anammox reaction, illustrated in Equation 4.2. The DAMOb reaction rate ($r_{\text{DAMOb } NO_2^-}$) was calculated using the measured NO_2^- consumption rate ($r_{NO_2^-}$) by considering the Anammox NO_2^- consumption rate ($r_{\text{Anammox } NO_2^-}$) and the DAMOa production rate of NO_2^- which is equal to ($r_{\text{DAMOa } NO_3^-}$) (Hu et al., 2015), as shown in Equation 4.3.

4.2.2.3 Determination of the Contribution of Each Target Microorganism to the Available TN Removed

The contribution of each of the target microorganisms to the TN removal was assessed to examine their activity and to further understand the composition of the

consortium in correlation with the molar ratio calculations and the molecular analysis. A sample calculation is displayed in APPENDIX H. The TN removed by each target microorganism, namely Anammox, DAMOb and DAMOa was calculated by considering the consumed and produced nitrogen with respect to each reaction (Equations 2.4, 2.5 and 2.6 in Section 2.3.2 and Section 2.4.2). Equations 4.4-4.14 were used in the calculations of the percent contribution of each microorganism to the TN removed. This was calculated as a percentage from the available TN that takes into consideration the produced nitrogen in the intermediate reactions, which cannot be observed by only considering the initial and final nitrogen concentrations. The initial TN was calculated by the summation of the initial concentrations of the nitrogen species analyzed experimentally (Equation 4.4). The final TN was calculated by the summation of the final concentrations of the nitrogen species (Equation 4.5).

The available TN is a term used via this thesis study for the first time. $TN_{available}$ is the summation of the initial nitrogen species and the produced nitrogen species via the reactions taking place, such as NO_3^- from Anammox and NO_2^- from DAMOa (Equation 4.6). Utilizing the available TN is critical since it allows the calculation of the actual consumption of each of the target species, otherwise, the real activity of DAMOa and DAMOb would not be recognized by just monitoring the initial and final concentrations of the nitrogen species. While the percentage contribution to the available TN removed ($\%CATN_{removed}$) was computed according to Equation 4.7.

$$TN_i=[NH_4^+\text{-}N]_i+[NO_2^-\text{-}N]_i+[NO_3^-\text{-}N]_i \quad \text{Equation 4.4}$$

$$TN_f=[NH_4^+\text{-}N]_f+[NO_2^-\text{-}N]_f+[NO_3^-\text{-}N]_f \quad \text{Equation 4.5}$$

$$TN_{available}=[NH_4^+\text{-}N]_i+[NO_2^-\text{-}N]_i+[NO_3^-\text{-}N]_i+\Delta[NO_3^-\text{-}N]_{AMX}+\Delta[NO_2^-\text{-}N]_{DAMOa} \quad \text{Equation 4.6}$$

$$\%CATN_{removed}^{microorganism}=(TN_{removed}^{microorganism}/TN_{available})*100 \quad \text{Equation 4.7}$$

where,

TN_i: initial TN concentration at each cycle, the sum of the initial concentrations of all the nitrogen species, (mg N/L)

$[NH_4^+\text{-}N]_i$: initial NH_4^+ concentration at each cycle, (mg N/L)

$[NO_2^-\text{-}N]_i$: initial NO_2^- concentration at each cycle, (mg N/L)

$[NO_3^-\text{-}N]_i$: initial NO_3^- concentration at each cycle, (mg N/L)

TN_f: final TN concentration at each cycle, the sum of the final concentrations of all the nitrogen species, (mg N/L)

$[NH_4^+\text{-}N]_f$: final NH_4^+ concentration at each cycle, (mg N/L)

$[NO_2^-\text{-}N]_f$: final NO_2^- concentration at each cycle, (mg N/L)

$[NO_3^-\text{-}N]_f$: final NO_3^- concentration at each cycle, (mg N/L)

$TN_{available}$: available TN concentration that is available for consumption by the target microorganisms which includes the summation of any nitrogen species to be produced via the target microorganisms, (mg N/L)

$\Delta[NO_3^-\text{-}N]_{AMX}$: NO_3^- concentration to be produced stoichiometrically by Anammox in each cycle computed regarding the consumed NH_4^+-N, (mg N/L)

$\Delta[NO_2^-\text{-}N]_{DAMOa}$: NO_2^- concentration to be produced stoichiometrically by DAMOa in each cycle, (mg N/L)

$TN_{removed}^{microorganism}$: TN removed by each microorganism calculated in Equations 4.11, 4.12 and 4.14, (mg N/L)

$\%CATN_{removed}^{microorganism}$: Percentage contribution of each microorganism to the available TN removal (%)

Since NH_4^+ is only consumed by Anammox and the Anammox bacteria were observed to be the most active of the three microorganisms, NH_4^+ was chosen to be the starting point of this calculation. The consumed NH_4^+ by Anammox was computed (Equation 4.8). While the corresponding consumed NO_2^- and produced

NO_3^- by Anammox was then computed, according to Equations 4.9 and 4.10, respectively. Hence the summation of the consumed nitrogen species while deducting the produced nitrogen yields the TN removed by Anammox (Equation 4.11).

AMX:

$\Delta[NH_4^+\text{-}N]=[NH_4^+\text{-}N]_i-[NH_4^+\text{-}N]_f$……..…….…... Equation 4.8

$\Delta[NO_2^-\text{-}N]_{AMX}= 1.32*\Delta[NH_4^+\text{-}N]$….....……..…...……..... Equation 4.9

$\Delta[NO_3^-\text{-}N]_{AMX}= 0.11*(\Delta[NH_4^+\text{-}N]+\Delta[NO_2^-\text{-}N]_{AMX})$……...…….... Equation 4.10

$TN_{removed}^{AMX}=\Delta[NH_4^+\text{-}N]+\Delta[NO_2^-\text{-}N]_{AMX}-\Delta[NO_3^-\text{-}N]_{AMX}$……..…..... Equation 4.11

where,

$\Delta[NH_4^+\text{-}N]$: NH_4^+ concentration consumed by Anammox in each cycle, (mg N/L)

$\Delta[NO_2^-\text{-}N]_{AMX}$: NO_2^- concentration consumed by Anammox in each cycle, (mg N/L)

$TN_{removed}^{AMX}$: TN concentration consumed by Anammox in each cycle, (mg N/L)

The available NO_3^- for DAMOa consumption includes the initial NO_3^- concentration and the produced NO_3^- by Anammox. Accordingly, the consumed NO_3^- by DAMOa can be computed, and subsequently the TN removed by DAMOa can be computed as well (Equation 4.12).

DAMOa:

$TN_{removed}^{DAMOa}=\Delta[NO_3^-\text{-}N]_{DAMOa}=[NO_3^-\text{-}N]_i-[NO_3^-\text{-}N]_f+\Delta[NO_3^-\text{-}N]_{AMX}$.. Equation 4.12

$\Delta[NO_2^-\text{-}N]_{DAMOa}=\Delta[NO_3^-\text{-}N]_{DAMOa}$…….…….....…... Equation 4.13

where,

$\Delta[NO_3^-\text{-}N]_{DAMOa}$: NO_3^- concentration consumed by DAMOa in each cycle, (mg N/L)

$TN_{removed}^{DAMOa}$: TN concentration consumed by DAMOa in each cycle, (mg N/L)

On the other hand, the available NO_2^- for DAMOb consumption is the remaining NO_2^- after the Anammox reaction, since Anammox has a higher affinity to NO_2^- in comparison to DAMOb, and the produced NO_2^- by DAMOa. Hence, the consumed NO_2^- by DAMOb can be computed, hence, the TN removed by DAMOb can be deduced (Equation 4.14).

DAMOb:

$TN_{removed}^{DAMOb}=\Delta[NO_2^-N]_{DAMOb}=[NO_2^-N]_i-\Delta[NO_2^-N]_{AMX}+\Delta[NO_2^-N]_{DAMOa}-[NO_2^-N]_f$ …….……... Equation 4.14

where,

$\Delta[NO_2^-N]_{DAMOb}$: NO_2^- concentration consumed by DAMOb in each cycle, (mg N/L)

$TN_{removed}^{DAMOb}$: TN concentration consumed by DAMOb in each cycle, (mg N/L)

4.2.2.4 Determination of the Stoichiometric Ratio of the Consortium

DAMO SBR

Since the target microorganisms for this reactor are DAMOa and DAMOb and no NH_4^+ was added, the theoretical cases considered were different than the DAMO-Anammox SBR. Only one stoichiometric molar ratio was considered and discussed, namely, $\Delta NO_2^-/\Delta NO_3^-$. The molar ratio was examined under four different cases that might be occurring in the reactor. The assumptions followed in these cases are given below:

- The cases are as follows: DAMOa, DAMOb and DAMO, (Equations 4.15, 4.16 and 4.17);
    i. DAMOa: The SBR contains only DAMOa.
    ii. DAMOb: The SBR contains only DAMOb.
    iii. DAMO: The SBR contains both DAMOb and DAMOa.
- For all cases, (i.e., for all the potential combinations of cultures)

- The change of concentration in each cycle was calculated as follows $\Delta C = C_{initial} - C_{final}$. Therefore, consumption of the nitrogen species is positive, while production is negative.

The theoretical ratios were calculated according to the stoichiometry present in the reaction equations (Equations 2.5 and 2.6 in Section 2.3.2 and Section 2.4.2). For Equations 2.5 and 2.6, the limiting reagent in each reaction was considered. The limiting reagent in each reaction is NO_3^- and NO_2^- for DAMOa and DAMOb reactions, respectively. Accordingly, the equations were adjusted for 1 mole of the specified limiting reagent.

In addition to the three main cases mentioned above, a special incident, namely, *DAMO where DAMOb activity is double the DAMOa activity, as displayed in Equation 4.18. In this case, the activity of DAMOa was not assumed to be 100%. Incorporating this special case may improve the characterization of the co-culture composition via the molar ratio calculation.

All calculations of each culture combination (four cases) are given in Equations 4.15-4.18 and accordingly, the theoretical stoichiometric molar values were obtained in Table 4.2.

DAMOa: $NO_3^- \rightarrow NO_2^-$……. Equation 4.15

DAMOb: $NO_2^- \rightarrow 0.5\ N_2$…….……...…… Equation 4.16

DAMO: $NO_2^- + NO_3^- \rightarrow NO_2^- + 0.5N_2$……..……. Equation 4.17

*DAMO: $2\ NO_2^- + NO_3^- \rightarrow NO_2^- + N_2$……....…… Equation 4.18

Table 4.2 Theoretical stoichiometric molar ratio calculations of nitrogen species for the different consortium cases in the DAMO SBR

Microbial consortium cases	ΔNO_2^-	ΔNO_3^-	$\Delta NO_2^-/\Delta NO_3^-$
DAMOa	1	-1	-1
DAMOb	-1	0	∞
DAMO	0	-1	0
*DAMO	-1	-1	1

DAA SBR

The consortium cases utilized in Section 3.2.2.4 of the DAMO-Anammox SBR, was also employed for the DAA SBR. The reactor performance was assessed in comparison to the theoretical molar ratios. Four different molar ratios were calculated and compared to the theoretical stoichiometric molar ratios, $\Delta NO_2^-/\Delta NH_4^+$, $\Delta NH_4^+/\Delta NO_3^-$, $\Delta NO_2^-/\Delta NO_3^-$ and $(\Delta NO_2^- + \Delta NH_4^+)/\Delta NO_3^-$. These ratios were examined under nine different cases that might be occurring in the reactor. The assumptions followed in these cases are given below:

- The nine cases are as follows: AMX, DAMOa, DAMOb, AMX & DAMOa, AMX & DAMOb, *AMX & DAMOa, DAMX, *DAMX, and DAMO (Equations 4.19, 4.20, 4.22, 4.23, 4.25, 4.26 and 4.27);
    i. AMX: The SBR only contains Anammox culture.
    ii. DAMOa: The SBR only contains DAMOa culture.
    iii. DAMOb: The SBR only contains DAMOb culture.
    iv. AMX & DAMOa: The SBR contains both Anammox and DAMOa.
    v. AMX & DAMOb: The SBR contains both Anammox and DAMOb.
    vi. DAMO: The SBR contains both DAMOa and DAMOb.
    vii. DAMX: The SBR contains Anammox, DAMOa and DAMOb.

- For all cases, (i.e., for all the potential combinations of cultures)
- The change of concentration in each cycle was calculated as follows $\Delta C = C_{initial} - C_{final}$. Therefore, consumption of the nitrogen species is positive, while production is negative.

The theoretical ratios were calculated according to the stoichiometry present in the reaction equations (Equations 2.4, 2.5 and 2.6 in Section 2.3.2 and Section 2.4.2). For Equations 2.4, 2.5 and 2.6, the limiting reagent in each reaction was considered. The limiting reagent in each reaction is NH_4^+, NO_3^- and NO_2^- for Anammox, DAMOa and DAMOb reactions, respectively. Accordingly, the equations were adjusted for 1 mole of the specified limiting reagent.

Similarly, to the DAMO-Anammox SBR, a special incident was added to the seven main cases mentioned above, where DAMOa is able to consume only the NO_3^- produced by the Anammox, was constructed by equating the moles of NO_3^- consumed to the moles of NO_3^- produced in the two cases, namely, *AMX & DAMOa and *DAMX, as displayed in Equations 4.21 and 4.24, respectively. In these two cases, the activity of DAMOa was not assumed to be 100%. Incorporating this special case may improve the characterization of the co-culture composition via the molar ratio calculation.

All calculations of each culture combination (nine cases) are given in Equations 4.19-4.27 and accordingly, the theoretical stoichiometric molar values were obtained in Table 4.3.

AMX: $NH_4^+ + 1.32\ NO_2^- \rightarrow 0.26\ NO_3^- + 1.02\ N_2$…….……. Equation 4.19

AMX & DAMOa: $NH_4^+ + 0.32\ NO_2^- + 0.74\ NO_3^- \rightarrow 1.02\ N_2$…..… Equation 4.20

*AMX & DAMOa: $NH_4^+ + 1.06\ NO_2^- \rightarrow 1.02\ N_2$…….. Equation 4.21

AMX & DAMOb: $NH_4^+ + 2.32\ NO_2^- \rightarrow 0.26\ NO_3^- + 1.52\ N_2$…..… Equation 4.22

DAMX: $NH_4^+ + 1.32\ NO_2^- + 0.74\ NO_3^- \rightarrow 1.52\ N_2$……...… Equation 4.23

*DAMX: $NH_4^+ + 2.06\ NO_2^- \rightarrow 1.52\ N_2$……..… Equation 4.24

DAMOa: $NO_3^- \rightarrow NO_2^-$…….……. Equation 4.25

DAMOb: $NO_2^- \rightarrow 0.5\ N_2$…….…… Equation 4.26

DAMO: $NO_2^- + NO_3^- \rightarrow NO_2^- + 0.5N_2$……..…. Equation 4.27

Table 4.3 Theoretical stoichiometric molar ratio calculations of nitrogen species for the different consortium cases in the DAA SBR

Consortium cases	ΔNH_4^+	ΔNO_2^-	ΔNO_3^-	$\Delta NO_2^-/\Delta NH_4^+$	$(\Delta NO_2^-+\Delta NH_4^+)/\Delta NO_3^-$	$\Delta NO_2^-/\Delta NO_3^-$	$\Delta NH_4^+/\Delta NO_3^-$
AMX	1	1.32	-0.26	1.32	-8.92	-5.08	-3.85
AMX & DAMOa	1	0.32	0.74	0.32	1.78	0.43	1.35
*AMX & DAMOa	1	1.06	0	1.06	□	□	□
AMX & DAMOb	1	2.32	-0.26	2.32	-12.77	-8.92	-3.85
DAMX	1	1.32	0.74	1.32	3.14	1.78	1.35
*DAMX	1	2.06	0	2.06	□	□	□
DAMOa	0	1	-1	□	-1	-1	0
DAMOb	0	-1	0	□	□	□	undefined
DAMO	0	0	-1	□	0	0	0

4.2.3 Fluorescent In-Situ Hybridization Analysis

The FISH analyses were performed during the operation of the DAMO SBR and DAA SBR for morphological detection and determination of the relative abundance of the target species (Nielsen et al., 2009).

About 5 ml of sample was used, where the supernatant was separated by centrifugation at 10,000 g for 5 min and then it was discarded. The remaining sludge was fixed with an equal volume of 4% PFA in PBS, which was then stored overnight at 4°C. The next day the sample was centrifuged at 10,000 g for 5 min to separate the PFA, which was then discarded. The remaining fixed biomass was then dissolved in 5 mL of 1:1 PBS/Ethanol (Daims et al., 2009). The samples were then stored overnight at -20°C. The following day the samples were carefully placed on slides and dehydration of the samples on the slides was conducted. This was carried out with sequential washing with 50%, 80%, and 99% ethanol (Daims et al., 2009). The next step was permeabilization of the microbial cells which was performed by incubating the slides for 1 hr at 37°C after the addition of lysozyme (Daims et al., 2009).

Hybridization solutions of different probes targeting *M. nitroreducens, M. oxyfera*, General Bacteria, General Archaea and Anammox were prepared considering their relative formamide and NaCl concentrations. The stringency conditions (formamide and NaCl concentrations) were optimized prior to the FISH analyses to ensure better results of probe hybridization. The probes used in the scope of these experiments are summarized in Table 4.4. Five hybridization mixtures were prepared using different combinations of the previously described solutions (Table 4.5). The mixtures containing only General Archaea and General Bacteria were counterstained with DAPI to determine the content of bacteria and archaea in the microbial consortium. Five slides were prepared for each biomass sample analyzed. The hybridization mixtures were added carefully on the slides and the slides were incubated at 46°C for about 5 hr (Daims et al., 2009). After hybridization, the slides were washed at

48°C for 15 min with a washing buffer containing the same formamide concentration as the hybridization buffer (Daims et al., 2009).

After washing and drying the slides, imaging can commence. FISH imaging was performed using Carl Zeiss Axio Vision A1 UV microscope under suitable filters of the chosen probes. At least 3 representative microscopy images were chosen for each slide. The images were analyzed via the ImageJ software. The obtained images from the microscope were then processed using ImageJ, where the colored areas were converted to pixels. The pixel areas represent the presence of the probe and hence the target cell. The average area occupied by the pixels in the three chosen images and the relative abundance of each slide was computed. These computations were conducted in relativeness to the area occupied by the General Bacteria and General Archaea which were performed in relativeness to DAPI counterstaining. A summary of the steps performed using ImageJ, the resulting images and the obtained relative abundance in each slide are illustrated in APPENDIX I.

Table 4.4 Sequences, labels and formamide concentrations of chosen FISH probes

Target Species	Probe	Label	Formamide Concentration (%)	Reference
M. nitroreducens	S-*-Darc-872-a-A-18-GGC TCC ACC CGT TGT AGT	GFP and Cy5	40	Hu et al. (2015)
M. oxyfera	S-*-DBACT-0193-a-A-18-CGC TCG CCC CCT TTG GTC	Alexa Fluor 350	40	Ettwig et al. (2009)
General Anammox	S-*-Amx-0368-a-A-18-CCT TTC GGG CAT TGC GAA	Cy5	20	Schmid et al. (2005)
General Bacteria	EUB1 -GCT GCC TCC CGT AGG AGT	GFP	40	Daims et al. (2009)
	EUB2 -GCA GCC ACC CGT AGG TGT			
	EUB3-GCT GCC ACC CGT AGG TGT			
General Archaea	S-Darc-0915-a-A-20-GTG CTC CCC CGC CAA TTC CT	GFP	40	Knittel et al. (2005)

Table 4.5 The hybridization mixture and aim of each slide

Slide	Hybridization mixture content	Aim
1	General Bacteria and DAPI counterstaining	Determine the content of bacteria in the microbial consortium
2	General Archaea and DAPI counterstaining	Determine the content of archaea in the microbial consortium
3	*M. oxyfera*, Anammox and General Bacteria	Determine the abundance of *M. oxyfera* and Anammox relative to General Bacteria
4	*M. nitroreducens* and General Archaea	Determine the abundance of *M. nitroreducens* relative to General Archaea
5	*M. oxyfera*, *M. nitroreducens* and Anammox	Determine the relative abundance of the target species among each other

4.3 Results and Discussion

4.3.1 The Results of DAMO SBR Operation

The DAMO SBR was established aiming to enrich a DAMO co-system (DAMO bacteria and DAMO archaea). This reactor would also provide a source of inoculum for the reactor described in Chapter 5. The DAMO SBR was inoculated with AD sludge and supplied with only NO_2^- and NO_3^-, as the nitrogen source, at initial concentrations of 10 and 25 mg N/L, respectively, at an HRT was 4 days. Limited NO_2^- was supplied in comparison to NO_3^- to provide the DAMOa a competitive advantage since they can be outcompeted by DAMOb. The reactor performance and the population dynamics of the microbial consortium enriched in the DAMO SBR were evaluated throughout the operation of the reactor. The DAMO SBR was operated for about 180 days (89 cycles) and the results are presented in two main sections, namely, results of reactor performance and results of molecular analyses.

4.3.1.1 Results of DAMO SBR Performance

The pH of the influent was maintained at a pH of 7.2-7.6. The effluent pH ranged from 7.38-8.03, throughout 89 cycles, as seen in Figure 4.3. The average pH of the 89 cycles of operation was 7.7±0.2. The pH values were slightly higher than the most commonly applied pH throughout DAMO-Anammox enrichment studies (7.3-7.5) (Luesken et al., 2011; Haroon et al., 2013; Ding et al., 2014; Ding et al., 2017; Cai et al., 2015; Xie et al., 2016; Fu et al., 2017; Hu et al., 2015). The pH higher than 7.6 signifies that there might be heterotrophic denitrification taking place, although no source of COD was supplied in the feed. Nevertheless, this heterotrophic denitrification did not seem to be occurring in all the cycles of the DAMO SBR.

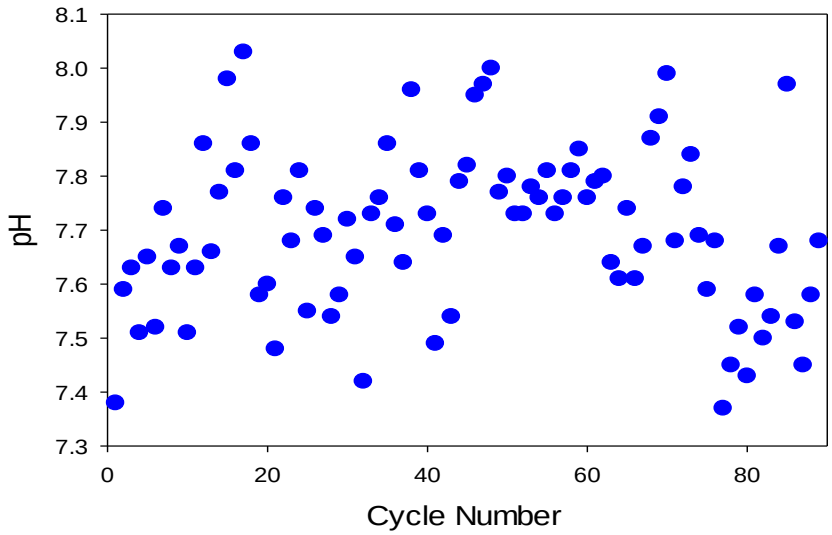

Figure 4.3 pH results of the effluent samples of the DAMO SBR

The TOC of Cycle 0 was found to be 309 mg/L; therefore, denitrification activity was expected to occur until the TOC was consumed (Figure 4.4). At Cycle 10, the initial TOC was measured to be 168 mg/L, while at the end of that cycle it was measured as 119 mg/L. At the Cycle 22, the initial TOC concentration was 121 mg/L while the final concentration of the same cycle was 113 mg/L. The TOC concentration at Cycle 80 reached 12 mg/L (Figure 4.4). It seems from the pH and TOC results that heterotrophic denitrification kept occurring till around Cycle 70, due to the presence of organic carbon, which seemed to be produced in the reactor since it was not supplied in the feed. Experimental TOC concentrations do not

comply with the theoretical effluent concentration trend line, which was produced considering only the hydraulics of the SBR operation without any biological TOC degradation. On the other hand, cyclic analysis on Cycle 22 and Cycle 55 reveal that there is no TOC production and there is neglibile TOC degradation.

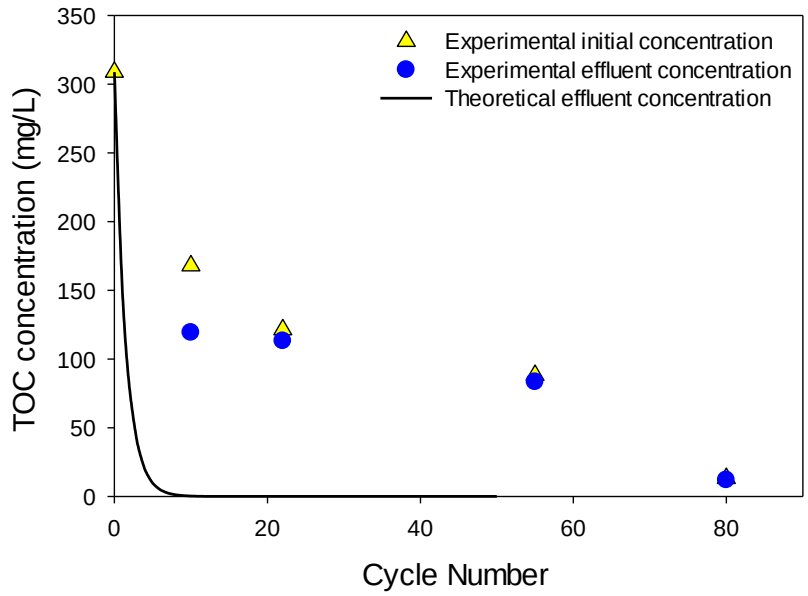

Figure 4.4 TOC results of the DAMO SBR

The TSS and VSS of the DAMO SBR was measured at the initial inoculation and at Cycle 80. The results show that the TSS and VSS decreased about four-fold, but the VSS/TSS percentage stayed approximately the same, as seen in Table 4.6. This suggests that the relevant active microorganisms with respect to the conditions provided might have remained in the reactor while the others were degraded. Furthermore, the degradation of these cells might have released organic carbon, explaining the TOC content in the samples withdrawn from the SBR.

Table 4.6 TSS and VSS results of the sludge from the DAMO SBR

Sludge	TSS (g/L)	VSS (g/L)	VSS/TSS (%)
Mixed initial sludge	36.1±1.0	15.1±0.4	42
Cycle 80	9.4±0.4	3.8±0.2	40

4.3.1.1.1 Nitrogen Removal Performance of DAMO SBR

The reactor was operated at initial concentrations of NO_2^- and NO_3^- of 10 and 25 mg N/L, respectively, to provide DAMOa an advantage over DAMOb. Since DAMOb has higher CH_4 affinity compared to DAMOa, therefore a lower concentration of NO_2^- is required to sustain a high activity of DAMOa (Luesken et al., 2011b; Zhu et al., 2011; Ding et al., 2014; Fu et al., 2017a). In this regard, DAMOa would be the rate-determining step in providing the extra NO_2^- for DAMOb to consume. The theoretical NLR was 17.5 mg N/L·day throughout the operation of the DAMO SBR, corresponding to the applied HRT of 4 days. The average experimental initial concentrations of NO_2^- and NO_3^- during the operation of the DAMO SBR were 10.1±2.5 and 24.2±5.3 mg N/L, respectively, while the experimental NLR was 17.1±3.5 mg N/L·day and the influent TN concentration was 68.5±14 mg N/L.

The NH_4^+ concentration at cycle 0 was found to be 250 mg N/L and decreased to a concentration of 0 mg N/L at the end of the 17th cycle (Figure 4.5a). No NH_4^+ was produced at any of the cycles after Cycle 17, this signifies that there was no DNRA activity. This means that any NO_2^- or NO_3^- was not converted to NH_4^+, concluding that the oxidized forms of nitrogen (NO_2^- and NO_3^-) were removed by other like means such as DAMO and heterotrophic denitrification.

The removal efficiencies, removal rates and consumption ratios were calculated to assess the performance of the system in comparison to the theoretical ratios of DAMOa and DAMOb. From Cycle 1-17, the DAMO SBR experienced fluctuations in terms of nitrogen species removal efficiencies and removal rates. With the consumption of NH_4^+, NO_2^- and NO_3^- removal efficiencies and removal rates became more stable (Figure 4.6 and Figure 4.7). This period can be referred to an acclimation period. The average removal efficiency of NO_2^- (Cycle 18-89) was calculated as 78±18 % (Figure 4.6b). While the average removal efficiency of NO_3^- (Cycle 18-89) was found to be 93±11 % (Figure 4.6c). The average removal rates of NO_2^- and NO_3^- (Cycle 18-89) was found to be 4.2±1.2 mg N/L·day (Figure 4.7b) and 11.6±2.3 mg N/L·day (Figure 4.7c), respectively.

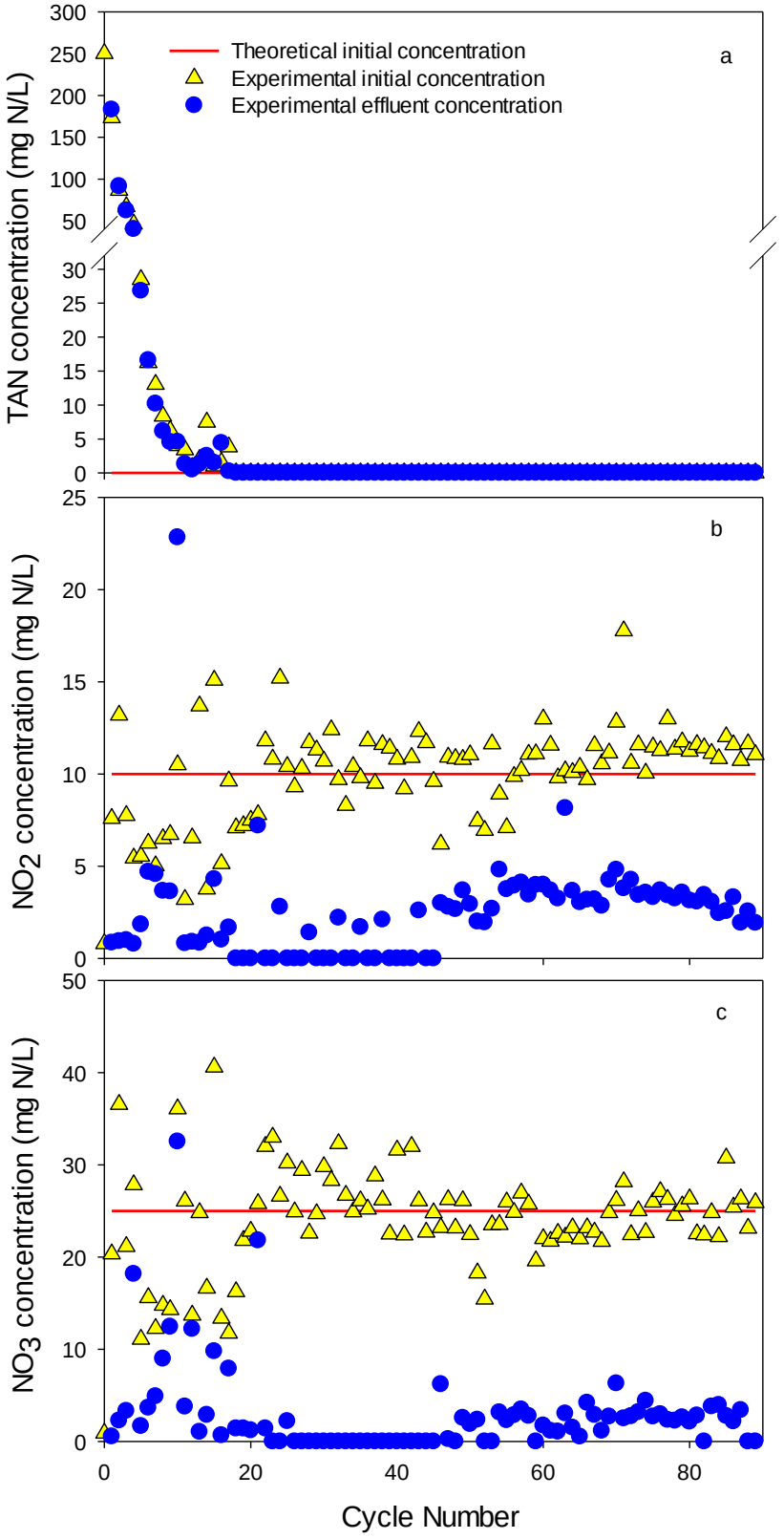

Figure 4.5 Initial and final concentrations of (a) TAN, (b) NO_2^--N and (c) NO_3^--N during each cycle of the DAMO SBR (the S.D of each measurement was <5%)

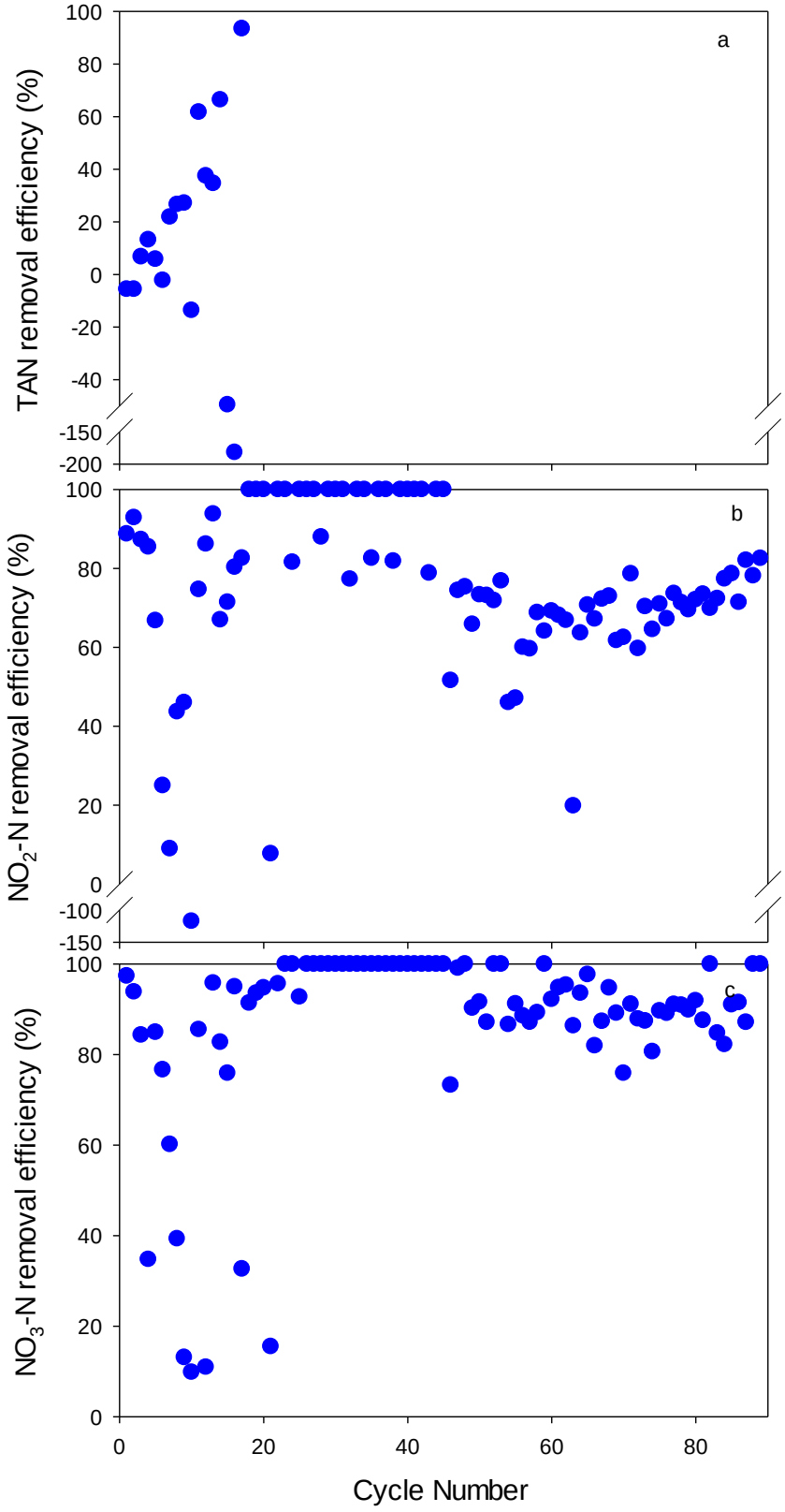

Figure 4.6 Removal efficiencies of (a) TAN, (b) NO_2^- and (c) NO_3^- in the DAMO SBR (The negative values emphasize production)

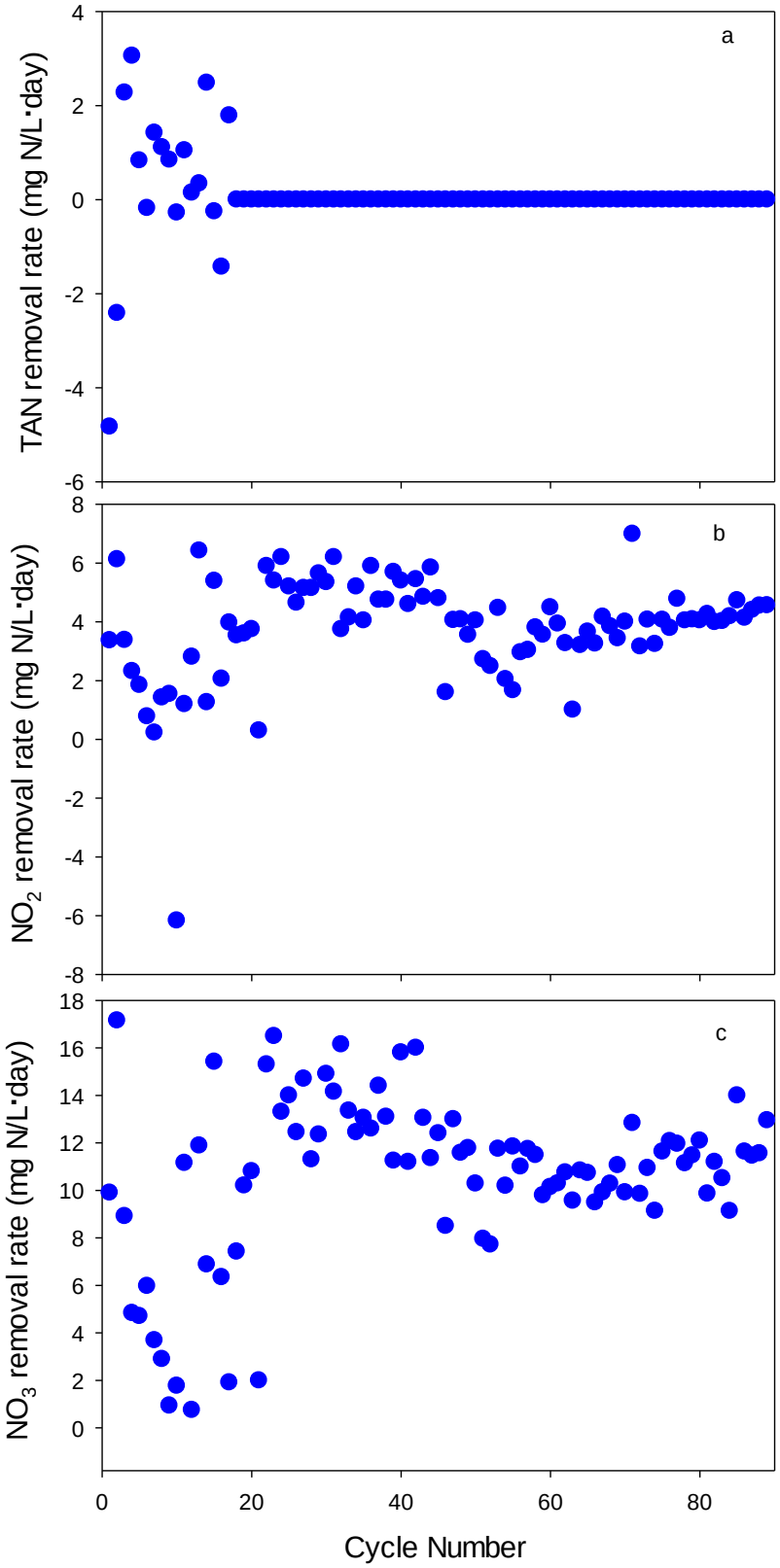

Figure 4.7 Removal rates of (a) TAN, (b) NO_2^- and (c) NO_3^- in the DAMO SBR (The negative values imply production)

The average TN removed from Cycle 18-89 was found to be 31.4±6.4 mg N/L (Figure 4.8). and the average percentage of TN removed of the same period was calculated as 88±12 %. The $\%CATN_{removed}$ of the intended target microorganisms to be enriched in the DAMO SBR were calculated. Since no NH_4^+ was added in the feed, the Anammox activity was not considered in the calculation. For the DAMO SBR, only DAMOa and DAMOb contributions were calculated from the available nitrogen species namely, NO_2^- and NO_3^-. The average $\%CATN_{removed}$ was found to be 39±4 %, while that of the DAMOb was computed to be 53±6 % (Figure 4.9). This suggests that DAMOb exhibited dominance over the DAMOa throughout the operation of the DAMO SBR.

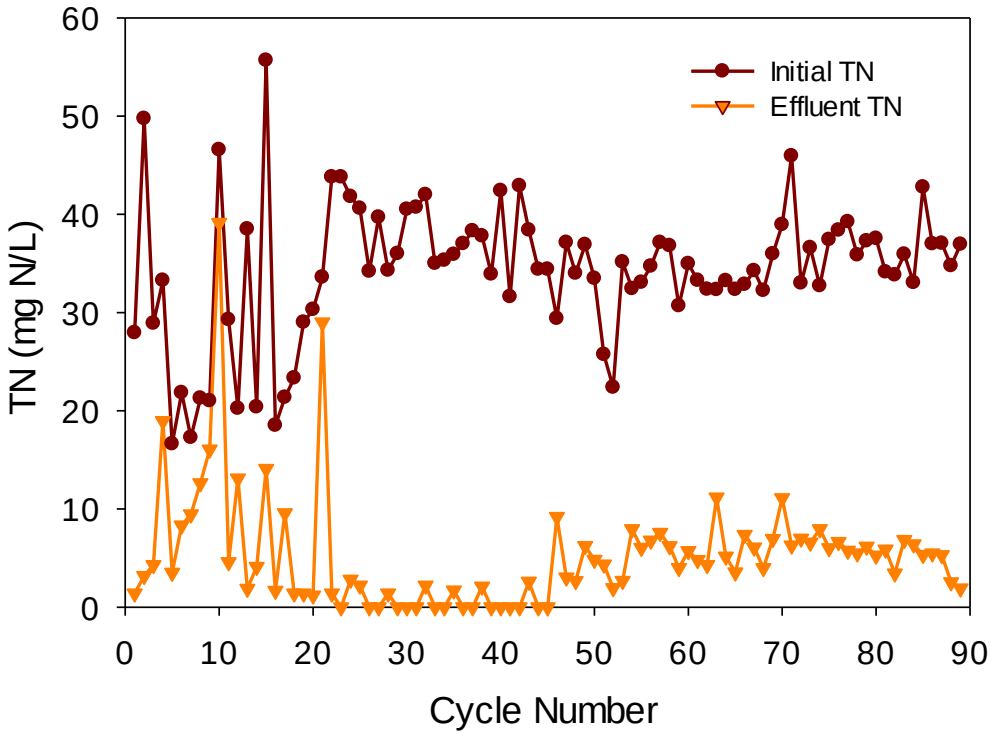

Figure 4.8 Initial and final TN concentrations of the DAMO SBR in each cycle

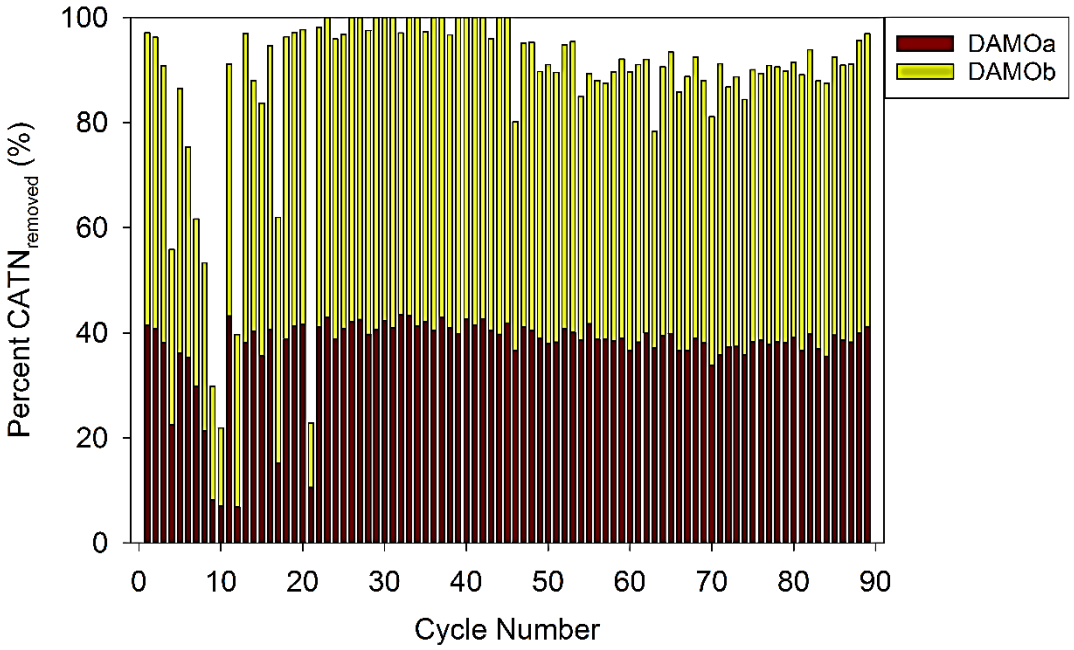

Figure 4.9 The %CATN$_{removed}$ in each cycle of the DAMO SBR

The NO_2^-- and NO_3^--based reaction rates of each of the target microorganisms were calculated and displayed in Figure 4.10. Since no NH_4^+ was added and it was completely consumed by Cycle 18, and was not produced after that, the Anammox activity was not visible. The average $r_{DAMOb\ NO_2^-}$ and $r_{DAMOa\ NO_3^-}$ (Cycle 18-89) were 15.8±3.2 mg N/L·day and 11.6±2.2 mg N/L·day, respectively, as seen in Figure 4.10. The results show that the average $r_{DAMOb\ NO_2^-}$ was about 1.5-fold than the average $r_{DAMOa\ NO_3^-}$, which is in accord with the results of the contribution to the available TN removed.

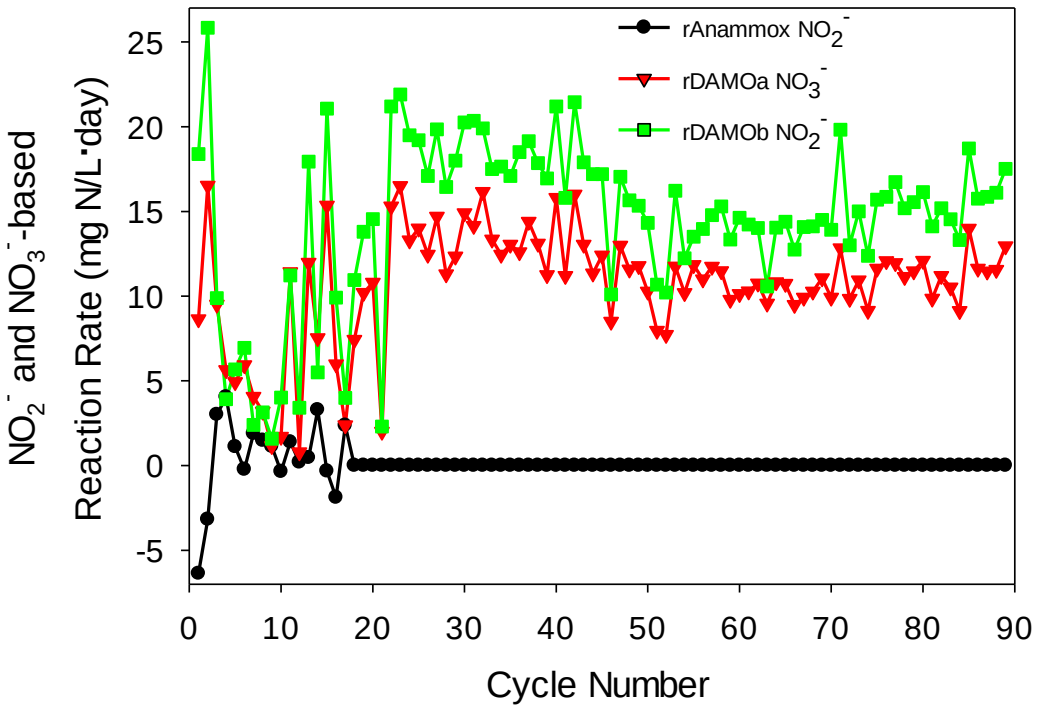

Figure 4.10 The calculated NO_2^- and NO_3^--based reaction rates of each target microorganism throughout the operation of the DAMO SBR

4.3.1.1.2 Determination of the Stoichiometric Ratio of the Microbial Consortium in DAMO SBR

Since only NO_2^- and NO_3^- were supplied in the feed, the experimental stoichiometric molar ratio, $\Delta NO_2^-/\Delta NO_3^-$ was computed and compared to the theoretical ratio in four different possible scenarios assumed to occur in the DAMO SBR, as illustrated in Figure 4.11. Since the $\Delta NO_2^-/\Delta NO_3^-$ ratio of the DAMOb case is equal to ∞, it was not shown in Figure 4.11. The higher the $\Delta NO_2^-/\Delta NO_3^-$ ratio, the more the DAMOb is dominant in the culture. From Cycle 1-17 the cyclic $\Delta NO_2^-/\Delta NO_3^-$ ratio was fluctuating in the acclimation, however, after Cycle 18 the cyclic $\Delta NO_2^-/\Delta NO_3^-$ ratio stabilized and it can be said that steady state was achieved. The average cyclic $\Delta NO_2^-/\Delta NO_3^-$ ratio of the DAMO SBR from Cycles 18-89 was calculated to be 0.36. This indicates that the culture contained both DAMOb and DAMOa, but DAMOb at about 1.5-fold the DAMOa. This result concurs with the result of the contribution percentage of each microorganism.

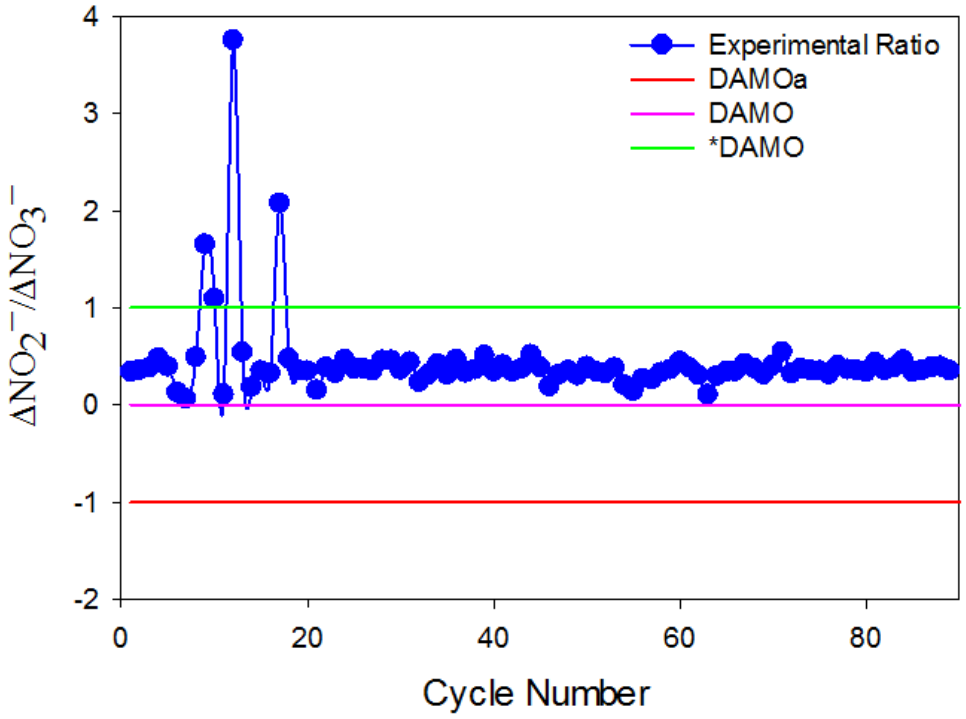

Figure 4.11 The cyclic $\Delta NO_2^-/\Delta NO_3^-$ ratio achieved in the DAMO SBR compared to the theoretical ratio of each case

4.3.1.2 FISH Analyses Results of DAMO SBR

Sludge samples from the DAMO SBR were taken at different intervals, at Cycle 0, (the initial seed sludge), at Cycle 50 and at Cycle 80 to perform the FISH analysis. This was performed to observe the change in the microbial composition existing in the reactor with respect to time. The target cells were tested with the corresponding probes from Table 4.4 that can visually distinguish *M. oxyfera*, *M. nitroreducens* and Anammox. General bacteria, general archaea and DAPI probes were used to quantify the relative abundance of the target species in the reactor. Hence, the enrichment progress was assessed. The samples were analyzed, and the microscope images are shown in Figure 4.12.

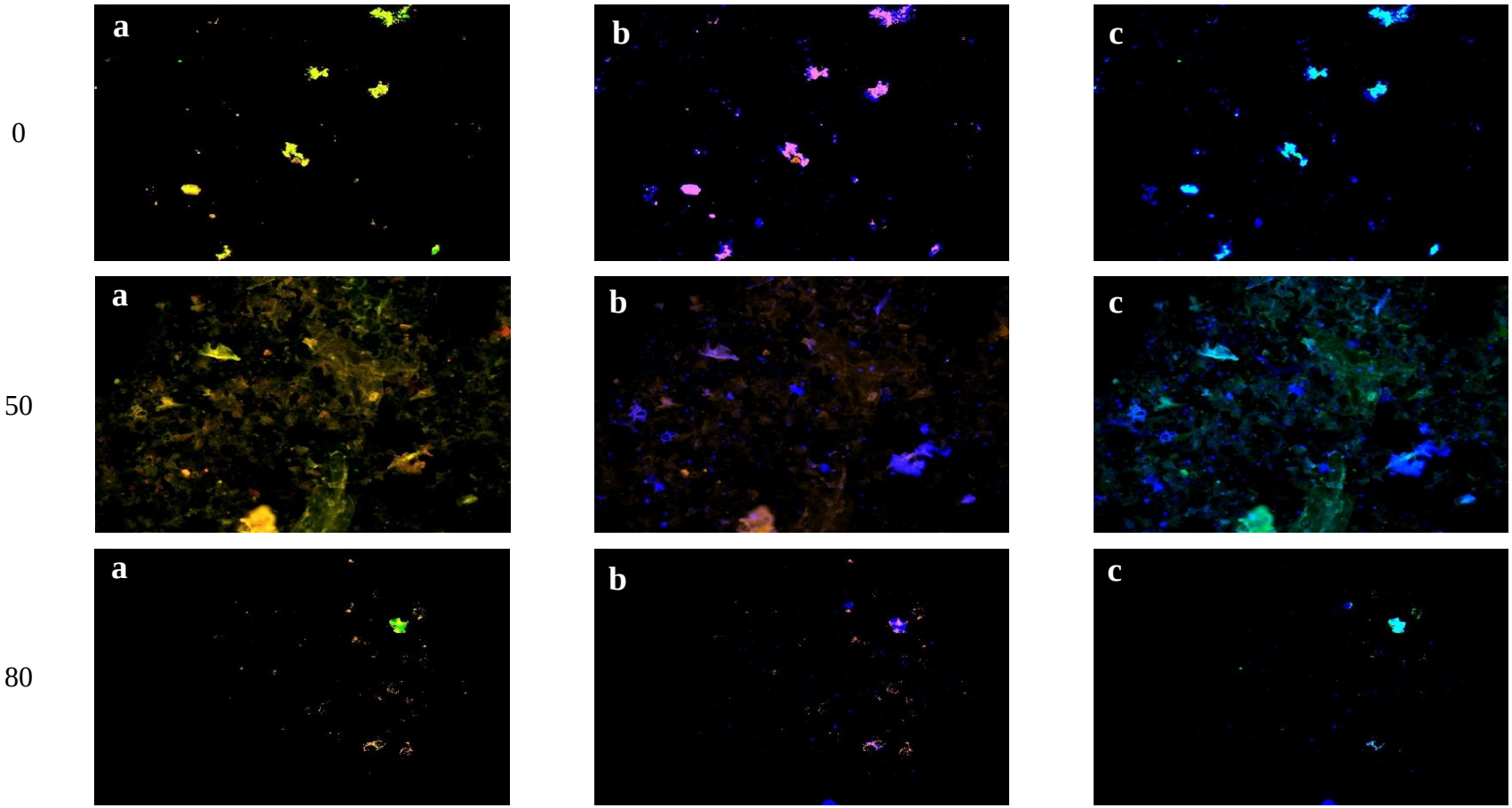

Figure 4.12 FISH images of DAMO SBR sludge samples withdrawn at Cycles 0, 50 and 80 (a) Orange: AMX-368 - general Anammox and green: DARCH-872 - *M. nitroreducens* (b) Orange: AMX-368 - general Anammox and blue: DBACT-193 - *M. oxyfera* (c) Blue: DBACT-193 - *M. oxyfera* and green: DARCH-872 - *M. nitroreducens*

The FISH results of the initial sludge sample illustrated that the relative abundance of Anammox, *M. oxyfera* and *M. nitroreducens* were 35±1 %, 25±2 % and 40±3 %, respectively (Figure 4.13). By Cycle 50, the relative abundance of Anammox and *M. nitroreducens* decreased to 21±5 % and 30±2 %, respectively, while that of *M. oxyfera* increased to 49±7 %. Moreover, at Cycle 80, the relative abundance of Anammox, *M. oxyfera* and *M. nitroreducens* did not change much, and reached 24±1 %, 44±2 % and 32±1 %, respectively. The results displayed that the *M. oxyfera* was the dominant species of the three target microorganisms reaching an abundance relatively 2-fold the abundance of *M. nitroreducens* from Cycle 0 to 80, as shown in Figure 4.13. This is in accordance with the results of the $\%CATN_{removed}$ and the stoichiometric molar ratio of the microbial consortium in Section 4.3.1.1.1 and Section 4.3.1.1.2.

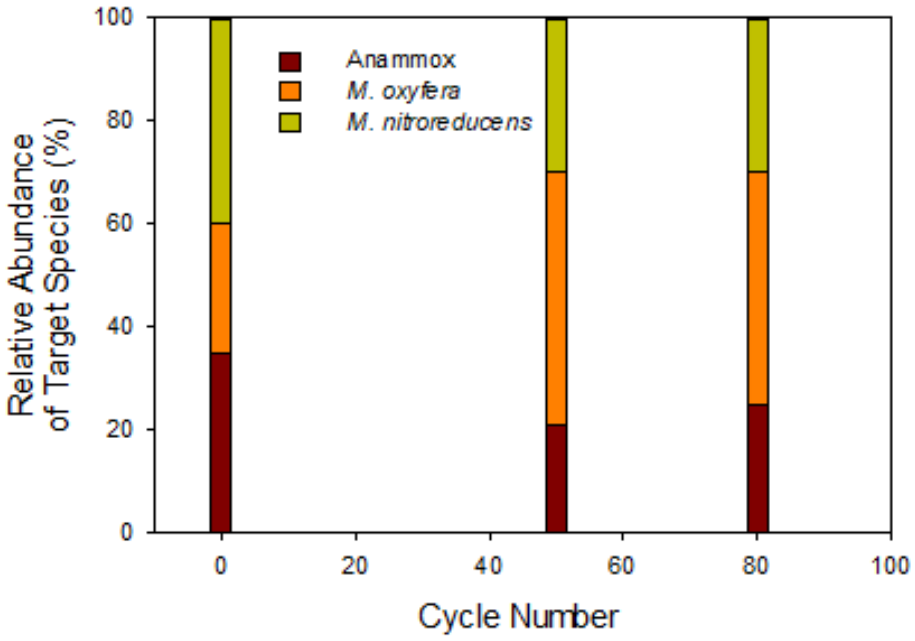

Figure 4.13 The relative abundance of target species with respect to the total microbial consortium in the DAMO SBR

The major outcome is that both DAMO are enriched. Despite the 2.5 fold higher influent NO_3^- to NO_2^- concentration, higher DAMOb abundance was observed in comparison to DAMOa. This resulted in 88±12 % removal of TN with an average

TN removal rate (Cycle 18-89) of 15.7±3.2 mg N/L·day, while the average removal rates of NO_2^- and NO_3^- were found to be 4.2±1.2 mg N/L·day and 11.6±2.3 mg N/L·day, respectively.

Although NH_4^+ was absent in the feed, yet Anammox bacteria were detected in the DAMO SBR. This might be due to the release of NH_4^+ via cell degradation that might have sustained the remaining Anammox in the reactor. NH_4^+ was not detected in the effluent of the DAMO SBR so it might have been consumed by Anammox.

4.3.2 The Results of DAA SBR Operation

The DAA SBR was established aiming to enrich DAMO archaea and Anammox and possibly DAMOb to improve the enrichment process of the DAMO-Anammox co-culture and investigate the effect of the different nitrogen sources on the enrichment of the co-culture. Moreover, this reactor would also provide a source of inoculum for the reactor described in Chapter 5. The DAA SBR was supplied with only NH_4^+ and NO_3^-, as the nitrogen source, at initial concentrations of 12 and 25 mg N/L, respectively, at an HRT was 4 days. Therefore, HRT and the NO_3^- concentration were the same as those applied in the DAMO SBR study, as well as DAMO-Anammox SBR (Phase IV). Limited NH_4^+ was supplied in comparison to NO_3^- to provide the DAMOa a competitive advantage since they can be outcompeted by DAMOb. The reactor performance and the population dynamics of the microbial consortium enriched in the DAA SBR were evaluated throughout the operation of the reactor. The DAA SBR was operated for about 170 days (82 cycles) and the results are presented in two main sections, results of reactor performance and results of molecular analyses.

4.3.2.1 Results of DAA SBR Performance

The pH of the influent was maintained at a pH of 7.2-7.6. The effluent pH ranged from 7.0-7.93, throughout 82 cycles, as seen in Figure 4.14. The average pH of the

82 cycles of operation was 7.32±0.15. The pH values were in the range of the most commonly applied pH throughout DAMO-Anammox enrichment studies (7.3-7.5) (Luesken et al., 2011; Haroon et al., 2013; Ding et al., 2014; Ding et al., 2017; Cai et al., 2015; Xie et al., 2016; Fu et al., 2017; Hu et al., 2015). This pH range was defined as the optimal pH range for the enrichment of the DAMO-Anammox co-culture.

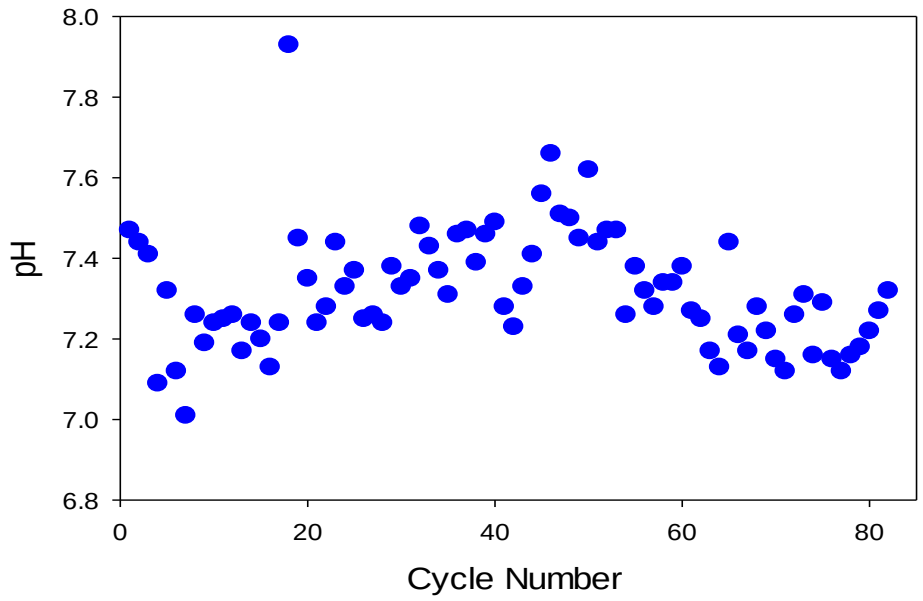

Figure 4.14 pH results of the effluent samples of the DAA SBR

The TOC concentration of Cycle 0 was found to be 309 mg/L; therefore, denitrification activity was expected to occur until the TOC is consumed (Figure 4.15). At cycle 10, the initial TOC was measured to be 196 mg/L and the at the end of the same cycle it was measured as 129 mg/L. At Cycle 22, the initial TOC concentration was 117 mg/L while the final concentration of the same cycle was 116 mg/L. Experimental TOC concentrations do not comply with the theoretical effluent concentration trend line, which was produced considering only the hydraulics of the SBR operation without any biological TOC degradation. This result reveals that there might be TOC production during the operation. This might be due to either the production of EPS or the degradation of cells that are not favored in the conditions provided in the reactor. On the other hand, cyclic analysis on Cycle 22 and Cycle 55

reveal that there is almost no TOC production and there is neglibile TOC degradation. Nevertheless, TOC concentration decreased down to 14.4 mg/L by Cycle 80. It can be concluded that, although it was not observed through the cycles where initial and final TOC analyses were performed TOC concentration decreased through the operational period of Cycles 20-82. This was attributed to heterotrophic denitrification. The TOC results of the DAA SBR were similar to the DAMO SBR, yet heterotrophic denitrification activity was less evident in the DAA SBR in comparison to the DAMO SBR in terms of pH increase, as seen in Figure 4.14.

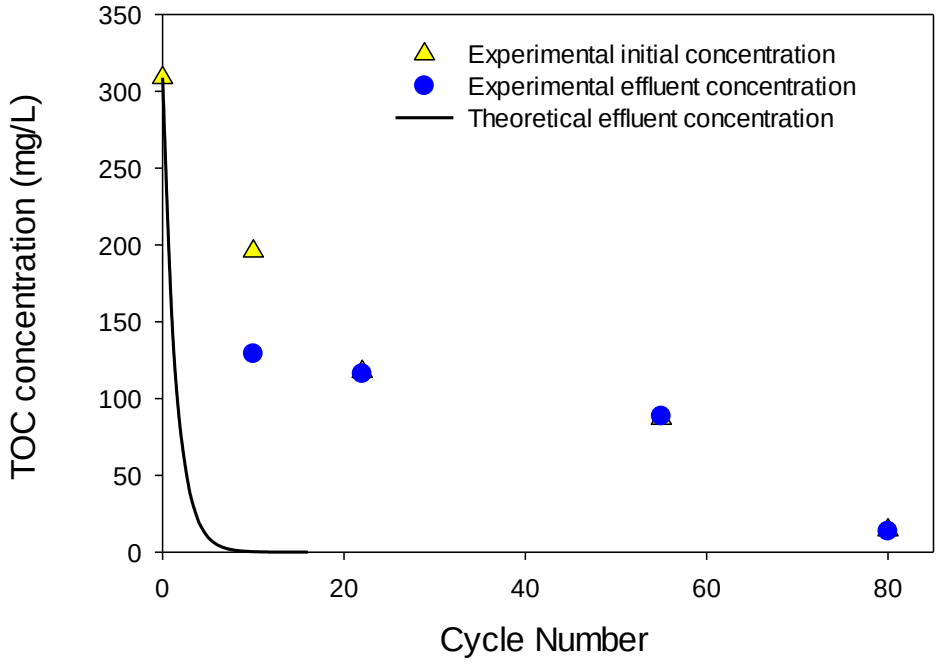

Figure 4.15 TOC results of the effluent samples of the DAA SBR

The TSS and VSS of the DAA SBR was measured at the initial inoculation and at Cycle 80. The results show that the TSS and VSS decreased about nine-fold, but the VSS/TSS percentage stayed approximately the same (Table 4.7). This signifies that the relevant microorganisms with the respect to the conditions provided remained in the reactor while the others degraded. The degradation of these cells might have released organic carbon and that may have caused slower decrease in TOC concentration the hydraulics of the SBR operation throughout the operation of the DAA SBR.

Table 4.7 Average TSS and VSS results of the sludge from the DAA SBR

Sludge	TSS (g/L)	VSS (g/L)	VSS/TSS (%)
Mixed initial sludge	36.1±1.0	15.1±0.4	42
Cycle 80	4.8±0.4	2.0±0.1	41

4.3.2.1.1 Nitrogen Removal Performance of DAA SBR

The reactor was operated at initial theoretical concentrations of NH_4^+ and NO_3^- of 12 and 25 mg N/L, respectively, while the theoretical NLR was 18.5 mg N/L·day. The DAMOa in this reactor would also be the rate-determining step in providing NO_2^- for possible Anammox or DAMOb activity. The experimental analyses revealed that the average initial NH_4^+ concentration (Cycle 6-82) was 13.1±3 mg N/L. The NH_4^+ concentration at Cycle 0 was found to be 250 mg N/L and decreased to a concentration of 17 mg N/L by the end of the 5th cycle (Figure 4.16a). At Cycle 6 and onwards, NH_4^+ was added to the feed to fulfill the theoretical initial NH_4^+ concentration.

NO_2^- was detected in the reactor but at Cycle 18 the cyclic initial and final concentrations of NO_2^- reached 0 mg N/L and did not change throughout the operation of the DAA SBR so its removal efficiency and removal rate were not calculated after Cycle 18 (Figure 4.16b). At Cycle 18 the IC was in a period of maintenance, therefore, the initial concentration of NO_3^- reached levels higher than the desired theoretical concentration of 25 mg N/L. So the initial NO_3^- concentrations were considered in three different phases, Cycle 1-16, Cycle 17-59 and Cycle 60-82 and were 20.6±5.2, 57.2±8.3 and 24.4±6.3 mg N/L, respectively. The experimental influent TN concentration were 67.1±8.4 mg N/L for Cycle 6-16, 138.6±16.7 mg N/L for Cycle 17-59 and 85.9±13.8 mg N/L for Cycle 60-82. The experimental NLR in Cycle 6-16, Cycle 17-59 and Cycle 60-82 were calculated as 16.8±2.1, 34.7±4.2 and 21.5±3.5 mg N/L·day, respectively. The increased initial NO_3^- did not negatively

affect the performance of the reactor, on the contrary, NO_3^- removal was high during this period.

The average removal efficiency of TAN was 62±19 % for Cycle 20-59 and 26±20 % for Cycle 60-82 (Figure 4.17a). While the average removal rate of TAN was 3.6±0.9 mg N/L·day for Cycle 20-59 and 2.1±1.5 mg N/L·day for Cycle 60-82 (Figure 4.18a). The removal efficiency and removal rate of NO_3^- did not experience any fluctuation as observed with NH_4^+ throughout the operation of the DAA SBR. The average removal efficiency of NO_3^- was 92±7 % for Cycle 1-16, 95±8 % for Cycle 17-59 and 97±6 % for Cycle 60-82 (Figure 4.17c). The average removal rate of NO_3^- was found to be 9.6±2.8 mg N/L·day for Cycle 1-16, 27.2±4.7 mg N/L·day for Cycle 17-59 and 11.9±3.4 mg N/L·day for Cycle 60-82 (Figure 4.18c).

During Cycle 20-59, the TAN removal efficiency was more than double the removal efficiency achieved in Cycle 60-82. Two possible speculations can be made, either the Anammox bacteria was consuming NO_3^- instead of NO_2^-, or that the production of NO_2^- by DAMOa increased providing Anammox a competition advantage over the other species consuming NO_2^- in the reactor, in turn facilitating the removal of NH_4^+ via Anammox. The latter seems more plausible since the TAN removal efficiency declined after the decrease in the initial NO_3^- in Cycle 60-82. Therefore, high NO_3^- concentration above the need of a potential heterotrophic denitrification (determined by the available organic carbon) might have favored the DAMOa activity and in turn the Anammox.

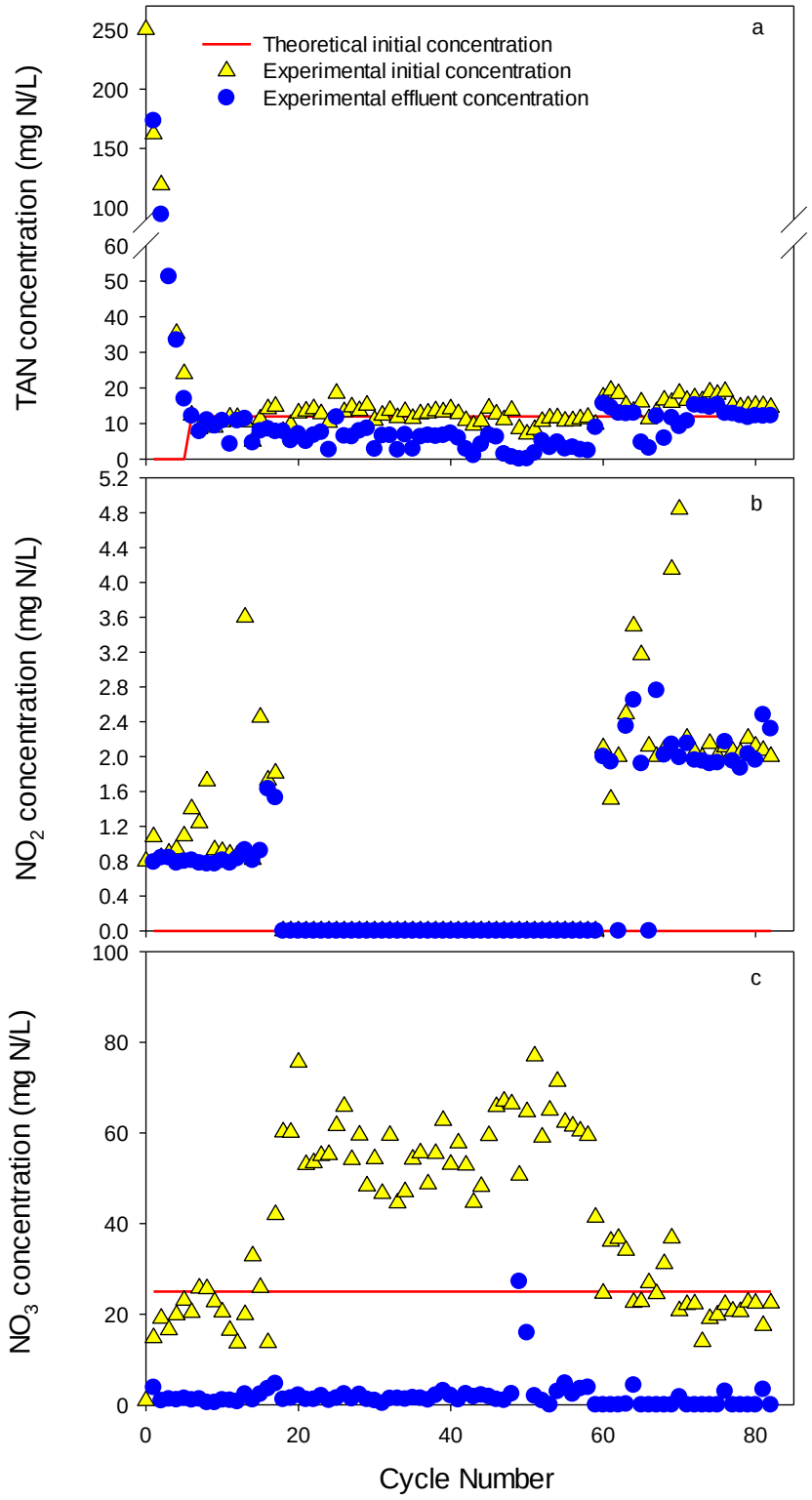

Figure 4.16 Initial and final concentrations of (a) TAN, (b) NO_2^--N and (c) NO_3^--N during each cycle of the DAA SBR (the S.D of each measurement was <5%)

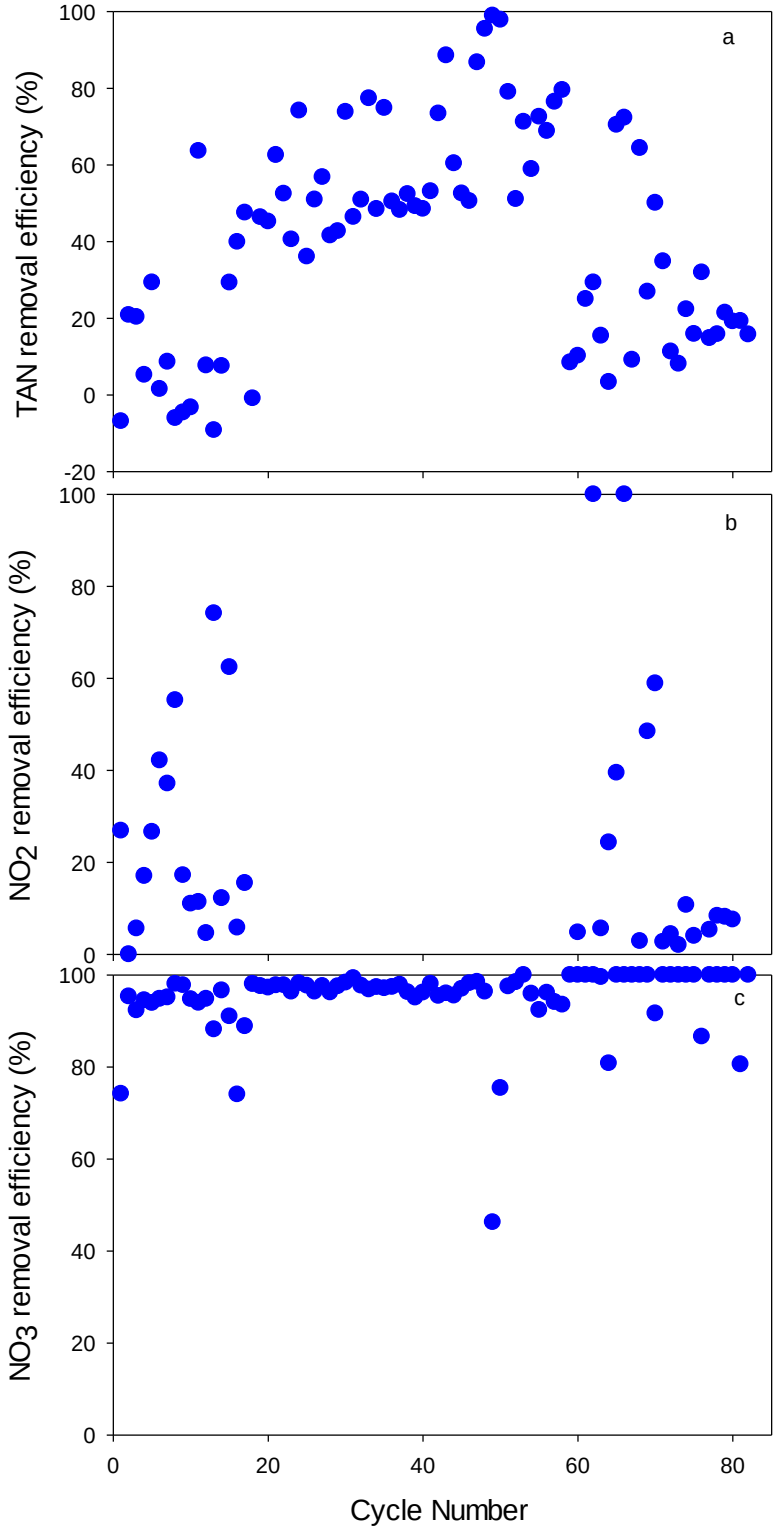

Figure 4.17 Removal efficiencies of (a) TAN, (b) NO_2^- and (c) NO_3^- in the DAA SBR (The negative values emphasize production)

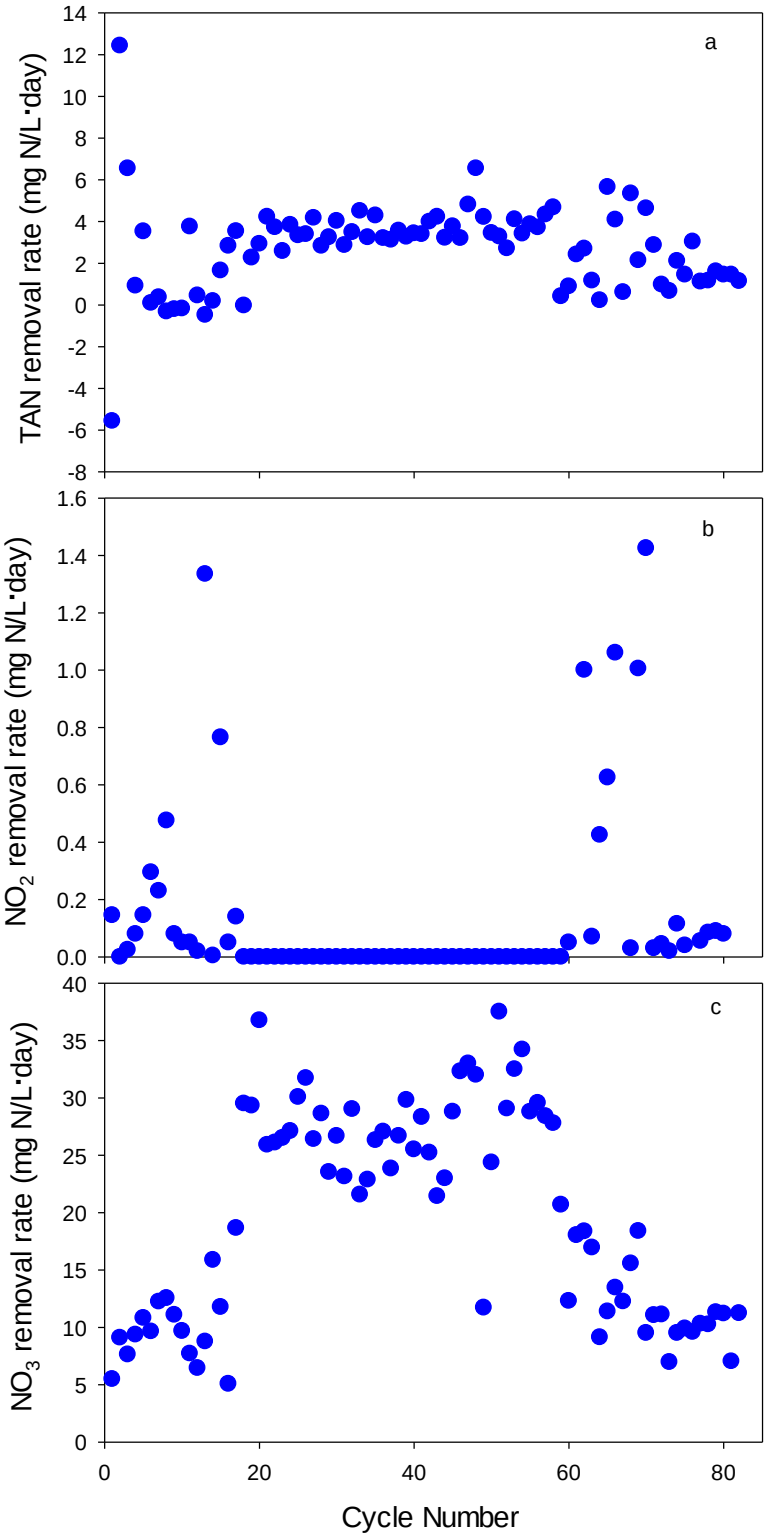

Figure 4.18 Removal rates of (a) TAN, (b) NO_2^- and (c) NO_3^- in the DAA SBR (The negative values imply production)

The average cyclic TN removed in the DAA SBR was 22.2±5.4 mg N/L for Cycle 6-16, 61.5±9.8 mg N/L for Cycle 17-59 and 28.6±8.4 mg N/L for Cycle 60-82 (Figure 4.19). While the average percentage of TN removed was 67±10 % for Cycle 6-16, 88±7 % for Cycle 17-59 and 66±12 % for Cycle 60-82 of the DAA SBR.

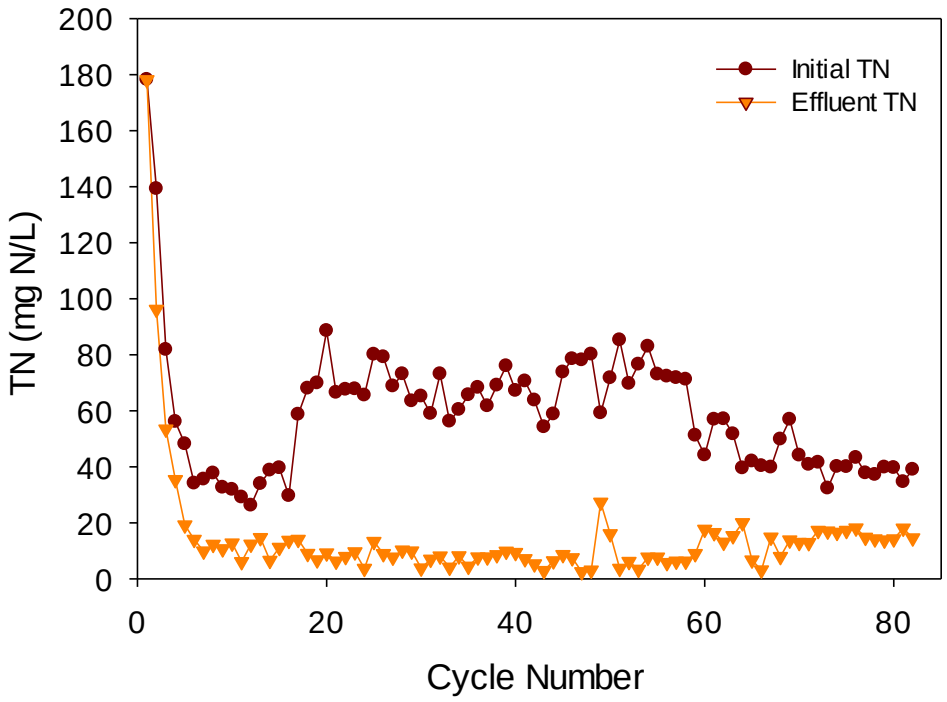

Figure 4.19 Initial and final TN concentrations of the DAA SBR

The %CATN$_{removed}$ of each of the target microorganisms in the DAA SBR was calculated as described in Section 4.2.2.3. For Cycle 6-16, the average %CATN$_{removed}$ of Anammox was fluctuating between 0% and 32%, while the %CATN$_{removed}$ of DAMOb and DAMOa were found to be 28±11 % and 31±5 %, respectively. For Cycle 17-59, the average %CATN$_{removed}$ of Anammox was more stable at 11±4 %, while the average %CATN$_{removed}$ of DAMOb and DAMOa increased to 34±5 % and 43±4 %, respectively. For Cycle 60-82, the average %CATN$_{removed}$ of Anammox remained roughly the same with slight increase in fluctuation at 11±8 %, whereas the average %CATN$_{removed}$ of DAMOb and DAMOa decreased to 23±5 % and 31±5 %, respectively (Figure 4.20). This suggests that DAMOa exhibited dominance over Anammox and DAMOb throughout the

operation of the DAA SBR. DAMOb activity was higher than that of Anammox due to the limited NH_4^+ added in the feed, causing the Anammox activity to be lower than that of DAMOa and DAMOb.

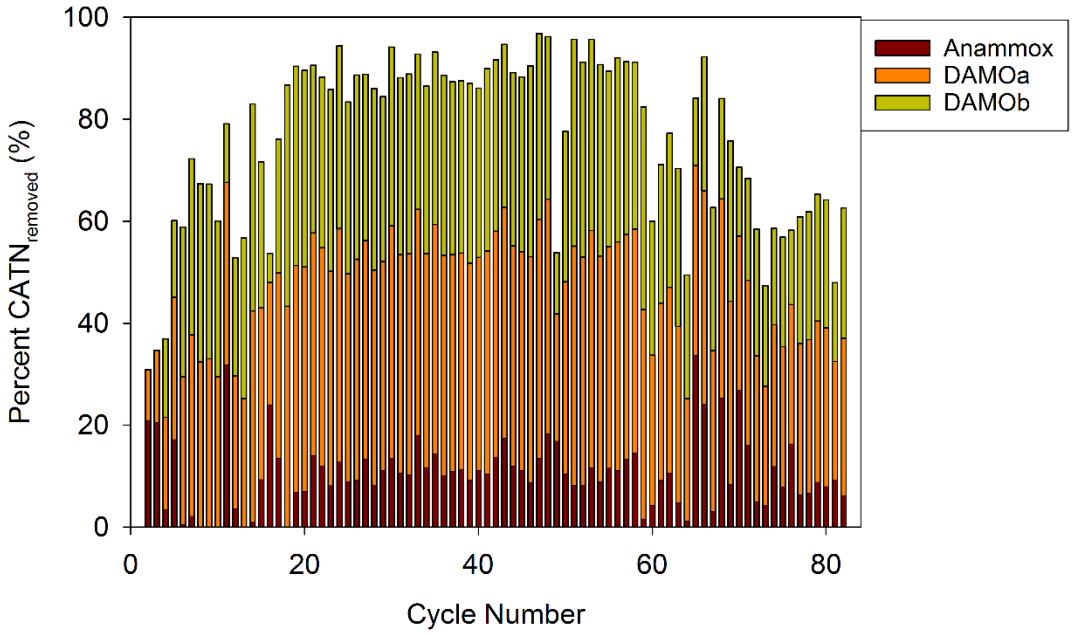

Figure 4.20 The $\%CATN_{removed}$ in the DAA SBR

The NO_2^- and NO_3^--based reaction rates of each of the target microorganisms were calculated and the results were revealed in Figure 4.21. Due to the fluctuations in the TAN removal rates and removal efficiencies, the $r_{Anammox\ NO_2^-}$ for Cycle 6-16 fluctuated between 0 and 3.8 mg N/L·day. While the average $r_{DAMOb\ NO_2^-}$ and $r_{DAMOa\ NO_3^-}$ were 9.5±4.0 mg N/L·day and 10.3±2.9 mg N/L·day, respectively, for Cycle 6-16. For Cycle 17-59, the average the $r_{Anammox\ NO_2^-}$, $r_{DAMOb\ NO_2^-}$ and $r_{DAMOa\ NO_3^-}$ were calculated as 4.6±1.4, 23.5±4.8 and 28.2±4.8 mg N/L·day, respectively. For Cycle 60-82, the average the $r_{Anammox\ NO_2^-}$, $r_{DAMOb\ NO_2^-}$ and $r_{DAMOa\ NO_3^-}$ were calculated as 2.8±2.0, 9.9±3.4 and 12.5±3.5 mg N/L·day, respectively. Although NO_2^- was not added in the feed the activity of DAMOb was higher than tat of Anammox due to the limited NH_4^+ in feed and the average $r_{Anammox\ NO_2^-}$ was the lowest of the three target microorganisms. Whereas the

average $r_{DAMOa\ NO_3^-}$ was higher than $r_{DAMOb\ NO_2^-}$. The results show that the average reaction rate of DAMOa was the highest but that of DAMOb was relatively close, which is in accordance with the $\%CATN_{removed}$ results.

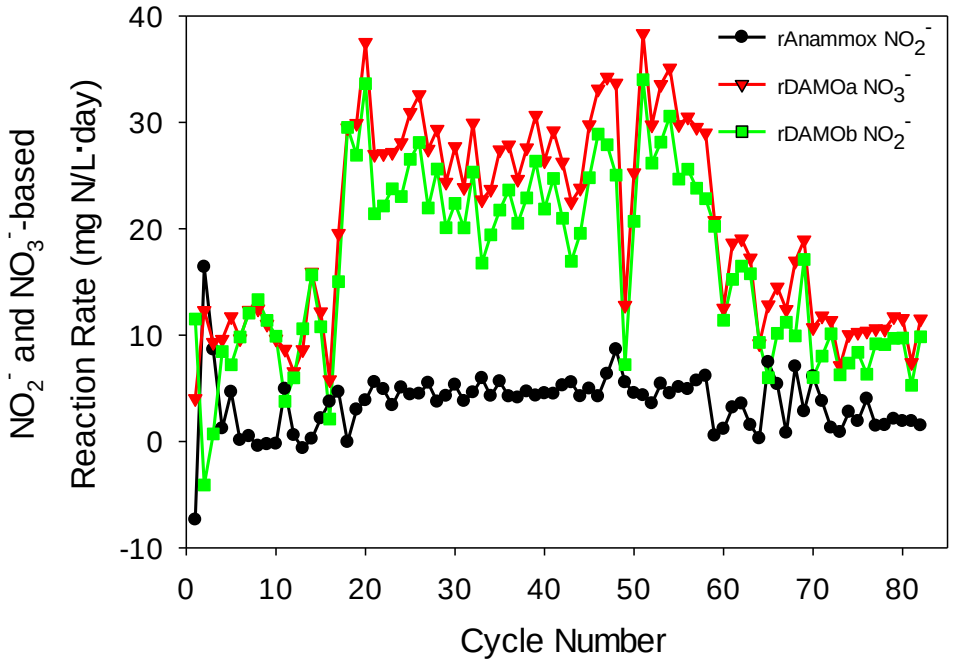

Figure 4.21 The calculated NO_2^- and NO_3^--based reaction rates of each target microorganism throughout the operation of the DAA SBR

4.3.2.1.2 Determination of the Stoichiometric Ratio of the Microbial Consortium in DAA SBR

The stoichiometric ratios were calculated according to Section 4.2.2.4 and the results are shown in Figure 4.22. For the $\Delta NO_2^-/\Delta NH_4^+$ molar ratio (Figure 4.22a), the DAA SBR was generally following the ratio of 0, on average the $\Delta NO_2^-/\Delta NH_4^+$ ratio was 0.03. The closest theoretical ratio was that of the AMX & DAMOa case which is 0.32. This indicates that the culture had more DAMOa than Anammox and DAMOb. Moreover, the average $(\Delta NO_2^- + \Delta NH_4^+)/\Delta NO_3^-$ ratio and $\Delta NO_2^-/\Delta NO_3^-$ ratio were 0.17 and 0.01, as shown in Figure 4.22b and Figure 4.22c, respectively. Both experimental ratios were closest to the theoretical ratio of DAMO which is 0 for both ratios. This suggests that the culture contained both DAMOa and DAMOb. As for the $\Delta NH_4^+/\Delta NO_3^-$ ratio, shown in Figure 4.22d, the average ratio during the operation of the DAA SBR was 0.16. This experimental ratio follows the cases of DAMOa or DAMOb or DAMO, hence signifies the presence of both DAMOa and DAMOb. Despite that the results of all the ratios exhibit the presence of three target microorganisms, DAMOa demonstrates dominance over the other two microorganisms in terms of the stoichiometric ratios. Moreover, DAMOb is second and Anammox is the least of the three target microorganisms. The results from the $\%CATN_{removed}$ by each species concur with the results presented by the stoichiometric molar ratio calculations.

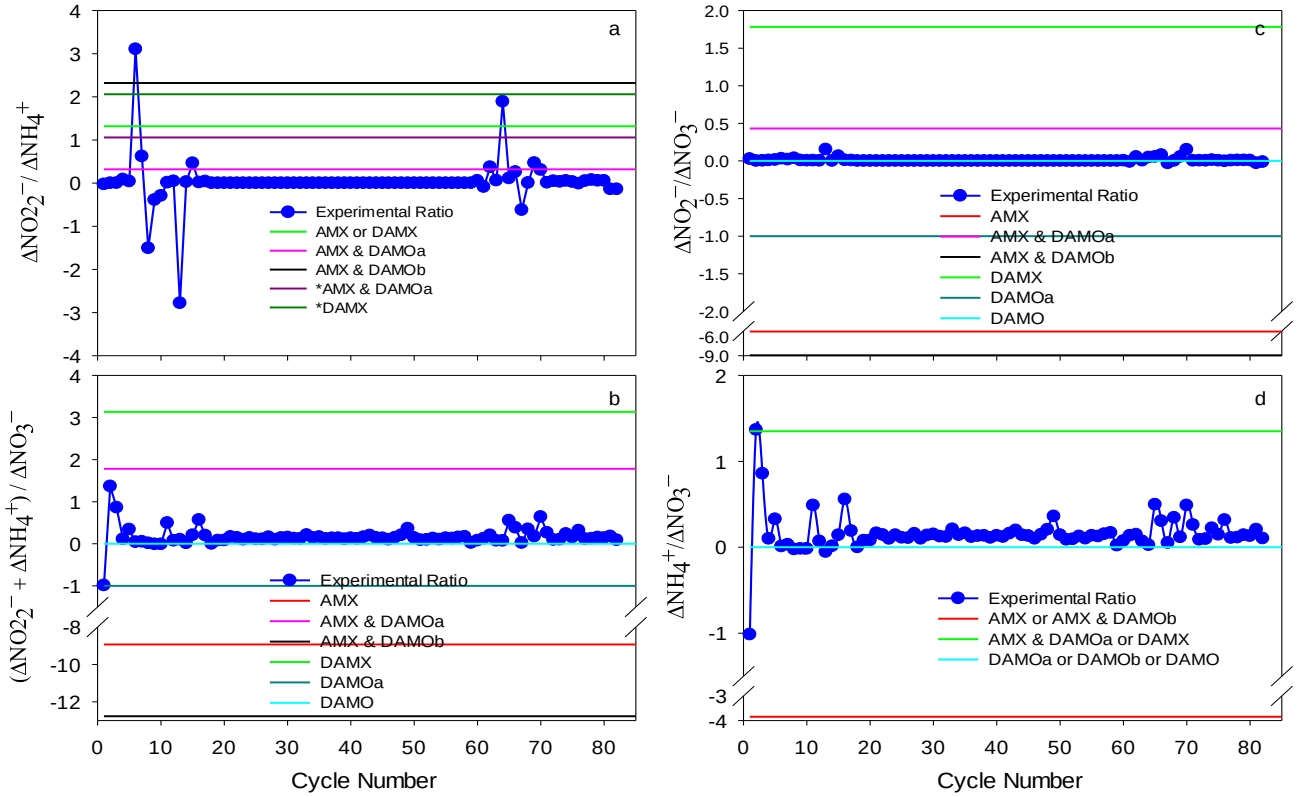

Figure 4.22 The cyclic (a) $\Delta NO_2^-/\Delta NH_4^+$, (b) $(\Delta NO_2^- + \Delta NH_4^+)/\Delta NO_3^-$, (c) $\Delta NO_2^-/\Delta NO_3^-$ and (d) $\Delta NH_4^+/\Delta NO_3^-$ ratios achieved in the DAA SBR compared to the theoretical ratio of each case

4.3.2.2 FISH Analyses Results of DAA SBR

Sludge samples from the DAA SBR were taken at the following intervals, at Cycle 0 (the initial seed sludge), at Cycle 50 and at Cycle 80 to perform the FISH analysis, to observe the change in the microbial composition existing in the reactor with respect to time. The target cells were identified with the corresponding probes from Table 4.4 that can visually distinguish *M. oxyfera*, *M. nitroreducens* and Anammox. General bacteria, general archaea and DAPI probes were used to quantify the relative abundance of the target species in the reactor. The samples were analyzed, and the microscope images are shown in Figure 4.23.

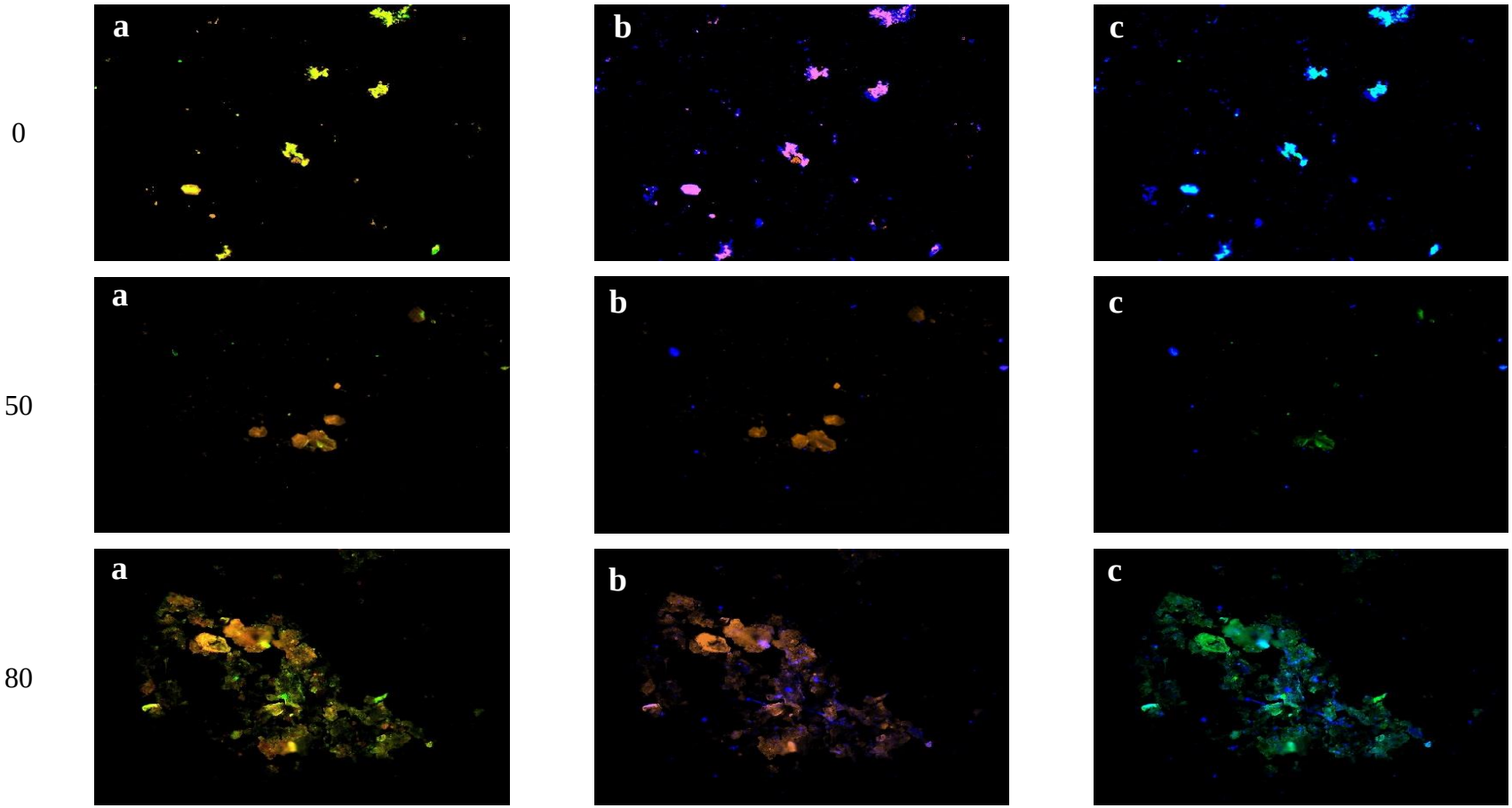

Figure 4.23 FISH images of DAA SBR sludge samples withdrawn at Cycles 0, 50 and 80 (a) Orange: AMX-368 - general Anammox and green: DARCH-872 - *M. nitroreducens* (b) Orange: AMX-368 - general Anammox and blue: DBACT-193 - *M. oxyfera* (c) Blue: DBACT-193 - *M. oxyfera* and green: DARCH-872 - *M. nitroreducens*

The FISH results of the initial sludge sample illustrated a relative abundance of Anammox, *M. oxyfera* and *M. nitroreducens* of 35±1 %, 25±2 %, and 40±3 %, respectively. This is the same sludge used in the DAMO SBR (Figure 4.13). At Cycle 50, the relative abundance of Anammox decreased to 22±9 %, while that of *M. oxyfera* and *M. nitroreducens* increased to 35±6 % and 43±7 %, respectively. Nevertheless, by Cycle 80, the relative abundance of Anammox slightly decreased to 19±2 %. On the other hand, the relative abundance of *M. oxyfera* and *M. nitroreducens* slightly increased to 38±1 % and 44±2 %, respectively. The relative abundance of the target species presented in Figure 4.24 shows *M. oxyfera* and *M. nitroreducens* dominance over Anammox which concurs with the results of $\%CATN_{removed}$ of DAMOa and the NO_3^--based DAMOa reaction rate in Section 4.3.2.1.2 and the results of the stoichiometric molar ratio in Section 4.3.2.1.2.

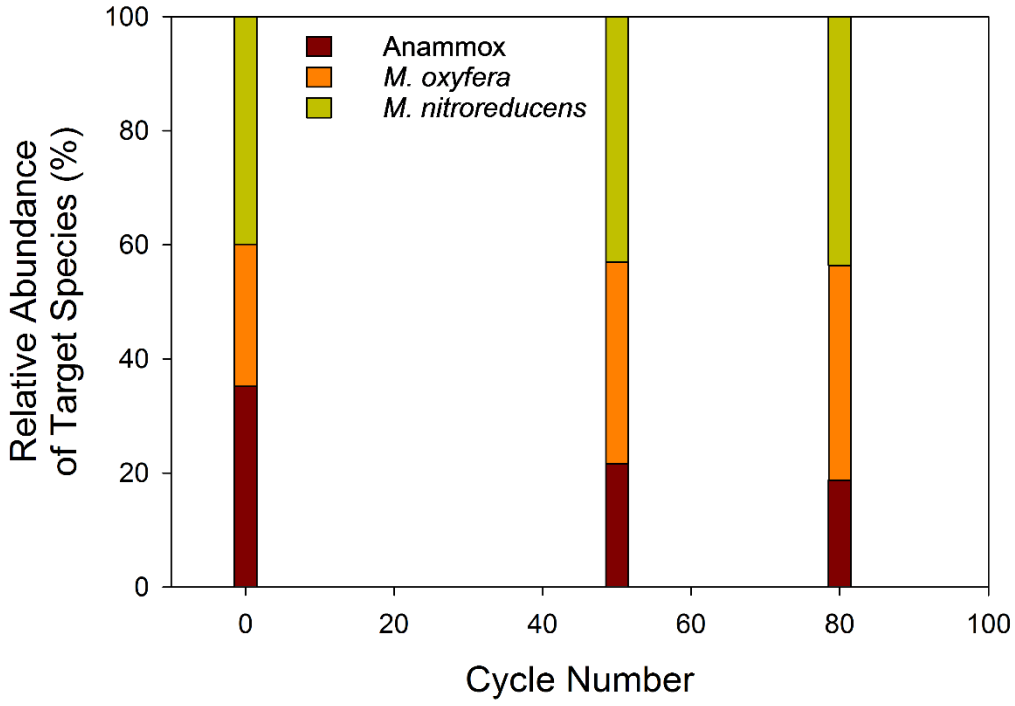

Figure 4.24 The relative abundance of target species with respect to the total microbial consortium in the DAA SBR

Although NH_4^+ was provided to the DAA SBR and absent in the DAMO SBR feed, at Cycle 80, the Anammox relative abundance was slightly higher in the DAMO SBR (24±1 %) than in the DAA SBR (19±2 %). On the other hand, NO_2^- was absent in the DAA SBR feed, yet the relative abundance of *M. oxyfera* and *M. nitroreducens* at Cycle 80 in both reactors was relatively similar, slightly higher abundance of *M. oxyfera* in the DAMO SBR and a slightly higher abundance of *M. nitroreducens* in the DAA SBR.

4.3.3 Comparison of the DAMO-Anammox, DAMO and DAA SBRs

In this section the DAMO SBR (Cycle 18-89) and the DAA SBR (Cycle 60-82) performances are compared with Phase IV of the DAMO-Anammox SBR since the HRT during this phase was the same in all reactors (4 days). The initial concentrations of NH_4^+, NO_2^- and NO_3^-, influent molar ratios, NLR and influent TN concentrations of the three reactors during the mentioned periods are shown in Table 4.8.

Among the three SBRs operated in this thesis study so far, the highest percentage of influent TN removed was achieved by the DAMO SBR (94±6 %), while that of the DAA SBR was the second highest (80±16 %). The lowest percentage of influent TN removed was achieved by the DAMO-Anammox (73±7 %) (Table 4.9).

Regarding NO_3^-, the highest average removal efficiency (97±6 %) and removal rate (11.9±3.4 mg N/L·day) was observed in the DAA SBR, while the DAMO SBR was not far behind with 93±11 % and 11.6±2.3 mg N/L·day, respectively (Table 4.9). The lowest NO_3^- removal efficiency (10±9 %) and removal rate (2.7±2.8 mg N/L·day) was attained in the DAMO-Anammox SBR (Table 4.9). This indicates that the DAMOa activity in the DAA SBR and DAMO SBR was much higher than that in the DAMO-Anammox SBR.

The NO_2^- removal efficiencies achieved in the DAMO SBR (78±18 %) and DAMO-Anammox SBR (77±9 %) were similar, yet the NO_2^- removal rate in the DAMO-Anammox SBR (9.9±2.6 mg N/L·day) was more than double that of the DAMO SBR

(4.2±1.2 mg N/L·day) (Table 4.9), because the initial NO_2^- concentration of the DAMO-Anammox SBR is more than 2.5 fold higher than that of the DAMO SBR.

Regarding TAN, the average removal efficiency and removal rate in the DAMO-Anammox SBR (97±15 % and 6.9±1.6 mg N/L·day, respectively) was much higher than that of the DAA SBR (26±20 % and 2.1±1.5 mg N/L·day, respectively) (Table 4.9). This indicates that the Anammox activity was much lower in the DAA SBR which can be attributed to the absence of NO2- in the DAA SBR feed.

Table 4.8 The initial concentrations of NH_4^+, NO_2^- and NO_3^-, NLR and influent TN concentrations in the DAMO, DAA and DAMO-Anammox SBRs

Reactor	Initial Concentrations (mg N/L)			Influent Molar Ratios			NLR (mg N/L·day)	Influent TN (mg N/L)
	NH_4^+	NO_2^-	NO_3^-	NH_4^+/NO_2^-	NH_4^+/NO_3^-	NO_2^-/NO_3^-		
DAMO SBR (Cycle 18-89)	0	10.1±2.5	24.2±5.3	0	0	0.4	17.1±3.5	85.9±13.8
DAA SBR (Cycle 60-82)	13.1±3	0	24.4±6.3	-	0.5	0	21.5±3.5	68.5±14.0
DAMO-Anammox SBR (Phase IV)	13.2±4.4	26.3±7.5	25.0±2.8	0.5	0.5	1.1	32.2±4.8	128.9±19.1

Table 4.9 The removal efficiencies, removal rates and percentage of influent TN removed of the DAMO, DAA and DAMO-Anammox SBRs

Reactor	Removal Efficiency (%)			Removal Rate (mg N/L·day)			Percent influent TN removal (%)
	TAN	NO_2^-	NO_3^-	TAN	NO_2^-	NO_3^-	
DAMO SBR (Cycle 18-89)	0	78±18	93±11	0	4.2±1.2	11.6±2.3	94±6
DAA SBR (Cycle 60-82)	26±20	0	97±6	2.1±1.5	0	11.9±3.4	80±16
DAMO-Anammox SBR (Phase IV)	97±15	77±9	10±9	6.9±1.6	9.9±2.6	2.7±2.8	73±7

Regarding the calculated average $\%CATN_{removed}$ in the three reactors, the highest average $\%CATN_{removed}$ of Anammox, expectedly, was calculated in the DAMO-Anammox SBR (37±13 %), while the average $\%CATN_{removed}$ of Anammox in the DAA SBR was found to be 11±8 % (Table 4.10). On the other hand, the highest average $\%CATN_{removed}$ of DAMOa was computed in the DAMO SBR (39±4 %), while that in the DAA SBR was closely behind (31±5 %). The average $\%CATN_{removed}$ of DAMOa in the DAMO-Anammox SBR was the lowest of the three reactors (4±4 %) (Table 4.10). Whereas, the highest average $\%CATN_{removed}$ of DAMOb was found in the DAMO SBR (53±6 %) and the second highest was observed in the DAA SBR (23±5 %). The average $\%CATN_{removed}$ of DAMOb was the lowest in the DAMO-Anammox SBR at 8±7 % (Table 4.10).

Similarly, the highest average $r_{DAMOa\ NO_3^-}$ was observed in the DAA SBR (12.5±3.5 mg N/L·day), while the second highest and the lowest average $r_{DAMOa\ NO_3^-}$ were observed in the DAMO SBR (11.6±2.2 mg N/L·day) and the DAMO-Anammox SBR (1.3±1.3 mg N/L·day), respectively. While the highest average $r_{DAMOb\ NO_2^-}$ was calculated in the DAMO SBR (15.8±3.2 mg N/L·day). The average $r_{DAMOb\ NO_2^-}$ in the DAA SBR (9.9±3.4 mg N/L·day) was lower than that in the DAMO SBR, while the DAMO-Anammox SBR experienced the lowest average $r_{DAMOb\ NO_2^-}$ of the three reactors (3.0±2.9 mg N/L·day) (Table 4.10). Regarding Anammox activity, the highest Anammox activity was observed in the DAMO-Anammox SBR with an average $r_{Anammox\ NO_2^-}$ of 8.3 mg N/L·day, while the average $r_{Anammox\ NO_2^-}$ in the DAA SBR was found to be 4.6±1.4 mg N/L·day (Table 4.10).

Table 4.10 The $\%CATN_{removed}$ and NO_2^- and NO_3^--based reaction rates of the DAMO, DAA and DAMO-Anammox SBRs

Reactor	$\%CATN_{removed}$ (%)			NO_2^- and NO_3^--based reaction rates (mg N/L·day)		
	AMX	DAMOb	DAMOa	$r_{Anammox\ NO_2^-}$	$r_{DAMOb\ NO_2^-}$	$r_{DAMOa\ NO_3^-}$
DAMO SBR (Cycle 18-89)	0	53±6	39±4	0	15.8±3.2	11.6±2.2
DAA SBR (Cycle 60-82)	11±8	23±5	31±5	4.6±1.4	9.9±3.4	12.5±3.5
DAMO-Anammox SBR (Phase IV)	37±13	8±7	4±4	8.3±3.2	3.0±2.9	1.3±1.3

The highest DAMOb activity was observed in the absence of Anammox activity, in the DAMO SBR, and the NO_2^- removal efficiency was nearly the same as in the DAMO-Anammox SBR. Moreover, the presence of a highly active Anammox culture negatively affected the removal of NO_3^-. Theoretically, the production of NO_3^- by Anammox can support the activity of DAMOa, if the DAMOa content in the sludge is not sufficient to begin with, its activity will be masked. It seems that the enrichment of a DAMO culture in the DAMO and DAA SBRs was achieved in a shorter time and with higher efficiencies compared to DAMO-Anammox SBR. The reason is that the DAMO composition in the initial sludge was low, so the DAMOb could not compete with an enriched Anammox culture and the DAMOa could not overcome the masking effect imposed by the Anammox. On the other hand, in the absence of Anammox their activity was more evident. This outcome contradicts the findings of Zhu et al. (2012) which claims that using Anammox as the base of a DAMO-Anammox co-culture enrichment reduces the enrichment period. Enriching the DAMO cultures and Anammox culture separately using multiple nitrogen sources seems to reduce the enrichment period.

The results were compared to a similar study performed by Fu et al. (2017a) investigating the effect of providing different combinations of nitrogen sources. In the study, a reactor named N1, was provided with NH_4^+, NO_2^-, NO_3^- and CH_4 resembling the DAMO-Anammox SBR in this thesis study (Chapter3), while the N2 reactor was supplied with NH_4^+, NO_3^- and CH_4 resembling the DAA SBR. Reactors N3 (NO_3^- and CH_4), N4 (NH_4^+, NO_2^- and CH_4), N5 (NO_2^- and CH_4) were also setup in the scope of the study conducted by Fu et al. (2017a). The initial concentrations of NH_4^+, NO_2^- and NO_3^- were 50, 10 and 50 mg N/L, respectively. The initial concentrations and the influent molar ratios applied and the removal rates achieved in the study performed by Fu et al. (2017a) are shown in Table 4.11.

Table 4.11 Influent concentrations, influent molar ratios and removal rates from Fu et al. (2017a)

Reactors	Initital Concentrations (mg N/L)			Influent Molar Ratio			TN removal rate (mg N/L·day)
	NH_4^+	NO_2^-	NO_3^-	NH_4^+/NO_2^-	NH_4^+/NO_3^-	NO_2^-/NO_3^-	
N1	50	10	50	5	1	0.2	107
N2	50	0	50	-	1	0	<2
N3	0	0	50	-	0	0	<2
N4	50	10	0	5	-	-	97
N5	0	10	0	0	-	-	33

The N1 reactor achieved the highest TN removal rate (107 mg N/L·day) with the shortest enrichment period, while the N4 reactor achieved the second highest TN removal rate with 97 mg N/L·day, while the N5 reactor achieved the third highest TN removal rate at 33 mg N/L·day. The N2 reactor, which was provided with NH_4^+ and NO_3^- as the nitrogen source, thus resembling the DAA SBR, achieved the lowest TN removal rate along with the N3 reactor (<2 mg N/L·day). The addition of NH_4^+ in the N1 and N4 reactors led to an increase in Anammox bacteria dominance, which allowed for a higher TN removal rate. Nevertheless, unlike the DAMO-Anammox SBR, DAMOb still dominated in the reactors.

Similar to the results attained by Fu et al. (2017a), the DAMO-Anammox SBR achieved a higher average TN removal rate (15.7±5.4 mg N/L·day) than in the DAA SBR (14.3±4.2 mg N/L·day). However, the average TN removal rate in the DAA SBR (14.3±4.2 mg N/L·day) was much higher than that of the N2 reactor. DAMOa was not detected in any of the reactors established by Fu et al. (2017a), due to their absence in the inoculum. The DAMO SBR achieved an average TN removal rate (15.7±3.2 mg N/L·day) similar to that achieved in the DAMO-Anammox SBR.

Fu et al. (2017a) found that the TN removal rates for DAMO cultures enriched using multiple nitrogen sources were generally higher than for single nitrogen source enrichment. Yet, the highest DAMOb activity was observed in the N5 reactor which was provided with NO_2^- as the sole nitrogen source ($r_{DAMOb\ NO_2^-}$ of 33 mg N/L·day), while $r_{DAMOb\ NO_2^-}$ from the N1 and N4 reactors were 12 and 15 mg N/L·day, respectively. The $r_{DAMOb\ NO_2^-}$ calculated from the DAA and DAMO SBRs were relatively comparable to the N1 and N4 reactors (9.9±3.4 and 15.8±3.2 mg N/L·day, respectively). Regarding Anammox activity, the $r_{Anammox\ NO_2^-}$ calculated from the N1 and N4 reactors (25 and 43 mg N/L·day, respectively) were found to be higher than in the DAA and DAMO-Anammox SBRs (4.6±1.4 and 8.3±3.2). This was due to the higher NH_4^+ concentrations by Fu et al. (2017a).

Considering the influent molar ratios applied in this thesis study, a low influent NH_4^+/NO_2^- molar ratio of 0.5, applied in the DAMO-Anammox SBR, the consortium enriched contained a dominant Anammox culture over DAMOb. Yet, at a much higher influent NH_4^+/NO_2^- molar ratio of 5, applied in the N1 reactor a culture dominated by DAMOb was enriched (Fu et al., 2017a). This outcome does not seem intuitive, since theoretically, Anammox has a higher affinity to NO_2^- than DAMOb and a higher influent NH_4^+/NO_2^- molar ratio would favor Anammox over DAMOb. The only plausible reasoning would be that the composition of the initial inoculum is dominated by DAMOb.

4.3.4 Conclusion

Although, the removal efficiency and removal rate of NO_3^- was very similar in both the DAMO SBR and the DAA SBR, the percent influent TN removed in the DAMO SBR (94±6 %) was hgher than that achieved in the DAA SBR (80±16 %). Both reactors exhibited DAMOb and DAMOa activity, nevertheless, the DAMO SBR illustrated higher DAMOb activity while the DAA SBR illustrated higher DAMOa activity, as seen in the results of the NO_2^- and NO_3^--based reaction rates, stoichiometric molar ratios and FISH analysis.

In comparison to the DAMO-Anammox SBR, DAMO activity was higher in the absence of a dominant Anammox culture. Enrichment of a DAMO culture in the absence of a dominant Anammox culture occurred in a shorter period, yet, Anammox was detected in both the DAMO SBR and DAA SBR, but its activity was much lower than that of the DAMO-Anammox SBR. This signifies that different combinations of the nitrogen sources, their influent concentrations and corresponding influent molar ratios play a critical role in the enrichment of a DAMO-Anammox co-culture.

When contrasting the results obtained from the DAMO-Anammox, DAMO and DAA SBRs with the results from Fu et al. (2017a), the following outcomes could be deduced. Cultures enriched with multiple nitrogen sources seem to have generally higher removal

rates than cultures enriched using a single nitrogen source. Further investigation of the effect of different combinations of influent nitrogen molar ratios on the reactor performance and the microbial community is required. Yet, to enrich the three target microorganisms the choice of inoculum to remains very critical.

CHAPTER 5

DAMO-ANAMMOX CO-CULTURE TREATMENT OF ANAEROBIC DIGESTER EFFLUENT AND ITS INTEGRATION WITH MICROALGAL CULTURE

5.1 Introduction

Investigating the application of a DAMO-Anammox system on real wastewater is critical for understanding the potential applications of this co-culture system. Lim et al. (2021), the first and only to employ on a lab-scale, a DAMO-Anammox MBfR for the treatment of original AD effluent. Lim et al. (2021) investigates the treatment of main-stream and side-stream effluents using a DAMO-Anammox co-culture. The source of main-stream wastewater was the effluent of a HRAS, where three scenarios were studied. In Scenario I, nitritation was applied to the HRAS effluent then the effluent was sent to the DAMO-Anammox MBfR, operated at an HRT of 1 day. Scenario II included partial nitritation then a DAMO-Anammox MBfR, which was operated at an HRT of 1 day, while in Scenario III, partial nitritation and Anammox was performed prior to the DAMO-Anammox MBfR, operated at an HRT of 0.5 days. The main-stream scenarios were performed at a temperature of 22°C. On the other hand, AD liquor was used a side-stream wastewater and studied under Scenario IV. In this scenario, the AD effluent was partially nitrified and then provided to a DAMO-Anammox MBfR operated at a temperature of 35°C and HRT of 2 days. Table 5.1 illustrates the influent concentrations, removal rates, microbial composition, and NO_2^- and NO_3^--based reaction rates of Anammox, DAMOa and DAMOb achieved in each scenario.

Table 5.1 Influent concentrations, removal rates, microbial composition and reaction rates achieved in the DAMO-Anammox MBfR in each scenario (Lim et al., 2021)

		Scenario			
		I	II	III	IV
Influent Concentration (mg N/L)	NH_4^+	13	20	5	455
	NO_2^-	62	31	0.5	590
	NO_3^-	8	6	11	10
Removal Rate (mg N/L·day)	NH_4^+	12	16	4	225
	NO_2^-	62	31	1	290
	NO_3^-	1-22	0-14	14	-
Microbial composition (%)	DAMOa	29	29	22	20
	DAMOb	11	6	12	5
	Anammox	1	1	1	12
NO_2^- and NO_3^--based Reaction Rate (mg N/L·day)	DAMOa	10	8	15	52
	DAMOb	56	22	9	32
	Anammox	15	17	5	270

The influent NH_4^+/NO_2^- ratio to the DAMO-Anammox MBfR was in the range of 0.2-0.3 in Scenario I, 0.5-0.6 in Scenario II, 0.3-0.6 in Scenario III and in 0.7-0.8 Scenario IV. In all the scenarios the effluent TN concentration was at most 5 mg N/L. The relative abundance of DAMOa in the microbial consortium was 29% in both Scenarios I and II, 22% in Scenario III and 20% in Scenario IV. The relative abundance of DAMOb in the microbial consortium was 11% in Scenario I, 6% in Scenario II, 12% in Scenario III and 5% in Scenario IV. Whereas, the relative abundance of Anammox was about 1% in Scenarios I, II and III each, and 12% in Scenario IV. Regarding the sidestream treatment, up to 96% of the TN concentration was removed at a rate of 500 mg N/L·day.The study performed by Lim et al. (2021) illustrates the applicability of using a DAMO-Anammox MBfR for the treatment of both mainstream and sidestream wastewater.

Modifications of a DAMO-Anammox system might be explored to achieve the treatment of phosphorus as well, for instance, integrating this co-culture with microalgae (Harb et al., 2021) can target phosphorus. Such an integrated system might even increase the removal efficiency of residual ammonium. Microalgae are fast-growing microorganisms capable of achieving nutrient and carbon removal while concurrently mitigating GHG emissions. Microalgal systems have relatively low operation and maintenance costs and short start-up time compared to conventional wastewater treatment processes (Cai et al., 2013). Depending on the type of wastewater, intended treatment and application objective different metabolism modes can be employed in the growth of microalgae (Hammed et al., 2016). Hence, they can be utilized in the treatment of various wastewater types. Nevertheless, parameters such as temperature, pH, light intensity, illumination period, HRT, NLR, PLR and OLR may affect the enrichment and growth of microalgae. In comparison to other microalgae species, *C. Vulgaris* are more robust and resistant to varying environmental factors and they are capable of accumulating high lipid content. Furthermore, microalgae harvesting can yield numerous value-added products, such as, biofuel, vitamins, proteins, and drugs. Such a configuration might close the energy cycle making it self-sustainable and energy efficient.

In this chapter the capability of the DAMO-Anammox co-culture enriched would be put to the test of treating an original AD effluent which would be done in two steps. The first step was performing a batch test where different dilutions of the AD effluent and their corresponding synthetic wastewater (SWW) equivalents were tested to determine a favorable dilution to apply to the SBR. The second step was applying the chosen dilution on an established SBR and monitoring the reactor performance in treating the AD effluent along with the changes in the population dynamics. Furthermore, the effluent of this SBR was provided to a *C. vulgaris* PBR for further treatment. In this step the applicability of an integrated DAMO-Anammox-Microalgae to treat AD effluent was assessed. The established SBR, namely DAMMOX SBR, was inoculated with

sludge from the three reactors, DAMO-Anammox SBR in Chapter 3 and DAMO SBR and DAA SBR in Chapter 4.

5.2 Materials and Methods

5.2.1 Reactor Setup and Operational Conditions

5.2.1.1 BATCH SET: SWW Versus AD Effluent Application

It was aimed in this batch reactor study to investigate the effect of AD effluent on both the removal performance and microbial consortium of a DAMO-Anammox co-culture, in comparison to synthetic feed application. The AD effluent would contain a matrix that is not provided in the synthetic feed, which can prove beneficial to the growth of the microorganisms. On the other hand, AD effluent does have many different microbial groups that may affect the enriched co-culture's activity directly or indirectly. Thus, it is worth investigating the feed type effect.

The AD effluent was obtained from ASKI Ankara Central WWTP, Tatlar. It was settled to retrieve the supernatant which was then centrifuged at 13,000 g for 10 min to remove the suspended solids that may affect the co-culture through introducing new unwanted microorganisms. After analysis of the AD effluent, it was observed that minute amounts of NO_2^- were present but no NO_3^- was found, the characteristics of the AD effluent are displayed in Table 5.2. The pH of the AD effluent was found to be 7.53.

Table 5.2 AD effluent characteristics after supernatant extraction and centrifugation

Compound	Concentration (mg/L)
TAN-N	750 ±5
NO_2^--N	4.9±0.1
NO_3^--N	0±0.03
PO_4^{3-}-P	40.8±0.3
SO_4^{2-}	694 ±5
TOC	925±15
tCOD	568±36
sCOD	435±34
Volatile Fatty Acids (VFA) (mM)	
Acetic Acid	1.069 ± 0.006
Propionic Acid	0.368 ± 0.002
Iso-butyric Acid	0.231 ± 0.001
Butyric Acid	0.309 ± 0.002
Iso-valeric Acid	0.269 ± 0.001
N-valeric Acid	0.311 ± 0.001
Iso-caproic Acid	0.351 ± 0.003
N-caproic Acid	0.386 ± 0.001

Eight batch reactor types, each run in triplicate, were setup (24 reactors) (Table 5.3). Four reactor types (12 in total) were operated with real AD effluent subject to different dilution factors, while the other four reactor types (12 in total) were operated with corresponding NH_4^+ concentrations, as that of the AD effluent reactors yet this time with synthetic feed (Table 5.6). The dilution factors chosen are 1/4, 1/8, 1/20 and 1/40 Table 5.3), which include one (1/40) that corresponds to the current NH_4^+ initial concentration provided to the DAMO-Anammox SBR in Phase V (12 mg N/L). These dilution factors were chosen, whilst taking into consideration the PO_4^{3-} concentration and the TN/P ratio

that will be available to the microalgae. Since at a later stage (Section 5.2.1.3) the effluent of the DAMMOX will be supplied to a microalgae PBR.

Table 5.3 Different reactor types operated in the batch reactor study

Reactor type	Nitrogen Content in Each Reactor Type		
	NH_4^+ (mg N/L)	NO_2^- (mg N/L)	NO_3^- (mg N/L)
AD 1/4	153±1	95±4	5.2±0.5
AD 1/8	71.1±1.4	50.6±1.1	3.8±0.5
AD 1/20	27.5±0.4	23.3±1.0	0.6±0.5
AD 1/40	13.2±0.9	29.6±2.0	20.7±2.2
SWW 1/4	152±1	96±4	0.4±0.3
SWW 1/8	77.1±0.9	49.4±1.8	0.4±0.3
SWW 1/20	28.9±1.0	23.3±1.7	3.1±0.7
SWW 1/40	14.5±0.5	27.6±1.1	23.3±3.1

As seen in Table 5.2, NO_2^- was not present in the AD effluent at concentrations that create a NO_2^-:NH_4^+ ratio between 1-2, which is preferential for the Anammox process. Such a ratio might be achieved after partial nitritation by ammonium oxidizing bacteria (AOB), which converts half of the NH_4^+ to NO_2^-, thus making Anammox possible. In this thesis study, the treatment of the AD effluent without any pretreatment, such as Anammox, was to be assessed. Therefore, it was decided to supplement NO_2^- externally to each reactor type. However, since the Anammox activity in the co-culture was dominant, the option of providing improved conditions for the Anammox bacteria may cause further imbalance in the currently enriched co-culture which may lead to the loss of the remaining DAMOb. Therefore, instead of a NO_2^-:NH_4^+ ratio of 1.32, favoring the Anammox reaction, a lower ratio of 0.5 applied to all the reactors, so NO_2^- was added accordingly (Table 5.3). On the other hand, NO_3^- was not added, except for reactors AD 1/40 and SWW 1/40, since the aim of the experiment was to treat AD effluent with no

pretreatment and minimal changes. In reactors AD 1/40 and SWW 1/40, NO_2^- and NO_3^- were added at concentrations similar to the DAMO-Anammox SBR in Phase V.

Each batch reactor has a total volume of 56 mL, and the operated effective volume was 35 mL, making a headspace volume of 21 mL. Each reactor was inoculated with 15 mL of DAMMOX SBR initial mixed sludge that was previously washed multiple times with nitrogen-free synthetic feed, to ensure that the concentrations of the nitrogen species in the sludge were approximately 0 mg N/L. The DAMMOX SBR initial mixed sludge consisted of a mixture of sludge from the DAMO-Anammox SBR (Phase V), discussed in Chapter 3, the DAMO SBR (Cycle 80) and the DAA SBR (Cycle 80), discussed in Chapter 4. The details of the sludge charcteristics such as TSS and VSS concentrations are displayed in Section 5.2.1.2.

The pH values of the sludge and feed were adjusted separately to 7.5 by purging with Ar and CO_2 before seeding the reactors. After inoculating the reactors, they were purged with 4 L/min of Ar for 4 min and then purged with 0.2 L/min of CH_4/CO_2 gas mixture for 1 min. The reactors were tightly closed, and the headspace was purged for 1 min with CH_4/CO_2 gas mixture and pressurized to achieve about 1.14 atm CH_4 partial pressure. By performing this procedure, DO was maintained as low as possible, pH was adjusted to around 7.5 and the headspace was pressurized with CH_4.

The reactors placed on an orbital shaker at an rpm of 127 and were operated for the duration of 7 days (168 hours) under the operational conditions shown in Table 5.4. Liquid samples were taken at the start of the experiment, the 48^{th} hour (2^{nd} day), 120^{th} hour (5^{th} day) and 168^{th} hour (7^{th} day). The samples were filtered and analyzed for the different nitrogen species. Similarly, gas samples were taken at the same time intervals.

Table 5.4 The operational conditions of the batch reactor study

Parameter	Condition
Operation period (day)	7
Total Volume (mL)	56
Headspace (mL)	21
Effective Volume (mL)	35
Inoculum (mL)	15
Medium (mL)	20
Total pressure in the headspace (atm)	1.20
Methane partial pressure (atm)	1.14
Initial pH	7.50
rpm	127

5.2.1.2 DAMMOX SBR

The aim of setting such a reactor was to proceed with the treatment of anaerobic digester effluent, where the effluent of the DAMMOX SBR was supplied to a culture of microalgae. The aim was to investigate the effect of AD effluent on the microbial consortium of the enriched DAMO-Anammox co-culture. It was also aimed to treat the effluent of DAMO-Anammox system sequentially with a microalgae PBR to test the applicability of a novel integrated DAMO-Anammox-Micoralgae system to treat nitrogen and phosphorus nutrients of an original AD effluent, as a proof of concept.

The DAMMOX SBR was operated after the DAMO SBR and DAA SBR in Chapter 4. After observing improved activity in the DAMO and DAA SBRs, a new reactor, namely the DAMMOX SBR was set up using the sludge of the DAMO-Anammox, DAMO and DAA SBRs. The DAMMOX SBR was inoculated with 0.2 L of sludge, 0.1 L from the DAMO-Anammox SBR, 0.05 L from the DAMO SBR and 0.05 L from the DAA SBR. Before inoculation the sludge mixture was washed with nitrogen-free feed, in order to

remove any residual NH_4^+, NO_2^- and NO_3^- from the previous reactors. The TSS and VSS of the sludge from each of the reactors (DAMO-Anammox, DAMO and DAA) was analyzed (Table 5.5) before seeding the DAMMOX SBR and accordingly the volume of each sludge was decided. The initial VSS/TSS percentage in the DAMMOX SBR was found to be 35%.

Table 5.5 TSS and VSS results of the sludges used to seed the DAMMOX SBR

Sludge obtained from related reactors[a]	TSS (g/L)	VSS (g/L)	VSS/TSS %
DAMO-Anammox SBR (Cycle 192)	7.9±0.6	1.9±0.2	24
DAMO SBR (Cycle 80)	9.4±0.4	3.8±0.2	40
DAA SBR (Cycle 80)	4.8±0.4	2.0±0.1	41
DAMMOX SBR (initial seed sludge)	5.9±0.2	2.1±0.1	35

[a] Cycles at which the sludge was withdrawn for inoculation of DAMMOX SBR

The DAMMOX SBR was an air-tight stainless steel reactor with total volume of 0.4 L (Figure 5.1). The effective volume was 0.3 L creating a headspace volume of 0.1 L. The exchange volume ratio for the DAMMOX SBR was set at 0.5 corresponding to an exchange volume of 0.15L. The cycle period of the reactor was 72 hr, making an HRT of 6 days.

Figure 5.1 DAMMOX SBR

The operation temperature and initial pH were set as 35°C and 7.0-7.5, respectively; mixing was done using an orbital shaker at 120 rpm. DO was maintained close to 0 mg/L by purging the reactor with an Ar/CO_2 mixture (95%:5%) for about 3-5 min every cycle.

The synthetic wastewater was purged with the Ar/CO_2 mixture for 10-15 min and its pH was adjusted, before being fed into the reactor. Then the reactor was purged with a mixture of CH_4: CO_2 at 95%:5% to flush the Ar out and the pressure of the headspace was stabilized at 1.5 atm (absolute pressure) at the beginning of each cycle (Ettwig et al., 2009; Zhu et al., 2012; He et al., 2014, He et al., 2015a; Zhao et al., 2017).

The reactor was initially fed with the same feed constituents as the DAMO-Anammox SBR (Table 5.6) including the same concentrations of NH_4^+ (12 mg N/L), NO_2^- (25 mg N/L) and NO_3^- (25 mg N/L), as in Phase V (Cycle 189-202) (Ettwig et al., 2009; Luesken et al., 2011; Cai et al., 2015). Once steady state conditions in terms of the removal efficiencies were observed, the second phase (Phase A1) started with the application of a 1/10 diluted AD effluent, establishing initial concentrations in the DAMMOX SBR similar to those of the AD 1/20 batch reactors in the batch test. In Phase A2 the dilution to the AD effluent was reduced to 1/5 dilution, in turn increasing the initial concentrations (Table 5.7).

The AD effluent used in the batch study was stored at 4ºC before using it in this study. Therefore, before administrating the diluted AD effluent, the characteristics were measured again, to ensure the consistency of the constituents. All the constituents remained the same as shown in Table 5.2, except for the TAN concentration which was was found to be 614±5 mg N/L. The dilutions to the AD effluent were accordingly adjusted.

Table 5.6 Modified DAMO-Anammox feed (Ettwig et al., 2009; Luesken et al., 2011b; Lu et al., 2018).

Compound	Concentration (g/L)
NH_4Cl	0.0535
$NaNO_2$	0.1479
KNO_3	0.2167
$KHCO_3$	0.5
KH_2PO_4	0.05
$CaCl_2 \cdot 2H_2O$	0.3
$MgSO_4 \cdot 7H_2O$	0.2
Acidic Trace Elements 0.5 mL/L (100 mM HCl)	
$FeSO_4 \cdot 7H_2O$	55.602
$ZnSO_4 \cdot 7H_2O$	0.068
$CoCl_2 \cdot 6H_2O$	0.12
$MnCl_2 \cdot 4H_2O$	0.5
$CuSO_4$	6.384
$NiCl_2 \cdot 6H_2O$	0.095
H_3BO_3	0.014
Alkali Trace Elements 0.2 mL/L (10 mM NaOH)	
SeO_2	0.067
$Na_2WO_4 \cdot 2H_2O$	0.05
Na_2MoO_4	0.242

Table 5.7 Operational details and phase changes of the DAMMOX SBR with respect to the feed source

Phase	Feed Source	Cycle No.	Influent NH_4^+ (mg N/L)	Influent NO_2^- (mg N/L)	Influent NO_3^- (mg N/L)	Influent Molar Ratio		
						NH_4^+/NO_2^-	NH_4^+/NO_3^-	NO_2^-/NO_3^-
S	SWW	1-10	24	50	50	0.48	0.48	1
A1	AD 1/10	11-24	60	30	0	2	-	-
A2	AD 1/5	25-28	120	60	0	2	-	-

5.2.1.3 *C. vulgaris* PBR

A semi-continuous 800 mL microalgae PBR was established and operated for at least 1 month prior to the start of the experiments in this section, namely, microalgae seed culture PBR (MSC PBR) (Figure 5.2). The MSC PBR contained an axenic *C. Vulgaris* culture, previously enriched from a culture obtained from "Istanbul Microalgae Biotechnologies Research and Development Centre" in an agar plate. This culture was cultivated in the 800 mL PBR under sterile conditions liquid 3-Fold Bold's Basal Medium with vitamins (3N BBM +V) in accordance with the recommendation of "UTEX Culture Collection of Algae" (Table 5.8). The MSC PBR was operated at an HRT of 4 days, which was previously established as the optimum HRT of the culture, considering the highest nitrogen and phosphorus removal efficiencies (Subaşı, 2022). Moreover, according to Subaşı (2022) the optimum influent TN/P ratio applied to this *C. vulgaris* culture was 8 g N/ g P, in the range of 5-15 g N/ g P (Aslan and Kapdan, 2006). Therefore, the theoretical influent TAN and PO_4^{3-} concentrations of the MSC PBR were 32 mg N/L and 4 mg P/L, respectively.

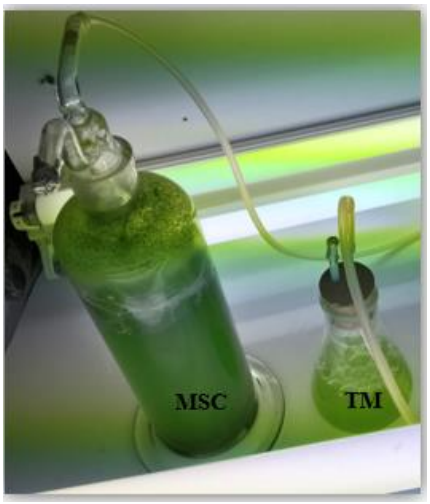

Figure 5.2 The MSC PBR shown on the left and the TM PBR shown on the right

Table 5.8 3N-BBM + Vitamins synthetic wastewater prepared for MSC PBR (UTEX Culture Collection of Algae)

Compound	Concentration (g/L)
NH_4Cl	0.122
KH_2PO_4	0.018
K_2HPO_4	0.008
$CaCl_2 \cdot 2H_2O$	0.025
$MgSO_4 \cdot 7H_2O$	0.075
NaCl	0.025
$NaHCO_3$	2.5
P-IV Metal Solution 6 mL/L	
$Na_2EDTA \cdot 2H_2O$	125
$FeCl_3 \cdot 6H_2O$	16.17
$MnCl_2 \cdot 4H_2O$	6.83
$ZnCl_2$	0.83
$CoCl_2 \cdot 6H_2O$	0.33
$Na_2MoO_4 \cdot 2H_2O$	0.67
Vitamins 1 mL/L for each	
Biotin	0.025
Thiamine HCl	0.335
Cyanocobalamin	0.135

A new test microalgae PBR (TM PBR) was established (Figure 5.2), inoculated with 135 mL of culture from the MSC PBR (Day 23). The effective volume of the TM PBR was 180 mL, while the exchange volume was 45 mL, corresponding to an exchange volume ratio of 0.25. The TM PBR was supplied with only the DAMMOX effluent running under diluted AD effluent. The MSC PBR was operated throughout the operation of the TM PBR as a stock for the microalgae culture and for comparison

between the two reactors in terms of removal performance. Moreover, similar to the MSC PBR, the TM PBR was operated at an HRT of 4 days.

Both PBRs were operated with a PAR of 150-200 PAR using an 18 W cool-white, fluorescent lamps (OSRAM, L 18W/685). The operation temperature was 19-24°C, while the aeration was applied using an air pump (RESUN Air Pump AC-9602) at a flowrate of 0.5 L/min (2.8 L/L/min, vvm). Filters with 0.45 μm pore size (Hydrophobic Minisart Syringe Filter) were mounted at the ends of the air inlet and outlet tubings to avoid contamination.

The DAMMOX SBR effluent was provided to the TM PBR after being filtered through 0.2 μm filters (Sartorius). Each DAMMOX SBR cycle effluent (150 mL) was divided after filtration and provided as influent for the TM PBR for 3 days. 15 mL were used for the various analysis conducted, 45 mL were supplied in the first day, while the remaining 90 mL were stored at 4°C for the next 2 days.

Parameters such as pH, temperature, TAN, NO_2^-, NO_3^-, PO_4^{3-}, dry cell weight, optical density were monitored throughout the operation of the PBRs. Alkalinity provided to the MSC PBR in the form of $NaHCO_3$, however, since the TM PBR was to be supplied with the effluent of the DAMMOX SBR, the total alkalinity of this effluent was assessed to ensure that it would be in the desired range.

The total alkalinity supplied to the MSC PBR was about 1500 mg $CaCO_3$/L, in the form of $NaHCO_3$. On the other hand, the total alkalinity of the DAMMOX SBR effluent was measured, in case it was necessary to supply an external source of alkalinity. The alkalinitiy was found to be 355 mg $CaCO_3$/L in the form of HCO_3^-, which was sufficient for the operation of the *C. vulgaris*.

Table 5.9 DAMMOX SBR (Phases A1 and A2) effluent characteristics that were supplied to the TM PBR

Compound	Concentration (mg/L)
TAN-N	20.9-47.7
NO_2^--N	0-5.6
NO_3^--N	0-34.5
PO_4^{3-}-P	4.7-9.6
Alkalinity ($CaCO_3$)	355-365 (HCO_3^-)
TN/P (g N/g P)	3.6-12.6
pH	7.0-7.63
sCOD	89.9-454.9

5.2.2 Analytical Methods

The activity of the DAMMOX SBR was assessed to evaluate the microbial composition. This was performed through the assessment of the removal rates, removal efficiencies, removal molar ratios of the nitrogen species and total nitrogen removal in comparison to the theoretical values present in the literature. The concentrations of sCOD and phosphate were monitored to follow the change in their concentrations before providing the effluent to the TM PBR. Furthermore, molecular analysis through FISH and NGS 16S Metagenome Analysis were performed to assess the change in the microbial consortium focusing on the DAMO and Anammox microorganisms.

The performance of the TM PBR was assessed through the assessment of the removal rates and removal efficiencies of the nitrogen species, phosphate and sCOD. The performance of the TM PBR was compared to the MSC PBR in terms of optical density and dry cell weight to determine the effect of AD effluent on the microalgae culture in comparison to SWW.

5.2.2.1 Volumetric and Chromatographic Analyses

Anions such as NO_2^-, NO_3^- and SO_4^{2-} were analyzed using IC (IC -Shimadzu Prominence HIC-SP). The IC was operated under the following conditions, highest pressure limit of 150 bar, oven temperature of 45°C, and a flow rate of 0.8 mL/min. The analyses were performed in duplicates or triplicates, depending on the presence of enough sample volume. The calibration curves, the limit of detection LOD and LOQ are shown in APPENDIX C.

TAN (NH_4^+-N + NH_3-N) was analyzed using the Hach Nessler Method (Hach, 2012). The analyses were performed in triplicates. The calibration curves, LOD and LOQ are illustrated in APPENDIX D.

The soluble ortho-phosphate (SOP) was measured using a spectrophotometer at a wavelength of 880 nm (HACH. DR 2800), according to the Ascorbic Acid Method indicated in the Standard Methods 4500-P (APHA, AWWA, WEF, 2005). All samples were filtered using 0.20 μm filters (Sartorius) before ion analysis. The analyses were performed as triplicates. The calibration results, LOD and LOQ are displayed in APPENDIX G.

sCOD was evaluated using medium range kits and low range kits (Hach, 2012). The analyses were performed in duplicates or triplicates, depending on the presence of enough sample volume. TOC was analyzed using the TOC analyzer. The analyses were performed in triplicates. The calibration, LOD and LOQ of the sCOD and TOC tests are shown in APPENDIX E.

TS, VS, TSS and VSS were analyzed using Standard Method (APHA, AWWA, WEF, 2005). The analyses were performed in triplicates. On the other hand, the pH and DO of the feed and the effluent of each reactor was measured using a pH-meter and DO-meter, as well as the temperature of the room was recorded.

CO_2, CH_4 and N_2 gases were analyzed using the TCD equipped in the GC (Trace GC Ultra: Thermo Electron Corporation). The following settings were applied in the GC, injector temperature 80°C, oven temperature 40°C, detector temperature 80°C, while the carrier gas used was He maintained at a pressure of 100 kPa. The analyses were performed in triplicates. The calibration and the LOD and LOQ of the GC analyses were performed and shown in APPENDIX F.

Regarding the analyses performed for the PBR setup, the photosynthetically active radiation (PAR) was measured using a PAR meter (Light SCOUT). The optical density was measured using the HACH spectrophotometer DR 2800 with 1-cm light path at the optimum wavelength of 680 nm which was previously determined for the enriched *C. Vulgaris* culture. Moreover, the dry cell weight (DCW) was measured according to the Standard Method (APHA, AWWA, WEF, 2005), where 10 mL of microalgae samples were filtered onto 1.2 μm porous filters, placed into 30 mL crucibles and dried at 105˚C

overnight. The analyses were performed in triplicates. The total alkalinity of the effluent of the DAMMOX SBR was assessed by titrating sulfuric acid as described in the Standard Method 2320 (APHA, AWWA, WEF, 2005).

5.2.2.2 Determination of the Reaction Rate of Each Target Microorganism in DAMMOX SBR

The NO_2^- and NO_3^--based reaction rates of the target microorganisms, namely Anammox, DAMOa and DAMOb were calculated throughout the operation of the SBR and the batch test. These reaction rates were computed according to the stoichiometric Equations 2.4, 2.5 and 2.6 in Section 2.3.2 and Section 2.4.2 (Hu et al., 2015). Equations 5.1, 5.2 and 5.3 were used to compute the reaction rates of each microorganism.

- $r_{Anammox\ NO_2^-} = -1.32 * r_{NH_4^+}$ ..... Equation 5.1
- $r_{DAMOa\ NO_3^-} = -r_{NO_3^-} + (0.26/1.32) * r_{Anammox\ NO_2^-}$ ..... Equation 5.2
- $r_{DAMOb\ NO_2^-} = -r_{NO_2^-} - r_{Anammox\ NO_2^-} + r_{DAMOa\ NO_2^-}$ ..... Equation 5.3

The Anammox and DAMOb reaction rates were calculated based on the NO_2^- consumption. Since Anammox is the only species among the three target microorganisms that oxidizes NH_4^+, the consumed NO_2^- by Anammox was computed using the measured NH_4^+ consumption rate ($r_{NH_4^+}$), and the NO_2^- removal reaction rate of Anammox ($r_{Anammox\ NO_2^-}$) was computed accordingly, as shown in Equation 5.1. The reaction rate of DAMOa ($r_{DAMOa\ NO_3^-}$) was calculated using the measured NO_3^- ($r_{NO_3^-}$) consumption rate, that includes the produced NO_3^- ($(0.26/1.32) * r_{Anammox\ NO_2^-}$) from the Anammox reaction, illustrated in Equation 5.2. The DAMOb reaction rate ($r_{DAMOb\ NO_2^-}$) was calculated using the measured NO_2^- consumption rate ($r_{NO_2^-}$) by considering the Anammox NO_2^- consumption rate ($r_{Anammox\ NO_2^-}$) and the DAMOa production rate of NO_2^- which is equal to ($r_{DAMOa\ NO_3^-}$) (Hu et al., 2015), as shown in Equation 5.3.

5.2.2.3 Determination of the Contribution of Each Target Microorganism Contribution to the Available TN Removed

The contribution of each of the target microorganisms to the TN removal was assessed to examine their activity and to further understand the composition of the consortium in correlation with the molar ratio calculations and the molecular analysis. A sample calculation is displayed in APPENDIX H. The TN removed by each target microorganism, namely Anammox, DAMOb and DAMOa was calculated by considering the consumed and produced nitrogen with respect to each reaction (Equations 2.4, 2.5 and 2.6 in Section 2.3.2 and Section 2.4.2). Equations 5.4-5.14 were used in the calculations of the percent contribution of each microorganism to the TN removed. This was calculated as a percentage from the available TN that takes into consideration the produced nitrogen in the intermediate reactions, which cannot be observed by only considering the initial and final nitrogen concentrations. The initial TN was calculated by the summation of the initial concentrations of the nitrogen species analyzed experimentally (Equation 5.4). The final TN was calculated by the summation of the final concentrations of the nitrogen species (Equation 5.5).

The available TN is a term used via this thesis study for the first time. $TN_{available}$ is the summation of the initial nitrogen species and the produced nitrogen species via the reactions taking place, such as NO_3^- from Anammox and NO_2^- from DAMOa (Equation 5.6). Utilizing the available TN is critical since it allows the calculation of the actual consumption of each of the target species, otherwise, the real activity of DAMOa and DAMOb would not be recognized by just monitoring the initial and final concentrations of the nitrogen species. While the percentage contribution to the available TN removed ($\%CATN_{removed}$) was computed according to Equation 5.7.

$$TN_i=[NH_4^+\text{-}N]_i+[NO_2^-\text{-}N]_i+[NO_3^-\text{-}N]_i \quad \text{Equation 5.4}$$

$$TN_f=[NH_4^+\text{-}N]_f+[NO_2^-\text{-}N]_f+[NO_3^-\text{-}N]_f \quad \text{Equation 5.5}$$

$TN_{available}=[NH_4^+\text{-}N]_i+[NO_2^-\text{-}N]_i+[NO_3^-\text{-}N]_i+\Delta[NO_3^-\text{-}N]_{AMX}+\Delta[NO_2^-\text{-}N]_{DAMOa}$

.....Equation 5.6

$\%CATN_{removed}^{microorganism}=(TN_{removed}^{microorganism}/TN_{available})*100$……. Equation 5.7

where,

TN_i: initial TN concentration at each cycle, the sum of the initial concentrations of all the nitrogen species, (mg N/L)

$[NH_4^+\text{-}N]_i$: initial NH_4^+ concentration at each cycle, (mg N/L)

$[NO_2^-\text{-}N]_i$: initial NO_2^- concentration at each cycle, (mg N/L)

$[NO_3^-\text{-}N]_i$: initial NO_3^- concentration at each cycle, (mg N/L)

TN_f: final TN concentration at each cycle, the sum of the final concentrations of all the nitrogen species, (mg N/L)

$[NH_4^+\text{-}N]_f$: final NH_4^+ concentration at each cycle, (mg N/L)

$[NO_2^-\text{-}N]_f$: final NO_2^- concentration at each cycle, (mg N/L)

$[NO_3^-\text{-}N]_f$: final NO_3^- concentration at each cycle, (mg N/L)

$TN_{available}$: available TN concentration that is available for consumption by the target microorganisms which includes the summation of any nitrogen species to be produced via the target microorganisms, (mg N/L)

$\Delta[NO_3^-\text{-}N]_{AMX}$: NO_3^- concentration to be produced stoichiometrically by Anammox in each cycle computed regarding the consumed NH_4^+-N, (mg N/L)

$\Delta[NO_2^-\text{-}N]_{DAMOa}$: NO_2^- concentration to be produced stoichiometrically by DAMOa in each cycle, (mg N/L)

$TN_{removed}^{microorganism}$: TN removed by each microorganism calculated in Equations 5.11, 5.12 and 5.14, (mg N/L)

$\%CATN_{removed}^{microorganism}$: Percentage contribution of each microorganism to the available TN removal (%)

Since NH_4^+ is only consumed by Anammox and the Anammox bacteria were observed to be the most active of the three microorganisms, NH_4^+ was chosen to be the starting point of this calculation. The consumed NH_4^+ by Anammox was computed (Equation 5.8). While the corresponding consumed NO_2^- and produced NO_3^- by Anammox was then computed, according to Equations 5.9 and 5.10, respectively. Hence the summation of the consumed nitrogen species while deducting the produced nitrogen yields the TN removed by Anammox (Equation 5.11).

AMX:

$\Delta[NH_4^+\text{-}N]=[NH_4^+\text{-}N]_i-[NH_4^+\text{-}N]_f$……..…….. Equation 5.8

$\Delta[NO_2^-\text{-}N]_{AMX}= 1.32*\Delta[NH_4^+\text{-}N]$…..……..…..…….... Equation 5.9

$\Delta[NO_3^-\text{-}N]_{AMX}= 0.11*(\Delta[NH_4^+\text{-}N]+\Delta[NO_2^-\text{-}N]_{AMX})$……..... Equation 5.10

$TN_{removed}^{AMX}= \Delta[NH_4^+\text{-}N]+\Delta[NO_2^-\text{-}N]_{AMX}-\Delta[NO_3^-\text{-}N]_{AMX}$……..…..... Equation 5.11

where,

$\Delta[NH_4^+\text{-}N]$: NH_4^+ concentration consumed by Anammox in each cycle, (mg N/L)

$\Delta[NO_2^-\text{-}N]_{AMX}$: NO_2^- concentration consumed by Anammox in each cycle, (mg N/L)

$TN_{removed}^{AMX}$: TN concentration consumed by Anammox in each cycle, (mg N/L)

The available NO_3^- for DAMOa consumption includes the initial NO_3^- concentration and the produced NO_3^- by Anammox. Accordingly, the consumed NO_3^- by DAMOa can be computed, and subsequently the TN removed by DAMOa can be computed as well (Equation 5.12).

DAMOa:

$TN_{removed}^{DAMOa}=\Delta[NO_3^-\text{-}N]_{DAMOa}=[NO_3^-\text{-}N]_i-[NO_3^-\text{-}N]_f+\Delta[NO_3^-\text{-}N]_{AMX}$.. Equation 5.12

$\Delta[NO_2^-\text{-}N]_{DAMOa}=\Delta[NO_3^-\text{-}N]_{DAMOa}$……..…….....….... Equation 5.13

where,

$\Delta[NO_3^-\text{-}N]_{DAMOa}$: NO_3^- concentration consumed by DAMOa in each cycle, (mg N/L)

$TN_{removed}^{DAMOa}$: TN concentration consumed by DAMOa in each cycle, (mg N/L)

On the other hand, the available NO_2^- for DAMOb consumption is the remaining NO_2^- after the Anammox reaction, since Anammox has a higher affinity to NO_2^- in comparison to DAMOb, and the produced NO_2^- by DAMOa. Hence, the consumed NO_2^- by DAMOb can be computed, hence, the TN removed by DAMOb can be deduced (Equation 5.14).

DAMOb:

$TN_{removed}^{DAMOb}=\Delta[NO_2^-\text{-}N]_{DAMOb}=[NO_2^-\text{-}N]_i-\Delta[NO_2^-\text{-}N]_{AMX}+\Delta[NO_2^-\text{-}N]_{DAMOa}-[NO_2^-\text{-}N]_f$

…..……...…….... Equation 5.14

where,

$\Delta[NO_2^-\text{-}N]_{DAMOb}$: NO_2^- concentration consumed by DAMOb in each cycle, (mg N/L)

$TN_{removed}^{DAMOb}$: TN concentration consumed by DAMOb in each cycle, (mg N/L)

5.2.2.4 Determination of the Stoichiometric Ratio of the Consortium in DAMMOX SBR

The different combinations of nitrogen ratios were examined to further assess the performance and status of the reactor in terms of the co-culture present. In other words, it was aimed to reveal the potential culture combinations and dominance by following the theoretical stoichiometric ratios of the nitrogen species, which might be the indicator of the reactions of the target microorganisms. Four different ratios were calculated and compared to the stoichiometric molar ratios, $\Delta NO_2^-/\Delta NH_4^+$; $\Delta NO_3^-/\Delta NH_4^+$; $\Delta NO_3^-/\Delta NO_2^-$ and $\Delta NO_3^-/(\Delta NO_2^- + \Delta NH_4^+)$. These ratios were examined under six different

cases of the co-cultures that might be occurring in the reactor. The assumptions followed in these cases are given below:

- The main four cases are as follows: AMX, AMX & DAMOa, AMX & DAMOb and DAMX, (Equations 5.15, 5.16, 5.18 and 5.19);
    j. AMX: The SBR only contains Anammox culture.
    v. AMX & DAMOa: The SBR contains both Anammox and DAMOa.
    vi. AMX & DAMOb: The SBR contains both Anammox and DAMOb.
    vii. DAMX: The SBR contains Anammox, DAMOa and DAMOb.
- For all cases (i.e., for all the potential combinations of cultures)
    j. Each culture is 100% active.
    iii. Anammox is present since they have been enriched and provided with the necessary conditions to thrive.
- The change of concentration in each cycle was calculated as follows $\Delta C = C_{initial} - C_{final}$. Therefore, consumption of the nitrogen species is positive, while production is negative.

The theoretical stoichiometric ratios were calculated according to the stoichiometry present in the reaction equations (Equations 2.4, 2.5 and 2.6 in Section 2.3.2 and Section 2.4.2). For Equations 2.4, 2.5 and 2.6, the limiting reagent in each reaction was considered. The limiting reagent in each reaction is NH_4^+, NO_3^- and NO_2^- for Anammox, DAMOa and DAMOb reactions, respectively. Accordingly, the equations were adjusted for 1 mole of the specified limiting reagent.

In addition to the four main cases mentioned above, a special incident, where DAMOa is able to consume only the NO_3^- produced by the Anammox, was constructed by equating the moles of NO_3^- consumed to the moles of NO_3^- produced in the two cases, namely, *AMX & DAMOa and *DAMX, as displayed in Equations 5.17 and 5.20, respectively. In these two cases, the activity of DAMOa was not assumed to be 100%. Incorporating this special case may improve the characterization of the co-culture composition via the molar ratio calculation.

All calculations of each culture combination (six cases) are given in Equations 5.15-5.20 and accordingly, the theoretical stoichiometric molar values were obtained in Table 5.10.

AMX: $NH_4^+ + 1.32\ NO_2^- \rightarrow 0.26\ NO_3^- + 1.02\ N_2$…….…... Equation 5.15

AMX & DAMOa: $NH_4^+ + 0.32\ NO_2^- + 0.74\ NO_3^- \rightarrow 1.02\ N_2$……..... Equation 5.16

*AMX & DAMOa: $NH_4^+ + 1.06\ NO_2^- \rightarrow 1.02\ N_2$……...…….…….. Equation 5.17

AMX & DAMOb: $NH_4^+ + 2.32\ NO_2^- \rightarrow 0.26\ NO_3^- + 1.52\ N_2$……..... Equation 5.18

DAMX: $NH_4^+ + 1.32\ NO_2^- + 0.74\ NO_3^- \rightarrow 1.52\ N_2$……..…… Equation 5.19

*DAMX: $NH_4^+ + 2.06\ NO_2^- \rightarrow 1.52\ N_2$……..…...…. Equation 5.20

Table 5.10 Theoretical stoichiometric molar ratio calculations of nitrogen species for the different microbial consortium cases

Microbial consortium cases	ΔNH_4^+	ΔNO_2^-	ΔNO_3^-	$\Delta NO_2^-/\Delta NH_4^+$	$\Delta NO_3^-/(\Delta NO_2^-+\Delta NH_4^+)$	$\Delta NO_3^-/\Delta NO_2^-$	$\Delta NO_3^-/\Delta NH_4^+$
AMX	1.00	1.32	-0.26	1.32	-0.11	-0.2	-0.26
AMX & DAMOa	1.00	0.32	0.74	0.32	0.56	2.31	0.74
*AMX & DAMOa	1.00	1.06	0	1.06	0	0	0
AMX & DAMOb	1.00	2.32	-0.26	2.32	-0.08	-0.11	-0.26
DAMX	1.00	1.32	0.74	1.32	0.32	0.56	0.74
*DAMX	1.00	2.06	0	2.06	0	0	0

5.2.3 Molecular Analysis Methods

Two molecular analyses methods were employed in this study, the FISH and the NGS 16S Metagenome. The FISH method was performed periodically to detect, identify, and determine the relative abundance of the target species among the whole microbial consortium. On the other hand, the NGS 16S Metagenome method was performed to determine all the microorganisms present in the consortium and their relative abundance.

5.2.3.1 Fluorescent In-Situ Hybridization Analysis

The FISH analyses were performed during the different phases of operation of the DAMMOX SBR for morphological detection and determination of the relative abundance of the target species (Nielsen et al., 2009).

About 5 ml of sample was used, where the supernatant was separated by centrifugation at 10,000 g for 5 min and then it was discarded. The remaining sludge was fixed with an equal volume of 4% PFA in PBS, which was then stored overnight at 4°C. The next day the sample was centrifuged at 10,000 g for 5 min to separate the PFA, which was then discarded. The remaining fixed biomass was then dissolved in 5 mL of 1:1 PBS/Ethanol (Daims et al., 2009). The samples were then stored overnight at -20°C. The following day the samples were carefully placed on slides and dehydration of the samples on the slides was conducted. This was carried out with sequential washing with 50%, 80%, and 99% ethanol (Daims et al., 2009). The next step was permeabilization of the microbial cells which was performed by incubating the slides for 1 hr at 37°C after the addition of lysozyme (Daims et al., 2009).

Hybridization solutions of different probes targeting *M. nitroreducens*, *M. oxyfera*, General Bacteria, General Archaea and Anammox were prepared considering their relative formamide and NaCl concentrations. The stringency conditions (formamide and NaCl concentrations) were optimized prior to the FISH analyses to ensure better results of probe hybridization. The probes used in the scope of these experiments are

summarized in Table 5.11. Five hybridization mixtures were prepared using different combinations of the previously described solutions (Table 5.12). The mixtures containing only General Archaea and General Bacteria were counterstained with DAPI to determine the content of bacteria and archaea in the microbial consortium. Five slides were prepared for each biomass sample analyzed. The hybridization mixtures were added carefully on the slides and the slides were incubated at 46°C for about 5 hr (Daims et al., 2009). After hybridization, the slides were washed at 48°C for 15 min with a washing buffer containing the same formamide concentration as the hybridization buffer (Daims et al., 2009).

After washing and drying the slides, imaging can commence. FISH imaging was performed using Carl Zeiss Axio Vision A1 UV microscope under suitable filters of the chosen probes. At least 3 representative microscopy images were chosen for each slide. The images were analyzed via the ImageJ software. The obtained images from the microscope were then processed using ImageJ, where the colored areas were converted to pixels. The pixel areas represent the presence of the probe and hence the target cell. The average area occupied by the pixels in the three chosen images and the relative abundance of each slide was computed. These computations were conducted in relativeness to the area occupied by the General Bacteria and General Archaea which were performed in relativeness to DAPI counterstaining. A summary of the steps performed using ImageJ, the resulting images and the obtained relative abundance in each slide are illustrated in APPENDIX I.

Table 5.11 Sequences, labels and formamide concentrations of chosen FISH probes

Target Species	Probe	Label	Formamide Concentration (%)	Reference
M. nitroreducens	S-*-Darc-872-a-A-18-GGC TCC ACC CGT TGT AGT	GFP and Cy5	40	Hu et al. (2015)
M. oxyfera	S-*-DBACT-0193-a-A-18-CGC TCG CCC CCT TTG GTC	Alexa Fluor 350	40	Ettwig et al. (2009)
General Anammox	S-*-Amx-0368-a-A-18-CCT TTC GGG CAT TGC GAA	Cy5	20	Schmid et al. (2005)
General Bacteria	EUB1 -GCT GCC TCC CGT AGG AGT	GFP	40	Daims et al. (2009)
	EUB2 -GCA GCC ACC CGT AGG TGT			
	EUB3-GCT GCC ACC CGT AGG TGT			
General Archaea	S-Darc-0915-a-A-20-GTG CTC CCC CGC CAA TTC CT	GFP	40	Knittel et al. (2005)

Table 5.12 The hybridization mixture and aim of each slide

Slide	Hybridization mixture content	Aim
1	General Bacteria and DAPI counterstaining	Determine the content of bacteria in the microbial consortium
2	General Archaea and DAPI counterstaining	Determine the content of archaea in the microbial consortium
3	*M. oxyfera*, Anammox and General Bacteria	Determine the abundance of *M. oxyfera* and Anammox relative to General Bacteria
4	*M. nitroreducens* and General Archaea	Determine the abundance of *M. nitroreducens* relative to General Archaea
5	*M. oxyfera, M. nitroreducens* and Anammox	Determine the relative abundance of the target species among each other

5.2.3.2 Next-Generation Sequencing 16S Metagenome Analysis

PCR amplification of specific genes of interest also referred to as "16S ribosomal RNA gene" allows achieving a taxonomic distribution profile and sequencing of the 16S rRNA gene. The taxonomic distribution can be linked with environmental data obtained from the sample under study and subsequently, allowing for a quick and detailed generation of a genomic profile of that environmental sample (Oulas et al., 2015).

Two sludge samples were withdrawn from the DAMMOX SBR at the initial cycle (Cycle 0) and at Cycle 24, each representing a different phase of the reactor operation. The samples were stored at -20°C and then sent for NGS analysis to be performed by BM LABOSIS and the change in the population dynamics was examined at the cycles stated above. The NGS 16S Metagenome Analysis procedure followed by BM

LABOSIS is the procedure described by Boylen et al. (2019) and is summarized in the following text.

1. Sample preparation: DNA isolation and quality control are performed to create libraries.
2. Creating a library: The 16S rRNA gene is used with specific primers, which were then replicated and purified. The concentration of libraries generated by real time PCR is diluted to 4 nM and normalization is done.
3. Sequencing: After the library is prepared sequencing using the synthesis method is done with each new dNTP added. The added base fluoresces are optically observed and recorded.
4. Raw Data Processing: The data generated after sequencing is analyzed in FASTA format.
5. Raw Data Quality Control: The quality of the fastqc files (FASTQC) are examined using QIIME2.
6. Determination of Chimeric Readings using DADA2
7. Filtering: Reads, primers and barcodes with Phred quality scores less than 20 are filtered out using DADA2.
8. Determination of Taxonomy: Determination of taxonomic species for each sample using QIIME2.
9. Diversity Analysis: Alpha and Beta Rarefaction Analysis using QIIME2 is performed.

5.3 Results and Discussion

5.3.1 Results of BATCH SET: SWW Versus AD Effluent Application

The initial TN concentrations in the reactors provided with AD effluent were similar to their equivalent reactors provided with SWW, as shown in Figure 5.3. The TN removal and removal efficiency in each reactor type are shown in Table 5.13. SWW 1/4 reactor type exhibited the highest TN removal of 127 mg N/L corresponding to a removal efficiency of 51%, meanwhile its counterpart AD 1/4 exhibited a TN removal of 79 mg N/L, which corresponds to the lowest removal efficiency of 31%. SWW 1/8 reactor types removed 67 mg N/L TN at a removal efficiency of 53%, lower than its counterpart AD 1/8, which removed 79 mg N/L TN at a removal efficiency of 63%. Similarly, AD 1/20 removed slightly higher TN at a higher removal efficiency than SWW 1/20. On the other hand, SWW 1/40, which was provided with similar concentrations as the DAMO-Anammox SBR, achieved a higher TN removal of 46 mg N/L corresponding to 71% than its counterpart AD 1/40, which removed 37 mg N/L corresponding to 58%.

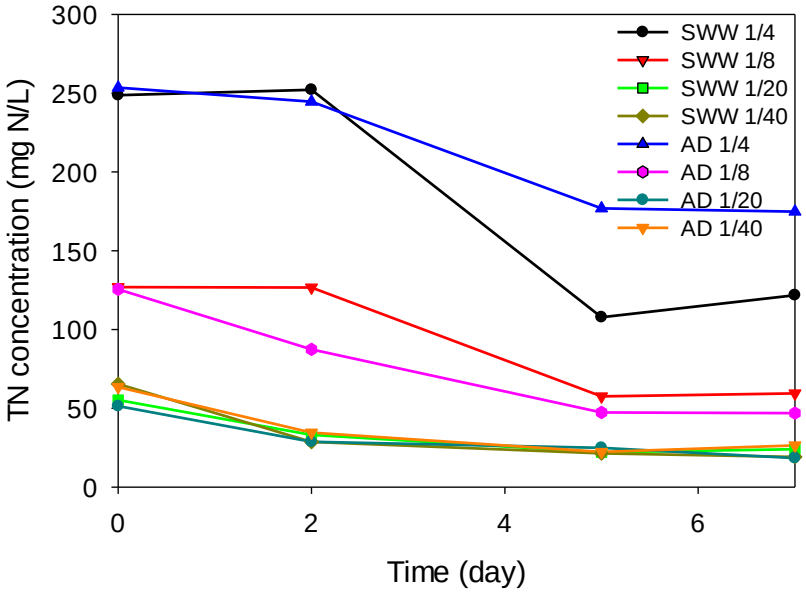

Figure 5.3 The TN concentrations in each reactor type

Table 5.13 TN removed and removal efficiency in each reactor type

Reactor Type	SWW 1/4	SWW 1/8	SWW 1/20	SWW 1/40	AD 1/4	AD 1/8	AD 1/20	AD 1/40
TN removed (mg N/L)	127	67	31	46	79	79	33	37
Percent of TN removal (%)	51	53	57	71	31	63	64	58

The removal efficiency of SWW 1/40 was the highest amongst all reactor types. The second and third highest reactor types in terms of TN removal efficiency were AD 1/20 and AD 1/8, respectively, which indicates that the constituents of the AD effluent supported the co-culture activity better than their counterparts SWW 1/20 and SWW 1/8. On the other hand, the difference in TN removal between SWW 1/4 and AD 1/4 may be due to the presence of about 173 mg/L of SO_4^{2-} in AD 1/4 reactor types. AD 1/8, AD 1/20 and AD 1/40 contained about 87, 35 and 17 mg SO_4^{2-} /L, respectively. The percent TN removal in reactors AD 1/8, AD 1/20 and AD 1/40 were close to one another, yet the percent N removal in AD 1/4 reactors was evidently lower, this might have been due to the effect of the high SO_4^{2-} concentration as suggested by Li et al. (2020a), where the highest denitrification rate of DAMO microorganisms was observed at 80 mg SO_4^{2-} /L while concentrations above that inhibited the DAMO process.

Regarding AD 1/40, the TN removal efficiency achieved was higher than SWW 1/8 and SWW 1/20 but could not match that of SWW 1/40, AD 1/20 and AD 1/8 reactor types. This was probably caused by the limited availability of vital components present in the feed due to the higher dilution factor applied in the AD 1/40 reactor types.

According to the results found in a modelling study performed by He et al. (2018a), a COD concentration of 24 mg COD/L forming a COD/N ratio of 0.34 mg COD/mg N achieved the highest DAMOb activity. The release of growth factors by heterotrophic denitrifiers indirectly supported the activity of DAMOb. The initial sCOD concentration in AD 1/4, AD 1/8, AD 1/20 and AD 1/40 was 109, 54, 22 and 11 mg/L, respectively.

Respectively, the sCOD/TN ratio of the AD 1/4, AD 1/8 and AD 1/20 reactor types was 0.43, while the sCOD/TN ratio of AD 1/40 was 0.17. Hence the results of the TN removal efficiency that show higher removal efficiency in AD 1/20 and AD 1/8 reactor types than AD 1/40 and AD 1/4 concur with the result from He et al. (2018a).

Due to the high sCOD and SO_4^{2-} concentrations present in AD 1/4 reactor type, inhibited Anammox activity is evident (Figure 5.4b) in comparison to SWW 1/4 reactor type (Figure 5.4a). Anammox bacteria was able to remove more TAN in SWW 1/4 (49 mg N/L) than in AD 1/4 (31 mg N/L) (Figure 5.4a). On the other hand, NO_3^- removal was lower in SWW 1/8 (Figure 5.4c) in comparison to AD 1/8 (Figure 5.4d) from Day 2 to Day 7. In addition, the NO_3^- removal in SWW 1/40 (Figure 5.4g) was higher than AD 1/40 (Figure 5.4h).

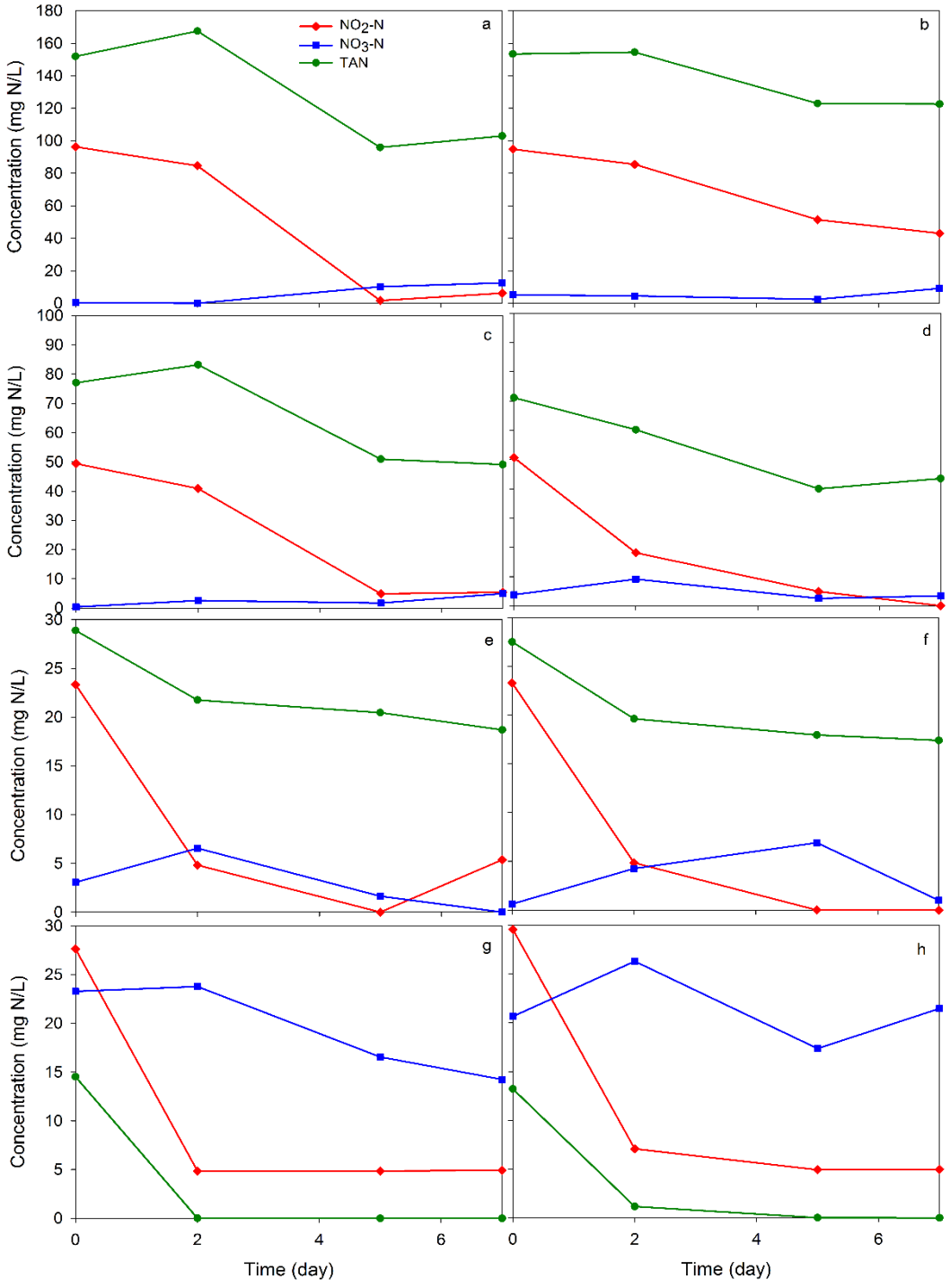

Figure 5.4 The concentrations of TAN, NO_2^--N and NO_3^--N in each reactor type (a) SWW 1/4, (b) AD 1/4, (c) SWW 1/8, (d) AD 1/8, (e) SWW 1/20, (f) AD 1/20, (g) SWW 1/40 and (h) AD 1/40

In all reactor types Anammox was responsible of removing most of the TN (Figure 5.5). The $r_{Anammox\ NO_2^-}$ was higher than $r_{DAMOb\ NO_2^-}$ and $r_{DAMOa\ NO_3^-}$ in all reactor types (Figure 5.6). The difference in Anammox activity between SWW 1/4 and AD 1/4 is evident in Figure 5.5 and Figure 5.6. In SWW 1/4, the $\%CATN_{removed}$ of Anammox was 56% and the $r_{Anammox\ NO_2^-}$ attained was 9.2 mg N/L·day. On the other hand, the $\%CATN_{removed}$ of Anammox and $r_{Anammox\ NO_2^-}$ in AD 1/4 reactor type was 26% (Figure 5.5) and 5.8 mg N/L·day (Figure 5.6), respectively. As mentioned above, the presence of SO_4^{2-} at such high concentrations may have negatively affected the Anammox activity, resulting in almost 50% decrease in NO_2^- removal rate and removal efficiency.

In the reactors supplied with NO_3^-, that is SWW 1/40 and AD 1/40, the highest $\%CATN_{removed}$ of DAMOa was observed (18% and 14%, respectively) followed by SWW 1/20 and AD 1/20 (13% and 11%, respectively). Nevertheless, the highest $r_{DAMOa\ NO_3^-}$, 1.8 mg N/L·day, was observed in the SWW 1/40 reactor type. However, the second and third highest $r_{DAMOa\ NO_3^-}$ were observed in AD 1/8 (1.1 mg N/L·day) and SWW 1/20 (0.8 mg N/L·day), respectively (Figure 5.6).

The highest $\%CATN_{removed}$ of DAMOb was observed in reactor types SWW 1/20 (30%), AD 1/20 (30%). Yet the highest $r_{DAMOb\ NO_2^-}$ was observed in SWW 1/4 (3.7 mg N/L·day), followed by AD 1/8 (3.1 mg N/L·day), then SWW 1/40 (2.3 mg N/L·day) and AD 1/4 (2.2 mg N/L·day). In terms of the NO_2^- and NO_3^--based reaction rates SWW 1/40 showed the most balanced activity among the three target microorganisms. This also leads to the highest TN removal of 71%. An Anammox $\%CATN_{removed}$ of about 40% might be advantageous for supporting the activity of DAMOa. Yet, an Anammox $\%CATN_{removed}$ above 50% as in SWW 1/4 and AD 1/8, is unbalancing the DAMO activitythus leading to a decrease in the TN removal.

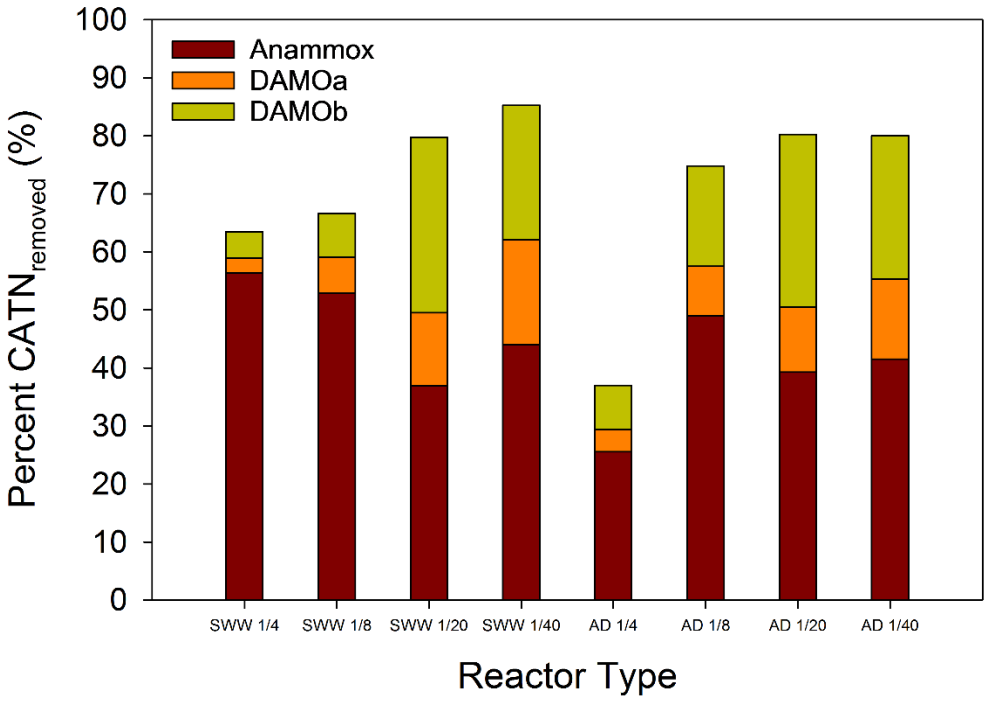

Figure 5.5 The %CATN$_{removed}$ in each reactor type

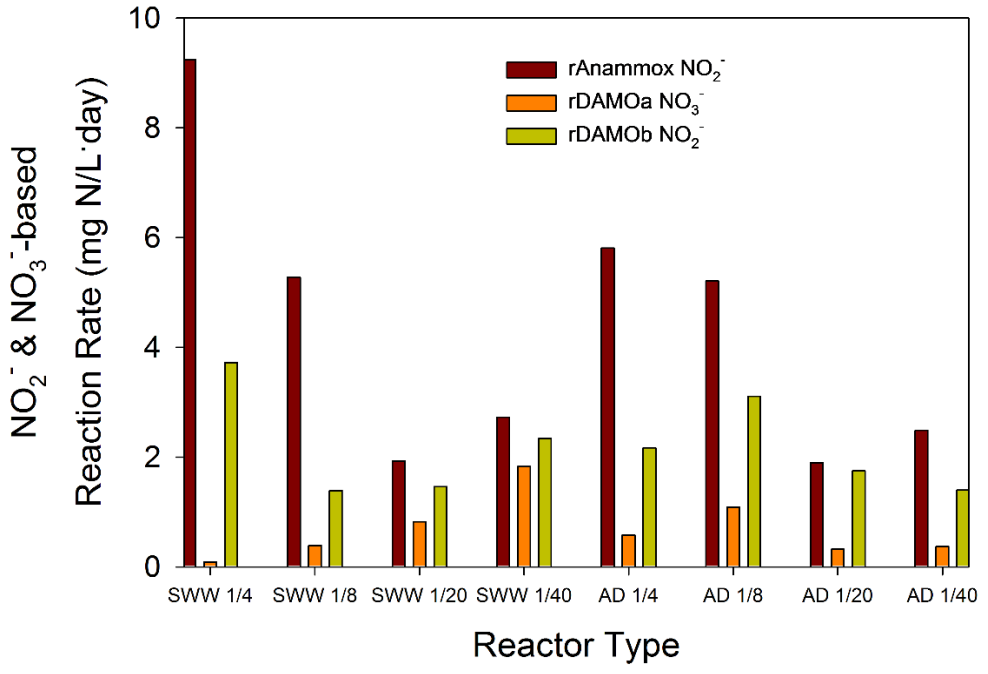

Figure 5.6 The NO_2^- and NO_3^--based reaction rate of each target microorganism in the different reactor types

In regard to CH_4 consumption, all reactor types exhibited similar consumption trends, as shown in Figure 5.7. Although CH4 was generally consumed, yet it was also produced due to the presence of methanogenic archaea in the sludge. The highest net consumption was observed in AD 1/40 reactors (211 μmole) and AD 1/4 (209 μmole). In the AD 1/20 reactors the highest consumption (306 μmole) occurred in the first two days. In terms of N_2 production, the highest production was exhibited in SWW 1/4, while the lowest production was observed in SWW 1/40, as illustrated in Figure 5.7a. The N_2 production in SWW 1/8 (Figure 5.7c) and SWW 1/20 (Figure 5.7e) were alike and lower than their counterparts AD 1/8 (Figure 5.7d) and AD 1/20 (Figure 5.7f), which had similar N_2 production. On the other hand, N_2 production in AD 1/4 (Figure 5.7b) and AD 1/40 (Figure 5.7h) reactor types was second to SWW 1/4. In addition, the CO_2 production, all reactor types exhibited similar production trends, as shown in Figure 5.7.

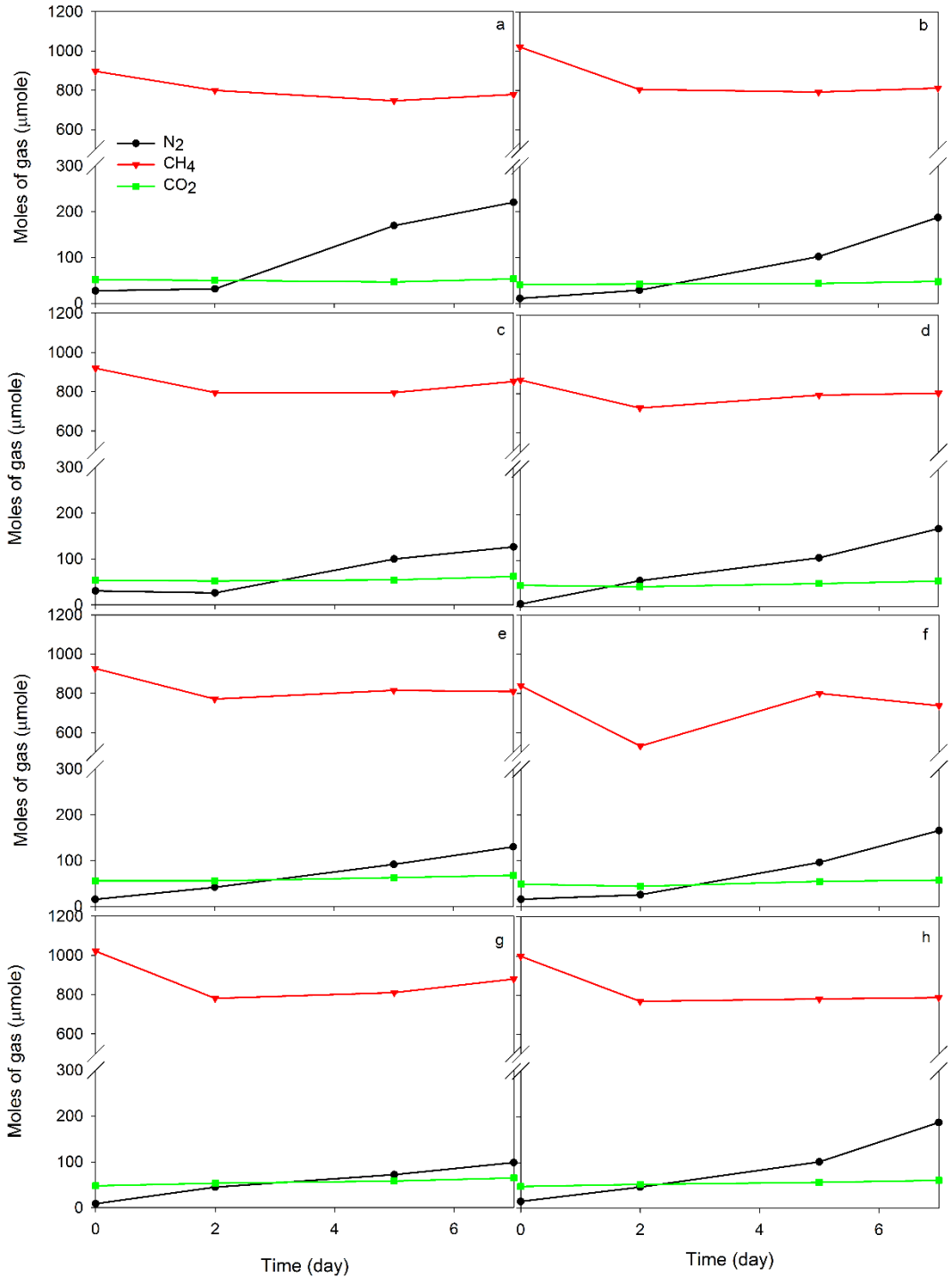

Figure 5.7 The gas composition of the headspace of each reactor type (a) SWW 1/4, (b) AD 1/4, (c) SWW 1/8, (d) AD 1/8, (e) SWW 1/20, (f) AD 1/20, (g) SWW 1/40 and (h) AD 1/40

5.3.2 DAMMOX SBR

The DAMMOX SBR was established aiming to treat anaerobic digester (AD) effluent using the DAMO-Anammox co-culture enriched in the DAMO-Anammox, DAMO and DAA SBRs discussed in Chapter 3 and Chapter 4. The DAMMOX SBR was operated with synthetic wastewater (SWW) in Phase S (Cycle 1-10), then with 1/10 diluted AD effluent in Phase A1 (Cycle 11-24) and finally with 1/5 diluted AD effluent in Phase A2 (Cycle 25-28), (Table 5.7). The effect of AD effluent application on the reactor performance and the population dynamics of the microbial consortium was assessed in the DAMMOX SBR. The DAMMOX SBR was operated for about 85 days (28 cycles) and the results are presented in two main sections, namely, results of reactor performance and results of molecular analyses.

5.3.2.1 Results of DAMMOX SBR Performance

The results of the reactor performance were divided into two sections, a section discussing the pH, TOC and TSS and VSS analyses conducted (Section 5.3.2.1.1) and a section discussing the results of the nitrogen species analyses (5.3.2.1.2), including the removal efficiencies, removal rates, TN removal and the contribution of each of the target species and reaction rates of each of the target species.

5.3.2.1.1 pH, TSS and VSS

The DAMMOX SBR was operated at a temperature of 35°C, while the pH of the influent was maintained at a pH of 7.2-7.6. The effluent pH ranged from 7.0-7.63, throughout 28 cycles, as shown in Figure 5.8. The average pH in the different phases of operation was 7.40±0.10, 7.25±0.15 and 7.51±0.09, in Phases S, A1 and A2, respectively. These pH values were in the range of the most commonly applied pH throughout DAMO-Anammox enrichment studies (7.3-7.5) (Luesken et al., 2011; Haroon et al., 2013; Ding et al., 2014; Ding et al., 2017; Cai et al., 2015; Xie et al., 2016; Fu et al., 2017; Hu et al.,

2015). This pH range was defined as the optimal pH range for DAMO-Anammox co-culture activity. Due to the initial pH of the AD effluent, 7.53, the application of the AD effluent did not have an effect on the pH of the DAMMOX SBR effluent.

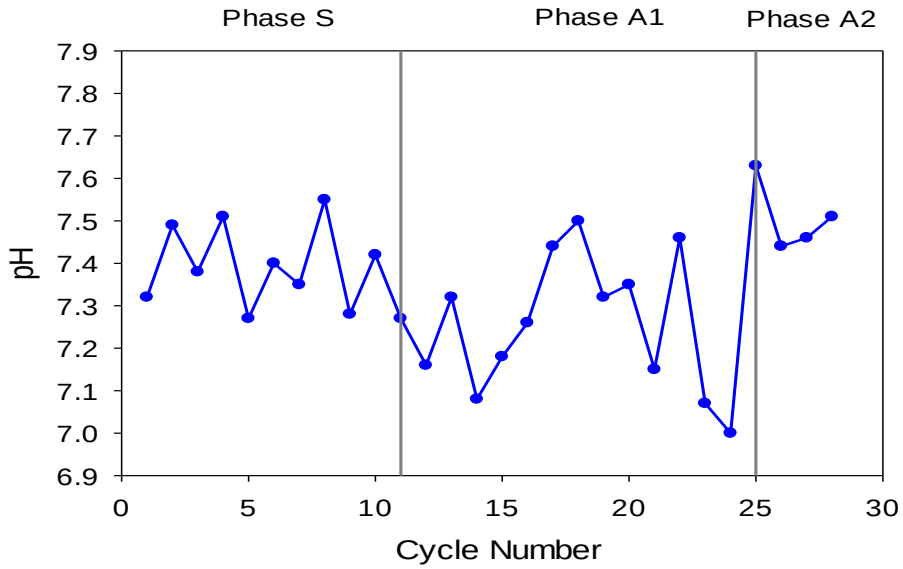

Figure 5.8 pH results of the effluent samples of the DAMMOX SBR

Before mixing the sludge from the three reactors the TSS and VSS were measured, (Table 5.14), and accordingly the volumes to be used of each of the sludges were determined. The initial TSS and VSS of the DAMMOX SBR were 5.9±0.2 and 2.1±0.1 g/L, respectively, corresponding to a VSS/TSS ratio of 36%. At Cycle 28 the TSS and VSS reached concentrations of 3.9±0.1 and 1.6±0.1 g/L, respectively, corresponding to a VSS/TSS ratio of 42%.

Table 5.14 TSS and VSS concentrations of the sludge in the DAMMOX SBR

Sludge	TSS (g/L)	VSS (g/L)	VSS/TSS (%)
DAMO-Anammox SBR (Cycle)	7.9±0.6	1.9±0.2	24
DAMO SBR (Cycle)	9.4±0.4	3.8±0.2	40
DAA SBR (Cycle)	4.8±0.4	2.0±0.1	41
Mixed initial DAMMOX seed	5.9±0.2	2.1±0.1	36
DAMMOX SBR Cycle 28	3.9±0.1	1.6±0.1	42

5.3.2.1.2 Results of Nitrogen Species Analyses

The results of the analyses conducted show the activity of the DAMO-Anammox co-culture fed with SWW feed and AD effluent. The $\%CATN_{removed}$ each of the target microorganisms, stoichiometric molar ratios of the nitrogen species and the NO_2^- and NO_3^--based reaction rates of the target microorganisms were computed. The results of Phase S were compared with the results of the other SBR performances to interpret the status of the DAMO-Anammox co-culture before the application of the AD effluent. Phase S illustrated the activity of the three target microorganisms, with the least activity shown by the Anammox bacteria.

Phase S

Phase S corresponds to the first 10 cycles where SWW was supplied at initial concentrations of NH_4^+, NO_2^- and NO_3^- of 13.2±1.0, 26.5±3.0 and 25.8±3.8 mg N/L, respectively, as shown in Figure 5.9. These concentrations were similar to the concentrations applied to the DAMO-Anammox SBR during Phases III and V. It should be noted that, the corresponding influent concentrations of NH_4^+, NO_2^- and NO_3^- were 26.4±1.9, 52.9±5.9 and 51.7±7.6 mg N/L, respectively, since the exchange volume to effective volume ratio was 0.5. The applied HRT was 6 days, which was the HRT of the DAMO-Anammox SBR during Phases III and V, consequently, the NLR was 21.8±2.2 mg N/L·day. The average removal efficiencies of TAN, NO_2^- and NO_3^- during Phase S

were 82±0.1% (Figure 5.10a), 90±0.04% (Figure 5.10b) and 94±0.1% (Figure 5.10c), respectively. While the average removal rates of TAN, NO_2^- and NO_3^- during Phase S were 3.6±0.5 mg N/L·day (Figure 5.11a), 8.0±1.1 mg N/L·day (Figure 5.11b) and 8.0±1.4 mg N/L·day (Figure 5.11c), respectively.

The HRT, NLR and initial NH_4^+, NO_2^- and NO_3^- concentrations applied to the DAMMOX SBR during Phase S were similar to Phase III and Phase V of the DAMO-Anammox SBR, discussed in Chapter 3. The attained average removal efficiency and average removal rate of TAN during Phase S of the DAMMOX SBR were lower than that of the DAMO-Anammox SBR in Phase III (96±3 % and 4.3±1.0 mg N/L·day) and Phase V (96±13 % and 4.8±0.7 mg N/L·day). Moreover, they were higher than that achieved in the DAA SBR (Cycle 60-82) (26±20 % and 2.1±1.5 mg N/L·day), discussed in Chapter 4. On the other hand, the average removal efficiency and average removal rate of NO_2^- achieved in the DAMMOX SBR in Phase S were higher than that achieved by the DAMO-Anammox SBR in Phase III (84±6 % and 7.2±1.3 mg N/L·day) and Phase V (81±10 % and 7.7±1.7mg N/L·day) and that of the DAMO SBR (78±18 % and 4.2±1.2 mg N/L·day), discussed in Chapter 4. Relatively lower TAN yet higher NO_2^- removal efficiencies and rates might reveal a relatively lower Anammox activity yet higher DAMOb activity in the DAMMOX SBR. Since the initial TOC concentration in the initial cycle (Cycle 0) of the DAMMOX SBR was found to be about 13.5±0.3 mg/L, the main mechanisms of NO_2^- removal can be attributed to the activities of Anammox and DAMOb. Nevertheless, this does not mean that heterotrophic does not occur, rather its activity can be considered neglibile compared to the activity of the DAMO-Anammox co-culture.

The average removal efficiency and average removal rate of NO_3^- in Phase S of the DAMMOX SBR reached much higher levels than that of the DAMO-Anammox SBR during Phase III (13±12 % and 4.6±4.9 mg N/L·day) and Phase V (14±14 % and 3.3±2.8 mg N/L·day). However, the NO_3^- average removal efficiency in Phase S of the DAMMOX SBR was slightly lower than in the DAA SBR (Cycle 60-82) (97±6 %) and higher than that of the DAMO SBR (93±11 %). The NO_3^- average removal rate in the

DAMMOX SBR was lower than both the DAMO SBR (11.6±2.3 mg N/L·day) and the DAA SBR (Cycle 60-82) (11.9±3.4 mg N/L·day). The higher NO_2^- and NO_3^- removal rates in DAA and DAMO SBRs compared to the DAMMOX SBR was mainly attributed to the shorter cycle period and thus shorter HRT (4 days) applied in the DAA and DAMO SBRs.

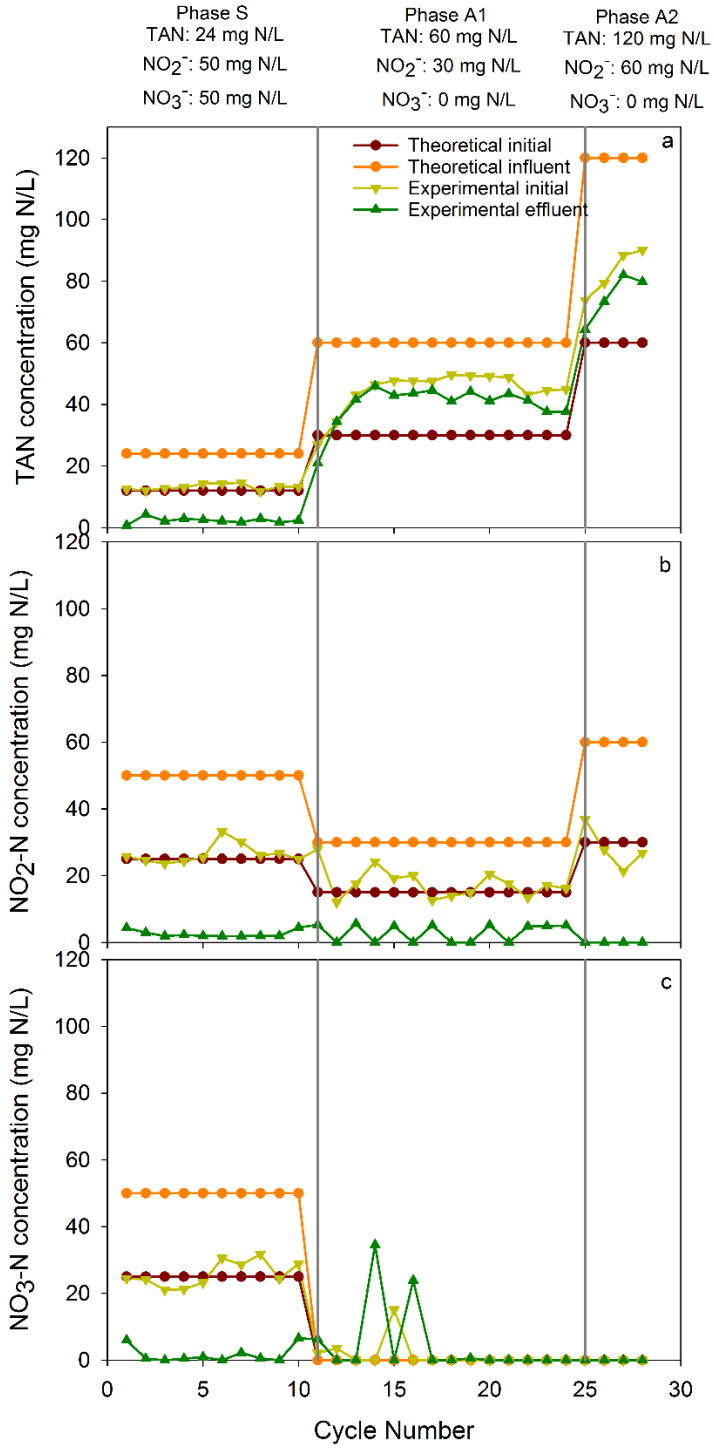

Figure 5.9 Influent, initial and final concentrations of (a) TAN, (b) NO_2^--N and (c) NO_3^--N during each cycle of the DAMMOX SBR (The values given at the top of the figure reveal the influent concentrations; the S.D of each measurement was <5%)

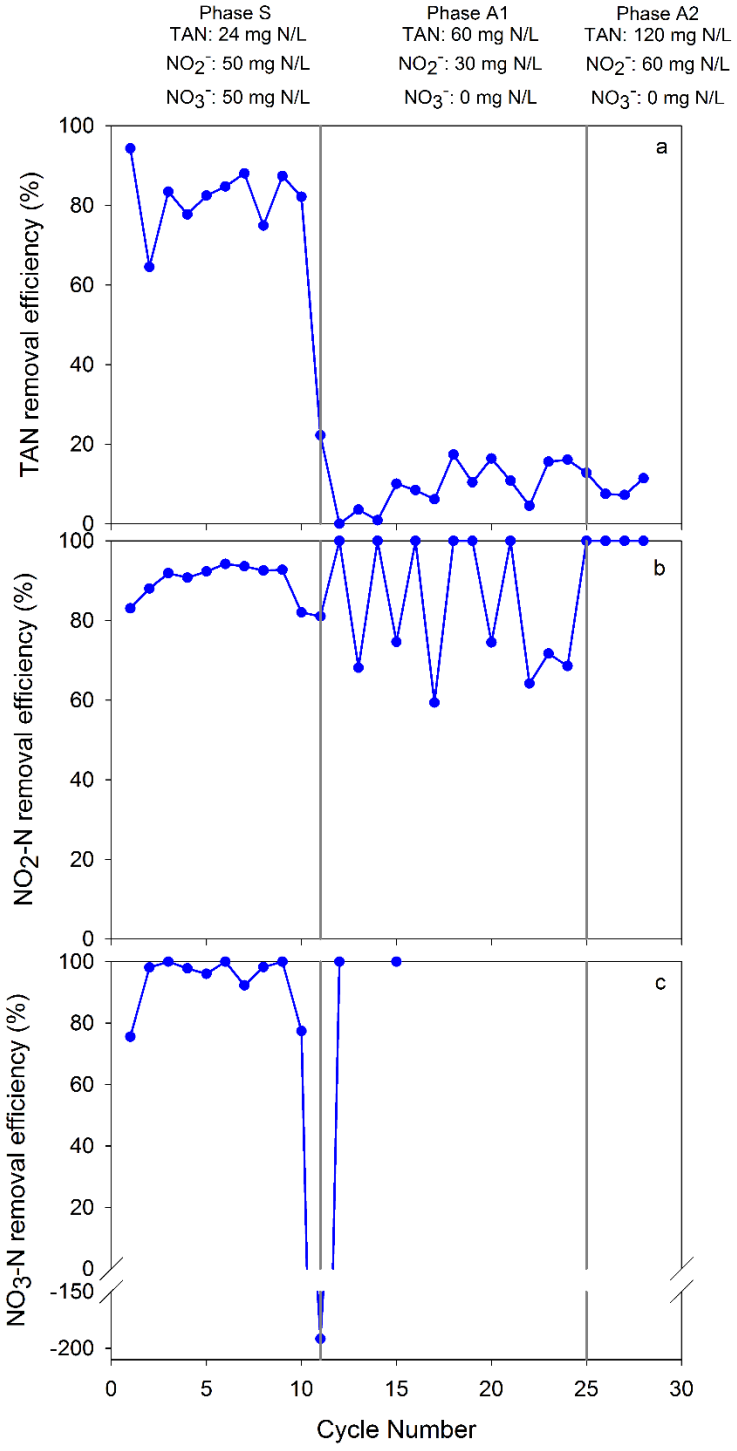

Figure 5.10 The removal efficiencies of (a) TAN, (b) NO_2^- and (c) NO_3^- in each cycle of the DAMMOX SBR (The values given at the top of the figure reveal the influent concentrations; the negative values signify production)

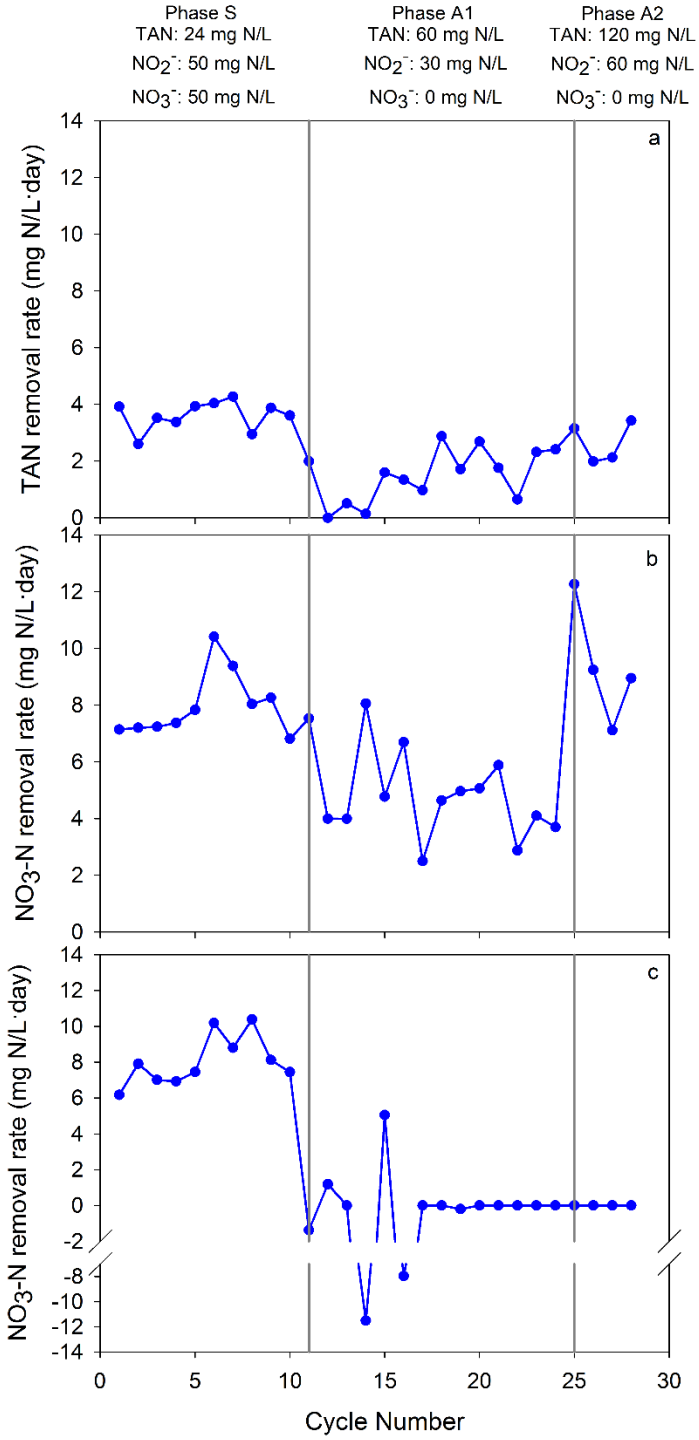

Figure 5.11 The removal rates of (a) TAN, (b) NO_2^- and (c) NO_3^- in each cycle of the DAMMOX SBR (The values given at the top of the figure reveal the influent concentrations; the negative values signify production)

The average TN removal was 90±5 % in Phase S. The average %CATN$_{removed}$ of Anammox, DAMOa and DAMOb was calculated as 24±4 %, 28±2 % and 38±4 %, respectively (Figure 5.13). The average TN removal rate during Phase S of the DAMMOX SBR was calculated as 19.6±2.5 mg N/L, which was higher than the average TN removal rate during Phases III and V of the DAMO-Anammox SBR, the DAMO SBR and the DAA SBR.

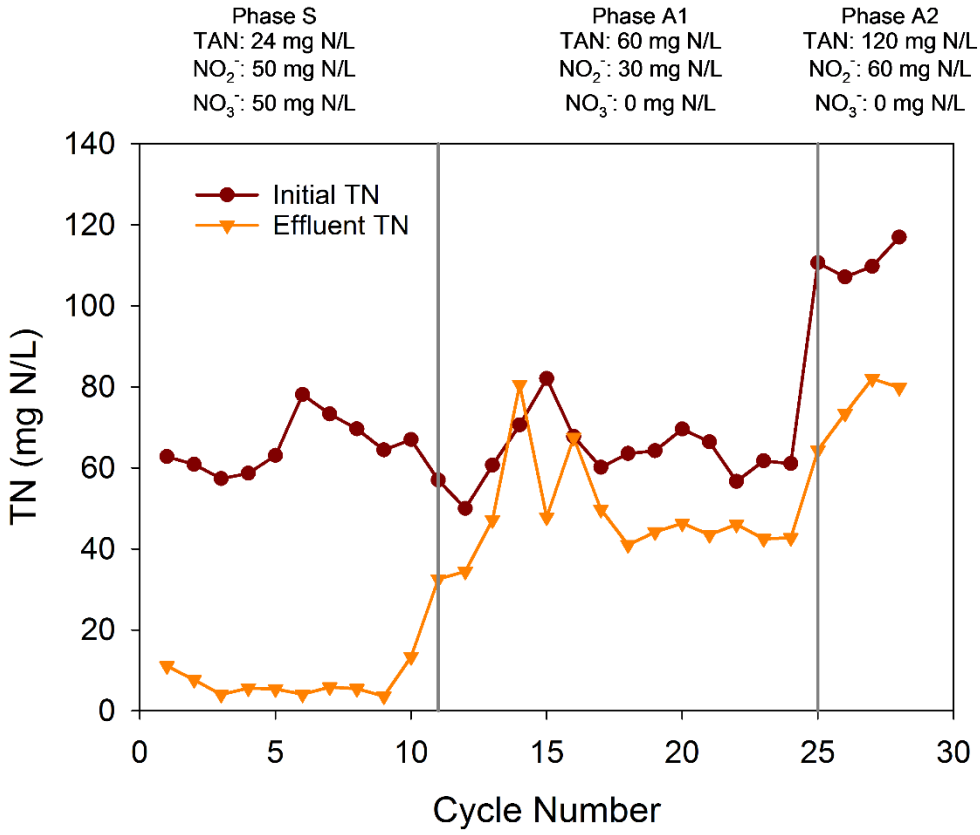

Figure 5.12 The initial and final TN of the DAMMOX SBR (The values given at the top of the figure reveal the influent concentrations)

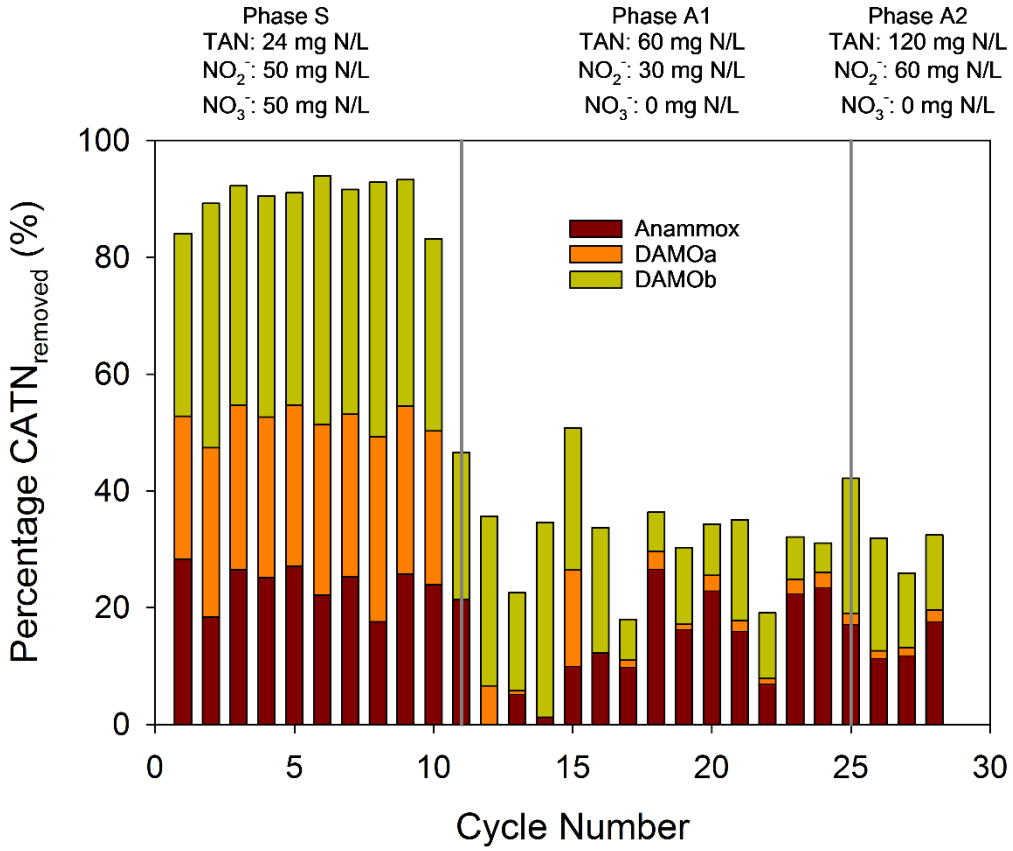

Figure 5.13 The %CATN$_{removed}$ of each microorganism in the DAMMOX SBR (The values given at the top of the figure reveal the influent concentrations)

During Phase S of the DAMMOX SBR operation, the average $r_{Anammox\ NO_2^-}$, $r_{DAMOb\ NO_2^-}$ and $r_{DAMOa\ NO_3^-}$ were found to be 4.8±0.7 mg N/L·day, 12.2±2.3 mg N/L·day, and 9.0±1.4 mg N/L·day, respectively. The results of Phase S of the DAMMOX SBR demonstrate higher performance in terms of removal efficiencies and removal rates of TAN, NO_2^- and NO_3^-, as well as higher activity of the DAMO-Anammox co-culture in comparison to the DAA, DAMO and DAMO-Anammox SBRs. The results of the removal efficiencies, removal rates, %CATN$_{removed}$, NO_2^- and NO_3^--based reaction rates signify that the DAMMOX SBR has a higher nitrogen removal performance and higher activity of the target microorganisms compared to the DAA, DAMO and DAMO-Anammox SBRs.

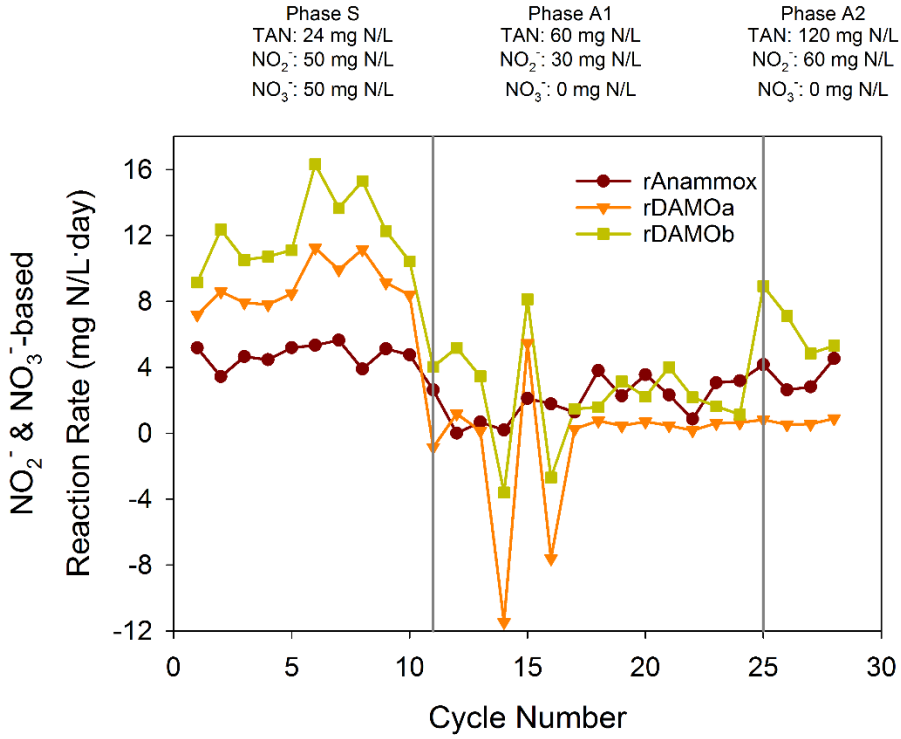

Figure 5.14 The calculated NO_2^- and NO_3^--based reaction rates of each target microorganism throughout the operation of the DAMMOX SBR

Phase A1

At Cycle 11, the application of diluted AD effluent commenced. The theoretical influent concentrations of the AD effluent after a 1/10 dilution factor and the addition of NO_2^- were 60 mg N/L of TAN, 30 mg N/L of NO_2^- and 0 mg N/L of NO_3^- (Figure 5.9). These concentrations were decided according to the results of the AD effluent batch test in Section 5.3.1, which demonstrated the highest TN removal percentage in the AD 1/20 reactor type. The HRT was kept constant at 6 days, so the new theoretical NLR of this phase was 15 mg N/L·day, which is slightly lower than in Phase S. The theoretical influent NH_4^+/ NO_2^- molar ratio changed from 0.5 in Phase S to 2 in Phase A1.

The average experimental influent concentrations of TAN and NO_2^- during Phase A1 were 89.0±12.8 and 35.3±9.0 mg N/L, respectively. The average removal rates of TAN and NO_2^- decreased to half the rates in Phase S. In Phase A1, the average removal

efficiencies of TAN and NO_2^- decreased to 10±0.1 % (Figure 5.10a) and 83±0.2 % (Figure 5.10b), respectively, and the average removal rates of TAN and NO_2^- decreased to 1.5±0.9 mg N/L·day (Figure 5.11a) and 4.9±1.6 mg N/L·day (Figure 5.11b), respectively. It was expected that the removal rates and efficiencies would decrease since the nitrogen source (absence of NO_3^-) and the influent molar ratios changed in this phase. The removal of TAN presumably decreased due to the presence of COD in the AD effluent which allowed for the heterotrophic denitrification to take place in turn decreasing the Anammox activity. Moreover, the presence of the dissimilatory nitrate reduction to ammonia (DNRA) process may have contributed to the conversion of NO_2^- to NH_4^+, therefore, net TAN consumption was not observed.

Since the initial concentration of NO_3^- was 0 mg N/L in the majority of the cycles after Cycle 11, the removal efficiency was not calculated. On the other hand, net production of NO_3^- was observed in Cycles 11, 14 and 16, the highest occurring in Cycle 14 with a net production of 34.5 mg N/L. The calculated produced NO_3^- due to Anammox activity was 1.4, 0.1 and 1 mg N/L in Cycles 11, 14 and 16, respectively. This did not correspond to the net production observed in those cycles; therefore, another process has caused this increase in NO_3^- concentration. Since this phenomenon only occurred in these cycles and did not occur later on during the application of the AD effluent, the release of NO_3^- concentration might be attributed to cell death.

During Phase A1, the average TN removal decreased to 25%, as illustrated in Figure 5.12. The average $\%CATN_{removed}$ of Anammox declined to 14±9%, while that of DAMOa declined the most to an average of 2.8% (Figure 5.13). Whereas the average $\%CATN_{removed}$ of DAMOb decreased to 16±%. The average TN removed during this period decreased to 5.6±3.7 mg N/L·day.

The average $r_{\text{Anammox } NO_2^-}$ and $r_{\text{DAMOb } NO_2^-}$ in Phase A1 significantly decreased to reach 2.0±1.2 mg N/L·day, 2.3±2.2 mg N/L·day, respectively. Since NO_3^- was not present in the AD effluent and the Anammox activity decreased, therefore the lack of NO_3^- caused the $r_{\text{DAMOa } NO_3^-}$ to become negligible. The Anammox and DAMOb activity decreased

since the influent NH_4^+/NO_2^- molar ratio increased from 0.5 in Phase S to 2 in Phase A1 and less NO_2^- was provided in comparison to Phase S. Due to the absence of NO_3^- in the influent, DAMOa activity was immensely affected.

Kinetic Sampling in Phase A1

Samples were taken from the DAMMOX SBR in each day of the three-day cycle period at Cycle 24 to assess the kinetics of the reactor, and assess the change in concentration of NH_4^+, NO_2^-, NO_3^-, and PO_4^{3-}. The results are illustrated in Figure 5.15. The initial concentrations of NH_4^+, NO_2^-, NO_3^-, and PO_4^{3-} were 44.9 mg N/L, 16.2 mg N/L, 0 mg N/L and 3.2 mg P/L, respectively. The concentrations of NH_4^+ and NO_2^- decreased to 32.6 and 6.1 mg N/L, respectively, in the first day. However, in the second day the concentrations of NH_4^+ and NO_2^- increased to 39 and 8.4 mg N/L, respectively. On the other hand, in the third day of the cycle the concentrations of NH_4^+ and NO_2^- decreased once again to 37.6 and 5.1 mg N/L, respectively. Meanwhile, the concentration of PO_4^{3-} in the first day slightly decreased to 2.9 mg P/L, then increased to 3.8 mg P/L in the second day and further increased to 4.7 mg P/L in the third day. The concentration of NO_3^-, on the other hand, remained 0 mg N/L throughout all the days of Cycle 24, indicating no production at the sampling periods. The consumption of NH_4^+ and NO_2^- in the first day can be mainly attributed to the Anammox activity, considering the specific activity tests performed in Chapter 3, which indicates that the Anammox reaction takes place before the occurrence of the DAMO reactions. Yet, the increase in NO_3^- concentration was not observed in the first day. Since the Anammox activity diminished significantly during Phase A1, the expected produced NO_3^- was at most 2 mg N/L, which would be probably consumed nearly instantly. PO_4^{3-} production or release can be observed within the 3-day cycle. This PO_4^{3-} release is further discussed in Section 5.3.2.1.3 and the microorganisms contributing to this activity are discussed in the results of the NGS analysis in Section 5.3.3.2

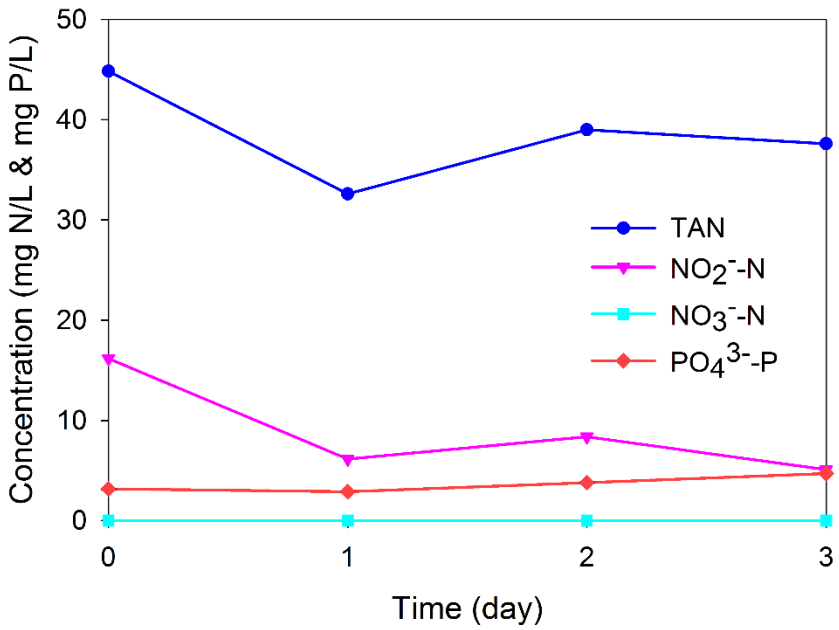

Figure 5.15 The results of the daily analysis of Cycle 24 of the DAMMOX SBR

Phase A2

After observing steady-state in Phase A1, at Cycle 25, the influent concentrations of NH_4^+ and NO_2^- were increased to 165±15 mg N/L and 56.3±12.8 mg N/L, respectively, using a 5-dilution of the AD effluent (Figure 5.9) and Phase A2 commenced. In Phase A2, the average removal efficiencies of TAN and NO_2^- were 9±3% (Figure 5.10a) and 100% (Figure 5.10b), respectively, while the average removal rates of TAN and NO_2^- were 2.7±0.7 mg N/L·day (Figure 5.11a) and 9.4±2.1 mg N/L·day (Figure 5.11b), respectively. During Phase A2, the initial and effluent NO_3^- concentrations were 0 mg N/L, therefore the removal efficiency and removal rate of NO_3^- were not calculated. The further decrease in the TAN removal efficiency and removal rate and the increase in NO_2^- removal efficiency and removal suggests that the Anammox activity further decreased after decreasing the dilution of the AD effluent. This occurred due to the increase in sCOD concentration which favors the activity of heterotrophic denitrification as well as the increase of the SO_4^{2-} concentration which has an inhibitory effect on Anammox and DAMOb at concentrations above 50 mg/L.

The average TN removal in Phase A2 slightly increased to reach 33±7 %. In Phase A2, the average $r_{Anammox\ NO_2^-}$, $r_{DAMOb\ NO_2^-}$ and $r_{DAMOa\ NO_3^-}$ increased to 3.5±1.0 mg N/L·day, 6.6±1.7 mg N/L·day, and 0.7±0.2 mg N/L·day, respectively, compared to Phase A1. Although the influent NH_4^+/NO_2^- molar ratio was unchanged from Phase A1, the increased concentrations of NH_4^+ and NO_2^- led to an increase in the average NO_2^- and NO_3^--based reaction rates of all the target microorganisms.

In Phases A1, the removal efficiency and removal rate of TAN were negatively affected the most among the nitrogen species since they experienced the greatest decrease (from 82% to 10% and from 3.6 mg N/L·day to 1.5 mg N/L·day), especially after a dominant presence of Anammox in Phase S. However, in Phase A2, the TAN removal rate slightly increased from 1.5 mg N/L·day to 2.4 mg N/L·day, due to the increased TAN influent concentrations, hence the TAN loading rate. Yet the TAN removal efficiency remained relatively the same as in Phase A1.

The TN removal in the DAMMOX SBR was low in comparison to the AD 1/4, AD 1/8 and AD 1/20 reactors from the AD batch test conducted discussed in Section 5.3.1, as shown in Table 5.15. Table 5.15 illustrates the initial concentrations, TN removal, contribution of the target microorganisms to the available TN removal and the NO_2^- and NO_3^--based reaction rates of the target microorganisms. Since the operation period of the batch reactors was 7 days, the effect of the COD and SO_4^{2-}concentrations was not as evident as in Phases A1 and A2, noting that the sludge used in the batch test was the same as the DAMMOX SBR. The batch reactors were fed once, yet in the DAMMOX SBR COD accumulation from one cycle may have caused an elevated effect on the Anammox activity more than that observed in the batch test. Moreover, the NO_2^- and NO_3^--based reaction rates of the target microorganisms in the AD 1/20 batch reactors were relatively similar to those in Phase A1 of the DAMMOX SBR. Yet the NO_2^- and NO_3^--based reaction rates of the target microorganisms in the AD 1/4 and AD 1/8 reactors were higher than those of the DAMMOX SBR. A decrease in the Anammox activity allowed for an increase in the DAMOb activity as observed in the AD 1/4 and AD 1/8 batch reactors and in Phase A2 of the DAMMOX SBR.

Table 5.15 Comparison between Phases A1 and A2 of the DAMMOX SBR and the AD 1/4, AD 1/8 and AD 1/20 batch reactors

Phase	Average Experimental Initial Concentrations (mg N/L)				TN removal (mg N/L)	Percentage TN removal (%)	Contribution to TN removal (%)			NO_2^- & NO_3^--based reaction rates (mg N/L·day)		
	NH_4^+	NO_2^-	NO_3^-	TN			AMX	DAMOb	DAMOa	$r_{Anammox\ NO_2^-}$	$r_{DAMOb\ NO_2^-}$	$r_{DAMOa\ NO_3^-}$
A1	44.5	17.7	1.5	64	16.1	25	14	16	2.8	2.0	2.3	-0.7
A2	82.9	28.2	0	111	36.2	33	15	17	1.6	3.5	6.6	0.7
Batch Reactors												
AD 1/4	153	95	5.2	253	79	31	26	7	4	5.8	2.2	0.6
AD 1/8	71	51	3.8	191	79	63	52	18	9	5.2	3.1	1.1
AD 1/20	27.5	23.3	0.6	51	33	64	41	21	12	1.9	1.8	0.3

5.3.2.1.3 COD and Phosphate in Phases A1 and A2

Since sCOD was present in the AD effluent, the influent and effluent concentrations of sCOD were tracked and are illustrated in Figure 5.16. It is evident that sCOD production occurred in the DAMMOX SBR. Moreover, sCOD accumulation from one cycle to the next and production within each cycle indicates that heterotrophic denitrification was not dominant in the reactor. The NGS analysis results in Section 5.3.3.2 would illustrate the species behind this increase in sCOD. Although the presence of sCOD may have diminished the Anammox activity by favoring microorganisms that perform heterotrophic denitrification, the decrease in Anammox activity in the DAMMOX SBR was also influenced by the influent NH_4^+/NO_2^- ratio, which was 2 instead of 0.76, which is the stoichiometric molar ratio of the Anammox reaction.

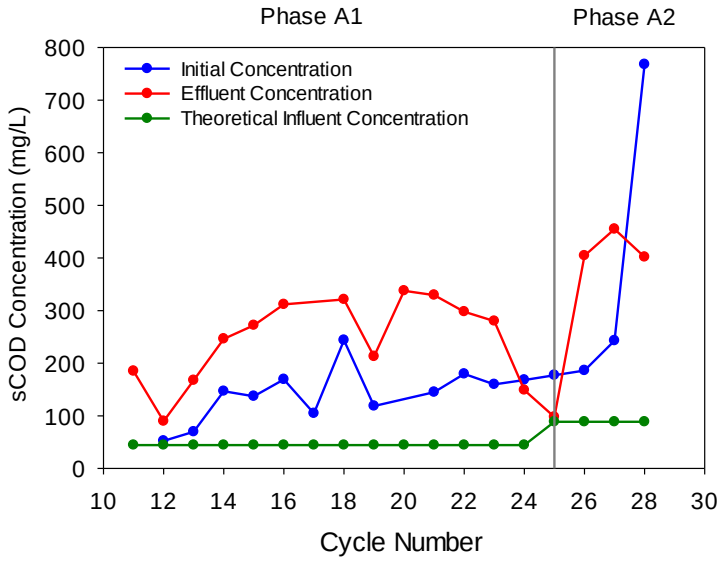

Figure 5.16 sCOD concentrations of the DAMMOX SBR during Phases A1 and A2

According to Chen et al. (2016c), COD concentrations below 100 mg/L could improve the nitrogen removal through coexistence of heterotrophic denitrification and Anammox. But at elevated concentrations of about 280 mg/L, could completely inhibit

the Anammox activity. Conversely, the anammox activity can be recovered by decreasing the COD/TN ratio from 2.33 to 1.25 (Chen et al., 2016c).

The initial sCOD concentrations ranged between 53-244 mg/L during Phase A1, averaging 141±51 mg/L. In Cycles 25-27 of Phase A2, the initial sCOD concentration ranged between 177-243 mg/L, with an average of 202±36 mg/L, yet, in Cycle 28 the initial sCOD was measured to be 768 mg/L. Correspondingly, the initial sCOD/TN ratio during Phase A1 ranged between 1.1-3.8, with an average of 2.2±0.8, whereas during Phase A2 (excluding Cycle 28) the initial sCOD/TN ranged between 1.6-2.2, with an average of 1.9±0.3. With the exception of Cycle 28, during Phases A1 and A2, the initial sCOD concentration remained below 280 mg/L. Moreover, since the initial sCOD/TN ratio was varying between 1.1 and 2.2 during Phases A1 and A2 (excluding Cycle 28), the Anammox activity was not expected to be completely inhibited, but was evidently lower than in Phase S. The sCOD indirectly affected the activity of the DAMO microorganism by favoring the heterotrophic denitrification.

Since the effluent of the DAMMOX SBR was planned to be supplied to a microalgae PBR, the initial and effluent concentrations of PO_4^{3-} were tracked to examine its fate before and after the microalgae PBR. The initial and effluent soluble ortho-phosphate (SOP) concentrations were measured and recorded as shown in Figure 5.17. The initial SOP concentration ranged from 2.8-5.7 mg P/L, averaging 4.2±0.8 mg P/L, while the effluent SOP concentration ranged from 4.7-9.6 mg P/L, with an average of 7.0±1.6 mg P/L. The concentration of PO_4^{3-} increased after each cycle of the DAMMOX SBR in Phases A1 and A2. The phenomenon of ortho-phosphate release could be attributed to either microbial decay or phosphate-solubilizing bacteria (PSB) or phosphate-accumulating organisms (PAO) which release PO_4^{3-} under anaerobic conditions. According to the NGS analysis, PSB species were not detected, but a species belonging to the genus *Candidatus Methylophosphatis* was detected. These species are methylotrophic capable of NO_2^- and NO_3^- reduction, as well as, exhibiting phosphate-accumulation characteristics (Singleton et al., 2021).

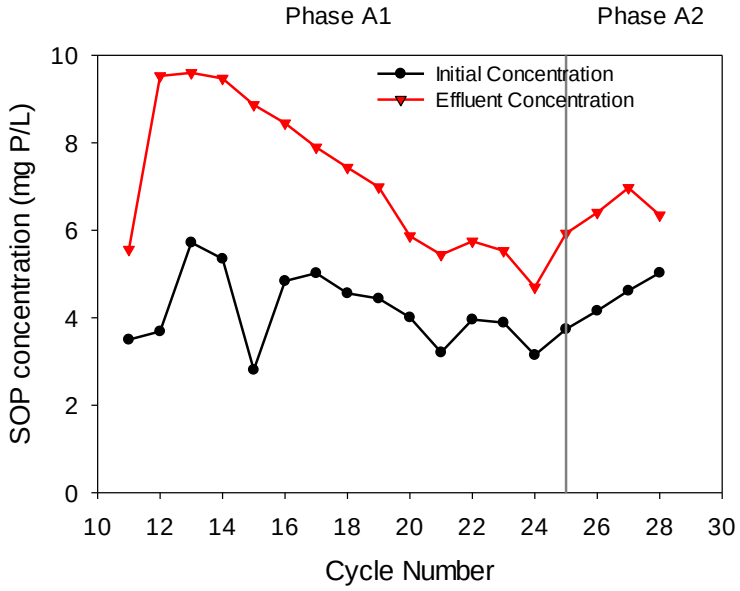

Figure 5.17 The initial and effluent SOP concentrations in the DAMMOX SBR after the application of the AD effluent (the S.D of each measurement was <5%)

Lim et al. (2021) established an MBfR operated at influent NH_4^+ and NO_2^- concentrations of 455 mg N/L and 590 mg N/L, respectively, and achieved removal rates of TAN (225 mg N/L·day) and NO_2^- (290 mg N/L·day). These rates were much higher than that of the DAMMOX SBR. This was due to the partial nitritation applied to the AD effluent that allowed a lower influent NH_4^+/NO_2^- ratio of about 0.77 in comparison to Phases A1 and A2 along with the removal of organic carbon. This in turn, did not negatively affect the Anammox activity. Moreover, this is evident in the fact that $r_{Anammox\ NO_2^-}$ was more than double the $r_{DAMOb\ NO_2^-}$ and $r_{DAMOa\ NO_3^-}$. The calculated average $r_{Anammox\ NO_2^-}$, $r_{DAMOb\ NO_2^-}$ and $r_{DAMOa\ NO_3^-}$ of the DAMO-Anammox MBfR were 270 mg N/L·day, 32 mg N/L·day and 52 mg N/L·day, respectively. These NO_2^- and NO_3^--based reaction rates calculated from Lim et al. (2021) were much higher than those of the DAMMOX SBR during Phases S, A1 and A2.

5.3.2.2 Determination of the Stoichiometric Ratio of the Consortium in DAMMOX SBR

Figure 5.18 shows the stoichiometric ratios under each case and the experimentally calculated ratios. During Phase S, the reactor was experiencing very little fluctuation and followed similar trends throughout the 10 cycles. The average $\Delta NO_2^-/\Delta NH_4^+$ stoichiometric molar ratio during Phase S was 2.2 (Figure 5.18a), where the microbial consortium was varying between the AMX & DAMOb and *DAMX theoretical cases. This was similar to Phase II of the DAMO-Anammox SBR (2.11). For the $\Delta NO_3^-/(\Delta NO_2^- + \Delta NH_4^+)$ stoichiometric molar ratio (Figure 5.18b), the reactor activity was stoichiometrically moving along the theoretical ratio of AMX & DAMOa in Phase S. The average $\Delta NO_3^-/ (\Delta NO_2^- + \Delta NH_4^+)$ ratio in Phase S was 0.7 which was much higher than that of the DAMO-Anammox SBR. This shows that the DAMOa activity in the DAMMOX SBR was much higher than that of the DAMO-Anammox SBR. As for the $\Delta NO_3^-/\Delta NO_2^-$ stoichiometric molar ratio (Figure 5.18c), the stoichiometric activity of the reactor was stable at an average ratio of about 1, between the theoretical ratios AMX & DAMOa and DAMX. The average $\Delta NO_3^-/\Delta NO_2^-$ stoichiometric molar ratio of Phase S of the DAMMOX SBR operation was much higher than that achieved in the DAMO-Anammox SBR, again illustrating the higher DAMOa activity in the DAMMOX SBR. In addition, for the $\Delta NO_3^-/\Delta NH_4^+$ stoichiometric molar ratio (Figure 5.18d), the stoichiometric ratio was stable at an average ratio of 2.2 in Phase S. The stoichiometric activity of the reactor was above the theoretical cases assumed.

Upon the application of the diluted AD effluent, the reactor stoichiometric activity started fluctuating immensely in all the stoichiometric ratios(Figure 5.18). This was due to the abrupt change in influent conditions, in terms of nitrogen species, COD and SO_4^{2-} concentrations. In this period of the activity of the microbial consortium was unstable, after a few cycles stability in the microbial consortium was observed. The average $\Delta NO_2^-/\Delta NH_4^+$ stoichiometric molar ratio in Phase A1 increased to 7.5. Towards the end of Phase A1 the $\Delta NO_2^-/\Delta NH_4^+$ stoichiometric molar ratio decreased and gradually the

reactor activity stoichiometrically went back to the fluctuate along the theoretical ratios of AMX & DAMOb and *DAMX. This indicates a decrease in the DAMOa activity and an increase in DAMOb activity. In Phase A2, the average $\Delta NO_2^-/\Delta NH_4^+$ stoichiometric molar ratio decreased to 3.6 which was similar to the trend shown between Cycles 16-24. All the other stoichiometric molar ratios fluctuated at the start of Phase A1 but by Cycle 17 they became 0 since there was no change in the NO_3^- concentration for the remainder of Phase A1 and Phase A2. For the $\Delta NO_3^-/(\Delta NO_2^- + \Delta NH_4^+)$ stoichiometric molar ratio, this was the theoretical ratio of *AMX & DAMOa or *DAMX. Moreover, for the $\Delta NO_3^-/\Delta NO_2^-$ the stoichiometric activity stabilized at the theoretical ratio of *AMX & DAMOa or *DAMX and the stoichiometric molar ratio of $\Delta NO_3^-/\Delta NH_4^+$ stabilized at the theoretical ratio of *AMX & DAMOa or *DAMX. This further indicated that the activity of DAMOa diminished in Phase A1 compared to Phase S.

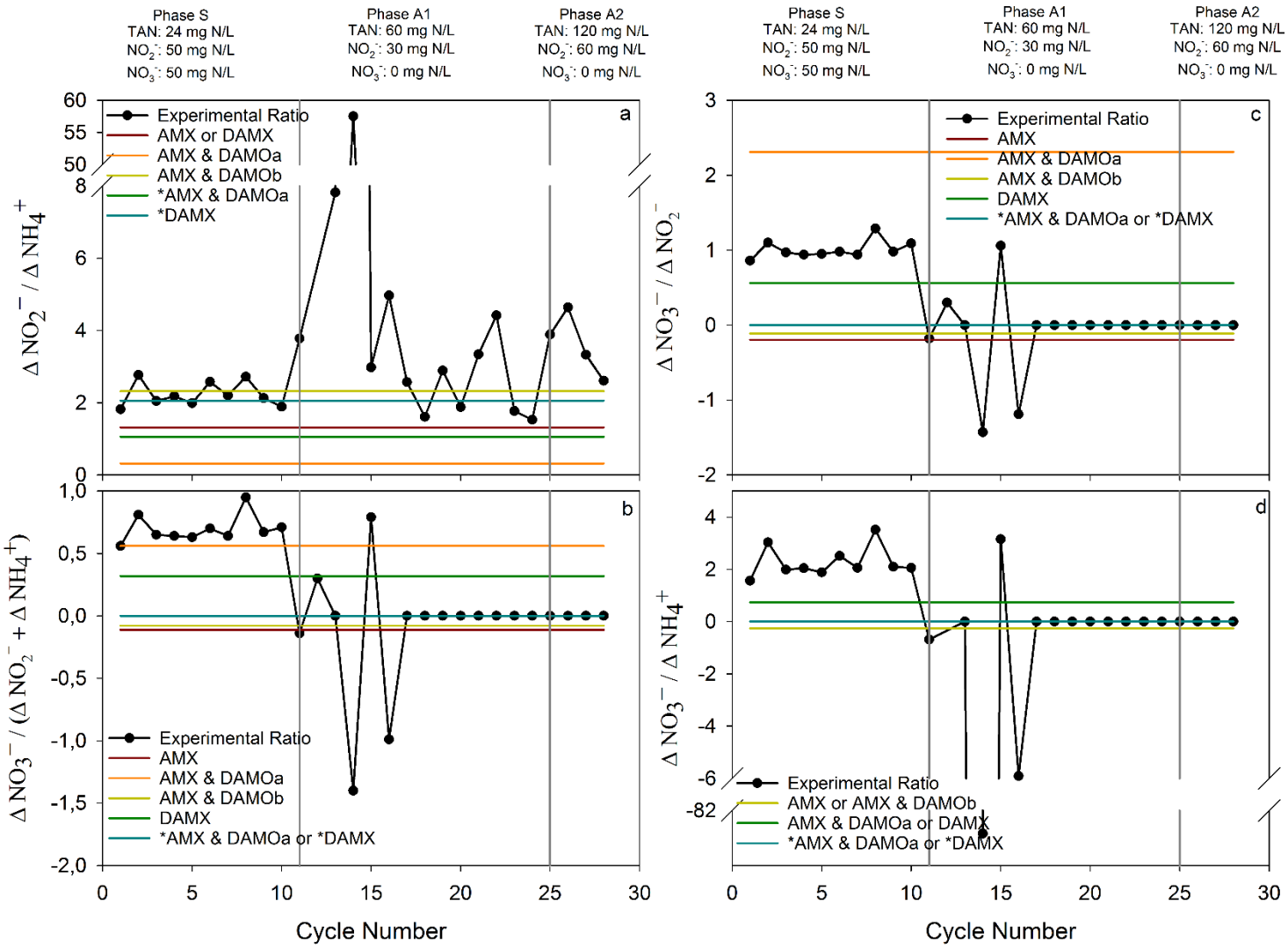

Figure 5.18 The ratios of (a) $\Delta NO_2^-/\Delta NH_4^+$, (b) $\Delta NO_3^-/(\Delta NO_2^- + \Delta NH_4^+)$, (c) $\Delta NO_3^-/\Delta NO_2^-$ and (d) $\Delta NO_3^-/\Delta NH_4^+$ in the effluent of the DAMMOX SBR compared to the theoretical ratio of each case

5.3.2.3 Molecular Analyses Results

5.3.2.3.1 FISH Results

Sludge was sampled at cycles 0, 24 and 28 for FISH analysis, to observe the changes in the microbial composition in the reactor with respect to influent changes. The images are shown in Figure 5.19. The target cells were identified with the corresponding probes given in Table 5.11 that can visually distinguish *M. oxyfera*, *M. nitroreducens* and Anammox bacteria. General bacteria, general archaea and DAPI probes were used to quantify the relative abundance of the target species in the DAMMOX SBR. It is noticeable in Figure 5.19 that Anammox bacteria and DAMOa are relatively in closer proximity to one another compared to DAMOb probably due to the fact that DAMOa consumes the NO_3^- produced by the Anammox bacteria.

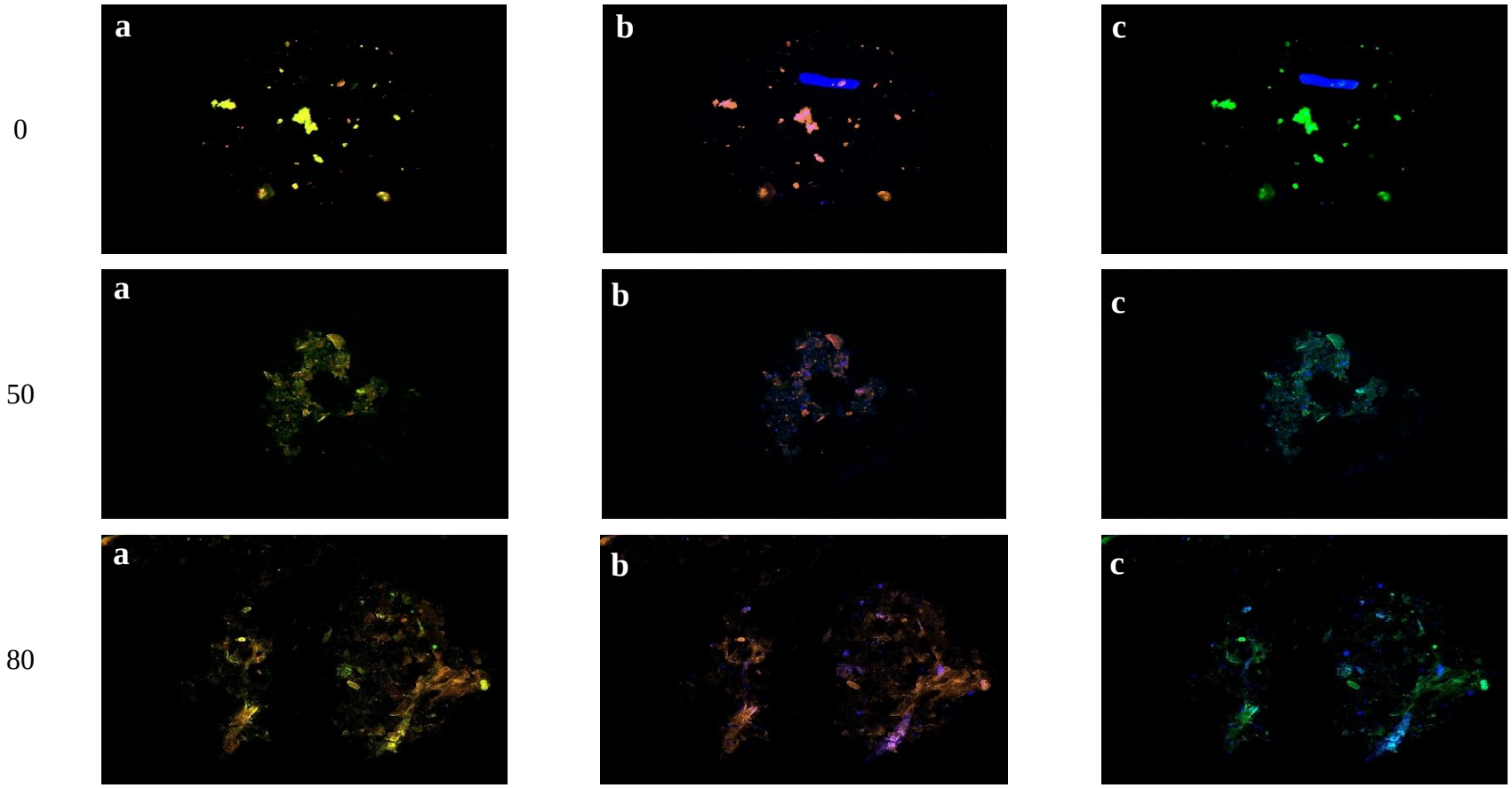

Figure 5.19 FISH images of DAMMOX SBR sludge samples withdrawn at Cycles 0, 24 and 28 (a) Orange: AMX-368 - general Anammox and green: DARCH-872 - *M. nitroreducens* (b) Orange: AMX-368 - general Anammox and blue: DBACT-193 - *M. oxyfera* (c) Blue: DBACT-193 - *M. oxyfera* and green: DARCH-872 - *M. nitroreducens*

Figure 5.20 illustrates the relative change in abundance of the target microorganisms in the DAMMOX SBR. At the beginning of Phase S, which corresponds to the initial mixed sludge of the DAMMOX SBR, the relative abundance of Anammox, *M. oxyfera* and *M. nitroreducens* were 57±5 %, 20±3 % and 23±2 %, respectively (Figure 5.20). By the end of Phase A1, the relative abundance of Anammox and *M. oxyfera* decreased to 43±3 % and 18±2 %, respectively, while that of *M. nitroreducens* increased to 39±1 %. The increase in abundance of *M. nitroreducens* might be due to the increased activity of S-DAMO which might have aided the activity of *M. nitroreducens*. By the end of Phase A2 the relative abundance of Anammox, *M. oxyfera* and *M. nitroreducens* were relatively the same as the end of Phase A1 at 44±1 %, 15±2 % and 40±1 %, respectively.

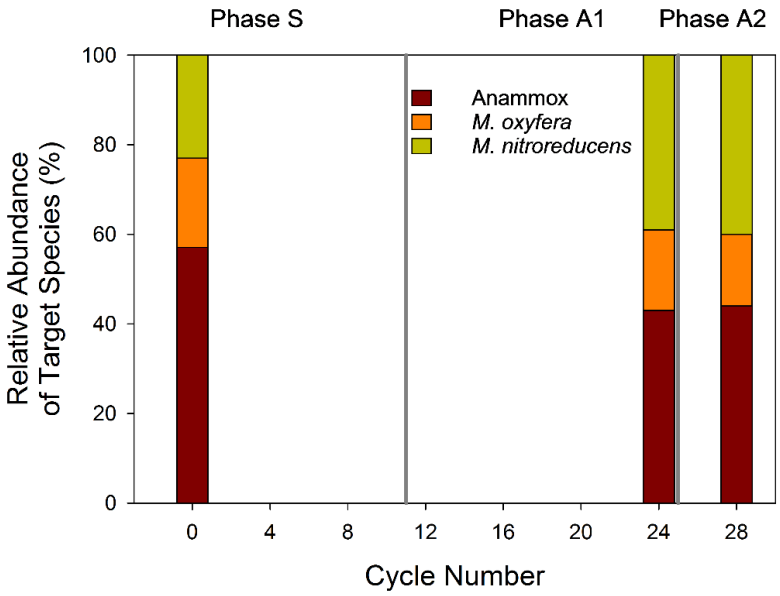

Figure 5.20 The relative abundance of target species in the DAMMOX SBR

5.3.2.3.2 NGS 16S Metagenome Analysis Results

The results involving the target microorganisms and their relative target phyla were analyzed at the genus level, while the general results of the samples analyzed were discussed at the order level with respect to the main metabolic activities detected in

the DAMMOX SBR. These activities include methanotrophic, methylotrophic, denitrification, and non-methanotrophic anaerobic chemoorganotrophic.

The results of the NGS analysis displayed that the target phyla, *Planctomycetota*, NC10 and *Euryarchaeota*, were present in the microbial consortium. Figure 5.21 illustrates the actual percentages of the target phyla at Cycle 0 and Cycle 24 of the DAMMOX SBR. In the initial cycle the microbial consortium consisted of 7% *Planctomycetota*, 0.2% NC10 and 0.3% *Euryarchaeota*. At the end of Phase A1 (Cycle 24), the content of *Planctomycetota*, NC10, and *Euryarchaeota* in the microbial consortium remained the same.

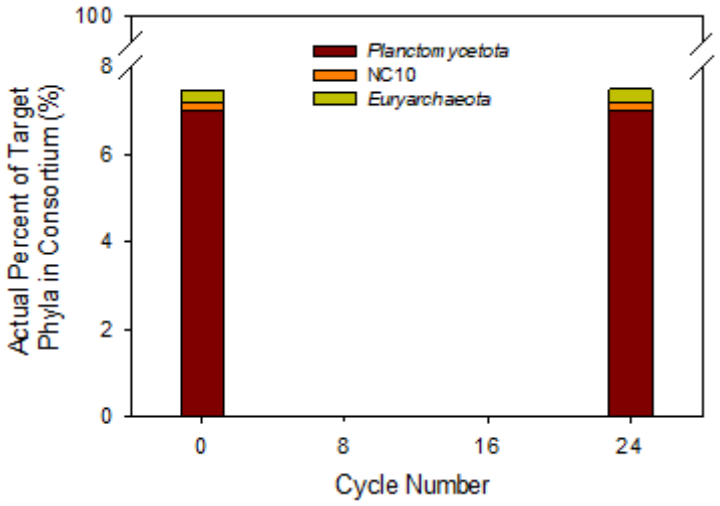

Figure 5.21 The actual percentage of the target phyla in the DAMMOX SBR

The NGS analysis results illustrated the existence of species from the classes *Candidatus Brocadiae*, *Phycisphaerae* and *Planctomycetia*, in the phylum *Planctomycetota*. The percentage of *Candidatus Brocadiae* increased from 9% at the initial cycle to 18% at the end of Phase A1, while *Phycisphaerae* decreased from 76% to 59% (Figure 5.22). On the other hand, *Planctomycetia* increased from 15% to 22%.

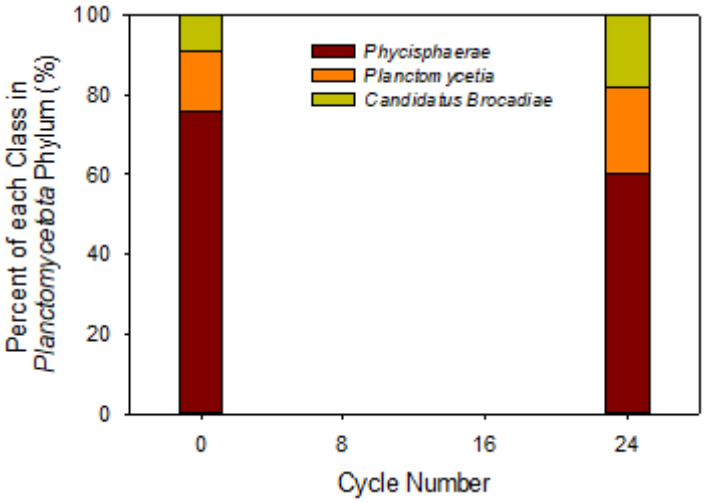

Figure 5.22 The percentage of each class in the phylum *Planctomycetota* from the DAMMOX SBR

Within the *Euryarchaeota* phylum, there are various classes that consist of methanotrophic, methylotrophic and methanogenic archaea. *Methanomicrobia*, *Methanobacteria*, *Candidatus Methanofastidiosia* and *Thermoplasmata* are classes within the phylum *Euryarchaeota* that contain methanotrophic and methylotrophic archaea that were detected in the DAMMOX SBR. The class *Methanomicrobia* includes *Methanoperedens nitroreducens* along with other methanotrophic archaea (Evans et al., 2019).

At the initial cycle, *Euryarchaeota* was distributed as 78% *Methanobacteria*, 15% *Methanomicrobia*, and 7% *Thermoplasmata*, as shown in Figure 5.23. By the end of Phase A1, the composition of *Euryarchaeota* was distributed as 86% *Methanobacteria*, 8% *Methanomicrobia* and 6% *Thermoplasmata*.

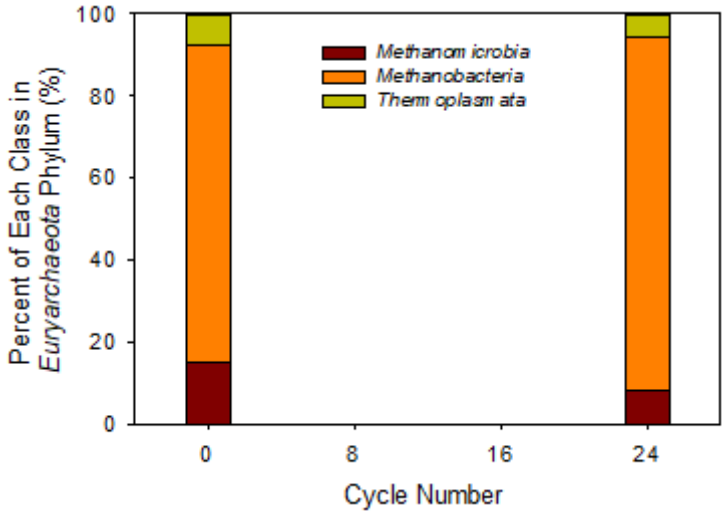

Figure 5.23 The percentage of each class in the phylum *Euryarchaeota* from the DAMMOX SBR

The general NGS analyses results of the consortium is presented at the phylum level in Figure 5.24 and Figure 5.25. Although the abundance of the target microorganisms decreased after the application of the AD effluent, the results illustrate an Anammox dominance over the DAMOa and DAMOb during the operation of the DAMMOX SBR. The NGS analysis illustrates that DAMO along with other denitrifying methanotrophs and methylotrophs belonging to the phyla *Proteobacteria*, *Verrucomicrobiota* and archaeal classes *Methanobacteria*, and *Thermoplasmata* decreased in the DAMMOX SBR with the application of the AD effluent in comparison to the DAMO-Anammox SBR. The presence of COD and SO_4^{2-} in the DAMMOX SBR promoted the growth of various distinct microorganisms in comparison to the DAMO-Anammox SBR.

Proteobacteria was the dominant phylum in the initial mixed sludge (Cycle 0) at 21%, followed by the superphylum *Candidatus Patescibacteria* (19%) and the phylum *Chloroflexota* (12%) (Figure 5.24). *Planctomycetota* was the fourth most dominant phylum at 7% of the microbial consortium. At Cycle 24 representing Phase A1, *Proteobacteria* was the dominant phylum, at 19%, followed by *Bacteroidota* (18%) and *Chloroflexota* (14%) (Figure 5.25), while *Planctomycetota* was the fourth

most phylum reaching 8% of the microbial consortium. An increase in *Planctomycetota* content of the microbial consortium is visible from the NGS results.

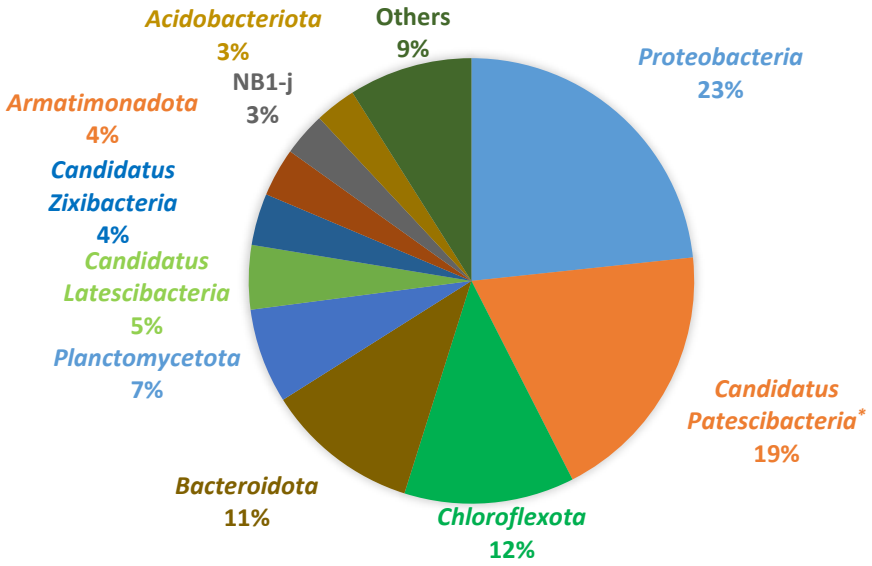

Figure 5.24 Phylum level composition of the DAMMOX SBR sludge at Cycle 0

**Candidatus Patescibacteria* is a superphylum

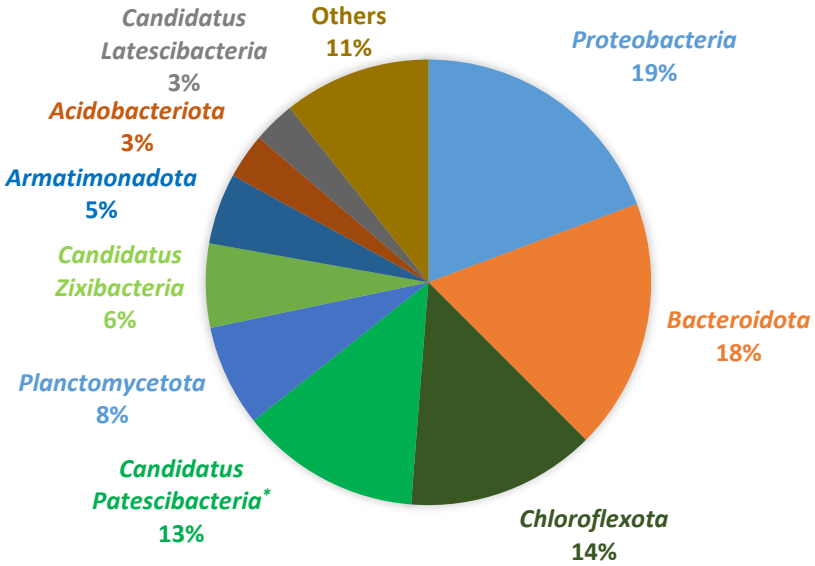

Figure 5.25 Phylum level composition of the DAMMOX SBR sludge at Cycle 24

**Candidatus Patescibacteria* is a superphylum

In the context of the study, the general results of the NGS analysis were interpreted and described within six main metabolic groups that were the highest in abundance. The six main metabolic groups are methanotrophic and methylotrophic, non-methanotrophic anaerobic chemoorganotrophic, fermenters, denitrifiers, sulfur-oxidizing bacteria (SOB) and sulfate-reducing bacteria (SRB) and phosphate-accumulating organisms.

Apart from the methanotrophic and methylotrophic species belonging to the phyla NC10 and *Euryarchaeota*, species belonging to the phyla *Proteobacteria* were detected in the DAMOMOX SBR. *Proteobacteria* also known as *Pseudomonadota* was one of the most dominant phyla detected in the DAMMOX SBR. This phylum is one of the largest phyla and is a diverse phylogenetic division that constitutes of Gram-negative bacteria. Some of the numerous methanotrophic and methylotrophic species in the phylum *Proteobacteria* belong to the orders *Hyphomicrobiales*, *Rhodobacterales*, *Nitrosomonadales*, *Burkholderiales* and *Methylococcales*. These species act as denitrifying methylotrophs in the absence of oxygen (Chistoserdova et al., 2010). *Hyphomicrobiales* and *Rhodobacterales* belong to the class *Alphaproteobacteria*, while *Burkholderiales* and *Nitrosomonadales* belong to the class *Betaproteobacteria* and *Methylococcales* belongs to the class *Gammaproteobacteria*.

The only microorganisms detected in the DAMMOX SBR that exhibit phosphate-accumulating characteristics were species belonging to the genus *Candidatus Methylophosphatis* and *Burkholderiales* order. These species are methylotrophic capable of NO_2^- and NO_3^- reduction, as well as, exhibiting phosphate-accumulation characteristics (Singleton et al., 2021). The activity of such microorganisms might be the cause of the rise in PO_4^{3-} concentration in each cycle.

Non-methanotrophic anaerobic chemoorganotrophic bacteria were detected in the initial mixed sludge sample and those microorganisms increased in their abundance after the application of AD effluent. This group includes species from the phyla *Proteobacteria*, *Bacteroidota*, *Chloroflexota* and *Acidobacteriota*. The reason

behind the proliferation of this group of microorganisms is the presence of COD in the AD effluent and the production of COD in the form of acetate and succinate by some of the microorganisms.

The anaerobic chemoorganotrophic species belonging to the phylum *Proteobacteria* belonged to the orders *Burkholderiales, Nitrosomonadales, Rhodocyclales, Pseudomonadales, Myxococcales* and *Syntrophobacterales*. *Burkholderiales, Nitrosomonadales* and *Rhodocyclales* belong to the class *Betaproteobacteria,* while *Pseudomonadales* belong to the class *Gammaproteobacteria*. On the other hand, *Myxococcales* and *Syntrophobacterales* belong to the class *Deltaproteobacteria*.

In addition, the phylum *Chloroflexota* consists of microorganisms that perform anaerobic chemoorganotrophic activities was detected in the DAMMOX SBR. The main classes detected in this phylum were *Anaerolineae, Chloroflexia,* and *Dehalococcoidia*. Microorganisms from the class *Anaerolineae* are anaerobic chemoorganotrophs but *Chloroflexia* can perform nitrite oxidation. Species from the classes *Acidobacteriia, Holophagae,* and *Thermoanaerobaculia* from the *Acidobacteriota* phylum were found in the DAMMOX SBR, which are mainly anaerobic chemoorganotrophic heterotrophs (Boone et al., 2005).

The presence of COD in the DAMMOX SBR led to the rise in abundance of some denitrifiers and ammonium oxidizers. Species from the genera *Denitratisoma* and *Nitrosomonas* belonging to the order *Nitrosomonadales* were detected. *Denitratisoma* can perform denitrification by reducing NO_2^- or NO_3^- utilizing organic carbon (Fahrbach et al., 2006). While *Nitrosomonas* which are capable of ammonia oxidation under aerobic conditions, however, under anoxic conditions they are capable of denitrifying with ammonia as an electron donor or using hydrogen or organic compounds or using N_2O_4 as an oxidant for ammonia oxidation under both oxic and anoxic conditions (Schmidt et al., 2002). Moreover, denitrifying species from the genus *Thauera* belonging to the order Rhodocyclales were detected in the DAMMOX SBR after the application of the AD effluent (Mechichi et al., 2002). On the other hand, microorganisms belonging to the order *Hydrogenophilales* which are

chemoautotrophic capable of performing denitrification by respiring NO_3^- and oxidizing H_2 were also detected (Ontiveros-Valencia et al., 2013).

The presence of various by-products of anaerobic digestion in the AD effluent, the release of chitin-like polysaccharides, such as poly-N-acetylglucosamine (PGA), by Anammox and other biofilm forming microorganisms, created a suitable environment for the rise of species belonging to the superphylum *Candidatus Patescibacteria*, and the phyla *Candidatus Latescibacteria*, *Candidatus Zixibacteria* and *Bacteroidota*. Since these species were either not detected or detected in very low abundance in the DAMO-Anammox SBR, they presumably came from the DAMO and DAA SBRs.

Chitinophagales is an order under the phylum *Bacteroidota*, they are mostly anaerobic and saccharolytic microorganisms that perform fermentation to produce mainly succinate and acetate (Boone et al., 2005) and as their name suggests can convert chitin-like polysaccharides to N-acetylglucosamine (Fuji et al., 2022). Microorganisms from the superphylum *Candidatus Patescibacteria*, also known as candidate phyla radiation (CPR). These microorganisms belonged to various phyla such as *Candidatus Microgenomates*, *Candidatus Gracilibacteria*, *Candidatus Parcubacteria*, *Candidatus Pacebacteria*, ABY1, *Candidatus Komeilibacteria* and *Candidatus Saccharibacteria*.

The species from the phylum *Candidatus Parcubacteria* are capable of producing H_2, SO_4^{2-} reduction and NO_2^- reduction, however, the majority of the microorganisms belonging to the other phyla are obligate fermenters that use heterolactic fermentation pathways, such as glycolysis and the pentose phosphate pathway but lack the tricarboxylic acid cycle and release fermentation by-products such as acetate, lactate, and formate utilizing chitin-like polysaccharides (Danczak et al., 2017; Chaudhari et al., 2021; Hosokawa et al., 2021; Fujii et al., 2022). In addition, the high abundance of peptidases in *Candidatus Gracilibacteria* implies that they have a role in cell lysis (Fujii et al., 2022). Whereas species from the phylum *Candidatus Latescibacteria* are anaerobic fermentative bacteria that degrade

multiple polysaccharides and glycoproteins (Youssef et al., 2015). In addition, the NGS analysis showed the presence of species from the phylum *Candidatus Zixibacteria* that mainly perform fermentation (Castelle et al., 2013).

Hosokawa et al. (2021) found that microorganisms belonging to the superphylum *Candidatus Patescibacteria* can utilize chitin-like polysaccharides and produce fermentation by-products of lactate and formate in anammox reactors. The coexistence of species from the superphylum *Candidatus Patescibacteria* along with other heterotrophic bacteria that utilize chitin-like polysaccharides produced by Anammox may a stable environment with reduced by-products (Hosokawa et al., 2021). Fujii et al. (2022) identified metabolic interactions between *Candidatus Saccharibacteria* and *Chitinophagales* through N-acetylglucosamine, between *Candidatus Gracilibacteria* and *Chitinophagales* through phospholipids, and between *Candidatus Parcubacteria* and *Chitinophagales* through nitrogen compounds involved in denitrification.

The increase in sCOD concentrations shown in Figure 5.16 can be explained by the release of organic compounds, such as lactate, formate, and acetate, as by-product of reactions performed by species mainly from the superphylum *Candidatus Patescibacteria* and the phyla *Candidatus Latescibacteria* and *Candidatus Zixibacteria*. Furthermore, species from the genus *Romboustia*, belonging to the phylum *Bacillota*, were detected in the DAMMOX SBR. These species are also capable of producing acetate, formate, and lactate as metabolic products (Gerritsen et al., 2014).

The presence of high sulfate concentrations in the AD effluent in comparison to the SWW allowed for the increase of abundance of SRB species, in turn allowing the rise of SOB species. The species belonging to the order *Desulfobacterales*, *Syntrophobacterales* and *Desulfuromonadales* were detected in much more abundance in the DAMMOX SBR than in the DAMO-Anammox SBR. Sulfide production from sulfate reduction may have caused Anammox activity reduction (Ontiveros-Valencia et al., 2013). Concurrently, species from the genera

Thiobacillus and *Sulfuritalea* belonging to the order *Nitrosomonadales* and the genus *Sulfurifustis* belonging to the order *Acidiferrobacterales* that are capable of performing thiosulfate or elemental sulfur oxidation to sulfate were also detected in the DAMMOX SBR after the application of the AD effluent (Smith et al., 1980; Kojima and Fukui, 2011; Kojima et al., 2015). Moreover, microorganisms belonging to the phylum *Armatimonadota* were detected in the reactor, such species utilize various carbohydrates as a carbon and energy source (Cheng et al., 2017). In addition, species belonging to the phylum *Candidatus Kapaibacteria,* which are capable of performing sulfur assimilation and chemolithoheterotrophic metabolism were also found in the DAMMOX SBR. However, carbon fixation pathways are absent in those species (Al-Saud et al., 2020).

After the application of partially nitrified AD effluent, Lim et al. (2021) achieved a microbial consortium in the DAMO-Anammox MBfR that contained *Methanoperedenaceae*, *Brocadiaceae*, *Methylomirabilaceae* and *Phycisphaeraceae* of about 20%, 12%, 5% and 8%, respectively. Although the influent NH_4^+/NO_2^- ratio was about 0.8, the high NO_2^- removal by Anammox bacteria did not allow DAMOb proliferation. The partial nitritation step applied to the AD effluent prior to the DAMO-Anammox reactor, allowed for a higher influent NH_4^+/NO_2^- ratio and a negligible organic carbon concentration than that applied to the DAMMOX SBR. This allowed the DAMOa to become dominant in the reactor with the help of Anammox that provided NO_3^- and outcompeted the DAMOb. Nevertheless, various similar microorganisms were detected in the MBfR in comparison to the DAMMOX SBR, such as *Thiobacillus*, *Hydrogenophilales*, *Denitratisoma, Candidatus Patescibacteria* and *Anaerolineaceae*.

5.3.3 Results of *C. vulgaris* PBR Study

Although both the MSC and TM PBRs were operated next to each other, as shown in Figure 5.2, the recorded temperatures of each reactor were slightly different. The temperature of MSC PBR was in the range of 19.1-20.7°C, while that of the TM PBR was in the range of 19.7-24°C (Figure 5.26). The temperatures recorded for both reactors were within the range described in the literature for the best photosynthesis and cell division performance (Falkowski and Owens, 1980; Deniz, 2020).

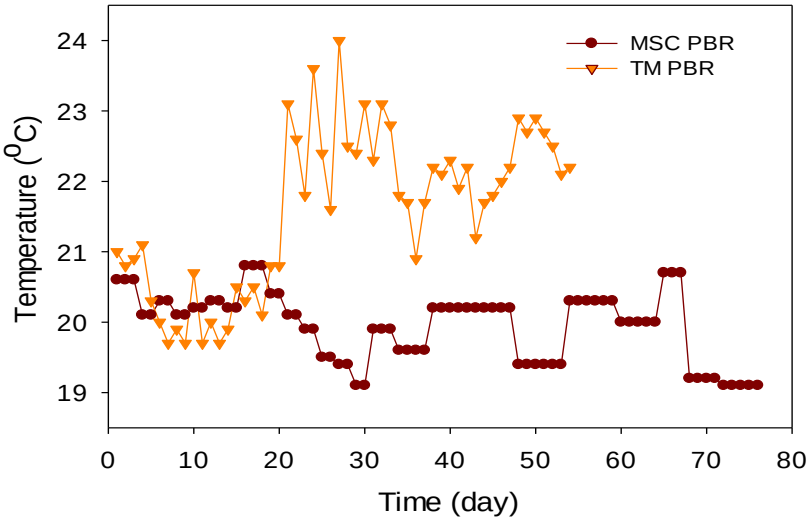

Figure 5.26 The temperature of the MSC PBR and TM PBR

The influent pH of the SWW provided to the MSC PBR was between 9.28-9.79, while the effluent pH was found to be in the range 10.23-10.81 (Figure 5.27). Conversely, the influent pH of the TM PBR, which is the effluent of the DAMMOX SBR, was in the range of 7.0-7.63, while the effluent pH of the TM PBR was between 9.09-10.05 (Figure 5.28). Both reactors were operated in a pH range of 6.5-10.0 that is suitable for *C. vulgaris* growth, according to the literature (Deniz, 2020).

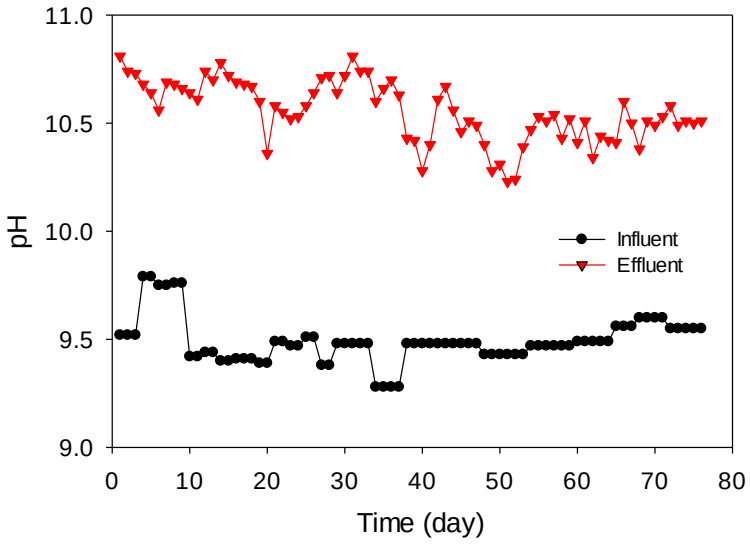

Figure 5.27 The influent and effluent pH of the MSC PBR

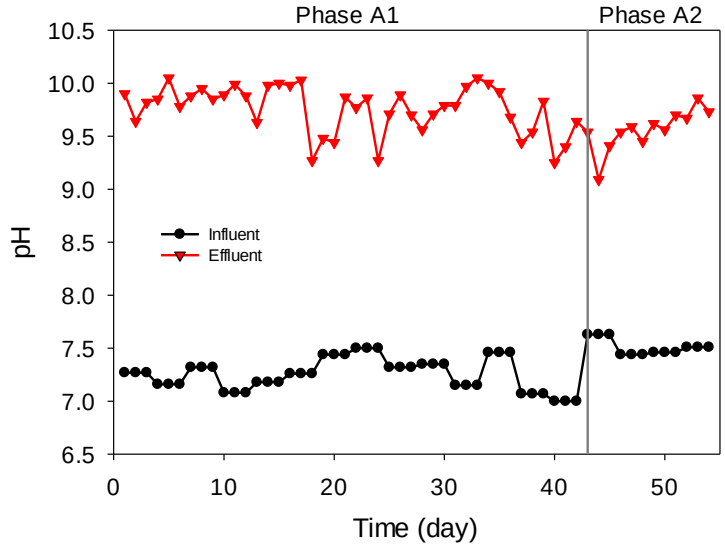

Figure 5.28 The influent and effluent pH of the TM PBR

The OD of the MSC PBR increased from 1.44 to a maximum of 1.55 by Day 31 and then decreased to a minimum of 0.62 by Day 64, as illustrated in Figure 5.29. The OD then increased to 0.92 by Day 76. Similarly, the DCW of the MSC PBR increased from 640 mg/L to a maximum of 790 mg/L by Day 32 and then the DCW decreased to reach a minimum of 280 mg/L by Day 56 (Figure 5.29). The DCW then increased to 460 mg/L by Day 74.

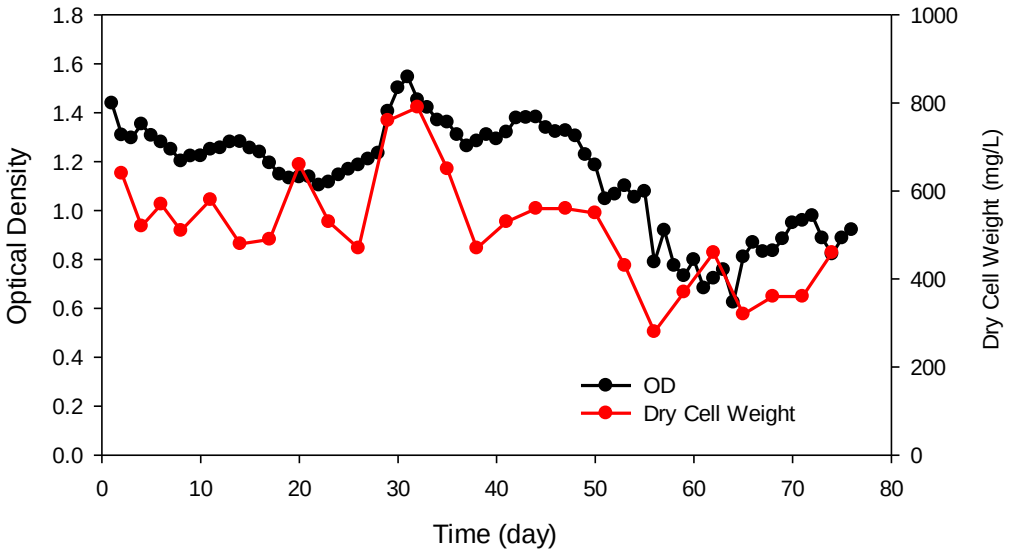

Figure 5.29 The OD and DCW of the MSC PBR

On the other hand, the OD and DCW of the TM PBR at Day 0 was 1.15 and 600 mg/L, respectively. By Day 33, the OD increased to 2.83 and then decreased to 1.95 by Day 47. From Day 47 to Day 54 the OD increased once again to reach a maximum of 2.89. The DCW followed a similar trend, increasing to a maximum of 2070 mg/L at Day 33 and then decreasing to 1350 mg/L by Day 54. The much higher OD and DCW values achieved in the TM PBR indicates that the *C. vulgaris* cell growth and reproduction was higher than in the MSC PBR, implying that AD effluent constituents may sustain higher *C. vulgaris* growth than SWW. Figure 5.31 illustrates the darkening of the *C. vulgaris* culture from Day 35 to Day 50, signifying growth and reproduction of the *C. vulgaris* cells.

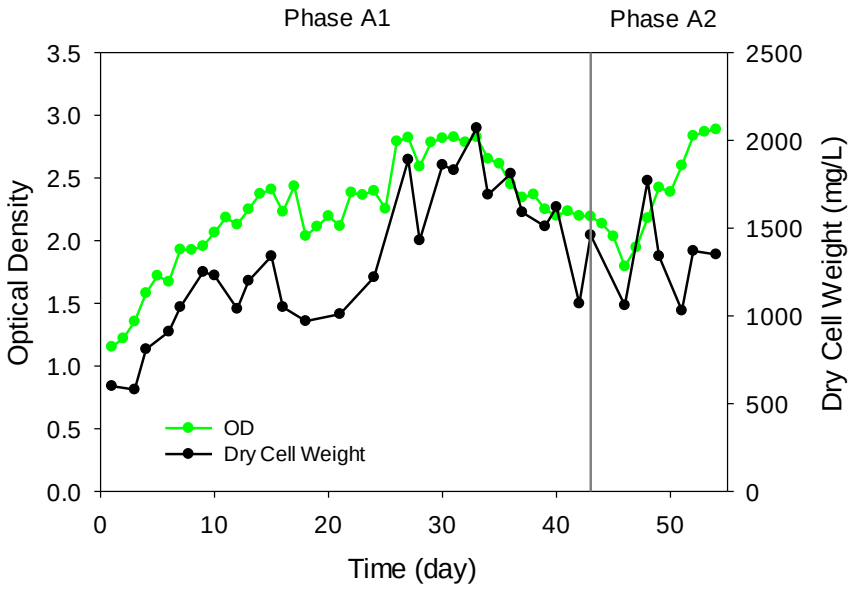

Figure 5.30 The OD and DCW of the TM PBR

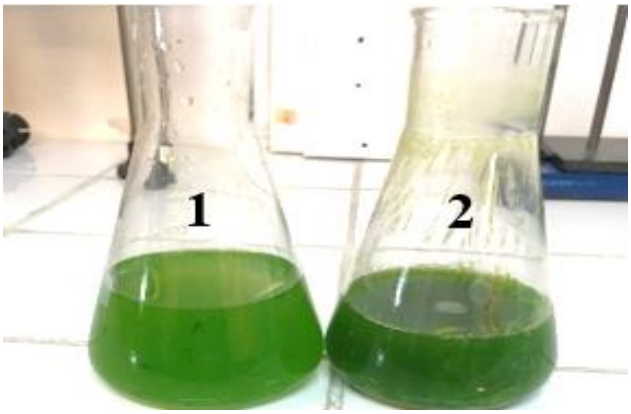

Figure 5.31 TM PBR change in color. (The photo of erlenmeyer 1 was taken at Day 35 and erlenmeyer 2 at Day 50)

The average experimental influent TAN and PO_4^{3-} concentrations of the MSC PBR were 30.6±2.0 mg N/L (Figure 5.32a) and 4.0±0.3 mg P/L (Figure 5.32b), respectively. Corresponding to an average experimental influent TN/P ratio of 7.8±0.6 g N/ g P (Figure 5.33). The effluent TAN and PO_4^{3-} concentrations were about 0 mg N/L and 0 mg P/L throughout the operation of the MSC PBR. Consequently, the TAN and PO_4^{3-} removal efficiencies achieved in the MSC SBR were about 100% (Figure 5.32c). Due to the near total removal of TAN and PO_4^{3-} in the MSC PBR, the $\Delta TN/\Delta P$ ratio was 7.8±0.6 g N/ g P, similar to the influent TN/P ratio.

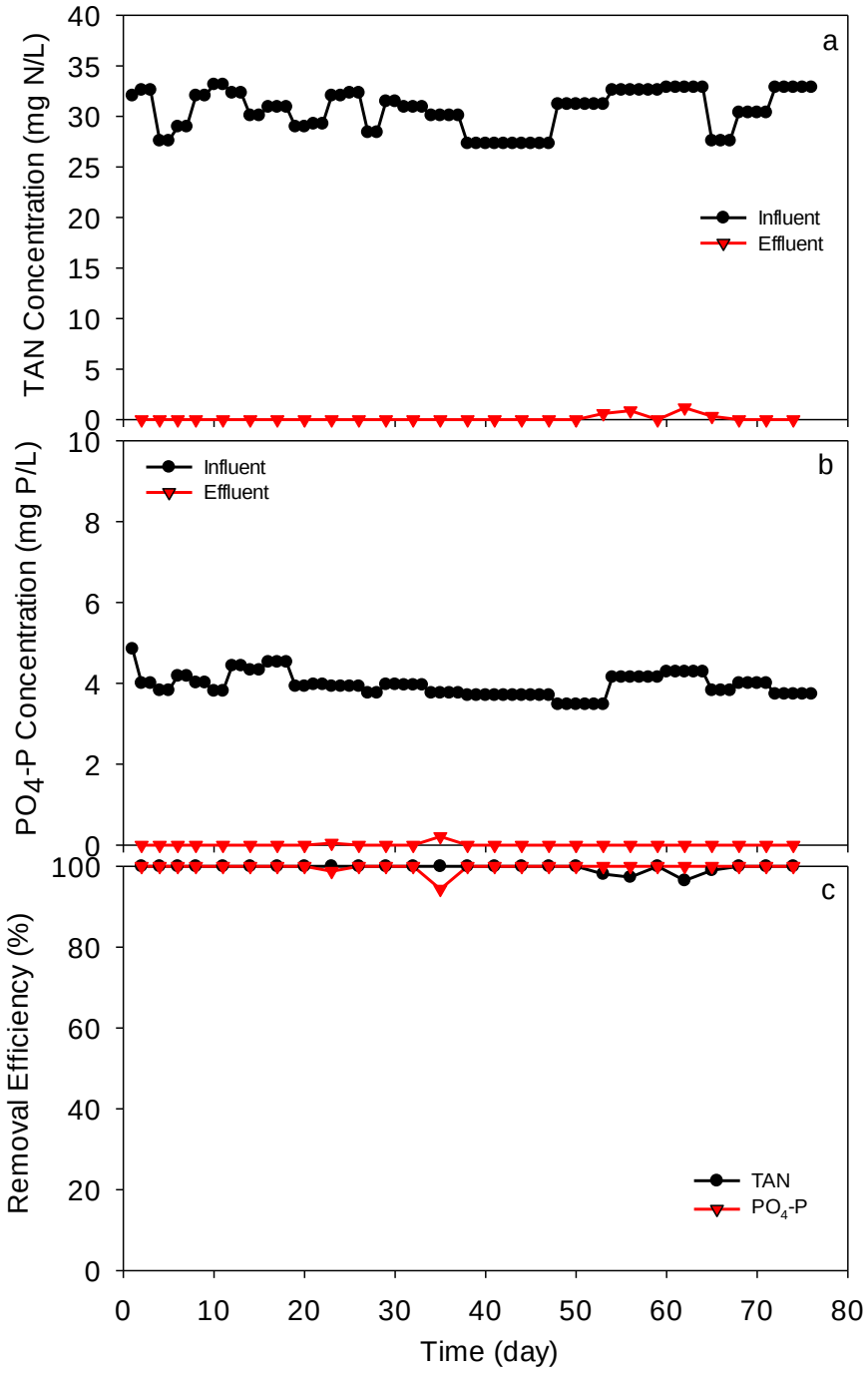

Figure 5.32 Influent and effluent concentrations of (a) TAN and (b) PO_4^{3-}-P and (c) the TAN and PO_4^{3-}-P removal efficiencies, during each cycle of the MSC PBR (the S.D of each measurement was <5%)

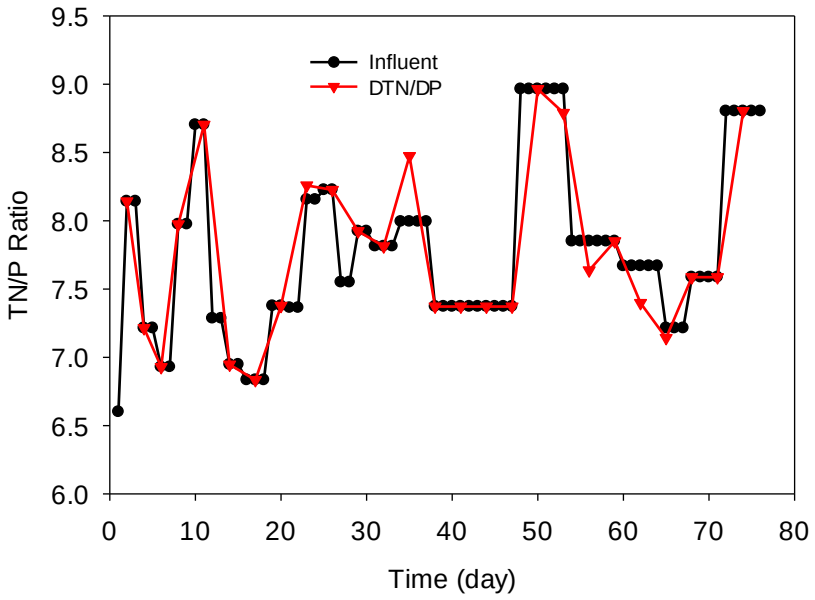

Figure 5.33 The influent and ΔTN/ΔP ratio during the operation of the MSC PBR

The influent TAN, NO_2^-, NO_3^- and PO_4^{3-} concentrations were measured after filtration of the DAMMOX SBR effluent. Each DAMMOX SBR cycle effluent was the influent to 3 cycles of the TM PBR. The average influent TAN concentration in Phase A1 was 40.0±6.3 mg N/L (Figure 5.34a). Meanwhile the influent NO_2^- concentration fluctuated between about 5 and 0 mg N/L, during the same period, averaging 2.9±2.6 mg N/L (Figure 5.34b). TAN and NO_2^- were nearly fully consumed by the *C. vulgaris* and were not detected in the effluent of the TM PBR during Phase A1. On the other hand, the average TAN influent concentration for Phase A2 was 74.9±7.9 mg N/L, due to the lower removal efficiency of the DAMMOX SBR with less diluted AD effluent (AD 1/5). The influent NO_2^- concentration for the same period was 0 mg N/L due to the removal in the DAMMOX SBR. TAN was nearly fully consumed by the *C. vulgaris* and was not detected in the effluent of the TM PBR in Phase A2.

The influent NO_3^- concentration for nearly all the operation period of the TM PBR was 0 mg N/L (Figure 5.34c). In the first 3 days, the concentration was about 6 mg N/L, then decreased to 0 mg N/L from Day 4-9. From Day 10-12 and Day 16-18, due to the production of NO_3^- in the DAMMOX SBR, the NO_3^- influent

concentration was 35 and 24 mg N/L, respectively. For the remaining days of operation of the TM PBR, the influent NO_3^- concentration was 0 mg N/L. Moreover, NO_3^- was not detected in nearly all the effluent samples throughout the operation of the TM PBR.

The influent PO_4^{3-} concentration varied between 4.7-9.6 mg P/L during Phases A1 and A2, averaging 7.2±1.8 mg P/L in Phase A1 and 6.4±0.4 mg P/L in Phase A2 (Figure 5.34d). The *C. vulgaris* was able to consume all the PO_4^{3-} present throughout the operation of the TM PBR. The TAN, NO_2^-, NO_3^- and PO_4^{3-} removal efficiencies achieved in the TM SBR were about 100% as illustrated in Figure 5.35. *C. vulgaris* was capable of achieving near total nitrogen and phosphorus and removal.

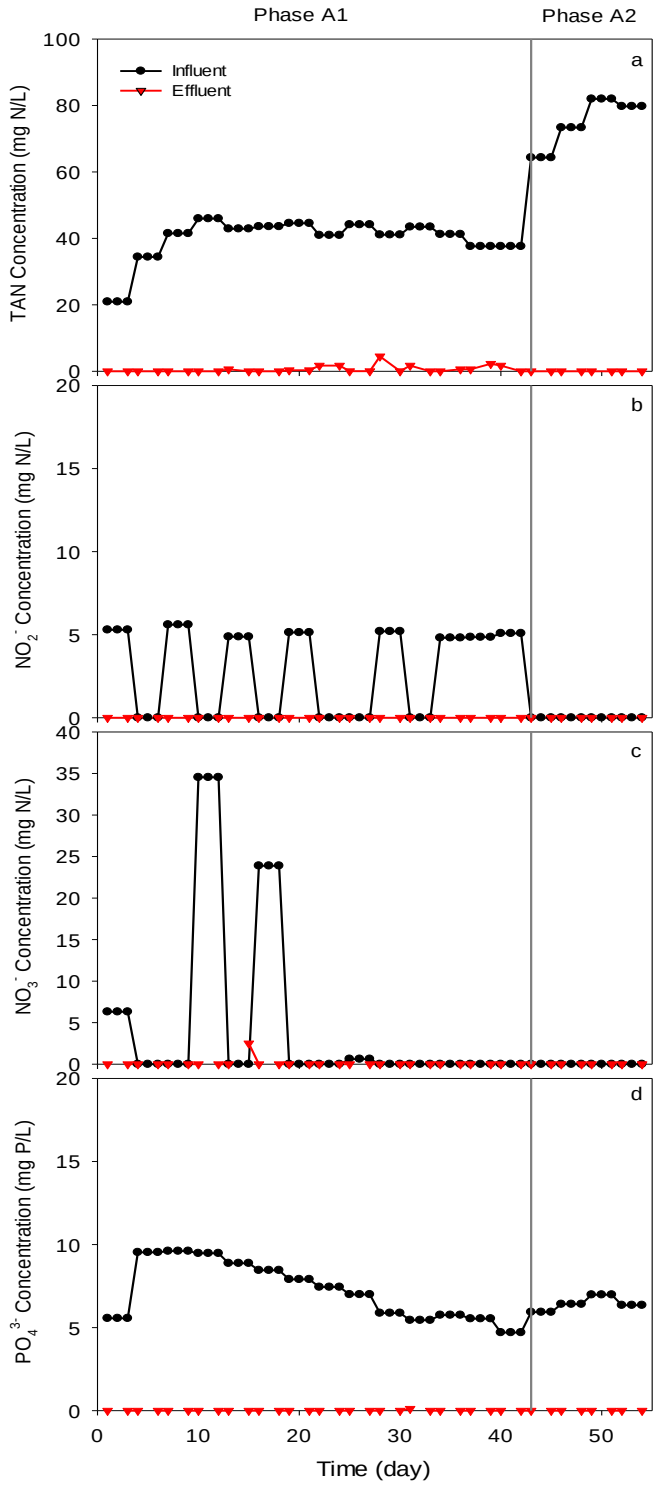

Figure 5.34 Influent and effluent concentrations of (a) TAN, (b) NO_2^--N, (c) NO_3^--N and (d) PO_4^{3-}-P, during each cycle of the TM PBR (the S.D of each measurement was <5%)

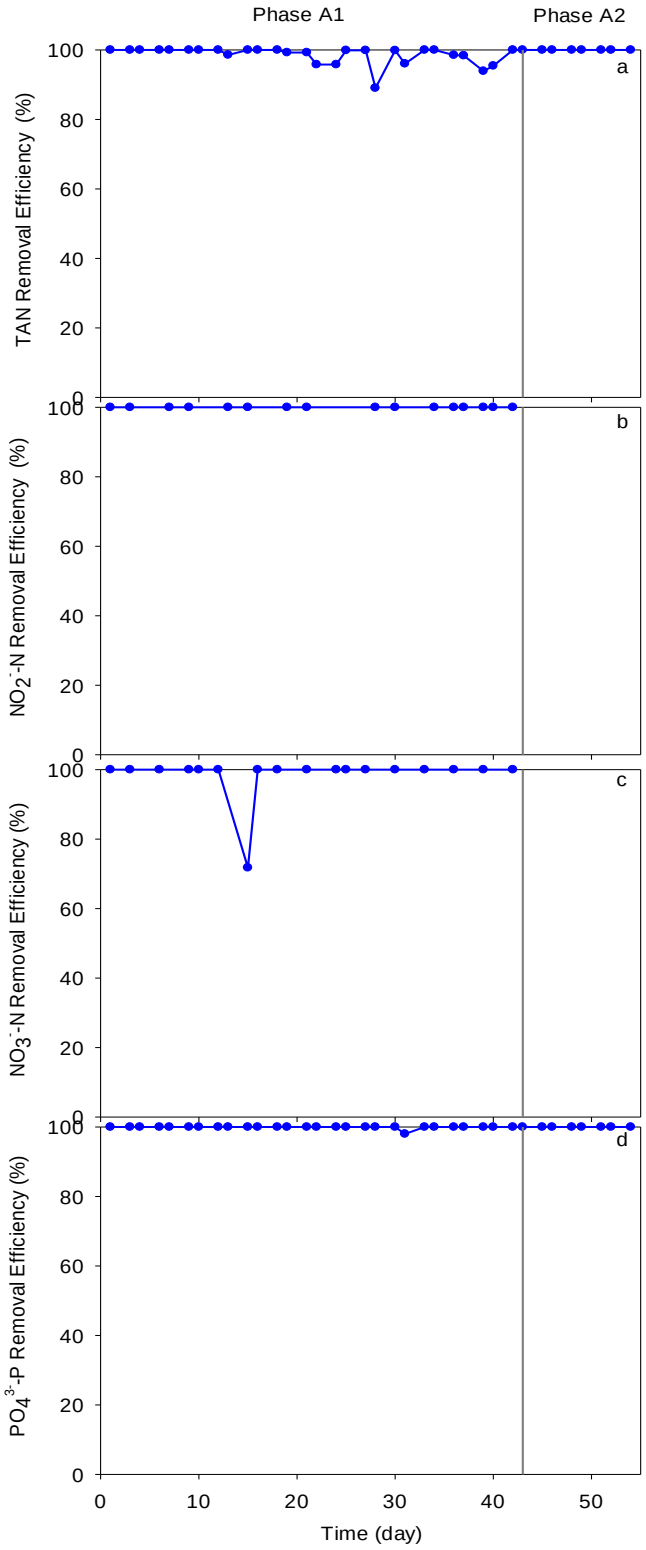

Figure 5.35 The removal efficiencies of (a) TAN, (b) NO_2^--N, (c) NO_3^--N and (d) PO_4^{3-}-P, during each cycle of the TM PBR

The influent TN/P ratio ranged from 3.6-12.6 g N/ g P throughout the operation of the TM PBR, with an average of 6.8±1.6 g N/ g P in Phase A1 and 11.7±0.7 g N/ g P in Phase A2 (Figure 5.36). The increase in the influent TN/P ratio was due to the reduced removal of nitrogen by the DAMMOX SBR in Phase A2, while the effluent PO_4^{3-} concentration did not change much from Phase A1 to Phase A2. Due to the near total removal of TN and PO_4^{3-} in the TM PBR, the ΔTN/ΔP ratio was similar to the influent TN/P ratio. The influent TN/P ratio, except for Day 4, 5 and 6, was in the range of 5-15 g N/ g/ P, as described in the literature (Aslan and Kapdan, 2006; Subaşı, 2022). Therefore, the effluent of the DAMMOX SBR was suitable for the *C. vulgaris* in this regard.

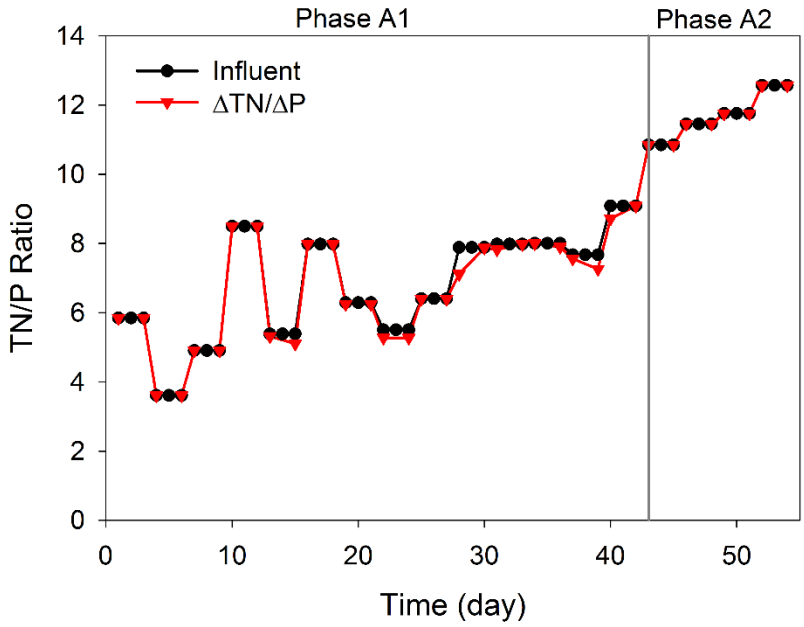

Figure 5.36 The influent and effluent TN/P ratio during each cycle of the TM PBR

The influent sCOD concentration of the TM PBR during Phase A1 ranged from 90-338 mg/L, with an average of 262±77 mg/L (Figure 5.37). The effluent of the same period ranged from 217-496 mg/L, with an average of 338±84 mg/L. During Phase A2, the influent sCOD concentration ranged from 98-455 mg/L, with an average of 319±172 mg/L. While the effluent of this period ranged from 321-456 mg/L, with an average of 389±47 mg/L. At Day 33, 36, 46, 51 and 52 of the TM PBR, sCOD

consumption was observed, while sCOD production was observed at all the other days. The sCOD removal efficiency for the majority of the TM PBR operation was negative, implying that production of sCOD usually occurred in the TM PBR. The removal efficiencies achieved at Day 33, 36, 46, 51 and 52 were 8, 27, 21, 15 and 10%, respectively (Figure 5.38). In heterotrophic or mixotrophic metabolism modes, where the microalgae is exposed to dark periods, organic carbon (sCOD) removal can take place. While under constant illumination, autotrophic metabolism will take place, where the microalgae will only remove inorganic carbon via photosynthesis. Since the TM PBR was supplied with continuous lighting, the dominant metabolism mode was autotrophy. Moreover, the *C. vulgaris* culture used in this study was acclimated to autotrophic conditions and was not exposed to COD prior to the experiment. This is further displayed in the low or none sCOD removal efficiencies. Only after self-shading became more prominent, which occurred after Day 46, did mixotrophic metabolism slowly started and sCOD was slightly degraded. Self-shading is a phenomenon where light penetration decreases into the center of the reactor causing the cells present there to undergo mixotrophic metabolism, as displayed in Figure 5.31 by the darker color of the microalgae.

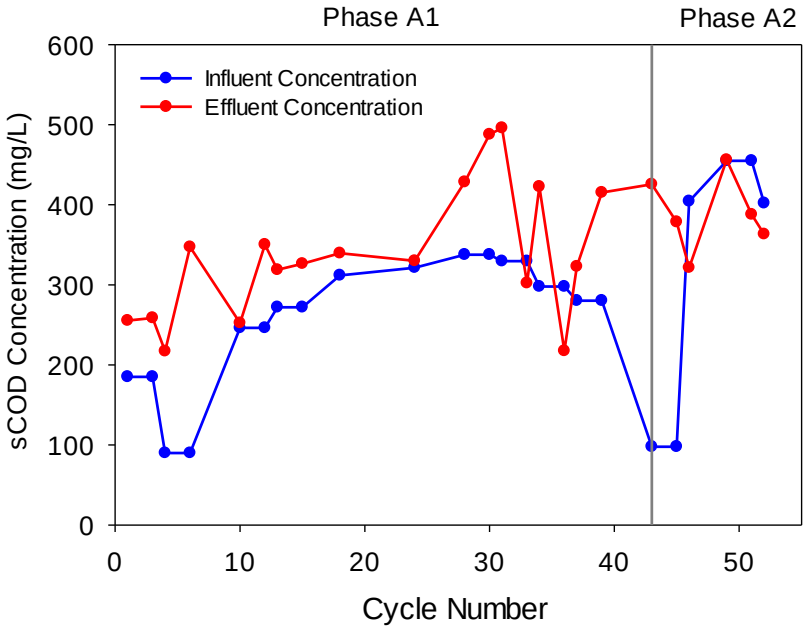

Figure 5.37 The influent and effluent sCOD concentrations of the TM PBR

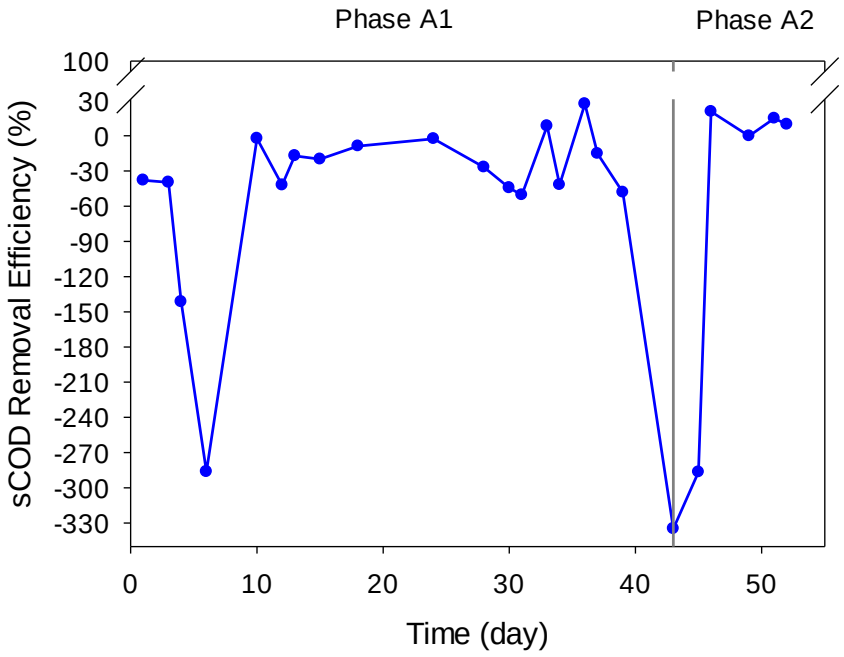

Figure 5.38 sCOD removal efficiency in the TM PBR

Samples from the TM PBR were taken at different Days (0, 35 and 50) and viewed under a light microscope to check if the *C. vulgaris* cells were healthy or experiencing any contamination. The images displayed in Figure 5.39 show that cells seemed healthy, and no contamination occurred during the operation of the TM PBR.

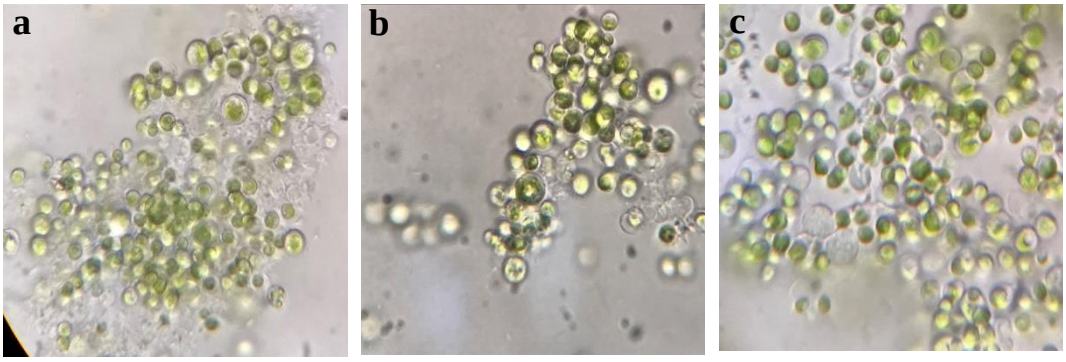

Figure 5.39 Microalgae under the light microscope 40X magnification (a) initial inoculation of TM PBR Day 0 (b) TM PBR Day 35 (c) TM PBR Day 50

5.3.4 Integrated DAMO-Anammox-Microalgae System

As an integrated DAMO-Anammox-Microalgae system nearly full TN removal was achieved in comparison to the influent concentration. Figure 5.40 illustrates the contribution of each of the DAMMOX and the TM PBR to the TN removal. During Phase A1, the DAMMOX SBR removed on average 51±10% of the TN, while the TM PBR removed on average 49±11% of the TN. Moreover, during Phase A2, the average contribution of the DAMMOX SBR to the TN removal increased to 56±4%, while the average contribution of the TM PBR to the TN removal decreased to 44±4%.

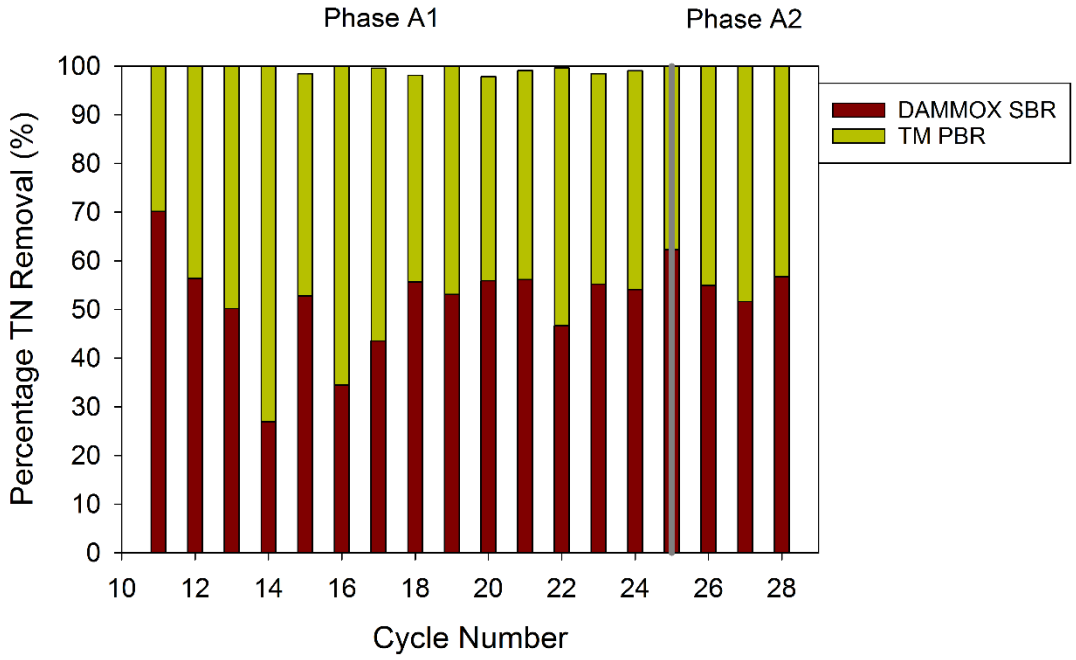

Figure 5.40 Percentage TN removal in DAMMOX SBR and in TM PBR

The integrated DAMO-Anammox-Microalgae system also achieved near full PO_4^{3-} removal in comparison to the influent concentration. Figure 5.41 illustrates the contribution of each of the DAMMOX SBR and the TM PBR to the PO_4^{3-} removal, the latter being the main contributor to the removal as expected. During Phase A1, the DAMMOX SBR removed on average 24±19% of the PO_4^{3-}, while the TM PBR removed on average 76±19% of the PO_4^{3-}. At Cycle 12 and 15, net PO_4^{3-} production

occurred in the DAMMOX SBR. Furthermore, during Phase A2, the average contribution of the DAMMOX SBR to the PO_4^{3-} removal increased to 37±5%, while the average contribution of the TM PBR to the PO_4^{3-} removal decreased to 63±5%.

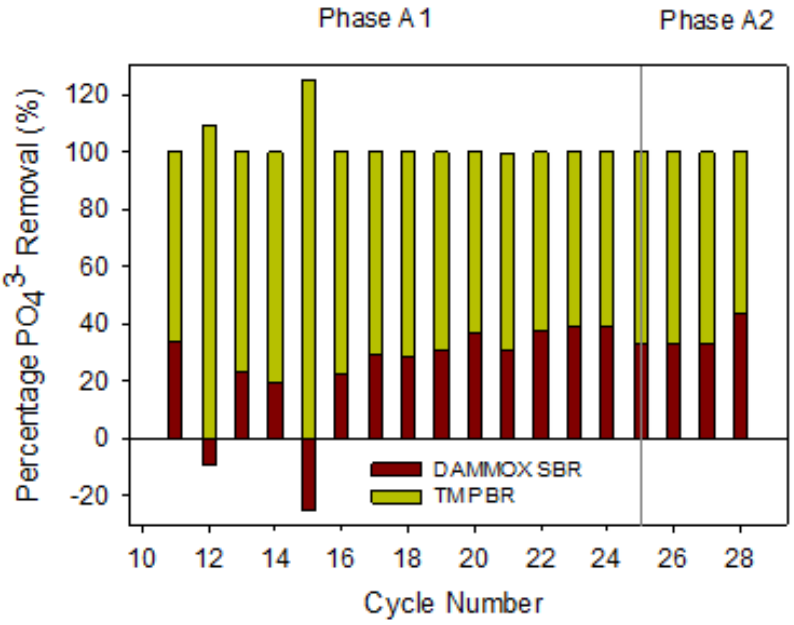

Figure 5.41 Percentage PO_4^{3-} removal in DAMMOX SBR and in TM PBR

The sCOD was not consumed in the DAMMOX SBR (Figure 5.16) but rather production of sCOD was observed for the majority of the cycles. On the other hand, sCOD consumption was expected to occur by the *C. vulgaris* using the mixotrophic metabolism. Nevertheless, sCOD production was observed in the TM PBR and it took the TM PBR 45 days to exhibit sCOD consumption (Figure 5.38), most probably due to the continuous illumination. In other words, it took 45 days for the TM PBR to darken in color decreasing the light penetration into the center of the reactor which in turn would promote mixotrophic metabolism.

As for the performance of the DAMO-Anammox-Microalgae integrated system, the sCOD concentration increased for the majority of the cycles with the exception of the last few cycles (Figure 5.42). Moreover, the contribution of the DAMMOX SBR to sCOD removal can only be seen in Cycle 25 with 45% and Cycle 28, with 48%, while that of the TM PBR only occurred in Phase A2, Cycle 26 with 21%, Cycle 27

with 7% and Cycle 28 with 10%. Hence, major sCOD removal did not occur in the system, since mixotrophic metabolism was not facilitated in the TM PBR.

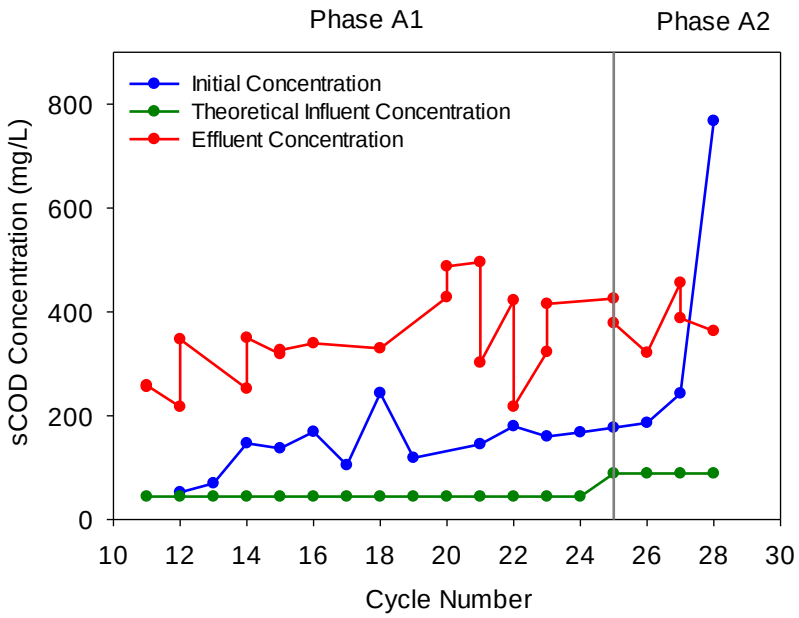

Figure 5.42 Initial and effluent sCOD concentrations of the integrated system

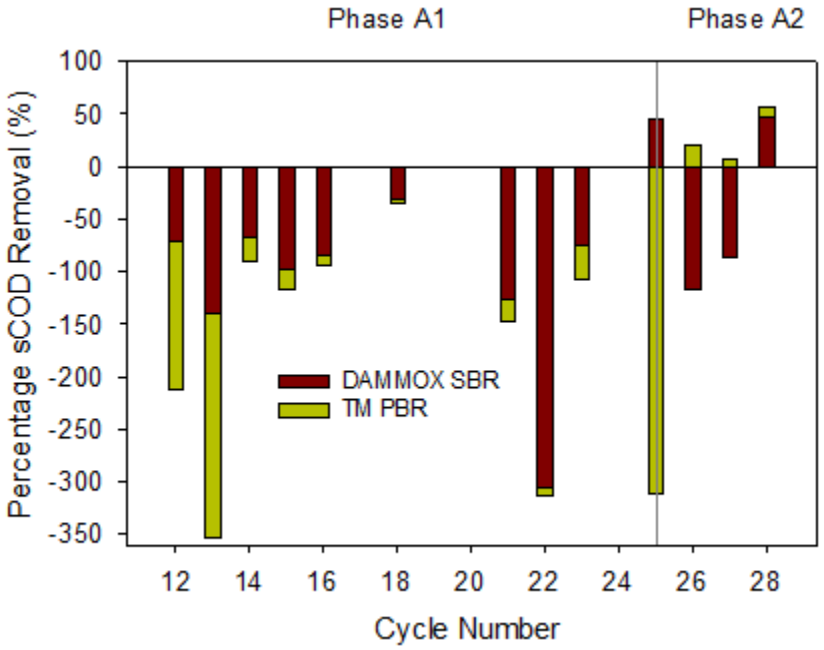

Figure 5.43 Percentage sCOD removal in DAMMOX SBR and in TM PBR

The maximum influent concentrations applied to the integrated system were in Phase A2 with average TN, PO_4^{3-}, SO_4^{2-} and sCOD concentrations about 222±8 mg N/L (166±15 mg TAN-N/L and 56±6 mg NO_2^--N/L), 10±1 mg P/L, 139±5 mg/L, 113±7 mg sCOD/L, respectively. The integrated DAMO-Anammox-Microalgae system achieved complete nitrogen and phosphorus removal but could not achieve major removal in the sCOD of the diluted AD effluent. The DAMO-Anammox co-culture was negatively affected by the presence of the sCOD and SO_4^{2-} in the AD effluent, especially in Phase A2, and the influent sCOD/TN ratio along with the influent NH_4^+/ NO_2^- were higher than the preference of the Anammox bacteria. Therefore, a partial nitritation step should be opted for prior to the DAMO-Anammox reactor, in order to provide higher NO_2^- concentrations, hence a suitable influent NH_4^+/NO_2^- ratio and meanwhile assuring the removal of any sCOD present in the wastewater as presented by Lim et al. (2021).

5.4 Conclusion

The DAMMOX SBR achieved near complete nitrogen removal during Phase S, that indicates the capability of the co-culture. Employing the enriched DAMO-Anammox co-culture, treatment of AD effluent was conducted. According to the results obtained, the main factors that need to be taken into consideration for the treatment of AD effluent are the sCOD concentration, the influent COD/TN ratio, SO_4^{2-} concentration and the influent NH_4^+/NO_2^- ratio. The presence of sCOD and a high influent COD/TN may cause a shift in the microbial consortium favoring heterotrophic denitrification and non-methanotrophic chemoorganotrophs. The effects of COD were not as evident in the short-term batch test as in the DAMMOX SBR, since the TN removal was higher in the batch test. Therefore, employing partial nitritation prior to the DAMO-Anammox reactor is a suitable solution that can address these factors by keeping the COD concentration lower 280 mg/L, stabilizing the influent COD/TN ratio below 2 and sustaining an influent NH_4^+/NO_2^- ratio of about 0.8-1.5.

The application of microalgae following the DAMO-Anammox reactor succeeded in achieving complete removal of residual nitrogen and phosphorus, however COD removal was not attained since the conditions provided to the *C. vulgaris* favored autotrophic metabolism rather than mixotrophic. The application of mixotrophic microalgal metabolism should be tested to improve COD removal.

CHAPTER 6

CONCLUSION

6.1 Conclusion

The main aim of this PhD research was to investigate the enrichment of a DAMO-Anammox co-culture in an SBR and employ the co-culture to treat AD effluent. Moreover, the potential of a novel integrated DAMO-Anammox-Microalgae system for complete nutrient removal from an AD effluent was assessed as a proof of concept.

- DAMO-Anammox co-culture was enriched in an SBR, using a mixture of previously enriched Anammox granular sludge, AD sludge and freshwater lake sediment as the inocula.
- Enrichment was evaluated via employing various methods that illustrate the percentage of contribution to the available TN removal, stoichiometric molar ratios, NO_2^- and NO_3^--based reaction rates and molecular analyses such as FISH and 16S NGS Metagenome analysis throughout the different phases of operation of the DAMO-Anammox SBR.
- Anammox was the most dominant of the three target microorganisms in the DAMO-Anammox SBR. Yet increasing the influent NO_2^-/NH_4^+ ratio (Phase II) allowed the DAMOb an advantage over the Anammox.
- *Planctomycetota*, NC10, and *Euryarchaeota* were found to be 8%, 0.5%, and 0.16% of the microbial consortium, respectively, in Phase V. The NGS Metagenome analysis illustrated other denitrifying methanotrophs and methylotrophs belonging to the phyla *Proteobacteria*, *Verrucomicrobiota*, and archaeal classes *Methanobacteria*, *Candidatus Methanofastidiosia* and *Thermoplasmata* were present in the DAMO-Anammox SBR.

- The main factors that were tested, affecting the enrichment of the target microorganisms were nitrogen source, influent nitrogen molar ratios (NH_4^+/NO_2^-, NH_4^+/NO_3^- and NO_2^-/NO_3^-), and HRT.
    - The choice of reactor configuration allows for the accommodation of a higher HRT which permits more reaction time especially for the DAMO microorganisms, that have long doubling time. Since Anammox bacteria was dominant in the reactor, the decrease in HRT from 6 to 4 days, had no effect on their activity and a decline in the DAMO activity. Reverting the HRT to 6 days, reverted the activities of the three target microorganisms to levels relatively similar prior to the decrease in HRT.
    - The reactor configuration also plays a critical role in the CH_4 availability to the DAMO microorganisms and in retaining the microorganisms thus increasing the SRT. Considering the selection reason of the SBR configuration in this study which provides a longer SRT, CH_4 availability seems to be more critical for the enrichment of DAMO microorganisms.
    - The presence of the DAMO microorganisms in the inoculum is critical therefore the choice of the inoculum is important.
    - The short-term effect of the NH_4^+ to dissolved CH_4 ratio (0, ¼, 1) in batch reactors was investigated and the results illustrated that, at ratios of 0 and ¼, DAMOb was dominant while at the ratio of 1, balanced activity of the DAMO-Anammox co-culture was observed. The increase in Anammox activity constrained the DAMOb activity hence allowing the increase in DAMOa activity.
    - DAMO (DAMOb and DAMOa) activity was higher in the absence of a dominant Anammox culture. Therefore, enrichment of a DAMO culture in the absence of a dominant Anammox culture may occur in a shorter period.

- Different combinations of the nitrogen sources, their influent concentrations and corresponding influent molar ratios play a critical role in the enrichment of a DAMO-Anammox co-culture.
- DAMO-Anammox co-cultures enriched with multiple nitrogen sources seem to have generally higher removal rates than cultures enriched using a single nitrogen source.
- The best indicatory stoichiometric molar ratios for a DAMO-Anammox co-culture are $\Delta NO_2^-/\Delta NH_4^+$ and $\Delta NO_3^-/ (\Delta NO_2^- + \Delta NH_4^+)$ and should be used together when defining the combination of target species.
- The increase in Fe^{2+} and Cu^{2+} initial concentrations to 50 μM and 10 μM, respectively, improved the activity of the three target microorganisms. The specific activity tests clearly illustrated the increase in the DAMOb and DAMOa activity.

- The DAMMOX SBR used to treat AD effluent was inoculated with sludge from the three reactors, DAMO-Anammox SBR, DAMO SBR and DAA SBR. Prior to the application of the diluted AD effluent (Phase S), the DAMMOX SBR achieved near complete nitrogen removal DAMO-Anammox co-culture in the DAMMOX SBR.
    - The main factors that need to be taken into consideration for the treatment of AD effluent are the sCOD concentration, the influent COD/TN ratio, SO_4^{2-} concentration and the influent NH_4^+/NO_2^- ratio. The presence of sCOD and a high influent COD/TN favored non-methanotrophic chemoorganotrophs and more importantly heterotrophic denitrifiers.
    - Employing partial nitritation prior to the DAMO-Anammox reactor seems to be a suitable solution that addresses the sCOD concentration, the COD/TN ratio and the NH_4^+/NO_2^- ratio.
- Employing a sequential microalgae PBR after the DAMO-Anammox reactor was successful in completely removing nitrogen and phosphorus from an AD

effluent. Yet, COD removal was not attained since the dominant metabolism mode of the *C. vulgaris* was autotrophic rather than mixotrophic. Such a configuration may close the energy cycle making this treatment system self-sustainable and energy-efficient.

6.2 Future Recommendations

In the application of a DAMO-Anammox co-culture for the treatment of an AD effluent or landfill leachate, the effects of SO_4^{2-}, H_2S, excessive CO_2 which can cause acidification, in-situ (original) biogas produced from an AD, heavy metals, salinity and the long-term effect of the NH_4^+/ dissolved CH_4 ratio, on a DAMO-Anammox co-culture with respect to the reactor performance and the microbial consortium should be investigated.

With respect to the integration of *C. vulgaris* with a DAMO-Anammox reactor, mixotrophic metabolism mode should be investigated by supplying dark periods which will have the potential for improved COD removal. Moreover, the effect of the COD content and their relative concentrations on the microalgae culture should be investigated.

Implementing pilot-scale or full-scale DAMO-based technologies for side-stream or main-stream wastewater treatment, scaling-up is required. Supplementing high-pressure combustible methane, optimizing dissolved methane concentration and biomass retention are some of the major concerns. These issues may be addressed by employing sensors and safety measures and reactor selection such as HfMBR or MAMBR which improves CH_4 availability. Furthermore, the start-up time of a DAMO-Anammox reactor should be taken into consideration along-side construction and operational costs.

6.3 Innovative municipal wastewater treatment

There are various limitations to conventional biological wastewater treatment processes that include extensive aeration requirement, GHG emissions, external carbon requirement, excessive sludge production and minimal energy recovery efficiency (Gu et al., 2018; Liu et al., 2018). Implementing anaerobic treatment as the central biological unit can address these limitations. For instance, utilizing Anammox for mainstream wastewater treatment can be beneficial in terms of the energy requirement and diminish sludge production. Yet, there are some fundamental obstacles that may arise from employing mainstream Anammox, which include limited Anammox activity at low temperatures, maintaining stable partial nitritation and controlling the C/N ratio (Liu et al., 2018).

The first stage of the proposed system comprises of anaerobic conversion of organics into CH_4, as shown in Figure 6.1. Various reactor configurations such as anaerobic fixed bed reactor (AFBR), anaerobic hybrid (AH) reactor, up-flow anaerobic sludge blanket (UASB) can be employed in this step. UASB-digester combined system demonstrated COD removal and CH_4 recovery at temperatures of 10-20°C (Zhang, 2016). Optimizing sludge recirculation, concentrating recirculated sludge, operating the digester at 30°C are important factors to consider for this reactor configuration. Moreover, reduction of installation and operational costs will be achieved since a primary sedimentation tank and aeration basin will not be required as in conventional municipal WWTPs (Zhang, 2016).

In the next stage, the NH_4^+ present in the wastewater should be converted to NO_2^-. This can be performed by partial nitritation using controlled aeration or by employing complete ammonium oxidation (COMAMMOX) (Figure 6.1). The NH_4^+/ NO_2^- ratio in the feed sent to the DAMO-Anammox reactor should be stabilized within the range of 1-1.3. COMAMMOX is advantageous over partial nitritation since it takes place under limited DO concentrations (<0.5 mg/L), where more than half of the TKN can be removed to NO_2^- and NO_3^- (Şenol and Kocamemi, 2011). The COMAMMOX process would require less energy for aeration in comparison to

partial nitritation and present no issues in terms of DO concentration entering into the DAMO-Anammox reactor.

The best reactor configuration for the DAMO-Anammox co-culture that provides biomass retention and maximizes the availability of dissolved CH_4 for the DAMO microorganisms seems to be the HfMBR. Dissolved CH_4 along with NH_4^+ will be provided from the effluent of the UASB-digester system while NO_2^- will be supplied from the partial nitritation or COMAMMOX stage, as shown in Figure 6.1. In case not enough NH_4^+ is present in the UASB effluent, AD effluent may be sent to the DAMO-Anammox HfMBR taking into account the resulting NH_4^+/ NO_2^- ratio.

The effluent of the DAMO-Anammox HfMBR will be provided to a tubular microalgae PBR (Figure 6.1). In this stage CO_2 will sequestered, while residual nitrogen will be removed along with the removal of phosphorus. Moreover, if necessary mixotrophic metabolism of microalgae will also be capable of removing of COD.

Microalgae can be either harvested to produce value-added products (VAPs), such as pigments and biofuels or sent to the anaerobic digester for the production of biogas. This wastewater treatment design has the potential to convert organics to biogas, in turn reducing GHG emissions, while achieving nitrogen and phosphorus removal and carbon sequestration, at the same time, recovering energy and VAPs in the form of biogas and microalgae, respectively. The proposed wastewater treatment system can treat main-stream and/or side-stream wastewater. Furthermore, the proposed WWTP has the prospective to achieve a paradigm shift in wastewater treatment by transforming this industry from the notion of pollutant removal to resource and energy recovery.

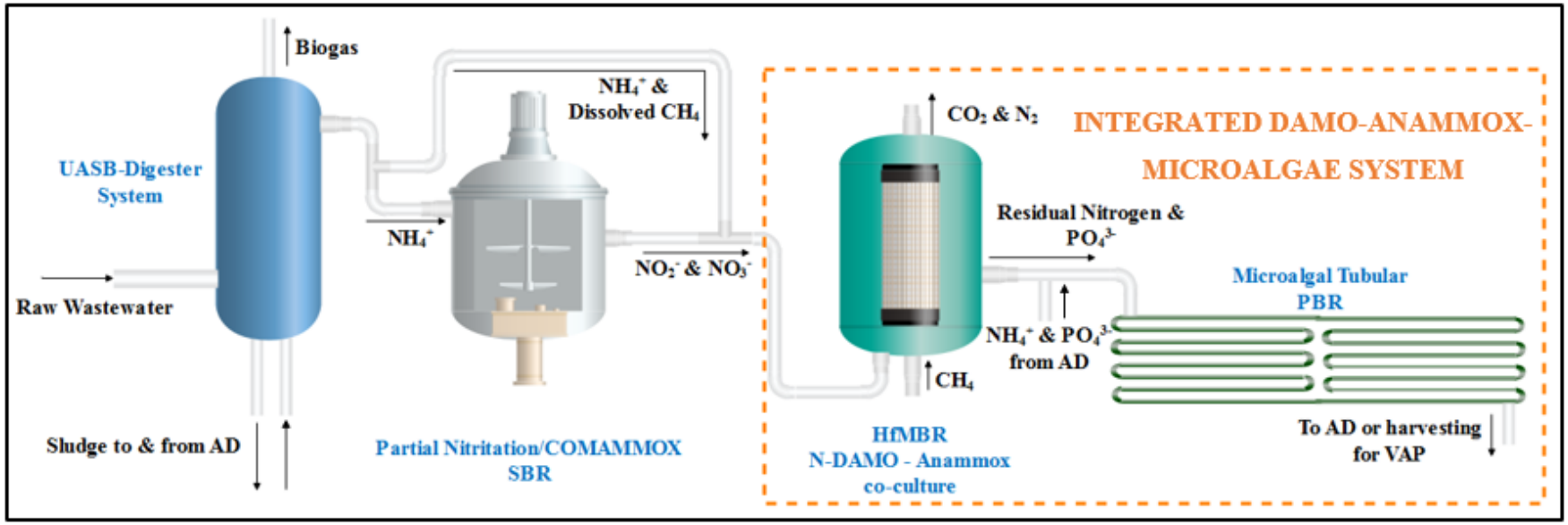

Figure 6.1 The proposed mainstream and/or sidestream wastewater treatment system

REFERENCES

Abdel-Raouf, N., Al-Homaidan, A. A., and Ibraheem, I. (2012). Microalgae and wastewater treatment. *Saudi Journal of Biological Sciences*, 19(3), 257-275.

Ahn, Y. (2006). Sustainable Nitrogen Elimination Biotechnologies: A Review. *Process Biochemistry*, vol. 41, no. 8, pp. 1709–1721., doi: 10.1016/j.procbio.2006.03.033.

Ahn, J. H., Kim, S., Park, H., Katehis, D., Pagilla, K., and Chandran, K. (2010). Spatial and temporal variability in atmospheric nitrous oxide generation and emission from full- scale biological nitrogen removal and non- BNR processes. *Water Environment Research*, 82(12), 2362-2372.

Al-Jabri, H., Das, P., Thaher, M., Khan, S., and AbdulQuadir, M. (2021). Potential utilization of waste nitrogen fertilizer from a fertilizer industry using marine microalgae. *Science of The Total Environment*, 755, 142532.

Al-Saud, S., Florea, K. M., Webb, E. A., and Thrash, J. C. (2020). Metagenome-Assembled Genome Sequence of Kapabacteriales Bacterium Strain Clear-D13, Assembled From a Harmful Algal Bloom Enrichment Culture. *Microbiology Resource Announcements*, 9(49). https://doi.org/10.1128/mra.01118-20

Anbalagan, A., Schwede, S., Lindberg, C. F., and Nehrenheim, E. (2016). Influence of hydraulic retention time on indigenous microalgae and activated sludge process. *Water Research*, 91, 277-284.

Anjos, M., Fernandes, B. D., Vicente, A. A., Teixeira, J. A., and Dragone, G. (2013). Optimization of CO_2 bio-mitigation by Chlorella vulgaris. *Bioresource Technology*, 139, 149-154.

APHA, AWWA, WEF (2005). *Standard Methods for the Examination of Water and Wastewater*. 21st Edition. Washington, DC.

Aslan, S., and Kapdan, I. K. (2006). Batch kinetics of nitrogen and phosphorus removal from synthetic wastewater by algae. *Ecological Engineering*, 28(1), 64-70.

Bae, H., Park, K. S., Chung, Y. C., and Jung, J. Y. (2010). Distribution of anammox bacteria in domestic WWTPs and their enrichments evaluated by real-time quantitative PCR. *Process Biochemistry*, 45(3), 323-334.

Barreiro, D. L., Prins, W., Ronsse, F., and Brilman, W. (2013). Hydrothermal liquefaction (HTL) of microalgae for biofuel production: state of the art review and future prospects. *Biomass and Bioenergy*, 53, 113-127.

Bashir, K. M. I., Mansoor, S., Kim, N. R., Grohmann, F. R., Shah, A. A., and Cho, M. G. (2019). Effect of organic carbon sources and environmental factors on cell growth and lipid content of Pavlova lutheri. *Annals of Microbiology*, 69(4), 353-368.

Bennion, E. P., Ginosar, D. M., Moses, J., Agblevor, F., and Quinn, J. C. (2015). Lifecycle assessment of microalgae to biofuel: comparison of thermochemical processing pathways. *Applied Energy*, 154, 1062-1071.

Bhattacharjee, A. S., Motlagh, A. M., Jetten, M. S., and Goel, R. (2016). Methane dependent denitrification- from ecosystem to laboratory-scale enrichment for engineering applications. *Water Research*, 99, 244-252. doi: 10.1016/j.watres.2016.04.070

Bian, L., Hinrichs, K., Xie, T., Brassell, S. C., Iversen, N., Fossing, H., Jørgensen B. B., and Hayes, J. M. (2001). Algal and archaeal polyisoprenoids in a recent marine sediment: Molecular isotopic evidence for anaerobic oxidation of

methane. *Geochemistry, Geophysics, Geosystems,* 2(1). doi:10.1029/2000gc000112

Boetius, A., Ravenschlag, K., Schubert, C. J., Rickert, D., Widdel, F., Gieske, A., Amann, R., Jørgensen, B. B., Witte, U., and Pfannkuche, O. (2000). A marine microbial consortium apparently mediating anaerobic oxidation of methane. *Nature*, 407, 623-626.

Boone, D. R., Castenholz, R. W., and Garrity, G. M. (2005). *Bergey's Manual of systematic bacteriology*. Springer.

Bolyen, E., Rideout, J. R., Dillon, M. R., Bokulich, N. A., Abnet, C. C., Al-Ghalith, G. A., Alexander, H., Alm, E.J., Arumugam, M., Asnicar, F., Bai, Y., Bisanz, J.E., Bittinger, K., Brejnrod, A., Brislawn, C.J., Brown, C.T., Callahan, B.J., Caraballo-Rodríguez, A.M., Chase, J.,… Caporaso, J. G. (2019). Reproducible, interactive, scalable and extensible microbiome data science using QIIME 2. *Nature Biotechnology*, 37(8), 852-857.

Brandes, J. A., Devol, A. H., and Deutsch, C. (2007). New developments in the marine nitrogen cycle. *Chemical reviews*, 107(2), 577-589.

Brennan, L., and Owende, P. (2010). Biofuels from microalgae—A review of technologies for production, processing, and extractions of biofuels and co-products. *Renewable and Sustainable Energy Reviews*, 14(2), 557-577. doi:10.1016/j.rser.2009.10.009

Burgin, A. J., and Hamilton, S. K. (2007). Have we overemphasized the role of denitrification in aquatic ecosystems? A review of nitrate removal pathways. *Frontiers in Ecology and the Environment*, 5, 89–96.

Bussmann, I. (2005). Methane Release through Resuspension of Littoral Sediment. *Biogeochemistry*, 74(3), 283-302. doi:10.1007/s10533-004-2223-2

Cabeen, M. T., and Jacobs-Wagner, C. (2005). Bacterial cell shape. *Nature Reviews Microbiology,* 3:601– 610.

Cai, C., Hu, S., Chen, X., Ni, B., Pu, J., and Yuan, Z. (2018). Effect of methane partial pressure on the performance of a membrane biofilm reactor coupling methane-dependent denitrification and anammox. *Science of The Total Environment, 639,* 278-285. doi: 10.1016/j.scitotenv.2018.05.164

Cai, C., Hu, S., Guo, J., Shi, Y., Xie, G., and Yuan, Z. (2015). Nitrate reduction by denitrifying anaerobic methane oxidizing microorganisms can reach a practically useful rate. *Water Research,* 87, 211-217. doi: 10.1016/j.watres.2015.09.026

Cai, T., Park, S. Y., and Li, Y. (2013). Nutrient recovery from wastewater streams by microalgae: status and prospects. *Renewable and Sustainable Energy Reviews,* 19, 360-369.

Campos, J. L., Valenzuela-Heredia, D., Pedrouso, A., Val del Río, A., Belmonte, M., and Mosquera-Corral, A. (2016). Greenhouse gases emissions from wastewater treatment plants: minimization, treatment, and prevention. *Journal of Chemistry*, 2016.

Carvalho, A. P., Meireles, L. A., and Malcata, F. X. (2006). Microalgal reactors: a review of enclosed system designs and performances. *Biotechnology Progress*, 22(6), 1490-1506.

Castelle, C. J., Hug, L. A., Wrighton, K. C., Thomas, B. C., Williams, K. H., Wu, D., Tringe, S. G., Singer, S. W., Eisen, J. A., and Banfield, J. F. (2013). Extraordinary phylogenetic diversity and metabolic versatility in aquifer sediment. *Nature Communications*, 4(1). https://doi.org/10.1038/ncomms3120

Castro-Barros, C. M., Ho, L. T., Winkler, M. K., and Volcke, E. I. (2017). Integration of methane removal in aerobic anammox-based granular sludge reactors. *Environmental Technology*, 39 (13), 1615-1625. doi:10.1080/09593330.2017.1334709

Chakraborty, R., Oconnor, S. M., Chan, E., and Coates, J. D. (2005). Anaerobic Degradation of Benzene, Toluene, Ethylbenzene, and Xylene Compounds by Dechloromonas Strain RCB. *Applied and Environmental Microbiology*, 71(12), 8649-8655. doi:10.1128/aem.71.12.8649-8655.2005

Chamchoi, N., and Nitisoravut, S. (2007). Anammox enrichment from different conventional sludges. *Chemosphere*, 66(11), 2225–2232. doi: 10.1016/j.chemosphere.2006.09.036

Chaudhari, N. M., Overholt, W. A., Figueroa-Gonzalez, P. A., Taubert, M., Bornemann, T. L., Probst, A. J., Hölzer, M., Marz, M., and Küsel, K. (2021). The Economical Lifestyle of CPR Bacteria in Groundwater Allows Little Preference for Environmental Drivers. *Environmental Microbiome*. https://doi.org/10.1101/2021.07.28.454184

Chen, F., Zheng, Y., Hou, L., Zhou, J., Yin, G., and Liu, M. (2020). Denitrifying anaerobic methane oxidation in MARSH sediments of Chongming EASTERN intertidal flat. *Marine Pollution Bulletin*, 150, 110681. https://doi.org/10.1016/j.marpolbul.2019.110681.

Chen, X., Guo, J., Shi, Y., Hu, S., Yuan, Z., and Ni, B. (2014). Modeling of Simultaneous Anaerobic Methane and Ammonium Oxidation in a Membrane Biofilm Reactor. *Environmental Science and Technology*, 48(16), 9540-9547. doi:10.1021/es502608s

Chen, X., Guo, J., Xie, G., Liu, Y., Yuan, Z. and Ni, B. (2015). A new approach to simultaneous ammonium and dissolved methane removal from anaerobic

digestion liquor: A model-based investigation of feasibility. *Water Research*, 85, 295-303.

Chen, X., Guo, J., Xie, G., Yuan, Z. and Ni, B. (2016a). Achieving complete nitrogen removal by coupling nitritation-anammox and methane-dependent denitrification: A model-based study. *Biotechnology and Bioengineering*, 113(5), 1035-1045

Chen, X., Liu, Y., Peng, L., Yuan, Z. and Ni, B. (2016b). Model-Based Feasibility Assessment of Membrane Biofilm Reactor to Achieve Simultaneous Ammonium, Dissolved Methane, and Sulfide Removal from Anaerobic Digestion Liquor. *Scientific Reports*, 6 (25114).

Chen, C., Sun, F., Zhang, H., Wang, J., Shen, Y., and Liang, X. (2016c). Evaluation of COD effect on ANAMMOX process and microbial communities in the anaerobic baffled reactor (ABR). *Bioresource Technology*, 216, 571–578. https://doi.org/10.1016/j.biortech.2016.05.115

Cheng, C., Zhou, Z., Niu, T., An, Y., Shen, X., Pan, W., Chen, Z., and Liu, J. (2017). Effects of side-stream ratio on sludge reduction and microbial structures of anaerobic side-stream reactor coupled membrane bioreactors. *Bioresource Technology*, 234, 380–388. https://doi.org/10.1016/j.biortech.2017.03.077

Chinnasamy, S., Ramakrishnan, B., Bhatnagar, A., and Das, K. C. (2009). Biomass production potential of a wastewater alga *Chlorella vulgaris* ARC 1 under elevated levels of CO_2 and temperature. *International Journal of Molecular Sciences*, 10(2), 518-532.

Chisti, Y., (2007). Biodiesel from Microalgae. *Biotechnology Advances*, 25(3) 294–306.

Chisti, Y. (2008). Biodiesel from microalgae beats bioethanol. *Trends in Biotechnology*, 26(3), 126-131.

Chistoserdova, L., Vorholt, J., and Lidstrom, M. A. (2005). A genomic view of methane oxidation by aerobic bacteria and anaerobic archaea. *Genome Biology*, Volume 6, Issue 2, Article 208, 6:208. Doi: http://genomebiology.com/2005/6/2/208

Choi, H. J., and Lee, S. M. (2015). Biomass and oil content of microalgae under mixotrophic conditions. *Environmental Engineering Research*, 20(1), 25-32.

Chu, L.M., Cheung, K.C., and Wong, M.H. (1994). Variations in the chemical properties of landfill leachate. *Environmental Management*. 18 (1), 105–117. https://doi.org/10.1007/ bf02393753.

Cogert, K. I., Ziels, R. M., and Winkler, M. K. H. (2019). Reducing cost and environmental impact of wastewater treatment with denitrifying methanotrophs, ANAMMOX, and mainstream anaerobic treatment. *Environmental Science and Technology*, 53(21), 12935–12944. https://doi.org/10.1021/acs.est.9b04764

Collet, P., Hélias, A., Lardon, L., Ras, M., Goy, R., and Steyer, J. (2010). Life-cycle assessment of microalgae culture coupled to biogas production. *Bioresource Technology*, 102, 207-214.

Cookney, J., Mcleod, A., Mathioudakis, V., Ncube, P., Soares, A., Jefferson, B., and Mcadam, E. (2016). Dissolved methane recovery from anaerobic effluents using hollow fibre membrane contactors, *Journal of Membrane Science*, 502(2016), 141-150

Cromar, N. J., and Fallowfield, H. J. (1997). Effect of nutrient loading and retention time on performance of high rate algal ponds. *Journal of Applied Phycology*, 9(4), 301-309.

Crone, B. C., Garland, J. L., Sorial, G. A., and Vane, L. M. (2016). Significance of dissolved methane in effluents of anaerobically treated low strength

wastewater and potential for recovery as an energy product: A review. *Water Research*, 104, 520-531.

Cui, M., Ma, A., Qi, H., Zhuang, X., and Zhuang, G. (2015). Anaerobic oxidation of methane: an "active" microbial process. *Microbiology Open*, 4(1), 1–11. doi: 10.1002/mbo3.232

Daelman, M. R. J., van Voorthuizen, E. M., van Dongen, U. G. J. M., Volcke, E. I. P., and van Loosdrecht, M. C. M. (2012). Methane emission during municipal wastewater treatment. *Water Research*, 46(11), 3657–3670. https://doi.org/10.1016/j.watres.2012.04.024

Daims, H. (2009). Use of fluorescence in situ hybridization and the *daime* image analysis program for the cultivation-independent quantification of microorganisms in environmental and medical samples. *Cold Spring Harbor Protocols*, 2009(7). https://doi.org/10.1101/pdb.prot5253

Daliry, S., Hallajisani, A., Mohammadi Roshandeh, J., Nouri, H., and Golzary, A. (2017). Investigation of optimal condition for Chlorella vulgaris microalgae growth. *Global Journal of Environmental Science and Management*., 3(2), 217-230. doi: 10.22034/gjesm.2017.03.02.010

Dalsgaard, T., Canfield, D. E., Petersen, J., Thamdrup, B., and Acuña-González, J. (2003). N_2 production by the anammox reaction in the anoxic water column of Golfo Dulce, Costa Rica. *Nature*, 422(6932), 606-608.

Dalsgaard, T., Thamdrup, B., and Canfield, D. E. (2005). Anaerobic ammonium oxidation (anammox) in the marine environment. *Research in Microbiology*, 156(4), 457-464. doi:10.1016/j.resmic.2005.01.011

Danczak, R. E., Johnston, M. D., Kenah, C., Slattery, M., Wrighton, K. C., and Wilkins, M. J. (2017). Members of the candidate phyla radiation are

functionally differentiated by carbon- and nitrogen-cycling capabilities. *Microbiome*, 5(1). https://doi.org/10.1186/s40168-017-0331-1

Danesh, A. F., Mooij, P., Ebrahimi, S., Kleerebezem, R., and van Loosdrecht, M. (2020). Chemostat Based Enrichment System: Nitrogen Loading Rates Impacts on Microalgal Communities and Intracellular Storage Compounds. *Authorea Preprints*.

Dapena-Mora, A., Fernández, I., Campos, J., Mosquera-Corral, A., Méndez, R., and Jetten, M. (2007). Evaluation of activity and inhibition effects on Anammox process by batch tests based on the nitrogen gas production. *Enzyme and Microbial Technology*, *40*(4), 859–865. doi: 10.1016/j.enzmictec.2006.06.018

De Godos, I., Blanco, S., García-Encina, P. A., Becares, E., and Muñoz, R. (2009). Long-term operation of high rate algal ponds for the bioremediation of piggery wastewaters at high loading rates. *Bioresource Technology*, 100(19), 4332-4339.

Deniz, İ. (2020). Determination of growth conditions for Chlorella vulgaris. *Marine Science and Technology Bulletin*, 9(2), 114-117.

Deutzmann, J. S., and Schink, B. (2011). Anaerobic Oxidation of Methane in Sediments of Lake Constance, an Oligotrophic Freshwater Lake. *Applied and Environmental Microbiology*, 77(13), 4429-4436. doi:10.1128/aem.00340-11

Diamantis, V., Erguder, T.H., Aivasidis, A., Verstraete, W., and Voudrias, E. (2013). Wastewater disposal to landfill-sites: a synergistic solution for centralized management of olive mill wastewater and enhanced production of landfill gas. *Journal of Environmental Management*, 128, 427–434. https://doi.org/10.1016/j.jenvman.2013.05.051.

Di Caprio, F., Scarponi, P., Altimari, P., Iaquaniello, G., and Pagnanelli, F. (2018). The influence of phenols extracted from olive mill wastewater on the heterotrophic and mixotrophic growth of Scenedesmus sp. *Journal of Chemical Technology & Biotechnology*, 93(12), 3619-3626.

Ding, J., and Zeng, R.J. (2021). Fundamentals and potential environmental significance of denitrifying anaerobic methane oxidizing archaea. *Science of the Total Environment*, 757, 143928. https://doi.org/10.1016/j.scitotenv.2020.143928.

Ding, Z., Ding, J., Fu, L., Zhang, F., and Zeng, R. J. (2014). Simultaneous enrichment of denitrifying methanotrophs and anammox bacteria. *Applied Microbiology and Biotechnology*, 98(24), 10211-10221. doi:10.1007/s00253-014-5936-8

Ding, Z., Lu, Y., Fu, L., Ding, J., and Zeng, R. J. (2017). Simultaneous enrichment of denitrifying anaerobic methane-oxidizing microorganisms and anammox bacteria in a hollow-fiber membrane biofilm reactor. *Applied Microbiology and Biotechnology*, 101(1), 437-446. doi:10.1007/s00253-016-7908-7

Du, R., Peng, Y., Ji, J., Shi, L., Gao, R., and Li, X. (2019). Partial denitrification providing nitrite: opportunities of extending application for anammox. *Environment International*, 131, 105001. https://doi.org/10.1016/j.envint.2019.105001.

Duce, R. A., LaRoche, J., Altieri, K., Arrigo, K. R., Baker, A. R., Capone, D. G., Cornell, S., Dentener, F., Galloway, J., Ganeshram, R. S., Geider, R. J., Jickells, T., Kuypers, M. M., Langlois, R., Liss, P. S., Liu, S. M., Middelburg, J. J., Moore, C. M., Nickovic, S.,… Zamora, L. (2008). Impacts of atmospheric anthropogenic nitrogen on the open ocean. Science, 320, 893–897.

Dutta, P., Rabaey, K., Yuan, Z., Rozendal, R., and Keller, J. (2010). Electrochemical sulfide removal and recovery from paper mill anaerobic treatment effluent, *Water Research*, 44(8), 2563-2571

Eliassen R. and Tcnosanoglous G. (1968). Chemical processing of waste water for nutrient removal. *Journal of the Water Pollution Control Federation*, 40, May, Part 2, R171

Engelbrecht, S., Mozooni, M., Rathsack, K., Böllmann, J., and Martienssen, M. (2018). Effect of increasing salinity to adapted and non-adapted anammox biofilms. *Environmental Technology*, 40 (22), 2880–2888. https://doi.org/10.1080/09593330.2018.1455748.

Engelhardt, H. (2007). Are S-layers exoskeletons? The basic function of protein surface layers revisited. *Journal of Structural Biol*ogy, 160, 115-124.

Escapa, C., Coimbra, R. N., Paniagua, S., García, A. I., and Otero, M. (2015). Nutrients and pharmaceuticals removal from wastewater by culture and harvesting of Chlorella sorokiniana. *Bioresource Technology*, 185, 276-284.

Ettwig, K. F., Alen, T. V., Pas-Schoonen, K. T., Jetten, M. S., and Strous, M. (2009). Enrichment and Molecular Detection of Denitrifying Methanotrophic Bacteria of the NC10 Phylum. *Applied and Environmental Microbiology*, 75(11), 3656-3662. doi:10.1128/aem.00067-09

Ettwig, K.F., Butler, M.K., Paslier, D.L., Pelletier, E., Mangenot, S., Kuypers, M.M., Schreiber, F., Dutilh, B.E., Zedelius, J., de Beer, D., Gloerich, J., Wessels, H.J.C.T., van Alen, T., Luesken, F., Wu, M.L., van de Pas-Schoonen, K.T., Op den Camp, H.J.M., Janssen-Megens, E.M., Francoijs, K.J.,… Strous, M. (2010). Nitrite-driven anaerobic methane oxidation by oxygenic bacteria. *Nature*, 464 (7288), 543–548. https://doi.org/10.1038/nature08883.

Ettwig, K.F., Shima, S., van de Pas-Schoonen, K.T., Kahnt, J., Medema, M.H., Op den Camp, H.J.M., Jetten, M.S., and Strous, M. (2008). Denitrifying bacteria anaerobically oxidize methane in the absence of Archaea. *Environmental Microbiology*, 10, 3164–3173.

Evans, P. N., Boyd, J. A., Leu, A. O., Woodcroft, B. J., Parks, D. H., Hugenholtz, P., and Tyson, G. W. (2019). An evolving view of methane metabolism in the Archaea. *Nature Reviews Microbiology*, *17*(4), 219–232. https://doi.org/10.1038/s41579-018-0136-72

Fahrbach, M., Kuever, J., Meinke, R., Kämpfer, P., and Hollender, J. (2006). Denitratisoma oestradiolicum gen. nov., sp. nov., a 17β-oestradiol-degrading, denitrifying betaproteobacterium. *International Journal of Systematic and Evolutionary Microbiology*, 56(7), 1547–1552. https://doi.org/10.1099/ijs.0.63672-0

Falkowski. P. G. and Owens, T. G. (1980). Light-shade adaptation. Two strategies in marine phytoplankton. *Plant Physiology*, 66: 592-595

Fernandez, E., and Galvan, A. (2008). Nitrate assimilation in Chlamydomonas. *Eukaryotic Cell*, 7(4), 555-559.

Frank, E. D., Elgowainy, A., Han, J., and Wang, Z. (2013). Life cycle comparison of hydrothermal liquefaction and lipid extraction pathways to renewable diesel from algae. *Mitigation and Adaptation Strategies for Global Change*, 18(1), 137-158.

Fu, L., Ding, J., Lu, Y., Ding, Z., Bai, Y., and Zeng, R. J. (2017b). Hollow fiber membrane bioreactor affects microbial community and morphology of the DAMO and Anammox co-culture system. *Bioresource Technology*, 232, 247-253. doi: 10.1016/j.biortech.2017.02.048

Fu, L., Ding, J., Lu, Y., Ding, Z., and Zeng, R.J. (2017a). Nitrogen source effects on the denitrifying anaerobic methane oxidation culture and anaerobic ammonium oxidation bacteria enrichment process. *Applied Microbiology and Biotechnology*, 101 (9), 3895–3906. https:// doi.org/10.1007/s00253-017-8163-2.9

Fu, L., Ding, Z., Ding, J., Zhang, F., and Zeng, R.J. (2015). The role of paraffin oil on the interaction between denitrifying anaerobic methane oxidation and Anammox processes. *Applied Microbiology and Biotechnology*, 99 (19), 7925–7936. https://doi.org/10.1007/s00253-015- 6670-6.

Fu, L., Zhang, F., Bai, Y., Lu, Y., Ding, J., Zhou, D., Liu, Y., and Zeng, R.J. (2019). Mass transfer affects reactor performance, microbial morphology, and community succession in the methane-dependent denitrification and anaerobic ammonium oxidation co-culture. *Science of the Total Environment*, 651, 291–297. https://doi.org/10.1016/j.scitotenv.2018.09.184.

Fujii, N., Kuroda, K., Narihiro, T., Aoi, Y., Ozaki, N., Ohashi, A., and Kindaichi, T. (2022). Metabolic Potential of the Superphylum *Patescibacteria* Reconstructed from Activated Sludge Samples from a Municipal Wastewater Treatment Plant. *Microbes and Environments*, 37(3). https://doi.org/10.1264/jsme2.me22012

Gabor, E., Vries, E., and Janssen, D. (2003). Efficient recovery of environmental DNA for expression cloning by indirect extraction methods. *FEMS Microbiology Ecology*, *44*(2), 153–163. doi: 10.1016/s0168-6496(02)00462-2

Gao, D.W., and Tao, Y. (2011). Versatility and application of anaerobic ammonium-oxidizing bacteria. *Applied Microbiology and Biotechnology*, 91 (4), 887–894. https://doi.org/10.1007/ s00253-011-3411-3

Garcia, J., Mujeriego, R., and Hernandez-Marine, M. (2000). High rate algal pond operating strategies for urban wastewater nitrogen removal. *Journal of Applied Phycology*, 12(3), 331-339.

Gerritsen, J., Fuentes, S., Grievink, W., van Niftrik, L., Tindall, B. J., Timmerman, H. M., Rijkers, G. T., and Smidt, H. (2014). Characterization of Romboutsia ilealis gen. nov., sp. nov., isolated from the gastro-intestinal tract of a rat, and proposal for the reclassification of five closely related members of the genus clostridium into the genera Romboutsia gen. Nov., Intestinibacter gen. Nov., Terrisporobacter gen. Nov. and asaccharospora gen. nov.. *International Journal of Systematic and Evolutionary Microbiology*, 64(Pt_5), 1600–1616. https://doi.org/10.1099/ijs.0.059543-0

Glass, J. B., and Orphan, V. J. (2012). Trace Metal Requirements for Microbial Enzymes Involved in the Production and Consumption of Methane and Nitrous Oxide. *Frontiers in Microbiology*,*3*. doi:10.3389/fmicb.2012.00061

Glória, R. M., Motta, T. M., Silva, P. V. O., Costa, P. D., Brandt, E. M. F., Souza, C. L., and Chernicharo, C. A. L. (2016). Stripping And Dissipation Techniques For The Removal Of Dissolved Gases From Anaerobic Effluents. *Brazilian Journal of Chemical Engineering*, 33(4), 713–721. doi: 10.1590/0104-6632.20160334s20150291

González, L. E., Cañizares, R. O., and Baena, S. (1997). Efficiency of ammonia and phosphorus removal from a Colombian agroindustrial wastewater by the microalgae Chlorella vulgaris and Scenedesmus dimorphus. *Bioresource Technology*, 60(3), 259-262.

Graf, J. S., Mayr, M. J., Marchant, H. K., Tienken, D., Hach, P. F., Brand, A., Schubert, C., Kuypers, M., and Milucka, J. (2018). Bloom of a denitrifying methanotroph, ‘Candidatus Methylomirabilis limnetica’, in a deep stratified

lake. *Environmental Microbiology*, 20(7), 2598-2614. doi:10.1111/1462-2920.14285

Gu, J., Yang, Q., and Liu, Y. (2018). Mainstream anammox in a novel A-2B process for energy-efficient municipal wastewater treatment with minimized sludge production. *Water Research*, 138, 1–6. https://doi.org/10.1016/j.watres.2018.02.051

Guerrero, M. G., Vega, J. M., and Losada, M. (1981). The assimilatory nitrate-reducing system and its regulation. *Annual Review of Plant Physiology*, 32(1), 169-204.

Guerrero-Cruz, S., Stultiens, K., Van Kessel, M.A., Versantvoort, W., Jetten, M.S., Op den Camp, H.J., and Kartal, B. (2019). Key physiology of a nitrite-dependent methane-oxidizing enrichment culture. *Applied Environment and Microbiology*, 85 (8). https://doi.org/10.1128/aem. 00124-19.

Gutwinski, P., and Cema, G. (2016). Removal of Nitrogen and Phosphorus From Reject Water Using *Chlorella vulgaris* Algae After Partial Nitrification/Anammox Process. *Water Environment Research*, 88(1), 63–69. https://doi.org/10.2175/106143015x14362865227634

Hach. (2012). Water Analysis Handbook, 7th Edition. Colorado: Hach Company.

Hallam, S. J., Girguis, P. R., Preston, C. M., Richardson, P. M., and DeLong, E. F. (2003). Identification of methyl coenzyme M reductase A (mcrA) genes associated with methane-oxidizing archaea. *Applied Environment and Microbiology*, 69:5483-5491.

Halim, D. (2012). Energy Recovery in Wastewater Treatment. report for *City College of New York Department of Civil Engineering*.

Hammed, A. M., Prajapati, S. K., Simsek, S., and Simsek, H. (2016). Growth Regime and Environmental Remediation of Microalgae. *Algae*, 31(3), 189-204.

Han, P., and Gu, J. (2013). A newly designed degenerate PCR primer based on pmoA gene for detection of nitrite-dependent anaerobic methane-oxidizing bacteria from different ecological niches. *Applied Microbiology and Biotechnology*, 97(23), 10155-10162. doi:10.1007/s00253-013-5260-8

Han, W., Jin, W., Li, Z., Wei, Y., He, Z., Chen, C., Qin, C., Chen, Y., Tu, R. and Zhou, X. (2021). Cultivation of microalgae for lipid production using municipal wastewater. *Process Safety and Environmental Protection*, 155, 155-165.

Hanson, R. S., and Hanson, T. E. (1996). Methanotrophic bacteria. *Microbiology Reviews*, 60, 439-471.

Harb, R., Laçin, D., Subaşı, I., and Erguder, T. H. (2021). Denitrifying anaerobic methane oxidation (DAMO) cultures: Factors affecting their enrichment, performance and integration with anammox bacteria. *Journal of Environmental Management*, 295, 113070. https://doi.org/10.1016/j.jenvman.2021.113070

Haroon, M. F., Hu, S., Shi, Y., Imelfort, M., Keller, J., Hugenholtz, P., Yuan, Z., and Tyson, G. W. (2013). Anaerobic oxidation of methane coupled to nitrate reduction in a novel archaeal lineage. *Nature*, 500(7464), 567-570. doi:10.1038/nature12375

Hatamoto, M., Kimura, M., Sato, T., Koizumi, M., Takahashi, M., Kawakami, S., Araki, N., and Yamaguchi, T. (2014). Enrichment of Denitrifying Methane-Oxidizing Microorganisms Using Up-Flow Continuous Reactors and Batch Cultures. *PLoS ONE*, 9(12). doi: 10.1371/journal.pone.0115823

Hatamoto, M., Nemoto, S., and Yamaguchi, T. (2018). Effects of Copper and PQQ on the Denitrification Activities of Microorganisms Facilitating Nitrite- and Nitrate-Dependent DAMO Reaction. *International Journal of Environmental Research, 12*(5), 749-753. doi:10.1007/s41742-018-0118-7

Hatamoto, M., Sato, T., Nemoto, S., and Yamaguchi, T. (2017). Cultivation of denitrifying anaerobic methane-oxidizing microorganisms in a continuous-flow sponge bioreactor. *Applied Microbiology and Biotechnology*, 101(14), 5881-5888. doi:10.1007/s00253-017-8315-4

He, Z., Cai, C., Geng, S., Lou, L., Xu, X., Zheng, P., and Hu, B. (2013). Modeling a nitrite-dependent anaerobic methane oxidation process: Parameters identification and model evaluation. *Bioresource Technology*, 147, 315–320. https://doi.org/10.1016/j.biortech.2013.08.001

He, Z., Cai, C., Shen, L., Lou, L., Zheng, P., Xu, X., and Hu, B. (2014). Effect of inoculum sources on the enrichment of nitrite-dependent anaerobic methane-oxidizing bacteria. *Applied Microbiology and Biotechnology*, 99(2), 939-946. doi:10.1007/s00253-014-6033-8

He, Z., Feng, J., Wei, Z., Wu, S., Zou, J., and Pan, X. (2018a). Optimization of methane-dependent oxygenic denitrification in sequencing batch reactors by insights into the microbial interactions. *Science of the Total Environment*, 643, 623–631. https://doi.org/10.1016/j. scitotenv.2018.06.238.

He, Z., Feng, Y., Zhang, S., Wang, X., Wu, S., and Pan, X. (2018b). Oxygenic denitrification for nitrogen removal with less greenhouse gas emissions: microbiology and potential applications. *Science of the Total Environment*, 621, 453–464. https://doi.org/10.1016/j.scitotenv. 2017.11.280.

He, Z., Geng, S., Pan, Y., Cai, C., Wang, J., Wang, L., Liu, S., Zheng, P., Xu, X., and Hu, B. (2015a). Improvement of the trace metal composition of medium

for nitrite-dependent anaerobic methane oxidation bacteria: iron (II) and copper (II) make a difference. *Water Research*, 85, 235–243. https://doi.org/10.1016/j.watres.2015.08.040.

He, Z., Geng, S., Shen, L., Lou, L., Zheng, P., Xu, X., and Hu, B. (2015b). The short- and long-term effects of environmental conditions on anaerobic methane oxidation coupled to nitrite reduction. *Water Research, 68,* 554-562. doi:10.1016/j.watres.2014.09.055

He, Z., Wang, J., Zhang, X., Cai, C., Geng, S., Zheng, P., Xu, X., and Hu, B. (2015c). Nitrogen removal from wastewater by anaerobic methane-driven denitrification in a lab-scale reactor: Heterotrophic denitrifiers associated with denitrifying methanotrophs. *Applied Microbiology and Biotechnology*, 99(24), 10853–10860. https://doi.org/10.1007/s00253-015-6939-9

Heller, C., Hoppert, M., and Reitner, J. (2008). Immunological localization of coenzyme M reductase in anaerobic methane-oxidizing archaea of ANME 1 and ANME 2 type. *Geomicrobiology Journal*. 25, 149–156.

Hernández, D., Riaño, B., Coca, M., Solana, M., Bertucco, A., and García-González, M. C. (2016). Microalgae cultivation in high rate algal ponds using slaughterhouse wastewater for biofuel applications. *Chemical Engineering Journal*, 285, 449-458.

Hildebrand, M., Abbriano, R. M., Polle, J. E., Traller, J. C., Trentacoste, E. M., Smith, S. R., and Davis, A. K. (2013). Metabolic and cellular organization in evolutionarily diverse microalgae as related to biofuels production. *Current Opinion in Chemical Biology*, 17(3), 506-514.

Hinrichs, K.U., Hayes, J.M., Sylva, S.P., Brewer, P.G., and DeLong, E.F. (1999). Methane-consuming archaebacteria in marine sediments. *Nature*, 398, 802–805.

Hosokawa, S., Kuroda, K., Narihiro, T., Aoi, Y., Ozaki, N., Ohashi, A., and Kindaichi, T. (2021). Cometabolism of the Superphylum *Patescibacteria* with Anammox Bacteria in a Long-Term Freshwater Anammox Column Reactor. *Water*, 13(2), 208. https://doi.org/10.3390/w13020208

Hu, B., He, Z., Geng, S., Cai, C., Lou, L., Zheng, P., and Xu, X. (2014). Cultivation of nitrite-dependent anaerobic methane-oxidizing bacteria: impact of reactor configuration. *Applied Microbiology and Biotechnology*, 98 (18), 7983–7991. https://doi.org/10.1007/s00253-014-5835- z.

Hu, S., Zeng, R. J., Haroon, M. F., Keller, J., Lant, P. A., Tyson, G. W., and Yuan, Z. (2015). A laboratory investigation of interactions between denitrifying anaerobic methane oxidation (DAMO) and anammox processes in anoxic environments. *Scientific Reports,5*, 8706.

Hu, S., Zeng, R.J., Burow, L.C., Lant, P., Keller, J., and Yuan, Z. (2009). Enrichment of denitrifying anaerobic methane oxidizing microorganisms. *Environmental Microbiology*, Rep. 1, 377–384.

Hu, S., Zeng, R.J., Keller, J., Lant, P.A., and Yuan, Z. (2011). Effect of nitrate and nitrite on the selection of microorganisms in the denitrifying anaerobic methane oxidation process. *Environmental Microbiology*, Rep. 3, 315–319.

Hu, Q., Sommerfeld, M., Jarvis, E., Ghirardi, M., Posewitz, M., Seibert, M., and Darzins, A. (2008). Microalgal triacylglycerols as feedstocks for biofuel production: perspectives and advances. *The Plant Journal*, 54(4), 621-639. doi:10.1111/j.1365-313x.2008.03492.x

Islas-Lima, S., Thalasso, F., and Gómez-Hernandez, J. (2004). Evidence of anoxic methane oxidation coupled to denitrification. *Water Research*, 38 (1), 13–16. https://doi.org/10.1016/ j.watres.2003.08.024.

Jetten, M. S. (2008). The microbial nitrogen cycle. *Environmental Microbiology*, 10(11), 2903-2909. doi:10.1111/j.1462-2920.2008.01786.x

Jetten, M. S. M., Cirpus, I., Kartal, B., van Niftrik, L. A. M. P., van De Pas-Schoonen, K. T., Sliekers, O., Haaijer, S., van der Star, W., Schmid, M., van de Vossenberg, J. L. C. M. and Schmidt, I., (2005). 1994–2004: 10 years of research on the anaerobic oxidation of ammonium. *Biochemical Society Transactions*, 33(1), 119-123.

Jiang, L., Hu, Z., Wang, Y., Ru, D., Li, J., and Fan, J. (2018). Effect of trace elements on the development of co-cultured nitrite-dependent anaerobic methane oxidation and methanogenic bacteria consortium. *Bioresource Technology*, 268, 190–196. https://doi.org/ 10.1016/j.biortech.2018.07.139.

Jin, R., Ma, C., Mahmood, Q., Yang, G., and Zheng, P. (2011). Anammox in a UASB reactor treating saline wastewater. *Process Safety and Environmental. Protection*, 89 (5), 342–348. https://doi. org/10.1016/j.psep.2011.05.001.

Jin, R., Yang, G., Zhang, Q., Ma, C., Yu, J., and Xing, B. (2013). The effect of sulfide inhibition on the Anammox process. *Water Research*. 47 (3), 1459–1469. https://doi.org/10.1016/j. watres.2012.12.018.

Kadam, K. L. (2001). (technical report). *Microalgae Production from Power Plant Flue Gas: Environmental Implications on a Life Cycle Basis* (pp. 1–55). Golden, Colorado: National Renewable Energy Laboratory.

Kampman, C., Hendrickx, T.L., Luesken, F.A., van Alen, T.A., Op den Camp, H.J., Jetten, M.S., Zeeman, G., Buisman, C.J.N., and Temmink, H. (2012). Enrichment of denitrifying methanotrophic bacteria for application after direct low-temperature anaerobic sewage treatment. *Journal of Hazardous Materials*, 227–228, 164–171. https://doi.org/10.1016/j.jhazmat. 2012.05.032.

Kampman, C., Piai, L., Temmink, H., Hendrickx, T.L., Zeeman, G., and Buisman, C.J. (2018). Effect of low concentrations of dissolved oxygen on the activity of denitrifying methanotrophic bacteria. *Water Science Technology*, 77 (11), 2589–2597. https://doi.org/10. 2166/wst.2018.219.

Kampman, C., Temmink, H., Hendrickx, T.L.G., Zeeman, G., and Buisman, C.J.N. (2014). Enrichment of denitrifying methanotrophic bacteria from municipal wastewater sludge in a membrane bioreactor at 20 °C. *Journal of Hazardous Materials*, 274, 428–435.

Kamyab, H., Md Din, M. F., Lee, C. T., Keyvanfar, A., Shafaghat, A., Majid, M. Z. A., Ponraj, M. and Yun, T. X. (2015). Lipid production by microalgae Chlorella pyrenoidosa cultivated in palm oil mill effluent (POME) using hybrid photo bioreactor (HPBR). *Desalination and Water Treatment*, 55(13), 3737-3749.

Kang, R., Wang, J., Shi, D., Cong, W., Cai, Z., and Ouyang, F. (2004). Interactions between organic and inorganic carbon sources during mixotrophic cultivation of Synechococcus sp. *Biotechnology Letters*, 26(18), 1429-1432.

Kartal, B., van Niftrik, L., Rattray, J., van De Vossenberg, J. L., Schmid, M. C., Damsté, J. S., Jetten, M. S. M. and Strous, M. (2008). Candidatu s 'Brocadia fulgida': an autofluorescent anaerobic ammonium oxidizing bacterium. *FEMS microbiology ecology*, 63(1), 46-55.

Khalil, Z. I., Asker, M. M., El-Sayed, S., Kobbia, I. A. (2010). Effect of pH on growth and biochemical of Donaliella and Chlorella. *World Journal of Microbiology and Biotechnology*, 26, 1225-1231.

Khalili, A., Najafpour, G. D., Amini, G., and Samkhaniyani, F. (2015). Influence of nutrients and LED light intensities on biomass production of microalgae

Chlorella vulgaris. *Biotechnology and Bioprocess Engineering*, 20(2), 284-290.

Khan, A., Gaur, R., Lew, B., Mehrotra, I., and Kazmi, A. (2011). Effect of Aeration on the Quality of Effluent from UASB Reactor Treating Sewage", *Journal of Environmental Engineering*, 137(6), 464-471.

Khan, S. A., R., Hussain, M. Z., Prasad, S., and Banerjee, U. (2009). Prospects of Biodiesel Production from Microalgae in India. *Renewable and Sustainable Energy Reviews*, 13(9), 2361-2372.

Khanzada, Z. T. (2020). Phosphorus removal from landfill leachate by microalgae. *Biotechnology Reports*, 25, e00419.

Kindaichi, T., Awata, T., Suzuki, Y., Tanabe, K., Hatamoto, M., Ozaki, N., and Ohashi, A. (2011). Enrichment using an up-flow column reactor and community structure of marine anammox bacteria from coastal sediment. *Microbes and Environments*, 26(1), 67-73.

Kitanou, S., Ayyoub, H., Touir, J., Zdeg, A., Benabdallah, S., Taky, M., and Elmidaoui, A. (2021). A comparative examination of MBR and SBR Performance for Municipal Wastewater treatment. *Water Practice and Technology*, 16(2), 582–591. https://doi.org/10.2166/wpt.2021.016

Knittel, K., and Boetius, A. (2009). Anaerobic oxidation of methane: Progress with an unknown process. *Annual Review of Microbiology*, 63(1), 311–334. https://doi.org/10.1146/annurev.micro.61.080706.093130

Knittel, K., Lösekann, T., Boetius, A., Kort, R., and Amann, R. (2005). Diversity and Distribution of Methanotrophic Archaea at Cold Seeps. *Applied and Environmental Microbiology*, 71(1), 467-479.

Kocamemi, B. A., Dityapak, D., Semerci, N., Keklik, E., Akarsubası, A., Kumru, M., and Kurt, H. (2018). Anammox start-up strategies: the use of local mixed activated sludge seed versus Anammox seed. *Water Science and Technology*, 78(9), 1901-1915.

Koch, H., van Kessel, M. A., and Lücker, S. (2019). Complete Nitrification: Insights into the Ecophysiology of Comammox Nitrospira. *Applied Microbiology and Biotechnology*, 103(1), 177-189.

Kojima, H., and Fukui, M. (2011). Sulfuritalea hydrogenivorans gen. nov., sp. nov., a facultative autotroph isolated from a freshwater lake. *International Journal of Systematic and Evolutionary Microbiology*, 61(7), 1651–1655. https://doi.org/10.1099/ijs.0.024968-0

Kojima, E., and Zhang, K. (1999). Growth and hydrocarbon production of microalga Botryococcus braunii in bubble column photobioreactors. *Journal of Bioscience and Bioengineering*, 87(6), 811-815. doi:10.1016/s1389-1723(99)80158-3

Kojima, H., Shinohara, A., and Fukui, M. (2015). Sulfurifustis variabilis gen. Nov., sp. nov., a sulfur oxidizer isolated from a lake, and proposal of Acidiferrobacteraceae Fam. nov. and Acidiferrobacterales Ord. Nov. *International Journal of Systematic and Evolutionary Microbiology*, 65(Pt_10), 3709–3713. https://doi.org/10.1099/ijsem.0.000479

Kojima, H., Tsutsumi, M., Ishikawa, K., Iwata, T., Mußmann, M., and Fukui, M. (2012). Distribution of putative denitrifying methane oxidizing bacteria in sediment of a freshwater lake, Lake Biwa. *Systematic and Applied Microbiology*, 35 (4), 233–238. https://doi.org/10. 1016/j.syapm.2012.03.005.

Kong, W., Song, H., Cao, Y., Yang, H., Hua, S., and Xia, C. (2011). The characteristics of biomass production, lipid accumulation and chlorophyll biosynthesis of Chlorella vulgaris under mixotrophic cultivation. *African Journal of Biotechnology*, 10(55), 11620-11630.

Konopka, A., and Brock, T. D. (1978). Effect of temperature on blue-green algae (cyanobacteria) in Lake Mendota. *Applied and Environmental Microbiology*, 36(4), 572-576.

Kuenen, J. (2008). Anammox bacteria: From discovery to application. *Nature Reviews Microbiology*, 6, 320-326.

Kumar, D., Chaturvedi, M. K., Sharma, S. K., and Asolekar, S. R. (2015). Sewage-fed aquaculture: a sustainable approach for wastewater treatment and reuse. *Environmental Monitoring and Assessment*, 187(10), 1-10.

Laçin, D. (2021). *Denitrifying Anaerobic Methane Oxidation (DAMO) Microorganisms: Investigation of Their Occurrence And Enrichment* [M.S. - Master of Science]. Middle East Technical University.

Langone, M., Yan, J., Haaijer, S.C., Op Den Camp, H.J.M., Jetten, M.S., and Andreottola, G. (2014). Coexistence of nitrifying, anammox and denitrifying bacteria in a sequencing batch reactor. *Frontiers in Microbiology*, 5. https://doi.org/10.3389/fmicb.2014.00028.

Larsdotter, K. (2006). Wastewater treatment with microalgae-a literature review. *Vatten*, 62(1), 31.

Latham, E. A., Anderson, R. C., Pinchak, W. E., and Nisbet, D. J. (2016). Insights on Alterations to the Rumen Ecosystem by Nitrate and Nitrocompounds. *Frontiers in microbiology*, 7, 228.

Lee, Y. K. (2001). Microalgal mass culture systems and methods: Their limitation and potential. *Journal of Applied Phycology*, 13,307. doi: 10.1023/A:1017560006941

Leliaert, F., Smith, D. R., Moreau, H., Herron, M. D., Verbruggen, H., Delwiche, C. F., and De Clerck, O. (2012). Phylogeny and molecular evolution of the green algae. *Critical Reviews in Plant Sciences*, 31(1), 1-46.

Li, J., Lou, J., and Lv, J. (2020a). The effect of sulfate on nitrite-denitrifying anaerobic methane oxidation (nitrite-DAMO) process. *Science of the Total Environment*, 731, 139160. https://doi.org/10. 1016/j.scitotenv.2020.139160.

Li, W., Lu, P., Chai, F., Zhang, L., Han, X., and Zhang, D. (2018a). Long-term nitrate removal through methane-dependent denitrification microorganisms in sequencing batch reactors fed with only nitrate and methane. *AMB Express*, 8 (1). https://doi.org/10. 1186/s13568-018-0637-9.

Li, W., Lu, P., Zhang, L., Ding, A., Wang, X., Yang, H., and Zhang, D. (2020b). Long-term performance of denitrifying anaerobic methane oxidation under stepwise cooling and ambient temperature conditions. *Science of the Total Environment*, 713, 136739. https://doi.org/10. 1016/j.scitotenv.2020.136739.

Li, X., Klaus, S., Bott, C., and He, Z. (2018b). Status, Challenges, and Perspectives of Mainstream Nitritation–Anammox for Wastewater Treatment. *Water Environment Research*, 90(7), 634-649.

Liang, Y., Sarkany, N., and Cui, Y. (2009). Biomass and lipid productivities of *Chlorella vulgaris* under autotrophic, heterotrophic and mixotrophic growth conditions. *Biotechnology Letters*, 31(7), 1043-1049. doi:10.1007/s10529-009-9975-7

Lim, Z. K., Liu, T., Zheng, M., Yuan, Z., Guo, J., and Hu, S. (2021). Versatility of nitrite/nitrate-dependent anaerobic methane oxidation (N-DAMO): First

demonstration with real wastewater. *Water Research*, 194, 116912. https://doi.org/10.1016/j.watres.2021.116912

Lin, L., Pratt, S., Rattier, M., and Ye, L. (2020). Individual and combined effect of salinity and nitrite on freshwater anammox bacteria (FAB). *Water Research*, 169, 114931. https://doi.org/ 10.1016/j.watres.2019.114931.

Liu, T., Hu, S., and Guo, J. (2019). Enhancing mainstream nitrogen removal by employing nitrate/nitrite-dependent anaerobic methane oxidation processes. *Critical Reviews in Biotechnology*, 39 (5), 732–754. https://doi.org/10.1080/07388551.2019.1598333.

Liu, J., Mao, X., Zhou, W., and Guarnieri, M. T. (2016a). Simultaneous production of triacylglycerol and high-value carotenoids by the astaxanthin-producing oleaginous green microalga *Chlorella zofingiensis*. *Bioresource Technology*, 214, 319-327.

Liu, X., Xu, Z., Peng, J., Song, Y., and Meng, X. (2016b). Phosphate recovery from anaerobic digester effluents using $CaMg(OH)_4$. *Journal of Environmental Sciences*, 44(2016), 260–268.

Lopes, F., Viollier, E., Thiam, A., Michard, G., Abril, G., Groleau, A., Prévot, F., Carrias, J. F., Albéric, P., and Jézéquel, D. (2011). Biogeochemical modelling of anaerobic vs. aerobic methane oxidation in a meromictic crater lake (Lake Pavin, France). *Applied Geochemistry*, 26 (12), 1919–1932. https://doi.org/10.1016/j.apgeochem.2011.06.021.

Lopez, H., Puig, S., Ganigué, R., Ruscalleda, M., Balaguer, M. D., and Colprim, J. (2008). Start-up and enrichment of a granular anammox SBR to treat high nitrogen load wastewaters. *Journal of Chemical Technology & Biotechnology*, 83(3), 233-241. doi:10.1002/jctb.1796

Lotti, T., Kleerebezem, R., Lubello, C., and van Loosdrecht, M. (2014). Physiological and kinetic characterization of a suspended cell anammox culture. *Water Research*, 60, 1–14. https://doi.org/10.1016/j.watres.2014.04.017.

Lou, J., Jin, H., Li, J., Lv, J., Xu, F., and Wang, R. (2022). The mechanism of sulfate on a nitrate denitrifying anaerobic methane oxidation system. *Environmental Science: Water Research and Technology*, 8(12), 2884–2894. https://doi.org/10.1039/d2ew00336h

Lou, J., Wang, X., Li, J., and Han, J. (2019). The short- and long-term effects of nitrite on denitrifying anaerobic methane oxidation (DAMO) organisms. *Environmental Science Pollution Research*, 26 (5), 4777–4790. https://doi.org/10.1007/s11356-018-3936-4.

Lu, P., Liu, T., Ni, B., Guo, J., Yuan, Z., and Hu, S. (2019). Growth kinetics of Candidatus 'Methanoperedens nitroreducens' enriched in a laboratory reactor. *Science of the Total Environmental*, 659, 442–450. https://doi.org/10.1016/j.scitotenv.2018.12.351.

Lu, Y., Fu, L., Li, N., Ding, J., Bai, Y., Samaras, P., and Zeng, R.J. (2018). The content of trace element iron is a key factor for competition between anaerobic ammonium oxidation and methane-dependent denitrification processes. *Chemosphere 198*, 370–376. https:// doi.org/10.1016/j.chemosphere.2018.01.172.

Luesken, F., Sánchez, J., Alen, T., Sanabria, J., Op Den Camp, H., Jetten, M., and Kartal, B. (2011b). Simultaneous Nitrite-Dependent Anaerobic Methane and Ammonium Oxidation Processes. *Applied and Environmental Microbiology*, 77(19), 6802-6807. doi:10.1128/aem.05539-11

Luesken, F., van Alen, T., Biezen, E., Frijters, C., Toonen, G., Kampman, C., Hendrickx, T., Zeeman, G., Temmink, H., Strous, M., Op den Camp, H., and Jetten, M. (2011a). Diversity and enrichment of nitrite-dependent anaerobic methane oxidizing bacteria from wastewater sludge. *Applied Microbiology and Biotechnology*, 92 (4), 845–854. https://doi.org/10.1007/s00253- 011-3361-9.

Luesken, F., Wu, M., Op den Camp, H., Keltjens, J., Stunnenberg, H., Francoijs, K., Strous, M., and Jetten, M. (2012). Effect of oxygen on the anaerobic methanotroph "Candidatus Methylomirabilis oxyfera": kinetic and transcriptional analysis. *Environmental Microbiology*, 14 (4), 1024–1034. https://doi.org/10.1111/j.1462-2920.2011.02682.x.

Luo, G., Wang, W., and Angelidaki, I. (2014). A new degassing membrane coupled upflow anaerobic sludge blanket (UASB) reactor to achieve in-situ biogas upgrading and recovery of dissolved CH_4 from the anaerobic effluent, *Applied Energy*, 132(2014), 536-542.

Manser, N.D., Wang, M., Ergas, S.J., Mihelcic, J.R., Mulder, A., van de Vossenberg, J., van Lier, J.B., and van der Steen, P. (2016). Biological nitrogen removal in a photo-sequencing batch reactor with an algal-nitrifying bacterial consortium and anammox granules. *Environmental Science and Technology Letters*, 3 (4), 175–179. https://doi.org/10.1021/acs.estlett. 6b00034.

Mechichi, T., Stackebrandt, E., Gad'on, N., and Fuchs, G. (2002). Phylogenetic and metabolic diversity of bacteria degrading aromatic compounds under denitrifying conditions, and description of Thauera Phenylacetica sp. nov., Thauera aminoaromatica sp. nov., and Azoarcus Buckelii sp. nov.. *Archives of Microbiology*, 178(1), 26–35. https://doi.org/10.1007/s00203-002-0422-6

Meidensha Corporation. (2015). Single-stage ammonium removal treatment - DEMON® Deammonification System. Retrieved March 26, 2017, from

http://www.meidensha.com/products/water/prod_06/prod_06_03/index.html

Meyerdierks, A., Kube, M., Kostadinov, I., Teeling, H., Glöckner, F.O., Reinhardt, R., and Amann, R. (2010). Metagenome and mRNA expression analyses of anaerobic methanotrophic archaea of the ANME-1 group. *Environmental Microbiology*, 12 (2), 422–439. https://doi.org/10.1111/j.1462-2920.2009.02083.x.

Min, M., Wang, L., Li, Y., Mohr, M. J., Hu, B., Zhou, W., Chen, P. and Ruan, R. (2011). Cultivating Chlorella sp. in a pilot-scale photobioreactor using centrate wastewater for microalgae biomass production and wastewater nutrient removal. *Applied Biochemistry and Biotechnology*, 165(1), 123-137.

Modin, O., Fukushi, K., and Yamamoto, K. (2007). Denitrification with methane as external carbon source. *Water Research*, 41 (12), 2726–2738.

Molina Grima, E., Belarbi, E., Fernández, F. A., Medina, A. R., and Chisti, Y. (2003). Recovery of microalgal biomass and metabolites: process options and economics. *Biotechnology Advances*, 20(7-8), 491-515. doi:10.1016/s0734-9750(02)00050-2

Molinuevo-Salces, B., Riaño, B., Hernández, D., and Cruz García-González, M. (2019). Microalgae and wastewater treatment: advantages and disadvantages. In *Microalgae biotechnology for development of biofuel and wastewater treatment* (pp. 505-533). Springer, Singapore.

Morales-Sánchez, D., Martinez-Rodriguez, O. A., Kyndt, J., and Martinez, A. (2015). Heterotrophic growth of microalgae: metabolic aspects. *World Journal of Microbiology and Biotechnology*, 31(1), 1-9.

Morgenroth, E., Eberl, H. J., van Loosdrecht, M. C. M., Noguera, D. R., Pizarro, G. E., Picioreanu, C., Rittmann, B. E., Schwarz, A. O., and Wanner, O. (2004).

Comparing biofilm models for a single species biofilm system. *Water Science and Technology*, 49(11-12), 145–154. https://doi.org/10.2166/wst.2004.0826

Muñoz, R., and Guieysse, B. (2006). Algal–bacterial processes for the treatment of hazardous contaminants: a review. Water Research, 40(15), 2799-2815.

Nauhaus, K., Boetius, A., Kruger, M., and Widdel, F. (2002). In vitro demonstration of anaerobic oxidation of methane coupled to sulphate reduction in sediment from a marine gas hydrate area. *Environmental Microbiology*, 4 (5), 296–305. https://doi.org/10.1046/j.1462-2920. 2002.00299.x.

Nie, W., Xie, G., Ding, J., Lu, Y., Liu, B., Xing, D., Wang, Q., Han, H., Yuan, Z., and Ren, N. (2019). High performance nitrogen removal through integrating denitrifying anaerobic methane oxidation and Anammox: from enrichment to application. *Environment International*, 132 (May), 105107. https://doi.org/10.1016/j.envint.2019.105107.

Nie, W., Xie, G., Ding, J., Peng, L., Lu, Y., Tan, X., Yue, H., Liu, B., Xing, D., Meng, J., Han, H., and Ren, N. (2020). Operation strategies of N-DAMO and anammox process based on microbial interactions for high-rate nitrogen removal from landfill leachate. *Environment International*, 139, 105596. https://doi.org/10.1016/j.envint.2020.105596.

Noophan, P., Sripiboon, S., Damrongsri, M., and Munakata-Marr, J. (2009). Anaerobic ammonium oxidation by Nitrosomonas spp. and anammox bacteria in a sequencing batch reactor. *Journal of Environmental Management*, 90(2), 967-972. doi:10.1016/j.jenvman.2008.03.003

Noyola, A., Morgan-Sagastume, J., and López-Hernández, J. (2006). Treatment of biogas produced in anaerobic reactors for domestic wastewater: Odor control

and energy/resource recovery, *Reviews in Environmental Science and Biotechnology*, 5(2006) 93–114.

Nozhevnikova, A. N., Simankova, M. V., and Litti, Y. V. (2012). Application of the microbial process of anaerobic ammonium oxidation (ANAMMOX) in biotechnological wastewater treatment. *Applied Biochemistry and Microbiology*, 48(8), 667-684. doi:10.1134/s0003683812080042

Nyberg, U., Andersson, B., and Aspegren, H. (1996). Long-term experiences with external carbon sources for nitrogen removal. *Water Science Technologies*. 33, 109–116.

Ontiveros-Valencia, A., Ilhan, Z. E., Kang, D.-W., Rittmann, B., and Krajmalnik-Brown, R. (2013). Phylogenetic Analysis of Nitrate- and Sulfate-Reducing Bacteria in a Hydrogen-Fed Biofilm. *FEMS Microbiology Ecology*, 85(1), 158–167. https://doi.org/10.1111/1574-6941.12107

Op den Camp, H. J., Islam, T., Stott, M. B., Harhangi, H. R., Hynes, A., Schouten, S., Jetten, M. S., Birkeland, N.-K., Pol, A., and Dunfield, P. F. (2009). Environmental, genomic and taxonomic perspectives on Methanotrophic *Verrucomicrobia*. *Environmental Microbiology Reports*, *1*(5), 293–306. https://doi.org/10.1111/j.1758-2229.2009.00022.x

Oremland, R.S. (2010). Biogeochemistry: NO connection with methane. *Nature 464*, (7288), 500–501. https://doi.org/10.1038/464500a.

Oulas, A., Pavloudi, C., Polymenakou, P., Pavlopoulos, G. A., Papanikolaou, N., Kotoulas, G., Arvanitidis, C., and Iliopoulos, I. (2015). Metagenomics: Tools and insights for analyzing next-generation sequencing data derived from Biodiversity Studies. *Bioinformatics and Biology Insights*, 9. https://doi.org/10.4137/bbi.s12462

Park, J. E., Zhang, S., Han, T. H., and Hwang, S. J. (2021). The contribution ratio of autotrophic and heterotrophic metabolism during a mixotrophic culture of *Chlorella sorokiniana*. *International Journal of Environmental Research and Public Health*, 18(3), 1353.

Perez-Garcia, O., Escalante, F. M., De-Bashan, L. E., and Bashan, Y. (2011). Heterotrophic cultures of microalgae: metabolism and potential products. *Water Research*, 45(1), 11-36.

Posadas, E., García-Encina, P. A., Domínguez, A., Díaz, I., Becares, E., Blanco, S., and Munoz, R. (2014). Enclosed tubular and open algal–bacterial biofilm photobioreactors for carbon and nutrient removal from domestic wastewater. *Ecological Engineering*, 67, 156-164.

Pragya, N., Pandey, K. K., and Sahoo, P. K. (2013). A review on harvesting, oil extraction and biofuels production technologies from microalgae. *Renewable and Sustainable Energy Reviews*, 24, 159-171.

Qiang, H., and Richmond, A. (1996). Productivity and photosynthetic efficiency of Spirulina platensis as affected by light intensity, algal density and rate of mixing in a flat plate photobioreactor. *Journal of Applied Phycology*, 8(2), 139-145. doi:10.1007/bf02186317

Raghoebarsing, A., Pol, A., van de Pas-Schoonen, K., Smolders, A., Ettwig, K., Rijpstra, W., Schouten, S., Sinninghe Damsté, J., Op den Camp, H., Jetten, M., and Strous, M. (2006). A microbial consortium couples anaerobic methane oxidation to denitrification. *Nature 440*, 918–921.

Rattray, J. E., van de Vossenberg, J., Hopmans, E.C., Kartal, B., van Niftrik, L., Rijpstra, W. I. C., Strous, M., Jetten, M. S., Schouten, S., and Sinninghe Damsté, J. S. (2008). Ladderane lipid distribution in four genera of anammox bacteria. *Archives of Microbiology*, 190, 51–66.

Rawat, I., Kumar, R. R., Mutanda, T., and Bux, F. (2011). Dual role of microalgae: phycoremediation of domestic wastewater and biomass production for sustainable biofuels production. *Applied Energy*, 88(10), 3411-3424.

Reeburgh, W. (1976). Methane consumption in Cariaco Trench waters and sediments. *Earth and Planetary Science Letters*, 28, 337–344.

Reino, C., Suarez-Ojeda, M., Perez J., and Carrera, J. (2018). Stable long-term operation of an upflow anammox sludge bed reactor at mainstream conditions, *Water Research*, 128(2018), 331-341.

Renou, S., Givaudan, J., Poulain, S., Dirassouyan, F., and Moulin, P. (2008). Landfill leachate treatment: review and opportunity. *Journal of Hazardous Materials*, 150 (3), 468–493. https://doi.org/ 10.1016/j.jhazmat.2007.09.077.

Riaño, B., Molinuevo, B., and García-González, M. C. (2011). Treatment of fish processing wastewater with microalgae-containing microbiota. *Bioresource Technology*, 102(23), 10829-10833.

Richmond, A. (2004). *Handbook of microalgal culture: Biotechnology and applied phycology*. Oxford, OX, UK: Blackwell Science.

Rodrigues, D. B., Menezes, C. R., Mercadante, A. Z., Jacob-Lopes, E., and Zepka, L. Q. (2015). Bioactive pigments from microalgae Phormidium autumnale. *Food Research International*, 77, 273-279.

Rogelj, J., Schaeffer, M., Meinshausen, M., Shindell, D. T., Hare, W., Klimont, Z., and Schellnhuber, H. J. (2014). Disentangling the effects of CO_2 and short-lived climate forcer mitigation. *Proceedings of the National Academy of Sciences of the USA*, 111(46), 16325-16330. doi:10.1073/pnas.1415631111.

Ryu, B. G., Kim, J., Yoo, G., Lim, J. T., Kim, W., Han, J. I., and Yang, J. W. (2014). Microalgae-mediated simultaneous treatment of toxic thiocyanate and production of biodiesel. *Bioresource Technology*, 158, 166-173.

Safi, C., Zebib, B., Merah, O., Pontalier, P. Y., and Vaca-Garcia, C. (2014). Morphology, composition, production, processing and applications of *Chlorella vulgaris*: A review. *Renewable and Sustainable Energy Reviews*, 35, 265-278.

Sakarika, M., and Kornaros, M. (2016). Effect of pH on growth and lipid accumulation kinetics of the microalga Chlorella vulgaris grown heterotrophically under sulfur limitation. *Bioresource Technology*, 219, 694-701.

Sánchez, A., Rodríguez-Hernández, L., Buntner, D., Esteban-García, A., Tejero, I., and Garrido, J.M. (2016). Denitrification coupled with methane oxidation in a membrane bioreactor after methanogenic pre-treatment of wastewater. *Journal of Chemical Technology and Biotechnology*, 91 (12), 2950–2958. https://doi.org/10.1002/jctb.4913.

Saricheewin, K., Sirivithayapakorn, S., Noophan, P. L., Wantawin, C., Techkarnjanaruk, S., and Munakata-Marr, J. (2010). Nitrogen removal of anammox cultures under different enrichment conditions. *Journal of Environmental Science and Health, Part A*, 45(14), 1832-1838.

Scheller, S., Goenrich, M., Boecher, R., Thauer, R., and Jaun, B. (2010). The key nickel enzyme of methanogenesis catalyses the anaerobic oxidation of methane. *Nature 465*, 606–608.

Schmid, M. C., Risgaard- Petersen, N., van De Vossenberg, J., Kuypers, M. M., Lavik, G., Petersen, J., Hulth, S., Thamdrup, B., Canfield, D., Dalsgaard, T. and Rysgaard, S., (2007). Anaerobic ammonium- oxidizing bacteria in

marine environments: widespread occurrence but low diversity. *Environmental Microbiology*, 9(6), 1476-1484.

Schmidt, I., Sliekers, O., Schmid, M., Cirpus, I., Strous, M., Bock, E., Kuenen, J., and Jetten, M. (2002). Aerobic and anaerobic ammonia oxidizing bacteria – competitors or natural partners? *FEMS Microbiology Ecology*, 39(3), 175–181. https://doi.org/10.1016/s0168-6496(01)00208-2

Sharma, P. K., Saharia, M., Srivstava, R., Kumar, S., and Sahoo, L. (2018). Tailoring microalgae for efficient biofuel production. *Frontiers in Marine Science*, 5, 382.

Shen, L., He, Z., Zhu, Q., Chen, D., Lou, L., Xu, X., Zheng, P., and Hu, B. (2012). Microbiology, ecology, and application of the nitrite-dependent anaerobic methane oxidation process. *Frontiers in Microbiology*, 3, 1–5. https://doi.org/10.3389/fmicb.2012.00269.

Shen, L., Liu, S., He, Z., Lian, X., Huang, Q., He, Y., Lou, L., Xu, X., Zheng, P., and Hu, B. (2015). Depth-specific distribution and importance of nitrite-dependent anaerobic ammonium and methane-oxidising bacteria in an urban wetland. *Soil Biology and Biochemistry*, 83, 43–51. https://doi.org/10.1016/j.soilbio.2015.01.010.

Shen, L., Liu, S., Zhu, Q., Li, X., Cai, C., Cheng, D., Lou, L., Xu, X., Zheng, P., and Hu, B. (2013). Distribution and Diversity of Nitrite-Dependent Anaerobic Methane-Oxidising Bacteria in the Sediments of the Qiantang River. *Microbial Ecology*, 67 (2), 341–349. https://doi. org/10.1007/s00248-013-0330-0

Shen, L., Wu, H., and Gao, Z. (2014). Distribution and environmental significance of nitrite dependent anaerobic methane-oxidising bacteria in natural

ecosystems. *Applied Microbiology and Biotechnology*, 99 (1), 133–142. https://doi.org/10.1007/s00253- 014-6200-y

Shi, Y., Hu, S., Lou, J., Lu, P., Keller, J., and Yuan, Z. (2013). Nitrogen removal from wastewater by coupling anammox and methane-dependent denitrification in a membrane biofilm reactor. *Environmental Science and Technology*, 47 (20), 11577–11583.

Silva-Teira, A., Sánchez, A., Buntner, D., Rodríguez-Hernández, L., and Garrido, J. (2017). Removal of dissolved methane and nitrogen from anaerobically treated effluents at low temperature by MBR post-treatment. *Chemical Engineering Journal*, 326, 970–979. https://doi.org/10.1016/j.cej.2017.06.047.

Singh, D., Nedbal, L., and Ebenhöh, O. (2018). Modelling phosphorus uptake in microalgae. *Biochemical Society Transactions*, 46(2), 483-490.

Singh, S. P., and Singh, P. (2014). Effect of CO_2 concentration on algal growth: a review. *Renewable and Sustainable Energy Reviews*, 38, 172-179.

Singh, U. B., and Ahluwalia, A. S. (2012). Microalgae: A Promising Tool for Carbon Sequestration. *Mitigation and Adaptation Strategies for Global Change*, 18(1), 73-95.

Singleton, C. M., Petriglieri, F., Kristensen, J. M., Kirkegaard, R. H., Michaelsen, T. Y., Andersen, M. H., Kondrotaite, Z., Karst, S. M., Dueholm, M. S., Nielsen, P. H., and Albertsen, M. (2021). Connecting structure to function with the recovery of over 1000 high-quality metagenome-assembled genomes from activated sludge using long-read sequencing. *Nature Communications*, 12(1). https://doi.org/10.1038/s41467-021-22203-2

Sleytr, U., and Beveridge, T. (1999). Bacterial S-layers. *Trends in Microbiology*, 7 (6), 253–260. https://doi.org/10.1016/s0966-842x(99)01513-9.

Smemo, K., and Yavitt, J. (2007). Evidence for anaerobic CH_4 oxidation in freshwater peatlands. *Geomicrobiology*, 24 (7–8), 583–597. https://doi.org/10.1080/ 01490450701672083.

Smith, A. L., Kelly, D. P., and Wood, A. P. (1980). Metabolism of thiobacillus A2 grown under autotrophic, mixotrophic and heterotrophic conditions in chemostat culture. *Microbiology*, 121(1), 127–138. https://doi.org/10.1099/00221287-121-1-127

Solovchenko, A., Gorelova, O., Karpova, O., Selyakh, I., Semenova, L., Chivkunova, O., Baulina, O., Vinogradova, E., Pugacheva, T., Scherbakov, P., Vasilieva, S., Lukyanov, A. and Lobakova, E. (2020). Phosphorus feast and famine in cyanobacteria: is luxury uptake of the nutrient just a consequence of acclimation to its shortage?. *Cells*, 9(9), 1933.

Stocker, T. F., Qin, D., Plattner, G. -K., Tignor, M., Allen, S. K., Boschung, J., Nauels, A., Xia, Y., Bex, V., and Midgley, P. M. (2013). Anthropogenic and Natural Radiative Forcing. In *Climate change 2013: The Physical Science Basis.: Contribution of Working Group I to the Fifth Assessment Report of the Intergovernmental Panel on Climate Change* (pp. 659–740). Cambridge University Press.

Stokke, R., Roalkvam, I., Lanzen, A., Haflidason, H., and Steen, I.H. (2012). Integrated metagenomic and metaproteomic analyses of an ANME-1 dominated community in marine cold seep sediments. *Environmental Microbiology*, 14, 1333–1346.

Strous, M., Kuenen, J. G., Fuerst, J. A., Wagner, M., and Jetten, M. S. (2002). The anammox case–a new experimental manifesto for microbiological eco-physiology. *Antonie van Leeuwenhoek*, 81(1-4), 693-702.

Strous, M., Pelletier, E., Mangenot, S., Rattei, T., Lehner, A., Taylor, M. W., Horn, M., Daims, H., Bartol-Mavel, D., Wincker, P., Barbe, V., Fonknechten, N., Vallenet, D., Segurens, B., Schenowitz-Truong, C., Médigue, C., Collingro, A., Snel, B., Dutilh, B.,… Le Paslier, D. (2006). Deciphering the evolution and metabolism of an anammox bacterium from a community genome. *Nature*, 440(7085), 790-794.

Subaşı, I. (2022). *Investigation of the growth and operational conditions for the enrichment of Chlorella vulgaris and its use in anaerobic digestate treatment* [M.S. - Master of Science]. Middle East Technical University.

Sun, W., Banihani, Q., Sierra-Alvarez, R., and Field, J. A. (2011). Stoichiometric and molecular evidence for the enrichment of anaerobic ammonium oxidizing bacteria from wastewater treatment plant sludge samples. *Chemosphere,* 84(9), 1262-1269.

Şenol, A. B., and Kocamemi, B. A. (2011). A Novel Nitrogen Removal Technology for Sewage: Complete Ammonium Oxidation (Comammox). In *5th EURASIA Waste Management Symposium, Istanbul, Turkey*.

Tang, Y., Zhou, C., Ziv-El, M., and Rittmann, B.E. (2011). A pH-control model for heterotrophic and hydrogen-based autotrophic denitrification. *Water Research,* 45 (1), 232–240. https:// doi.org/10.1016/j.watres.2010.07.049.

Thauer, R.K., and Shima, S. (2006). Biogeochemistry–methane and microbes. *Nature 440*, 878–879.

U.S. EPA, (2012). *Global Anthropogenic Emissions of Non-CO_2 Greenhouse Gases: 1990–2030* (EPA 430-R-12-006), http://www.epa.gov/climatechange/EPAactivities/economics/nonco2projections.html.

van Kessel, M.A., Stultiens, K., Slegers, M.F., Cruz, S.G., Jetten, M.S., Kartal, B., and Op den Camp, H.J. (2018). Current Perspectives on the Application of N-DAMO and Anammox in Wastewater Treatment. *Current Opinion in Biotechnology*, 50, 222–227. https://doi.org/10.1016/j. copbio.2018.01.031.

van Niftrik, L. A., Fuerst, J. A., Damsté, J. S., Kuenen, J., Jetten, M. S., and Strous, M. (2004). The anammoxosome: An intracytoplasmic compartment in anammox bacteria. *FEMS Microbiology Letters*, 233(1), 7-13. doi:10.1016/j.femsle.2004.01.044

van Niftrik, L., and Jetten, M. (2012). Anaerobic Ammonium-Oxidizing Bacteria: Unique Microorganisms with Exceptional Properties. *Microbiology and Molecular Biology Reviews*, 585-596.

van Niftrik, L., Geerts, W.J., van Donselaar, E.G., Humbel, B.M., Webb, R.I., Fuerst, J.A., Verkleij, A.J., Jetten, M.S.M., and Strous, M. (2008). Linking ultrastructure and function in four genera of anaerobic ammonium-oxidizing bacteria: cell plan, glycogen storage, and localization of cytochrome c proteins. *Journal of Bacteriology*, 190 (2), 708–717. https://doi.org/10. 1128/jb.01449-07.

van De Vossenberg, J., Rattray, J. E., Geerts, W., Kartal, B., van Niftrik, L., van Donselaar, E. G., Damsté, J. S. S., Strous M. and Jetten, M. S. (2008). Enrichment and characterization of marine anammox bacteria associated with global nitrogen gas production. *Environmental Microbiology*, 10(11), 3120-3129.

Vázquez-Padín, J. R., Figueroa, M., Fernández, I., Mosquera-Corral, A., Campos, J. L., and Méndez, R. (2009). Post-treatment of effluents from anaerobic digesters by the ANAMMOX process. *Water Science and Technology*, 60(5), 1135–1143. https://doi.org/10.2166/wst.2009.421

Wang, C., Li, H., Wang, Q., and Wei, P. (2010). Effect of pH on growth and lipid content of Chlorella vulgaris cultured in biogas slurry. *Chinese Journal of Biotechnology*, 26(8), 1074-1079.

Wang, D., Wang, Y., Liu, Y., Ngo, H. H., Lian, Y., Zhao, J., Chen, F., Yang, Q., Zeng, G., and Li, X. (2017a). Is denitrifying anaerobic methane oxidation-centered technologies a solution for the sustainable operation of wastewater treatment Plants? *Bioresource Technology*, 234, 456-465. doi:10.1016/j.biortech.2017.02.059

Wang, D., Yang, G., Li, X., Zheng, W., Wu, Y., Yang, Q., and Zeng, G. (2012). Inducing mechanism of biological phosphorus removal driven by the aerobic/extended-idle regime. *Biotechnology and Bioengineering*, 109(11), 2798-2807. doi:10.1002/bit.24543

Wang, G., Tang, Z., Wei, J., and Li, J. (2019). Effect of salinity on anammox nitrogen removal efficiency and sludge properties at low temperature. *Environmental Technology*, 41 (22), 2920–2927. https://doi.org/10.1080/09593330.2019.1588384.

Wang, J., Yang, H., and Wang, F. (2014). Mixotrophic cultivation of microalgae for biodiesel production: status and prospects. *Applied Biochemistry and Biotechnology*, 172(7), 3307-3329.

Wang, S., Wu, Q., Lei, T., Liang, P., and Huang, X. (2016). Enrichment of denitrifying methanotrophic bacteria from Taihu sediments by a membrane biofilm bioreactor at ambient temperature. *Environmental Science and Pollution Research*, 23(6):5627–5634

Wang, Y., Wang, D., Yang, Q., Zeng, G., and Li, X. (2017b). Wastewater opportunities for denitrifying anaerobic methane oxidation. *Trends in Biotechnology*, https://doi.org/10.1016/ j.tibtech.2017.02.010.

W.E.F. (2011). *Nutrient Removal: Manual of Practice No. 34: WEF manual of practice no. 34*. New York, NY: Mcgraw-Hill.

Winkler, M., Ettwig, K., Vannecke, T., Stultiens, K., Bogdan, A., Kartal, B., and Volcke, E. (2015). Modelling simultaneous anaerobic methane and ammonium removal in a granular sludge reactor. *Water Research*, 73, 323–331. https://doi.org/10.1016/j.watres.2015.01.039.

Winkler, M., and Straka, L. (2019). New Directions in biological nitrogen removal and recovery from wastewater. *Current Opinion in Biotechnology*, 57, 50–55. https://doi.org/10.1016/j.copbio.2018.12.007

Wu, M., Ettwig, K., Jetten, M., Strous, M., Keltjens, J., and van Niftrik, L. (2011). A new intra-aerobic metabolism in the nitrite-dependent anaerobic methane-oxidizing bacterium Candidatus 'Methylomirabilis oxyfera. *Biochemical Society Transactions*, 39 (1), 243–248.

Wu, M., van Alen, T.A., van Donselaar, E., Strous, M., Jetten, M., and van Niftrik, L. (2012a). Co-localization of particulate methane monooxygenase and cd1 nitrite reductase in the denitrifying methanotroph 'Candidatus Methylomirabilis oxyfera'. *FEMS Microbiology Letters*, 334 (1), 49–56.

Wu, M.L., van Teeseling, M.C., Willems, M.J., van Donselaar, E.G., Klingl, A., Rachel, R., Geerts, W.J., Jetten, M.S., Strous, M., and van Niftrik, L. (2012b). Ultrastructure of the denitrifying methanotroph "Candidatus Methylomirabilis oxyfera", a novel polygon-shaped bacterium. *Journal of Bacteriology*, 194, 284–291.

Xie, G., Cai, C., Hu, S., and Yuan, Z. (2016). Complete Nitrogen Removal from Synthetic Anaerobic Sludge Digestion Liquor through Integrating Anammox and Denitrifying Anaerobic Methane Oxidation in a Membrane Biofilm

Reactor. *Environmental Science and Technology*, 51(2), 819-827. doi:10.1021/acs.est.6b04500

Xie, G., Liu, T., Cai, C., Hu, S., and Yuan, Z. (2018). Achieving high-level nitrogen removal in mainstream by coupling anammox with denitrifying anaerobic methane oxidation in a membrane biofilm reactor. *Water Research*, 131, 196–204. https://doi.org/10.1016/j.watres. 2017.12.037.

Xu, M., Li, P., Tang, T., and Hu, Z. (2015). Roles of SRT and HRT of an algal membrane bioreactor system with a tanks-in-series configuration for secondary wastewater effluent polishing. *Ecological Engineering*, 85, 257-264.

Xu, S., Lu, W., Muhammad, F.M., Liu, Y., Guo, H., Meng, R., and Wang, H. (2018). New molecular method to detect denitrifying anaerobic methane oxidation bacteria from different environmental niches. *Journal of Environmental Science*, 65, 367–374. https://doi.org/10.1016/j. jes.2017.04.016.

Xu, S., Lu, W., Mustafa, M.F., Caicedo, L.M., Guo, H., Fu, X., and Wang, H. (2017). Co-existence of anaerobic ammonium oxidation bacteria and denitrifying anaerobic methane oxidation bacteria in sewage sludge: community diversity and seasonal dynamics. *Microbial Ecology*, 74 (4), 832–840. https://doi.org/10.1007/s00248-017-1015-x.

Yamamoto, M., Fujishita, M., Hirata, A., and Kawano, S. (2004). Regeneration and maturation of daughter cell walls in the autospore-forming green alga *Chlorella vulgaris* (Chlorophyta, Trebouxiophyceae). *Journal of Plant Research*, 117(4). doi:10.1007/s10265-004-0154-6

Yamamoto, M., Kurihara, I., and Kawano, S. (2005). Late type of daughter cell wall synthesis in one of the Chlorellaceae, Parachlorella kessleri (Chlorophyta,

Trebouxiophyceae). *Planta*, 221(6), 766-775. doi:10.1007/s00425-005-1486-8

Yang, J., Jiang, H., Wu, G., Hou, W., Sun, Y., Lai, Z., and Dong, H. (2012). Co-occurrence of nitrite-dependent anaerobic methane oxidizing and anaerobic ammonia oxidizing bacteria in two Qinghai-Tibetan saline lakes. *Frontiers of Earth Science*, 6, 383–391.

Yi, Y., Yong, H., and Hui Ping, D. (2011). Effect of salt on anammox process. *Procedia Environmental Sciences 10*, 2036–2041. https://doi.org/10.1016/j.proenv.2011.09. 319.

Youssef, N. H., Farag, I. F., Rinke, C., Hallam, S. J., Woyke, T., and Elshahed, M. S. (2015). *In Silico* Analysis of the Metabolic Potential and Niche Specialization of Candidate Phylum "*Latescibacteria*" (WS3). *PLOS ONE*, 10(6). https://doi.org/10.1371/journal.pone.0127499

Yu, H., Kashima, H., Regan, J.M., Hussain, A., Elbeshbishy, E., and Lee, H. (2017). Kinetic study on anaerobic oxidation of methane coupled to denitrification. *Enzyme and Microbial Technology*, 104, 47–55. https://doi.org/10.1016/j.enzmictec.2017.05.005.

Zedelius, J., Rabus, R., Grundmann, O., Werner, I., Brodkorb, D., Schreiber, F., Ehrenreich, P., Behrends, A., Heinz, W., Kube, M., Reinhardt, R., and Widdel, F. (2011). Alkane degradation under anoxic conditions by a nitrate-reducing bacterium with possible involvement of the electron acceptor in substrate activation. *Environmental Microbiology Reports*, 3 (1), 125–135. https://doi.org/10.1111/j.1758-2229.2010. 00198.x.

Zekker, I., Artemchuk, O., Rikmann, E., Ohimai, K., Dhar Bhowmick, G., Madhao Ghangrekar, M., Burlakovs, J., and Tenno, T. (2021). Start-up of Anammox

SBR from non-specific inoculum and process acceleration methods by hydrazine. *Water*, 13(3), 350. https://doi.org/10.3390/w13030350

Zekker, I., Kivirüüt, A., Rikmann, E., Mandel, A., Jaagura, M., Tenno, T., Artemchuk, O., Rubin, S. dC., and Tenno, T. (2019). Enhanced efficiency of nitritating-anammox sequencing batch reactor achieved at low decrease rates of oxidation–reduction potential. *Environmental Engineering Science*, 36(3), 350–360. https://doi.org/10.1089/ees.2018.0225

Zhang, K., Miyachi, S., and Kurano, N. (2001). Evaluation of a vertical flat-plate photobioreactor for outdoor biomass production and carbon dioxide bio-fixation: effects of reactor dimensions, irradiation and cell concentration on the biomass productivity and irradiation utilization efficiency. *Applied Microbiology and Biotechnology*, 55(4), 428-433. doi:10.1007/s002530000550

Zhang, L. (2016). Anaerobic Treatment of Municipal Wastewater in a UASB-Digester System: Temperature effect on system performance, hydrolysis and methanogenesis (*Thesis*).

Zhang, L., Yang, J., Hira, D., Fujii, T., Zhang, W., and Furukawa, K. (2011). High-rate nitrogen removal from anaerobic digester liquor using an up-flow anammox reactor with polyethylene sponge as a biomass carrier, *Journal of Bioscience and Bioengineering*, 111(3), 306-311.

Zhang, L., Zheng, P., He, Y., and Jin, R. (2009). Performance of sulfate-dependent anaerobic ammonium oxidation. *Science in China Series B: Chemistry*, 52 (1), 86–92. https://doi.org/10. 1007/s11426-008-0161-x.

Zhang, X., Liu, Y., and Gu, J. (2018). A global analysis on the distribution pattern of the bacteria coupling simultaneous methane oxidation to nitrite reduction.

International Biodeterioration and Biodegradation, 129, 123–132. https://doi.org/10.1016/j.ibiod.2018.01.014.

Zhou, L., Wang, Y., Long, X., Guo, J., and Zhu, G. (2014). High abundance and diversity of nitrite-dependent anaerobic methane-oxidizing bacteria in a paddy field profile. *FEMS Microbiology Letters*, 360 (1), 33–41. https://doi.org/10.1111/ 1574-6968.12567.

Zhu, B., Dijk, G. V., Fritz, C., Smolders, A. J., Pol, A., Jetten, M. S., and Ettwig, K. F. (2012). Anaerobic Oxidization of Methane in a Minerotrophic Peatland: Enrichment of Nitrite-Dependent Methane-Oxidizing Bacteria. *Applied and Environmental Microbiology*, 78(24), 8657-8665. doi:10.1128/aem.02102-12

Zhu, B., Sánchez, J., Alen, T. A., Sanabria, J., Jetten, M. S., Ettwig, K. F., and Kartal, B. (2011). Combined anaerobic ammonium and methane oxidation for nitrogen and methane removal. *Biochemical Society Transactions*, 39(6), 1822-1825. doi:10.1042/bst20110704

Zhu, Q., Shen, L., Hu, B., Lou, L., and Cheng, D. (2013). Molecular detection of denitrifying anaerobic methane oxidizing bacteria in the sediment of West Lake. *Acta Scientiae. Circumstantiae*, 33, 1321–1325.

Znad, H., Naderi, G., Ang, H. M., and Tade, M. O. (2012). CO_2 biomitigation and biofuel production using microalgae: photobioreactors developments and future directions. *Advances in Chemical Engineering*, 230-244.

Zuccaro, G., Steyer, J. P., and van Lis, R. (2019). The algal trophic mode affects the interaction and oil production of a synergistic microalga-yeast consortium. *Bioresource Technology*, 273, 608-617.

APPENDICES

A. Results of the Anammox SBR

Table A-1 TSS and VSS in the sludge of the Anammox SBR

Sludge	TSS (g/L)	VSS (g/L)	VSS/TSS (%)
Cycle 0	9.65 ± 0.31	7.33 ± 0.05	76
Cycle 10	4.22 ± 0.4	2.60 ± 0.3	62
Cycle 13	3.63 ± 0.5	3.08 ± 0.5	85
Cycle 95	2.21 ± 0.05	1.73 ± 0.03	78
Cycle 156	2.91 ± 0.27	2.34 ± 0.28	80

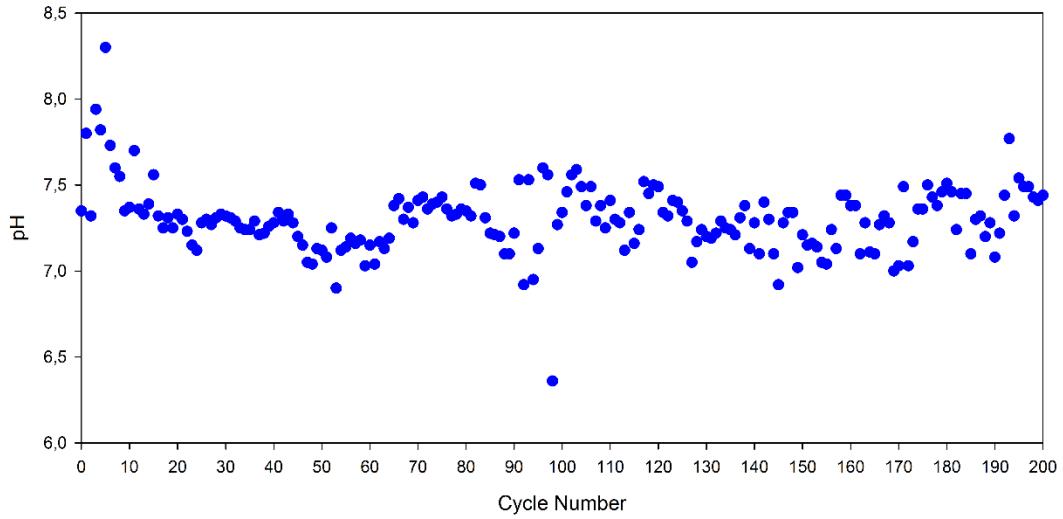

Figure A-1 pH results of the effluent samples of the Anammox reactor

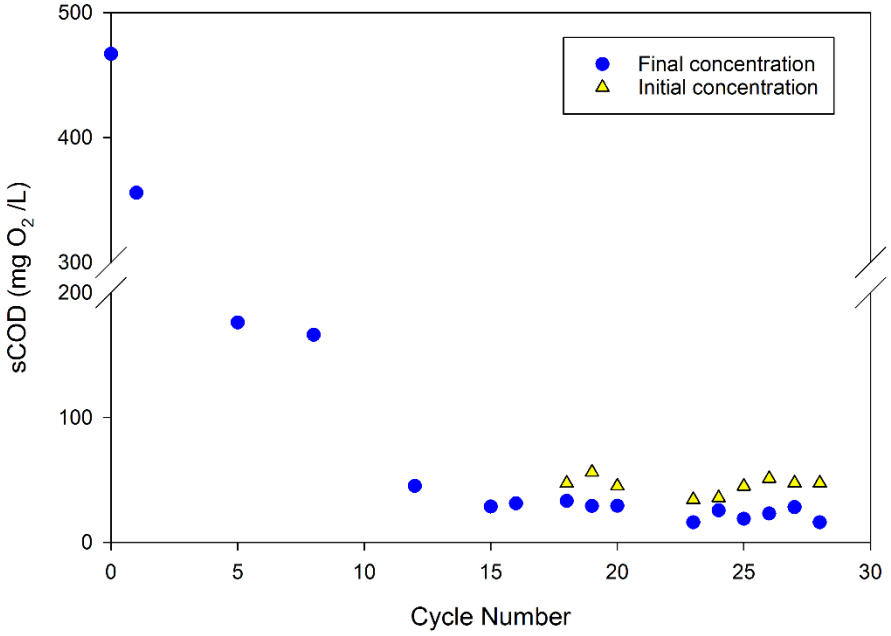

Figure A-2 sCOD results of the Anammox SBR samples

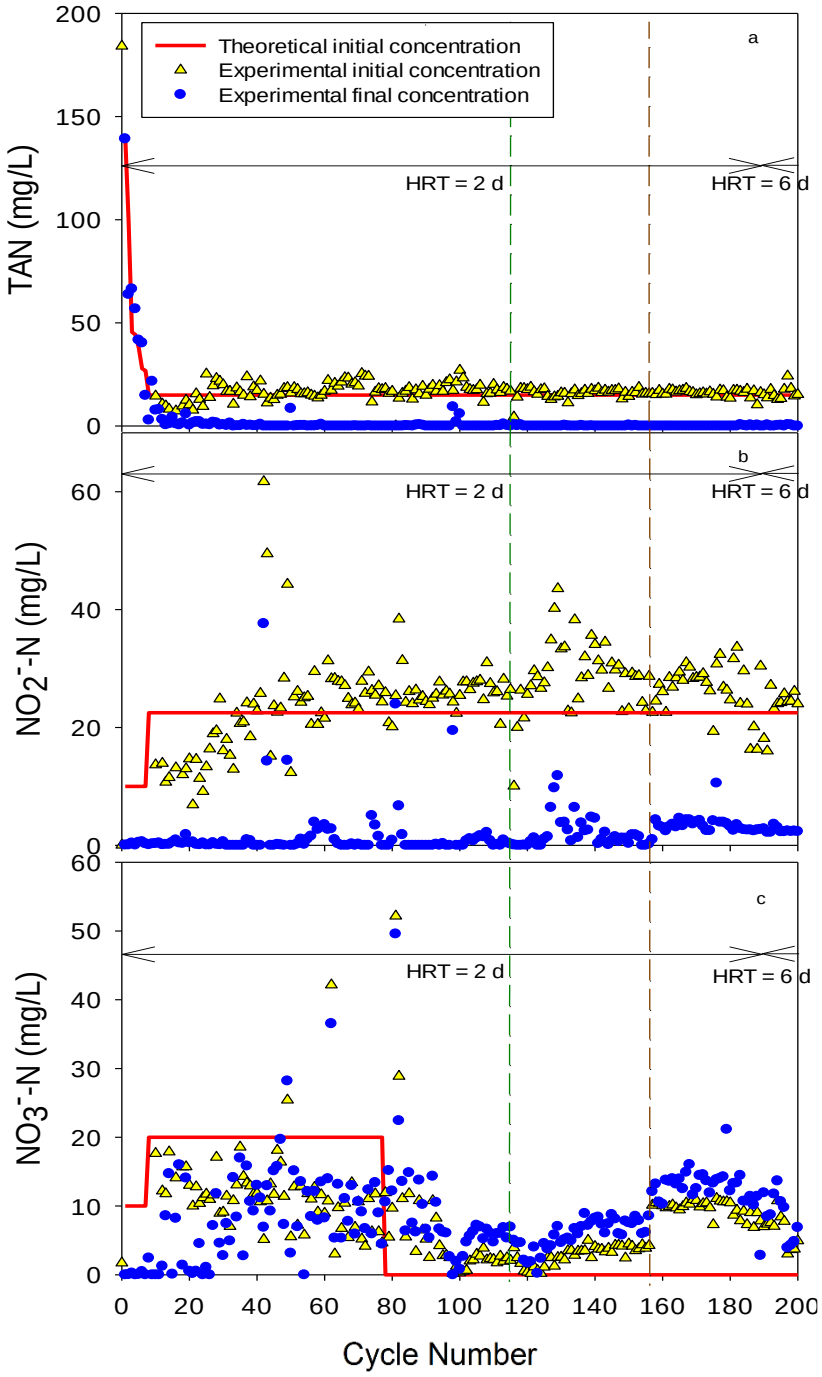

Figure A-3 Initial and final concentrations of (a) NH_4^+-N, (b) NO_2^--N and (c) NO_3^--N during each cycle in the Anammox SBR (green dashed line at cycle 115 refers to removal of 0.25 L of sludge from the reactor; brown dashed line at cycle 156 refers to removal of 0.6 L of sludge for DAMO-Anammox SBR seeding; the S.D of each measurement was <5%)

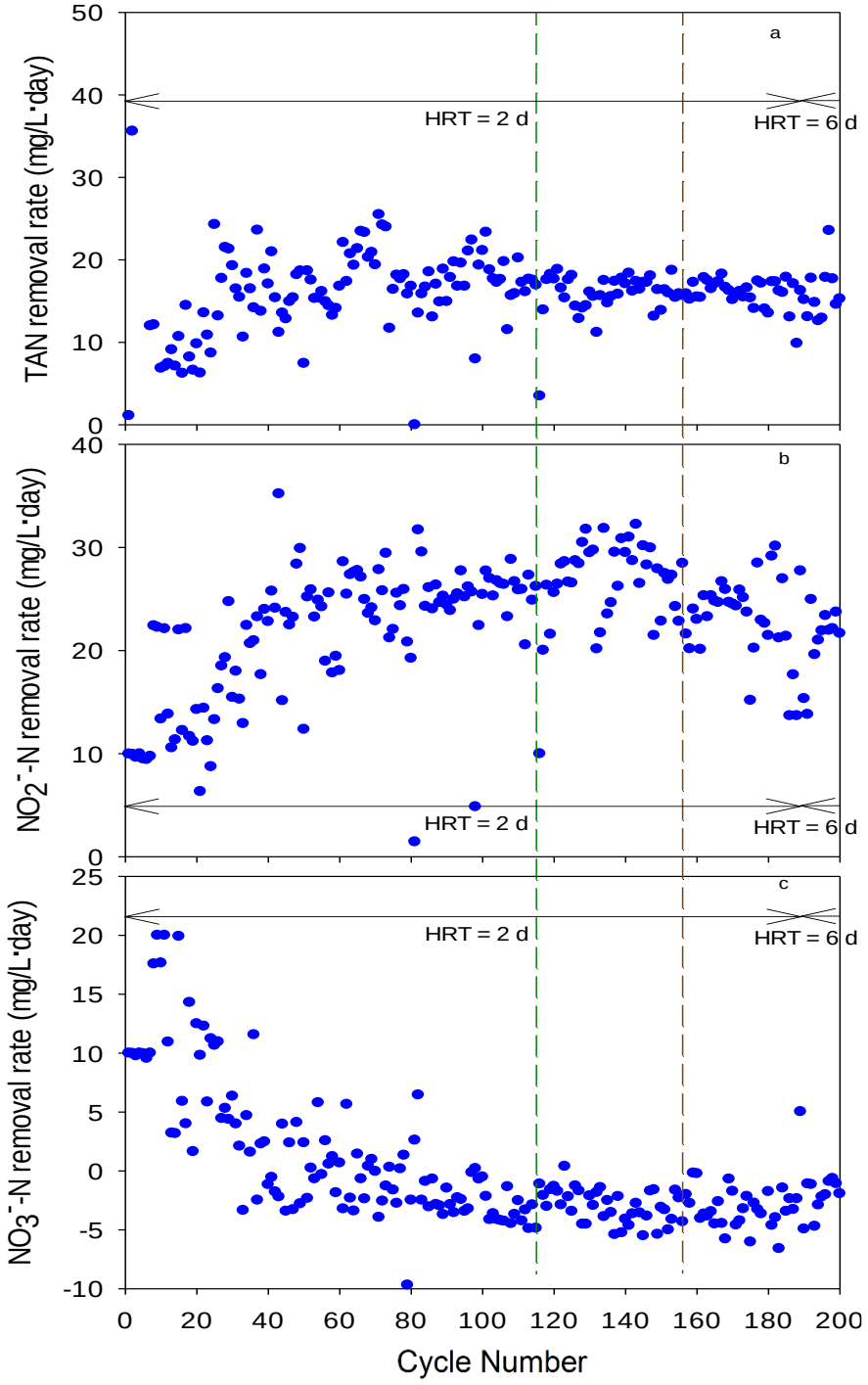

Figure A-4 Removal rates of (a) NH_4^+, (b) NO_2^- and (c) NO_3^- in the Anammox SBR (the negative values imply production of the ion; green dashed line at cycle 115 refers to removal of 0.25 L of sludge from the reactor; brown dashed line at cycle 156 refers to removal of 0.6 L of sludge for DAMO-Anammox SBR seeding)

B. Specific Activity Test Results of DAMO-Anammox SBR

Phase I

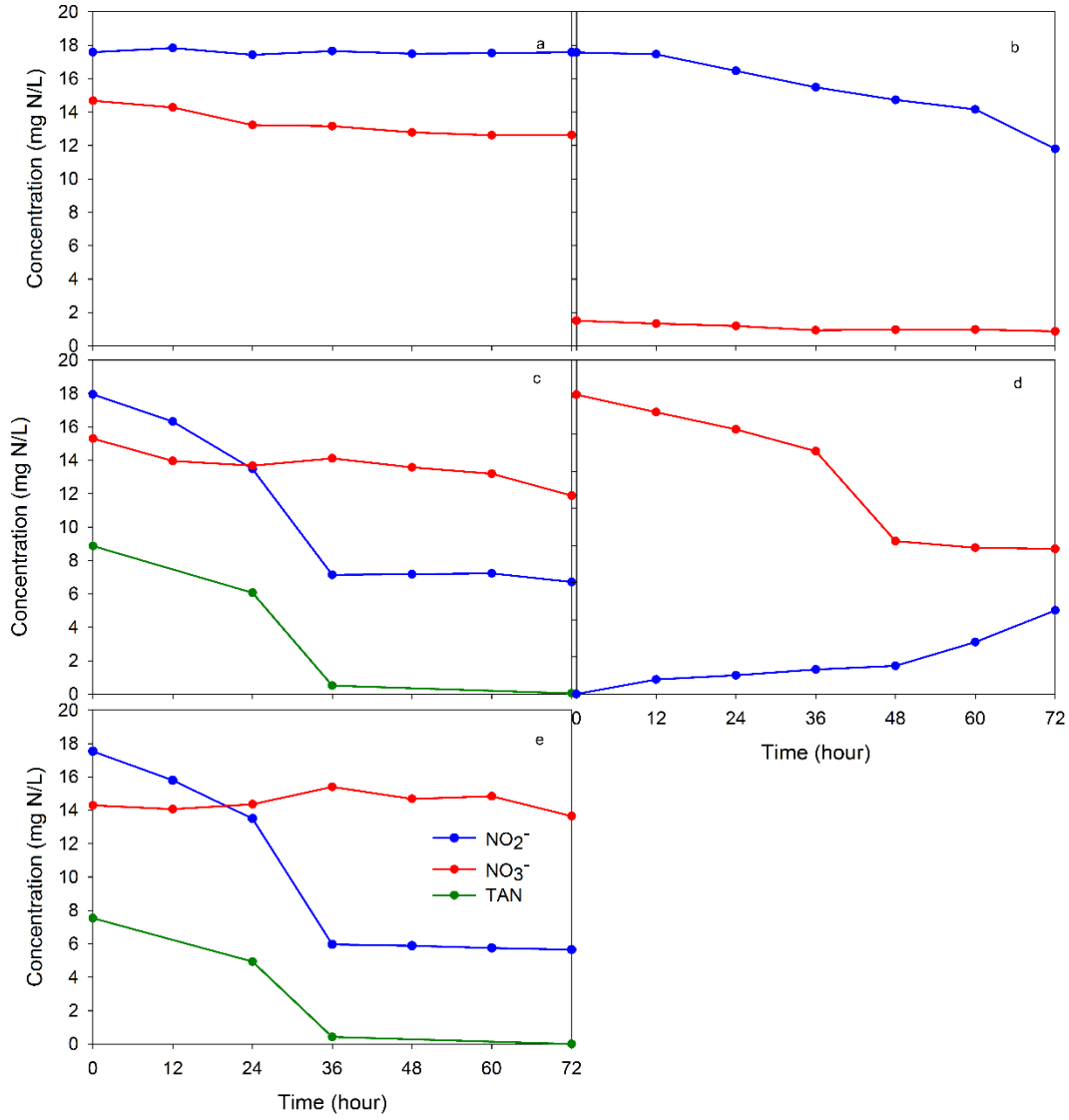

Figure B-1 The concentration changes in each reactor type of Phase I specific activity test (a) DEN (Denitrifiers), (b) DAMOb, (c) DAMX (DAMO-Anammox co-culture), (d) DAMOa and (e) AMX (Anammox)

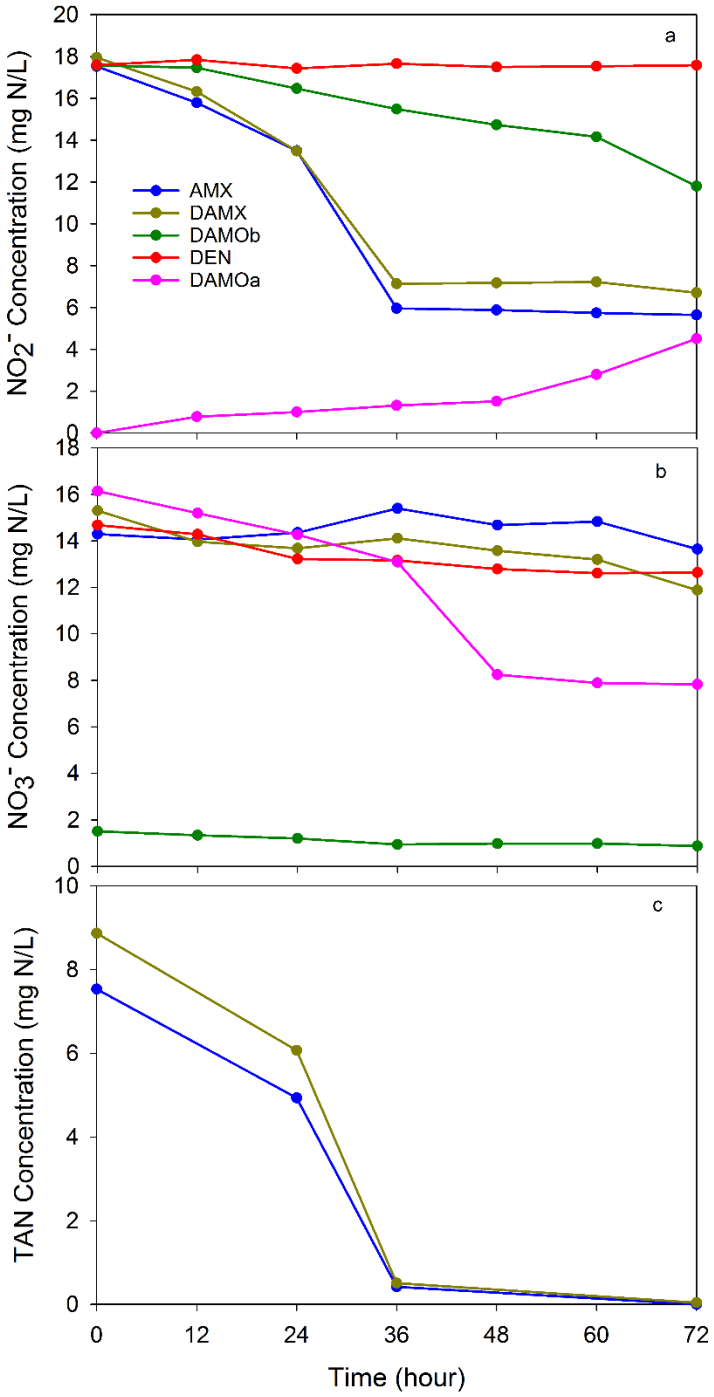

Figure B-2 Comparison of the concentration changes in the different reactor setups of Phase I specific activity test (a) NO_2^--N, (b) NO_3^--N, (c) TAN

DEN (Denitrifiers), DAMOb, DAMX (DAMO-Anammox co-culture), DAMOa and AMX (Anammox)

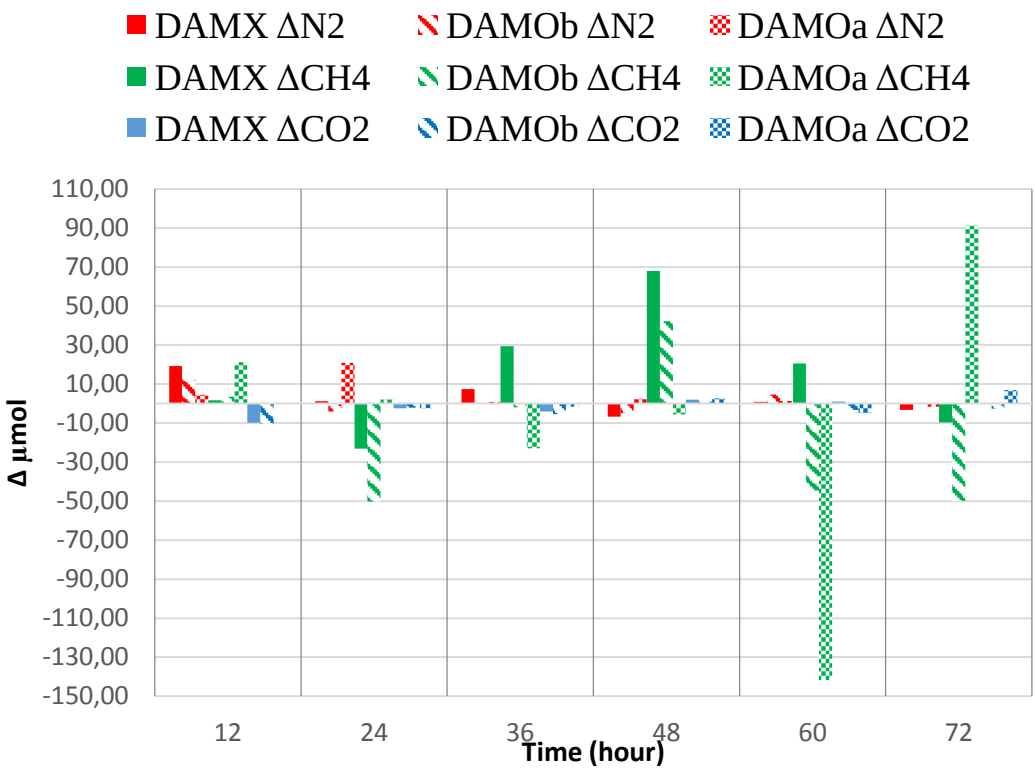

Figure B-3 GC results of Phase I specific activity test

DAMX (DAMO-Anammox co-culture), DAMOb and DAMOa

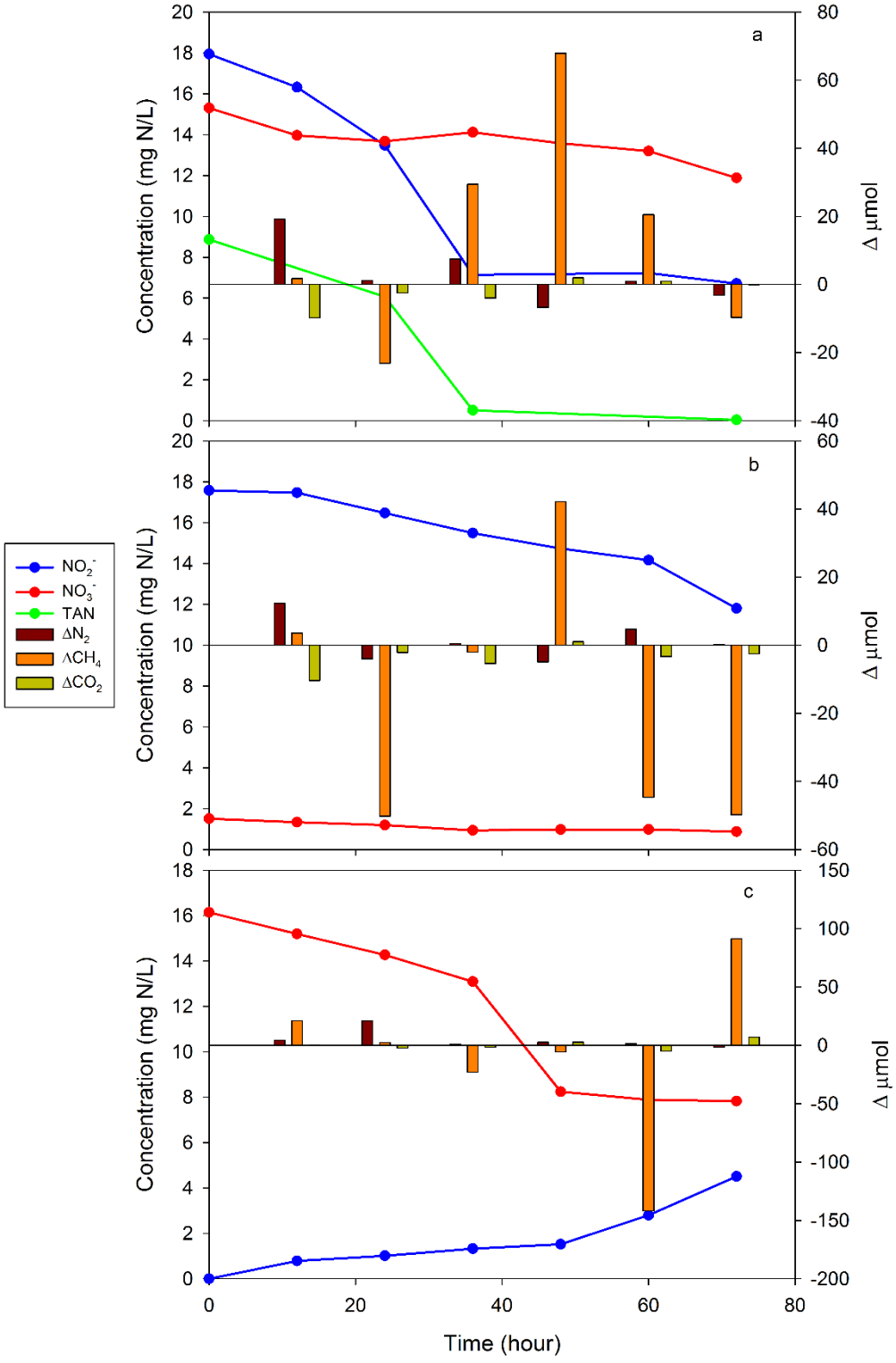

Figure B-4 Correlation of the GC and nitrogen results of Phase I specific activity test (a) DAMX (DAMO-Anammox co-culture) (b) DAMOb (c) DAMOa reactors

Phase II

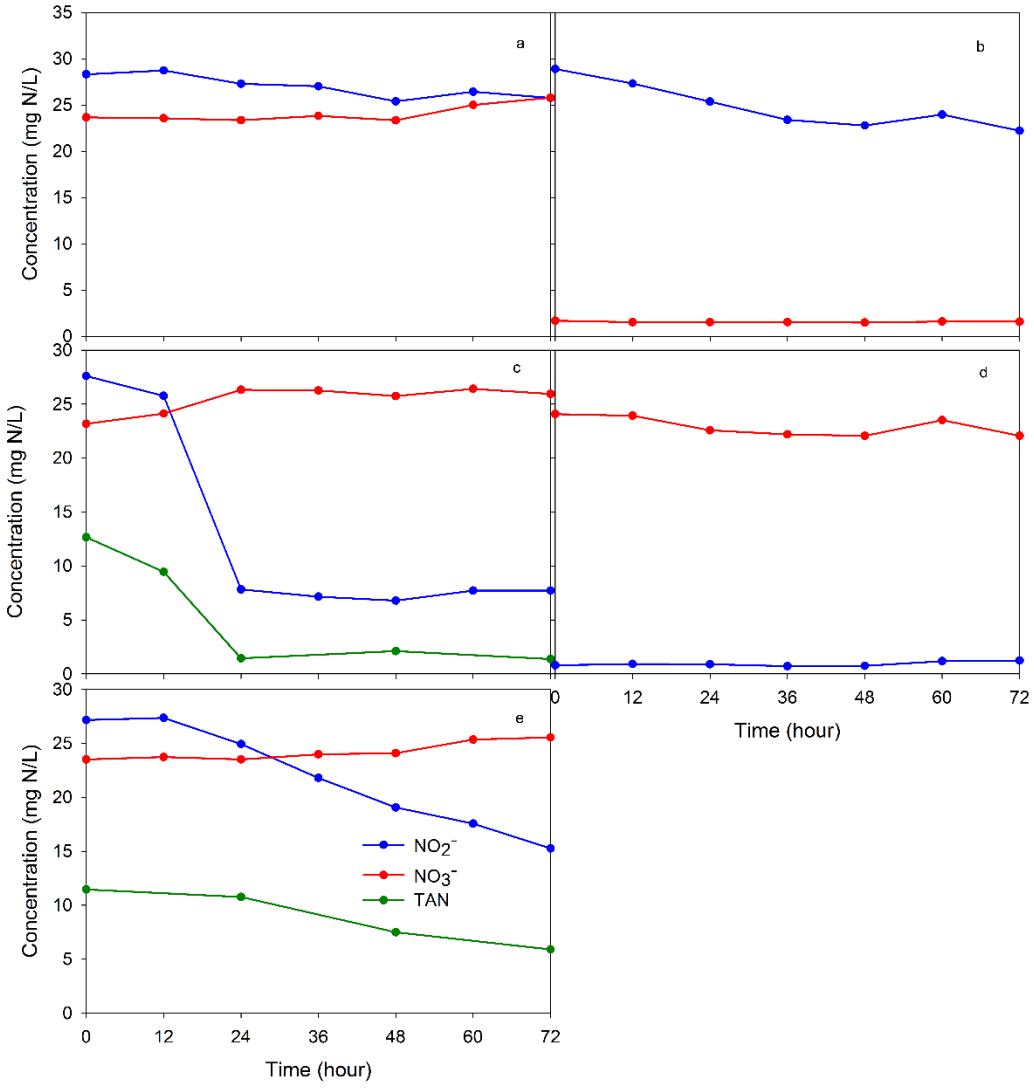

Figure B-5 The concentration changes in each reactor type in Phase II specific activity test (a) DEN (Denitrifiers), (b) DAMOb, (c) DAMX (DAMO-Anammox co-culture), (d) DAMOa and (e) AMX (Anammox)

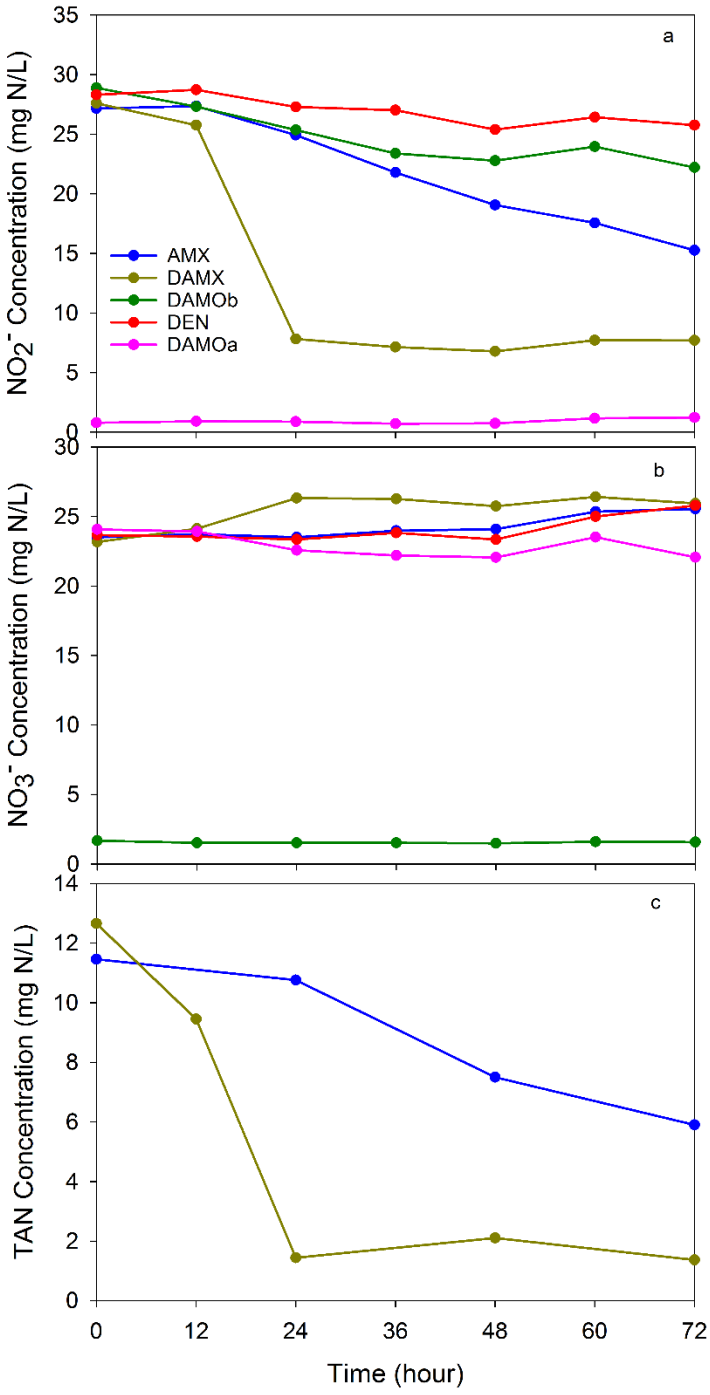

Figure B-6 Comparison of the concentration changes in the different reactor setups of Phase II specific activity test (a) NO_2^--N, (b) NO_3^--N, (c) TAN

DEN (Denitrifiers), DAMOb, DAMX (DAMO-Anammox co-culture), DAMOa and AMX (Anammox)

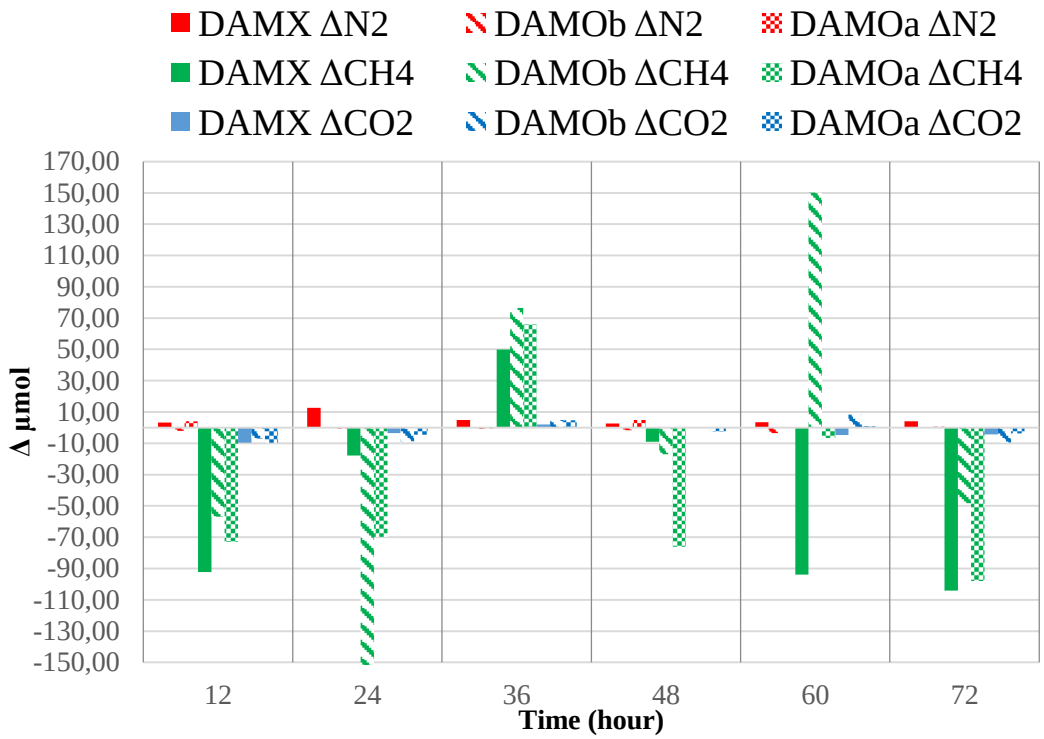

Figure B-7 GC results of Phase II specific activity test

DAMX (DAMO-Anammox co-culture), DAMOb and DAMOa

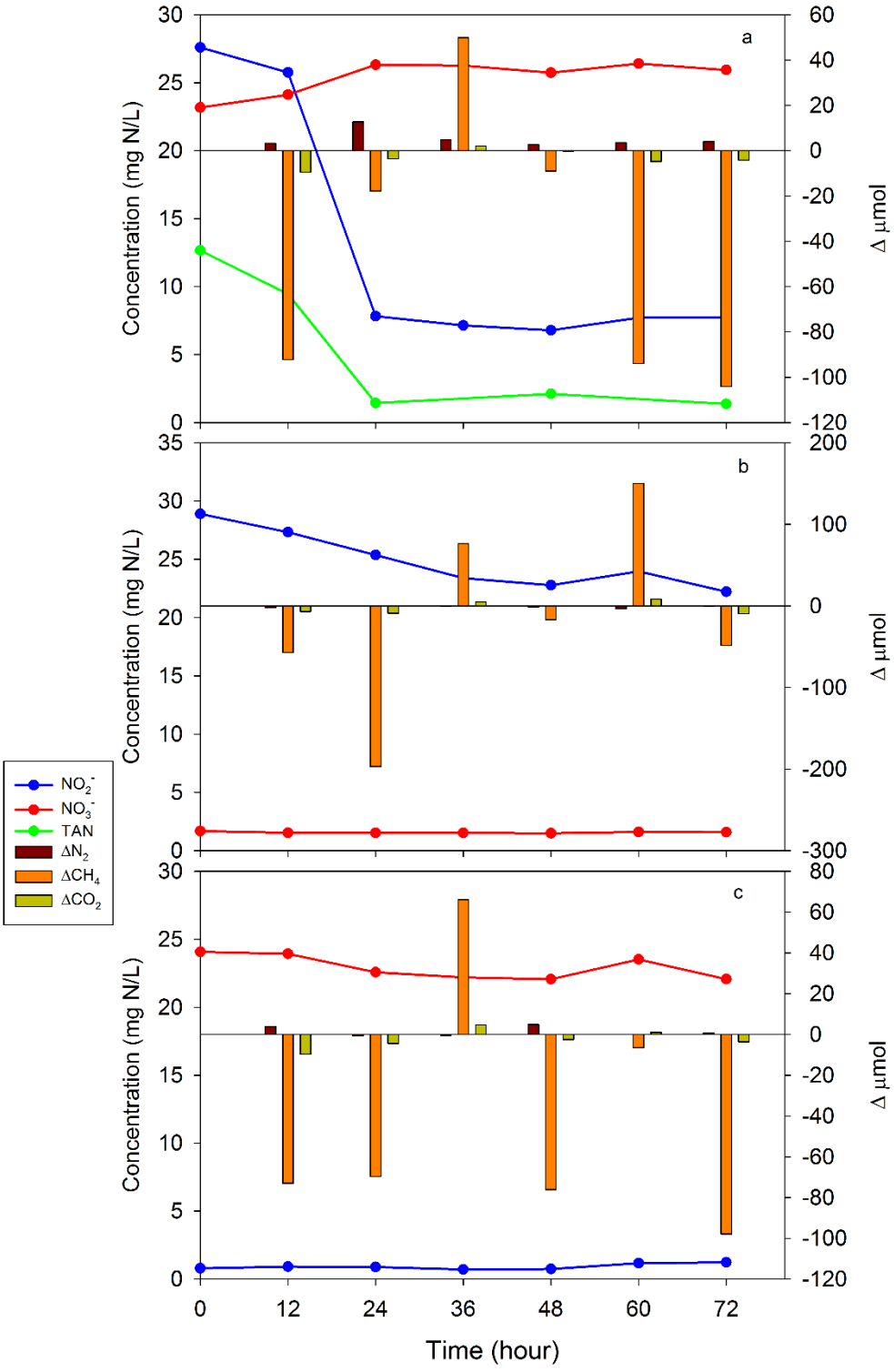

Figure B-8 Correlation of the GC and nitrogen results of Phase II specific activity test (a) DAMX (DAMO-Anammox co-culture) (b) DAMOb (c) DAMOa reactors

Phase III

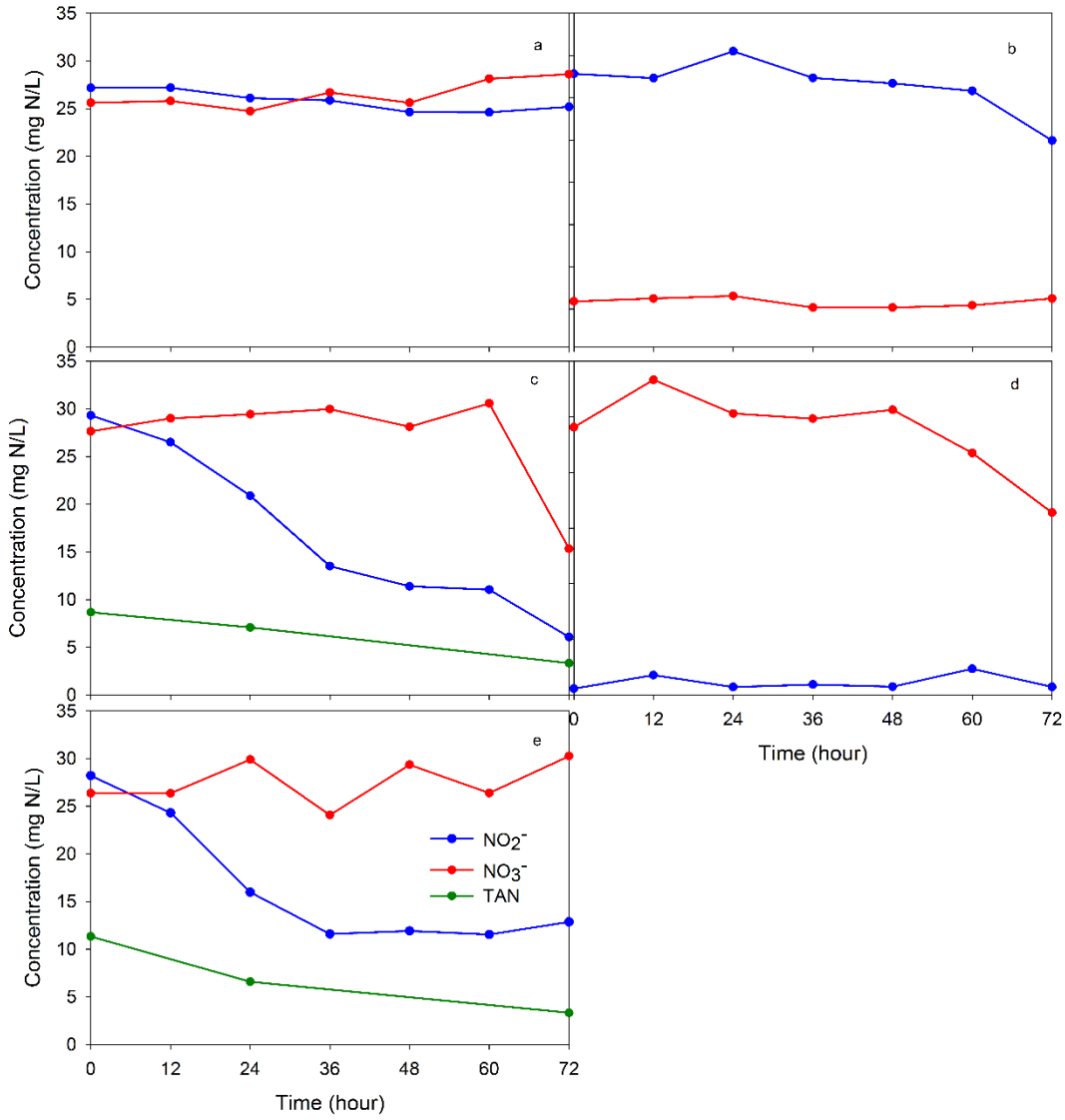

Figure B-9 The concentration changes in each reactor type of Phase III specific activity test (a) DEN (Denitrifiers), (b) DAMOb, (c) DAMX (DAMO-Anammox co-culture), (d) DAMOa and (e) AMX (Anammox)

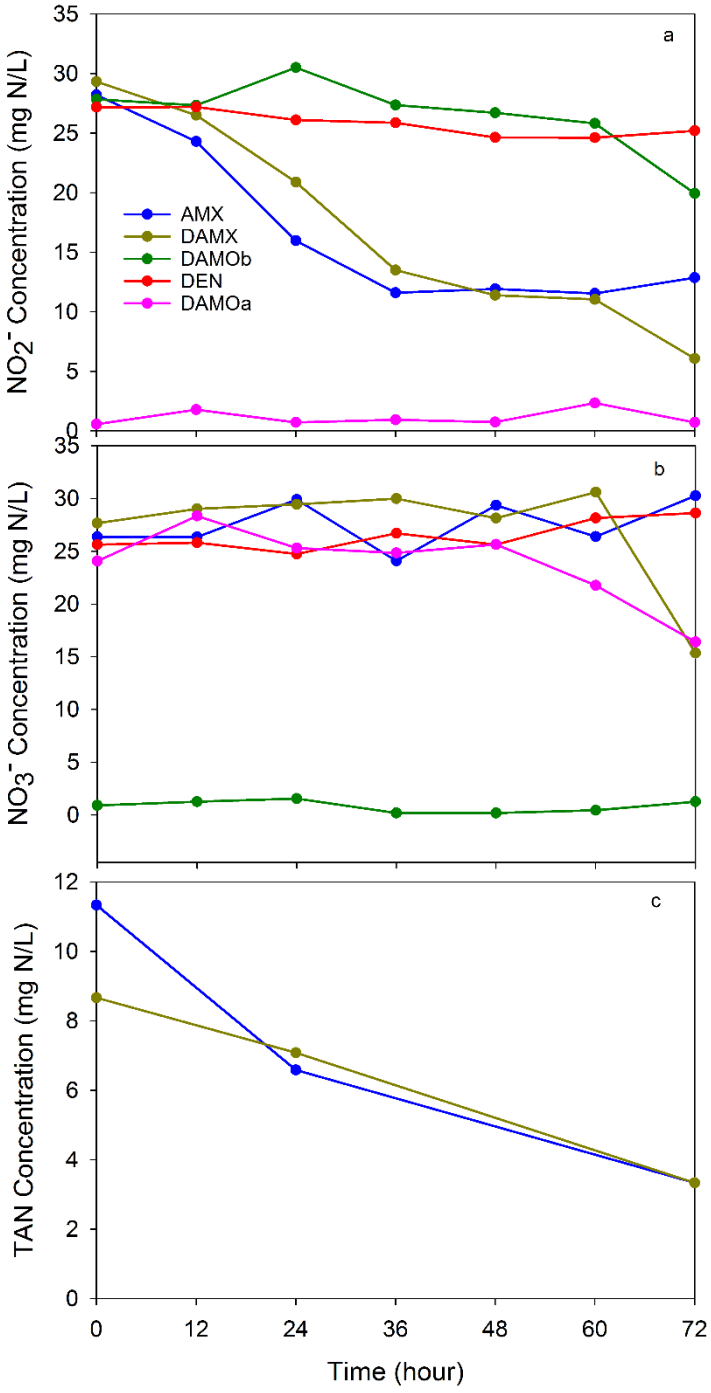

Figure B-10 Comparison of the concentration changes in the different reactor setups of Phase III specific activity test (a) NO_2^--N, (b) NO_3^--N, (c) TAN

DEN (Denitrifiers), DAMOb, DAMX (DAMO-Anammox co-culture), DAMOa and AMX (Anammox)

C. Ion Chromatography Calibration

The IC calibration curves using the anion standard solution (Shimadzu PIA Std. Sample Anion) of NO_2^-, NO_3^- and SO_4^{2-} are shown in Figure C-1, Figure C-2, and Figure C-3, respectively. The maximum pressure limit was set at 150 bar, the oven temperature was set as 45ºC and at a flow rate of 0.8 mL/min. The LOD of NO_2^-, NO_3^- and SO_4^{2-} were calculated as 0.015, 0.09 and 0.003 mg/L, respectively. The LOQ of NO_2^-, NO_3^- and SO_4^{2-} were calculated as 0.045, 0.027, and 0.01 mg/L, respectively.

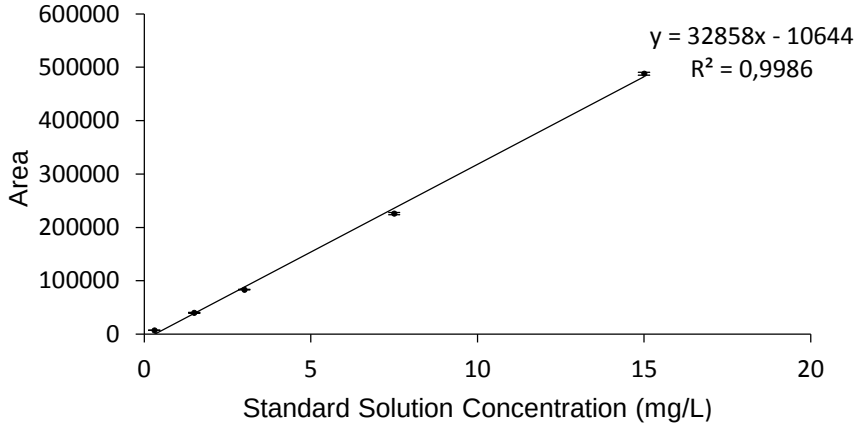

Figure C-1 NO_2^- Calibration

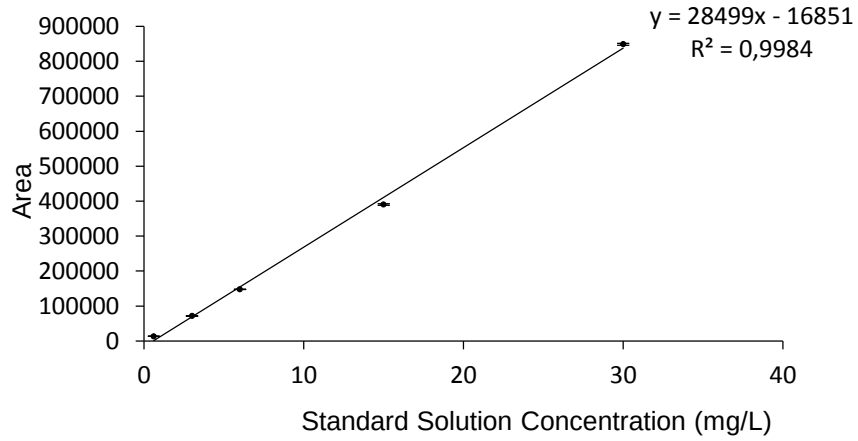

Figure C-2 NO_3^- Calibration

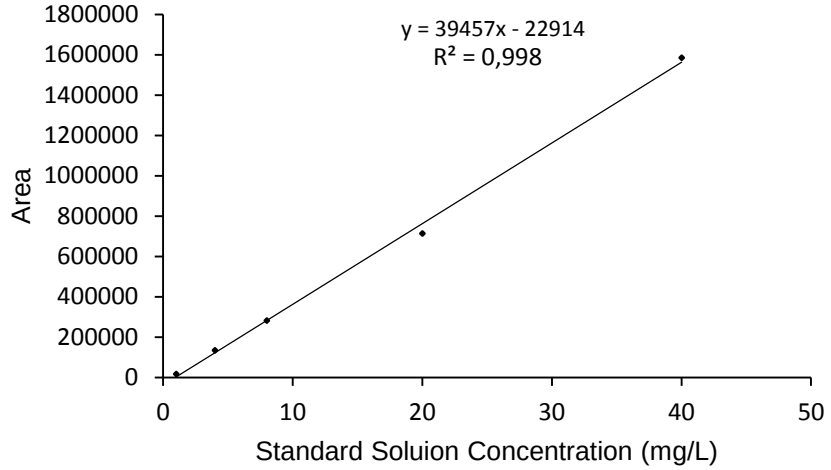

Figure C-3 SO_4^{2-} Calibration

D. Total Ammonium Nitrogen Calibration

NH_4Cl was used as the calibration solution of the Hach Nessler Method (Figure D-1). The LOD and LOQ for the TAN analyses were calculated as , respectively.

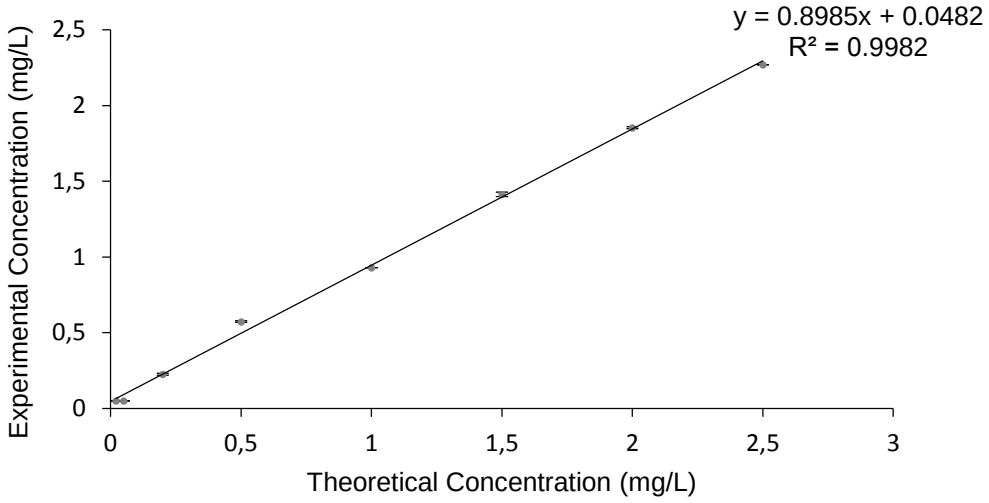

Figure D-1. Nessler-TAN Calibration Curve

E. Soluble Chemical Oxygen Demand and Total Organic Carbon Calibration

Potassium hydrogen phthalate ($C_8H_5KO_4$) was used as the calibration solution for the sCOD and TOC calibrations. The sCOD calibration curve is shown in Figure E-1, and the LOD and LOQ were calculated as 60 mg/L and 182 mg/L, respectively.

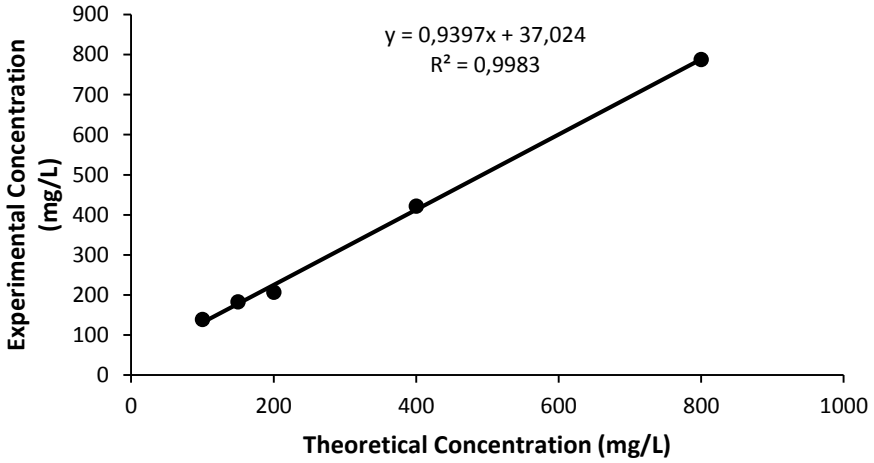

Figure E-1 sCOD

The non-purgable TOC referring calibration curve is in shown in Figure E-2, and the LOD and LOQ were calculated as 0.02 mg/L and 0.07 mg/L, respectively.

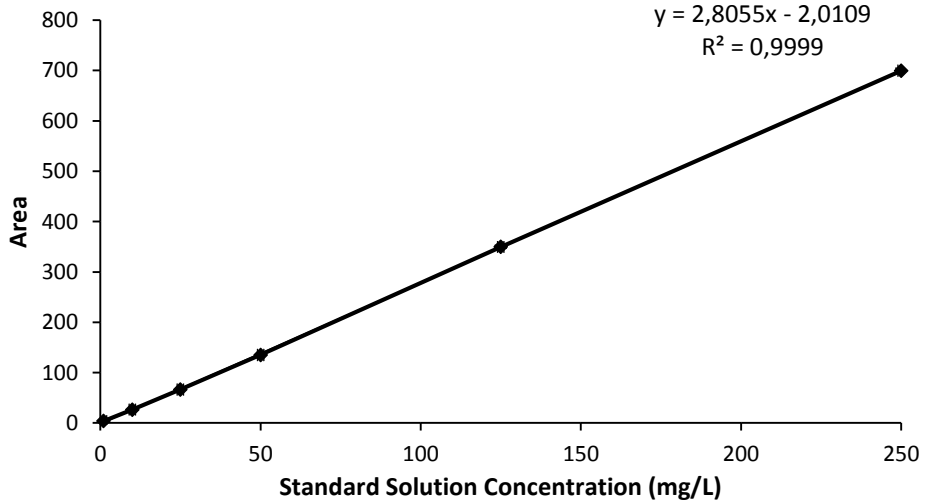

Figure E-2 Non-purgable TOC calibration curve of the Shimadzu TOC analyzer

F. Gas Chromatography Calibration

The calibration gas mixture used for the GC calibration had the concentrations of 10% H_2, 10% N_2, 30% CO_2 and 50% CH_4. The calibration curves for N_2, CH_4 and CO_2 are displayed in Figure F-1, F-2 and F-3, respectively. The temperatures of the injector, furnace and detector were set at 80°C, 40°C and 80°C, respectively. He gas was used as the carrier gas at a constant pressure of 100 kPa. The column used was the serial connected CP7429: CPmolsieve 5A/CP-porabond Q column. The LOD of N_2, CH_4 and CO_2 were calculated as 0.04, 0.38 and 0.07, respectively. The LOQ of N_2, CH_4 and CO_2 were calculated as 0.11, 1.15 and 0.21, respectively.

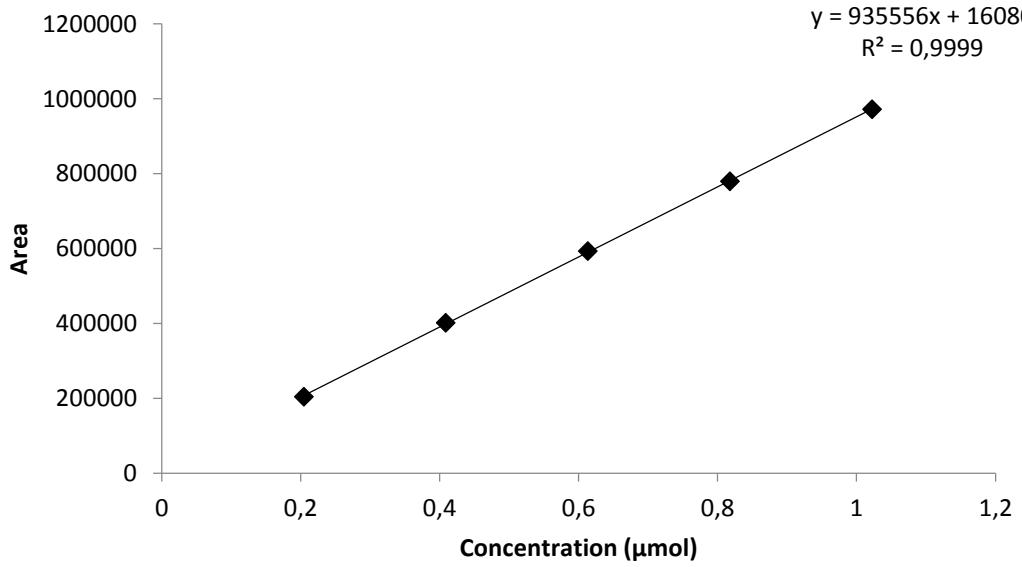

Figure F-1 N_2 calibration curve

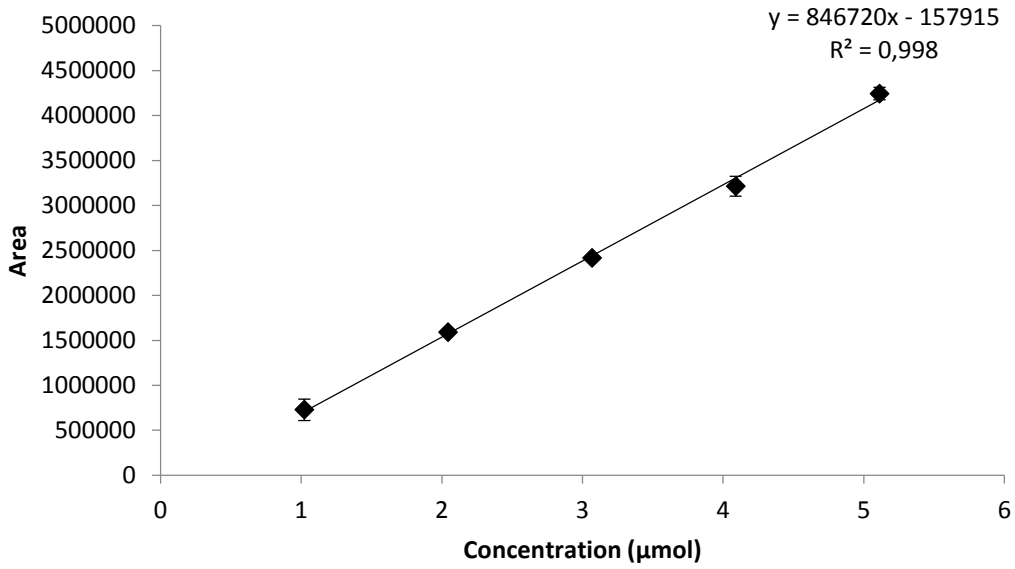

Figure F-2 CH_4 calibration curve

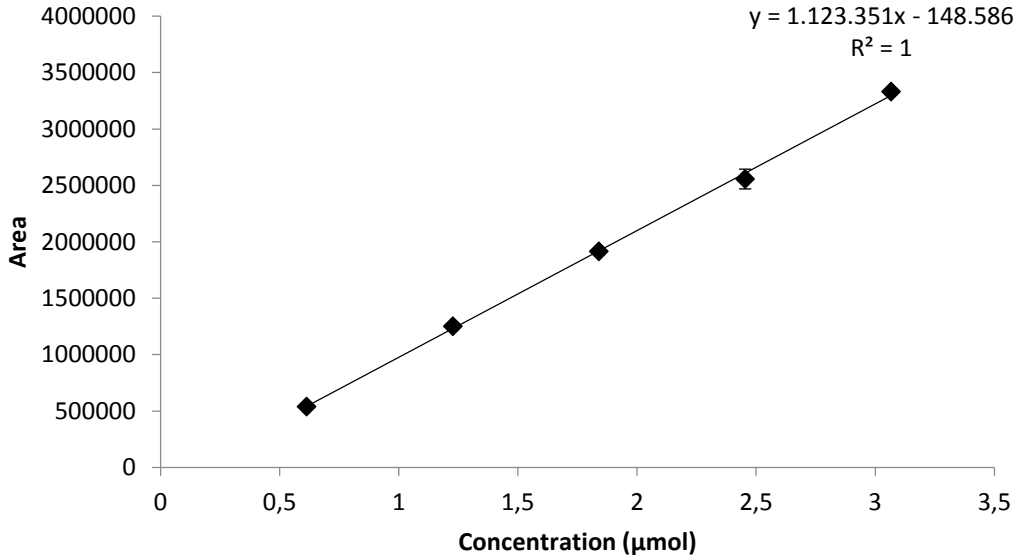

Figure F-3 CO_2 calibration curve

G. Soluble Ortho-Phosphate Calibration

A solution of potassium dihydrogen phosphate (KH_2PO_4) was used to perform the SOP calibration (Figure G-1). The LOD and LOQ were calculated as 0.0021 mg P/L and 0.0069 mg P/L, respectively.

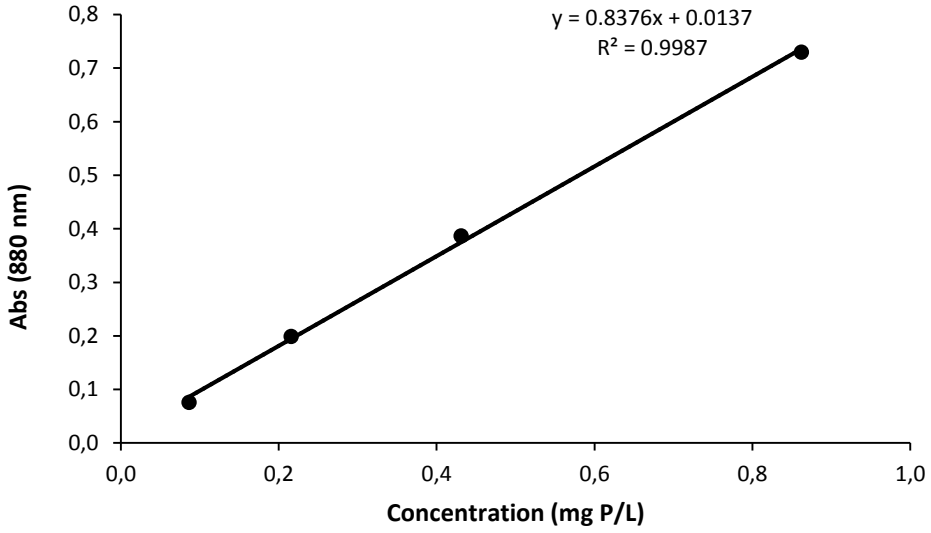

Figure G-1 SOP Calibration

H. Sample Calculation of Percent Contribution of Each Microorganism to the Available TN Removed

Cycle 128 from the DAMO-Anammox SBR was used in the calculcations.

The initial NH_4^+, NO_2^- and NO_3^- concentrations in Cycle 128,

$[NH_4^+\text{-}N]_i$ = 13.8 mgN/L

$[NO_2^-\text{-}N]_i$ = 24.6 mg N/L

$[NO_3^-\text{-}N]_i$ = 26.6 mg N/L

$TN_i=[NH_4^+\text{-}N]_i+[NO_2^-\text{-}N]_i+[NO_3^-\text{-}N]_i$ = 13.8+24.6+26.6 = 65 mg N/L

The final NH_4^+, NO_2^- and NO_3^- concentrations in Cycle 128,

$[NH_4^+\text{-}N]_f$ = 0 mgN/L

$[NO_2^-\text{-}N]_f$ = 1.5 mg N/L

$[NO_3^-\text{-}N]_f$ = 16.5 mg N/L

$TN_f=[NH_4^+\text{-}N]_f+[NO_2^-\text{-}N]_f+[NO_3^-\text{-}N]_f$ = 0+1.5+16.5 = 18 mg N/L

Since Anammox is the only target microorganism removing NH_4^+ and Anammox has higher affinity to NO_2^- than DAMOb, the starting point of the calculations will be Anammox. According to the stoichiometry of the Anammox reaction, the amount of NO_2^- consumed and NO_3^- produced are calculated according to the NH_4^+ consumed. The TN removed by Anammox is calculated as the sum of the NH_4^+ and NO_2^- consumed, deducting the NO_3^- produced.

AMX:

$\Delta[NH_4^+\text{-}N]=[NH_4^+\text{-}N]_i-[NH_4^+\text{-}N]_f$ = 13.8–0 = 13.8 mg N/L

$\Delta[NO_2^-\text{-}N]_{AMX}=1.32*\Delta[NH_4^+\text{-}N]$= 1.32*13.8 = 18.2 mg N/L

$\Delta[NO_3^-\text{-}N]_{AMX}=0.11*(\Delta[NH_4^+\text{-}N]+\Delta[NO_2^-\text{-}N]_{AMX})$= 0.11(13.8+18.2)= 3.5 mg N/L

$TN_{removed}^{AMX}=\Delta[NH_4^+\text{-}N]+\Delta[NO_2^-\text{-}N]_{AMX}-\Delta[NO_3^-\text{-}N]_{AMX}$ =13.8+18.2–3.5= 28.5 mg N/L

The next step would be calculating the TN removed by DAMOa. Here, the NO_3^- produced by the Anammox will be considered along with the initial NO_3^- concentration and the consumed NO_3^- by DAMOa is calculated. According to the stoichiometry of the DAMOa reaction, the NO_2^- produced by DAMOa is calculated.

DAMOa:

$TN_{removed}^{DAMOa}=\Delta[NO_3^-\text{-}N]_{DAMOa}=[NO_3^-\text{-}N]_i-[NO_3^-\text{-}N]_f+\Delta[NO_3^-\text{-}N]_{AMX}$ = 26.6–16.5+3.5 = 13.6 mg N/L

$\Delta[NO_2^-\text{-}N]_{DAMOa}=\Delta[NO_3^-\text{-}N]_{DAMOa}$ = 13.6 mg N/L

To calculate the TN removed by DAMOb, the NO_2^- left which was not consumed by the Anammox reaction and the NO_2^- produced from the DAMOa reaction are used along with the initial and final concentrations of NO_2^-.

DAMOb:

$TN_{removed}^{DAMOb}=\Delta[NO_2^-\text{-}N]_{DAMOb}=[NO_2^-\text{-}N]_i-\Delta[NO_2^-\text{-}N]_{AMX}+\Delta[NO_2^-\text{-}N]_{DAMOa}-[NO_2^-\text{-}N]_f$ = 24.6–18.2+13.6–1.5 = 18.5 mg N/L

The available TN is the initial NH_4^+, NO_2^- and NO_3^- concentrations along with the NO_3^- produced by the Anammox and NO_2^- produced by DAMOa.

$TN_{available}=[NH_4^+\text{-}N]_i+[NO_2^-\text{-}N]_i+[NO_3^-\text{-}N]_i+\Delta[NO_3^-\text{-}N]_{AMX}+\Delta[NO_2^-\text{-}N]_{DAMOa}$ = 13.8+24.6+26.6+3.5+13.6 = 82.1 mg N/L

To calculate the contribution of each microorganism to the available TN removed the following equations are employed.

$\%CATN_{removed}^{AMX}=(TN_{removed}^{AMX}/TN_{available})*100$= (28.5/82.1)*100= 35%

$\%CATN_{removed}^{DAMOa}=(TN_{removed}^{DAMOa}/TN_{available})*100$= (13.6/82.1)*100= 17%

$\%CATN_{removed}^{DAMOb}=(TN_{removed}^{DAMOb}/TN_{available})*100$= (18.5/82.1)*100= 23%

İ. FISH Imaging

Microscopy

The Carl Zeiss Axio Vision A1 UV microscope was used to view the prepared stained slides under the 40X magnification lense, in a dark room. The General Bacteria, General Archaea, and *M. nitroreducens* (DAMOa) labelled with GFP probes were viewed under the blue filter and appeared green in color. *M. oxyfera* (DAMOb) labelled with the Alexa-Fluor 350 probe was viewed under the UV filter and appeared blue in color. While General Anammox and *M. nitroreducens* (DAMOa) labelled with the Cy5 probe was viewed under the gren filter and appeared orange in color. Two different probes were used for the *M. nitroreducens* (DAMOa), the Cy5 probe was used in the slide aimed at determining the the abundance of *M. nitroreducens* relative to General Archaea, while the GFP probe was used in the slide aimed at determining the relative abundance of the target species among each other. The DAPI counterstaining was viewed under the UV filter and appeared as blue in color. The microscope camera captured black and white images, therefore, the necessary coloring was done through the Axio Vision software.

Imaging

For each slide at least 3 representative images were captured for each slide. These images were then processed using the ImageJ software (Schneider et al., 2012). The target microorganisms were classified depending on their fluorescence signal intensity which was compared to the threshold intensity (Zhou et al., 2007). The images were converted to 8-bit images (Figure I-1b), then the image was inverted to a white background and black pixels representing the fluorescent areas. The threshold was then adjusted to resemble the original image (Figure I-1c). The pixels were then analyzed using “Analyze Particles” to obtain a summary of the total area occupied by the pixels (Figure I-1d). Finally, the average of the total area occupied by the pixels of the three images was taken.

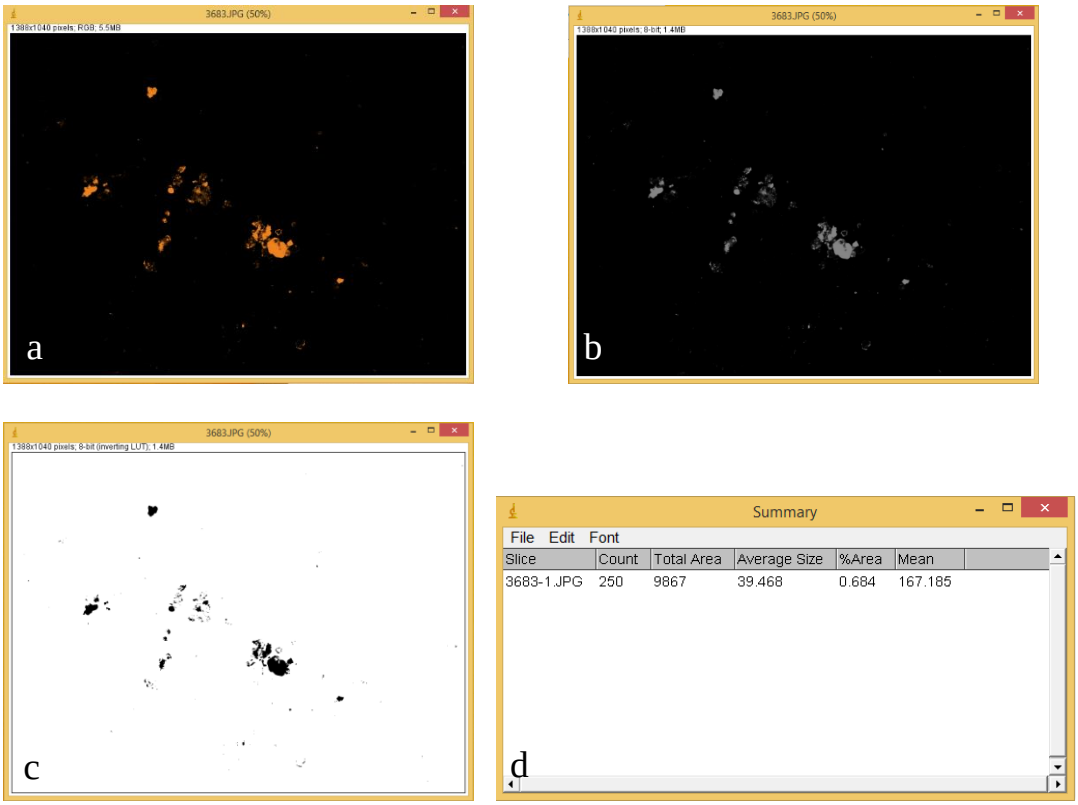

Figure I-1 (a) Original image taken from the microscope (b) Image converted to 8-bit (c) Inverted image and threshold adjustment administred (d) Summary of total area occupied by pixels

Relative Abundance Calculations

The relative abundances of microbial communities were calculated by assuming that the total microbial population included Bacteria and Archaea, which added up to 100%.

General Bacteria to DAPI ratio and General Archaea to DAPI ratio were calculated using the image taken. These ratios were subsequently used to normalization of the content of General Bacteria and General Archaea in the total microbial population (100%). The formulas used in the calculations are shown below.

$$\frac{General\ Bacteria}{DAPI}(\%) = \frac{Pixel\ Area\ of\ General\ Bacteria}{Pixel\ Area\ of\ DAPI} x100$$

$$\frac{General\ Archaea}{DAPI}(\%) = \frac{Pixel\ Area\ of\ General\ Archaea}{Pixel\ Area\ of\ DAPI} x100$$

$$\frac{General\ Bacteria}{Total\ Microbial\ Population}(\%)$$

$$= \frac{\frac{General\ Bacteria}{DAPI}}{\frac{General\ Bacteria}{DAPI}(\%) + \frac{General\ Archaea}{DAPI}(\%)}$$

$$\frac{General\ Archaea}{Total\ Microbial\ Population}(\%)$$

$$= \frac{\frac{General\ Archaea}{DAPI}}{\frac{General\ Bacteria}{DAPI}(\%) + \frac{General\ Archaea}{DAPI}(\%)}$$

The percentage of DAMOa in General Archaea Population (%) was calculated as shown below.

$$\frac{DAMOa}{General\ Archaea}(\%) = \frac{Pixel\ Area\ of\ DAMOa}{Pixel\ Area\ of\ General\ Archaea} x100$$

The following ratios are used to calculate Anammox to General Bacteria (%) and DAMOb to General Bacteria (%).

$$\frac{Anammox}{General\ Bacteria}(\%) = \frac{Pixel\ Area\ of\ Anammox}{Pixel\ Area\ of\ General\ Bacteria} x100$$

$$\frac{DAMOb}{General\ Bacteria}(\%) = \frac{Pixel\ Area\ of\ DAMOb}{Pixel\ Area\ of\ General\ Bacteria} x100$$

Finally, the percentage of target species (DAMOb, DAMOa, and Anammox) in the total microbial population (%) was calculated using the following formulas:

$$\frac{DAMOb}{Total\ Microbial\ Population}(\%) = \frac{\frac{General\ Bacteria}{Total\ Microbial\ Population}(\%) x \frac{DAMOb}{General\ Bacteria}(\%)}{100}$$

$$\frac{DAMOa}{Total\ Microbial\ Population}(\%) = \frac{\frac{General\ Archaea}{Total\ Microbial\ Population}(\%) x \frac{DAMOa}{General\ Archaea}(\%)}{100}$$

$$\frac{Anammox}{Total\ Microbial\ Population}(\%) = \frac{\frac{General\ Bacteria}{Total\ Microbial\ Population}(\%) x \frac{Anammox}{General\ Bacteria}(\%)}{100}$$

CURRICULUM VITAE

Surname, Name: Harb, Rayaan

EDUCATION

Degree	Institution	Year of Graduation
MS	METU-NCC Sustainable Environment and Energy Systems	2015
BS	AUB Biology	2012
High School	International School of Choueifat, Abu Dhabi	2007

FOREIGN LANGUAGES

Fluent English, Fluent Arabic, Average Turkish

PUBLICATIONS

Harb, R., Laçin, D., Subaşı, I., and Erguder, T. H. (2021). Denitrifying anaerobic methane oxidation (DAMO) cultures: Factors affecting their enrichment, performance and integration with anammox bacteria. *Journal of Environmental Management*, 295, 113070. https://doi.org/10.1016/j.jenvman.2021.113070

Football, Boxing, Percussions, Chess